

Lecture Notes in Management and Industrial Engineering

Ruhul Sarker

Hussein A. Abbass

Simon Dunstall

Philip Kilby

Richard Davis

Leon Young *Editors*

Data and Decision Sciences in Action

Proceedings of the Australian Society
for Operations Research Conference
2016

 Springer

Lecture Notes in Management and Industrial Engineering

Series editor

Adolfo López-Paredes, Valladolid, Spain

This book series provides a means for the dissemination of current theoretical and applied research in the areas of Industrial Engineering & Engineering Management. The latest methodological and computational advances that both researchers and practitioners can widely apply to solve new and classical problems in industries and organizations constitute a growing source of publications written for and by our readership.

The aim of this book series is to facilitate the dissemination of current research in the following topics:

- Strategy and Entrepreneurship;
- Operations Research, Modelling and Simulation;
- Logistics, Production and Information Systems;
- Quality Management;
- Product Management;
- Sustainability and Ecoefficiency;
- Industrial Marketing and Consumer Behavior;
- Knowledge and Project Management;
- Risk Management;
- Service Systems;
- Healthcare Management;
- Human Factors and Ergonomics;
- Emergencies and Disaster Management; and
- Education.

More information about this series at <http://www.springer.com/series/11786>

Ruhul Sarker · Hussein A. Abbass
Simon Dunstall · Philip Kilby
Richard Davis · Leon Young
Editors

Data and Decision Sciences in Action

Proceedings of the Australian Society
for Operations Research Conference 2016

 Springer

Editors

Ruhul Sarker
School of Engineering and Information
Technology
University of New South Wales
Canberra, ACT
Australia

Philip Kilby
Data 61
Commonwealth Scientific and Industrial
Research Organisation (CSIRO)
Melbourne, VIC
Australia

Hussein A. Abbass
School of Engineering and Information
Technology
University of New South Wales
Canberra, ACT
Australia

Richard Davis
Strategic Capability Analysis Department
Defence Science and Technology Group
Canberra, ACT
Australia

Simon Dunstall
Data 61
Commonwealth Scientific and Industrial
Research Organisation (CSIRO)
Melbourne, VIC
Australia

Leon Young
Department of Defence
War Research Centre
Canberra, ACT
Australia

ISSN 2198-0772

ISSN 2198-0780 (electronic)

Lecture Notes in Management and Industrial Engineering

ISBN 978-3-319-55913-1

ISBN 978-3-319-55914-8 (eBook)

DOI 10.1007/978-3-319-55914-8

Library of Congress Control Number: 2017935836

© Springer International Publishing AG 2018

This work is subject to copyright. All rights are reserved by the Publisher, whether the whole or part of the material is concerned, specifically the rights of translation, reprinting, reuse of illustrations, recitation, broadcasting, reproduction on microfilms or in any other physical way, and transmission or information storage and retrieval, electronic adaptation, computer software, or by similar or dissimilar methodology now known or hereafter developed.

The use of general descriptive names, registered names, trademarks, service marks, etc. in this publication does not imply, even in the absence of a specific statement, that such names are exempt from the relevant protective laws and regulations and therefore free for general use.

The publisher, the authors and the editors are safe to assume that the advice and information in this book are believed to be true and accurate at the date of publication. Neither the publisher nor the authors or the editors give a warranty, express or implied, with respect to the material contained herein or for any errors or omissions that may have been made. The publisher remains neutral with regard to jurisdictional claims in published maps and institutional affiliations.

Printed on acid-free paper

This Springer imprint is published by Springer Nature

The registered company is Springer International Publishing AG

The registered company address is: Gewerbestrasse 11, 6330 Cham, Switzerland

Preface

The Australian Society for Operations Research (ASOR) was established on the 1 January 1972. ASOR is associated with the International Federation of Operational Research Society (IFORS). Today, the society has more than 400 members nationwide and is expanding. The society runs an annual conference. 2016 witnessed the 24th edition of the ASOR conference with 120+ attendees and a programme spanning four days of interesting presentations and workshops.

This book is the culmination of the papers accepted at the conference. The event witnessed 72 technical presentations, out of which this book contains 29 chapters representing the papers accepted as full papers. Each submission was reviewed by two independent reviewers.

The conference was held at the University of New South Wales, Canberra Campus, located at the Australian Defence Force Academy. The event also hosted the Defence Operations Research Symposium (DORS). Four high calibre speakers gave plenary talks. These were Dr. Pamela Blechinger, Director US Army TRA-DOC Analysis Center; Dr. Stephan De Spiegeleire, Principal Scientist, Haque Centre for Strategic Studies, the Netherlands; Dr. Jamie Morin, Director, Cost Assessment and Program Evaluation (CAPE); and Dr. Haris Aziz, Senior Research Scientist, Data 61 (CSIRO), and Conjoint Senior Lecturer (UNSW).

The Editors of this book wish to take this opportunity to thank all attendees and the operations research community in Australia for supporting the event. Our deep appreciations go to members of the organising committee of the event, who made this happen: Mr. Arvind Chandran, Dr. Sharon Boswell, Dr. Sondoss El-Sawah, Dr. George Leu, Dr. Donald Lowe, and Dr. Jiangjun Tang.

We also wish to thank the organisations that supported this year's conference: the University of New South Wales, Canberra Campus, located at the Australian

Defence Force Academy; the Defence Science and Technology Group, Department of Defence, Australia; Data 61, Commonwealth Scientific and Industrial Research Organisation (CSIRO), Australia; and the Australian Society for Operations Research.

Australia
October 2016

Ruhul Sarker
Hussein A. Abbass
Simon Dunstall
Philip Kilby
Richard Davis
Leon Young

Contents

What Latin Hypercube Is Not	1
Oleg Mazonka and Charalambos Konstantinou	
A BDI-Based Methodology for Eliciting Tactical Decision-Making Expertise	13
Rick Evertsz, John Thangarajah and Thanh Ly	
Analysis of Demand and Operations of Inter-modal Terminals	27
Rodolfo García-Flores, Soumya Banerjee, George Mathews, Blandine Vacher, Brian Thorne, Nazanin Borhan, Claudio Aracena and Yuriy Tyshetskiy	
Efficient Models, Formulations and Algorithms for Some Variants of Fixed Interval Scheduling Problems	43
D. Niraj Ramesh, Mohan Krishnamoorthy and Andreas T. Ernst	
The Value of Flexible Road Designs Through Ecologically Sensitive Areas	71
Nicholas Davey, Simon Dunstall and Saman Halgamuge	
Local Cuts for 0–1 Multidimensional Knapsack Problems	81
Hanyu Gu	
An Exact Algorithm for the Heterogeneous Fleet Vehicle Routing Problem with Time Windows and Three-Dimensional Loading Constraints	91
Vicky Mak-Hau, I. Moser and Aldeida Aleti	
Automated Techniques for Generating Behavioural Models for Constructive Combat Simulations	103
Matt Selway, Kerry R. Owen, Richard M. Dexter, Georg Grossmann, Wolfgang Mayer and Markus Stumptner	

Analytic and Probabilistic Techniques for the Determination of Surface Spray Patterns from Air Bursting Munitions	117
Paul A. Chircop	
Reformulations and Computational Results for the Uncapacitated Single Allocation Hub Covering Problem	133
Andreas T. Ernst, Houyuan Jiang, Mohan Krishnamoorthy and Davaatseren Baatar	
Search Strategies for Problems with Detectable Boundaries and Restricted Level Sets	149
Hanyu Gu, Julia Memar and Yakov Zinder	
Alternative Passenger Cars for the Australian Market: A Cost–Benefit Analysis	163
Jason Milowski, Kalyan Shankar Bhattacharjee, Hemant Kumar Singh and Tapabrata Ray	
A Quick Practical Guide to Polyhedral Analysis in Integer Programming	175
Vicky Mak-Hau	
Towards a Feasible Design Space for Proximity Alerts Between Two Aircraft in the Conflict Plane	187
Mark Westcott, Neale Fulton and Warren F. Smith	
Constructing a Feasible Design Space for Multiple Cluster Conflict and Taskload Assessment	201
Neale L. Fulton, Mark Westcott and Warren F. Smith	
Open-Pit Mine Production Planning and Scheduling: A Research Agenda	221
Mehran Samavati, Daryl L. Essam, Micah Nehring and Ruhul Sarker	
A Comparative Study of Different Integer Linear Programming Approaches for Resource-Constrained Project Scheduling Problems	227
Ripon K. Chakraborty, Ruhul Sarker and Daryl L. Essam	
A Recovery Model for Sudden Supply Delay with Demand Uncertainty and Safety Stock	243
Sanjoy Kumar Paul and Shams Rahman	
Applying Action Research to Strategic Thinking Modelling	259
Leon Young	
Regression Models for Project Expenditures	271
Terence Weir	

SimR: Automating Combat Simulation Database Generation 291
 Lance Holden, Richard M. Dexter and Denis R. Shine

Battlespace Mobile/Ad Hoc Communication Networks: Performance, Vulnerability and Resilience. 303
 Vladimir Likic and Kamran Shafi

Using Multi-agent Simulation to Assess the Future Sustainability of Capability 315
 A. Gore and M. Harvey

Application of Field Anomaly Relaxation to Battlefield Casualties and Treatment: A Formal Approach to Consolidating Large Morphological Spaces 327
 Guy E. Gallasch, Jon Jordans and Ksenia Ivanova

Network Analysis of Decision Loops in Operational Command and Control Arrangements. 343
 Alexander Kalloniatis, Cayt Rowe, Phuong La, Andrew Holder, Jamahl Bennier and Brice Mitchell

Impact of Initial Level and Growth Rate in Multiplicative HW Model on Bullwhip Effect in a Supply Chain 357
 H.M. Emrul Kays, A.N.M. Karim, M. Hasan and R.A. Sarker

The *p*-Median Problem and Health Facilities: Cost Saving and Improvement in Healthcare Delivery Through Facility Location 369
 Michael Dzator and Janet Dzator

A Bi-level Mixed Integer Programming Model to Solve the Multi-servicing Facility Location Problem, Minimising Negative Impacts Due to an Existing Semi-obnoxious Facility. 381
 Ahmed W.A. Hammad, David Rey and Ali Akbarnezhad

Can Three Pronouns Discriminate Identity in Writing? 397
 David Kernot

What Latin Hypercube Is Not

Oleg Mazonka and Charalambos Konstantinou

Abstract Simulation methods play a key role in the modelling of theoretical or actual physical systems. Such models can approximate the behaviour of the real system and provide insights into its operation. Well-determined input parameters are of prime importance for obtaining reliable simulations due to their impact on the performance of the simulation design. Among various strategies for producing input parameter samples is Latin hypercube design (LHD). LHDs are generated by Latin hypercube sampling (LHS), a type of stratified sampling that can be applied to multiple variables. LHS has proven to be an efficient and popular method; however, it misses some important elements. While LHS focuses on the parameter space aspects, this paper highlights five more aspects which may greatly impact the efficiency of sampling. In this paper, we do not provide solutions but rather bring up unanswered questions which could be missed during strategy planning on model simulation.

Keywords Latin hypercube · Experimental design · Computer simulations

1 Introduction

Computer simulations aim to emulate a physical system through a computer model. The design and modelling of computer experiments allows to reproduce and capture the behaviour of the replicated system and thus make inferences about its characteristics. In science fields, many of these emulated processes need spatially distributed values to be used in computer simulation models as input. Latin hypercube sampling (LHS) has been used worldwide in such computer modelling applications.

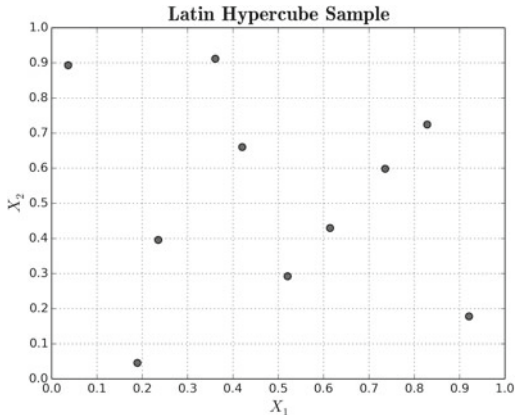
O. Mazonka (✉)

Defence Science and Technology (DST) Group, Department of Defence,
Edinburgh, SA 5111, Australia
e-mail: Oleg.Mazonka@defence.gov.au

C. Konstantinou

Department of Electrical and Computer Engineering, New York University
School of Engineering, Brooklyn, NY 11201, USA
e-mail: ckonstantinou@nyu.edu

Fig. 1 A Latin hypercube sample with $N = 10$, for two independent random variables X_1 and X_2 distributed uniformly on the unit square



LHS, introduced by McKay, Beckman, and Conover in 1979 [5], is a stratified random procedure which simultaneously samples on all input dimensions. Stratified sampling is a probability sampling technique in which the population is divided into non-overlapping segments, i.e. strata, and a sample is selected within each stratum. In Latin hypercube designs (LHDs), a sample is maximally stratified when the number of strata is equal to the sample size N and when the probability of falling in each of the strata is N^{-1} . Figure 1 shows a LHD sample drawn from two independent variables X_1 and X_2 distributed uniformly in $U[0, 1]$.

LHDs have always been particularly popular in computer simulations. For instance, LHDs have been used in a wide range of applications such as hurricane loss projection modelling, assessment for nuclear power plants and geologic isolation of radioactive waste, reliability analyses for manufacturing equipment, petroleum industry, and transmission of HIV [6]. There exist several reasons for the popularity of LHS. For example, Latin hypercube samples can cover design spaces regardless of their size and the requirements about the location and density of the data. The orthogonality of such samples allows also to construct non-collapsing, space-filling designs [4]. Hence, even if a subset of dimensions need to be discarded, the design remains a LHD allowing the samples to be reused. In addition, LHDs provide flexibility as they can adjust to the statistical assumptions of the experimental model.

LHDs often face problems to control the sampling of combinations of distributions and fill the design space, as the sampling of each distribution is handled separately to provide even distribution coverage. In many instances, optimization techniques to improve space-filling (e.g. minimizing some form of distance measure) or orthogonality (e.g. considering column-wise correlations) are challenging and expensive [11]. Other drawbacks of LHDs include the loss of statistical independence of sample values and the requirements in memory to hold the samples for each distribution. Also, there are practical scenarios in which LHS does not appear to be significantly superior to random sampling for computational sensitivity analysis [1, 9]. LHS lacks the ability to accommodate any prior knowledge of the model. To

overcome this problem, sequential sampling techniques, where a set of sample values are chosen so that certain criteria of the next experiment are satisfied, could be used. The yielded data is evaluated as it is collected, and further sampling is performed based on pre-defined rules of the resulted model performance.

In this paper, we show that some aspects of analysis during strategy planning on model simulation can be missed. While LHS focuses on the parameter space aspects, we present five more aspects worth considering before committing to a particular methodology of sampling design. We believe that there exist rigorous and correct solutions, of which the authors are not aware at the time of writing. Whether the solutions be known or ad hoc methods applied, they all remain outside of the scope of the paper.

The following section introduces a few techniques employed in experimental designs. The contribution of this paper—the different aspects of an experimental design—is described in Sect. 3.

2 Background and Overview

In experimental design, one studies a model (possibly stochastic) which depends on a number of parameters. These parameters are also called *factors*. Each factor can be set at a particular value. All such possible values are called *levels*. For example, a binary factor can take only two values: yes/no, true/false, etc.; a continuous factor can take values within a range of real numbers. If all factors are fixed to some values, then this set is called a *design point*. And the whole set of design points represent the experimental design. A design point is a deterministic input to the model, to which the model outputs the result either in a deterministic or probabilistic fashion.¹

In this section, we present the most notable techniques used for experimental designs.

2.1 *Randomized Complete Block Design (RCBD)*

In RCBDs, used in agricultural experiments, the field is divided into blocks and each block is further divided into units. The number of units is equal to the number of treatments. Treatments are then assigned randomly to the subjects in the blocks so that a different treatment is applied to each unit. This procedure ensures that all treatments are observed within each block. A simple layout of a RCBD is presented in Fig. 2. The defining characteristic of RCBD is that each block sees each treatment exactly once [13].

¹Note that randomness in probabilistic models cannot be included into the input to make the model deterministic, since the results represented as distributions rather than fixed values may reflect smoothness of the model which would be broken by fixing the seed to the random generator.

Fig. 2 Randomized complete block design (RCBD): each row represents a block in which the colours illustrate different treatments (4 blocks and 4 units/treatments within each block)



Fig. 3 Examples of a 3×3 and a 4×4 Latin square (LS) designs

A	B	C
C	A	B
B	C	A

(a) 3×3 LS.

A	C	B	D
D	A	C	B
B	D	A	C
C	B	D	A

(b) 4×4 LS.

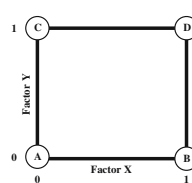
2.2 Latin Square (LS)

LS experimental designs follow the same concept of RCBDs with the main difference of conducting a single experiment in each block, so LS allows the existence of two factors [13]. In the previous agricultural example, the fertility of the land might vary in two directions (x -axis and y -axis) that can be used as the factors (e.g. due to soil type and water stagnation). The k levels of each factor can be represented in a square with k rows and k columns. In order to achieve a $k \times k$ LS design, then k treatments must be applied exactly once in each column and each row. Examples of a 3×3 and a 4×4 LS designs are shown in Fig. 3.

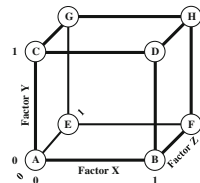
2.3 Factorial Designs

Such experimental designs consider all possible combinations of levels across all the design factors, i.e. the sample size N of factorial designs is equal to $N = \prod_{i=1}^n L_i$, where n the number of factors and L_i the levels of each factor [13]. In some cases, each factor has two levels ($L = 2$), resulting in 2^n treatment combinations. Figure 4 presents two such examples with two and three levels.

Fig. 4 Examples of a 2^2 and a 2^3 full factorial designs; factors X, Y, Z



(a) 2^2 full factorial.



(b) 2^3 full factorial.

Although factorial designs include at least one trial for each possible combination of factors and levels, they come at a high cost in terms of experimental resources. In order to reduce the cost, a set of possible combinations can be excluded resulting in a fractional factorial design.

2.4 Central Composite Design (CCD)

A CCD experimental design is a factorial or fractional factorial design with centre points, supplemented with a group of *star points* [3]. A CCD always contains twice as many star points as there are factors in the design. Those extra points allow the estimation of the second-order interactions between factors; otherwise, only linear dependencies can be assumed. Figure 5 presents the generation of a CCD for two factors.

2.5 Box–Behnken Design (BBD)

In contrast with the previous CCD design, BBD experimental designs do not contain all the embedded factorial points [2]. Specifically, BBDs is a class of rotatable or nearly rotatable second-order designs based on three-level incomplete factorial designs. The points in such designs exist at the centre and at the mid-points of edges of the parameter space. Figure 6 illustrates a BBD for three factors.

Fig. 5 Representation of the *star points* being added to factorial points



Fig. 6 The graphical representation of a Box–Behnken design (BBD) for three factors

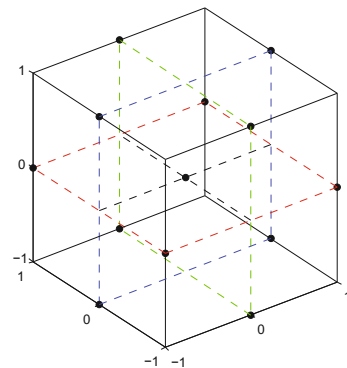


Table 1 A 12-run PB design matrix

Run	A	B	C	D	E	F	G	H	I	J	K
1	+	+	-	+	+	+	-	-	-	+	-
2	-	+	+	-	+	+	+	-	-	-	+
3	+	-	+	+	-	+	+	+	-	-	-
4	-	+	-	+	+	-	+	+	+	-	-
5	-	-	+	-	+	+	-	+	+	+	-
6	-	-	-	+	-	+	+	-	+	+	+
7	+	-	-	-	+	-	+	+	-	+	+
8	+	+	-	-	-	+	-	+	+	-	+
9	+	+	+	-	-	-	+	-	+	+	-
10	-	+	+	+	-	-	-	+	-	+	+
11	+	-	+	+	+	-	-	-	+	-	+
12	-	-	-	-	-	-	-	-	-	-	-

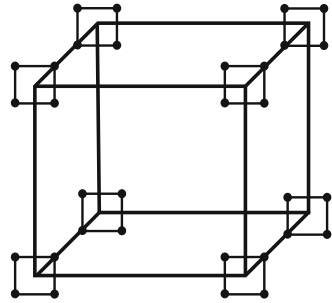
2.6 Plackett–Burman Design (PBD)

PBD is an efficient screening design when only particular effects are of interest. This experimental method is often used in ruggedness tests with the purpose: (a) to find the factors that strongly affect the outcome of an analytical procedure, and (b) to determine how closely one needs to control these factors [10]. PBD always involves $4n$ experiments ($n \geq 1$), and in each experiment, the maximum number of factors that can be studied is $4n - 1$. For instance, in a 12-run design, one can study up to 11 factors. A PBD matrix is shown in Table 1 in which the PB pattern is given in the first run. The other rows are generated by shifting one cell right the elements of the previous runs, and at the end, a row of minus signs is added. PBDs utilize two levels for each factor, the higher level being denoted ‘+’ and the lower ‘-’. Note that for any pair of factors, the number of combinations ‘++’, ‘+-’, ‘-+’, and ‘--’ is exactly the same.

2.7 Taguchi’s Idea

Taguchi procedures often refer to the experimental design as ‘offline quality control’ since they provide a good level of performance of products or processes occurred in the design space. Taguchi designs take into consideration that there exist factors (called noise factors) which cannot be controlled in the normal operation of a product [8]. The other factors identifying as controllable parameters are able to control the variability and minimize the effect of the noise factors (robust parameter design problem).

Fig. 7 Example of Taguchi design of experiment for 2^3 full factorial controllable factors and 2^2 full factorial noise factors



In the world of simulations, these parameters are called *exploration parameters* (controllable factors) and *sensitivity analysis parameters* (noise/uncontrollable factors). Studies often aim to compare the performance between different sets of exploration parameters as well as to compare the variation of performances due to noise factors. For example, the best performance may not be ‘the best’ choice because of variability, where some suboptimal result is better because it is less affected by uncontrollable factors.

Figure 7 shows a scenario of five parameters, two of which are uncontrollable and three are controllable. Two-level full factorial experimental designs can be considered for both types of factors. One design point—a corner in the cube—can be the optimal point whatever optimality is defined. However, this point may not be ‘the best’ choice because the variations of noise parameters—the four points around the corner—make worse on average results than another corner.

2.8 Monte Carlo

Such designs rely on random or pseudo-random samples of an input probability distribution [7]. The two main strengths on Monte Carlo methods are the following: first, the sampling process does not depend on number of factors—dimensionality, which means that any number of factors can be thrown into the design. Secondly, the data obtained from the running simulations can be analysed, while new simulations are being conducted. Thus, to obtain better knowledge about the model, one needs to run more simulations.

2.9 Latin Hypercube Designs (LHDs)

A type of stratified Monte Carlo sampling is LHS which simultaneously stratifies on all input dimensions [3]. LHDs, already presented in Sect. 1, require fewer iterations compared to Monte Carlo methods in order to recreate the input distribution. To recapitulate, the features of LHDs rely on both random and stratified sampling.

3 Experimental Design Considerations

The purpose of experimental designs is to study the performance of systems and processes. The choice of experiments as a series of tests is performed in a way to maximize efficiency. The problem in such design models is how to select a number of certain experiments from a possible infinite number of options in order to (a) gain as much valuable information as possible, and (b) satisfy the constraints of limited resources because each experiment bears cost and requires time.

Computer models are typically characterized by the input parameters (factors). All factors can be seen as dimensions of a parameter space S . A single experiment requires all factors to be set at particular values. Such set of values corresponds to a single point $\xi \in S$ —a design point. LHD generates a set of design points uniformly distributed within the multidimensional box in S , which is defined by the ranges of parameter values. This can be expressed via the following formula:

$$E[S] \rightarrow D$$

where E is an abstract engine which takes the definition of parameter space S as input and produces the experimental design D . LHD is an example of such engine.

The choice of point ξ in the experimental space determines the outcomes $\{\phi_i\}$ of the experiment from a variety of observable results ϕ in space O . Each replication, the repetition of the experiment aiming to acquire a more precise outcome distribution, is represented by the index i . For each selected ξ , several replications can be executed and each replication results in possibly different ϕ_i . In stochastic simulations, this variability is achieved by supplying different random seeds. In physical experiments, this variability may come from measurement errors or the inability to control all factors that determine the outcome. For each point ξ , the desired, and practically not achievable, outcome is to draw the real probability distribution of ϕ . The probability distribution can be approached with the growth of the number of replications executed at point ξ .

There is a dilemma, however, in how to obtain the distribution of the observable outcomes: whether to increase the number of replications in each point ξ or to increase the number of points ξ . In the first case, more replications at fewer points ξ can result in information of higher granularity. On the other hand, a greater number of points with fewer replications can provide a better illustration of the overall information. Finding an optimal balance between these two elements is outside of the scope of the paper. Had this question been resolved, a new engine,

$$E[S, O] \rightarrow D$$

taking into account the space of observables O , would provide a better design.

Besides the trade-off between the number of points ξ and the number of replications, the simulation cost C is also important. If different points ξ and different replications require the same amount of resources, then the cost is proportional to the number of simulations. In the general case, however, not all the areas of the

experimental space S would have the same cost effect: certain zones can be less expensively explored than others in terms of cost $C(\xi)$. Additionally, in complex experimental designs, the cost $C(\xi)$ may not be known in advance but obtained as one of the results O . Clearly, the knowledge of the cost function would influence the optimal design:

$$E[S, O, C] \rightarrow D$$

Similarly with the simulation cost C , the value $V(\xi)$ of information obtained as a result of simulation at point ξ defines another aspect that influences D . Some areas of the experimental space S , for instance, might be of greater importance for the system compared to other points ξ in the design. In addition, as with the simulation cost case, the value $V(\xi)$ of particular areas may depend on the obtained experimental results. For example, in combat simulations, a balance between forces strongly governs winning or losing outcomes [12]. In the parameter space, there may be vast areas of no particular interest because the outcome is predictable. The valuable information is the transition area where the probability to lose or win is not definite. An optimal design would have all design points in this transition area; then, the engine E including function $V(\xi)$ becomes:

$$E[S, O, C, V] \rightarrow D$$

At first glance, the value V constraint can be interpreted as quite artificial. One can assume to tolerate some extra experiments in not important areas as trade-off for simplicity of having a multidimensional box with flat boundaries. However, multidimensional spaces can be very counter-intuitive. For example, an n -dimensional unit ball submerged into a n -dimensional cube with edge equal to 2 (the ball touches each face of the cube) has its volume about 80% of the volume of the cube in *two* dimensions—a circle and a square. In *three*-dimensional space, this value is around 50%, in 10 dimensions $\approx 1.6\%$, and in 20-dimensional space, the ratio of the ball's volume to the cube's volume is 2.5×10^{-8} . For the latter case of the 20-parameter space, a randomly chosen point within the smallest enclosing box will almost always be outside of the ball. In this example, having 20 factors requires more than 40 million points in order to get at least one point inside the ball—representing a constraint on factors.

Another aspect that needs to be taken into account is the information I already obtained from the experiment. This information depends on the set of points which have been evaluated $\{\xi_i \rightarrow \{\phi\}\}$, plus the set of points which are being evaluated but do not have yet the result $\{\xi_j\}$. In general, the information I is a function of those two sets: $I = I(\{\xi_i \rightarrow \{\phi\}\}, \{\xi_j\})$. Design engine E has to wisely produce more points where not enough information has been or expecting to be accumulated and less where the space is already explored:

$$E[S, O, C, V, I] \rightarrow D$$

This idea is known as sequential sampling.

The last aspect we consider in this paper is the resources R required to conduct the new experiment. In the simple scenario for which the cost C follows a uniform distribution, the resources R are equivalent to the total number of samples, i.e. the sum of the number of replications N_ξ over the number of points ξ : $R = \sum_\xi N_\xi$. The resource R in many cases influences the implementation of the design E . When the design points are evaluated sequentially, the order of evaluation is important, because depending on the intermediate outcomes, the evaluation can be simply interrupted, redesigned and/or re-evaluated. The design engine E therefore should include this aspect as well:

$$E[S, O, C, V, I, R] \rightarrow D$$

In its simplicity, LHD, besides the non-collapsing and filling properties in the experimental space S , ignores all the other aspects:

$$E[S, \emptyset, \emptyset, \emptyset, \emptyset, R] \rightarrow D$$

observational space O , cost C and value V functions, prior information I , and the experimentation resources R . From this point of view, applicability of LHD appears sound only after considering and consciously ignoring these five aspects.

4 Conclusions

LHD is a useful and practical tool which can provide exceptional benefits in experimental design. In this paper, we have highlighted aspects which are important in experimental design but, except parameter space S , are not present in the Latin hypercube method. Awareness of those aspects brings justification of proper usage of LHD and sets up the boundaries where LHD can be safely utilized.

Considering these aspects brings up a question: Is there a method taking all known information and giving the optimal design? The authors believe that such a method—the perfect engine E —exists, derived from the basic principles of probability theory. At the same time, it is possible that each aspect raised in this paper can be addressed by a simple ad hoc solution which may not be very far from optimal.

5 Rev2 Replies

First, the definition of resource R seems to overlap with the other aspects, notably space O and cost C . Does the knowledge of O and C is enough to know R ? (In which case R is redundant). Or does R provide some information not already included in O and C ? (And if yes, what is it?).

No. Assume that O and C are known and well defined. If we allow to run only one point, then the engine gives us the most useful position of the design point. If we

allow to run two points, then the most useful points will likely be both different from the one before (when we have the resources to run only one point). In this sense, the optimal position of design points depends on the number of points we are able to run.

Second, the shortcomings of LHD described here (that $E[S]$ ignores, O , C , V , I and R) are not specific to LHD. More generally, all general quasi-random generators (classical random sampling, low-discrepancy sampling, etc.) used as is without input from the system at hand will suffer from the same limitations.

This is correct. However, many Latin hypercube promoters consider LHS as so powerful that great effort is spent on improving the method within LHDs. The purpose of this paper is to provide an alternative point of view, especially for a less experienced audience (not to fall into conclusion that LHD solves the problem).

Following the previous remark, it could be interesting to come back to the list of most notable techniques for experimental designs listed in Sect. 2 (RCBD, LS, Factorial, CCD, BBD, PBD, Taguchi, Monte Carlo, LHD) in the light of the list of desirable elements that experimental designs should take into account (S , O , C , V , I , R) established in Sect. 3. This can be summarized in a table, for example, and could help to establish clusters of similar methods, and would point out to the best existing experimental design (according to the criteria from Sect. 3). This would be consistent with the idea of searching for the optimal design discussed in the Conclusion. At the same time, LHD would be even less the real focus of the paper (the title might need to be changed).

In this paper, we discuss only about LHD. Other methods are provided as a background material. In the context of the paper, LHD is superior to other designs (except Taguchi, which is not a design, but is a relevant observation). Hence, we would like to point the reader exactly to ‘What Latin Hypercube is not’.

References

1. Becker, D.A.: Overview of advantages and drawbacks of different methods for sensitivity analysis in the context of performance assessment. In: 5th IGD-TP Technical Exchange Forum, Kalmar, Sweden (2014)
2. Ferreira, S.C., Bruns, R., et al.: Box-Behnken design: an alternative for the optimization of analytical methods. *Anal. Chim. Acta* **597**(2), 179–186 (2007)
3. Giunta, A., Wojtkiewicz, S., et al.: Overview of modern design of experiments methods for computational simulations. In: Proceedings of the 41st AIAA Aerospace Sciences Meeting and Exhibit, AIAA-2003-0649 (2003)
4. Kleijnen, J., Sanchez, S., et al.: A user’s guide to the brave new world of designing simulation experiments. Center for Economic Research Discussion Paper (1) (2003)
5. McKay, M., Beckman, R., Conover, W.: A comparison of three methods for selecting values of input variables in the analysis of output from a computer code. *Technometrics* **42**(1), 55–61 (2000)
6. Melnick, E., Everitt, B.: *Encyclopedia of Quantitative Risk Analysis and Assessment*, vol. 1. Wiley (2008)
7. Paxton, P., Curran, P., et al.: Monte carlo experiments: design and implementation. *Struct. Equ. Model.* **8**(2), 287–312 (2001)

8. Roy, R.K.: Design of experiments using the Taguchi approach: 16 steps to product and process improvement. Wiley (2001)
9. Saltelli, A., Chan, K., et al.: Sensitivity Analysis, vol. 1. Wiley, NY (2000)
10. Vanaja, K., Shobha Rani, R.: Design of experiments: concept and applications of Plackett Burman design. *Clin. Res. Regul. Aff.* **24**(1), 1–23 (2007)
11. Viana, F.A.: Things you wanted to know about the Latin hypercube design and were afraid to ask. In: 10th World Congress on Structural and Multidisciplinary Optimization, Orlando, Florida, USA (cf. p. 69) (2013)
12. Williams, P., Bowden, F.: Dynamic morphological exploration. In: Proceedings of the 22nd National Conference of the Australian Society for Operations Research (2013)
13. Winer, B.J., Brown, D.R., Michels, K.M.: Statistical Principles in Experimental Design, vol. 2. McGraw-Hill (1971)

A BDI-Based Methodology for Eliciting Tactical Decision-Making Expertise

Rick Evertsz, John Thangarajah and Thanh Ly

Abstract There is an ongoing need to computationally model human tactical decision-making, for example in military simulation, where the tactics of human combatants are modelled for the purposes of training and wargaming. These efforts have been dominated by AI-based approaches, such as production systems and the BDI (Beliefs, Desires, Intentions) paradigm. Typically, the tactics are elicited from human domain experts, but due to the pre-conscious nature of much of human expertise, this is a non-trivial exercise. Knowledge elicitation methods developed for expert systems and ontologies have drawbacks when it comes to tactics modelling. Our objective has been to develop a new methodology that addresses the shortcomings, resulting in an approach that supports the efficient elicitation of tactical decision-making expertise and its mapping to a modelling representation that is intuitive to domain experts. Rather than treating knowledge elicitation, as a process of *extracting* knowledge from an expert, our approach views it as a collaborative modelling exercise with the expert involved in critiquing the models as they are constructed. To foster this collaborative process, we have employed an intuitive, diagrammatic representation for tactics. This paper describes TEM (Tactics Elicitation Methodology), a novel synthesis of knowledge elicitation with a BDI-based tactics modelling methodology, and outlines three case studies that provide initial support for our contention that it is an effective means of eliciting tactical decision-making knowledge in a form that can be readily understood by domain experts.

R. Evertsz (✉) · J. Thangarajah
RMIT University, Melbourne, VIC, Australia
e-mail: rick.evertsz@rmit.edu.au

J. Thangarajah
e-mail: john.thangarajah@rmit.edu.au

T. Ly
Defence Science and Technology Group, Perth, Australia
e-mail: thanh.ly@dsto.defence.gov.au

Keywords BDI · Cognitive modelling · Knowledge elicitation · Tactical decision making

1 Introduction

AI has been central to the computational modelling of tactical decision-making for over 20 years; early applications include air combat [10], and more recently, autonomous live-fire robot targets [6]. Previously, we have argued that these efforts have all been at the *implementation* level, and that tactics need to be represented at the *design* level in order to facilitate maintenance and sharing amongst developers, as well as comprehension by domain experts [7]. As part of that work, we proposed TDF (Tactics Development Framework) as a means of addressing this shortcoming and extended agent-oriented software engineering approaches such as Prometheus [14] to better handle the demands of tactical modelling.

Whereas TDF allows models of tactics to be captured, it does not support the elicitation of those tactics, and this is a challenging and important aspect that has not been addressed until now. In this work, we propose a methodology for the elicitation of tactical decision-making that maps directly to TDF concepts.

In theory, tactics can be automatically generated if the domain can be sufficiently well formalised. However, this is not practical in complex, real-world domains, and so the dominant approach to tactics modelling is to study domain experts. Unfortunately, eliciting knowledge from experts is a non-trivial exercise. The so-called *knowledge acquisition bottleneck* was recognised very early on as a key problem in the construction of intelligent systems [8]. Pioneering work on the knowledge acquisition problem was performed predominantly by those developing *expert systems*—computer models that were intended to be comparable in domain-specific competence to human experts.

Our experience, collaborating for over 20 years with military analysts modelling tactics in areas such as undersea warfare, air combat, tank battles, and special forces, suggests that knowledge elicitation continues to be a very significant problem. Across these groups of analysts, various techniques are employed, e.g. Cognitive Task Analysis [4], with varying degrees of success. It is difficult to critique these approaches collectively because they tend to be idiosyncratic, with a wide range of elicitation objectives and products. However, what they do have in common is the absence of a well-defined representation language for tactics that is readily understood by domain experts. The elicitation products tend to be static and result in an informal snapshot of the knowledge elicitation sessions that quickly becomes divorced from the tactics models. It is very difficult for domain experts to critique the resulting tactics implementation, because all they can do is observe the behaviour without a straightforward means of mapping that behaviour back to the elicited tactics.

Our research objective is to develop a methodology that supports the efficient elicitation of tactical decision-making expertise and its mapping to a tactics repre-

sentation that is intuitive to domain experts. To this end, we have developed TEM (Tactics Elicitation Methodology), which advances the state of the art in knowledge elicitation to better handle the demands of tactics modelling. Rather than treating knowledge elicitation as a process of *extracting* knowledge from an expert, our approach views it as a collaborative modelling exercise with the expert involved in critiquing the models as they are constructed. To foster this collaborative process, we have employed an intuitive, diagrammatic representation for tactics. We argue that knowledge elicitation is intimately bound to the target conceptual framework. For example, elicitation methods that work well when building an ontology may need to be quite different to those that suit a diagnostic expert system. The former is likely to focus on teasing out the fine detail of conceptual structures, whereas the latter will be more concerned with cues and problem-solving methods. Likewise, tactics elicitation focuses on particular factors such as the events that trigger the adoption of goals, the methods used to achieve those goals, and the conditions that indicate that a goal should be dropped in favour of a more pressing one.

This paper makes several contributions to the field of behaviour modelling in intelligent systems: (i) it offers a novel synthesis of knowledge elicitation with a BDI-based tactics modelling methodology; (ii) it focuses knowledge elicitation on the aspects that are important to tactics modelling; and (iii) the elicitation methodology's application to three domains is evaluated.

2 Background

Military science definitions of the term, *tactics*, tend to emphasise their adversarial nature. More generally, tactics can be viewed as the means of achieving an immediate objective in a manner that can be adapted to handle unexpected changes in the situation. Tactics are distinguished from *strategy* in that the latter is concerned with a general approach to the problem, rather than the means of achieving a more short-term goal. A submarine commander's use of stealth to approach a target is a strategy, whereas the particular method used, for example hiding in the adversary's baffles (a blind spot), is a tactic. Tactics are concerned with the current, unfolding situation—that is, how to deflect threats and exploit opportunities to achieve victory. This view of tactics, as the means of achieving a short-term goal in a manner that can respond to unexpected change, seems to be common to all definitions, whether in military science, game theory, or management science.

2.1 Knowledge Elicitation

Over the years, a significant proportion of the effort to construct intelligent systems has adopted a *knowledge-based* approach. In contrast to general problem-solving methods, the knowledge-based approach relies on encoding a large quantity

of domain-specific knowledge. This was motivated by the observation that expert human performance achieves its efficacy by applying domain-specific strategies and knowledge to the problem at hand. The computational modelling of expert competence came to be known as *knowledge engineering*, with the term *knowledge elicitation* being used to denote the initial process of extracting the knowledge from the expert before encoding it in a suitable knowledge representation language.

Practitioners generally agree that the elicitation of expertise is a challenging endeavour. Musen identified a number of reasons [11]; perhaps the most significant is that expert knowledge is largely tacit. It is generally agreed that *knowledge compilation* [12] is central to the human cognitive architecture's ability to efficiently process large amounts of information as smaller, composite items that functionally expand working memory. The downside is that it is difficult, if not impossible, for experts to decompile such knowledge to understand the basis of their decision-making. Consequently, experts can be inaccurate when recounting their thought processes, and may unintentionally fabricate reasoning steps in order to bridge the gaps in their conscious understanding of their own decision-making [9].

2.2 *BDI and the Theory of Mind*

Our experience of eliciting tactical knowledge from experts, in domains including air combat, infantry tactics, air traffic flow management, and undersea warfare, suggests that the outcome is greatly influenced by whether the experts find the conceptual framework in which the knowledge is cast to be intuitive. Experts are better able to describe their reasoning if the emerging tactical model corresponds to how they *think they think*. In the field of cognitive science, it is generally accepted that human beings employ a *theory of mind* to explain and predict the actions of others, as well as to provide a narrative for their own reasoning processes. According to the *intentional stance* [5], we attribute intentions to ourselves and others, and believe them to arise from a combination of our beliefs and desires.

Through the work of Bratman [2] on practical reasoning, this philosophical perspective gave rise to the BDI paradigm, a modelling approach that has been popular for many years in the multi-agent systems community. It has been claimed that the BDI paradigm is a good *folk psychology* model of human reasoning, i.e. a model of how we think [13].

The BDI model is a particularly parsimonious conception of rational agency, characterising agents as reasoning in terms of their *beliefs* about the world, *desires* that they would like to achieve and the *intentions* that they are committed to. Apart from its intuitive appeal to domain experts, it is a powerful computational abstraction for building sophisticated, goal-directed, and reactive reasoning systems, and consequently is well suited to tactics modelling.

Put very succinctly, a BDI agent performs a continuous loop in which it updates its beliefs to reflect the current state of the world, deliberates about what to achieve next, finds a plan for doing so, and executes the next step in that plan. Each time around

this cycle, it effectively reconsiders its options, yielding goal-oriented behaviour that is also responsive to environmental change.

Our research objective is to develop a tactics elicitation methodology that is easier to master than Cognitive Task Analysis, and offers an intuitive representation of decision-making—one that is compatible with experts’ intuitions about how they reason tactically. With this in mind, we have developed a BDI-based elicitation methodology.

2.3 Tactics Development Framework (TDF)

TEM targets TDF, a BDI-based tactics design methodology founded on agent-oriented software engineering principles. In TDF, the tactical environment is represented in terms of the important *percepts* received, *actions* performed, and the *actors* the system interacts with. Methods of achieving *goals* using *plans* are encapsulated in terms of *tactics*. These in turn are encapsulated by the *missions* that the system can undertake. The other concepts that are relevant to TEM are *messages* passed between *agents*, *scenarios* outlining the different ways that a mission can play out, the *roles* embodied by the system, and the *data* maintained by the system.

TDF divides modelling into three major stages: (i) *System Specification* of system-level artefacts, (ii) *Architectural Design* of the internal structure of the tactical system, and (iii) *Detailed Design* of the internals of the agents in the system. In addition, *tactics design patterns* span the three stages, providing a reusable template from which new tactics can be built. TDF has been used to model undersea warfare, Apache attack helicopter tactics, UAS decision-making, and infantry tactics. Further detail on the methodology can be found in [7].

3 Tactics Elicitation Methodology (TEM)

TEM’s artefacts all map directly to the corresponding TDF concepts (apart from TEM’s *concept maps*, which TDF does not include). Some of the TDF artefacts have been renamed so that they are more meaningful to domain experts within the context of knowledge elicitation, namely *mission* becomes *vignette*, *agent* becomes *character*, *actor* becomes *environmental entity*, *scenario* becomes *storyline*, and *data* is now *belief*.

The TEM artefacts are as follows: (i) *Concept Map*—a diagrammatic graph-like structure that informally represents concepts and their interrelationships; (ii) *Vignette*—a succinct description of a tactical situation, as per [3]; (iii) *Tactic*—specifies how to achieve a goal in a situation that might change in unexpected ways, and comprises a goal/sub-goal structure, the methods used to achieve goals, and the conditions under which goals are adopted, dropped, suspended or resumed; (iv) *Storyline*—a specification of the key cues and decision points that occur as

the vignette unfolds; (v) *Goal Structure*—a goal/sub-goal hierarchy; (vi) *Plan*—a method of achieving a goal, or responding to an event; (vii) *Character*—a behavioural entity embodying some combination of tactics, goals, and plans; (viii) *Team*—an aggregation of characters and/or teams; (ix) *Role*—functionality assigned to a character or team; (x) *Percept/Action*—a character receives information in the form of percepts and affects its environment by performing actions; (xi) *Environmental Entity*—source of percepts or the target of actions; (xii) *Belief*—each character or team has a set of beliefs that defines its declarative knowledge.

3.1 TEM Steps

TEM is an interview-based elicitation methodology, as this is the most efficient method in terms of time and resources [4].

The following account is necessarily abbreviated to fit within the confines of this paper, but all of the steps are included, if not in great detail. The examples are based on a study [1] in which an HVU (High Value Unit) is protected by four destroyers (Screen Ships) from attack by a submarine.

TEM comprises six sequential steps that are repeated until the requisite information has been acquired: (i) Scope Requirements; (ii) Expand Modelling Objective; (iii) Construct Storylines; (iv) Populate Concept Map from Storylines; (v) Develop TDF Design; and (vi) Plan Next Session.

3.1.1 Scope Requirements

- *Elicit Stakeholder Objective.* If required, interview the stakeholder to determine the question to be answered by the modelling exercise, for example, ‘*How many screen ships are required to protect an aircraft carrier from submarine attack?*’.
- *Elicit Modelling Objective.* The stakeholder objective is usually not sufficiently specific for the purposes of modelling and needs refining to derive the *modelling objective*—ideally a testable hypothesis relating independent to dependent variables. If the modelling objective can be expressed quantitatively, determine the MOEs.¹
- *Study Background Material.* Ensures interviewer has sufficient grounding in the domain to efficiently interview the domain expert.
- *Scope Interview Sessions.* Purpose is to determine how much time is available, and to plan the sessions so that the stakeholder objective is adequately addressed.

¹An MOE (Measure of Effectiveness) is a quantitative impact assessment, e.g. ‘*Dollar value of aircraft carrier damage saved per screen ship deployed*’. In simulation applications, the values for a dependent variable are typically aggregated across multiple simulation runs to yield an MOP (Measure of Performance), e.g. ‘*average dollar value of aircraft carrier damage*’. The MOE combines the MOPs into an impact statement.

3.1.2 Expand Modelling Objective

The modelling objective is central to the TEM process and is used to ensure that the elicitation does not drift off into interesting but irrelevant detail. This step results in a concept map representation of the modelling objective properties and related attributes, such as independent variables, dependent variables, and MOEs. This step comprises three activities:

- Create a concept map with the modelling objective at its root.
- Link MOEs to the modelling objective in the concept map.
- Add any modelling objective preferences to the concept map, e.g. variables that define the optimality of a given solution.

The concept map is a graph that acts as a shared diagrammatic representation of the domain. It does not constrain the interviewer to a particular set of artefacts, and this notational freedom is instrumental in fostering rapid elicitation. However, structure is added to the concept map after each elicitation session, by identifying relevant TDF artefacts (Fig. 1 shows part of a bushfire concept map after the TDF artefacts have been identified).

3.1.3 Construct Storylines

- *Elicit Relevant Vignettes.* Prompt the domain expert for vignettes that he/she has personal decision-making experience of, and that address the modelling objective. Identify those vignettes that are most likely to provide useful information about the modelling objective. Add the selected vignette(s) to the concept map. Where appropriate, employ diagrams to document the spatial layout of the key entities in the vignette, for the purposes of discussion with the domain expert.
- *Generate Relevant Storylines.* The domain expert selects the vignette that reveals the most about the modelling objective, and recounts a related storyline, for which he/she was the primary decision-maker. Failing this, the domain expert should generate a hypothetical storyline.
- *Verify Selected Storyline.* Verify that the storyline addresses the modelling objective *before* too much time is spent eliciting the details. Establish that the outcomes (as characterised by the MOEs) will depend upon the identified dependent variables. If the relationship between the storyline and modelling objective is not convincing, choose a new storyline. If the domain expert cannot come up with a more effective storyline, select a new vignette.
- *Fill Out Storyline.* Map out the key decision-making cues and decision points in the storyline. Link the storyline to the vignette in the concept map. Elicit missing information and significant storyline variations that will be needed to build the tactics, i.e. (i) key decision points, (ii) the goal being tackled in each episode of the storyline, (iii) conditions that need to be maintained during storyline episodes, (iv) goals adopted/dropped/suspended/resumed and the conditions under which this

happens, (v) the name of the tactic adopted to achieve the goal, (vi) other courses of action considered, (vii) actions performed as part of the tactical approach, (viii) significant roles/characters/teams involved in the storyline, (ix) communications between characters, teams, and environmental entities, (x) timing information (relative and/or absolute) that relates to the events in the storyline.

3.1.4 Populate Concept Map from Storylines

This step's purpose is to identify concepts that arise from the storylines and elicit further detail about those concepts. To do so, label concepts in the storyline that relate to goals, tactics, roles, teams, characters, key conditions, and domain-specific terminology. Figure 1 shows an annotated concept map from a firefighting case study (with actions, beliefs, goals, percepts, plans, and roles).

3.1.5 Develop TDF Design

This step occurs after the elicitation session is over.

- *Develop Storyline Diagrams.* Results in a diagrammatic representation of each storyline, to be used in subsequent elicitation sessions, and as input to the TDF design process. Figure 2 shows an example of an *episode* of a storyline (a storyline can be made up of a number of episodes).

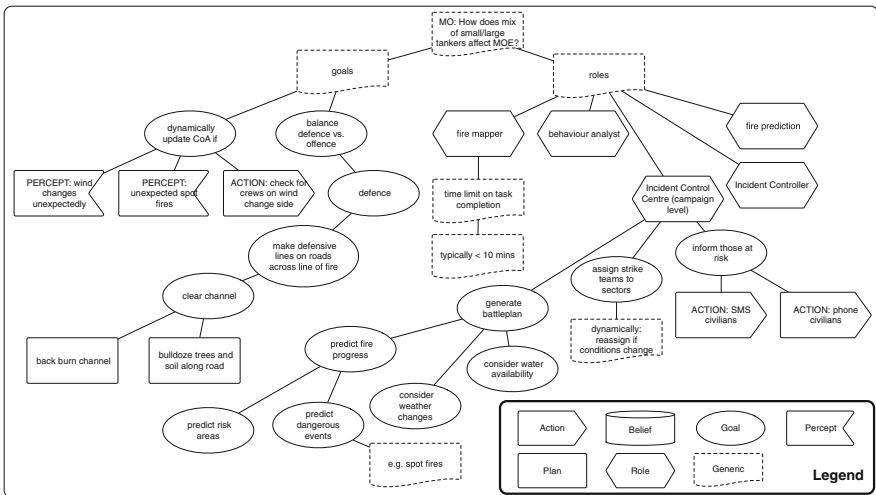


Fig. 1 Part of bushfire concept map (after artefact classification)

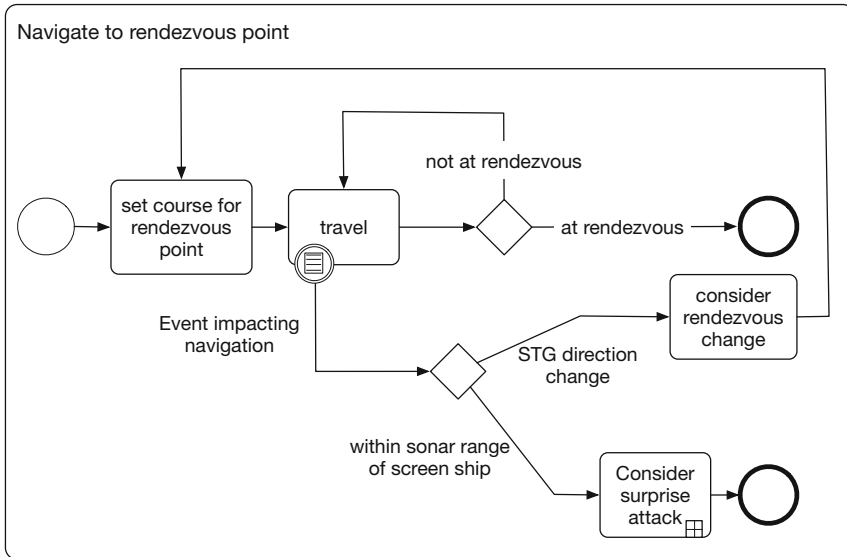


Fig. 2 Navigate to rendezvous (example storyline episode)

- *Develop Initial TDF Design.* This involves identifying and labelling TDF artefacts in the concept map and storylines (goals, plans, roles, percepts, etc.), using a palette of predefined TDF icons. Underspecified concepts are highlighted so that they can be addressed at the next elicitation session. An initial TDF design is constructed as outlined in the *System Specification, Architectural Design,* and *Detailed Design* stages, described fully in [7].

3.1.6 Plan Next Session

This step identifies missing information so that gaps can be filled during the next elicitation session. It comprises the following activities:

- Work through any artefacts that were marked as underspecified while developing the initial TDF design.
- Verify that there is sufficient information to build a goal structure for each of the decision points in the storylines.
- Verify that there is enough information to build the plans required to achieve the goals.
- Identify missing artefacts, for example, percepts that are needed to discriminate between alternative plans for achieving a goal.
- Identify areas of focus for the next elicitation session.

4 Preliminary Case Studies

The evaluation of knowledge elicitation methodologies continues to be a problematic and challenging endeavour. An extensive discussion of the issues can be found in [15]. Impediments include the difficulty of accessing a large enough sample of domain experts for statistical significance, the lack of homogeneity in domain expert opinions, how to quantify coverage and depth of knowledge elicited, and how to compare the content of disparate knowledge representations. Although it would be feasible to conduct a quantitative evaluation using a restricted and formal board game, such as chess, this would be unenlightening with respect to the domains TEM is designed for. TEM targets dynamic, real-world domains and so focuses on eliciting the goal-directed and reactive aspects of decision-making that rely on complex and varied contextual cues and broad repertoires of tactical actions. With these caveats in mind, a preliminary evaluation of TEM was performed, using three distinct domains to broaden the coverage: (i) firefighting of bushfires, (ii) undersea warfare, and (iii) the League of Legends real-time, multi-player tactical game.

4.1 *Bushfire Tactics (Pilot Study)*

The objective of the initial evaluation of TEM was to investigate its efficacy. The domain expert had many years of experience fighting bushfires, both on the ground and from the control centre. After a number of knowledge elicitation sessions, totalling 5 h, a TDF design was produced from the elicited storyline and concept map. The domain expert judged the design to be a clear and accurate representation of the elicited firefighting tactics. He volunteered that he found the whole process to be very rewarding and was highly motivated to provide accurate and detailed information about tactical alternatives because he felt that he fully understood how his expertise was being represented and so felt ownership of the models as they were being developed. This feedback provides encouraging support for TEM's collaborative approach to elicitation.

4.2 *Undersea Warfare Tactics*

The undersea warfare environment is characterised by a high degree of uncertainty about the true tactical situation. Situation awareness is time consuming to acquire and often unreliable, and this makes it difficult to predict the outcome of a particular course of action. Many factors have to be considered when trying to eliminate hypotheses, and this, taken together with the high level of uncertainty, makes it difficult to elicit the submarine commander's tactical knowledge. An analyst, attempting to elicit and build a model of submarine commander decision-making, is faced with

a very wide and potentially confusing array of options, and this was the original motivation for developing TEM.

A number of 90-min undersea warfare tactics elicitation sessions were conducted over the course of three consecutive days, amounting to about 18 h. Six domain experts took part in the sessions, which focused on submarine evasion of helicopter(s) equipped with dipping sonar. Some of the experts had extensive knowledge of the performance of active sonar, which is highly relevant to the modelling objective (dipping sonar is active, not passive), and one of the domain experts, a submarine commander, had direct experience of operating against helicopters with dipping sonar. The two interviewers had experience of informally interviewing domain experts, and one had been an observer in the bushfire elicitation sessions. Neither had any experience leading a TEM session, and relied solely on reading the TEM documentation beforehand.

The interviewers provided general feedback on TEM, but due to security considerations, were not able to provide us with the concrete products of the elicitation sessions. They reported that:

- the methodology was straightforward and very successful in guiding their elicitation of the requisite information;
- the methodology should include a step recommending diagramming of the spatial layout of the problem;
- the methodology's focus on working immediately from the vignettes/storylines was vital because the domain experts resisted discussing abstractions, preferring instead to discuss specific instances;
- the elicitation sessions exposed novel information that was not in any written material about the domain;
- the storyline mechanism was very effective in eliciting key perceptual cues, decisions, and sequences of actions; and
- the identification of tactical goals was instrumental in the elicitation of alternative courses of action.

The feedback from the interviewers and domain experts was overwhelmingly positive, and the interviewers reported that the methodology was easy to follow, and the outcome was successful. There were two recommendations for change: (i) add a methodological step for creating one or more diagrams of the spatial layout of the tactical situation, and (ii) emphasise the need to begin with concrete vignettes and storylines, rather than abstract questions about the domain.

4.3 League of Legends Tactics

The final case study applied TEM to the elicitation of League of Legends tactics, and apart from investigating the efficacy of the methodology, it focused on the comprehensibility of the resulting TDF designs.

League of Legends² is a fast-paced, multi-player, online strategic/tactical game, with tens of millions playing it daily. Each player takes on the role of a *summoner* who controls a champion. Each game comprises two teams of five players, with each team battling the other to destroy their *nexus*. The League of Legends domain is particularly rich, with a wide range of characters possessing very different capabilities, many classes of weaponry, only partial situation awareness, team tactics, and frequent unexpected changes in the tactical situation. Although the tactics are goal-directed, there is a large reactive component and a good player must be able to respond quickly to significant changes, based only on partial information about the situation.

Three domain experts took part in the study; one was interviewed over the course of seven 90-min sessions, and the other two assessed the comprehensibility of the resulting TDF tactics diagrams. All three experts have a world ranking in the top few per cent of the League of Legends Elo rating system, but none of them were familiar with TEM or TDF. During the storyline phase, TEM helped elicit cues for adopting and dropping goals, with some complex interactions between *achievement goals* and *maintenance goals* (the latter are goals that are eligible for adoption when their maintenance condition is violated).

Comprehension was assessed by giving the two experts, who were not involved in the elicitation sessions, a two-page introduction to TDF's goal diagram notation, 13 goal diagrams representing some of the elicited League of Legends tactics, and a questionnaire comprising ten questions. The questions probed understanding of the meaning of the diagrams and how to change the diagrams to produce a different tactical outcome. One of the diagrams included a deliberate omission, which both experts were able to identify; they were also able to provide suggestions on how to extend the tactics to handle a wider range of cases. The expert used for the elicitation sessions assessed their level of comprehension as high, with a mean score of 85% correct. Their high scores were very encouraging, given that they had no previous exposure to TDF.

5 Discussion

This paper introduced TEM, a new approach to tactics elicitation that targets the BDI-based framework, TDF. The BDI paradigm was chosen because it is intuitive to domain experts, and the literature suggests that it maps well to their *theory of mind*. A major contribution of this paper is TEM's specific methodological steps and how they focus the interview process on the information required to build BDI-based tactics, namely roles, characters, teams, goals adopted/dropped/suspended/resumed, tactics, key decision points, and so on. The central role played by the modelling objective is another important contribution of this work to tactics modelling because it ensures that the elicitation process remains focused on the desired outcome,

²<http://leagueoflegends.com/>.

thereby ameliorating a common problem in knowledge elicitation—that of drifting off point and wasting time on interesting detail that ultimately does not contribute to the requirements of the study. This was a significant factor in the efficiency of the elicitation sessions in the three case studies.

The evaluation of TEM, though preliminary, was quite broad in scope and provides some confidence in the efficacy of the methodology. The bushfire case study revealed a few important deficiencies in the original methodology, and these were addressed before the undersea warfare case study. The undersea warfare study provides initial support for our claim that TEM is easy to learn and apply effectively; one of the two interviewers had only been an observer in the bushfire case study, and the other had no experience of TEM but had many years of experience in eliciting and modelling tactics for undersea warfare. His feedback on the effectiveness of TEM is particularly encouraging (see the five points at the end of Sect. 4.2). The League of Legends case study provides support for the claim that the TEM/TDF combination produces models that are easily understood by domain experts that were not part of the elicitation sessions. TEM's emphasis on collaboration between the modeller and domain expert is an important contribution of this work. The domain experts in the case studies all expressed that they found this aspect highly motivating and that they felt confident that the resulting models were a valid reflection of their tactical expertise.

A key contribution of this work is the fact that the elicitation methodology is closely tied to an effective and intuitive tactics modelling framework (TDF). This helps keep the sessions focused on the desired modelling products and provide continuity from elicitation, through to modelling, and ultimately implementation. We believe that, after two years of development and evaluation, this work is now sufficiently mature to warrant wider dissemination to those building intelligent decision-making systems that need to be based on human expertise. However, further work remains.

5.1 Further Work

This research has ongoing support from our undersea warfare sponsor, and now has funding from a different sponsor to investigate its application to team-based air combat tactics. Wider adoption of TEM would be greatly facilitated by the provision of appropriate tool support, and tool development is now underway. The case studies were conducted by adapting publicly available BPMN and concept mapping tools, but this is less than ideal because they are not sufficiently tailored to TEM, and there is no integration with the TDF tool. Our TEM tool development will support the construction of concept maps and storylines. Linking the TEM tool with the TDF tool will provide an opportunity for verification and validation of the elicitation and design artefacts, as well as TDF-generated code. Artefacts identified in the concept

maps and storylines could be linked to their counterparts in the TDF design; storylines could also be mapped to TDF plan diagrams. Integration of this sort would help with traceability from elicitation right through to the behaviour that results from running code.

References

1. Akbori, F.: Autonomous-agent based simulation of anti-submarine warfare operations with the goal of protecting a high value unit. Master's Thesis (2004)
2. Bratman, M.E.: *Intention, Plans, and Practical Reasoning*. Harvard University Press, Cambridge, MA (USA) (1987)
3. CLAMO.: *Rules of Engagement (ROE) Handbook for Judge Advocates*. Center for Law and Military Operations, Charlottesville, Virginia (2000)
4. Crandall, B., Klein, G.A., Hoffman, R.R.: *Working Minds: a Practitioner's Guide to Cognitive Task Analysis*. MIT Press (2006)
5. Dennett, D.C.: *The Intentional Stance*. MIT press (1987)
6. Evertsz, R., Lucas, A., Smith, C., Pedrotti, M., Ritter, F.E., Baker, R., Burns, P.: Enhanced behavioral realism for live fire targets. In: St. Amant, R.S., Reitter, D., Stacy, E.W. (eds.) *Proceedings of the 23rd Annual Conference on Behavior Representation in Modeling and Simulation*. BRIMS Society, Washington DC (2014)
7. Evertsz, R., Thangarajah, J., Yadav, N., Ly, T.: A framework for modelling tactical decision-making in autonomous systems. *J. Syst. Softw.* **110**(C), 222–238 (2015). [10.1016/j.jss.2015.08.046](https://doi.org/10.1016/j.jss.2015.08.046)
8. Feigenbaum, E.A.: Themes and case studies of knowledge engineering. In: *Expert Systems in the Micro-Electronic Age*, pp. 3–25 (1979)
9. Johnson, P.E.: What kind of expert should a system be? *J. Med. Philos.* **8**(1), 77–97 (1983)
10. Laird, J.E., Jones, R.M., Jones, O.M., Nielsen, P.E.: Coordinated behavior of computer generated forces in Tacair-Soar. In: *Proceedings of the Fourth Conference on Computer Generated Forces And Behavioral Representation* (1994)
11. Musen, M.A.: *An Overview of Knowledge Acquisition*. Springer (1993)
12. Neves, D.M., Anderson, J.R.: Knowledge compilation: mechanisms for the automatization of cognitive skills. In: *Cognitive Skills and Their Acquisition*, pp. 57–84 (1981)
13. Norling, E.: Folk psychology for human modelling: Extending the bdi paradigm. In: *Proceedings of the Third International Joint Conference on Autonomous Agents and Multiagent Systems-Volume 1*, pp. 202–209. IEEE Computer Society (2004)
14. Padgham, L., Winikoff, M.: *DEveloping Intelligent Agent Systems: a Practical Guide*, vol. 1. Wiley (2004)
15. Shadbolt, N., O'Hara, K., Crow, L.: The experimental evaluation of knowledge acquisition techniques and methods: history, problems and new directions. *Int. J. Hum. Comput. Stud.* **51**(4), 729–755 (1999)

Analysis of Demand and Operations of Inter-modal Terminals

Rodolfo García-Flores, Soumya Banerjee, George Mathews,
Blandine Vacher, Brian Thorne, Nazanin Borhan, Claudio Aracena
and Yuriy Tyshetskiy

Abstract Inter-modal terminals (IMT) reduce road congestion and exploit economies of scale by pooling demand from surrounding areas and using rail to transport containers to and from ports. The alternative to using IMTs is using trucks to transport containers directly to and from the port. Trucks increase road congestion, but rail requires additional handling of containers (lift on and lift off). The attractiveness of truck versus rail is dependent on a number of variables such as costs, total travel time, frequency of services, risk and material resources. To date, the use of open data to analyse and model freight movements has been minimal, primarily because of the shortage of open data focusing on freight movements across cities, regions or countries. In this paper, we leverage open government data for the Port Botany rail network and use it to develop exible and dynamic simulation and optimisation tools that enable various stakeholders including IMT operators, port authorities and government policy makers to make more informed decisions not only about pricing, but also about operation scheduling and internal operations.

Keywords Open data · Simulation · Optimisation · Transport

1 Introduction

Multi-modal transportation is defined as the transportation of goods by at least two different modes of transport (e.g. ships, barges, trains or trucks). In the Greater Sydney freight network, inter-modal terminals (IMT) are equipped for the transshipment of containers between rail and road transport modes. In 2014, there were 2.3 million movements of twenty-foot equivalent units (TEU) through Port Botany, of which over 80% correspond to imports. The land transportation of these containers was

R. García-Flores (✉) · B. Vacher
CSIRO Data61, Private Bag 10, Clayton South, VIC 3168, Australia
e-mail: Rodolfo.Garcia-Flores@csiro.au

S. Banerjee · G. Mathews · B. Thorne · N. Borhan · C. Aracena · Y. Tyshetskiy
CSIRO Data61, Australian Technology Park Level 5, 13 Garden Street, Eveleigh,
NSW 2015, Australia

© Springer International Publishing AG 2018
R. Sarker et al. (eds.), *Data and Decision Sciences in Action*,
Lecture Notes in Management and Industrial Engineering,
DOI 10.1007/978-3-319-55914-8_3

2 million carried by truck and 0.3 million carried by rail, corresponding to a 14% share of total transported TEUs, a figure that the NSW State Government is trying to increase in order to reduce congestion and extend the life of valuable road infrastructure [12]. Forecasts indicate that total volume will increase fourfold in the next 25 years and that there will be an increase in the proportion of containers destined to Sydney's western and south-western suburbs driven by a combination of availability of large parcels of land and lower land prices.

On the one hand, these IMTs reduce road congestion and exploit economies of scale by pooling demand from surrounding areas and using rail to transport containers to and from ports, although additional handling of containers is necessary. On the other hand, trucks may transport containers directly to port without the need to transfer containers at IMTs, but this increases road congestion. The attractiveness of truck versus rail is dependent on a number of variables such as costs, demand, total travel time, frequency of services, risk and material resources, which must be analysed and understood in order to maximise the value of existing infrastructure.

The objective of the present paper was to introduce tools to determine whether the existing network of railway lines and inter-modal terminals is adequate to support future growth of the Port Botany freight system. To that end, we introduce and analyse the results of a simulation and an optimisation model, which leverage on newly available open government data. These models complement each other: the simulation aims at understanding the demand and cost structures of individual, competing IMTs, whereas the optimisation model seeks the greater benefit for all participants in the system. In the remainder of the present paper, we review existing work dedicated to the analysis of operations in IMTs in Sect. 1.1 and describe the Port Botany bi-modal transportation system in Sect. 2. We then describe the simulation and optimisation models in Sects. 3 and 4, respectively, and present and discuss their results (Sect. 5). We round up the discussion and present ideas for further analysis in Sect. 6.

1.1 Previous Work

Literature related to IMTs is mostly concerned with the problem of selecting the optimal location of these facilities. Sørensen et al. [13] explained that different transport modes have different environmental footprints, but it is hard for other transport modes to compete with the cost, flexibility and service level of road transport. A consequence of this is that infrastructure and connectivity at IMTs are still relatively poor. Sørensen et al. [13] presented two efficient meta-heuristics for the fast solution of the IMT location problem. In follow-up papers, Lin et al. [10] improved on Sørensen et al.'s model by removing redundant constraints and improving solution times, while also introducing matheuristics to obtain near-optimal solutions quickly. Lin and Lin [11] performed a decomposition of IMT selection and transportation flows for the same problem.

Regarding the optimisation of IMT operations, Alické [1] presented a constraint satisfaction model to minimise maximum tardiness of operating a single IMT known

as *Mega Hub*. The IMT under study had a novel design, and as a consequence, the model was customised for the configuration of the terminal. The resulting model turned out to be very flexible and could be solved quickly. Caris and Janssens [6] optimised the drayage plans at IMTs, that is they created efficient vehicle routes performing all loaded and empty container transports in the service area of one or several container terminals during a single day. A local search heuristic was proposed to address the problem, whereas in a following paper by the same team [4], this is achieved by minimising two objectives: number of vehicles and total distance travelled, using two heuristic algorithms. Gundersen et al. [8] presented a data envelopment analysis to compare the performance in terms of security of a set of 18 IMTs, identifying opportunity areas in most of them. Holguín-Veras and Jara-Díaz [9] derive formulae for optimal space allocation and pricing for storage at container terminals, motivated by the increasing service and price differentiation, as the industry is more willing to implement different types of services tailored to customer needs.

Regarding the combined use of simulation and optimisation, Gambardella and Rizzol [7] provided a short review of the main classes of problems at IMTs whose instances can be found in the operations of container terminals, and advocated for the combined use of simulation and optimisation. Vidović et al. [15] addressed the problem of optimally locating inter-modal freight terminals in Serbia by combining optimisation for locating facilities, and simulation for validating the solution.

2 The Port Botany Bi-modal System

In Sydney's Port Botany freight system, containers can be transported directly between the premises of the freight owners and the port with trucks via the road network. Alternatively, they can be transported via an intermediate inter-modal rail terminal. The system comprises the Greater Sydney metropolitan region that extends out 50 km from the port. For this study, it must be determined whether the existing network of railway lines and inter-modal terminals is adequate to support future growth. The system comprises the following components:

1. **Production/consumption areas.** These areas contain producers that send containers with goods for export and also contain the end customers for imports. The areas aggregate the total supply of containers for export as well as demand of containers imported, to the suburb level. Customers within each suburb area determine their transport choice by selecting the service provider that best satisfies their price and service time requirements. The simulation part of the study considered 233 postcode locations as origin of exports and destination of imports. By contrast, the optimisation study aggregates these into ten production areas.
2. **Inter-modal terminals.** An IMT is a transfer facility with road and rail access, and on-site warehousing. In the model presented here, each IMTs run its own rail assets (wagons/locomotives) and container-handling assets (forklifts or cranes);

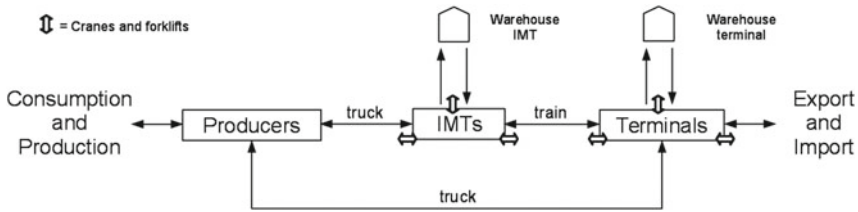


Fig. 1 Schematic of Port Botany freight system. Containers are transported by truck between producers and IMTs and between producers and terminals. Transport by rail occurs only between IMTs and terminals. IMTs and terminals count with warehousing space to store containers. Cranes or forklifts are necessary to load and unload containers to and from trucks and train consists

in the real world, trains are operated by train companies that may or not own an IMT. For example, some logistics companies own trains and an IMT, but Cooks River IMT does not own any trains. Import containers change from trains to trucks at the IMT facilities on their way to the production areas, and export containers are assembled into consists (i.e. the rolling stock, exclusive of the locomotive) from trucks on their way to the port terminals for shipping. The rate at which containers can be processed by a facility is determined by the number of handling assets, while the rate at which containers can be transported to and from the port is determined by the rail assets. Five IMTs are considered. Additional information on the features of the set of IMTs servicing the Port Botany freight system can be found in [14].

- 3. Port terminals.** Terminals are export-shipping points and entry points for imports, and also have warehousing facilities available. Two terminals are included in the case study.

A schematic of the system is depicted in Fig. 1. Producers have the option to send containers for export and receive imports directly from terminals by truck, or to use IMTs. If this is the case, containers are transferred from trains to trucks and vice versa in the IMTs for imports and exports, respectively. Storage facilities exist at terminals and IMTs, which require container transfer equipment (cranes and forklifts). Currently, Port Botany is serviced by trains from existing IMTs located in Cooks River, McArthur and Yennora and the recently opened terminals at Chullora and Enfield [12]. A proposed facility in Moorebank will be able to service the increasing demand in Sydney's south-west. Figure 2 indicates the location of these sites and shows the spatial distribution of the destination of deliveries of imported containers into the Greater Sydney area.

The importance of understanding this system resides in the fact that, on the one hand, IMTs reduce road congestion and exploit economies of scale by pooling demand from surrounding areas and using rail to transport containers to and from ports. Additionally, it may be in the interest of local government authorities to encourage rail transport in order to reduce congestion and extend the life of valuable road infrastructure. On the other hand, rail requires additional handling of containers (lift on and lift off), while direct transport from and to ports by truck may be more

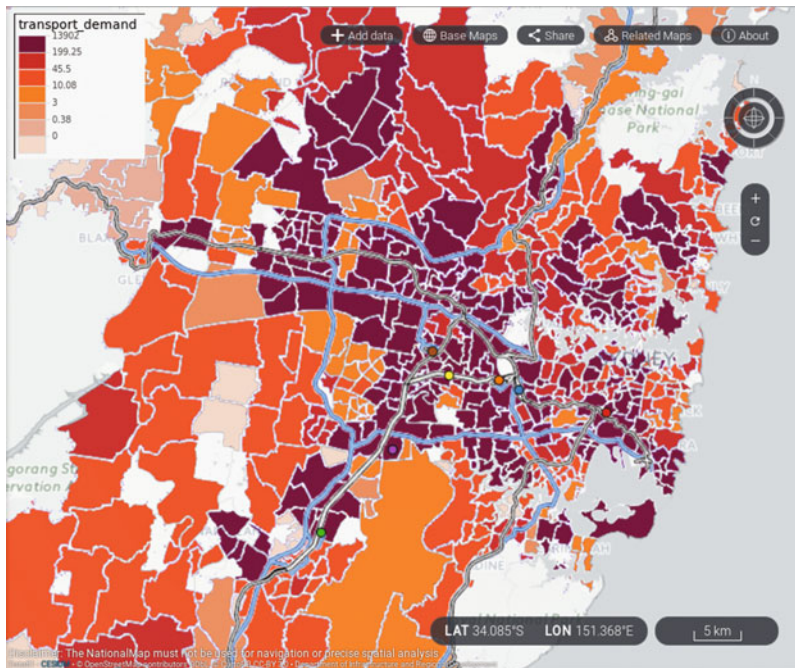


Fig. 2 IMTs and spatial distribution of the delivery destination of imported containers into the Sydney metropolitan region. The IMTs shown are McArthur (*green*), Yennora (*brown*), Villawood (*yellow*, closed and not operating), Chullora (*orange*), Enfield (*blue*), Cooks River (*red*) and Moorebank (*purple*, proposed and not operating). The *grey lines* in this map represent rail and the *blue lines* represent the main roads

convenient and save the need for extra-handling in IMTs. In other words, there is a trade-off to be analysed in the attractiveness of truck versus rail that depends on a number of variables such as cost, total travel time, frequency of services and risk.

In the remainder of this paper, we describe and present initial results from the simulation and optimisation models, the former focused on understanding the demand and cost structures of individual, competing IMTs, and the latter aimed at obtaining the greater benefit for all participants in the system. In this sense, the optimisation and simulation models described complement each other.

3 Simulation of Rail Demand

We simulated computationally the operations of IMTs and their resulting container throughput, and generated an underlying demand for container imports and exports in the Greater Sydney region based on real data provided by the Australian Bureau of Statistics [2]. The goal of this simulator, of which a more detailed description

can be found in [3], is to improve the efficiency and profitability of IMTs. In order to achieve this objective, we built a model of internal operation of IMTs within a value-driven modelling framework. The model of internal operations can be used to predict profit based on different asset mixes such as number of trains and wagons and number of forklifts and different pricing structures.

The value-driven model framework incorporates (1) a detailed operational model of IMTs including costs, capacities and service times for different asset mixes within an IMT; (2) a model of spatial demand for containers; (3) competition from direct truck transport or other IMTs. The components of the model are calibrated based on internal operational data and publicly available data, and the decision to use an IMT is based on price, transportation time and the frequency of delays [5]. The model allows analysts to perform what-if analyses, predict the outcome of different investment and operational decisions, and compare individual IMTs. On the one hand, the simulation model takes into account the travel times and demand for containers at level of suburbs. On the other hand, it only considers imports, which account for the majority of container movements in the Sydney region.

4 Optimisation of Operations

The aim of the linear optimisation model is to maximise the net economic benefit, defined as the sales of all containers minus the total costs of operating the entire supply chain. These costs comprise transportation costs, the costs of violating the soft inventory limits at warehouses, the costs of moving containers to and from warehouses and the costs of hiring extra trains and container-handling equipment if the available resources are not sufficient. The full formulation can be found in the Appendix.

Profit as described above is expressed in Eq. (1). A summary of the constraints is as follows:

1. The *soft inventory capacity constraints* (2) impose a penalty for exceeding the desirable limits to the amount of containers that may be stored in the IMT and terminal warehouses.
2. The *hard inventory capacity constraints* (3) state the maximum number of containers that can be stored at sites with warehousing capability.
3. The *crane capacity constraints for IMTs* (4) impose a limit on how many containers the cranes (or forklifts) can move at any time period, and a penalty when the available container moving resources are not sufficient. For IMTs, containers must be moved in and out of the warehouses, as well as to trucks or trains if they are going to be brought into and sent out of the facility at the current planning period.
4. The *crane capacity constraints for terminals* (5) are similar to the constraints for IMTs described above, but in addition to all the containers moved into and out of the warehouses and the train and truck loading and unloading operations,

we need to consider that the containers for export must be loaded into the ships, and containers for import must be unloaded from the ships.

5. The amount of containers that can be imported or exported is constrained by expressions (6) and (7).
6. The *conservation constraints at IMTs* (8) define the flow of containers at IMTs and their warehouses. We consider that the initial inventory level at all warehouses is zero.
7. The *conservation constraints at terminals* (10) define the flow of containers at terminals and their warehouses.
8. The *conservation constraints at producers* (12) assume that the producers do not hold inventory and that all containers produced must enter the supply chain.
9. The *constraints for consist assembly* (14) and (16) state that the space for containers in the trains is limited. Wagons have room for three TEUs (slots). Containers can be 40 foot and occupy two TEUs, or 20 foot and occupy one TEU. The current version of the optimisation model distinguishes four commodities, 20ft-EXP, 40ft-EXP, 20ft-IMP and 40ft-IMP. Knapsack-like constraints state that the number of containers transported by rail in a road segment is not more than the capacity of all the trains travelling in that road segment at any given period. The model assumes that every truck can only carry one container.
10. *Road capacity constraints*: We assume that roads have a fixed capacity.

In contrast to the simulation model, the optimisation model is a strategic planning tool and does not take into account travel times. Demand for containers is modelled at an aggregate level, at least in the current stage of development. However, the optimisation model does calculate the optimal flows for import and export containers that maximise the net economic benefit to the region.

5 Results and Discussion

The simulation was coded in Python¹ version 3.5.2, and we obtained the results of Sect. 5.1 in a desktop computer using an Intel® i7-4712HQ CPU at 2.27 GHz. We implemented the optimisation problem in version 1.5 of the Clojure² language with an Excel interface. We obtained all the results in Sect. 5.2 using version 12.4 of the CPLEX³ optimiser in a 64-bit Intel Xeon CPU with two processors of eight cores (2.27 GHz) each and 48 GB of RAM. The problem has 32220 integer variables and 55352 constraints. A typical run takes around 10 min to complete.

¹<https://www.python.org/downloads/release/python-352/>, accessed on the 28 of July 2016.

²<http://clojure.org/>, accessed on the 8 of April 2016.

³<http://www-01.ibm.com/software/commerce/optimization/cplex-optimizer/index.html>, accessed on the 16 of May 2016.

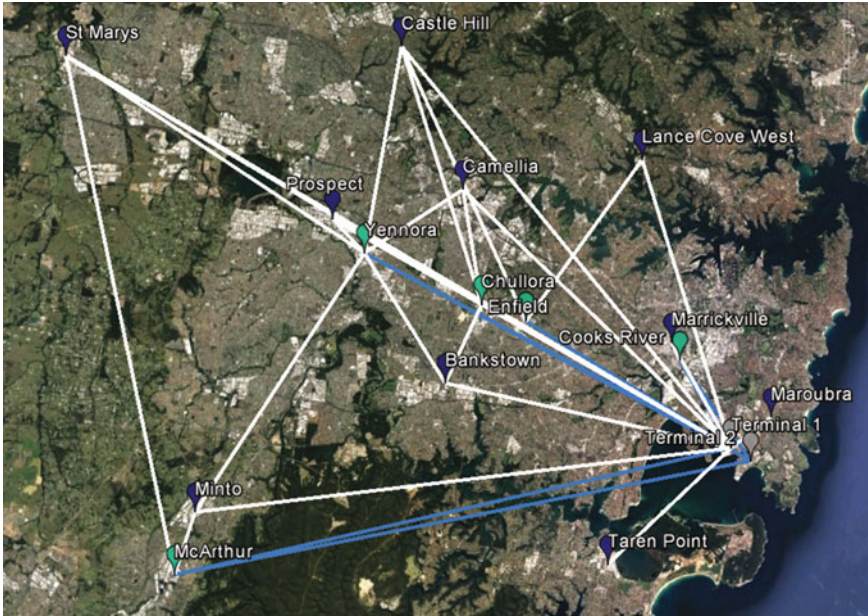


Fig. 3 Location of all sites that form the optimisation case study. Producers are marked in *blue*, IMTs in *green* and terminals in *grey*. The model considers that all producers are connected to all terminals and to all IMTs by road (*white lines*), and that all IMTs are connected to all terminals by rail (*blue lines*). Only the road segments used at some point of the time horizon are shown

As mentioned above, the simulation considered 233 postcode locations as origin of exports and destination of imports. By contrast, the optimisation study aggregated these locations into ten production/consumption areas, as shown in Fig. 3. A fleet of ten trains was considered.

5.1 Operations

The results from the simulation model indicate that the median transportation time is almost the same for both transport modes, at 2.30 days for trucks and 2.31 days for rail, even when there is a delay in changing modes at IMTs. Rail has an advantage in the most distant regions of the area under study, with the fastest 5% of containers travelling by rail taking 3.5 h less time to move through the system than the fastest 5% travelling by road.

The base scenario was configured using data corresponding to the transport system as it was configured in 2014. During this year, 2.3 million TEUs were transported in the system, and five IMTs were in operation: McArthur, Chullora, Enfield, Yennora and Cooks River. The configured simulation model can reproduce the observed

Table 1 Modelled market equilibrium for services offered by the inter-modal terminals

	Railing price (\$/TEU)	Trains per day
McArthur	240	3
Chullora	240	3
Cooks River	230	3
Yennora	250	3
Enfield	230	3

Table 2 Outputs of simulation for one year for the base 2014 scenario

	TEUs handled	Market share	Average road distance travelled
Direct truck service	945,028	85.8	30.0
McArthur	25,373	2.3	10.6
Chullora	31,563	2.8	21.8
Cooks River	4043	0.4	26.4
Yennora	63,715	5.8	14.6
Enfield	31,760	2.9	25.8

characteristics of the system, in particular the existing 14% market share of rail transport. The market equilibrium determined by the model is shown in Table 1, and the model outputs for this base scenario are displayed in Table 2.

5.2 Rail Demand

The optimisation model serves as a complement to the simulation model, so instead of calculating the equilibrium prices for individual IMTs, in this case, we considered a time horizon of 60 days and that the cost of railing was a fixed parameter with value \$200.00. Other data used was as close to the data used on the simulation as possible, although in some cases it had to be aggregated, as in the case of the producers, or estimated, as in the case of the train fleet size. Fleet size was estimated to get as close to the rail transportation share of 14%; in the optimisation model, the share of total rail transport is 14.73%. The fraction of exports transported by rail is 16.88%, and for imports, this is 14.19%.

Tables 3 and 4 show the optimal flows of exports and imports, respectively. The model indicates that, given the current production and consumption data, all producing and consuming areas (except Castle Hill and St. Marys) import and export around 10% of their needs directly by road to terminal 1. Castle Hill and St. Marys have a lower share of road transport at around 3–5%. Yennora and McArthur are the IMTs with the highest share of rail transport, a result that is compatible with the

Table 3 Total number of export containers and percentage received at terminals from IMTs or directly from producers for base case

	Terminal 1	Terminal 2	% Terminal 1	% Terminal 2
McArthur	1107	287	1.56	5.05
Yennora	5501	5014	7.75	88.21
Chullora	471	329	0.66	5.79
Enfield	170	0	0.24	0.00
Cooks River	0	54	0.00	0.95
Lane Cove West	7724	0	10.89	0.00
Marrickville	7546	0	10.64	0.00
Maroubra	6884	0	9.70	0.00
Taren point	6890	0	9.71	0.00
Minto	6675	0	9.41	0.00
Bankstown	7752	0	10.93	0.00
Camellia	7785	0	10.97	0.00
Prospect	2588	0	3.65	0.00
St. Marys	3386	0	4.77	0.00
Castle Hill	6472	0	9.12	0.00
TOTAL:	70,951	5684	100.00	100.00

Table 4 Total number of import containers and percentage sent from terminals to IMTs or directly to producers for base case

	Terminal 1	Terminal 2	% Terminal 1	% Terminal 2
McArthur	3922	1450	1.30	38.00
Yennora	35,494	2270	11.72	59.49
Chullora	288	96	0.10	2.52
Enfield	0	0	0.00	0.00
Cooks River	6	0	0.00	0.00
Lane Cove West	33,175	0	10.95	0.00
Marrickville	31,268	0	10.32	0.00
Maroubra	25,585	0	8.45	0.00
Taren Point	30,251	0	9.99	0.00
Minto	25,714	0	8.49	0.00
Bankstown	28,492	0	9.41	0.00
Camellia	31,593	0	10.43	0.00
Prospect	10,124	0	3.34	0.00
St Marys	16,321	0	5.39	0.00
Castle Hill	30,617	0	10.11	0.00
Total	302,850	3816	100.00	100.00

simulation results in Table 2. The model also indicates that most containers should be handled at terminal one: 92.6% of exports and 98.8% of imports should pass through this terminal. This is probably an aspect of the model that could be improved, but at present, we do not have information regarding the actual handling capacities or operating rules of these terminals.

6 Concluding Remarks

Inter-modal terminals reduce road congestion and exploit economies of scale by pooling demand from surrounding areas and using rail to transport containers to and from ports. In the Port Botany freight system, trains and trucks supply the Greater Sydney metropolitan area with 2.3 million containers per year, with forecasts indicating that total volume will increase fourfold in the next 25 years. In the present paper, we introduce and analyse the results of a simulation and an optimisation model, which leverage on newly available open government data [2] in order to determine whether the existing network of railway lines and inter-modal terminals is adequate to support future growth of the Port Botany freight system.

These two complementary models offer a holistic approach that moves away from simple capacity considerations and assesses the effect of changes on the behaviour of key market players. Both models capture the logistic processes from port to final delivery destination, with the simulation model also taking into account a more detailed set of production/consumption areas, transportation time and the frequency of delays. The optimisation model is not as detailed, but provides insights on the greater benefit and more efficient use of resources for all participants in the system. Our simulation results indicate that the median transportation time is almost the same for both transport modes, at 2.30 days for trucks and 2.31 days for rail, even when there is a delay in changing modes at IMTs. The optimisation results indicate that terminal 2 is underutilised and that, indeed, McArthur and Yennora should be the IMTs with the largest inter-modal transfers. We have introduced the models and presented preliminary results, but many improvements are possible as more data becomes available. Some of these include adding imports to the simulation model, considering commodity level characteristics (e.g. perishables), refinement of delivery time and reliability, refining the transport decision model in the simulation and attempting a more detailed description of individual producer/consumer areas for optimisation.

Appendix

Let us define the decision variables x_{ijkt}^E and y_{ijkt}^E as the containers for export that travel between sites i and j carrying commodity k at period t by truck and by rail, respectively; x_{ijkt}^I and y_{ijkt}^I as the containers for import that travel between sites i and

j carrying commodity k at period t by truck and by rail, respectively; z_{ikt}^E and z_{jkt}^I the containers that go to export and that come as import at terminal i , respectively; u_{ikt}^+ and u_{ikt}^- the containers that are moved into and out of the IMTs' warehouses, respectively; v_{ikt}^+ and v_{ikt}^- the containers that are moved into and out of the terminals' warehouses, respectively; w_{ikt} and w_{ikt}^{\downarrow} the containers that are stored in the IMT and terminal warehouses, respectively; α_{ikt}^{\uparrow} and $\alpha_{ikt}^{\downarrow}$ the amount by which the minimum and maximum desired inventory levels at sites with warehouses (i.e. IMTs and terminals) are violated, respectively; γ_t the number of additional trains needed at time t and δ_{it} the number of additional container-handling equipment at IMT i at time t . Also, let N be the number of wagons in a consist (normally 32), n_{ijt} the number of trains that travel between sites i and j and γ_t the number of additional trains needed in excess of the total available, $MAXNT$. We can now define the objective function as

$$\begin{aligned}
\text{Maximise} \quad & \sum_{i \in \mathcal{P}} \sum_{k \in \mathcal{K}} \sum_{t \in \mathcal{T}} SP_{kt} z_{ikt}^I + \sum_{i \in \mathcal{P}} \sum_{k \in \mathcal{K}} \sum_{t \in \mathcal{T}} SP_{kt} z_{ikt}^E \\
& - \sum_{(i,j) \in \mathcal{L}_R^E} \sum_{k \in \mathcal{K}} \sum_{t \in \mathcal{T}} RTC_{ijkt} x_{ijkt}^E - \sum_{(i,j) \in \mathcal{L}_R^I} \sum_{k \in \mathcal{K}} \sum_{t \in \mathcal{T}} RTC_{ijkt} x_{ijkt}^I \\
& - \sum_{(i,j) \in \mathcal{L}_P^E} \sum_{t \in \mathcal{T}} PTC_{ijt} n_{ijt} - \sum_{i \in \mathcal{R} \cup \mathcal{P}} \sum_{t \in \mathcal{T}} SVC_{it} \sum_{k \in \mathcal{K}} (\alpha_{ikt}^{\uparrow} - \alpha_{ikt}^{\downarrow}) \\
& - \sum_{i \in \mathcal{R}} \sum_{k \in \mathcal{K}} \sum_{t \in \mathcal{T}} CM_{ikt} \left[u_{ikt}^+ + u_{ikt}^- + \sum_{j \in \mathcal{S}} (x_{jikt}^E + x_{ijkt}^I) + \sum_{j \in \mathcal{P}} (y_{ijkt}^E + y_{jikt}^I) \right] \\
& - \sum_{i \in \mathcal{P}} \sum_{k \in \mathcal{K}} \sum_{t \in \mathcal{T}} CM_{ikt} \left[v_{ikt}^+ + v_{ikt}^- + \sum_{j \in \mathcal{S}} (x_{jikt}^E + x_{ijkt}^I) + \sum_{j \in \mathcal{R}} (y_{ijkt}^E + y_{jikt}^I) + z_{ikt}^E + z_{ikt}^I \right] \\
& - \sum_{t \in \mathcal{T}} FC_t \gamma_t - \sum_{i \in \mathcal{R}} CC_i \sum_t \delta_{it} . \tag{1}
\end{aligned}$$

where SP_{kt} is the sales price of commodity k at period t , RTC_{ijkt} and PTC_{ijkt} are the transportation costs per km from i to j by road and rail, respectively, SVC_{it} is the cost of violating soft inventory limits at site i , CM_{ikt} is the cost of moving containers within a site i , FC_t is the cost of setting up additional trains at period t and CC_i is the cost of additional container movements.

Subject to:

$$WDES_i^{\min} - \sum_{k \in \mathcal{K}} \alpha_{ikt}^{\downarrow} \leq \sum_{k \in \mathcal{K}} w_{ikt} \leq WDES_i^{\max} + \sum_{k \in \mathcal{K}} \alpha_{ikt}^{\uparrow} \quad \forall i \in \mathcal{R} \cup \mathcal{P}, \quad \forall t \in \mathcal{T} . \tag{2}$$

$$WDES_i^{\max} + \sum_{k \in \mathcal{K}} \alpha_{ikt}^{\uparrow} \leq WLIM_i \quad \forall i \in \mathcal{R} \cup \mathcal{P}, \quad \forall t \in \mathcal{T} . \tag{3}$$

$$\begin{aligned}
& \sum_{k \in \mathcal{K}} (u_{ikt}^+ + u_{ikt}^- + \sum_{j \in \mathcal{S}} x_{jikt}^E + \sum_{j \in \mathcal{S}} x_{ijkt}^I + \sum_{j \in \mathcal{P}} y_{ijkt}^E \\
& + \sum_{j \in \mathcal{P}} y_{jikt}^I) - \delta_{it} \leq W_i^{\max} \quad \forall i \in \mathcal{R}, \quad \forall t \in \mathcal{T} . \tag{4}
\end{aligned}$$

$$\sum_{k \in \mathcal{K}} (v_{ikt}^+ + v_{ikt}^- + \sum_{j \in \mathcal{S}} x_{jikt}^E + \sum_{j \in \mathcal{S}} x_{ijkt}^I + \sum_{j \in \mathcal{R}} y_{jikt}^E + \sum_{j \in \mathcal{R}} y_{ijkt}^I + z_{ikt}^E + z_{ikt}^I) - \delta_{it} \leq W_i^{\max} \quad \forall i \in \mathcal{P}, \forall t \in \mathcal{T}, \quad (5)$$

where δ_{it} is the number of additional container-handling operations needed at site i at time t and

$$z_{ikt}^E \leq EXP_{ikt} \quad \forall i \in \mathcal{P}, \forall k \in \mathcal{K}^E, \forall t \in \mathcal{T}, \quad (6)$$

$$z_{ikt}^I \leq IMP_{ikt} \quad \forall i \in \mathcal{P}, \forall k \in \mathcal{K}^I, \forall t \in \mathcal{T}. \quad (7)$$

$$\sum_{j \in \mathcal{S}} x_{jikt}^E + \sum_{j \in \mathcal{P}} y_{jikt}^I + u_{ikt}^- = \sum_{j \in \mathcal{S}} x_{ij'kt}^I + \sum_{j \in \mathcal{P}} y_{ij'kt}^E + u_{ikt}^+ \quad \forall i \in \mathcal{R}, \forall k \in \mathcal{K}, \forall t \in \mathcal{T}, \quad (8)$$

$$w_{ik,t+1} = w_{ikt} + u_{ikt}^+ - u_{ikt}^- \quad \forall i \in \mathcal{R}, \forall k \in \mathcal{K}, \forall t \in \mathcal{T}. \quad (9)$$

$$\sum_{j \in \mathcal{S}} x_{jikt}^E + \sum_{j \in \mathcal{R}} y_{jikt}^E + v_{ikt}^- + z_{ikt}^I = \sum_{j \in \mathcal{S}} x_{ij'kt}^I + \sum_{j \in \mathcal{R}} y_{ij'kt}^I + v_{ikt}^+ + z_{ikt}^E \quad \forall i \in \mathcal{P}, \forall k \in \mathcal{K}, \forall t \in \mathcal{T}, \quad (10)$$

$$w_{ik,t+1} = w_{ikt} + v_{ikt}^+ - v_{ikt}^- \quad \forall i \in \mathcal{P}, \forall k \in \mathcal{K}, \forall t \in \mathcal{T}. \quad (11)$$

$$\sum_{j \in \mathcal{R} \cup \mathcal{P}} x_{jikt}^I = CONS_{ikt} \quad \forall i \in \mathcal{S}, \forall k \in \mathcal{K}^I, \forall t \in \mathcal{T}, \quad (12)$$

$$\sum_{j \in \mathcal{R} \cup \mathcal{P}} x_{ijkt}^E = PROD_{ikt} \quad \forall i \in \mathcal{S}, \forall k \in \mathcal{K}^E, \forall t \in \mathcal{T}, \quad (13)$$

where $PROD_{ikt}$ and $CONS_{ikt}$ are the amounts of produced and consumed containers of export and import commodities, respectively, in producer i .

$$\sum_{k \in \mathcal{K}^I} NS_k y_{ijkt}^I - 3 N n_{ijt} \leq 0 \quad \forall (i,j) \in \mathcal{L}_p^I, \forall t \in \mathcal{T}, \text{ and} \quad (14)$$

$$\sum_{k \in \mathcal{K}^E} NS_k y_{ijkt}^E - 3 N n_{ijt} \leq 0 \quad \forall (i,j) \in \mathcal{L}_p^E, \forall t \in \mathcal{T}, \quad (15)$$

where NS_k is the number of slots a container of type k takes.

$$\sum_{(i,j) \in \mathcal{L}_p} n_{ijt} - \gamma_t \leq MAXNT \quad \forall t \in \mathcal{T}. \quad (16)$$

$$\sum_{k \in \mathcal{K}} x_{ijkt}^E \leq Q_{ij} \quad \forall (i,j) \in \mathcal{L}_R^E, \forall t \in \mathcal{T}, \quad (17)$$

$$\sum_{k \in \mathcal{K}} x_{ijkt}^I \leq Q_{ij} \quad \forall (i,j) \in \mathcal{L}_R^I, \forall t \in \mathcal{T}, \quad (18)$$

where Q_{ij} is the capacity of the road segment (i,j) .

References

1. Alicke, K.: Modeling and optimization of the intermodal terminal mega hub. *OR Spectr.* **24**, 1–17 (2002)
2. Australian Government: Experimental statistics on international shipping container movements. Technical Report 5368.0.55.018, Australian Bureau of Statistics, ABS House 45 Benjamin Way, Belconnen ACT 2617 (2016). <http://www.abs.gov.au/AUSSTATS/abs@.nsf/Lookup/5368.0.55.018Main+Features12009-10?OpenDocument>
3. Banerjee, S., Mathews, G., Aracena, C., Thorne, B., Tyshetskiy, Y., Vitsounis, T.: Computationally simulating intermodal terminal attractiveness and demand. In: Proceedings of the 23 Intelligent Transport Systems World Congress. Melbourne, Australia (2016)
4. Braekers, K., Caris, A., Janssens, G.: Bi-objective optimization of drayage operations in the service area of intermodal terminals. *Transp. Res. Part E* **65**, 50–69 (2014)
5. Brooks, M., Puckett, S., Hensher, D., Sammons, A.: Understanding mode choice decisions: a study of Australian freight shippers. *Marit. Econ. Logisti.* **14**(3), 274–299 (2012)
6. Caris, A., Janssens, G.: A local search heuristic for the pre- and end-haulage of intermodal container terminals. *Comput. Oper. Res.* **36**, 2763–2772 (2009)
7. Gambardella, L., Rizzoli, A.: The role of simulation and optimisation in intermodal container terminals. In: D. Moller (ed.) Proceedings of the 12th European Simulation Symposium (ESS 2000), pp. 422–426. Society for Computer Simulation, PO BOX 17900, San Diego, CA 92177 USA, Hamburg, Germany (2000)
8. Gundersen, E., Kaiser, E., Scarlatos, P.: Assessing container terminal safety and security using data envelopment analysis. In: Mastorakis, N., Jha, M. (eds.) Proceedings of the Second WSEAS International Conference on Urban Planning and Transportation, Mathematics and Computers in Science and Engineering, pp. 125–130. WSEAS, World Scientific and Engineering Academic Society, Ag Loannou Theologou 17–23, 15773 Zographou, Athens, Greece (2009)
9. Holguín-Veras, J., Jara-Díaz, S.: Preliminary insights into optimal pricing and space allocation at intermodal terminals with elastic arrivals and capacity constraint. *Netw. Spat. Econ.* **6**(1), 25–38 (2006)
10. Lin, C., Chang, Y., Lin, S.: Efficient model and heuristic for the intermodal terminal location problem. *Comput. Oper. Res.* **51**, 41–51 (2014)
11. Lin, C., Lin, S.: Two-stage approach to the intermodal terminal location problem. *Comput. Oper. Res.* **67**, 113–119 (2016)
12. New South Wales Government: navigating the future: NSW Ports' 30 year master plan. Technical report NSW Ports (2015). <http://www.nswports.com.au/assets/Publications/NSW-Ports-Master-Plan-2015.pdf>

13. Sörensen, K., Vanovermeire, C., Busschaert, S.: Efficient metaheuristics to solve the inter-modal terminal location problem. *Comput. Oper. Res.* **39**, 2079–2090 (2012)
14. Thai, C.: Metropolitan Intermodal Terminal Study 2011. Tech. rep., Shipping Australia Limited (2011). <http://www.transport.nsw.gov.au/sites/default/files/b2b/freight/rail-access-review-shipping-aust-mits-attachment.pdf>
15. Vidović, M., Sečević, S., Kilibarda, M., Vlajić, J., Bjelić, Tadić, S.: The p-hub model with hub-catchment areas, existing hubs, and simulation: A case study of serbian intermodal terminals. *Netw. Spat. Econ.* **11**, 295–314 (2011)

Efficient Models, Formulations and Algorithms for Some Variants of Fixed Interval Scheduling Problems

D. Niraj Ramesh, Mohan Krishnamoorthy and Andreas T. Ernst

Abstract The fixed interval scheduling problem—also known as the personnel task scheduling problem—optimizes the allocation of available resources (workers, machines, or shifts) to execute a given set of jobs or tasks. We introduce a new approach to solve this problem by decomposing it into separate subproblems. We establish the mathematical basis for optimality of such a decomposition and thereafter develop several new techniques (exact and heuristic) to solve the resulting subproblems. An extensive computational analysis of the new techniques proves the efficacy of these approaches when compared to other established techniques in the literature. Specifically, a hybrid integer programming formulation presented in this paper solves several larger problem instances that were not amenable to exact techniques previously. In addition, a constructive heuristic approach (based on quantification metrics for tasks and resources) gives solutions equal to the optimal. We demonstrate that our decomposition approach is applicable for several important variants within the topic of fixed interval scheduling including tactical fixed interval scheduling problem and operational fixed interval scheduling problem.

Keywords Fixed interval scheduling problem · Personnel task scheduling problem · Machine scheduling · Decomposition approach

D. Niraj Ramesh · M. Krishnamoorthy (✉)
Department of Mechanical and Aerospace Engineering, Monash University,
Clayton, VIC 3800, Australia
e-mail: mohan.krishnamoorthy@monash.edu

D. Niraj Ramesh
e-mail: niraj.ramesh@monash.edu

A.T. Ernst
School of Mathematical Sciences, Monash University, Clayton,
VIC 3800, Australia
e-mail: andreas.ernst@monash.edu

1 Introduction

Decision support models often seek efficient distribution of resources in order to satisfy a set of conflicting requirements. The term *resource* has been used in various different contexts. It is commonly used to represent machines (including cars, aeroplanes, or cranes). It may also be used to represent crew or workforce as ‘personnel,’ ‘staff,’ or ‘workers’. Problems of allocating such resources to a fixed set of conflicting tasks appear in diverse domains such as rostering of staff at large enterprises (airline, hospitals, and hotels), allocation of computational processes to processors, planning of logistic operations such as crane scheduling at shipping ports, and scheduling of utility services (like rental cars) for customers bookings. To solve these problems, the OR community has developed a rich set of algorithms and approaches (e.g., see [5, 11] or [17]). But the increasing size of problem instances and the inclusion of complicating side constraints drive the need for novel approaches to address such problems.

Consider the *fixed interval scheduling problem* of optimally allocating a set of non-identical workers or resources to perform a set of conflicting tasks or activities without preemption. The problem restricts that only certain identified workers or resources may be qualified to execute specific tasks. Further, every task has a specific known time window (with a fixed start time and duration) within which it must be completed. Within this broad topic of fixed interval scheduling, the *tactical fixed interval scheduling problem* (hereafter abbreviated as *TFISP*) intends to minimize the number of workers used, such that all given tasks are executed. There exist several variants within this category; they attempt to minimize quantities such as the weighted total cost of usage of resources, weighted penalty for operations not executed, total working time, and spread time. For example, spread time refers to a restriction on the time duration (or shift timing) for which a specific machine, resource, or worker will remain usable starting from the starting time of the earliest job assigned to it. Further consideration that may apply includes the sequence-dependent or precedence-dependent non-uniform changeover time spent by any resource between a pair of tasks assigned to it, priority of jobs or costs of workers, etc.

In this paper, we develop algorithms and procedures that apply to the tactical fixed interval scheduling problem (*TFISP*). Our discussion can be extended further to cover several side constraints including sequence dependence and also some alternative objective functions. More specifically, this paper primarily addresses the shift minimization personnel task scheduling problem (*SM-PTSP*).

We explicitly acknowledge the semantic similarity of *TFISP* and *SM-PTSP*. The only difference is that *SM-PTSP* relates to personnel allocation only, whereas *TFISP* has a broader sense and it falls within the generic interval scheduling domain. We discuss our paper in terms of interval scheduling and not *SM-PTSP*. However, we will use some data instances from *SM-PTSP* to demonstrate the efficacy of our algorithms against comparable techniques.

This paper is organized as follows: The remainder of Sect. 1 formally defines the tactical fixed interval scheduling problem (TFISP) and thereafter reviews the relevant literature. Section 2 introduces new methods to decompose the TFISP and interlink the resulting subproblems. The actual formulations and solution techniques for TFISP are presented in Sect. 3. Section 4 discusses the results from applying these techniques to a large number of TFISP data instances.

1.1 Problem Definition

To maintain consistency with existing literature, we adapt and combine the nomenclature as defined previously. This includes [19, 21, 22]. We consider a set J of tasks that must be executed by allocating them to parallel unrelated non-uniform resources (machines or workers) from set W . Every task $j \in J$ must be executed by exactly one (unique) resource $w \in W$ without interruption or *preemption*. The term ‘preemption’ refers to a situation where one resource w performs some part of a task j , and the remaining part of that task j is performed by some other resource w' . This paper assumes that preemption is strictly not permitted.

Every task $j \in J$ has a predefined start time (or ready time) S_j and an end time E_j , such that the task j must be performed during the entire interval $[S_j, E_j]$. Obviously, the resource w allocated to task j cannot perform any other task during interval $[S_j, E_j]$ (noting that any resource can only perform a maximum of one task at a time). Not all resources are qualified to perform all tasks. The subset $J_w \subseteq J$ covers the tasks that any resource w is ‘qualified’ to perform. Conversely, the subset $W_j \subseteq W$ gives the resources qualified to perform task $j \in J$. The following parameters formally define the fixed interval scheduling problem:

$J :=$ Set of tasks to be assigned $\{1, 2, \dots, n\}$

$W :=$ Set of workers that can perform the tasks $\{1, 2, \dots, m\}$

$[S_j, E_j] :=$ Interval of time for executing task $j \in J$

$J_w \subseteq J :=$ Subset of tasks that can be allocated to worker $w \in W$

$W_j \subseteq W :=$ Subset of workers capable (qualified) of executing task $j \in J$

We assume that all resources/workers W have uniform (fixed) cost of usage. Similarly, all tasks J have uniform fixed cost of execution with no special preferential ordering or priority. There is no additional variable cost for allocating a specific task to a specific worker. The objective for TFISP is to minimize the size of the (minimal) set of workers w^* for whom a feasible allocation plan can be determined to execute all tasks in J without preemption.

1.2 Literature Review

Problems related to interval scheduling have received considerable attention in the literature. Detailed surveys of the interval scheduling domain are presented in [17, 18, 25]. Some of the earliest contributions to this topic have been in the area of fixed interval scheduling or the ‘fixed job schedule problem’ (FJSP). The FJSP is a special case of TFISP where resource qualifications are identical and uniform. Also, the permissible time window matches the required processing time for every job. See [6, 13, 14] for some of the earliest contributions to the FJSP. Interesting polynomial time approximation algorithms for some variants of the fixed job schedule problem are discussed in [12]. An updated repository of data instances, best-known results, and other resources is maintained at [28].

[1, 21] are two of the seminal works that specifically address the TFISP and prove its computational complexity arising from qualification restrictions. The current literature has referred to TFISP by several different names including ‘heterogeneous workforce assignment problem,’ ‘personnel task scheduling problem,’ and others. Krishnamoorthy et al. [19, 20] discuss the ‘personnel task scheduling problem’ (PTSP) which includes additional restrictions on the availability of workers. However, [20] explains the equivalence of PTSP to TFISP by noting that the time restrictions on worker availability are quite simply considered as another facet of a worker qualification constraint. The PTSP was derived from a two-stage personnel rostering approach in [8] which employed a simulated annealing algorithm to handle the rostering of staff and shifts at airports. In the first stage, worker shifts are derived over a two-week planning horizon, and in the second stage, tasks are allocated to shifts/workers. [34] refer to TFISP as a problem of assigning ‘heterogeneous workforce’ and present a coloring approach to identify possible allocations along with bounds on the branch-and-bound search tree. Eitzen et al. [9] present strategies based on a set covering approach for optimizing the use of multi-skilled workforce. Greedy heuristic algorithms for TFISP (in terms of manpower shift planning) are presented by [23]. A genetic algorithm is used to solve the TFISP in [31]. Heuristic algorithms based on specialization of tasks and capacities of workers are discussed in [29]. Very recent results for PTSP are reported in [26, 37].

Currently, the best performing exact solution approach to solve TFISP is by [2, 7]. Here, the idea of a ‘triplet’ of tasks is introduced and used in a column generation algorithm. Meta-heuristic approaches developed by [32, 33] currently offer the best heuristic techniques. They have solved the larger problem data instances within reasonable computational time.

Other interesting variants of fixed interval scheduling problems include cases where individual resources incur non-uniform costs, especially when allocated to specific tasks (see [10]). Another variant widely studied is the minimization of spread time for all tasks [30]. Although we do not propose to address any such variant in the current paper, we note that some solution techniques discussed for solving these variants in [4, 15, 16, 24, 36] apply very well for our version of TFISP.

2 Decomposition Approach

In this section, we introduce a new decomposition approach for the TFISP. We begin with the premise that the procedure to solve TFISP can be divided into the following distinct phases:

1. *Selection phase for identifying suitable resources*: Identify the minimal subset $w^* \subseteq W$ with the expectation that a feasible allocation of tasks J to w^* must exist. However, this phase does not give the actual allocation of w^* to J .
2. *Allocation phase for assigning unique resource to every task*: Given a subset $w^* \subseteq W$, find the feasible allocation of all tasks J to workers w^* .

Looking at the existing literature on the TFISP, we note that exact approaches attempt to solve both the phases (listed above) simultaneously. Heuristic approaches tend to find suitable task allocations first and then look for solutions where the number of workers required can be reduced. The central or governing hypothesis of our paper is that it is possible and desirable to solve the two phases listed above separately. Further, we propose that the selection phase must be independently solved first. Then, given the result of the selection phase, the allocation phase should later try to find suitable allocations of tasks to resources. If an exact procedure for the selection phase can actually be found (and proved to be exact), then the allocation phase becomes comparatively easier because we only need to find one single feasible allocation; if the selection phase was optimally solved, then any feasible solution from the allocation phase is inherently assured to be optimal for the overall TFISP. We will prove this hypothesis in Theorem 4 and use it to develop algorithms employing the two-phase decomposition approach.

Please Note: The selection phase *attempts* to find a set w^* . However, it does not include a strict proof or guarantee that this proposed set w^* is indeed sufficient in all cases. In fact, some Remedial-corrections are always expected during subsequent stages. These corrections can potentially add some more workers over and above the starting set w^* . Although the selection phase can be solved independently, its result may not necessarily constitute a feasible solution to the overall problem. The first phase gives a lower bound, which will be validated or corrected in subsequent stages.

We first study the TFISP to identify conditions under which a set $w^* \subset W$ obtained from the selection phase is feasible for the overall TFISP.

2.1 Feasibility Conditions for Selection Phase

Consider that the selection phase has yielded a solution w^* . We will use the following terminology: For any set s of workers ($s \subset W$), the subset ($s \cap w^*$) is denoted as s^* . For example, for a task $j \in J$, the subset of applicable qualified workers that are selected in w^* would be $W_j \cap w^* = W_j^*$.

The first requirement for feasibility is that for every task $j \in J$, at least one worker from set W_j must be included among the chosen set of (selected) workers w^* . We refer to this as *Condition 1* and define the condition below:

$$\text{Condition 1} \Rightarrow |W_j^*| \geq 1 \quad \forall j \in J \quad (1)$$

Even if Condition 1 is satisfied by w^* , these available workers may still not be sufficient for J . Often, there may exist two or more tasks in J that overlap in time. Even if a certain worker $w \in w^*$ is qualified to execute both of these tasks, only one task can be actually allocated to w at a time. Such interference or overlap of tasks is represented in terms of *cliques*. A clique is defined as a set of overlapping tasks: For any given clique c , there must exist some time interval when all the tasks in that clique are ongoing (started but not completed). The concept of cliques has also been discussed in the TFISP and related literature under many different terminologies and notations including ‘Interval graph,’ ‘conflict graph’ (see [18] for details). The terminology used in this paper for cliques is presented below. Please note that our definition and notations are slightly different from several seminal papers of TFISP.

1. *General-clique*: Any clique of two or more overlapping tasks in a given TFISP instance is called as a *general-clique*. Unless otherwise specified, any usage of the term ‘clique’ refers to a ‘general-clique’ with no further conditions imposed on it. We denote the set of all general-cliques as C .
2. *Pair-clique*: A clique comprising of only two tasks is referred to as *pair-clique*. We denote the set of all pair-cliques as C^2 .
3. *Maximal clique*: A *maximal clique* is defined as a clique κ for which there does not exist any task $j \notin \kappa, j \in J$ where $\{j\} \cup \kappa$ is also a clique. The set of all maximal cliques κ is denoted as \mathbb{K} .
4. *Clique-capable workers*: For a clique c , the set of Clique-capable workers $W_c \subset W$ is defined as the set of workers such that any worker $w \in W_c$ can execute at least one task $j \in c$. In a sense, the term W_c is merely a generalization of the term W_j which indicated the set of workers qualified to execute task j .
5. *Worker-specific clique*: For any worker $w \in W$, a clique $c \in C$ is said to be a *worker-specific clique* for w if worker w is qualified to execute absolutely all tasks in c . This means $c \subset J_w$. For the given worker w , we denote the set of all worker-specific cliques for w as Θ_w .

For a clique $c \in C$, the clique-capable workers available in w^* would be $W_c \cap w^*$. Using the terminology defined above in this section, we denote $W_c \cap w^*$ as W_c^* . Then, we now have a condition on w^* . For any clique $c \in C$, at least $|c|$ workers from among W_c must be included in w^* . We define this *Condition 2* as follows:

$$\text{Condition 2} \Rightarrow |W_c^*| \geq |c| \quad \forall c \in C \quad (2)$$

Notation of covering workers: Consider a set of tasks $\bar{j} \subseteq J$ and a set of workers $\bar{w} \subseteq W$, such that for any given task $j \in \bar{j}$, there is at least one qualified worker $w \in \bar{w}$, where $w \in W_j$. Then, we will designate this situation as: \bar{w} covers \bar{j} and denote

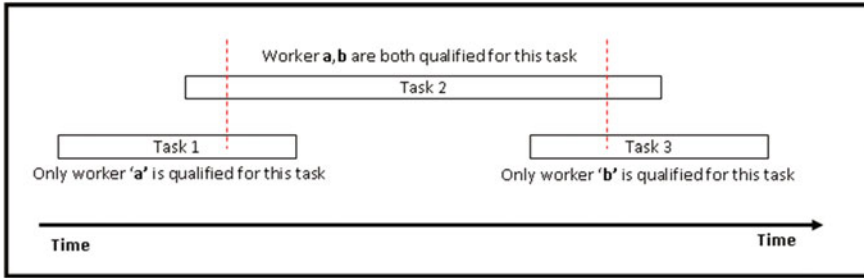


Fig. 1 A sample problem instance of CSRP

it as $\bar{w} \supseteq \bar{j}$. The symbol \supseteq implies that the preceding set of workers *covers* the set of tasks mentioned. We point out that this covering set \bar{w} was not defined to be a unique or even a minimal set of workers. Further, if either \bar{w} , or \bar{j} , or both involve one element only, then the notation will simply be stated for the element instead of the entire set. For example, $w \supseteq j$ implies that a worker w is qualified to execute task j . With this definition, conditions 1 and 2 are succinctly stated as: $w^* \supseteq j \forall j \in J$ and $w^* \supseteq c \forall c \in C$ respectively.

We argue that conditions 1 and 2 (together) are necessary but still not sufficient to assure that w^* is feasible for the allocation. For example, consider the situation shown in Fig. 1. Figure 1 shows a TFISP instance containing three tasks 1, 2, and 3 where the qualifications of some workers a, b are such that a can execute tasks 1, 2 (i.e., $a \supseteq \{1, 2\}$) and b can execute tasks 2,3, i.e., $b \supseteq \{2, 3\}$. Then, the feasibility conditions 1 and 2 are satisfied by the proposed solution $w^* = a, b$. But no feasible allocation of w^* to 1, 2, 3 exists; if a were to be allocated to task 1, then only b is available for task 2. Since tasks 2, 3 form a clique, it is not possible to execute task 3 by b . Also, a is not qualified to execute task 3 at all. So, even though $w^* = \{a, b\}$ satisfied both feasibility conditions stated above, it is not a feasible solution.

We notice that w^* would have been a feasible solution if preemption of tasks (or allocation of partial tasks) was permitted. In that case, worker b starts with some initial part of task 2 but interrupts it to take up task 3, whereas worker a executes task 1 and then takes up the remainder of task 2. The conditions 1 and 2 effectively gave a selection of workers that can only execute the given tasks if preemption is permitted. So, we need to restrict and reject the preemption possibility from the selection phase. If we can identify, curtail and avoid such situations from the selection phase, then the resultant w^* must be feasible for the allocation phase. We now study the features of a specific proposed solution w^* that necessarily lead to preemption during allocation.

Lemma 1 *Preemption cannot occur on any task $j \in J$ if j is not part of at least one pair-clique*

Proof We prove this by contradiction. Let us assume that there exists some task $j \in J$ such that it is not a part of any pair-clique $c \in C^2$. Then, j does not overlap with any other task at any time. We consider that preemption is still occurring on j .

This means that the only feasible allocation of w^* on J necessitates that at least two workers $a, b \in w^*$ must each execute some part of j . Without loss of generality, let us suppose that worker a first executes some part of task j and then worker b takes up the remaining part of j . Now if worker a was allocated to some part of task j , then it must be true that worker a is qualified and available for the entirety of task j . Then, the only reason why worker a must interrupt task j halfway through can be that a is assigned some other task say j' . If worker a needs to interrupt j to take up j' , then j' must overlap with j for some time. Then, j and j' constitute a pair-clique. This violates our assumption of j not being a part of any clique.

So, preemption only needs to be constrained on tasks that participate in at least one clique. However, this statement does not help much, because we expect typical large TFISP problems to involve tasks that participate in a very large number of cliques. We build upon Lemma 1 to make a stronger statement about preemption.

Lemma 2 *Preemption can only occur on some task $j \in J$ if j is in the intersection of two different pair-cliques.*

Proof By Lemma 1, we already know that j is a part of at least one pair-clique. Thus, $\exists c \in C^2 : j \in c$. Let us assume that preemption does occur on j but j is not a part of any other pair-clique except c . Now, if preemption occurs on j , there exist at least two workers $a, b \in w^*$ assigned to j . Without loss of generality, let us suppose that worker a first executes some part of task j and then worker b must take up the remaining part of j . Repeating the arguments from the proof of Lemma 1, a needs to interrupt j halfway through and move off because a was assigned some other task j' . So, $\{j, j'\}$ must constitute the clique c . Now, let us consider the actions of worker b . We needed to allocate worker b to j because the earlier worker a handling j had interrupted j to take up some other task. But the question arises why we could not allocate b for the entirety of j . Since b must necessarily be qualified for j , the only reason why b was not allocated to j from the beginning itself can only be that b was blocked in executing some other task j'' . Again j and j'' must then overlap; i.e., they constitute another pair-clique. So j is in the intersection of two separate pair-cliques.

Note: The overlapping pattern of tasks j, j', j'' as discussed here bears resemblance to the concept of triplets discussed in [2, 7]. However, our subsequent analysis and utilization differ significantly from the work of [2, 7].

Lemmas 1 and 2 have only made statements concerning the overlap of tasks. Since preemption can only occur for qualified workers, we further strengthen our observation to include another restriction on occurrence of preemption:

Theorem 3 *Preemption can only occur on some task $j \in J$ if all the following conditions hold:*

1. $\exists c_1, c_2 \in C^2 : j \in c_1 \cap c_2$
2. $\exists w_1, w_2 \in W_j : w_1 \neq w_2$
3. $w_1 \in W_{c_1 \setminus \{j\}}$ and $w_2 \in W_{c_2 \setminus \{j\}}$

Proof The first condition in the theorem follows from Lemma 2. The second statement holds because preemption necessarily needs two unique workers to share a task. The third statement states that if the exchange of a specific task j has indeed occurred between workers w_1, w_2 then only one of them is qualified to handle the remaining task from the two intersecting cliques. This must be true because otherwise there would be no reason for the workers to exchange any tasks at all.

We have identified situations under which permit preemption may occur. We now have two options to proceed: (1) We can enforce preventive constraints or precautionary conditions that explicitly identify and thereby avoid any preemption from within the selection phase itself. (2) We do not identify or restrict preemption within the selection phase, but we take the resulting w^* and estimate whether a feasible allocation without preemption is possible from this w^* . If not, we apply some remedial ‘corrections’ to w^* .

Option 1: Avoid preemption within selection phase: To develop constraints that prevent preemption over two pair-cliques c_1, c_2 we look at the clique-capable workers W_{c_1} and W_{c_2} . Theorem 3 states that preemption can only occur if $\exists j \in c_1 \cup c_2 : \exists w_1, w_2 \in W_j \cap W_{c_1} \cap W_{c_2}$. Consider the workers in a proposed solution w^* . For any of the terms W_j, W_{c_1} , and W_{c_2} , we denote the corresponding workers selected in w^* as $W_j^*, W_{c_1}^*$, and $W_{c_2}^*$, respectively. Then, to ensure that preemption does not occur on task j , the following condition must apply:

$$|(W_{c_1}^* \cup W_{c_2}^*) \setminus W_j^*| + |W_j^*| \geq |c_1 \cup c_2| \tag{3}$$

In larger problem instances, the task j might be in the intersection of many different pair-cliques as shown in Fig. 2.

Theorem 3 does not restrict that the pair-cliques c_1 or c_2 be maximal, so it predicts that preemption may occur in the case demonstrated. To avoid such situations, Eq. (3) is generalized to give the following condition on every task $j \in J$:

$$\text{Condition 3} \Rightarrow \left| \left(\bigcup_{c_k} W_{c_k}^* \right) \setminus W_j^* \right| + |W_j^*| \geq \left| \bigcup_{c_k} c_k \right| \quad \forall c_k \in C : j \in c_k \tag{4}$$

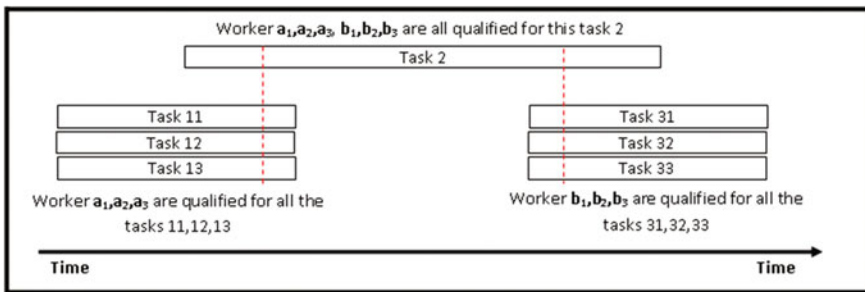


Fig. 2 Intersection of multiple pair-cliques

Theorem 3 assures that conditions 1, 2, 3 applied in conjunction within the selection phase will yield a solution w^* that is necessarily feasible for allocation phase also. Based on this, it is possible to formulate the selection phase as a standard integer program where the equations underlying conditions 1, 2, 3 are enforced as constraints. But the major concern with Condition 3 in Eq. (4) is that for any practical data instance of TFISP, the number of constraints induced would be prohibitively large. We may formulate a branch-and-cut algorithm where we enforce conditions 1, 2 as standard constraints and relax Condition 3 initially. After a solution is proposed by the solver, we can then enforce Eq. (4) as *lazy cuts* by specifically identifying the binding equations only. Even then, Eq. (4) is a very weak constraint. The computational effort expended in first separating the binding cuts and then getting newer solutions makes this approach ineffective. We must consider some other way of removing preemption.

Option 2: Allow preemption, but then make recursive Remedial-corrections:

In this approach, we first solve the selection phase enforcing conditions 1, 2 only. We totally neglect Eqs. (3)–(4) and acknowledge that preemption might exist. We then analyze w^* to identify if preemption actually occurs. Theorem 3 indicates that preemption is not really a task-specific concern but rather it is a clique-based phenomenon. So, given an initial solution w^* from selection phase, we only try to identify any cliques where preemption is unavoidable for any allocation. We defer the discussion of the actual procedure of identifying such cliques till Sect. 3.2. For now, we first consider the remedial actions that can be taken after some cliques are identified where preemption is unavoidable for a given w^* .

Consider that a single specific clique c has been identified such that preemption has been detected to occur only over tasks in c for a proposed solution w^* . Out of the clique-capable workers W_c for c , W_c^* were selected into w^* . Let $W_c^- := W_c \setminus W_c^*$ denote those clique-capable workers of c which were not selected in w^* . Now, preemption occurs on c only if it is impossible to feasibly and uniquely allocate all tasks in c using W_c^* only. This situation can be possibly avoided by two different approaches:

1. Change W_c^* by selecting and including some additional worker from W_c^- in addition to current W_c^* .
2. Remove some (at least one) of the workers from among current W_c^* . However, Condition 2 in Eq. (2) ensures that at least $|c|$ number of workers from among W_c are present in w^* . Then, removal of some worker(s) from W_c^* implies the inclusion of some other worker from W_c^- .

In either of the cases, we find that removal of preemption in clique c necessitates the inclusion of at least one additional worker from W_c^- . We designate the set W_c^- as a *Remedial-correction* for w^* . There may exist many tasks in many cliques where preemption occurs for w^* . Hence, several different Remedial-corrections may exist. We shall solve the selection phase again, but with the additional constraint that at least one worker from among every such Remedial-correction W_c^- be assuredly included in the new solution. We get a new solution and again check for preemption within the new solution. This repeats till no more preemption is detected. Then, the solution

w^* obtained eventually must satisfy conditions 1, 2, 3. This procedure is outlined in Algorithm 1 below.

Algorithm 1 Outline of overall solution procedure

Input: TFISP instance of tasks J and workers W with qualifications J_w and W_j pre-computed and cliques C^2 identified

- 1: Find minimal set $w^* : w^* \succeq j \in J$ and $w^* \succeq c \in C$ (This procedure will be discussed in Sect. 3.1)
- 2: Set \mathbb{R} of all Remedial-corrections \leftarrow Identify Remedial-corrections needed for w^* (will be discussed in Sect. 3.2)
- 3: **while** $\mathbb{R} \neq \text{Empty}$ **do**
- 4: **for all** $s \in \mathbb{R}$ **do**
- 5: Define remedial constraint that at least one worker from among s be used in w^*
- 6: Find set w^* satisfying all remedial constraints, so that $w^* \succeq j \in J$ & $w^* \succeq c \in C$ (This procedure will be given in Sect. 3.1)
- 7: Set \mathbb{R} of all Remedial-corrections \leftarrow Identify Remedial-corrections needed for w^* (will be discussed in Sect. 3.2)

Output: Minimal set w^* such that a feasible allocation to J without preemption must exist

Please Note: Every remedial constraint found in step no. 5 is a valid inequality applicable to w^* . This means that we can include the constraint as a ‘lazy cut’ to be passed to the MIP solver. Although the Algorithm 1 does not mention this explicitly, the understanding is that the valid inequalities discovered will not be discarded ever—they are used as ‘lazy cuts’ in all future iterations.

2.2 Definition of Subproblems

We claim that if the set w^* computed in lines 1 and 6 of Algorithm 1 is the minimal set satisfying conditions 1, 2 and also if the remedial constraints are rightly identified, then the underlying decomposition is a sound and complete procedure to get the optimal solution of TFISP. Algorithm 1 presented the outline of the decomposition procedure, but we now divide the steps in Algorithm 1 into three subproblems so that we can address each of them separately. We formally define the subproblems as follows:

Subproblem A Naive Selection: Given a TFISP instance involving tasks J and workers W , where qualifications J_w , W_j , and cliques C are known, determine the smallest possible set w^* that covers all tasks in J and all cliques in C .

This subproblem will be utilized at line 1 of Algorithm 1. It merely needs to satisfy conditions 1, 2. Further, we notice that if a set w^* covers all maximal cliques \mathbb{K} , then all general-cliques and pair-cliques are also covered. So, the ‘Naive selection subproblem’ only needs to select a minimal set of workers that cover all tasks and all

maximal cliques. This can be done by a standard IP formulation or also by heuristic procedures. We will present such formulations in Sect. 3.1.

Subproblem B Remedial-Corrections Identification: Given a set w^* of workers, find all Remedial-corrections needed wherever preemption can occur

This subproblem will be utilized at lines 2 and 7 of the Algorithm 1. It will give a *set of sets of workers* \mathbb{R} . Every set or group of workers $s \in \mathbb{R}$ is such that:

1. Absolutely no worker from set s of workers was present in w^* .
2. At least one worker from each set s should have been present in w^* to avoid preemption.
3. If \mathbb{R} is empty, then a feasible unique allocation of workers w^* to J must exist without preemption.

The crux of this Subproblem B is its third statement. If this subproblem cannot find any Remedial-correction set, then it must assure that a feasible allocation (without preemption) exists from w^* . The best way to prove that such a feasible solution exists is to actually give the said allocation. So, to solve the ‘Remedial-corrections identification subproblem,’ we search for feasible allocations of J to w^* . We formulate this subproblem as an integer program in Sect. 3.2.

Subproblem C Corrective Selection: Given a set of workers w^* and a set of remedial constraints \mathbb{R} , find the minimal set of workers \bar{w}^* , such that

1. $\bar{w}^* \succeq j \forall j \in J \rightarrow$: This implies that \bar{w}^* covers all tasks.
2. $\bar{w}^* \succeq c \forall c \in C \rightarrow$ This implies that \bar{w}^* covers all cliques.
3. \bar{w}^* includes at least one worker from every set $s \in \mathbb{R}$.

This subproblem will be utilized at line 6. It is merely an extension of the Naive selection subproblem A. It can be solved by a standard IP formulation or also by heuristic procedures. We will present such formulations in Sect. 3.1.

Assuming that each of three subproblems is solved optimally, we are now ready to prove our hypothesis that the decomposition approach gives an exact solution to TFISP.

Theorem 4 *If Subproblems A, B, and C are solved optimally, Algorithm 1 is an exact procedure to solve TFISP.*

Proof If no further Remedial-corrections are needed for a proposed w^* , then a feasible allocation of those workers for J is assured by Subproblem B. This proves the feasibility of w^* . If a Remedial-correction set is found, then it should be impossible to find any feasible allocation of w^* to J . This means that no solution having lesser number of workers than w^* can be feasible. These two conditions assure that the resulting w^* must be the minimal feasible set of workers that can execute J .

3 Formulations and Solution Techniques

This section gives several alternative formulations for each of the subproblems as defined in Sect. 2.2 earlier.

3.1 Selection Subproblem

We begin with the ‘Naive selection’ subproblem. This must find a minimal set w^* satisfying constraints (1) and (2). We model this as an integer program using the following binary decision variable:

$$Y_w := \begin{cases} 1 & \dots \text{ if worker } w \text{ is picked and included in } w^* \\ 0 & \dots \text{ otherwise} \end{cases}$$

To minimize the number of workers used, the objective is to minimize $|w^*|$, i.e., to

$$\text{Minimize } \sum_{w \in W} Y_w \quad (5)$$

The feasibility conditions 1, 2 stated in Eqs. (1) and (2) earlier lead to the following constraints:

$$\sum_{w \in W_j} Y_w \geq 1 \quad \forall j \in J \quad (6)$$

$$\sum_{w \in W_c} Y_w \geq |c| \quad \forall c \in \mathbb{K} \quad (7)$$

Eqs. (6) and (7) are sufficient to model the ‘Naive selection’ subproblem A.

We proceed to consider the extension of this formulation for subproblem C of ‘Corrective selection’ where a non-empty set \mathbb{R} of Remedial-corrections is known. The following linear constraint facilitates this requirement:

$$\sum_{w \in \mathbb{S}} Y_w \geq 1 \quad \forall s \in \mathbb{R} \quad (8)$$

Thus, we have presented an IP formulation to solve the Naive selection subproblem A and the Corrective selection subproblem C optimally. Such IP formulations using decision variables like Y_w have been used earlier in [20, 21] and others. However, all such formulations had attempted to handle task allocation at the same time as worker selection. They used a two-index decision variable to model the allocation of any task to a unique worker. For a TFISP instance of n tasks and m workers, our formulation uses only $O(m)$ number of variables with $O(n + |\mathbb{K}|)$ number of constraints. This (linear) number of variables and constraints is substantially less than

the (quadratic) $O(mn + m)$ number of variables with $O(n + m|C|)$ constraints used earlier. Thus, the decomposition approach has led to a much compact formulation for this subproblem. We also consider some ways to further tighten this formulation.

3.1.1 Alternative Approach to Solve the Selection Subproblem

The IP approach discussed above presented an exact way of finding w^* . Effectively, the feasibility conditions discussed earlier (implemented through Eqs. (6) and (7)) constrain the workers that must be selected within w^* . However, during computational experiments on several problem instances, it was noticed that the ‘Corrective selection’ subproblem was repeatedly needed many times before a feasible w^* without preemption could be found. We now propose an alternative heuristic algorithm to find w^* for Subproblems A and C. Contrary to the established practice in heuristic algorithms, the expectation from this algorithm is not that it should work faster than the exact IP. Rather, the intention is that the minimal set w^* found here should preferably not allow any preemption (thus avoiding repeated calls).

Heuristic algorithms developed to construct a set of desirable workers have often been used in interval scheduling problems. For example, see the ‘left-edge algorithm’ mentioned by [17] and in [14]. These algorithms essentially combine the task allocation decisions with the selection decision. We modify this approach by developing a procedure to construct w^* , such that we quantify the expected impact of the inclusion or exclusion of any specific worker $w \in W$ into w^* . We find a slightly analogous approach used in [29]. However, in our case, we neglect any task allocation decisions totally; this allows us to focus on selecting a suitable set w^* while deferring the allocation decisions to other algorithms better suited for allocations. Also, since our algorithm must solve Subproblem C, our intentions and procedure are fundamentally different from the cited works.

Consider staff rostering problem where some employees or workers are to be selected and allocated for a set of tasks. The person or system that makes these selection or allocation decisions would prefer workers who are capable/available for more number of tasks. They would seek workers with broad areas of expertise, so that they can handle several different tasks. Also, employees or workers who are available during ‘rush hours’ (i.e., when several different simultaneous tasks or cliques are to be executed simultaneously) would be preferred. Finally, the planners need some specialists—this implies the persons who can perform tasks that very few other persons can perform. Thus, the inclusion/exclusion of a worker in w^* depends on three factors: (a) specialization of tasks performed, (b) breadth of expertise, and (c) availability in cliques. We now quantify these factors:

- The specialization of tasks is determined by the number of workers that can do a specific task. If very few workers are capable/available to handle a specific task $j \in J$, then it is a very special task. We denote the speciality factor of the task $j \in J$ as S_j . It is defined as follows:

$$S_j := \frac{1}{|W_j|}$$

- The breadth of expertise of a worker is a quantification of the different tasks that may be allocated to that worker. We denote the expertise factor for worker $w \in W$ as E_w . The following definition of E_w inherently accounts for the speciality factor of tasks handled by that worker:

$$E_w := \sum_{j \in J_w} S_j$$

- Consider that a worker $w \in W$ is a clique-capable worker for maximal clique $\kappa \in \mathbb{K}$. Then, we assign a notional ‘bonus’ to the worker for being available during this maximal clique. We imagine that worker w is doing the most specialized possible task from κ . Hence, we allocate a bonus numerically equal to the speciality factor of the most specialized task in κ . We define the *total clique factor* F_w for the worker w as the sum of these notional bonuses over all maximal cliques for which w is clique-capable. The definition given below inherently accounts for the speciality factor of tasks handled by that worker for that maximal clique.

$$F_w := \sum_{\kappa \in \mathbb{K}} (\text{Max}_j S_j \forall j \in \kappa) : w \in W_\kappa$$

We note that F_w is not related to starting time of job j . It is a heuristic measure of how often a specific worker is available during cliques. The underlying logic is that A worker available during crunch times (cliques) is more valuable than another worker who is neither specially qualified nor available in times of special requirements. We combine these factors into a single metric denoting the *Value* V_w of any worker $w \in W$ as:

$$V_w := E_w + F_w \tag{9}$$

In practice, we can also use a nonlinear weighted functions to calculate V_w instead of the simple linear combination given in Eq. (9). This value for any worker $w \in W$ can be precomputed deterministically as a parameter for the problem instance. We then use it to build w^* in Algorithm 2. This algorithm addresses the ‘Naive selection’ subproblem as well as the ‘Corrective selection’ subproblem. The only difference is that the parameter \mathbb{R} (set of Remedial-corrections) would be empty for the ‘Naive selection’ subproblem.

Algorithm 2 Procedure to build w^* based on V_w values

Input: SMPTSP or TFISP instance of tasks J and workers W where V_w, J_w, S_j and W_j are pre-computed

Input: Set of Remedial-correction \mathbb{R} may optionally be given

```

1:  $w^* := \{\}$ 
2:  $J :=$  Set of all  $n$  tasks sorted in ascending order of speciality factor  $S_j$ 
3: for all  $s \in \mathbb{R}$  do
4:   if  $\nexists w \in w^* : w \in s$  then
5:      $w =$  Worker with maximum  $V_w$  such that  $w \in s$ 
6:      $w^* = w^* \cup \{w\}$ 
7: for all  $j \in J$  do
8:   if  $\nexists w \in w^* : w \in W_j$  then
9:      $w =$  Worker with maximum  $V_w$  such that  $w \in W_j$ 
10:     $w^* = w^* \cup \{w\}$ 
11:  $\mathbb{K} :=$  Set of all Maximal Cliques sorted in ascending order of clique-size
12: for all  $\kappa \in \mathbb{K}$  do
13:    $q := |\kappa| - |w^* \cap W_\kappa|$ 
14:   if  $q > 0$  then
15:      $W^+ :=$  Best  $q$  workers from  $W_\kappa \setminus w^*$  identified by highest values of  $V_w$ 
16:      $w^* = w^* \cup W^+$ 
17: return  $w^*$ 

```

Output: Set of workers w^*

In the above algorithm, we first selected the highest ‘value’ workers who fulfill the remedial constraints. Then, we selected the highest ‘value’ workers who could handle the most generalized (low speciality) tasks. We gradually moved to specialized tasks with the hope that some of the high value workers selected earlier might be capable/available for them. If not, we needed to add more workers. Finally, we checked whether all cliques were accounted for. Algorithm 2 runs within computational time of polynomial order for the data instance size.

3.1.2 Hybrid Procedure for Worker Selection

We combine the best features of the MIP formulation and the heuristic approach to form a ‘hybrid’ procedure as follows:

1. Major commercial MIP solvers typically perform better if an initial or starting solution is provided beforehand. The Algorithm 2 provides a heuristic w^* which may be used as the starting solution for MIP. So, we refine the MIP approach to first call Algorithm 2, get a heuristic solution (say hw^*), and then internally use this hw^* to get the exact w^* .
2. The MIP formulation discussed earlier did not give any prioritization or preference to any specific worker in the objective function—the coefficient for all terms Y_j in the objective function was uniform. On the contrary, Algorithm 2 introduced a quantification for the value or ‘desirability’ of any specific worker w . We use the concept of ‘value’ of a worker to improve the performance of the MIP formulation. For any worker $w \in W$, consider the term \bar{V}_w defined as follows:

$$\bar{V}_w = \frac{V_w}{\sum_w V_w} \quad (10)$$

The term \bar{V}_w is a scaled or weighted measure of the value of worker w , and it will always be significantly less than 1. We use \bar{V}_w to redefine Eq. (5) as follows:

$$\text{Minimize } \sum_{w \in W} (1 + \bar{V}_w) \times Y_w$$

This modified objective gives a preference to higher ‘value’ workers wherever possible.

3.2 Identifying Remedial-Corrections

Consider that the selection subproblem has been solved to get a set of workers w^* with the expectation that these workers should be sufficient for a feasible allocation to J . The subproblem B of ‘Remedial-corrections’ needs a procedure to get either one of the following: (1) a set of cliques, such that it is impossible to do unique allocation of tasks in those cliques without preemption within w^* or (2) a feasible allocation of all tasks in J without preemption within given w^* . Initially, let us assume that the feasible allocation is indeed possible for the given w^* . We devise an integer program to find this allocation based on the following decision binary variable:

$$Z_w^j := \begin{cases} 1 & \dots \text{ if worker } w \text{ is allocated to execute task } j \\ 0 & \dots \text{ otherwise} \end{cases}$$

We only want a feasible allocation in this subproblem, and the optimality of w^* is not a concern within this section. So, this integer program has no explicit objective function at all. The following constraint applies:

$$\sum_{j \in c} Z_w^j \leq 1 \quad \forall c \in \Theta_w \quad \forall w \in W \quad (11)$$

$$\sum_{w \in w^*} Z_w^j = 1 \quad \forall j \in J \quad (12)$$

Eq. (11) ensures that any worker can be allocated to (at the most) one task in any ‘worker-specific clique.’ The concept of ‘worker-specific cliques’ Θ_w was explained earlier in Sect. 2.1. Eq. (12) ensures that every task is assigned to exactly one worker from w^* . This MIP formulation can give a feasible allocation of tasks J to workers Eq. (11) if such an allocation exists. Further, the integrality condition of the decision variable Z_w^j along with Eq. (12) ensures that preemption is not permitted.

If no feasible allocation (without preemption) exists for a given w^* , then this formulation will yield infeasibility. But in such a case, we wish to find specific

Remedial-correction sets. In general, there may exist a separate Remedial-correction for every possible clique $c \in \mathcal{C}$. The computational cost of individually looking at every clique is considerable. We now devise a method to identify ‘sufficient’ remedial sets by looking at very few cliques only.

Consider a maximal clique κ . We define ψ_κ as the set of all tasks that meet at least one of the following two conditions:

1. The task should be included within κ or,
2. The task should overlap with at least one task within κ

Formally, we write this as $\psi_\kappa = \kappa \cup \{j \in J \setminus \kappa : \exists j' \in \kappa \text{ where } \{j, j'\} \in \mathcal{C}^2\}$. We term this set ψ_κ as the *cover* of the maximal clique κ . For all maximal cliques $\kappa \in \mathbb{K}$, it is possible to find the corresponding cover. We denote the set of all these *covers* as Ψ . Then, we assert the following statement on covers. The following statement may even be regarded as a corollary to previous theorems.

Theorem 5 *For any allocation of tasks J to a given set of workers w^* , preemption can occur only within the tasks of some cover ψ . Conversely, if preemption does not occur within any cover $\psi \in \Psi$, then a feasible allocation without preemption must exist.*

Proof Theorem 3 has already established that preemption can only occur on tasks in the intersection of a pair of cliques. So, if preemption is occurring on some task $j \in J$, then j must be a part of at least two cliques c_1, c_2 . If c_1, c_2 are both subsets of some maximal clique κ , then this theorem is already proved. Let us consider the other case: c_1 and c_2 are not the subsets of any single maximal clique. Even then, c_1 will still be part of at least one maximal clique (or c_1 itself will be a maximal clique). Then, the other task in c_2 overlaps with one task (j) in the maximal clique. So all the tasks in c_1, c_2 are still within some cover.

Theorem 5 indicates that we only need to check for preemption across tasks that exist in the same cover. We have two different ways to achieve this.

Alternative 1: Shortlisting infeasibility constraints within IP solver

Major commercially available mixed-integer programming solvers (including Cplex™ and Gurobi™) allow a programmatic analysis of any infeasible model to identify sets of constraint that cause the infeasibility. If preemption within a specific cover ψ causes infeasibility, then the constraints involving tasks and worker-specific cliques in that cover are collectively infeasible. We identify the Remedial-correction terms on every cover $\psi \in \Psi$ as follows:

1. For all tasks $j \in \psi$, mark the corresponding constraint from Eq. (12).
2. For all workers $w \in w^*$, consider all worker-specific cliques in Θ_w as referred in Eq. (11). If any of these cliques is a subset of ψ , then mark the corresponding constraint.
3. Check whether the constraints marked in steps 1 and 2 above are collectively infeasible. If not, then there is no preemption in cover ψ

4. If the marked constraints are collectively infeasible, we now wish to find the Remedial-correction. We build a set of workers W_ψ who are qualified to perform at least one task in ψ . Then, the set $W_\psi \setminus w^*$ gives the workers who could have avoided this preemption. So, we get the Remedial-correction $W_\psi \setminus w^*$ from ψ .

Alternative 2: Penalty terms in the objective

We point out that the MIP formulation presented above for this subproblem does not have any objective term at all. We propose a modification of the MIP formulation so that it directly identifies the unavoidable preemption and the covers within which it occurs. We imagine that for every cover $\psi \in \Psi$, there exists a new special additional worker ω_ψ . This additional imaginary worker (or phantom worker) is qualified to do any tasks within that cover. Further, ω_ψ can even execute more than one task at a time; preemption is permitted for ω_ψ . However, for every task j allocated to ω_ψ , we introduce a very large penalty term in the objective. In a sense, this is slightly similar to Lagrangian relaxation of preemption. An additional decision variable Z_ω to model the use of worker ω_ψ is introduced in Eq. (11). Now, if allocation of w^* to J without preemption is infeasible, then the modified MIP will yield a solution where some phantom worker(s) ω_ψ are allocated some tasks. We only make Remedial-corrections on the covers ψ where the corresponding phantom worker is used. The selection of workers for this Remedial-correction set is as mentioned in the Alternative 1 above.

Remarks:

1. Alternatives 1 and 2 were exact procedures that gave Remedial-correction sets for any cover ψ .
2. Alternatives 1 and 2 are logically equivalent to each other. We collectively term them as *standard MIP* approaches for identifying Remedial-corrections.
3. We can improve the performance of any these two alternative approaches by taking some partial allocation information from the heuristic procedure in Algorithm 2 at line 9.

A comparison of Algorithm 1 to the classical branch-and-cut procedure in MIP formulations seems inevitable. Superficially, it appears that any Remedial-corrections offered by any implementation for the subproblem **B** is effectively a ‘cut’ that eliminates some infeasible selection sets. But we still do not classify our algorithm 1 as a classical branch-and-cut approach. This is because the intent and function of the Subproblem **B** is not merely to provide the ‘cuts.’ Rather, it aims to either prove that no feasible allocation for a given w^* is possible *or* to find a feasible allocation if the proof of infeasibility cannot be made. If we had designed Algorithm 1 as a standard branch-and-cut procedure, then we would only get a set of workers w^* that the algorithm would claim to be optimal. But finding the actual allocation would still be an unsolved *NP*-hard problem.

4 Results

In this section, we present a rigorous computational analysis of the algorithms and procedures discussed in Sect. 3 to support the efficacy of the decomposition approach from Sect. 2. We have coded our algorithms in JavaTMSE (build 1.7) language. MIP formulations have been solved using IBTMCplexTM12.5 solver. The computer hardware is 16-core 64-bit IntelTMXeonTMprocessor at 2.93 GHz with 64 GB RAM.

We notice that an extensive family of 137 problem data instances for TFISP with increasing problem sizes is available in the OR-library (see [3]). Several recent papers and discussion on TFISP have used these instances as benchmarks, so we continue to work with them. It is very well possible to directly solve the problem using a plain MILP model in Cplex without any special procedures. But this works only for very few small-sized instances. For medium- to large-sized instances, the performance by the plain Cplex model alone is too poor to even report or compare—optimal solutions cannot be obtained for reasonably sized problems in meaningful time. The most recent and best-known results for exact approaches for TFISP are from [2, 7]; the best-known heuristics are by [32]. Since the current paper focuses on optimal techniques, we will benchmark the performance of our exact algorithms for the data instances from [27] against the results of [2, 7].

Out of the 137 data instances available in [27], ([2]/[7]) report that 83 instances had been optimally solved within time limit of 1800 s. On the contrary, our results from Algorithm 1 solve 104 of these instances optimally within the same time limit of 1800 s. This includes all 83 instances solved previously; we also manage to get the solutions considerably faster than the previous results in most cases. Table 1 presents the computational time needed by Algorithm 1 against the previous best results for individual data instances. While developing this table, we executed Algorithm 1 with a computational time limit of 1800 s. We repeated this using the various different options described for solving each of the three underlying subproblems. The results for all options (including the plain MIP formulation for worker selection, hybrid approach, heuristic approach) are listed individually in Table 1.

The results from [2, 7] are also provided for comparison purposes. In the interest of brevity, we have intentionally skipped the first 50 very small instances (that were almost trivial) and presented only the larger instances here. These smaller 50 instances were of course solved within very short time by our optimal procedures. We plot the results of our decomposition algorithm against the best-known previous (optimal) results in Fig. 3. This figure uses the data for the hybrid approach within the decomposition algorithm.

Table 1 and Fig. 3 conclusively demonstrate that the decomposition procedure surpasses the previous best (exact) algorithms. We conclude this section by looking at the performance of our decomposition approach for the *very hard* data instances proposed by [33]. Out of the ten new instances introduced, our algorithm (optimally) solves five instances within the time limit of 5000 s. Among these, three data instances were actually solved faster by the (optimal) decomposition algorithm than the best-known heuristic technique. The results are tabulated in Table 2.

Table 1 Details of data instances solved within 1800 s of computational time

Instance details		Time required to solve optimally (s)				Heuristic obj. value	
Name	No. of tasks	No. of workers	Optimal Obj. value	Previous best-known (exact)	By decomposition algorithm	Found by using Algorithm 2 Sect. 3.1.1	
					By hybrid selection (Sect. 3.1.2)	By plain MIP (Sect. 3.1)	
data_51_196_480_33	480	196	160	26.5	23.2	11.8	160
data_52_205_480_66	480	205	160	246.3	43.1	24.2	160
data_53_127_487_66	487	127	100	1113.6	36.3	172.4	100
data_54_175_492_66	492	175	140	154.5	189.2	87.7	140
data_55_85_493_66	493	85	70	425.6	126.1	126.5	70
data_56_163_500_66	500	163	140	1011.6	61.1	81.4	140
data_57_88_508_66	508	88	70	789.3	161.5	222.8	70
data_58_158_517_66	517	158	140	922.5	71.9	234.1	140
data_59_70_525_33	525	70	59	239	163.7	270.6	59
data_60_181_549_66	549	181	139	1424	255.3	101.9	139
data_61_121_557_66	557	121	100	764.4	37.5	253.2	100
data_62_101_571_33	571	101	80	573.6	131.7	140.6	80
data_63_97_577_66	577	97	80	622.7	69.1	309.7	80
data_64_176_595_66	595	176	160	1788.9	137.7	286.5	160
data_65_179_596_66	596	179	159	1967.5	130.0	276.8	159
data_66_348_600_33	600	348	300	15.8	32.4	33.2	300
data_67_371_600_66	600	371	300	272.8	68.6	85.4	300

(continued)

Table 1 (continued)

Instance details					Time required to solve optimally (s)		Heuristic obj. value
Name	No. of tasks	No. of workers	Optimal Obj. value	Previous best-known (exact)	By decomposition algorithm		Found by using Algorithm 2 Sect. 3.1.1
					By hybrid selection (Sect. 3.1.2)	By plain MIP (Sect. 3.1)	
data_68_359_613_66	613	359	300	115.9	138.7	187.5	300
data_69_148_614_33	614	148	120	427.3	172.6	287.8	120
data_70_192_623_66	623	192	160	2142.2	115.5	197.4	160
data_71_197_624_33	624	197	158	69.3	304.3	250.0	158
data_72_205_624_66	624	205	160	2219.3	180.2	263.0	160
data_73_155_661_66	661	155	120	-X-	742.8	1046.5	120
data_74_209_664_33	664	209	180	1106.9	297.6	219.3	180
data_75_72_665_33	665	72	60	398.3	121.1	277.4	60
data_76_162_683_66	683	162	140	1560.3	897.7	994.1	140
data_77_180_688_33	688	180	160	1195.1	463.8	253.8	160
data_78_199_688_66	688	199	160	4424.2	1185.6	648.8	160
data_79_94_689_33	689	94	80	427.8	255.0	660.6	80
data_80_112_691_33	691	112	99	411.9	629.5	661.6	99
data_81_97_692_66	692	97	80	1478	568.6	698.5	80
data_82_89_697_66	697	89	80	1760	50.6	769.4	80
data_83_222_700_66	700	222	180	-X-	121.3	1336.7	180
data_84_136_718_66	718	136	120	1061.5	51.2	511.6	120

(continued)

Table 1 (continued)

Instance details		Time required to solve optimally (s)			Heuristic obj. value		
Name	No. of tasks	No. of workers	Optimal Obj. value	Previous best-known (exact)	By decomposition algorithm	Found by using Algorithm 2 Sect. 3.1.1	
					By hybrid selection (Sect. 3.1.2)	By plain MIP (Sect. 3.1)	
data_85_217_720_66	720	217	180	1665.1	215.2	161.4	180
data_86_178_721_33	721	178	140	-X-	315.6	319.3	140
data_87_203_735_33	735	203	170	1851.4	637.3	1006.1	170
data_88_137_777_66	777	137	120	-X-	2496.9	1521.6	120
data_89_88_788_33	788	88	70	608.7	420.7	588.6	70
data_90_157_791_66	791	157	139	-X-	173.0	-X-	139
data_91_147_851_66	851	147	118	-X-	207.6	-X-	118
data_92_126_856_66	856	126	98	-X-	3517.9	-X-	98
data_93_141_856_66	856	141	119	-X-	352.0	-X-	119
data_94_93_881_33	881	93	80	1001.7	687.9	497.4	80
data_95_204_882_33	882	204	170	-X-	738.7	1475.0	170
data_96_98_886_66	886	98	80	-X-	656.7	523.9	80
data_97_383_895_33	895	383	300	1786	273.6	287.9	300
data_98_91_896_33	896	91	80	1022.5	895.9	488.8	80
data_99_176_956_66	956	176	160	-X-	1711.8	-X-	160
data_100_194_956_66	956	194	160	-X-	181.6	-X-	160

(continued)

Table 1 (continued)

Instance details		Time required to solve optimally (s)				Heuristic obj. value	
Name	No. of tasks	No. of workers	Optimal Obj. value	Previous best-known (exact)	By decomposition algorithm		Found by using Algorithm 2 Sect. 3.1.1
					By hybrid selection (Sect. 3.1.2)	By plain MIP (Sect. 3.1)	
data_101_166_997_66	997	166	140	-X-	283.8	-X-	140
data_102_179_997_66	997	179	138	-X-	10360.3	-X-	138
data_103_348_1024_33	1024	348	300	-X-	6936.2	-X-	300
data_104_181_1057_33	1057	181	146	-X-	23731.6	-X-	146
data_105_173_1075_66	1075	173	150	-X-	6939.7	-X-	150
data_106_121_1096_33	1096	121	100	-X-	1104.2	-X-	100
data_107_114_1112_33	1112	114	100	-X-	1318.1	-X-	100
data_109_205_1115_33	1115	205	157	-X-	3125.2	-X-	157
data_111_155_1211_33	1211	155	139	-X-	3264.4	-X-	139
data_112_200_1213_33	1213	200	169	-X-	6848.2	-X-	169
data_117_192_1285_33	1285	192	149	-X-	4737.8	-X-	149
data_121_147_1345_33	1345	147	120	-X-	5487.8	-X-	120
data_122_422_1358_66	1358	422	348	-X-	1634.4	-X-	348
data_123_187_1376_33	1376	187	159	-X-	352.3	-X-	159
data_125_157_1448_33	1448	157	130	-X-	4106.3	-X-	130
data_127_192_1472_66	1472	192	170	-X-	808.3	-X-	170

^aThe entry -X- indicates that the relevant value could not be found within 1800 s on the available systems

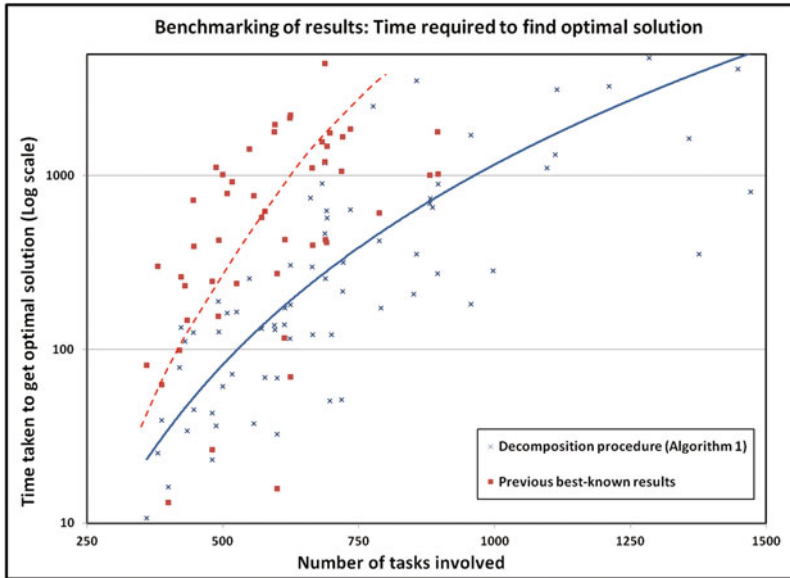


Fig. 3 Benchmarking of results versus previous best known

Table 2 Performance of decomposition approach for very hard data instances from [33]

Name of the data instance	Number of tasks involved	Optimum objective value	Time taken (s) to solve optimally by decomposition
data_1_50_258_20_90_100_200_300	258 ^a	40	33.8
data_2_44_510_20_90_0_100_200	510	40	3007.0
data_3_102_525_30_90_100_200_300	525 ^a	77	591.3
data_4_113_647_20_90_100_200_300	647 ^a	98	299.7
data_6_135_777_20_90_100_200_300	777	116	3691.8

^aThe decomposition approach optimally solves the identified instance faster than even the best known heuristic algorithm

We conclude that the logical decomposition of the TFISP—first into subproblems and later based on covers—has yielded very good benefits.

5 Conclusion and Future Work

In this paper, we have made three noteworthy contributions. The primary contribution is the decomposition of overall TFISP into subproblems through Algorithm 1. Not only have we proved an interesting result theoretically, but this algorithm has fulfilled also the expectations practically by easily surpassing other comparable exact

methods. The second contribution is the value-based heuristic in Algorithm 2. The efficacy of this in ‘guiding’ the MIP as well as in getting the optimal solution is shown.

We notice that the structure of constraint matrices induced by our formulations matches the discussion in [35]. So, we expect major saving in computational effort if we invest efforts in a custom LP solver based on [35] instead of using commercial solvers. We also expect that further improvements could be made in performance if meta-heuristic or constructive heuristic techniques could be developed to suit the requirements of Subproblem B only. In fact, by combining partial solutions as provided by Algorithm 2 and allocation decisions by heuristic techniques like [32], it might be possible to solve much larger TFISP instances also. We propose to explore these possibilities in future work.

References

1. Arkin, E.M., Silverberg, E.B.: Scheduling jobs with fixed start and end times. *Discrete Appl. Math.* **18**(1), 1–8 (1987)
2. Baatar, D., Krishnamoorthy, M., Ernst, A.T.: A triplet-based branch-and-bound algorithm for the shift minimisation personnel task scheduling problem. Submitted to Elsevier April 3, 2012
3. Beasley, J.E.: Or-library: distributing test problems by electronic mail. *J. Oper. Res. Soc.* 1069–1072 (1990)
4. Bekki, O.B., Azizoglu, M.: Operational fixed interval scheduling problem on uniform parallel machines. *Int. J. Prod. Econ.* **112**(2), 756–768 (2008)
5. den Bergh, J.V., Belin, J., Bruecker, P.D., Demeulemeester, E., Boeck, L.D.: Personnel scheduling: a literature review. *Eur. J. Oper. Res.* **226**(3), 367–385 (2013)
6. Dantzig, G.B., Fulkerson, D.R.: Minimizing the number of tankers to meet a fixed schedule. *Nav. Res. Logist. Q.* **1**(3), 217–222 (1954)
7. Davaatseren, B., Krishnamoorthy, M., Ernst, A.T.: A triplet-based exact method for the shift minimisation personnel task scheduling problem. In: *Proceedings of the European Symposium of Algorithms, Patras* (2015)
8. Dowling, D., Krishnamoorthy, M., Mackenzie, H., Sier, D.: Staff rostering at a large international airport. *Ann. Oper. Res.* **72**, 125–147 (1997)
9. Eitzen, G., Panton, D., Mills, G.: MultiSkilled workforce optimisation. *Ann. Oper. Res.* **127**, 359–372 (2004)
10. Erlebach, T., Spieksma, F.C.: Interval selection: applications, algorithms, and lower bounds. *J. Algorithms* **46**(1), 27–53 (2003)
11. Ernst, A., Jiang, H., Krishnamoorthy, M., Sier, D.: Staff scheduling and rostering: a review of applications, methods and models. *Eur. J. Oper. Res.* **153**(1), 3–27 (2004)
12. Fischetti, M., Martello, S., Toth, P.: Approximation algorithms for fixed job schedule problems. *Oper. Res.* **40**(1-Supplement-1), S96–S108 (1992)
13. Gertsbakh, I., Stern, H.I.: Minimal resources for fixed and variable job schedules. *Oper. Res.* **26**(1), 68–85 (1978)
14. Gupta, U.I., Lee, D.T., Leung, J.Y.T.: An optimal solution for the channel-assignment problem. *IEEE Trans. Comput.* **28**, 807–810 (1979)
15. Huang, Q., Lloyd, E.: Cost constrained fixed job scheduling. In: Blundo, C., Laneve, C. (eds.) *Theoretical Computer Science. Lecture Notes in Computer Science*, vol. 2841, pp. 111–124. Springer, Berlin (2003)
16. Huo, Y., Leung, J.Y.T.: Parallel machine scheduling with nested processing set restrictions. *Eur. J. Oper. Res.* **204**(2), 229–236 (2010)

17. Kolen, A.W., Lenstra, J.K., Papadimitriou, C.H., Spieksma, F.C.: Interval scheduling: a survey. *Nav. Res. Logist. (NRL)* **54**(5), 530–543 (2007)
18. Kovalyov, M.Y., Ng, C., Cheng, T.E.: Fixed interval scheduling: models, applications, computational complexity and algorithms. *Eur. J. Oper. Res.* **178**(2), 331–342 (2007)
19. Krishnamoorthy, M., Ernst, A.: The personnel task scheduling problem. In: Yang, X., Teo, K., Caccetta, L. (eds.) *Optimization Methods and Applications, Applied Optimization*, vol. 52, pp. 343–368. Springer, US (2001)
20. Krishnamoorthy, M., Ernst, A., Baatar, D.: Algorithms for large scale shift minimisation personnel task scheduling problems. *Eur. J. Oper. Res.* **219**(1), 34–48 (2012)
21. Kroon, L.G., Salomon, M., Van Wassenhove, L.N.: Exact and approximation algorithms for the tactical fixed interval scheduling problem. *Oper. Res.* **45**(4), 624–638 (1997)
22. Kroon, L.G., Salomon, M., Wassenhove, L.N.V.: Exact and approximation algorithms for the operational fixed interval scheduling problem. *Eur. J. Oper. Res.* **82**(1), 190–205 (1995)
23. Lagodimos, A., Leopoulos, V.: Greedy heuristic algorithms for manpower shift planning. *Int. J. Prod. Econ.* **68**(1), 95–106 (2000)
24. Lapgue, T., Bellenguez-Morineau, O., Prot, D.: A constraint-based approach for the shift design personnel task scheduling problem with equity. *Comput. Oper. Res.* **40**(10), 2450–2465 (2013)
25. Leung, J.Y.T., Li, C.L.: Scheduling with processing set restrictions: a survey. *Int. J. Prod. Econ.* **116**(2), 251–262 (2008)
26. Lin, S.W., Ying, K.C.: Minimizing shifts for personnel task scheduling problems: a three-phase algorithm. *Eur. J. Oper. Res.* **237**(1), 323–334 (2014)
27. OR-Library: Problem data instances for ‘shift minimization personnel task scheduling’ in the OR library. <http://people.brunel.ac.uk/~mastjjb/jeb/orlib/ptaskinfo.html> (2013). Accessed 10 July 2013
28. PTSP-Library: Homepage of ptsp library. <https://sites.google.com/site/ptsplib/sdptspe/home> (2013). Accessed 12 July 2013
29. Rafaeli, D., Mahalel, D., Prashker, J.N.: Heuristic approach to task scheduling: weight and improve algorithms. *Int. J. Prod. Econ.* **29**(2), 175–186 (1993)
30. Rossi, A., Singh, A., Sevaux, M.: A metaheuristic for the fixed job scheduling problem under spread time constraints. *Comput. Oper. Res.* **37**(6), 1045–1054 (2010)
31. Santos, E., Jr., Zhong, X.: Genetic algorithms and reinforcement learning for the tactical fixed interval scheduling problem (2001)
32. Smet, P., Vanden Berghe, G.: A matheuristic approach to the shift minimisation personnel task scheduling problem. In: *Proceedings of the 9th International Conference on the Practice and Theory of Automated Timetabling* (2012)
33. Smet, P., Wauters, T., Mihaylov, M., Vanden Berghe, G.: The shift minimisation personnel task scheduling problem: a new hybrid approach and computational insights. Technical report, KAH0 - KU Leuven (2013)
34. Valls, V., Prez, A., Quintanilla, S.: A graph colouring model for assigning a heterogeneous workforce to a given schedule. *Eur. J. Oper. Res.* **90**(2), 285–302 (1996)
35. Vavasis, S., Ye, Y.: A primal-dual interior point method whose running time depends only on the constraint matrix. *Math. Program.* **74**(1), 79–120 (1996)
36. Wright, P., Bretthauer, K., Cote, M.: Reexamining the nurse scheduling problem: staffing ratios and nursing shortages. *Decis. Sci.* **37**(1), 39–70 (2006)
37. Zhou, S., Zhang, X., Chen, B., Van De Velde, S.: Tactical fixed job scheduling with spread-time constraints. *Comput. Oper. Res.* **47**, 53–60 (2014)

The Value of Flexible Road Designs Through Ecologically Sensitive Areas

Nicholas Davey, Simon Dunstall and Saman Halgamuge

Abstract Mining haul road traffic can have significant impacts on nearby animal populations that can threaten an entity's licence to operate. As operators have the ability to control heavy vehicle traffic flow through mining road networks, opportunities exist to reroute traffic away from more damaging roads in response to uncertain animal population dynamics. The presence of this flexibility in turn has a positive effect on the future value of proposed road designs. In this paper, we present an approach for evaluating the flexibility of controlling traffic flow in proposed road designs between two locations separated by an intervening species habitat. We do this by treating the design problem as a Real Options Valuation (Stochastic Optimal Control) problem solved using Least-Squares Monte Carlo. Here, the different control actions are the discrete traffic flow rates, and the uncertain-state variables are the animal populations at each location in the region of interest. Because the control chosen has a direct impact on the path of the uncertain variables, we use the technique of control randomisation in generating the Monte Carlo paths and computing the costs-to-go in the Real Options Valuation. In addition, we use a state-reduction parameter called Animals at Risk to reduce the dimensionality of the problem to improve tractability. In an example scenario, the addition of routing flexibility resulted in an increase in project value over the case without flexibility while maintaining the animal population above a critical threshold.

Keywords Real Options · Stochastic control · Haul road design · Road ecology · Control randomisation

N. Davey (✉)

The University of Melbourne, Parkville, Australia
e-mail: ndavey@student.unimelb.edu.au

S. Dunstall

CSIRO Data 61, Docklands, Australia
e-mail: Simon.Dunstall@data61.csiro.au

S. Halgamuge

The Australian National University, Canberra, Australia
e-mail: saman.halgamuge@anu.edu.au

© Springer International Publishing AG 2018

R. Sarker et al. (eds.), *Data and Decision Sciences in Action*,
Lecture Notes in Management and Industrial Engineering,
DOI 10.1007/978-3-319-55914-8_5

1 Introduction

In mining operations, haul roads are increasingly traversing ecologically sensitive areas [5]. Therefore, designers must consider their effects on surrounding animal populations when evaluating different route designs. If they do not build sustainable roads, the mine risks losing its social licence to operate [19]. However, road operations are not static and operators have the ability to control traffic flow over time in response to inherently uncertain animal population dynamics. The presence of this flexibility is an important factor in determining the trade-off between value and ecological impact of a road. In this paper, we present an approach for incorporating this flexibility into haul road design using Real Options Valuation (ROV) based on Least-Squares Monte Carlo [16] and Control Randomisation [11], while simulating animal movement patterns with an empirically derived movement and road mortality model [21].

Vehicle movements pose a significant threat to animal populations, resulting in habitat fragmentation, declines in reproduction rates and collisions of vehicles with wildlife [6]. These effects have been studied in great detail since the mid-1990s [9], showing that traffic volumes, distribution of traffic through the region and road routes, have a profound impact on species survival [6, 9, 18, 21, 25]. Comprehensive stochastic models based on empirical data, such as those in [20, 25] have been developed to help policy-makers understand the migration behaviours of animal species through two-dimensional regions so as to make better-informed planning decisions. Models such as the ones in [18, 21] have extended these approaches to quantify the effects of vehicle collisions on species mortality. To date, this research has only considered the case of fixed or steadily increasing traffic flows along mostly public roads. However, these models are readily applicable to mining haul roads where operators can also control traffic flow rates along roads so as to mitigate the damage caused by a particular design.

A powerful technique for evaluating this flexibility under uncertainty is Real Options Valuation (ROV), which falls under the umbrella of Stochastic Optimal Control (Dynamic Programming). The ROV technique values each decision to switch from one operating state to another in the same way as one would for American-styled financial options [17]. In such cases, the decision-maker has the right, but not the obligation, to exercise an option at any time leading up to a particular date depending on the prevailing stochastic factors and switching costs. This valuation approach has been shown to yield more realistic present values of decisions than the more common discounted cash flow methods (DCF) as the latter approach fails to properly account for the true behaviour of decision-makers in the presence of uncertainty [8, 17, 23]. This is because typical DCF approaches result in unrealistic assumptions about the manner in which decisions are actually made by essentially assuming that all future outcomes of a decision occur, even when the decision-maker has a choice to avoid unprofitable decisions in the future [17]. ROV, on the other hand, assumes that as new information becomes available regarding the uncer-

tain parameters, decision-makers are free to make the most optimal choice, thereby avoiding undesirable outcomes.

In mining contexts, ROV has typically been used to evaluate strategic-level decisions such as the flexibility of opening and closing a mine based on the prevailing commodity price using traditional computation approaches such as finite difference methods [2] and multinomial trees [17]. However, as ROV is based on dynamic programming, it is plagued by the ‘curse of dimensionality’ [22], whereby increases in computational complexity scale exponentially with increases in the size and number of problem dimensions. For realistic applications, this is troublesome as dimension numbers can be quite high [16]. To alleviate this, Longstaff and Schwartz popularised the technique of Least-Squares Monte Carlo (LSMC) [16], which simulates the stochastic parameters forward in time using multiple Monte Carlo paths to reduce the computational overhead while retaining an accurate approximation of the true value. This technique has gained popularity in both financial options pricing and real options valuation for its ability to incorporate multiple uncertainties and decisions [3, 7, 11–15, 22].

As useful as it has been, the LSMC approach has typically only been applied to situations with exogenous uncertainty such as opening and closing a mine subject to prevailing commodity prices. However, in many real-world scenarios, uncertainty can be highly dependent upon the decisions taken by operators [7, 11]. Building a haul road through an ecologically sensitive region with variable traffic flow rates is one such important case, where different traffic flow rates will result in different expected animal mortalities. To address this shortcoming, Kharroubi et al. [11] developed the technique of Control Randomisation (CR), which involves randomising the control decision taken at each time step when generating the Monte Carlo paths. Next, when the optimal costs-to-go are computed at each stage using backward induction, the forward paths are regenerated using the computed optimal controls [14].

In this paper, we propose a framework to value a mining haul road that passes through an ecologically sensitive region that contains a switchable set of discrete traffic flow rates. We do this by using the animal migration model of [21] to model uncertain animal movement and mortality while computing the value of the switching flexibility using Least-Squares Monte Carlo [3] and Control Randomisation [11, 14]. To combat the curse of dimensionality, we introduce a dimensionality-reduction parameter, *Animals at Risk* [4], to reduce the spatial dimensionality of the animal populations to a manageable number in order to improve computational tractability when computing ROV using LSMC and CR.

The paper is organised as follows. Section 2 outlines the formulation of the optimisation problem. Section 3 describes the framework for solving the problem while Sect. 4 provides some numerical results showing how the method performs. Finally, Sect. 5 concludes the paper and presents an agenda for future work.

2 Problem Formulation

We study the effect of flexible traffic flow rates on operating value for a set of alternative roads designed to connect two locations that are separated by an ecologically sensitive region. Traffic along the road must be optimally controlled such that the animal population within the region is maintained at or above a critical threshold (\mathcal{P}_{min}). The spatial distribution of these animals is modelled by discretising the region into N discrete animal patches. Flexibility is provided by the ability to reroute some or all of the traffic from the proposed route to an existing road that is costlier to operate but has no negative ecological impacts. The single-period value of operating the proposed road is therefore the cost savings of using it instead of the existing road.

For consistency, each road has the same discrete set of flow options: $\alpha \in \mathcal{A} = \{\alpha_1, \dots, \alpha_m\}$. Each year ($t \in [0, T]$), management has the choice to select one of these scenarios for the next period based on the overall animal population $\mathcal{P} = \sum_{i=1}^N p_i$ as well as their distribution throughout the study region, which is represented by the dimensionality-reduction parameter, *Animals at Risk*, η [4] (see Sect. 3.2). Each time the operating policy is changed from one state, a , to another, b , a switching cost may also be incurred ($K^{a \rightarrow b}$).

We apply the method of Real Options Valuation with endogenous uncertainty using the technique developed in [14], treating the populations in each patch as the stochastic factors. These populations are simulated through time using the Monte Carlo-based animal movement model of [21]. As this is a mining context, we could also treat the commodity prices, input prices (fuel, maintenance, etc.) and remaining reserve level as stochastic [14]. However, to reduce the number of uncertain dimensions and focus on the effects of animal movement alone, we have kept them constant in this work.

The objective of the decision process, therefore, is to *maximise the present value of expected future cash flows less the road construction costs* for each road in order to determine the most valuable road to build.

3 Methodology

The methodology is similar to the problem of opening, closing and abandoning a mine in [14] but applied to road design, which contains highly dimensional and endogenous uncertainty in the form of discrete animal populations. Therefore, we must first reduce the dimensionality of the endogenous uncertainty before implementing the LSMC approach with Control Randomisation. To achieve this, we use the underlying animal movement and mortality model of [21] (Sect. 3.1) that models the endogenous spatial uncertainty, to find the proportion of animals at risk of dying under each control in the current period, η . This dimensionality reduction is described in Sect. 3.2. The value η is then used within the ROV approach, which values the road given flexible operating states as described in Sect. 3.3.

3.1 Simulating Stochastic Animal Movement Model

The uncertain component of the model, which must be optimally controlled so as to produce the maximum possible profit while meeting the minimum population threshold, \mathcal{P}_{min} , is the animal population in each of the N habitat patches at time t , $\mathbf{p}_t = [p_{1,t}, \dots, p_{N,t}]'$. This is simulated for the horizon $t \in [0, T]$ with the model of [21], which incorporates many empirically tested species characteristics such as habitat preferences, ranging behaviour and crossing speeds. In this model, the probabilities of animals moving from each discrete habitat patch to every other patch are captured in a $N \times N$ transition matrix, \mathbf{TP} , where the rows correspond to the originating patches. Each patch transition in this matrix also has a corresponding survival probability, \mathbf{SP} , that is related to the number of road crossings and the traffic flow rate along the road [21]. These two matrices are used to update the population in each patch after via Eq. 1, where \odot indicates element-wise multiplication.

$$\mathbf{p}_t^\alpha = \{ [\mathbf{TP} \odot \mathbf{SP}^\alpha] \mathbf{p}_t \} \quad (1)$$

The population growth rate in the i th patch, r_i , is modelled using a logistic growth model (Eq. 2), where $g_i \sim N(g_\mu, g_\sigma)$ and ζ_i is the capacity of patch i . Finally, the populations at the next time step are given by Eq. 3, where ξ is a column vector. Clearly, as the survival probability is dependent on the traffic flow rate, the population in each habitat patch is an *endogenous* risk factor.

$$\xi_i = 1 + g \frac{\zeta_i - p_i}{\zeta_i} \quad (2)$$

$$\mathbf{p}_{t+1}^\alpha = \mathbf{p}_t^\alpha \odot \xi \quad (3)$$

3.2 Dimensionality Reduction

The full state space at time t includes the number of animals in each of the N habitat patches. To understand the spatial dynamics of the animals over time and therefore the impact of road traffic, a large value of N is required. However, a large number of states would render the problem intractable. On the other hand, using only a single variable such as the overall animal population for the entire region would hide the spatial dynamics captured by the animal movement model.

To overcome this, we introduce a state-reduction parameter called *Animals at Risk* [4] (Eq. 4), which measures the total number of animals expected to perish between the start and end of the current time step based on the traffic flow level chosen (α) (i.e. before accounting for population growth). It is readily obtained by running the model from [21] for one time period to find the proportion of animals expected to perish for the time period for the given flow rate.

$$\eta_t^\alpha = 1 - \frac{\sum_{i=1}^N p_{i,t}^\alpha}{\sum_{i=1}^N p_{i,t}} \quad (4)$$

In this manner, the state space reduces from N (the population in habitat patch) to 2: the overall population, $\mathcal{P}_t = \sum_{i=1}^N p_{i,t}$, t and the proportion of animals expected to perish in the current time period due to road traffic, η_t^α . In this manner, we do not lose the effects of spatial distribution on mortality rates.

If it is expected that the population after movement and mortality at time t (which we shall call the *adjusted population*, Eq. 5) is above the minimum threshold, then that control is viable. In financial parlance, this path is said to be *in-the-money* [14, 16]. If it is not, then the control is not able to be considered for the next time period.

$$\mathcal{P}_t^{adj} = \mathcal{P}_t \times [1 - \eta_t^\alpha] \quad (5)$$

3.3 Valuation of Flexibility

To value the road's flexibility, we incorporate the animal movement and mortality model described in Sect. 3.1 and the dimensionality-reduction technique of Sect. 3.2 into the model described in [14].

We first let $\theta_t = [\mathcal{P}_t, \eta_t, \alpha_t]$ be the state vector at time t . The future operating value of the road at time t is thus given by the Bellman value function in Eq. 6.

$$V(t, \theta) = \sup_{\alpha \in \mathcal{A}} \mathbb{E} \left\{ \int_t^T e^{-r(s-t)} \Pi(s, \mathcal{P}_s, \eta_s, \alpha_s) ds - \sum_{t \leq \tau_n \leq T} e^{-r(\tau_n-t)} K(\tau_n, \alpha_{\tau_n^-}, \alpha_{\tau_n}) | \theta_t = \theta \right\} \quad (6)$$

In this equation, $\Pi(s, \alpha_s)$ is the cash inflow at time s of running the road with traffic control $\alpha \in \mathcal{A}$; $K(\tau_n, \alpha_{\tau_n^-}, \alpha_{\tau_n})$ is the cost of switching from traffic control $\alpha_{\tau_n^-}$ to traffic control α_{τ_n} ; and r is the required rate of return. Using this formula at time $t = 0$, the objective of finding a road's value can be expressed mathematically as follows:

$$V(0, \theta_0) = \sup_{\alpha \in \mathcal{A}} \mathbb{E} \left\{ \int_0^T e^{-rs} \Pi_{\hat{\alpha}_s}(s, \mathcal{P}_s, \eta_s) ds - \sum_{0 \leq \tau_n \leq T} e^{-r\tau_n} K(\tau_n, \alpha_{\tau_n^-}, \alpha_{\tau_n}) | \theta_0 = \theta \right\} \quad (7)$$

where the optimal profits-to-go ($\Pi_{\hat{\alpha}_s}(s, \mathcal{P}_s)$) and the optimal control at each time step ($\hat{\alpha}_s$) are given by Eqs. 8 and 9, respectively.

$$\Pi_{\hat{\alpha}_s}(s, \mathcal{P}_s, \eta_s) = \sup_{\alpha \in \mathcal{A}} \{f(s, \mathcal{P}_s, \eta_s, \alpha_s) + \Phi_s(\mathcal{P}_s, \eta_s, \alpha_s)\} \quad (8)$$

$$\hat{\alpha}_s = \arg \sup_{\gamma \in \Gamma} \{\Pi_{\hat{\alpha}_s}(s, \mathcal{P}_s, \eta_s)\} \quad (9)$$

where $f(s, \mathcal{P}_s, \eta_s, \alpha_s)$ is the single-period profit at time s and $\Phi_s(\mathcal{P}_s, \eta_s, \alpha_s)$ is the conditional expectation at time s under control α_s .

Typically, Eq. 7 would be computed with the Longstaff and Schwartz algorithm [16]. This algorithm uses a Monte Carlo approach to simulate the exogenous uncertain parameters for each path. Next, it applies backward induction, whereby the expected optimal pay-off for the viable paths are regressed onto the predictors using a locally linear kernel [14] to compute the Φ 's for each control and hence find the optimal control at that stage. In the case of controlling a road through an ecologically sensitive area, the predictor is the adjusted population for each path \mathcal{P}_t^{adj} .

However, the uncertainty in \mathcal{P}_t^{adj} is endogenous. To account for this, we use the algorithm of [14], which applies the Control Randomisation technique of [11]. To do this, when the Monte Carlo paths are generated, the control action taken at each time step along each path is sampled from a dummy distribution. Furthermore, when backward induction is used to find the optimal controls and profits-to-go, the resulting optimal controls alter the Monte Carlo paths. Therefore, the paths and the corresponding optimal profits-to-go are recomputed from the current stage in the backward induction up to time T for each path using the previously computed values of Φ . A detailed description of this algorithm is provided in [14].

4 An Example

For illustration purposes, we consider a flat terrain as shown in Fig. 1 where two points are separated by an ecologically sensitive region. It should be noted that this region is stylised for the sake of demonstrating the method and is not a true-to-life representation. The road set is such that roads that cost more to operate should have smaller impacts on the animal species when computed using the model in [21] under full traffic flow rates for the entire design horizon, T (See Table 1). There are two operating states: a high flow rate of 150 journeys per hour along the proposed road and a lower impact scenario where all of the traffic is diverted along the lower impact road. Switching between these rates is used to maintain the animal population (with an initial population of 1000 animals that is initially at full capacity) above a critical threshold of $\mathcal{P}_{min} = 900$. It is assumed that there are no switching costs between these two states, although in reality this may not be the case. The inclusion of switching costs is considered beyond the scope of this paper.

The set of roads for consideration is provided in Table 1. Here, the end population under full flow is computed using the method outlined in [21] assuming the high flow traffic volume for the entire time horizon (i.e. $\alpha = \alpha_1 \forall t \in [0, T]$). Within this model,

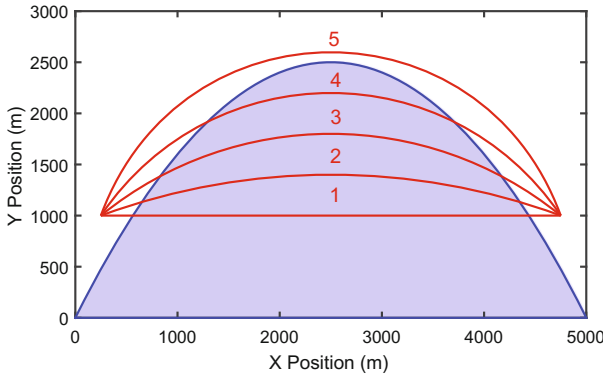


Fig. 1 Paths of candidate roads around habitat region

Table 1 Details of the five roads to be compared, listed in order of increasing ecological impact. Operating cost and benefit figures are in \$AUD, M per journey per hour per year. The remaining cost figures are in \$AUD, M

Road	Op. cost	Op. benefit	Full flow results		ROV
			End Pop.	Value	
1	0.334	0.114	474	209	67
2	0.342	0.107	523	196	71
3	0.362	0.086	625	158	75
4	0.395	0.054	827	98	81
5	0.438	0.010	1000	19	19

the animal ranging parameter (λ in [21]) is set to 5.0×10^{-4} , the average animal length is 0.7 m, the animal crossing speed is 10 km/hr and the average vehicle width is 7.5 m. The operating benefits per year per vehicle represent the savings of using the proposed road over an existing road that costs AUD 450,000 to operate per year. The project is run for 50 years, using a discount rate of 8%p.a. Finally, the animal population growth rate parameter is normally distributed ($g \sim N(1.4, 1.5)$ %p.a.) in each patch.

As column 5 in Table 1 shows, the present value of cost savings for the cheaper roads (1–4) is quite substantial when the full traffic flow is over the entire horizon. However, these roads are also far more damaging if operated in this manner, as shown in column 4. In contrast, the value of road 5, which is the only road that avoids the region and does not affect animal populations, is far lower. Furthermore, this is the only road that exceeds the minimum population of 900 animals when operated full time and would therefore be the only viable road in the absence of flexibility.

Using flexible traffic flows allows all roads to maintain the animal population above 900 for the design horizon. Using ROV, we find that the value of road 4 is the greatest, at \$81M. In fact, all four cheapest roads are more valuable than road 5. This

shows that having the flexibility on hand allows the operator to improve profits while preventing excessive damage to animal populations. This ensures that the mine does not risk losing its licence to operate.

Naturally, in a real-world application, operators would have access to more than just two flow states, which should further increase the values of the more damaging roads. Furthermore, there will also be uncertain macroeconomic factors that need to be taken into consideration. Most importantly, this work only considered a discrete set of five candidate roads that were created prior to valuation using ROV. For a truly optimal road route, the ROV approach will need to be incorporated into a global optimal road design algorithm. As such routines are often based on population-based optimisation schemes, the Real Options Valuation routine would have to be computed potentially thousands of times. This poses a severe tractability issue that could be addressed in future work by exploring the relationship between road path and the road's ROV.

5 Conclusion

This paper described an approach for valuing flexible traffic flow rates along haul roads built through ecologically sensitive regions using Least-Squares Monte Carlo with Control Randomisation. As the high-dimensionality of ecological dynamics can be a problem for stochastic control techniques such as ROV, a simple state-space reduction technique was introduced to reduce the number of dimensions (the population in discrete habitat patches) to just two uncertain variables: the overall population and the proportion of animals at risk of mortality. In a simple case study, the results show that flexibility can allow construction of cheaper roads without having animal populations fall below critical thresholds for managing local extinction risk. This work can be extended in the future by investigating the effect of more control levels as well its application to existing road network optimisation problems.

References

1. Bao, C., Mortazavi-Naeini, M., Northey, S., Tarnopolskaya, T., Monch, A., Zhu, Z.: Valuing flexible operating strategies in nickel production under uncertainty. In: MODSIM2013: 20th International Congress on Modelling and Simulation 16 (2013)
2. Brennan, M., Schwartz, E.: Evaluating natural resource investments. *J. Bus.* **58**, 135–157 (1985)
3. Chen, W., Tarnopolskaya, T., Langrené, N.: Switching surfaces for optimal natural resource extraction under uncertainty. In: 21st International Congress on Modelling and Simulation, pp. 1063–1069, Gold Coast (2015)
4. Davey, N., Dunstall, S., Halgamuge, S.: Optimal road design through ecologically sensitive areas considering animal migration dynamics. *Transp. Res. Part C Emerg. Technol.* **77**, 478–494 (2017). doi:[10.1016/j.trc.2017.02.016](https://doi.org/10.1016/j.trc.2017.02.016)

5. Duran, A., Rauch, J., Gaston, K.: Global spatial coincidence between protected areas and metal mining activities. *Biol. Conserv.* (2013). doi:[10.1016/j.biocon.2013.02.003](https://doi.org/10.1016/j.biocon.2013.02.003)
6. Fahrig, L., Rytwinski, T.: Effects of roads on animal abundance: an empirical review and synthesis. *Ecol. Soc.* **14**, 21–41 (2009)
7. Henry-Labordre, P.: The uncertain volatility model: a Monte Carlo approach. *J. Comput. Financ.* **14** (2011)
8. Hult, G., Craighead, C., Ketchen, D.: Risk uncertainty and supply chain decisions: a real options perspective. *Decis. Sci.* **41**, 435–458 (2010). doi:[10.1111/j.1540-5915.2010.00276.x](https://doi.org/10.1111/j.1540-5915.2010.00276.x)
9. Jaarsma, C.: Approaches for the planning of rural road networks according to sustainable land use planning. *Landsc. Urban Plan.* **39**, 47–54 (1997). doi:[10.1016/S0169-2046\(97\)00067-4](https://doi.org/10.1016/S0169-2046(97)00067-4)
10. Jong, C., Schonfeld, P.: An evolutionary model for simultaneously optimizing three-dimensional highway alignments. *Transp. Res. Part B Methodol.* **37**, 107–128 (2003). doi:[10.1016/S0191-2615\(01\)00047-9](https://doi.org/10.1016/S0191-2615(01)00047-9)
11. Kharroubi, I., Langren, N., Pham, H.: A numerical algorithm for fully nonlinear HJB equations: an approach by control randomization. *Monte Carlo Methods Appl.* **20**, 145–165 (2014)
12. Kitapbayev, Y., Moriarty, J., Mancarella, P.: Stochastic control and real options valuation of thermal storage-enabled demand response from flexible district energy systems. *Appl. Energy* **137**, 823–831 (2014). doi:[10.1016/j.apenergy.2014.07.019](https://doi.org/10.1016/j.apenergy.2014.07.019)
13. Kohler, M.: A review on regression-based Monte Carlo methods for pricing American options. *Recent Dev. Appl. Probab. Stat.* **1235** (2010). doi:[10.1007/978-3-7908-2598-5](https://doi.org/10.1007/978-3-7908-2598-5)
14. Langrené, N., Tarnopolskaya, T., Chen, W., Zhu, Z., Cooksey, M.: New regression monte carlo methods for high-dimensional real options problems in minerals industry. In: 21st International Congress on Modelling and Simulation, pp. 1077–1083. Gold Coast (2015)
15. Li, S., Knights, P.: Integration of real options into short-term mine planning and production scheduling. *Min. Sci. Technol.* **19**, 674–678 (2009). doi:[10.1016/S1674-5264\(09\)60125-3](https://doi.org/10.1016/S1674-5264(09)60125-3)
16. Longstaff, F., Schwartz, E.: Valuing American options by simulation: a simple least-squares approach. *Rev. Financ. Stud.* (2001). doi:[10.1093/rfs/14.1.113](https://doi.org/10.1093/rfs/14.1.113)
17. Miller, L., Park, C.: Decision making under uncertainty real options to the rescue? *Eng. Econ.* **47**, 105–150 (2002). doi:[10.1080/00137910208965029](https://doi.org/10.1080/00137910208965029)
18. Polak, T., Rhodes, J., Jones, D., Possingham, H.: Optimal planning for mitigating the impacts of roads on wildlife. *J. Appl. Ecol.* **51**, 726–734 (2014). doi:[10.1111/1365-2664.12243](https://doi.org/10.1111/1365-2664.12243)
19. Prno, J.: An analysis of factors leading to the establishment of a social license to operate in the mining industry. *Resour. Policy* (2013). doi:[10.1016/j.resourpol.2013.09.010](https://doi.org/10.1016/j.resourpol.2013.09.010)
20. Rhodes, J., McAlpine, C., Lunney, D., Possingham, H.: A spatially explicit habitat selection model incorporating home range behavior. *Ecology* **86**, 1199–1205 (2005). doi:[10.1890/04-0912](https://doi.org/10.1890/04-0912)
21. Rhodes, J., Lunney, D., Callaghan, J., McAlpine, C.: A few large roads or many small ones? How to accommodate growth in vehicle numbers to minimise impacts on wildlife. *PLoS One* (2014). doi:[10.1371/journal.pone.0091093](https://doi.org/10.1371/journal.pone.0091093)
22. Tarnopolskaya, T., Chen, W., Bao, C.: Switching boundaries for flexible management of natural resource investment under uncertainty. *IAENG Trans. Eng. Sci.* 1–14 (2015)
23. Trigeorgis, L.: Real options and interactions with financial flexibility. *Financ. Manag.* **22**, 202–224 (1993)
24. van Langevelde, F., Jaarsma, C.: Using traffic flow theory to model traffic mortality in mammals. *Landsc. Ecol.* **19**, 895–907 (2004). doi:[10.1007/s10980-005-0464-7](https://doi.org/10.1007/s10980-005-0464-7)
25. van Langevelde, F., Jaarsma, C.: Modeling the effect of traffic calming on local animal population persistence. *Ecol. Soc.* **14**(2), 39 (2009)

Local Cuts for 0–1 Multidimensional Knapsack Problems

Hanyu Gu

Abstract This paper investigates the local cuts approach for the multidimensional knapsack problem (MKP) which has more than one knapsack constraints. The implementation of the local cuts-based cutting plane algorithm is an extension of the exact knapsack separation scheme of Vasilyev et al. (J Glob Optim 1–24, [13]). Comparisons are made with the global lifted cover inequalities (GLCI) proposed in our recent paper in Computers & Operations Research (Gu, Comput Oper Res 71:82–89, [7]). Preliminary results show that the local cuts approach may be powerful for the MKP.

Keywords Multidimensional Knapsack Problem • Cutting plane • Local cuts

1 Introduction

The multidimensional knapsack problem (MKP) is a well-known strongly NP-hard combinatorial optimization problem which has been applied to various resource allocation-related practical problems [4]. Given m knapsacks with capacities b_i , $i = 1, \dots, m$, and n items contributing profits c_j , $j = 1, \dots, n$, the MKP maximizes the total profits of selected items under the knapsack capacity limitations. In MKP, an item j requires simultaneous resource consumption of a_{ij} units in the i th knapsack ($i = 1, \dots, m$, $j = 1, \dots, n$). The MKP can be formulated as an integer linear programming (ILP):

$$\text{(MKP)} \quad z^* = \max\{c^T x : Ax \leq b, x \in \{0, 1\}^n\} \quad (1)$$

where $c = [c_1, c_2, \dots, c_n]^T$ is the profit vector; $x = [x_1, x_2, \dots, x_n]^T$ is a vector of 0-1 decision variables; x_i is equal to 1 if item i is selected, otherwise 0; $A = [a_{ij}]$, $i = 1, 2, \dots, m$, $j = 1, 2, \dots, n$ is the resource consumption matrix; $b = [b_1, b_2, \dots, b_m]^T$

H. Gu (✉)

School of Mathematical and Physical Sciences, University of Technology Sydney,
15 Broadway, Ultimo, NSW 2007, Australia
e-mail: Hanyu.Gu@uts.edu.au

is the vector of knapsack capacities. For MKP, all parameters are assumed to be nonnegative integers.

A large amount of research efforts has been committed to MKP which is closely related to the classical knapsack problem (KP) [12]. In spite of the huge theoretical and computational progress in combinatorial optimization, MKP remains a challenging problem [5, 14]. It still takes many hours on a modern computer to obtain the best-known solutions for some of the well-known benchmark problems.

In this paper, we focus on the cutting plane approach which has found tremendous success in the commercial and open-source mixed integer programming (MIP) solvers. For knapsack problem, the cover-based valid inequalities are among the best-studied classes and have been shown useful, especially for solving difficult binary integer programming problems including the MKP [8, 11]. Recently, exact knapsack separation algorithms (EKSA) were proposed in [6, 11]. Although EKSA can produce stronger valid inequalities, they are more or less useless in the branch and cut paradigm due to much longer computation time. An efficient EKSA was implemented in [13] and was found useful for solving large instances of some classical MIP problems.

Recently, the global lifted cover inequalities (GLCI) [10] and its variants were proposed for MKP to take into account multiple knapsack constraints simultaneously when lifting the coefficients of a valid inequality. The face defined by GLCI may not be of higher dimensions than lifted cover inequalities (LCI) for MKP; however, computational results demonstrated that GLCI can be more effective in tightening the integrality gap, especially when the number of knapsack constraints increases. Furthermore, the computationally stronger GLCI can lead to improved performance of core-based heuristics [7]. This motivates the research in this paper to combine the power of exact separation and global lifting, which the authors' believe belongs to the local cuts paradigm which is very different from the traditional template paradigm [2].

This paper is organized as follows. We first describe the cutting plane algorithm based on the local cuts approach in Sect. 2. The details of the exact separation for the reduced problem is given in Sect. 3. The global lifting procedure is described in Sect. 4. Computational results are presented in Sect. 5. The conclusion is given in Sect. 6.

2 Cutting Plane Algorithm Based on Local Cuts

The cutting plane approach [15] can be used to strengthen the linear programming (LP) relaxation of MKP which is defined as

$$\text{(MKP-LP)} \quad \bar{z} = \max\{c^T x : Ax \leq b, x \in [0, 1]^n\} \quad (2)$$

MKP-LP is solved at each iteration of the cutting plane approach with additional constraints corresponding to the cuts generated from previous iterations. Assume

that an optimal continuous solution x^k is obtained at the k th iteration, an attempt will be made to generate a cut separating x^k from the convex hull of the MKP polytope. If cuts are successfully generated, they are added to MKP-LP and the process is repeated until some termination criteria are met. Since the separation algorithm can be time-consuming in practice, this process has to be terminated earlier without the exact description of the convex hull of the MKP polytope. In the local cuts approach, a reduced problem of MKP (RMKP) is created at each iteration which can be efficiently separated due to much lower dimension. A valid cut for the original problem can then be induced. The cutting plane algorithm based on local cuts (CPALC) is described as follows:

Algorithm 1: Cutting Plane Algorithm Based on Local Cuts (CPALC)

Input: MKP

Output: a set of valid inequalities for MKP

```

1  $k = 1$ ;
2 repeat
3   solve the cut strengthened MKP-LP with optimal solution  $x^k$ ;
4   if  $x^k$  is an integer solution then break;
5   generate the separation problem for the reduced MKP (RMKP) problem;
6   compute cuts for RMKP;
7   induce valid cuts for MKP to separate  $x^k$ ;
8   if no cut then break;
9   add cuts to MKP-LP;
10 until enough cuts or time limit reached;
11 return all the generated cuts;
```

The creation of the separation problem for RMKP is described in the next section. A cut for the original MKP can always be induced from a cut for RMKP through the global lifting procedure discussed in Sect. 4.

3 Exact Separation Algorithm for RMKP

Given x^k , the LP relation solution of MKP in CPALC, let $V^k = \{i | x_i^k = 1\}$, and $W^k = \{i | x_i^k = 0\}$. Denote $R^k = N \setminus (V^k \cup W^k) = \{r_1, r_2, \dots, r_p\}$, the RMKP is defined as

$$\begin{aligned}
 \text{RMKP} \quad \max \quad & z = \sum_{1 \leq j \leq p} c_{r_j} y_j \\
 \text{s. t.} \quad & \sum_{1 \leq j \leq p} a_{i r_j} y_j \leq \tilde{b}_i^k, \quad i = 1, \dots, m \\
 & y_j \in \{0, 1\}, \quad 1 \leq j \leq p
 \end{aligned}$$

with $\tilde{b}_i^k = b_i - \sum_{j \in V^k} a_{ij}$, $i = 1, \dots, m$.

The separation problem for RMKP is to separate y^k defined as $y_j^k = x_{r_j}^k, 1 \leq j \leq p$. The RMKP polytope has much lower dimension than that of MKP, which may be amenable to the exact separation approach. The exact separation formulation can take many different forms. Our implementation of the exact separation for RMKP is an adaptation of the source code of [13] for single knapsack problem and is based on the formulation below [13]:

$$\begin{aligned} \text{RMKP-S} \quad & \max_{\pi} \quad z = \pi^T y^k \\ \text{s. t.} \quad & h^T \pi \leq 1, \quad \forall h \in P \\ & \pi \in \Pi \end{aligned}$$

where $P \neq \emptyset$ is the feasible set of RMKP, and $\Pi \subset \mathcal{R}^p$ is a sufficiently large convex compact set containing the origin in its interior. Denote the optimal solution to RMKP-S by $\bar{\pi}^k$, then $y^T \bar{\pi}^k \leq 1$ is a valid cut separating y^k from the RMKP polytope if $y^{kT} \bar{\pi}^k > 1$. The nice property of RMKP-S is that the cut $y^T \bar{\pi}^k \leq 1$ also defines a facet of RMKP.

RMKP-S can be solved by row generation. At the l th iteration, π^l is solved as an optimal solution to

$$\begin{aligned} \text{RMKP-S}(l) \quad & \max_{\pi} \quad z = \pi^T y^k \\ \text{s. t.} \quad & h^T \pi \leq 1, \quad \forall h \in P^l \subset P \\ & \pi \in \Pi \end{aligned}$$

If $y^{kT} \pi^l \leq 1$, y^k is an interior point of the RMKP polytope since $y^{kT} \pi^l \geq y^T \bar{\pi}^k$. Otherwise, a new row may be obtained by solving

$$\begin{aligned} \text{Row-Gen} \quad & \max_h \quad z = h^T \pi^l \\ \text{s. t.} \quad & h \in P \end{aligned}$$

which has optimal objective value z^l and optimal solution h^l .

If $z^l \leq 1$, then $\bar{\pi}^k = \pi^l$ and $y^T \pi^l \leq 1$ is a cut for RMKP; otherwise, h^l can be added to P^l and a new row is generated for RMKP-S(l).

To avoid numerical errors, all coefficients in the cut need to be converted into integer. In [13], $\bar{\pi}^k$ is multiplied by a proper integer to make it an integer vector $\tilde{\pi}^k$ (within a tolerance of 10^{-5}). The separation procedure fails if no such integer multiplier can be found within the range $[1, \dots, 10^4]$. Then, the right-hand side can be calculated as

$$\pi_0^k = \max\{h^T \tilde{\pi}^k : h \in P\} \quad (3)$$

$y^T \tilde{\pi}^k \leq \pi_0^k$ is a valid cut for RMKP if it is violated by y^k .

If y_j can be fixed to 0 in RMKP, i.e., $\exists i \in [1, \dots, m], a_{i,r_j} > \tilde{b}_i^k$, we can generate a cut for RMKP in the form $y_j \leq 0$ instead of solving RMKP-S which will set $\tilde{\pi}_j^k$ to the largest value of π_j in Π .

The exact separation algorithm for RMKP (ESAR) can be described as follows:

Algorithm 2: Exact Separation Algorithm for RMKP (ESAR)

Input: RMKP, y^k

Output: a set of cuts separating y^k from RMKP polytope

- 1 compute $F = \{j \in [1, \dots, p] : a_{i,r_j} > \tilde{b}_i^k, \exists i \in [1, \dots, m]\}$;
 - 2 **if** $F \neq \emptyset$ **then**
 - 3 generate cuts $y_j \leq 0, \forall j \in F$;
 - 4 **return**
 - 5 $l = 1, P^l = \{e_1, \dots, e_p\}$ where e_i is the i th unit vector;
 - 6 **Loop**
 - 7 solve RMKP-S(l) with the optimal solution π^l ;
 - 8 **if** $y^{kT} \pi^l \leq 1$ **then return** // y^k is interior point
 - 9 solve Row-Gen with optimal value z^l and optimal solution h^l ;
 - 10 **if** $z^l \leq 1$ **then**
 - 11 $\tilde{\pi}^k = \pi^l$; // $y^T \pi^l \leq 1$ is a cut for RMKP
 - 12 **break**;
 - 13 $P^{l+1} = P^l \cup \{h^l\}, l = l + 1$;
 - 14 compute the integral inequality $y^T \tilde{\pi}^k \leq \pi_0^k$ according to (3);
 - 15 generate a cut $y^T \tilde{\pi}^k \leq \pi_0^k$ if it is violated by y^k ;
 - 16 **return**
-

4 Global Lifting Algorithm

The valid inequality for RMKP generated by ESAR can be sequentially lifted to become valid for MKP. We apply the same idea as for GLCI in [7] by considering all the constraints in MKP when lifting a variable.

Let K be the feasible set of MKP, and $S(V, W) = K \cap \{x \in \{0, 1\}^n | x_j = 0, \forall j \in W, x_j = 1, \forall j \in V\}$. A variable in V can be down-lifted according to the following proposition:

Proposition 1 *Given $\sum_{j \in N \setminus (V \cup W)} \pi_j x_j \leq \pi_0$ is valid for $S(V, W)$. For $i \in V$, if $S(V \setminus \{i\}, W) \neq \emptyset$, then $\gamma_i x_i + \sum_{j \in N \setminus (V \cup W)} \pi_j x_j \leq \pi_0 + \gamma_i$ is valid for $S(V \setminus \{i\}, W)$ for any $\gamma_i \geq \zeta - \pi_0$, where*

$$\zeta = \max \left\{ \sum_{j \in N \setminus (V \cup W)} \pi_j x_j | x_i = 0, x \in S(V \setminus \{i\}, W) \right\} \quad (4)$$

A variable in W can be up-lifted according to the following proposition:

Proposition 2 Given $\sum_{j \in N \setminus (V \cup W)} \pi_j x_j \leq \pi_0$ is valid for $S(V, W)$. For $i \in W$, if $S(V, W \setminus \{i\}) \neq \emptyset$, then $\alpha_i x_i + \sum_{j \in N \setminus (V \cup W)} \pi_j x_j \leq \pi_0$ is valid for $S(V, W \setminus \{i\})$ for any $\alpha_i \leq \pi_0 - \zeta$, where

$$\zeta = \max \left\{ \sum_{j \in N \setminus (V \cup W)} \pi_j x_j \mid x_i = 1, x \in S(V, W \setminus \{i\}) \right\} \quad (5)$$

For a cut generated by ESAR in the form of $y^T \tilde{\pi}^k \leq \pi_0^k$, we can have $\sum_{1 \leq j \leq p} x_{I_j}^T \hat{\pi}_{x_j}^k \leq \pi_0^k$ with $\hat{\pi}_{x_j} = \tilde{\pi}_j^k$, which is valid for $S(V^k, W^k)$. Then, the variables in V^k are down-lifted sequentially in the non-decreasing order of the reduced costs obtained when solving for x^k at step 3 of Algorithm 2. Finally, the variables in W^k are up-lifted sequentially in the non-increasing order of the reduced costs. To reduce computation time on lifting, we calculate the down-lifting coefficient according to $\gamma_i = \zeta_{LP} - \pi_0$, and the up-lifting coefficient according to $\alpha_i = \pi_0 - \zeta_{LP}$, where ζ_{LP} is the linear relaxation upper bound of ζ in (4) and (5).

Denote the valid inequality after lifting by $x^T \hat{\pi}^k \leq \hat{\pi}_0^k$, we have

$$x^{kT} \hat{\pi}^k - \hat{\pi}_0^k = y^{kT} \tilde{\pi}^k - \pi_0^k \quad (6)$$

Therefore, the cut for RMKP is also a cut for MKP after the lifting.

5 Computational Results

We first compare the exact knapsack separation algorithm (EKSA) of [13] with our implementations of GLCI and its variants [7]. Then, EKSA is compared with the local cuts (LC)-based separation algorithm CPALC implemented in this paper. All experiments are carried out on the comprehensive Cho test set in [1] and the widely used Chu and Beasley MKP test set in [3]. The algorithms presented in this paper were implemented in C++ and compiled with gcc 4.4. All tests were run on a computer with 2.3 GHz AMD CPU and Red Hat 4.4 operating system. We use CPLEX 12.5 to solve the LP and IP problems in CPALC with a time limit of 60 s and a limit on the maximum number of threads to 8. The number of cuts in CPALC is limited to 100 as for GLCI, but there is no limit for the number of cuts in EKSA which typically takes no more than a few seconds. In RMKP-S(l), Π is set to be $[-10^6, 10^6]^p$.

The Cho test set contains classes of randomly generated instances for each combination of $n \in \{50, 100, 250\}$ items and $m \in \{5, 10, 30\}$ constraints. Each class contains 30 instances. The Cho test set represents a much larger range of correlation values than the Chu and Beasley test set under the MKP structure and was created according to a well-designed comprehensive problem generation scheme [9]. The results of GLCIs and EKSA for the Cho test set are reported in Table 1. The columns in Table 1 are explained as follows: The first column $n.m$ represents the class of test cases where n is the number items and m is the number of knapsack constraints; the

Table 1 Comparison of GLCI and EKSA on the Cho test set [1]

$n.m$	z^*	\bar{z}	Δ_D	GSA-LP			GSA-IP			EKSA		
				I_C	N_c	T_v	I_C	N_c	T_v	I_C	N_c	T_v
50.5	1481.6	1494.6	0.91	51.9	13.0	–	49.5	12.9	0.2	78.6	43.7	0.1
50.10	1199.2	1214.9	1.32	50.2	19.9	0.1	53.4	22.6	1.3	66.2	53.7	0.1
50.25	968.7	984.6	1.63	46.9	29.8	0.2	49.6	37.9	7.4	57.2	63.8	0.4
100.5	2824.7	2830.8	0.22	41.8	9.2	–	44.2	10.0	0.5	83.3	62.6	0.2
100.10	2548.2	2558.8	0.42	33.3	15.8	–	33.5	18.6	1.9	59.9	76.1	0.4
100.25	1959.5	1972.3	0.64	34.1	23.6	0.2	37.4	30.0	8.2	50.7	82.5	0.6
250.5	7036.3	7040.2	0.05	41.2	9.1	0.1	42.3	9.3	0.7	74.8	90.6	0.7
250.10	6097.8	6103.2	0.09	26.2	12.5	0.2	28.2	13.2	2.2	58.7	107.6	0.9
250.25	4874.6	4882.7	0.16	22.0	17.7	0.6	23.9	22.2	17.5	38.6	113.1	1.3

second column reports the best-known objective value z^* found in the literature; the next column presents the objective value of the LP relaxation \bar{z} without additional cuts; the fourth column gives the relative integrality gap $\Delta_D = (\bar{z} - z^*) \times 100 / \bar{z}\%$; the next column reports the closed integrality gap in percentage; GSA-LP and GSA-IP are the different implementations of GLCI in [7]; and the next two columns present the total number of cuts generated by the corresponding separation scheme and the total CPU time spent T_v in seconds. The value of T_v is replaced with “–” if it is smaller than 0.1 s. For each class of test cases, the arithmetic mean of the 30 instances of the same class is reported. It can be seen that EKSA significantly outperforms GLCIs in terms of the percentage of integrality gap closed. The computation time of EKSA is only slightly higher than that of GSA-LP. The superiority of EKSA may be due to the weak interactions of the knapsack constraints in the instances.

The results of EKSA and CPALC for the Cho test set are reported in Table 2. The time for the exact separation in Sect. 3 and the time for the global lifting in Sect. 4 are

Table 2 Comparison of EKSA and CPALC on the Cho test set [1]

$n.m$	z^*	\bar{z}	Δ_D	EKSA			CPALC				
				I_C	N_c	T_v	I_C	N_c	T_v	T_c	T_l
50.5	1481.6	1494.6	0.91	78.6	43.7	0.1	100.0	48.2	11.7	11.5	0.1
50.10	1199.2	1214.9	1.32	66.2	53.7	0.1	100.0	55.6	18.3	18.2	0.1
50.25	968.7	984.6	1.63	57.2	63.8	0.4	98.7	70.9	69.6	69.3	0.3
100.5	2824.7	2830.8	0.22	83.3	62.6	0.2	100.0	64.1	13.4	12.6	0.8
100.10	2548.2	2558.8	0.42	59.9	76.1	0.4	92.8	80.8	61.0	60.1	0.9
100.25	1959.5	1972.3	0.64	50.7	82.5	0.6	86.4	88.7	125.9	124.5	1.5
250.5	7036.3	7040.2	0.05	74.8	90.6	0.7	92.8	82.4	41.8	38.1	3.7
250.10	6097.8	6103.2	0.09	58.7	107.6	0.9	84.4	95.0	64.3	60.4	3.9
250.25	4874.6	4882.7	0.16	38.6	113.1	1.3	64.6	101.0	176.7	170.0	6.7

Table 3 Comparison of GLCI, EKSA, and CPALC on 100-item instances from Chu and Beasley test set [3]

m, α	GSA-LP			GSA-IP			EKSA			CPALC		
	I_C	N_c	T_v	I_C	N_c	T_v	I_C	N_c	T_v	I_C	N_c	T_v
5. 25	6.99	15.8	–	6.80	16.3	0.4	19.18	119.5	1.6	41.85	101	239.5
5. 50	6.11	13	–	6.38	14.4	0.2	22.65	122.6	2.7	44.54	101	256.8
5. 75	6.50	12.7	–	7.46	12.7	0.2	23.52	121.4	3.7	51.33	101	241.1
10. 25	6.49	19	–	8.78	37.3	9.1	5.9	100.5	1.9	24.88	76.6	754.4
10. 50	6.96	21.8	–	10.28	30	4.5	7.83	120.7	3.7	28.06	80	1070.1
10. 75	4.18	13.2	–	5.07	14.8	2	7.62	97.5	3.5	32.15	79.2	908.4
30. 25	2.74	15.5	1.1	6.49	73.1	269.9	0.22	12.3	1.6	6.17	10.5	645.4
30. 50	5.30	33.5	2.3	7.79	90.5	233.1	0.55	38.4	2.8	5.89	8.4	323.7
30. 75	4.84	28.4	2.5	11.26	86.7	230.5	0.63	37	2.9	11.09	15.8	1286.8

reported as T_e and T_l in seconds. It can be seen that CPALC significantly outperforms EKSA in terms of closed integrality gap. The computation time of CPALC is much higher than that of EKSA. The global lifting is very efficient in terms of computation time. EKSA failed to close integrality gap on many instances even without the limit on the number of cuts. CPALC can always separate the LP solution which is consistent with the theory; however, the convergence can be slow on large instances with more constraints.

The Chu and Beasley test set contains a total of 270 instances randomly generated for 27 classes which are combinations of the number of items $n \in \{100, 250, 500\}$, the number of knapsack constraints $m \in \{5, 10, 25\}$, and knapsack capacity tightness ratios $\alpha \in \{0.25, 0.5, 0.75\}$. The results for the Chu and Beasley test set are reported in Table 3 for test cases with 100 items. For each class of test cases, the arithmetic mean of the 10 instances of the same class is reported. For cases with five constraints, EKSA closed much higher integrity gaps than GLCIs with marginally longer computation time. However, GLCIs perform significantly better than EKSA when $m = 30$. The reason could be that the intersection of single knapsack polytopes is not a good approximation of the MKP polytope as the number of constraints increases. The exact separation procedure of CPALC failed on many cases when $m = 10$ and $m = 30$ due to the difficulty to make integral the cutting plane obtained from RMKP-S(l). However, CPALC achieved similar amount of closed integrality gaps with many fewer cuts when compared with GSA-IP, which demonstrated the superior strength of the exact separation procedure for MKP.

6 Conclusion

The local cuts approach was implemented for the 0–1 multidimensional knapsack problem. Based on LP solution of MKP, a reduced separation problem is solved exactly with the row generation algorithm. The valid inequality for the reduced MKP

problem is then globally lifted to the original MKP problem. Computational experiments are carried out on a comprehensive set of MKP instances which demonstrate the superiority of the local cuts approach in terms of closed integrity gap. Further research is needed to reduce the computation time and investigate the possibility to combine the local cuts approach with a branch and bound algorithm or other meta-heuristics.

References

1. Cho, Y.K., Moore, J.T., Hill, R.R., Reilly, C.H.: Exploiting empirical knowledge for bi-dimensional knapsack problem heuristics. *Int. J. Ind. Syst. Eng.* **3**(5), 530–548 (2008)
2. Chvátal, V., Cook, W., Espinoza, D.: Local cuts for mixed-integer programming. *Math. Program. Comput.* **5**(2), 171–200 (2013). doi:[10.1007/s12532-013-0052-9](https://doi.org/10.1007/s12532-013-0052-9)
3. Chu, P.C., Beasley, J.E.: A genetic algorithm for the multidimensional knapsack problem. *J. Heuristics* **4**(1), 63–86 (1998)
4. Fréville, A.: The multidimensional 0–1 knapsack problem: an overview. *Eur. J. Oper. Res.* **155**(1), 1–21 (2004)
5. Fréville, A., Hanafi, S.: The multidimensional 0–1 knapsack problem—bounds and computational aspects. *Ann. Oper. Res.* **139**(1), 195–227 (2005)
6. Fukasawa, R., Goycoolea, M.: On the exact separation of mixed integer knapsack cuts. *Math. Program.* **128**(1), 19–41 (2011). doi:[10.1007/s10107-009-0284-7](https://doi.org/10.1007/s10107-009-0284-7)
7. Gu, H.: Improving problem reduction for 0–1 multidimensional knapsack problems with valid inequalities. *Comput. Oper. Res.* **71**(C), 82–89 (2016). doi:[10.1016/j.cor.2016.01.013](https://doi.org/10.1016/j.cor.2016.01.013)
8. Gu, Z., Nemhauser, G.L., Savelsbergh, M.W.P.: Lifted cover inequalities for 0–1 integer programs: computation. *INFORMS J. Comput.* **10**(4), 427–437 (1998)
9. Hill, R.R., Moore, J.T., Hiremath, C., Cho, Y.K.: Test problem generation of binary knapsack problem variants and the implications of their use. *Int. J. Oper. Quant. Manag.* **18**(2), 105–128 (2011)
10. Kaparis, K., Letchford, A.N.: Local and global lifted cover inequalities for the 0–1 multidimensional knapsack problem. *Eur. J. Oper. Res.* **186**(1), 91–103 (2008)
11. Kaparis, K., Letchford, A.N.: Separation algorithms for 0–1 knapsack polytopes. *Math. Program.* **124**(1–2), 69–91 (2010). doi:[10.1007/s10107-010-0359-5](https://doi.org/10.1007/s10107-010-0359-5)
12. Kellerer, H., Pferschy, U., Pisinger, D.: *Knapsack Problems*. Springer (2004)
13. Vasilyev, I., Boccia, M., Hanafi, S.: An implementation of exact knapsack separation. *J. Glob. Optim.* 1–24 (2015). doi:[10.1007/s10898-015-0294-3](https://doi.org/10.1007/s10898-015-0294-3)
14. Wilbaut, C., Hanafi, S., Salhi, S.: A survey of effective heuristics and their application to a variety of knapsack problems. *IMA J. Manag. Math.* **19**(3), 227–244 (2008)
15. Wolsey, L.A., Nemhauser, G.L.: *Integer and Combinatorial Optimization*. Wiley Series in Discrete Mathematics and Optimization. Wiley (1999)

An Exact Algorithm for the Heterogeneous Fleet Vehicle Routing Problem with Time Windows and Three-Dimensional Loading Constraints

Vicky Mak-Hau, I. Moser and Aldeida Aleti

Abstract One of our industry partners distributes a multitude of orders of fibre boards all over each of the Australian capital cities, a problem that has been formalised as the Heterogeneous Fleet Vehicle Routing Problem with Time Windows and Three-Dimensional Loading Constraints (3L-HFVRPTW). The fleet consists of two types of trucks with flat loading surfaces and slots for spacers that allow a subdivision into stacks of different sizes. A customer's delivery can be positioned on more than one partition, but the deliveries have to be loaded in a strict LIFO order. Optimising the truck loads beyond the 75% that can be achieved manually provides value to the company because the deliveries are generally last-minute orders and the customers depend on the deliveries for their contract work on refurbishments. This paper presents an exact integer linear programming model that serves two purposes: (1) providing exact solutions for problems of a modest size as a basis for comparing the quality of heuristic solution methodologies, and (2) for further exploration of various relaxations, stack generation, and decomposition strategies that are based on the ILP model. We solved a few real-life instances by obtaining the exact optimal solution using CPLEX 12.61, whereas previously, the problem was solved manually by staff members of the furniture company.

Keywords Delivery truck loading • Routing • Integer Programming

V. Mak-Hau (✉)

School of Information Technology, Deakin University, Waurn Ponds,
Geelong, Australia
e-mail: vicky.mak@deakin.edu.au

I. Moser

Department of Computer Science and Software Engineering,
Swinburne University of Technology, Melbourne, Australia
e-mail: imoser@swin.edu.au

A. Aleti

Faculty of Information Technology, Monash University, Caulfield, Australia
e-mail: aldeida.aleti@monash.edu

© Springer International Publishing AG 2018

R. Sarker et al. (eds.), *Data and Decision Sciences in Action*,
Lecture Notes in Management and Industrial Engineering,
DOI 10.1007/978-3-319-55914-8_7

1 Introduction

Our Australian industry partner manufactures and distributes particle boards, medium density fibre boards and high-pressure laminates. These stock keeping units (SKUs) exist in many colours and sizes and are used as building material for doors, kitchen cabinets, etc. The company has a distribution centre (DC) in each of the major Australian cities (Melbourne, Adelaide, Brisbane). This research captures the distribution problem faced by the Melbourne DC (MDC).

The MDC is equipped with two types of custom-made delivery trucks. There are eight 8-ton trucks, each with a loading area with a width of 2480 mm, a height of 2200 mm and a length of 6530 mm; and nine 12-ton trucks with same measurements except for the length: which is 7600 mm. A delivery truck can be configured into different *layouts*. Each layout is a way to divide the truck floor into rectangular *stacks* (or, *partitions*) of different sizes. In theory, there may be exponentially many ways to configure the layout of a truck. In practice, the majority of boards delivered have four different widths and two different lengths, which leads to subdivisions into two, three or four stacks.

Customer orders typically include different types of boards which may be of a slightly different size. The number of boards per type is typically small, in the range 1–10, but can be 100 boards or more. There are SKUs of all sizes, but typically, the widths are 1200, 1500, 1800 or 2400 mm and the length 2400 or 3600 mm. All boards of the same size, regardless of type, are bundled into a pack to be delivered to the customer. A pack may contain more than one size of board, with the larger boards always below. If the sizes are too diverse, several packs may have to be created with supports and cover sheets and then added in LIFO order to a suitable stack on the truck.

Larger boards can be placed on smaller boards if the overhang is no larger than one-third of the length or width of the smaller board. The number of packs has to be minimised to shorten the time needed for uploading. The load has to be balanced back-to-front with the proportion of total weight of goods loaded in the front section over the back section of a truck must be around 60% over 40%, and the ratio of total weight of goods loaded on the left side over the right side of a truck can be no more than 7:3 and no less than 3:7.

Customers make their orders by 4 pm, after which the deliveries are planned and the trucks loaded for the next day. Ideally, the company would not have to hire external delivery capacity, although this could not always be avoided in the past. Truck drivers must not work more than 10 h a day. If they return to the MDC in time, they can take another load and service another route if they can do so without exceeding their working hours. Some customers are available during certain parts of the day, leading to partial time windows.

We have investigated two different objective functions, total distance/time travelled and arrival time of the last truck. Melbourne traffic is heavy on certain roads and fluctuates greatly during the day, and hence, distances/times do not reflect the problem accurately. The assumption of minimising total distance/time is a simplification made for our first formulation.

2 Literature Review

The vehicle routing problem (VRP) has been studied extensively in different forms and with various constraints, such as orientation [4, 5, 23], cargo stability [4, 5, 23, 24], load bearing [4, 5, 19], weight limit [4, 5] and time windows [11]. Little work has been done on split deliveries [5] and specific pick up and delivery points [24]. The objective is usually defined as minimising the number of vehicles, or the total distance given a fixed number of vehicles [7, 13, 17]. The Capacitated Vehicle Routing Problem (CVRP) [21] is NP-hard, and it is often solved to acceptable quality using heuristics or metaheuristics. Examples are variable neighbourhood search [7], particle swarm optimisation [13], adaptive evolutionary approach [3], large neighbourhood search [9] and artificial bee colony [18].

The work by Baldacci et al. [2] is one of the successful applications of exact algorithms to CVRP. The method extends the TSP model introduced by Finke et al. [6], which is based on two-index flow formulation and uses a branch and cut algorithm with only rounded capacity inequalities. Recently, Rivera et al. [15] introduced a mathematical formulation and exact algorithm for the multitrip cumulative capacitated single-vehicle routing problem. The problem is inspired by disaster logistics, where a single vehicle can perform successive trips to serve a set of affected sites and minimise an emergency criterion, such as the sum of arrival times. The most sophisticated exact algorithm known today is able to solve problems with up to 135 customer drop-offs [8].

The integrated problem of CVRP and three-dimensional load construction (3D-CVRP) has only been considered by researchers very recently. One of the first examples is the work by Moura and Oliveira [14], which combines Vehicle Routing Problem with Time Windows and the Container Loading Problem using two different resolution methods: a sequential and a hierarchical approach. Wei et al. [22] model the problem with a heterogeneous fleet and use an Adaptive Variable Neighbourhood Search. The objective is to serve all customers by selecting a set of vehicles such that the total transportation cost is minimised.

All approaches to 3D-CVRP known to date use non-exact methods. Junqueira and Morabito [10] propose algorithms based on the combination of classical heuristics from vehicle routing and loading literatures, and two metaheuristics. Many works include a local search procedure; the most sophisticated methods use a combination of relocations of orders within and between routes, as well as swaps within and between routes [4, 20].

The heterogeneous fleet 3D-CVRP with time windows introduced by Pace et al. [16] is the closest example to our work. The paper proposes a specialised loading heuristic and uses a Simulated Annealing algorithm and Iterated Local Search for the routing phase. As far as we aware, thus far there is no exact methods or models. The major contribution of our paper is the introduction of a MILP model of the heterogeneous fleet 3D-CVRP with time windows and solves the problem with exact methods for the first time. In addition, unlike previous research in 2D/3D-CVRP, which solve the routing and loading problems independently and sequentially, our approach solves the two problems simultaneously.

3 A Mathematical Description of the Problem

We first define the notation we use in this section. Let:

- N be the index set of vertices with 0 denoting the depot and $N' = N \setminus \{0\}$ the set of customers;
- K be the index set of sheet types
- D_j^k the demand of customer j for type k sheets;
- \mathcal{P}_j be the index set of all feasible packs for customer j ;
- $\eta_{p,j}^k$ be the number of type k boards in pack p of customer j ;
- $h_{p,j}$ be the height of pack p of customer j ;
- Λ be the index set of all trucks;
- H_ν be the height of truck $\nu \in \Lambda$;
- \mathcal{L}_ν be the index set of all possible layouts for truck $\nu \in \Lambda$, where each layout is a 2D configuration associated with a set of partitions;
- Π_ℓ be the set of all partitions within a particular layout $\ell \in \mathcal{L}_\nu$ for Truck $\nu \in \Lambda$, where each partition is characterised by a length and a width;
- $\tau_{p,j}^L$ the length of the longest board in pack p of customer j ;
- $\tau_{p,j}^W$ the width of the widest board of pack p of customer j ;
- $\beta_{p,j}^L$ the length of the shortest board of pack p of customer j ;
- $\beta_{p,j}^W$ the width of the narrowest board of pack p of customer j ;
- $\omega_{p,j}$ the weight of pack p of customer j ;
- Δ_1 be the tolerance of proportion of total weight of goods in front section over the back section of the truck;
- \mathcal{F}_ν^ℓ and \mathcal{B}_ν^ℓ be the index sets of all partitions in the front and back in layout $\ell \in \mathcal{L}_\nu$ of truck ν ;
- \mathcal{C}_ν^ℓ and \mathcal{D}_ν^ℓ be the index sets of all partitions in the left and right in layout $\ell \in \mathcal{L}_\nu$ of truck ν .

We define the following decision variables. Let:

- $x_{p,j,\nu}^{\ell,\pi} \in \{0, 1\}$ be a decision variable with $x_{p,j,\nu}^{\ell,\pi} = 1$ if Pack p of Customer j is placed in Partition $\pi \in \Pi_\ell$ of Layout $\ell \in \mathcal{L}_\nu$ for Vehicle ν ;
- $\phi_j^\nu \in \{0, 1\}$ be a decision variable with $\phi_j^\nu = 1$ if Customer j is served by Vehicle ν ;
- $y_{j,\nu}^\pi \in \{0, 1\}$ be a decision variable with $y_{j,\nu}^\pi = 1$ if Customer j has packs in Partition $\pi \in \Pi^*$ for Vehicle ν , for $\Pi^* = \{1, \dots, \max_{\ell \in \mathcal{L}} \{|\Pi_\ell|\}\}$, and 0 otherwise;
- $t_j^\nu \geq 0$ be a decision variable that indicates the time customer j is visited by truck ν ;
- $\xi_{\ell,\nu} \in \{0, 1\}$ be a decision variable with $\xi_{\ell,\nu} = 1$ indicating layout ℓ is used for ν ;
- $z_{i,j}^\nu \in \{0, 1\}$ be a decision variable with $z_{i,j}^\nu = 1$ indicating Customer i is visited immediately before Customer j in the route of Vehicle ν , and 0 otherwise;
- $\Omega_{i,j}^\nu \in \{0, 1\}$ be a decision variable with $\Omega_{i,j}^\nu = 1$ indicating Customer i precedes Customer j in the route of Vehicle ν , and 0 otherwise.

- $\psi_{i,j,v}^\pi \in \{0, 1\}$ be a decision variable with $\psi_{i,j,v}^\pi = 1$ if Customer i precedes Customer j in Partition $\pi \in \Pi^*$ of Vehicle v , and 0 otherwise;
- $\Theta_{i,j,v}^\pi \in \{0, 1\}$ be a decision variable with $\Theta_{i,j,v}^\pi = 1$ indicating customer i 's pack is immediately above Customer j 's pack in Partition $\pi \in \Pi^*$ of truck v ;
- $\gamma_{ikj}^\pi \in \{0, 1\}$ be a decision variable used in logic constraints, explained in (19)–(22).

Model 1 *A Polynomial-sized Mixed-Integer Linear Programming Model*

$$\min \sum_{v \in \Lambda} \sum_{i \in N'} \sum_{j \in N' : j \neq i} c_{ij} z_{ij}^v \quad (1)$$

$$\text{s.t.} \quad \sum_{\ell \in \mathcal{L}_v} \xi_{\ell,v} = 1, \quad \forall v \in \Lambda \quad (2)$$

$$x_{p,j,v}^{\ell,\pi} \leq \xi_{\ell,v}, \quad \forall p \in \mathcal{P}_j, j \in N', \pi \in \Pi_\ell, \ell \in \mathcal{L}, v \in \Lambda \quad (3)$$

$$\sum_{p \in \mathcal{P}_j} x_{p,j,v}^{\ell,\pi} \leq \phi_j^v, \quad \forall j \in N', \pi \in \Pi_\ell, \forall \ell \in \mathcal{L}, \forall v \in \Lambda \quad (4)$$

$$\sum_{j \in N'} \sum_{p \in \mathcal{P}_j} h_{p,j} x_{p,j,v}^{\ell,\pi} \leq H_v, \quad \forall \pi \in \Pi_\ell, \ell \in \mathcal{L}, v \in \Lambda \quad (5)$$

$$\sum_{v \in \Lambda} \sum_{\ell \in \mathcal{L}} \sum_{\pi \in \Pi_\ell} \sum_{p \in \mathcal{P}_j} n_{p,j}^k x_{p,j,v}^{\ell,\pi} = D_j^k, \quad \forall k \in K, \forall j \in N' \quad (6)$$

$$\sum_{v \in \Lambda} \phi_j^v = 1, \quad \forall j \in N' \quad (7)$$

$$\sum_{j \in N} z_{ij}^v = \sum_{j \in N} z_{ji}^v = \phi_i^v, \quad \forall i \in N', v \in \Lambda \quad (8)$$

$$2(z_{ij}^v + z_{ji}^v) \leq \phi_i^v + \phi_j^v, \quad \forall i \neq j \in N', v \in \Lambda \quad (9)$$

$$\sum_{j \in N'} z_{0j}^v = \sum_{j \in N'} z_{j,0}^v = 1, \quad \forall v \in \Lambda \quad (10)$$

$$t_i^v + 1 - t_j^v \leq |N'| (1 - z_{ij}^v), \quad \forall i, j \in N' \ i \neq j, v \in \Lambda \quad (11)$$

$$t_j^v - t_i^v \leq (|N'| - 1) \Omega_{ij}^v, \quad \forall i, j \in N' \ i \neq j, v \in \Lambda \quad (12)$$

$$\Omega_{ij}^v + \Omega_{ji}^v \leq 1, \quad \forall i, j \in N' \ i \neq j, v \in \Lambda \quad (13)$$

$$\sum_{\ell \in \mathcal{L}} \sum_{p \in \mathcal{P}_i} x_{p,i,v}^{\ell,\pi} = y_{i,v}^\pi, \quad \forall i \in N', \pi \in \Pi^*, v \in \Lambda \quad (14)$$

$$3\psi_{i,j,v}^\pi \leq \Omega_{ij}^v + y_{i,v}^\pi + y_{j,v}^\pi, \quad \forall i, j \in N', i \neq j, \pi \in \Pi^*, v \in \Lambda \quad (15)$$

$$\Omega_{ij}^v + y_{i,v}^\pi + y_{j,v}^\pi \leq \psi_{i,j,v}^\pi + 2, \quad \forall i, j \in N', i \neq j, \pi \in \Pi^*, v \in \Lambda \quad (16)$$

The first set of constraints are vehicle/layout/partition and related logic constraints. Constraints (2) ensure that exactly one layout is used in each truck. Constraint (3) is a logic constraint to ensure that if a layout, ℓ , is not selected, then no allocation with respect to Layout ℓ will be made and that holds for all vehicles. Constraint (4) ensures that no more than one pack from a customer will be allocated to a partition in each vehicle. The rationale is that if two distinct packs are loaded for the same customer in a partition, they can be combined into one. Constraint (5) guarantees that the height of the goods in each partition of each truck will not exceed the height of a truck. The demand of a customer for each type of board is guaranteed to be satisfied by constraint (6).

The next set of constraints are to determine the vehicle routes. Each customer will be visited by exactly one vehicle (7). The in- and out-degree of a customer under a particular vehicle is either 0 or 1 and is logically determined whether the customer is visited by the vehicle (8). Constraint (9) enforces that Customer i can only be visited immediately before or after Customer j only when both of them are visited by the same vehicle. The in-degree and out-degree for each vehicle at the depot are exactly one, and hence, we have (10). Finally, to eliminate subtours that do not involve the depot, we use the classic Miller-Tucker-Zemlin [12] constraint (11) by using a variable that represents the time stamp when a customer is visited, and the same constraint infers the travel route of each vehicle. From the travel route of a vehicle, we are able to deduce the precedence relations of the customers for each vehicle, and these are achieved by constraints (12)–(14).

The next set of constraints are logic constraints that copy the precedence relations of the general route for each vehicle into each partition, but only for customers who have packs in that partition. We use a simple binary variable $y_{i,v}^\pi$ to capture whether a customer has a pack in Partition π of Vehicle v (see 14). If Customer i precedes Customer j in the route of vehicle v (even not immediately), and both customers have packs in the same partition of the same truck, the precedence relation must be preserved. This can be achieved by constraints (15) and (16), and such a requirement is needed for the size constraints which we will discuss later. Even though there are many variables and constraints, the largest set of variables $x_{p,j,v}^{\ell,\pi}$ contains at most $\tilde{\mathcal{L}}\tilde{\Pi}\tilde{\mathcal{P}}|N'| |A|$ variables, for $\tilde{\mathcal{L}} = \max_{v \in A} \{\mathcal{L}_v\}$; $\tilde{\Pi} = \max_{\ell \in \mathcal{L}_v, v \in A} \{\Pi_\ell\}$ and $\tilde{\mathcal{P}} = \max_{j \in N'} P_j$. A similar deduction can be made for the largest set of constraints. Hence, the MILP is polynomial in size.

Time Windows Constraint: If a time window exists for a customer, with s_j the earliest possible arrival time at customer j , and f_j the latest possible arrival time, we can add the following constraint

$$s_j \phi_j^v \leq t_j^v \leq f_j \phi_j^v, \quad \forall j \in N', \forall v \in A \quad (17)$$

Minimising the Latest Return Time: Should one wish to minimise the latest return time of all vehicles (which in theory will promote the distribution of the assignments more evenly, and shorten the total work time of truck drivers), one can replace the objective function by $\min T$ and add the following constraint:

$$\sum_{i \in N'} \sum_{j \in N': j \neq i} c_{ij} z_{ij}^v \leq T, \quad \forall v \in A \quad (18)$$

Preserving the Route in Partitions: Should the exact sequence in each partition for each vehicle be required, they can be deduced by using the following constraints. If i precedes j , and there exists a customer k such that i precedes k and k precedes j in Partition π of Vehicle v , we set $\gamma_{ikj}^{\pi,v}$ to 1, otherwise we set it to 0 (see 19 and 20).

If there does not exist such a vertex k , (21) sets $\Theta_{ij}^{\pi,v}$ to 1, otherwise it is set to 0. So $\Theta_{ij}^{\pi,v}$ preserves the general vehicle route sequence for each partition for only customers that have packs in the partition.

$$2\gamma_{ikj}^{\pi,v} \leq \psi_{i,k,v}^{\pi} + \psi_{k,j,v}^{\pi}, \quad \forall i, k, j \in N, i \neq k \neq j, v \in \Lambda \quad (19)$$

$$\psi_{i,k,v}^{\pi} + \psi_{k,j,v}^{\pi} \leq \gamma_{ikj}^{\pi,v} + 1, \quad \forall i, k, j \in N, i \neq k \neq j, v \in \Lambda \quad (20)$$

$$\psi_{i,j,v}^{\pi} - \sum_k \gamma_{ikj}^{\pi,v} \leq \Theta_{ij}^{\pi,v}, \quad \forall i, j, k \in N', i \neq j \neq k, \pi \in \Pi^*, v \in \Lambda \quad (21)$$

$$\sum_k \gamma_{ikj}^{\pi,v} - \psi_{i,j,v}^{\pi} + 1 \leq (|N'| - 1)(1 - \Theta_{ij}^{\pi,v}), \quad \forall i, j, k \in N', i \neq j \neq k, \pi \in \Pi^*, v \in \Lambda \quad (22)$$

Size Restrictions: There exist pack size restrictions for the loads in each partition. The dimension of the longest board of a pack cannot exceed that of the shortest one in any of the packs laid underneath it in the same partition by more than one-third of the shorter one. The same restriction applies for the width of each pack. We further assume that the packs are already packed in a way that these size restrictions are observed.

$$3 \sum_{p \in P_i} \tau_{p,i}^L X_{p,i,v}^{\ell,\pi} - 4 \sum_{p \in P_j} \beta_{p,j}^L X_{p,j,v}^{\ell,\pi} \leq M(1 - \psi_{jv}^{\pi}), \quad \forall i, j \in N', i \neq j, \pi \in \Pi_{\ell}, \ell \in \mathcal{L}_v, v \in \Lambda$$

$$3 \sum_{p \in P_i} \tau_{p,i}^W X_{p,i,v}^{\ell,\pi} - 4 \sum_{p \in P_j} \beta_{p,j}^W X_{p,j,v}^{\ell,\pi} \leq M(1 - \psi_{jv}^{\pi}), \quad \forall i, j \in N', i \neq j, \pi \in \Pi_{\ell}, \ell \in \mathcal{L}_v, v \in \Lambda$$

Front-Rear Weight Balance Constraints: There are also some weight balance restrictions to be observed. For example, the proportion of total weight of goods loaded in the front section over the back section of a truck must be around 60% over 40%. This can be fulfilled by the following constraints. Let Δ_1 be some tolerance.

$$2 \sum_{\ell \in \mathcal{L}_v} \sum_{\pi \in P_{\ell}^c} \sum_{j \in N'} \sum_{p \in P_j} \omega_{p,j} X_{p,j,v}^{\ell,\pi} \leq (3 + 2\Delta_1) \sum_{\ell \in \mathcal{L}_v} \sum_{\pi \in B_{\ell}^c} \sum_{j \in N'} \sum_{p \in P_j} \omega_{p,j} X_{p,j,v}^{\ell,\pi}, \quad \forall v \in \Lambda$$

$$2 \sum_{\ell \in \mathcal{L}_v} \sum_{\pi \in P_{\ell}^c} \sum_{j \in N'} \sum_{p \in P_j} \omega_{p,j} X_{p,j,v}^{\ell,\pi} \geq (3 - 2\Delta_1) \sum_{\ell \in \mathcal{L}_v} \sum_{\pi \in B_{\ell}^c} \sum_{j \in N'} \sum_{p \in P_j} \omega_{p,j} X_{p,j,v}^{\ell,\pi}, \quad \forall v \in \Lambda$$

Left-Right Weight Balance Constraints: Further, the ratio of total weight of goods loaded on the left side over the right side of a truck can be no more than 7:3 and no less than 3:7. This can be achieved by the following constraints:

$$3 \sum_{\ell \in \mathcal{L}_v} \sum_{\pi \in C_{\ell}^c} \sum_{j \in N'} \sum_{p \in P_j} \omega_{p,j} X_{p,j,v}^{\ell,\pi} \leq 7 \sum_{\ell \in \mathcal{L}_v} \sum_{\pi \in D_{\ell}^c} \sum_{j \in N'} \sum_{p \in P_j} \omega_{p,j} X_{p,j,v}^{\ell,\pi}, \quad \forall v \in \Lambda \quad (23)$$

$$7 \sum_{\ell \in \mathcal{L}_v} \sum_{\pi \in C_{\ell}^c} \sum_{j \in N'} \sum_{p \in P_j} \omega_{p,j} X_{p,j,v}^{\ell,\pi} \geq 3 \sum_{\ell \in \mathcal{L}_v} \sum_{\pi \in D_{\ell}^c} \sum_{j \in N'} \sum_{p \in P_j} \omega_{p,j} X_{p,j,v}^{\ell,\pi}, \quad \forall v \in \Lambda \quad (24)$$

Symmetry Elimination for Homogenous Vehicle Fleet: Should the vehicle fleet be homogenous, the MILP will contain a great deal of symmetry by permutation. This can be dealt with by including the following symmetry elimination constraints.

$$\sum_{i \in N^i} \sum_{j \in N^i: j \neq i} c_{ij} z_{ij}^v \leq \sum_{i \in N^i} \sum_{j \in N^i: j \neq i} c_{ij} z_{ij}^{v+1}, \quad \forall v \in A \setminus \{|A| - 1\} \tag{25}$$

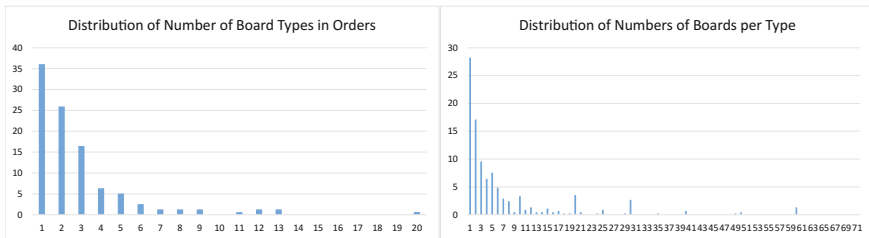
4 Preprocessing and Test Instances

One original test problem instance has been provided by our industry partner. It consists of a daily order of 158 deliveries destined for different customers all over Melbourne. Data sets with smaller numbers of deliveries are constructed from the original dataset by sampling the customers and boards randomly according to the distributions of the original order.

The distributions of different board types in an order were captured, and how many boards were ordered per type, leading to the histograms shown in Fig. 1. The data sets in our experiments were generated using the same distributions.

In this preprocessing phase, all possible combinations of boards were created as packs in the MILP model. If an order has three sizes of boards, one option would be to combine all sizes into a pack, another would be to have three packs with one size each, and another two options would be to either combine the largest and medium size while separating the smallest size into its own pack, or combining the medium and smallest boards into one pack while keeping the largest in a pack of its own.

In a similar way, the combinations of layouts on trucks were generated. Firstly, the maximum number of 8 and 12-ton trucks was determined by dividing the number of orders by four and then setting the maximum to this number or the total number of trucks available (8 for 8-ton trucks, 9 for 12-ton trucks), whichever is smaller. CPLEX was provided with data sets that contain between 1 and the maximum



(a) Percentage of orders that have the given number of board types. (b) Percentage of board types that are included in the given number.

Fig. 1 Distribution of boards in the 158 orders of the Laminex data set

number of 8-ton and 12-ton trucks. If the smallest number of trucks (one 8-ton truck and one 12-ton truck) would not yield a result, the programme would solve the same data set with an option of two 8tn trucks and one 12-ton truck and so on until it finds a feasible solution.

For each truck, a total of eight layouts were described and provided to CPLEX. There are two positions to divide the length of the trucks; the front of the loading platform can be designed to hold a 3600 mm long board or a 2400 mm board. This leads to two options of dividing the length of the platform. Each of these subdivisions can be used for four layouts; in the first, there are only two partitions, one in the front and one at the rear. The second has two partitions in both the front and the rear. The remaining two have two partitions in the front and one at the rear and vice versa.

5 Numerical Results

In Table 1, we present preliminary test results for Model 1. The model is tested on CPLEX Optimization Studio 12.6.2, with solution time limited to 3600 s. The data instances are listed in Column 1 of the table. The instances are numbered $n\text{del-}x\text{-}y\text{-}z$, where n is the number of deliveries (customers), x the problem instance number, y the number of 8-ton trucks and z the number of 12-ton trucks.

In Columns 2 and 3, we present the root node LP relaxation gap (if the optimal objective value is known) and solution time. In Columns 4 and 5, where an optimal

Table 1 Results for 10 deliveries instances and 20 deliveries instances

Instances	Root LPR		Optimal		1st FEA		Best FEA	
	Gap (%)	Time (s)	ItCnt	Time (s)	ItCnt	Gap (%)	ItCnt	Gap (%)
10del-1-1-1	24.37	0.22	358934	35.63		96.84		
10del-2-1-1	47.36	0.06	997363	116.39		97.54		
10del-3-1-1	13.89	0.03	207524	10.94		24.59		
10del-4-1-1	46.82	0.03	256704	12.28		51.33		
10del-7-1-1	45.01	0.05	139551	8.08		50.61		
10del-8-1-1	46.89	0.09	644308	64.18		64.15		
10del-9-1-1	30.87	0.20	678300	117.02		39.32		
10del-10-1-1	18.46	0.20	93566	9.30		27.25		
20del-1-2-2		0.89				98.87	869019	4.07
20del-2-2-3		1.42			406183	67.29	573590	66.53
20del-4-2-2		0.94			1385334	19.79	4044675	15.37
20del-5-1-2		1.78				99.73	5666152	78.64
20del-6-2-2		1.94				98.90		98.90
20del-6-2-3	60.06	1.34	733584	1748.07		99.57		
20del-6-3-3	65.64	1.73	458377	1468.87		99.57		

solution is obtained for a problem instance, we report the cumulative iteration count solving the subproblems (ItCnt) and solution time for the optimal solution.

In Columns 6 and 7, we report the ItCnt and percentage gap when the first feasible solution is obtained. Notice that the ItCnt is not always reported in CPLEX's Engine Log. Finally, in Columns 8 and 9, we report the ItCnt and percentage gap when the last feasible solution is obtained if the problem is not solved to optimality within 3600 s.

As for number of constraints and variables in the MILP, typically, for the 20 delivery problem instances with 2 vehicles, the MILP has around 492 K constraints and 102 K variables. With 5 vehicles, however, the MILP has around 1.35 million constraints and 2.8 million variables.

It is clear from the results that there are limitations in solving 20 delivery problems to optimality within an hour of computation time, hence the motivation to explore alternative formulations as well as other relaxations and decomposition schemes.

6 Future Research Directions

This paper presents a mixed-integer linear programming formulation for a vehicle routing problem with 3D-loading. From the preliminary result section, we can see that there are limitations to the size of problem that can be handled when running a full MILP model on CPLEX. There are a few areas one can explore. 1. Alternative formulations that use variables to determine the suitable packs, rather than using predetermined packs as variables. This option represents a more global approach, though we can expect the size of the MILP to become very large. 2. A column generation approach may be considered for creating the feasible pack configurations, although the column generation problem itself is not expected to be of polynomial complexity. 3. A number of various relaxation or decomposition methods in the manner of Akartunali, Mak and Tran [1] can be considered, given that there are two decision problems here: routing and loading. 4. One can also explore hybrid exact methods (integer programming, constraint programming) and heuristics (or meta-heuristics) methods for solving problems of real-life scale.

References

1. Akartunali, K., Mak-Hau, V., Tran, T.: A unified mixed-integer programming model for simultaneous fluence weight and aperture optimisation in vmat, tomotherapy, and cyberknife. *Comput. Oper. Res.* **56**, 134–150 (2015)
2. Baldacci, R., Hadjiconstantinou, E., Mingozzi, A.: An exact algorithm for the capacitated vehicle routing problem based on a two-commodity network flow formulation. *Oper. Res.* **52**(5), 723–738 (2004)
3. Barkaoui, M., Gendreau, M.: An adaptive evolutionary approach for real-time vehicle routing and dispatching. *Comput. Oper. Res.* **40**(7), 1766–1776 (2013)

4. Bortfeldt, A.: A hybrid algorithm for the capacitated vehicle routing problem with three-dimensional loading constraints. *Comput. Oper. Res.* **39**(9), 2248–2257 (2012)
5. Ceschia, S., Schaerf, A.: Local search for a multi-drop multi-container loading problem. *J. Heuristics* **19**(2), 275–294 (2013)
6. Finke, G., Claus, A., Gunn, E.: A two-commodity network flow approach to the traveling salesman problem. *Congressus Numerantium* **41**(1), 167–178 (1984)
7. Fleszar, K., Osman, I.H., Hindi, K.S.: A variable neighbourhood search algorithm for the open vehicle routing problem. *Eur. J. Oper. Res.* **195**(3), 803–809 (2009)
8. Fukasawa, R., Lysgaard, J., Poggi de Arago, M., Reis, M., Uchoa, E., Werneck, R.: Robust branch-and-cut-and-price for the capacitated vehicle routing problem. In: Bienstock, D., Nemhauser, G. (eds.) *Integer Programming and Combinatorial Optimization. Lecture Notes in Computer Science*, vol. 3064, pp. 1–15. Springer, Berlin (2004)
9. Hong, L.: An improved lns algorithm for real-time vehicle routing problem with time windows. *Comput. Oper. Res.* **39**(2), 151–163 (2012)
10. Junqueira, L., Morabito, R.: Heuristic algorithms for a three-dimensional loading capacitated vehicle routing problem in a carrier. *Comput. Ind. Eng.* **88**, 110–130 (2015)
11. Mak, V., Ernst, A.T.: New cutting-planes for the time-and/or precedence-constrained ATSP and directed VRP. *Math. Methods Oper. Res.* **66**(1), 69–98 (2007)
12. Miller, C., Tucker, A., Zemlin, R.A.: Integer programming formulations and travelling salesman problems. *J. ACM* **7**, 326–329 (1960)
13. MirHassani, S., Abolghasemi, N.: A particle swarm optimization algorithm for open vehicle routing problem. *Expert Syst. Appl.* **38**(9), 11547–11551 (2011)
14. Moura, A., Oliveira, J.F.: An integrated approach to the vehicle routing and container loading problems. *OR Spectrum* **31**(4), 775–800 (2009)
15. Rivera, J.C., Afsar, H.M., Prins, C.: Mathematical formulations and exact algorithm for the multitrip cumulative capacitated single-vehicle routing problem. *Eur. J. Oper. Res.* **249**(1), 93–104 (2016)
16. Pace, S., Turky, A., Moser, I., Aleti, A.: Distributing fibre boards: a practical application of the heterogeneous fleet vehicle routing problem with time windows and three-dimensional loading constraints. In: *International Conference On Computational Science*, pp. 2257–2266. ACM, NY, USA (2015). doi:[10.1016/j.procs.2015.05.382](https://doi.org/10.1016/j.procs.2015.05.382)
17. Subramanian, A., Uchoa, E., Ochi, L.S.: A hybrid algorithm for a class of vehicle routing problems. *Comput. Oper. Res.* **40**(10), 2519–2531 (2013)
18. Szeto, W., Wu, Y., Ho, S.C.: An artificial bee colony algorithm for the capacitated vehicle routing problem. *Eur. J. Oper. Res.* **215**(1), 126–135 (2011)
19. Tao, Y., Wang, F.: An effective tabu search approach with improved loading algorithms for the 3l-cvrp. *Comput. Oper. Res.* **55**(C), 127–140 (2015)
20. Tarantilis, C., Zachariadis, E., Kiranoudis, C.: A hybrid metaheuristic algorithm for the integrated vehicle routing and three-dimensional container-loading problem. *IEEE Trans. Intell. Transp. Syst.* **10**(2), 255–271 (2009)
21. Toth, P., Vigo, D.: Models, relaxations and exact approaches for the capacitated vehicle routing problem. *Discrete Appl. Math.* **123**(1), 487–512 (2002)
22. Wei, L., Zhang, Z., Lim, A.: An adaptive variable neighborhood search for a heterogeneous fleet vehicle routing problem with three-dimensional loading constraints. *IEEE Comput. Intell. Mag.* **9**(4), 18–30 (2014)
23. Zachariadis, E.E., Tarantilis, C.D., Kiranoudis, C.T.: The pallet-packing vehicle routing problem. *Transp. Sci.* **46**(3), 341–358 (2012)
24. Zachariadis, E.E., Tarantilis, C.D., Kiranoudis, C.T.: Designing vehicle routes for a mix of different request types, under time windows and loading constraints. *Eur. J. Oper. Res.* **229**(2), 303–317 (2013)

Automated Techniques for Generating Behavioural Models for Constructive Combat Simulations

Matt Selway, Kerry R. Owen, Richard M. Dexter, Georg Grossmann, Wolfgang Mayer and Markus Stumptner

Abstract Constructive combat simulation is widely used across Defence Science and Technology Group, typically using behavioural models written by software developers in a scripting or programming language for a specific simulation. This approach is time-consuming, can lead to inconsistencies between the same behaviour in different simulations, and is difficult to engage military subject matter experts in the elicitation and verification of behaviours. Therefore, a representation is required that is both comprehensible to non-programmers and is translatable to different simulation execution formats. This paper presents such a representation, the Hierarchical Behaviour Model and Notation (HBMN), which incorporates aspects of existing business process and behaviour representations to provide a hierarchical schema allowing an incremental approach to developing and refining behaviour models from abstract partial models to concrete executable models. The HBMN representation is combined with automated processes for translating written military doctrine texts to HBMN and from HBMN to executable simulation behaviours, providing a cohesive solution to modelling combat behaviours across all stages of development.

M. Selway · G. Grossmann · W. Mayer · M. Stumptner
University of South Australia, Adelaide, Australia
e-mail: Matt.Selway@unisa.edu.au

G. Grossmann
e-mail: Georg.Grossmann@unisa.edu.au

W. Mayer
e-mail: Wolfgang.Mayer@unisa.edu.au

M. Stumptner
e-mail: Markus.Stumptner@unisa.edu.au

K.R. Owen (✉) · R.M. Dexter
Land Simulation, Experimentation, and Wargaming, Land Capability Analysis,
Joint and Operations Analysis Division, Defence Science and Technology Group,
Edinburgh, Australia
e-mail: Kerry.Owen3@dsto.defence.gov.au

R.M. Dexter
e-mail: Richard.Dexter@dsto.defence.gov.au

© Springer International Publishing AG 2018
R. Sarker et al. (eds.), *Data and Decision Sciences in Action*,
Lecture Notes in Management and Industrial Engineering,
DOI 10.1007/978-3-319-55914-8_8

Keywords Behaviour modelling · Combat simulation · Language processing · Model Transformation

1 Introduction

Constructive combat simulation is widely used across Defence Science and Technology (DST) Group in support of operations research studies. Such simulations typically execute behavioural models written in a scripting or programming language that is authored and maintained by software developers dedicated to a specific combat simulation. This approach is time-consuming, requires specific expertise, and can create inconsistencies in representations of the same behaviour between multiple simulations. Furthermore, it is a desirable practice to engage military subject matter experts in the elicitation and verification of behaviours representing military doctrine and tactics (see [4, 5, 12]). This means there is a requirement to have a representation of behavioural models that is not specific to a particular simulation, is comprehensible to a non-programmer but translatable to a simulation execution format, and offers an intuitive interface as presented in [6].

The University of South Australia and DST Group have developed the Hierarchical Behaviour Model and Notation (HBMN) behaviour representation, an automated process for translating written military doctrine texts to HBMN, and an automated process for generating executable behaviours from HBMN to other modelling formats. This workflow is illustrated in Fig. 1.

The HBMN representation adheres to a strictly hierarchical schema allowing behaviours to be expressed at varying levels of abstraction. Therefore, HBMN models can be developed incrementally in a top-down approach by refining abstract partial behavioural models into concrete behaviours before execution in an existing simulation environment. The HBMN representation incorporates selected elements of existing business process and behaviour representations, including Business Process Execution Language [13], Business process Model and Notation [14], and Hierarchical Task Networks [7, 8].

HBMN models can be automatically generated from military doctrine texts via the following process. Natural Language Doctrine Analysis (NLDA) is performed using Natural Language Processing and Information Extraction techniques [15] using rule-based methods and general purpose lexical resources (i.e. dictionaries incorporating additional information), such as [10], to perform the extraction. A key feature is the contextual integration of analysed sentences, which supports the creation of more complete, integrated models rather than producing disconnected fragments.

Finally, HBMN models can be automatically transformed into other simulation formats using the Model Transformation and Code Generation (MTCG) framework. This framework takes an input model, executes a defined set of transformation rules, and outputs the results in a target model. The framework utilises visual contracts for defining the preconditions, post-conditions, and invariants that must hold for the exe-

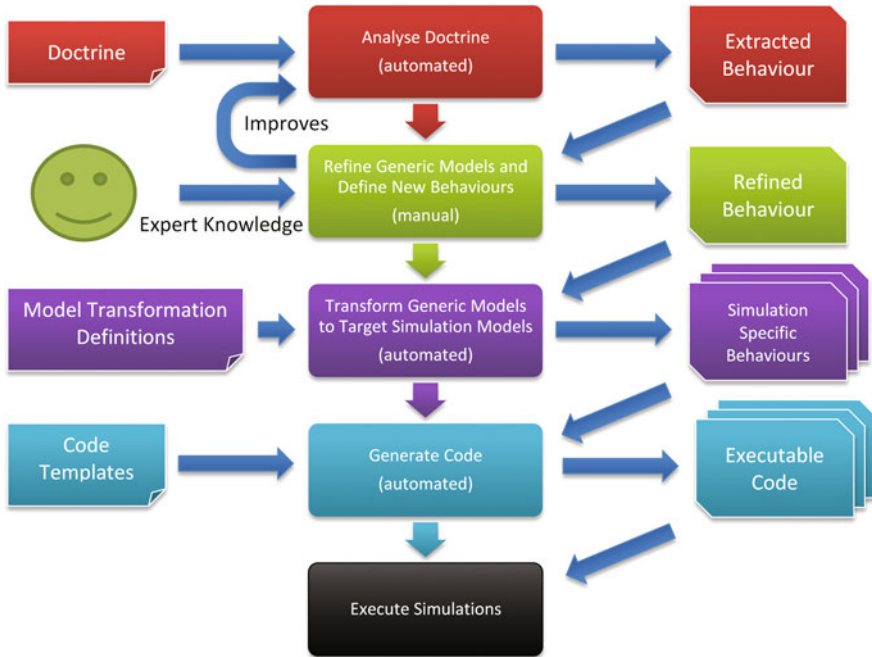


Fig. 1 Behaviour extraction and modelling workflow

cution of the model transformation [9]. In addition, the data transfer and manipulation for an invariant is defined using Visual Transformation Operators: an extensible set of operators for data manipulation built on a core library of operators [1].

This paper presents the HBMN schema and compares it with some of the more common behaviour representation schemas. In addition, the Natural Language Doctrine Analysis and the Model Transformation processes are introduced.

2 Hierarchical Behaviour Model and Notation

A behaviour representation appropriate for the specification of behavioural models for combat simulations in a simulation agnostic way needs to fulfil a number of requirements. These include the need to represent typical behaviour control flow (such as sequential, parallel, and exclusive branch activities), resource sharing, and information transfer, as well as support for modularity to allow the reuse of models. These requirements have evolved from those as described in [3]. Existing behaviour representations do not adequately cover all of the requirements; hence, the Hierarchical Behaviour Model and Notation was developed. HBMN incorporates selected elements of existing business process and behaviour representations, primarily:

- BPEL (Business Process Execution Language) [13]
- BPMN2 (Business process Model and Notation version 2) [14]
- HTN (Hierarchical Task Networks) [7]

Behaviours represented in HBMN adhere to a strictly hierarchical schema to provide structured models that can be expressed at varying levels of abstraction. The development of HBMN models can be performed incrementally using a top-down approach where abstract partial behavioural models are refined into concrete executable behaviours that can be run in existing simulation environments. HBMN models can also be developed in a bottom-up approach where a behaviour model is developed by combining previously defined lower-level models in new contexts.

Concrete executable behavioural models are developed through the collaboration of subject matter experts, such as military commanders, who specify behavioural models, and technical experts who refine abstract behaviours into detailed executable simulations. HBMN facilitates this collaboration by providing a visual representation for modelling suited to non-programmers and an encoding in a machine-readable format that enables automated processing of the models by software tools.

A hierarchical component-oriented approach to behaviour modelling enables modular composition of behaviours from existing behaviour modules which may be shared in a library of common behaviours and reused in subsequent models. Each behaviour module is described by a well-defined interface capturing essential properties such as entry and exit conditions, data input and outputs, and resource requirements. In addition, the interface includes signals for communication between behaviours, supporting the modelling of behaviours that are not strictly hierarchical where necessary. A common interface enables the composition of modules and facilitates the analysis and transformation of behavioural models to other representations, for example different visual and textual views of a model or program code for specific target simulation environments.

This approach has the potential to promote consistency of behavioural models across simulations as well as to streamline the implementation of simulations for a variety of target simulation environments when combined with Model Transformation capabilities. Benefits of the strictly structured model are as follows:

- The model eases interpretation and translation to and from other representations, including text and code.
- Compositionality and comprehensive interfaces facilitate the reuse of behaviour components.

The behaviour model is uniform across all modelling levels, from abstract to fully executable. It combines reactive modelling (i.e. looking only at the current state as opposed to planning ahead), hierarchical task network methods (hierarchical decomposition, preconditions, and effects), and prioritised and interruptible tasks. The following section outlines the basic elements of the HBMN schema.

2.1 HBMN Schema

HBMN models are composed of tasks using behaviour *combinators* (a term adopted from Process Algebras such as CSP [11]) to form composite behaviours. Tasks are either primitive tasks that have corresponding implementations in a simulation environment (possibly derivable through a transformation), or abstract tasks which may be realised through one or more composite behaviour models. Each task, whether it is primitive or composite, has a common interface. The main features include a label, one or more exit conditions, data inputs/outputs, and required resources and their capabilities. In addition, each task can be associated with preconditions that control the activation of the task, effects that enforce post-conditions on the execution, data values for data inputs that are known at design time, and signals or messages which support communication and can be used to model behaviour that is not strictly hierarchical. The common elements are shown in Fig. 2.

Primitive tasks are illustrated as a rounded rectangle with a circular exit condition (no icon), while composite tasks use diamond gateways containing an icon indicating the type of task (e.g. a Sequence uses a single arrow, a Parallel has a triple arrow, and Selection has a question mark, see Fig. 3).

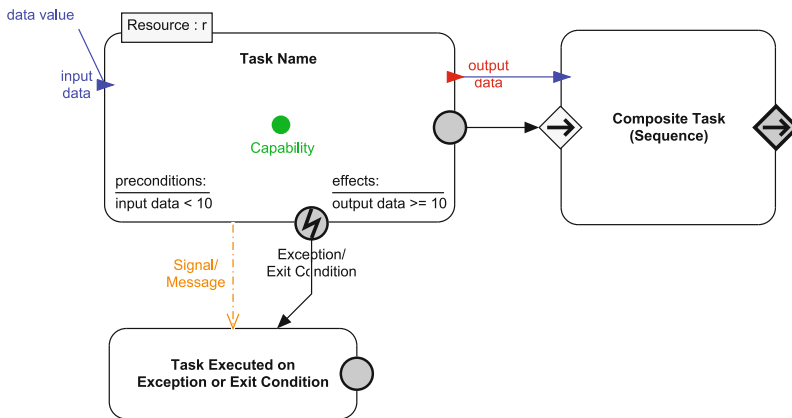


Fig. 2 Common HBMN task elements

Fig. 3 Task type icons

	Task		Repetition
	Sequence		Exception Handler
	Parallel		Time Trigger
	Selection		Conditional Trigger
	Interrupt		Message Trigger

Each task has a distinct exit condition that denotes the successful completion of the task, which may or may not be named. Exit conditions are the dark grey gateway for composite tasks. Additional (named) exit conditions represent alternative outcomes and exceptions that may have occurred during the execution of the task. All exit conditions may be the source of flow arcs denoting the subsequent task to be executed.

Input and output data parameters (blue and red triangles, respectively) can be associated with a task and are described by a label (unique among all data elements associated with the task) and a type (drawn from a taxonomy of data types). Moreover, data values can be explicitly supplied for input parameters if they are known in the context of the behaviour being specified. Data flows (blue lines) are used to connect explicit values to inputs, as well as to connect inputs and outputs between tasks. In addition, data flows may connect two inputs (or two outputs) together when modelling nested behaviours: the inputs of the higher-level task are mapped to inputs of the nested task(s) and vice versa for outputs. Data types and data flows (from values or outputs) are required for all data parameters of tasks in executable models.

Resources required by a task can be specified through resource parameters which define a label and the required resource type in the form 'Type : label'. Resource parameters may denote individual entities (e.g. a soldier) or aggregate entities such as squads. Moreover, the capabilities requested from the resource can be specified in terms of a shared capability model. Capabilities provide a locking mechanism on resources to prevent the possibility of tasks being executed concurrently by a single resource, for example if they require the same capability.

A task may be associated with precondition expressions (logical expressions formed from the input parameters of the task) that govern if a task may execute. While multiple precondition expressions can be specified, they are treated as a logical conjunction. Therefore, all the precondition expressions taken together must be satisfied before a task can be executed. While executable models require fully specified logical expressions, more abstract models can be provided with a description of the precondition. This facilitates understanding by subject matter experts, and refinement of the simple description into logical expressions can later be performed by technical experts.

Similarly, effects can be specified that govern the expected results of the task execution, i.e. logical expressions formed from the output parameters of the task. The logical conjunction of the effect expressions is expected to be satisfied as a result of the successful completion of the task.

Tasks can send and receive signals to other tasks. These can consist of arbitrary messages to other resources or tasks and typically block the execution of a task until the required signal is received.

2.1.1 Execution Semantics

A task can only be executed if the following conditions are met:

- its control entry point is enabled,
- all data input parameters have received a value,
- all required resource parameters have been assigned a resource,
- the capabilities of all required resources are available,
- any signals that are present have been received, and
- all specified precondition expressions are satisfied.

Resources (and their capabilities) are acquired when a task commences execution and released when the task ceases execution. Data output parameters are considered local to the task until the task completes. Values are propagated to the enclosing scope once a task has (successfully) completed execution. Signals are emitted on successful completion of a task.

If an exception or alternative exit condition is encountered, the output data values are propagated to the exception handler if they are of interest to it (by being assigned the appropriate input data parameter). Otherwise, they are assigned a special nil value, and signals are not emitted. The exception handler can then choose to propagate the data value further and/or emit signals as required.

2.1.2 Combinators

In total, there are 9 combinators, or composite task, types. For brevity, we will highlight five major combinators: Sequence, Parallel, Repetition, Selection, and Interruption. For each type of combinator, data inputs and outputs, exit conditions, and resource parameters are formed as the union of the respective parameters and conditions of the subtasks.

The most basic composite task is a Sequence, in which a number of subtasks are ordered by sequence flow connections between the exit point of one task and the entry point of the next. A Sequence completes once all of its subtasks have completed successfully (or an error handler leads to successful completion). In contrast, the Parallel combinator allows the representation of tasks that are performed concurrently with synchronisation: either the same resource performing concurrent actions or multiple resources (e.g. each soldier in a squad) performing actions at the same time. The Parallel task completes once all of the subtasks have completed. If an unhandled exit condition causes early termination of the parallel tasks, the incomplete subordinate tasks are terminated as well.

Task repetition (or loops) can be represented using the Repetition combinator in which a task is executed repeatedly in sequence governed by a loop condition. Loop conditions can control the Repetition by specifying a logical expression (which will cause the Repetition to occur for as long as it evaluates to true or until it evaluates to false), a specific number of repetitions (possibly the result of a calculation), or based on the result of executing a separate subordinate task. To support different types

of repetitive behaviour, the output parameters of a Repetition can output values after each Repetition or they can be combined using an aggregation expression and output once when the Repetition task completes. For example, this allows a repetitive task to continuously output values to another task running in parallel.

The Selection combinator allows a subordinate behaviour to be chosen from a set of alternatives. Unlike choices in other languages such as BPMN [14], the Selection combinator does not perform an exclusive choice by default. Instead, the default behaviour is that all enabled subordinate tasks are executed. In contrast to a Parallel combinator, subordinate tasks cannot be enabled and executed, while some tasks are still executing. Moreover, once the executing tasks are completed, the selection task completes. However, a termination condition can be provided that specifies the number of subordinate tasks to be executed. If the number of tasks required has not been met after some tasks have completed, the preconditions of remaining tasks are rechecked and any newly enabled tasks are executed until the required completion condition has been met. In addition, the subtasks of a Selection combinator can be given a priority, which is used to determine which task(s) will be executed when more tasks are enabled than can be executed (otherwise the choice of task(s) to execute is random).

Finally, HBMN provides an explicit representation of interruption behaviour through the Interruption Combinator. Interruptions are similar to Selections with priority, with a few key differences: only one subtask executes at a time; a task with higher priority than the currently executing task can become enabled and, if so, the current task is suspended and the higher priority task is executed; and once a subtask completes, the next highest priority suspended task is resumed. This is highly useful for modelling combat behaviour (e.g. where a squad behaviour must patrol an area, react to contact with an enemy, and then return to patrolling once the contact has been resolved) as it allows the direct representation of suspending and resuming some task without relying on complex combinations of loops and selections. As a result, it reduces the complexity of the models and improves their clarity for subject matter experts.

2.2 Comparison with Other Behaviour Representations

In general, HBMN provides several advantages over other approaches to modelling behaviour. These include the following:

- A strictly hierarchical, well-structured model with comprehensive interface definitions covering control, data, and resource aspects of primitive and composite behaviours
- Support for reactive behaviours including interruptions and prioritisation
- A layered approach that supports incremental collaborative definition of behaviours

- Simpler visual notation than comparable process modelling approaches (BPMN2, BPEL, YAWL)

The following briefly discusses the limitations of particular process/behaviour modelling approaches.

BPEL [13] is a language designed for orchestrating Web Service processes. It combines graph-based and structured hierarchical modelling primitives in a single language. The resulting language possesses complex execution semantics where control flow, exception handling, and data flow interact. Behaviour prioritisation, interruptions, resource sharing, and reactive features are not easily modelled in the language. The language is formally defined in terms of XML Schema, and mappings from visual notations to BPEL exist. Although interface specifications provide uniform descriptions of individual service operations, the underlying Web Service XML stack is exposed to the user and the web service centric model does not easily translate to hierarchical behaviour definitions.

BPMN2 [14] is a rich language for modelling conceptual business processes and workflows. However, the number of behaviour primitives is large, and aspects of the language lack a universally agreed upon execution semantics. The graph-based modelling approach requires careful thought to avoid unstructured behaviour models that are difficult to analyse and reuse. Simple hierarchical refinement of individual tasks is possible, yet resource sharing and the absence of a comprehensive data flow model make modular composition difficult. The complexity of the language renders analysis and translation to other representations challenging. Reactive behaviour traits are restricted to simple event-based triggers; interruptions are not covered.

Hierarchical Task Network (HTN) is one of the main approaches in automated planning [7, 8]. HTN planners refine abstract task graphs into more detailed (executable) plans using a library of available methods that may realise each abstract task. This approach is advantageous as domain-specific subprocesses can be incorporated easily. HTNs can represent concurrent behaviours but are not well suited for reactive behaviours where behaviours may be interrupted and prioritised dynamically.

(E)FFBDs and SysML/UML Activity Diagrams are two languages for modelling engineering functional decomposition of systems and processes [2]. Both languages can capture control flow, concurrency, data flow, (informal) triggering conditions, and multi-instance tasks. The languages are expressive yet care must be taken to avoid unstructured models which would be difficult to analyse and translate. Advanced reactive concepts, such as interruptions and signals, are not directly expressible in the language and must instead be simulated through other mechanisms.

3 Natural Language Doctrine Analysis (NLDA)

To support the development of behavioural models in a timely fashion, we have developed automated processes to extract HBMN models from military doctrine texts. This NLDA process uses Natural Language Processing and Information

Extraction techniques to identify tasks, resources, data parameters, and data values in doctrine texts. To perform the process extraction, we use rule-based methods based on a generalisation of previous work into the extraction of structural models from software requirements documents [15]. The extraction framework makes use of general purpose lexical resources, such as WordNet and VerbNet, through a common interface (Uby [10]) to support the extraction of behaviours from scratch. In addition, it integrates knowledge gained from previously extracted and refined models to improve the extraction of new models over time. That is, it reuses existing HBMN models and their components to enhance newly extracted models. The goal is to reduce the amount of manual refinement required as a repository of reusable high-quality models is developed.

4 Model Transformation and Code Generation (MTCG)

We have incorporated a Model Transformation and Code Generation (MTCG) framework to automate the process of generating simulation specific models and code from the HBMN models. The MTCG framework takes an input model, executes a defined set of transformation rules, and outputs the results in a target model—this could be the same or a different type of model to that which was input. The framework is based on the use of visual contracts for defining the preconditions, post-conditions, and invariants that should hold for the execution of the Model Transformation [9]. The contracts define patterns of elements that are to be matched in the source and/or target models, as well as constraint expressions that the matched elements must satisfy for the contract to be fulfilled; an example is shown in Fig. 4. When used for the

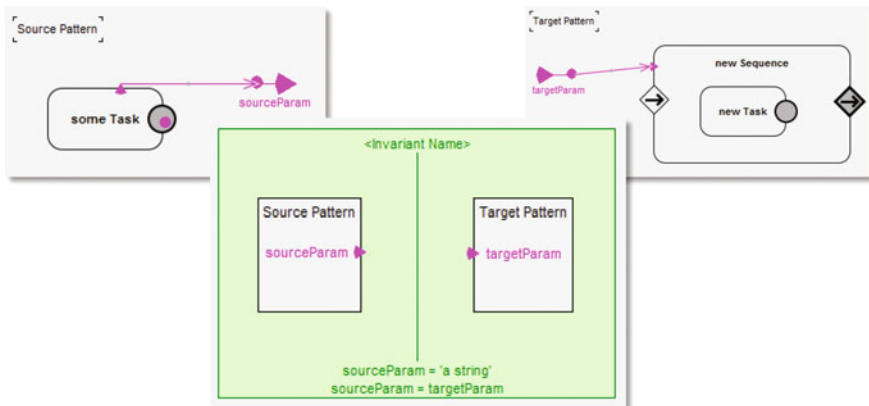


Fig. 4 MTCG positive invariant (*centre*) with the source pattern definition (*left*) and target pattern definition (*right*). The invariant defines a simple equality constraint between the parameters of the source and target patterns. The source and target pattern definitions utilise the concrete model notation augmented with mapping parameters (*pink nodes*)

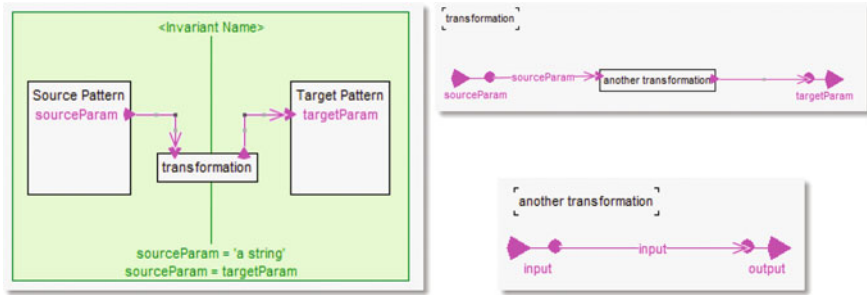


Fig. 5 MTCG positive invariant with transformation definition (*left*) and the hierarchical decomposition of the transformation (*top-right* and *bottom-right*)

execution of transformations, the target model patterns are instantiated with information carried across from model elements that match the source patterns. The transfer and manipulation of this data between source and target models is defined through the use of Visual Transformation Operators [1]: an extensible set of operators for data manipulation built on a core library of operators. Moreover, complex transformation definitions can be constructed hierarchically, allowing defined transformations to be modularised and reused. Figure 5 illustrates a contract with a nested transformation definition that copies the value of the source parameter to the target.

The use of visual contracts and operators for Model Transformations enables the transformations to be defined using the native notations of the source and target models. This allows transformation specification to be separated from transformation implementation; simpler and more concise definitions of transformations; and a major component of the transformation, the source and target patterns, to be developed by those familiar with the underlying notations. In addition, the checking of models can be performed independently from the transformation execution, for example, to check that the models conform to the pre-/post-conditions or that a pair of models satisfies the transformation conditions. This is useful to check previously transformed models against a modified transformation definition. Furthermore, the structure of the transformation rules allows the transformation itself to be checked for correctness, with various inconsistencies and their causes able to be reported to the transformation designer. These features facilitate the long-term maintenance and update of transformations by different people at different times and by those more familiar with the source and target notations than specific transformation notation.

5 Conclusion and Future Work

In modelling behaviours for constructive combat simulations, there is a need for a simulation agnostic modelling language that can be transformed into executable formats, facilitates collaboration with subject matter experts, and directly represents

reactive aspects such as interruptions. Such a representation would reduce the time taken to develop simulations and minimise inconsistencies between different simulations. The Hierarchical Behaviour Model and Notation, presented here, and the accompanying Natural Language Doctrine Analysis and Model Transformation and Code Generation processes address these concerns. It provides a simplified and well-structured behaviour representation that covers control, data, and resource aspects of primitive and composite behaviours, as well as direct representations of reactive behaviours such as interruptions. Furthermore, it supports the incremental definition of behaviours from abstract, including initial models automatically extracted from doctrine texts, to concrete definitions that can be transformed to executable formats using the Model Transformation and Code Generation framework.

The HBMN Schema, NLDA, and MTCG processes are packaged in the HBMN Modeller software, and further refinement of the software and techniques used is ongoing. At this stage, basic doctrine has been translated using NLDA and the MTCG is capable of producing executable code for the COMBATXXI simulation. Future work includes ongoing refinement of the NLDA and MTCG, building a library of HBMN behaviours, and disseminating the model to a wider user community.

References

1. Berger, S., Grossmann, G., Stumptner, M., Schrefl, M.: Metamodel-based information integration at industrial scale. In: Proceedings of ACM/IEEE International Conference on Model Driven Engineering Languages and Systems (MODELS), pp. 153–167 (2010)
2. Bock, C.: UML 2 activity model support for systems engineering functional flow diagrams. *Syst. Eng.* **6**(4), 249–265 (2003). doi:[10.1002/sys.10053](https://doi.org/10.1002/sys.10053)
3. Bowden, F.D.J., Davies, M.: Application of a role-based methodology to represent command and control processes using extended petri nets. In: Proceedings of 1997 IEEE International Conference on Systems, Man and Cybernetics. Orlando, Florida (1997)
4. Bowden, F.D.J., Davies, M., Dunn, J.M.: Representing role based agents using coloured petri nets. In: 5th Computer Generated Forces and Behavioral Representation Conference (1995)
5. Cox, A., Gibb, A., Page, I.: Army training and CGDs—a UK perspective. In: Proceedings of 5th Computer Generated Forces and Behavioral Representation Conference (1995)
6. Dexter, R.M., Piotta, J., Pash, K.M.: Bridging the gap: a generic behaviour framework for behaviour representation (extended abstract). In: Proceedings of MODSIM 2013. Australia (2013)
7. Georgievski, I., Aiello, M.: HTN planning: overview, comparison, and beyond. *Artif. Intell.* **222**, 124–156 (2015). doi:[10.1016/j.artint.2015.02.002](https://doi.org/10.1016/j.artint.2015.02.002)
8. Ghallab, M., Nau, D., Traverso, P.: Automated Planning: Theory & Practice. Morgan Kaufmann Publishers Inc., San Francisco, CA, USA (2004)
9. Guerra, E., de Lara, J., Wimmer, M., Kappel, G., Kusel, A., Retschitzegger, W., Schönböck, J., Schwinger, W.: Automated verification of model transformations based on visual contracts. *Autom. Soft. Eng.* **20**(1), 5–46 (2013). doi:[10.1007/s10515-012-0102-y](https://doi.org/10.1007/s10515-012-0102-y)
10. Gurevych, I., Eckle-Kohler, J., Hartmann, S., Matuschek, M., Meyer, C., Wirth, C.: Uby: a large-scale unified lexical-semantic resource based on LMF. In: Proceedings of 13th Conference of the European Chapter of the Association for Computational Linguistics, pp. 580–590 (2012)

11. Hoare, C.A.R.: *Communicating Sequential Processes*. Prentice Hall (1985)
12. Lewis, J.W.: Agents that explain their own actions. In: *Proceedings of 5th Computer Generated Forces and Behavioral Representation Conference*. Orlando, Florida (1994)
13. OASIS: Web services business process execution language version 2.0. Standard (2007). <http://docs.oasis-open.org/wsbpel/2.0/OS/wsbpel-v2.0-OS.html>
14. OMG: Business process model and notation, version 2.0. Standard formal/2011-01-03, Object Management Group (2011). <http://www.omg.org/spec/BPMN/2.0>
15. Selway, M., Grossmann, G., Mayer, W., Stumptner, M.: Formalising natural language specifications using a cognitive linguistic/configuration based approach. *Inf. Syst.* **54**, 191–208 (2015). doi:[10.1016/j.is.2015.04.003](https://doi.org/10.1016/j.is.2015.04.003)

Analytic and Probabilistic Techniques for the Determination of Surface Spray Patterns from Air Bursting Munitions

Paul A. Chircop

Abstract We present a methodological framework for the evaluation and comparison of surface spray fragmentation patterns from a range of medium-calibre air bursting munitions. The methodology is underpinned by both analytic and probabilistic modelling techniques. In particular, we present a fly-out model for the calculation of the terminal speed of a fragment on the impact plane. The fly-out model constitutes a trade-off between the computational efficiency of analytic models and the accuracy of detailed numerical methods extant in the literature. The methodology has been developed with the ability to readily adapt to modifications in the gun and ammunition parameters, with applications to controlled and naturally fragmenting munitions, as well as shrapnel-based warheads. This is demonstrated by comparing the surface spray patterns of two different ammunition types.

Keywords Fragment · Lethal energy · Probability map · Shrapnel · Spray pattern

1 Introduction and Contextual Background

Naval platforms such as destroyers and frigates are fitted with a variety of defensive weapons. These systems are generally able to utilize a variety of ammunition types. In particular, there is the potential to employ medium-calibre ammunition options against surface threats at extended engagement ranges before a ship's shorter range weapon systems are brought to bear. Motivated by this contextual background, we present a mathematical modelling approach and a methodological framework for evaluating and comparing the lethal effects of air bursting munitions via surface spray fragmentation patterns.

Medium-calibre munitions come with various fusing, shell fragmentation and shrapnel dispersion mechanisms. In surface warfare, proximity and timed fuses can be employed to detonate a munition above or ahead of a target/threat, thus determin-

P.A. Chircop (✉)

Defence Science and Technology Group, 13 Garden Street, Eveleigh, NSW, Australia
e-mail: paul.chircop@dst.defence.gov.au

ing the burst height. On detonation, the fragmenting payload is dispersed according to some distribution, with the intent of delivering a lethal effect to the target/threat via the kinetic energy imparted to the fragments from the explosive charge/filler. A fragment which strikes the target/threat above a certain energy threshold is considered to be lethal.¹

In order to determine the terminal kinetic energy of a fragment, a mathematical model for the ballistic fly-out is required. As a fragment flies through the air, its speed is attenuated according to its drag profile. There are two extant modelling paradigms for handling the drag profile of a fragment. The first assumes a constant drag coefficient and a straight-line trajectory from the burst position to the impact point (e.g. see [2, 13, 14]). The second paradigm assumes a detailed drag profile characterization with advanced numerical methods to compute the ballistic trajectory of each fragment (e.g. see [8]). For certain speed regimes, the first paradigm can be a simplistic approximation while the second is nearly always computationally intensive and time consuming.

As a key component of the methodological framework, we develop an alternative approach to the extant fragment fly-out models in the literature. Our modelling approach can be used in situations where the lethal energy threshold permits a straight-line approximation, but where the total variation in fragment speed is non-trivial (e.g. transitioning from the supersonic to the subsonic regime). This is accomplished by accounting for the complete drag profile via a piecewise combination of speed-dependent functions.

2 Input Data

The methodology requires input data from various sources. There are three main input components to the modelling framework. These are (in no particular order) the terminal ballistics data for the munition, the fragment dispersion data for the (static) munition and vulnerability/lethality analysis data for the target/threat. These input components can be fed into our modelling approach, producing a probabilistic surface spray pattern and a measure of effectiveness, called the Area Of Effect (AOE). This is summarized in Fig. 1.

Polar zones can be defined for a munition which characterize the distribution of the number, masses and ejection speeds of the fragments. Explosive arena testing (using flash panels) can be used to determine these distribution profiles for HE (High Explosive) munitions [6, 9, 14].² Figure 2 depicts the polar zones around an exploding HE munition.

¹The lethal effect depends on the target/threat being considered. See [13] for energy thresholds in the anti-materiel context and [12, 14] for anti-personnel applications.

²Historically, Mott [11] and Gurney [7] also developed analytical methodologies for determining fragment mass distributions and ejection speeds from exploding cylinders and spheres.

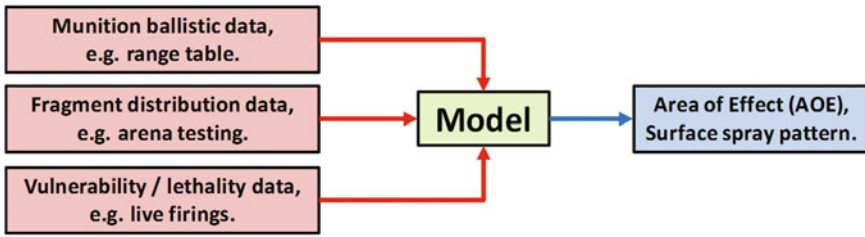


Fig. 1 The modelling framework requires input from three principal data sources



Fig. 2 The distributions of fragment numbers, masses and static ejection speeds from an exploding munition are dependent on the polar angle or zone, as measured from the nose (axially symmetric). In this example, the polar zones are numbered from 1 to 12

For a shrapnel-based munition like IKE-ET³ [1], there is a single polar zone emanating from the nose of the munition. The munition contains a payload of tungsten pellets which are sprayed forward in a cone of narrow beamwidth. For munitions like these, the constitution of the payload and burst mechanics can be determined by live firings or from the manufacturer.

The information pertaining to a munition’s terminal characteristics at a given engagement range and burst height is required to determine the dynamic fragment ejection speeds and angular distributions. The orientation and speed of the munition at detonation will result in the forward vectoring of the static ejection velocities of the fragments, thus increasing the lethal effect in some cases [9]. Terminal data for the munition can be obtained from range tables or through high-fidelity ballistic trajectory models.⁴

Lethality or vulnerability analysis of the target/threat is required to determine the energy threshold criterion for a lethal fragment.⁵ Depending on the context, this could be the energy required for a certain penetrative effect on a metal sheet, a fibre-glass panel, a layer of protective clothing or skin.

³The Improved Kinetic Energy—Electronically Timed advanced shotgun projectile.

⁴These models, which include detailed atmospheric data, usually require advanced numerical methods (e.g. fourth order Runge-Kutta) for their solution (see [5]).

⁵Also known as the injury criterion for anti-personnel applications [14].

3 Determination of Conical Boundaries on the Impact Plane

As outlined previously, the distribution of fragment numbers, masses and ejection speeds can be characterized by polar zones around a munition. The polar zones are regions in space bounded by *conical surfaces* emanating from the centroid of the munition [6]. In the context of an air bursting munition, the intersection of a conical surface with the impact plane will trace out a *conic section*. This insight provides the basis for our mathematical modelling approach. So long as the polar zone characterization satisfies the aforementioned geometrical construct, the modelling approach presented in this chapter should be fit for purpose.

3.1 General Representation

A conical surface with apex $(a, b, c) \in \mathbb{R}^3$, axis parallel to the vector \mathbf{d} and half-angle φ (aperture 2φ), where $0 < \varphi < \pi/2$, is given by:

$$(\mathbf{x} \cdot \mathbf{d})^2 - (\mathbf{d} \cdot \mathbf{d})(\mathbf{x} \cdot \mathbf{x}) \cos^2 \varphi = 0, \quad (1)$$

where $\mathbf{x} = (x - a)\mathbf{i} + (y - b)\mathbf{j} + (z - c)\mathbf{k}$ and $\mathbf{d} = \alpha\mathbf{i} + \beta\mathbf{j} + \gamma\mathbf{k}$.

The burst position of the projectile is the point $(0, 0, h)$ (where $h > 0$) with impact angle θ (angle of descent relative to the y -axis). Hence, $a = 0$, $b = 0$, $c = h$ and $\mathbf{x} = x\mathbf{i} + y\mathbf{j} + (z - h)\mathbf{k}$ and $\mathbf{d} = (h \cot \theta)\mathbf{j} - h\mathbf{k}$. Substituting into Eq. (1), we get:

$$(y \cot \theta - (z - h))^2 - (x^2 + y^2 + (z - h)^2) \csc^2 \theta \cos^2 \varphi = 0. \quad (2)$$

Alternatively, the same conical surface can be written in parametric form:

$$x(\ell, \omega) = \ell \cos \omega \tan \varphi, \quad (3)$$

$$y(\ell, \omega) = \ell \sin \omega \tan \varphi \sin \theta - \ell \cos \theta, \quad (4)$$

$$z(\ell, \omega) = h + \ell \sin \omega \tan \varphi \cos \theta + \ell \sin \theta, \quad (5)$$

where $\ell \in (-\infty, +\infty)$ and $\omega \in [0, 2\pi)$.⁶

In order to find the intersection of the conical surface with the x - y plane, Eq. (2) can be rewritten as a quadratic in z . Solving the quadratic gives two solutions z_+ and z_- . Setting $z_{\pm} = 0$ gives at most two solutions for the intersection of the conical surface with the x - y plane (with $\varphi \neq \theta$):

⁶To verify that the polar representation describes the same conical surface, the components may be substituted into the known cartesian equation given in Eq. (2). This can be verified with a computational algebra software package such as MAPLE®.

$$y_{\pm}(x) = \frac{-h \cos \theta \sin \theta \pm \cos \varphi \sqrt{h^2 \sin^2 \varphi + x^2 (\cos^2 \theta - \cos^2 \varphi)}}{\cos^2 \theta - \cos^2 \varphi}, \quad (6)$$

Rearranging Eq. (6) gives the equation of the conic section (with $\varphi \neq \theta$):

$$\frac{(y - y_0)^2}{a^2} - \frac{x^2}{b^2} = 1, \quad \text{where,} \quad (7)$$

$$a^2 = \frac{h^2 \cos^2 \varphi \sin^2 \varphi}{(\cos^2 \theta - \cos^2 \varphi)^2}, \quad b^2 = \frac{h^2 \sin^2 \varphi}{\cos^2 \theta - \cos^2 \varphi}, \quad y_0 = \frac{-h \cos \theta \sin \theta}{\cos^2 \theta - \cos^2 \varphi}.$$

When $\theta < \varphi < \pi/2$, Eq. (7) corresponds to a *North-South opening hyperbola*. When $\varphi < \theta < \pi/2$, Eq. (7) corresponds to an *ellipse*. When $\theta = \pi/2$, Eq. (7) corresponds to a *circle* of radius $h \tan \varphi$. The eccentricity e of the conic section is given by:

$$e = \sqrt{1 + \frac{b^2}{a^2}} = \left| \frac{\cos \theta}{\cos \varphi} \right|. \quad (8)$$

For $y_+(x)$, it can be seen that the numerator and denominator of Eq. (6) approach 0 as $\varphi \rightarrow \theta$. Hence, we can apply L'Hôpital's Rule to find the limit of $y_+(x)$ as $\varphi \rightarrow \theta$:

$$\lim_{\varphi \rightarrow \theta} y_+(x) = \left(\frac{1}{2h} \cot \theta \right) x^2 + h \cot 2\theta. \quad (9)$$

This corresponds to a *parabola* with vertex $(0, h \cot 2\theta)$ and focal parameter $h \tan \theta$.

Henceforth, we will write the equation of the conic section as a function of both the variable x and the conical angle φ , assuming that the height h and munition's angle of descent θ are held constant, that is, $y = y_{\pm}(x, \varphi)$. The subscript P is used in the case of a parabolic conic section ($\theta = \varphi$), that is, $y = y_P(x, \varphi)$.

3.2 Correction for Terminal Angle and Speed of Munition

As previously foreshadowed, a munition with terminal velocity \mathbf{v} , burst height h and terminal angle θ to the horizontal will influence the ejection speed and angle of each fragment. Let the static ejection velocity of a fragment be \mathbf{u} with static ejection angle φ , that is, the angle between \mathbf{v} and \mathbf{u} . The dynamic ejection velocity (\mathbf{u}_F) of a fragment will be determined by the forward vectoring of \mathbf{u} by the munition velocity \mathbf{v} . This will result in a new ejection speed $\|\mathbf{u}_F\|$ and angle φ_F for each fragment, where φ_F is the angle between \mathbf{v} and $\mathbf{u}_F = \mathbf{u} + \mathbf{v}$.

Given \mathbf{u} , \mathbf{v} and φ , the dynamic ejection speed $\|\mathbf{u}_F\|$ and angle φ_F can be calculated as follows:

$$\|\mathbf{u}_F\| = \sqrt{\|\mathbf{u}\|^2 + \|\mathbf{v}\|^2 + 2\|\mathbf{u}\|\|\mathbf{v}\|\cos\varphi}, \quad \varphi_F = \cos^{-1}\left(\frac{\|\mathbf{v}\| + \|\mathbf{u}\|\cos\varphi}{\|\mathbf{u}_F\|}\right). \quad (10)$$

A procedure for plotting the conic sections on the impact plane is given in Algorithm 1. Such a procedure can be used for quick and easy comparison of the possible angular distribution of fragments for a given burst height, terminal angle and speed.

Algorithm 1 Get Surface Conic Section Boundaries

```

1: Input: A burst height  $h$ , fragment static ejection speed  $\|\mathbf{u}\|$ , munition terminal speed and angle
   ( $\|\mathbf{v}\|, \theta$ ), a polar angle  $\varphi$ 
2: Compute  $\varphi_F = \cos^{-1}\left(\frac{\|\mathbf{v}\| + \|\mathbf{u}\|\cos\varphi}{\sqrt{\|\mathbf{u}\|^2 + \|\mathbf{v}\|^2 + 2\|\mathbf{u}\|\|\mathbf{v}\|\cos\varphi}}\right)$ 
3: if  $\theta < \varphi_F$  then
4:    $\mathcal{R} := \{(x, y) \in \mathbb{R}^2 \mid y = y_+(x, \varphi_F)\}$ 
5: else
6:   if  $\theta > \varphi_F$  then
7:      $\mathcal{R} := \{(x, y) \in \mathbb{R}^2 \mid y = y_-(x, \varphi_F)\} \cap \{(x, y) \in \mathbb{R}^2 \mid y = y_+(x, \varphi_F)\}$ 
8:     (Circular bounding area for  $\theta = \pi/2$ )
9:   else
10:    if  $\theta = \varphi_F$  then
11:       $\mathcal{R} := \{(x, y) \in \mathbb{R}^2 \mid y = y_p(x, \varphi_F)\}$ 
12:    end if
13:  end if
14: end if
15: Return  $\mathcal{R}$ 

```

4 Fragment Fly-Out Model

In this section, we develop a mathematical model for the ballistic fly-out of an individual fragment. The model is designed to account for the complete drag profile characterization of a fragment by approximating the drag coefficient with a piecewise combination of speed-dependent functions. We begin by presenting the general equation of motion.

The equation of motion for a fragment of mass m launched from an initial position $(0, 0, h)$ at an angle of depression ϕ_0 to the horizontal is:

$$m \frac{dv}{dt} = mg \sin \phi - kv^2. \quad (11)$$

The angle ϕ_0 is measured positive in the *clockwise* direction. We assume a straight-line trajectory, so that $\phi = \phi_0$ throughout. The drag factor k is given by $k = \rho AC_D/2$, where ρ is the density of dry air at sea level and A is the cross-sectional area of the fragment.⁷

⁷For example, the cross-sectional area of a spherical fragment is $A = \pi d^2/4$, where d is the diameter.

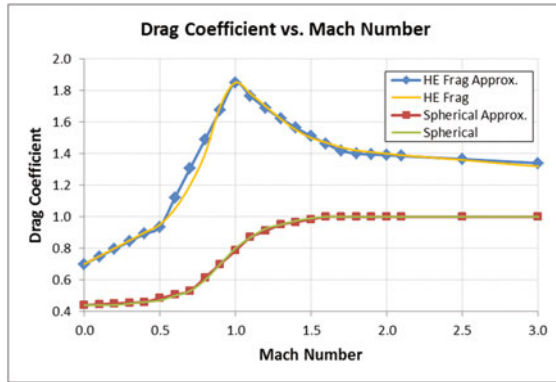


Fig. 3 Drag profiles for a generic HE shell fragment [4] and a spherical pellet [10]. In both cases, the drag profiles can be constructed piecewise with Regime I and II functions. The spherical pellet’s drag profile can be approximated solely with Regime I functions. For the HE fragment, Regime II is used for approximation in the low-supersonic flight interval of Mach 1.0 to 1.8 [3]

The drag coefficient C_D is a function of the Mach number M , the ratio of the fragment’s speed to the speed of sound in air (c_0): $C_D = C_D(M)$. We define two regimes for the drag coefficient profile. **Regime I**: the drag coefficient is an affine function of the Mach number, that is:

$$C_D(M) = K_1M + L_1, \tag{12}$$

where K_1 and L_1 are real numbers. **Regime II**: the drag coefficient varies inversely as the square root of the Mach number, that is, for $M \neq 0$, we have:

$$C_D(M) = K_2/\sqrt{M}, \tag{13}$$

where $K_2 \neq 0$ is a real number.⁸

Figure 3 depicts the drag profiles for a generic HE fragment and a spherical pellet. Each profile is approximated by a piecewise continuous combination of Regime I and II functions. The number of discrete regime segments can be chosen in accordance with the desired accuracy of the approximation.

In the following sections, we derive the equations to determine the terminal speed of a fragment on the impact plane. There are three cases to consider under Regime I, and one case for Regime II.

⁸See Chap. 8 of Carlucci and Jacobson [3] for further details on the approximation of drag profiles by analytic functions.

4.1 Regime I: C_D an Affine Function of M

Using the expression given in Eq. (12) for Regime I, the equation of motion for a fragment becomes:

$$\frac{dv}{dt} = k_1 - k_2v^2 - k_3v^3, \quad (14)$$

where: $k_1 = g \sin \phi$, $k_2 = \rho AL_1/(2m)$, $k_3 = \rho AK_1/(2mc_0)$. There are three cases to consider—Case I: $k_2, k_3 \neq 0$, Case II: $k_2 = 0, k_3 \neq 0$, Case III: $k_2 \neq 0, k_3 = 0$.

4.1.1 Case I: $k_2, k_3 \neq 0$

The equation of motion (14) can be written in terms of the displacement (the *slant range* s) instead of time by writing $dv/dt = v(dv/ds)$. Therefore, separation of variables gives:

$$\int \frac{v}{k_1 - k_2v^2 - k_3v^3} dv = \int ds. \quad (15)$$

Let the LHS of Eq. (15) be denoted by $I_{k_{2,3} \neq 0}(v)$. After factorizing the denominator of the integrand of $I_{k_{2,3} \neq 0}(v)$, we get the result:

$$I_{k_{2,3} \neq 0}(v) = \frac{\beta}{2E} \ln \left(\frac{-k_3v^2 - \frac{k_1}{\beta^2}v + \frac{k_1}{\beta}}{(v + \beta)^2} \right) - \frac{D}{2E} \int \frac{dv}{-k_3v^2 - \frac{k_1}{\beta^2}v + \frac{k_1}{\beta}}, \quad (16)$$

where $E = 2k_1/\beta - k_3\beta^2$, $D = -3k_1/\beta$ and β satisfies the cubic equation:

$$k_3\beta^3 - k_2\beta^2 + k_1 = 0. \quad (17)$$

Let $\Delta = (k_1^2 + 4k_1k_3\beta^3)/\beta^4$. Then the integral found in Eq. (16) is given by:

$$\int \frac{dv}{-k_3v^2 - \frac{k_1}{\beta^2}v + \frac{k_1}{\beta}} = \begin{cases} \frac{-2}{\sqrt{\Delta}} \coth^{-1} \left(\frac{-2k_3v - k_1/\beta^2}{\sqrt{\Delta}} \right) + C, & \text{for } \Delta > 0, \\ \frac{2}{2k_3v + k_1/\beta^2} + C, & \text{for } \Delta = 0, \\ \frac{2}{\sqrt{-\Delta}} \tan^{-1} \left(\frac{-2k_3v - k_1/\beta^2}{\sqrt{-\Delta}} \right) + C, & \text{for } \Delta < 0, \end{cases} \quad (18)$$

where C is a constant of integration.

4.1.2 Case II: $k_2 = 0, k_3 \neq 0$

In this case, the line segment defining the drag profile of the fragment passes through the origin. The equation of motion is therefore given by:

$$\int \frac{v}{k_1 - k_3 v^3} dv = \int ds. \quad (19)$$

Let the LHS of Eq. (19) be denoted by $I_{k_2=0}$ and let $p^3 = k_1/k_3$. By factorizing the denominator of the integrand of $I_{k_2=0}$, we get:

$$I_{k_2=0}(v) = \frac{1}{k_3} \left\{ \frac{1}{6p} \ln \left(\frac{p^2 + pv + v^2}{(p-v)^2} \right) - \frac{1}{p\sqrt{3}} \tan^{-1} \left(\frac{2v+p}{p\sqrt{3}} \right) \right\}. \quad (20)$$

4.1.3 Case III: $k_2 \neq 0, k_3 = 0$

In this case, the line segment defining the drag profile of the fragment is a horizontal line (zero gradient). In this case, we have:

$$\int \frac{v}{k_1 - k_2 v^2} dv = \int ds. \quad (21)$$

By writing the LHS of Eq. (21) as $I_{k_3=0}$, we get:

$$I_{k_3=0}(v) = -\frac{1}{2k_2} \ln(k_1 - k_2 v^2). \quad (22)$$

4.1.4 Summary

The equation of motion for Regime I is therefore given by:

$$I(v) = s + C, \quad (23)$$

where s is the slant range, C is a constant of integration and $I(v)$ is given by:

$$I(v) = \begin{cases} I_{k_2=0}(v) & \text{if } k_2 = 0, k_3 \neq 0, \\ I_{k_3=0}(v) & \text{if } k_2 \neq 0, k_3 = 0, \\ I_{k_{2,3} \neq 0}(v) & \text{if } k_2 \neq 0, k_3 \neq 0. \end{cases} \quad (24)$$

Equation (23) can be solved via a numerical method, such as Newton–Raphson.

4.2 Regime II: C_D Proportional to $1/\sqrt{M}$

The equation of motion for Regime II is:

$$v \frac{dv}{ds} = k_1 - k_4 v^{\frac{3}{2}}, \quad (25)$$

where: $k_1 = g \sin \phi$, $k_4 = \rho A K_2 \sqrt{c_0} / (2m)$.

Integrating the equation of motion via separation of variables gives:

$$\int \frac{v}{k_1 - k_4 v^{\frac{3}{2}}} dv = \int ds. \quad (26)$$

Consider the integral on the LHS of Eq. (26), which we denote by $\Pi(v)$. Using a suitable substitution and a partial fraction decomposition applied to the integrand of $\Pi(v)$, and by writing $q^3 = k_1/k_4$, we get:

$$\Pi(v) = \frac{1}{k_4} \left\{ \frac{q}{3} \ln \left(\frac{q^2 + q\sqrt{v} + v}{(q - \sqrt{v})^2} \right) + \frac{2q}{\sqrt{3}} \tan^{-1} \left(\frac{2\sqrt{v} + q}{q\sqrt{3}} \right) - 2\sqrt{v} \right\}. \quad (27)$$

Therefore, the equation of motion for Regime II is given by:

$$\Pi(v) = s + C, \quad (28)$$

where C is a constant of integration.

4.3 Terminal Speed of a Fragment at an Impact Point

The drag profile $C_D(M)$ of a fragment is a piecewise continuous combination of smooth functions from Regime I and II. Each segment of the drag profile \mathcal{C}_D^j is defined over an interval $[v_{j-1}, v_j]$, where $j = 1, \dots, n$, and $v_{j-1} < v_j \forall j \in \{1, \dots, n\}$. Each interval is assigned a binary value, depending on whether its drag profile describes Regime I or II. Therefore, we can define a mapping: $r : \{1, \dots, n\} \rightarrow \{0, 1\}$, where 0 corresponds to Regime I, and 1 to Regime II. Thus, segment $\mathcal{C}_D^j(M)$ of the drag profile can be expressed as follows:

$$\mathcal{C}_D^j(M) = \begin{cases} K_1^j M + L_1^j & \text{if } r(j) = 0, \\ K_2^j / \sqrt{M} & \text{otherwise.} \end{cases} \quad (29)$$

For the equations of motion (23) and (28), we write $I_j(v)$ and $\Pi_j(v)$, respectively, in order to specify the segment \mathcal{C}_D^j of a fragment's drag profile. Furthermore, Eqs. (23)

and (28) can be consolidated by defining:

$$J_j(v) = \begin{cases} I_j(v) & \text{if } r(j) = 0, \\ II_j(v) & \text{otherwise.} \end{cases} \quad (30)$$

Therefore, the terminal speed of a fragment on interval $[v_{j-1}, v_j]$ can be found by solving:

$$J_j(v) = s + C, \quad (31)$$

where C is a constant of integration.

Given a fragment's specifications and drag profile characterization, along with its initial dynamic speed $\|\mathbf{u}_F\|$, initial height h and an impact point (x_I, y_I) on the plane, an iterative application of Eq. (31) can be employed to determine the terminal speed. The iterative process, which is summarized in Algorithm 2, ensures that continuity is preserved at the boundaries of the various regime segments.

Algorithm 2 Get Fragment Impact Speed

```

1: Input: A burst height  $h$ , an impact point  $p_I = (x_I, y_I)$ , an initial fragment speed  $\|\mathbf{u}_F\|$ , fragment's
   specifications  $F = (A, m, \|\mathbf{u}\|, C_D)$ .
2: procedure GETIMPACTSPEED( $h, \|\mathbf{u}_F\|, x_I, y_I, F$ )
3:    $\phi \leftarrow \tan^{-1} \left( h / \sqrt{x_I^2 + y_I^2} \right)$ 
4:   Locate  $j$ , where  $1 \leq j \leq n$  and  $\|\mathbf{u}_F\| \in [v_{j-1}, v_j]$ 
5:    $k \leftarrow 1$ 
6:    $v_j \leftarrow \|\mathbf{u}_F\|$ 
7:    $C_k \leftarrow J_j(v_j)$ 
8:    $s_k \leftarrow J_j(v_{j-1}) - C_k$ 
9:   while  $s_k < h \csc \phi$  do
10:     $j \leftarrow j - 1$ 
11:     $k \leftarrow k + 1$ 
12:     $C_k \leftarrow J_j(v_j) - s_{k-1}$ 
13:     $s_k \leftarrow J_j(v_{j-1}) - C_k$ 
14:   end while
15:   Find  $v_I: J_j(v_I) - h \csc \phi - C_k = 0$   $\triangleright$  Newton–Raphson or other numerical method.
16:   Return:  $v_I$ 
17: end procedure

```

5 A Probabilistic Approach for the Determination of Surface Spray Patterns

An impact point can be generated for each fragment based on the fragment's ejection direction from the munition. The impact point can be determined probabilistically for fragments within a given polar zone. Recall that the conical surface generated by the polar angle φ can be represented by the parametric equations (3)–(5). Given that

the fragments within a polar zone are uniformly dispersed in the angle $\omega \in [0, 2\pi)$, we can use a random sampling technique with the parametric equations to generate impact points on the plane. This is given in Algorithm 3. Once an impact point has been determined from Algorithm 3, it can be used as input to Algorithm 2 to get the impact speed.

Algorithm 4 calls both Algorithm 3 and Algorithm 2 to obtain impact points and speeds for each fragment ejected from a munition. Algorithm 4 keeps track of the impact points which satisfy the required kinetic energy threshold, denoted by T . This is carried out with reference to a grid structure \mathbf{G} , which is composed of grid squares that are indexed by $w \in \{1, \dots, |\mathbf{G}|\}$, where $|\mathbf{G}|$ is the number of grid squares. The output for this procedure is a binary value for each grid square, which is 1 if there is at least one impact point with the required energy, and 0 otherwise. The notation for Algorithm 4 is as follows. Each polar zone is indexed by $q \in \{1, \dots, Q\}$ and defined by a minimum and maximum conical half-angle, φ_{\min}^q and φ_{\max}^q , respectively. The number of fragments in polar zone q is given by N_q , thereby giving a total of $M_Q = \sum_{q=1}^Q N_q$ fragments. Each polar zone is represented by a tuple $(\varphi_{\min}^q, \varphi_{\max}^q, N_q)$ and each fragment $i \in \{1, \dots, M_Q\}$ is specified by $F_i = (A_i, m_i, \|\mathbf{u}_i\|, C_D^i)$.

Algorithm 3 Get Fragment Impact Point

```

1: Input: A burst height  $h$ , fragment static ejection speed  $\|\mathbf{u}\|$ , munition terminal speed and angle
   ( $\|\mathbf{v}\|, \theta$ ), polar zone boundaries  $(\varphi_{\min}, \varphi_{\max})$ 
2: procedure GETIMPACTPOINT( $h, \|\mathbf{u}\|, \|\mathbf{v}\|, \theta, \varphi_{\min}, \varphi_{\max}$ )
3:    $\tilde{\omega} = \tilde{r} \times [0, 2\pi)$   $\triangleright \tilde{r} \sim U(0, 1)$ , where  $U$  is the uniform distribution.
4:    $\tilde{\varphi} = \tilde{r} \times [\varphi_{\min}, \varphi_{\max}]$ 
5:    $\|\mathbf{u}_F\| = \sqrt{\|\mathbf{u}\|^2 + \|\mathbf{v}\|^2 + 2\|\mathbf{u}\|\|\mathbf{v}\|\cos\tilde{\varphi}}$ 
6:    $\varphi_F = \cos^{-1}\left(\frac{\|\mathbf{v}\| + \|\mathbf{u}\|\cos\tilde{\varphi}}{\|\mathbf{u}_F\|}\right)$ 
7:    $\tilde{\ell} = -h/(\sin\tilde{\omega}\tan\varphi_F\cos\theta + \sin\theta)$   $\triangleright$  Set  $z = 0$  in Eq. (5).
8:   if  $\{(0 \leq \varphi_F < \pi/2) \wedge (\tilde{\ell} < 0)\} \vee \{(\varphi_F \geq \pi/2) \wedge (\tilde{\ell} \geq 0)\}$  then
9:      $x_I = \tilde{\ell} \cos\tilde{\omega} \tan\varphi_F$ 
10:     $y_I = \tilde{\ell} \sin\tilde{\omega} \tan\varphi_F \sin\theta - \tilde{\ell} \cos\theta$ 
11:   else
12:      $(x_I, y_I) \leftarrow \text{NULL}$ 
13:   end if
14:   Return:  $[\|\mathbf{u}_F\| (x_I, y_I)]$ 
15: end procedure

```

Algorithm 5 runs the procedure of Algorithm 4 a number of times given by the integer RUNS. The output of this iterative process is a probability value \mathbf{p}_w for each grid square $w \in \{1, \dots, |\mathbf{G}|\}$ over the structure \mathbf{G} , where \mathbf{p}_w is the probability that at least one lethal fragment will strike the grid square w . The Area of Effect (AOE) of the spray pattern is just the sum of the areas of the grid squares weighted by their respective probability values: $\text{AOE} = \sum_w \text{area}(w) \times \mathbf{p}_w$.

Algorithm 4 Get Fragment Spray Pattern

```

1: Input: A burst height  $h$ , munition terminal speed and angle ( $\|\mathbf{v}\|, \theta$ ), fragment specifications
    $\mathbf{F}$ , polar zone specifications  $\mathbf{Q}$ , a grid square map  $\mathbf{G}$ , a kinetic energy threshold  $T$ 
2: procedure GETIMPACTPATTERN( $h, \|\mathbf{v}\|, \theta, \mathbf{F}, \mathbf{Q}, \mathbf{G}, T$ )
3:    $i \leftarrow 0$ 
4:   for  $w = 1, \dots, |\mathbf{G}|$  do
5:      $\mathbf{g}_w \leftarrow 0$  ▷ Counter for the number of impact points in grid square  $w$ .
6:   end for
7:   for  $q = 1, \dots, Q$  do
8:     for  $l = 1, \dots, N_q$  do
9:        $i \leftarrow i + 1$ 
10:       $[\|\mathbf{u}_F^i\| (x_l^i, y_l^i)] \leftarrow \text{GETIMPACTPOINT}(h, \|\mathbf{u}_F\|, \|\mathbf{v}\|, \theta, \varphi_{\min}^q, \varphi_{\max}^q)$ 
11:      if  $(x_l^i, y_l^i) \neq \text{NULL}$  then
12:         $v_l^i \leftarrow \text{GETIMPACTSPEED}(h, \|\mathbf{u}_F^i\|, x_l^i, y_l^i, F_i)$ 
13:      else
14:        continue
15:      end if
16:      if  $\frac{1}{2}m_i(v_l^i)^2 \geq T$  then
17:         $\mathbf{g}_{W(x_l^i, y_l^i)} \leftarrow \mathbf{g}_{W(x_l^i, y_l^i)} + 1$  ▷  $W : \mathbb{R}^2 \rightarrow \mathbb{Z}^+$  maps impact points to grid squares.
18:      else
19:        continue
20:      end if
21:    end for
22:  end for
23:  for  $w = 1, \dots, |\mathbf{G}|$  do
24:     $\mathbf{g}_w \leftarrow \mathbb{1}_{\geq 1}(\mathbf{g}_w)$  ▷  $\mathbb{1}_{\geq 1} : \mathbb{R} \rightarrow \{0, 1\}$  is the indicator function.
25:  end for
26:  Return:  $(\mathbf{g}_1, \dots, \mathbf{g}_{|\mathbf{G}|})$ 
27: end procedure

```

Algorithm 5 Get Fragment Probability Map

```

1: Input: A burst height  $h$ , munition terminal speed and angle ( $\|\mathbf{v}\|, \theta$ ), fragment specifications
    $\mathbf{F}$ , polar zone specifications  $\mathbf{Q}$ , a grid square map  $\mathbf{G}$ , a kinetic energy threshold  $T$ , the number
   of runs ‘RUNS’
2: procedure GETPROBABILITYMAP( $h, \|\mathbf{v}\|, \theta, \mathbf{F}, \mathbf{Q}, \mathbf{G}, T, \text{RUNS}$ )
3:   for  $w = 1, \dots, |\mathbf{G}|$  do
4:      $\mathbf{h}_w \leftarrow 0$ 
5:   end for
6:   for  $R = 1, \dots, \text{RUNS}$  do
7:      $(\mathbf{g}_1, \dots, \mathbf{g}_{|\mathbf{G}|}) \leftarrow \text{GETIMPACTPATTERN}(h, \|\mathbf{v}\|, \theta, \mathbf{F}, \mathbf{Q}, \mathbf{G}, T)$ 
8:     for  $w = 1, \dots, |\mathbf{G}|$  do
9:        $\mathbf{h}_w \leftarrow \mathbf{h}_w + \mathbf{g}_w$ 
10:    end for
11:  end for
12:  for  $w = 1, \dots, |\mathbf{G}|$  do
13:     $\mathbf{p}_w = \mathbf{h}_w / \text{RUNS}$ 
14:  end for
15:  Return:  $(\mathbf{p}_1, \dots, \mathbf{p}_{|\mathbf{G}|})$ 
16: end procedure

```

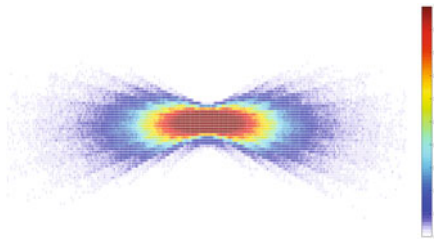


Fig. 4 The surface spray pattern for a static and level HE munition detonated from a given height and assuming a specified kinetic energy impact threshold. Notice the axial symmetry of the pattern and the faint outline of the hyperbolic boundaries between the different polar zones

6 Example Output and Discussion of Applications

The procedure given by Algorithm 5 may be used to generate a probabilistic spray pattern (or heat map) for an air bursting munition. An example of a surface spray pattern arising from the static and level detonation of a representative HE munition is shown in Fig. 4. The map was produced by using a large number of runs and a small grid size in order to produce a smooth map.⁹

In the context of calibrating the detonation trigger for electronically timed fuses, the methodology for generating surface spray patterns can be used to examine the effects produced by different ammunition types at various burst heights and angles of descent.¹⁰ Figure 5 compares the spray patterns produced by a generic HE munition at short/medium/long range with those produced by a representative IKE-ET advanced shotgun projectile [1]. From the top to the bottom of Fig. 5, the three chart-layers correspond to a short, medium and long range engagement for a given kinetic energy threshold. The AOE for both the HE and IKE-ET munition increases with range for the assumed kinetic energy impact threshold.¹¹

7 Summary and Conclusions

We have outlined a mathematical modelling approach to compare different medium-calibre ammunition options via the probabilistic spray pattern of lethal fragments on the surface (impact plane) and the calculation of the AOE. A key component of our approach is the mathematical modelling of the trajectories of individual

⁹Produced in MATLAB®.

¹⁰For example, comparing the hyper-ballistic trajectories to standard trajectories.

¹¹This is the so-called fragmentation blooming effect.

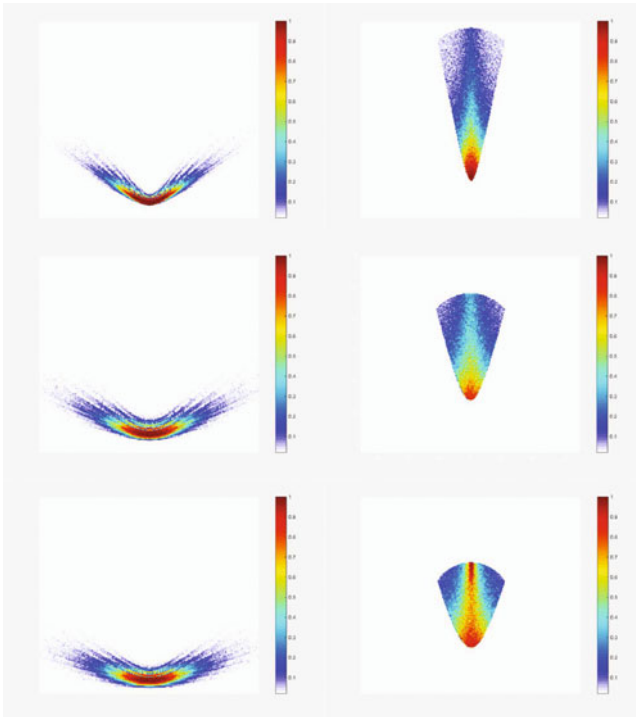


Fig. 5 A comparison between an HE munition and a representative IKE-ET shotgun projectile. Notice the forward vectoring of the HE fragments compared to the static case of Fig. 4. The enclosed pellets for the IKE-ET munition largely rely on the munition’s terminal speed for their kinetic energy. At longer range, the angle of attack increases, thus concentrating the pellets to a smaller region but with higher impact probability

fragments. The fly-out model developed in this chapter is a trade-off between analytic and detailed numerical methods and provides a good approximation to the terminal fragment speed for nearly straight line trajectories.

The methodology can be adapted to any air bursting munition for which the polar zone characterization of the fragment/shrapnel dispersion can be bounded by conical surfaces. The surface spray pattern depends on the detonation mechanism, the burst height and the munition’s terminal angle and speed. The AOE due to lethal fragments is a function of the choice of grid square size and the selection of a lethal kinetic energy threshold.

Future work could consider coupling/combining the methodology to error budgets of medium-calibre weapon systems in order to inform studies into the accuracy and effectiveness of various ammunition options.

References

1. Bland, G.: The development and testing of the improved kinetic energy electronic time (IKE-ET) round. In: Proceedings of the 2015 Armament Systems Forum. Defense Technical Information Center (2015)
2. Boon, J.K.: Probabilistic Models for Artillery Tactical Effects with Fragmentation Rounds. Technical Report DSTO-TR-1767. Defence Science and Technology Organisation, Edinburgh, South Australia (2005)
3. Carlucci, D.E., Jacobson, S.S.: Ballistics: Theory and Design of Guns and Ammunition. CRC Press, Boca Raton, Florida (2008)
4. Catovic, A., Zecevic, B., Serdarevic, S., Terzic, J.: Numerical simulations for prediction of aerodynamic drag on high velocity fragments from naturally fragmenting high explosive warheads. In: Proceedings of the 15th Seminar of New Trends in Research of Energetic Materials. Part II, pp. 475–484. University of Pardubice, Pardubice, Czech Republic (2012)
5. Chircop, P.: Projectile Trajectory Modelling for Surface Gunfire. Technical Note DSTO-TN-0914. Defence Science and Technology Organisation, Edinburgh, South Australia (2009)
6. Driels, M.R.: Weaponizing: Conventional Weapon Systems Effectiveness, 2nd edn. American Institute of Aeronautics and Astronautics Inc., Reston, Virginia (2013)
7. Gurney, R.M.: The Initial Velocities of Fragments from Bombs, Shell and Grenades. Technical Report, Defense Technical Information Center (1943)
8. Jelic, Z., Zagorecki, A., Hameed, A., Nandeecha, S.: Fragmentation and lethality analysis tool for natural and controlled fragmentation, and pre-fragmented warheads. In: Proceedings of the 27th International Symposium on Ballistics, pp. 665–675. Freiburg, Germany (2013)
9. Lloyd, R.M.: Conventional Warhead Systems Physics and Engineering Design. American Institute of Aeronautics and Astronautics Inc. (1998)
10. Miller, D.G., Bailey, A.B.: Sphere drag at Mach numbers from 0.3 to 2.0 at Reynolds numbers approaching 10^7 . *J. Fluid Mech.* **93**(3):449–464. Cambridge University Press (1979)
11. Mott, N.F.: A Theory of the fragmentation of shells and bombs. In: Fragmentation of Rings and Shells: The Legacy of N.F. Mott, pp. 243–294. Springer, Heidelberg (2006)
12. Nelhiebel, A., Paul, W.: Soldier vulnerability model. In: Proceedings of the 27th International Symposium on Ballistics, pp. 637–647. Freiburg, Germany (2013)
13. Payne, C.: Principles of Naval Weapon Systems, 2nd edn. United States Naval Institute, Annapolis, Maryland (2010)
14. Zaker, T.A.: Fragment and Debris Hazards. Technical Report, Defense Technical Information Center (1975)

Reformulations and Computational Results for the Uncapacitated Single Allocation Hub Covering Problem

Andreas T. Ernst, Houyuan Jiang, Mohan Krishnamoorthy
and Davaatseren Baatar

Abstract We study the *single allocation hub covering problem*, which is a special case of the general hub location problem and an important extension to traditional covering problems. Hubs are located at some nodes in the network and are used to facilitate (consolidate, transfer, distribute) flows. An important feature in hub location is that the transfer cost between hub nodes is discounted. The hub covering problem is to locate a minimum number of hubs such that the travel cost between each o–d pair in the network does not exceed a given threshold. We improve the best existing integer programming formulation for this problem by lifting constraints to produce facet-defining inequalities. We also develop a new formulation for the problem. The numerical results show that your new formulation performs better than existing formulations when using lifted constraints and paying special attention the number of non-zero coefficients used.

Keywords Hub cover · Location · Integer programming · Lifted constraints

A.T. Ernst (✉) · D. Baatar
School of Mathematical Sciences, Monash University, Clayton,
VIC, Australia
e-mail: Andreas.Ernst@monash.edu

D. Baatar
e-mail: Davaatseren.Baatar@monash.edu

H. Jiang
Judge Business School, University of Cambridge, Trumpington Street,
Cambridge CB2 1AG, UK
e-mail: h.jiang@jbs.cam.ac.uk

M. Krishnamoorthy
Department of Mechanical & Aerospace Engineering, Monash University,
Clayton, VIC, Australia
e-mail: Mohan.Krishnamoorthy@monash.edu

1 Introduction

Hubs form critical elements in many airline, transportation, postal, and telecommunications networks. Hubs are centralized facilities that consolidate, switch, and sort flows. Flow concentration and consolidation occur on the arcs that connect hub nodes. Hub networks provide a trade-off between cost of building and using the network: They require far less links than completely connected networks but limit the maximum number of arcs in a path to three. However, distances may still be large. Hub covering problems address this by adding a constraint on the maximum distance between any o–d pair. For recent reviews of hub location problems, see [2, 6, 7].

The most widely studied variant of hub location uses a median object to minimize total transportation cost. This can sometimes lead to large worst-case o–d distances. This is avoided in *hub center* models and in *hub covering* models, which are particularly important for delivery of perishable (time-sensitive) items. In the hub center problem, the main objective is one of minimizing the maximum distance or cost between o–d pairs. In the hub covering problem, the objective is to minimize the number of hubs that are selected in order to ensure that the maximum distance (or, cost) between o–d pairs does not exceed a given threshold.

The hub covering problem has been previously studied in [5, 13]. More recently, [16] introduced new formulations of the hub covering problem for quantity-dependent and independent discount factor. The single allocation hub covering problem (in incomplete hub networks) is considered in [1, 4]. The latest arrival hub covering problem is considered in [15]. Of these approaches, our view is that the model/approach of [16] is the most comprehensive and is considered the “state-of-the-art” approach for hub covering problems. In this current paper, we consider the uncapacitated single allocation p -hub covering problem (USAHCoP, we use “Co” (to indicate “covering”) rather than the “C” in USApHCP for hub center problems.). We show that the formulation in [16] can be tightened by lifting some of the constraints to produce facet-defining inequalities. We also introduce a new formulation and show that this performs even better.

Given a complete graph with N nodes and a *covering threshold* β , covering problems seek the minimum number of hubs so that the cost between each o–d pair does not exceed β . There are no capacities on hubs or arcs. In the USAHCoP, each non-hub node is allocated to a unique hub. Let d_{ik} be the distance between the nodes i and k . We assume that $d_{ik} = d_{ki}$ and the triangle inequality holds. Let $\alpha \in [0, 1]$ be the economic discount factor for hub arcs. The cost of any arc $[k, l]$ is αd_{kl} for hub arcs and d_{kl} otherwise. This problem has been shown to be NP-hard by [13].

2 The Uncapacitated Single Allocation Hub Covering Problem

The USAHCoP can be defined as a (quadratic) integer program using binary variables X_{ik} that are 1 iff i is allocated to hub k , with $X_{kk} = 1$ for any hub k [5]:

$$\text{USAHCoP} \quad \min \sum_{k=1}^N X_{kk} \quad (1)$$

$$\text{s.t. } X \in \mathcal{F} \equiv \{X \in \{0, 1\}^{N^2} \mid \sum_{k=1}^N X_{ik} = 1 \forall i; \text{ and } X_{ik} \leq X_{kk} \forall i, k\} \quad (2)$$

$$(d_{ik} + \alpha d_{kl} + d_{jl})X_{ik}X_{jl} \leq \beta, i, j, k, l = 1, \dots, N \quad (3)$$

The objective (1) is to minimize the total number of hubs to be used. The feasible set \mathcal{F} in (2) implies that each node is assigned to exactly one node k and k must be a hub. Constraint (3) enforces the maximum cost β between each o-d pair.

Several linearizations of (3) have been presented in the literature. For example, Campbell [5] uses binary variables $s_{ijkm} = X_{ik}X_{jm}$. [11] introduce HPC-Lin which replaces (3) with

$$(d_{ik} + \alpha d_{kl})X_{ik} + d_{jl}X_{jl} \leq \beta, \quad i, j, k, l = 1, \dots, N. \quad (4)$$

HCP-Lin has fewer variables than any other MILP formulations in the literature. Moreover, it is reported in [11] that this formulation is computationally more efficient than previous formulations. Constraint (4) can be replaced by the following strengthened constraint: $\sum_{k=1}^N (d_{ik} + \alpha d_{kl})X_{ik} + d_{jl}X_{jl} \leq \beta, \forall i, j, l = 1, \dots, N$. This strategy has been used for the hub center problem in [12], but not for USAH-CoP in [11]. We call this new formulation HCP-KT. HCP-KT is more compact than HCP-Lin since the HCP-KT has $O(N^3)$ constraints while the HCP-Lin has $O(N^4)$.

An improvement on HPC-Lin was introduced in [16], referred to as SAQI-W2. First only valid assignments (VA) are considered, based on a lower bound on cost:

$$VA = \{(i, k) \mid 2d_{ik} \leq \beta \text{ and } d_{ik} + \alpha \max_j d_{kj} \leq \beta\} \quad (5)$$

Then, some threshold constraints (4) are removed if $d_{ik} + \alpha d_{km} + d_{mj} \leq \beta$, since they are obsolete, and the remaining constraints are replaced by tighter constraints

$$X_{ik} + X_{jm} \leq 1 \quad \forall (i, k, j, m) \in IA \quad (6)$$

$$IA \equiv \{(i, k, j, m) \mid (i, k), (j, m) \in VA, i < j, \& d_{ik} + \alpha d_{km} + d_{mj} > \beta\}. \quad (7)$$

Constraints (6) are tightened by aggregating the constraints. A heuristic was proposed to aggregate the constraints in [16]. The resulting formulation consisting of (1) and (2) plus the constraints produced by Algorithm 2.1 is referred to as **SAQI-W2**.

Algorithm 2.1 Heuristic for Aggregating Constraints

Let $M = \{(k, m) \mid (i, k, j, m) \in IA\}$
while $M \neq \emptyset$ **do**
 $\bar{k} := \arg \max_k |\{(k, m) \mid (k, m) \in M\}|$, and $\bar{m} := \arg \max_m |\{(k, m) \mid (k, m) \in M\}|$
if $|\{m \mid (\bar{k}, m) \in M\}| < |\{k \mid (k, \bar{m}) \in M\}|$ **then**
 add constraints $\sum_{k:(k,\bar{m}) \in M} X_{ik} + X_{j\bar{m}} \leq 1$, and set $M := M \setminus \{(k, \bar{m}) \mid (k, \bar{m}) \in M\}$
else
 add constraints $X_{i\bar{k}} + \sum_{m:(\bar{k},m) \in M} X_{jm} \leq 1$, and set $M := M \setminus \{(\bar{k}, m) \mid (\bar{k}, m) \in M\}$
end if
end while

SAQI-W2 is, in our view, the current “state of the art.” It is smaller than HCP-Lin, and the constraints are tighter. Note that size depends on the value of β .

We now propose a new two-index formulation for the USAHCoP based on a concept which we define as the *radius of hubs* [8]. Let r_k be a nonnegative variable representing the radius of hub k (largest distance to any node allocated to k). Then, USAHCoP can be formulated as:

$$\text{USAHCoP-r} \quad \min \sum_{k=1}^N X_{kk} \quad (8)$$

$$\text{s.t.} \quad X \in \mathcal{F} \quad (9)$$

$$r_k \geq d_{ik} X_{ik}, \quad i, k = 1, \dots, N \quad (10)$$

$$r_k + r_m + \alpha d_{km} \leq \beta, \quad k, m = 1, \dots, N \quad (11)$$

Constraint (10) indicates that the radius of a hub is the maximum distance to any node allocated to the hub. Constraint (11) replaces (4). USApHCoP-r permits $r_k > 0$ for $X_{kk} = 0$. However for any optimal solution (X_{ik}^*, r_k^*) , we can construct a new optimal solution (X_{ik}^*, r_k^+) such that $r_k^+ = \max_j d_{jk} X_{jk}^*$. Constraint (11) is still valid $X_{kk} = 0$ or $X_{mm} = 0$ because $\alpha \leq 1$ and the triangle inequality holds.

3 Conflict Graph

Let us consider the *conflict graph* $\mathcal{G} = (\mathcal{V}, \mathcal{E})$ where the nodes represent the variables X_{ik} , and two nodes X_{ik} and X_{jm} are connected by an edge $e = (X_{ik}, X_{jm})$ iff those two assignments cannot be realized at the same time:

$$\mathcal{E} = \{(X_{ik}, X_{jm}) \mid (i, k, j, m) \in IA \text{ or } i = j, k \neq m \text{ or } k = j \neq m \text{ or } m = i \neq k\} \quad (12)$$

The first condition (IA) derives from the threshold β , the second from single allocation, and the last two prevent allocation to non-hubs. Conflict graphs can be used effectively to generate valid strong cuts and facet-defining inequalities. From the definition of \mathcal{E} , it is obvious that the following holds.

Proposition 1 *Let $\mathcal{S} \subseteq \mathcal{V}$ be a clique of \mathcal{G} , then all feasible solutions satisfy:*

$$\sum_{X_{ik} \in \mathcal{S}} X_{ik} \leq 1. \tag{13}$$

We refer to (13) as a *clique constraints*. One can easily show that the constraints obtained by the Algorithm 2.1 are indeed clique constraints. We expect larger cliques to provide tighter constraints. We say a clique is a *maximal clique* if it cannot be extended any further. We give a brief summary of the theory and show that maximal cliques give facet-defining inequalities, though similar results have been shown for set packing and clique polytopes previously (see [3, 14]). In order to make the exposition easier, we will consider the integer polytope

$$\mathcal{P} = \text{conv}(\{X \in \{0, 1\}^{N^2} \mid \sum_{k=1}^N X_{ik} \leq 1 \forall i; X_{ik} \leq X_{kk} \forall i, k; \text{ and (4) holds}\}) \tag{14}$$

This is a full-dimensional polytope and a slight relaxation of the original problem where nodes may not be allocated anywhere. It is equivalent to the original problem if we subtract a sufficiently large constant from all of the variable costs (effectively maximizing the number of nodes allocated and then minimizing hubs).

Theorem 1 *If \mathcal{S} is a maximal clique of the graph $\mathcal{G} = (\mathcal{V}, \mathcal{E})$ then the corresponding clique constraint (13) is a facet-defining inequality for the polytope \mathcal{P} .*

Proof First note that $0 \in \mathcal{P}$. Let $x(i, k)$ denote the vector x such that $x_{ik} = 1$ and $x_{kk} = 1$ (or $i = k$) but all other elements are zero. Assume w.l.o.g. that $x(i, k) \in \mathcal{P}$ for all $(i, k) \in \mathcal{V}$, as otherwise (i, k) and perhaps (k, k) can be removed from \mathcal{V} to give an equivalent problem. Hence, the number of dimensions of the set of convex combinations of points in \mathcal{P} is equal to the number of variables, i.e., $\dim(\text{conv}(\mathcal{P})) = |\mathcal{V}| \leq N^2$.

We will now show that there are $|\mathcal{V}|$ linearly independent solutions that satisfy (13) with equality. Clearly $x(i, k)$ lies on the constraint for $(i, k) \in \mathcal{S}$. Now

$$\forall (j, l) \in \mathcal{V} \setminus \mathcal{S}, \exists (p, q) \in \mathcal{S} : x(j, l) + x(p, q) \in \mathcal{P}.$$

This is easy to see since if no such (p, q) were to exist then (p, q) could be added to the clique, but \mathcal{S} is already maximal. Obviously the set of all such $x(i, k)$ and $x(j, l) + x(p, q)$ are linearly independent thus proving the result. ■

Generating all such maximal cliques is in general too computationally expensive and leads to an excessive number of constraints. For our computational experiments,

we will restrict ourselves to extending the constraints from Algorithm 2.1 into maximal clique constraints. A branch and cut approach would also be possible, though separating maximum clique cuts is non-trivial. This gives rise to the formulation:

$$\text{SAQI-Cliq} \quad \min \sum_{k=1}^N X_{kk} \quad (15)$$

$$\text{s.t.} \quad X \in \mathcal{F} \quad (16)$$

$$\sum_{(i,k) \in C} X_{ik} \leq 1 \quad C \in \mathcal{C} \quad (17)$$

The set of cliques \mathcal{C} is generated by starting with Algorithm 2.1 and performing lifting. We test all other (i, k) pairs in a random order to see if they can be are incompatible with existing $(j, l) \in \mathcal{C}$, i.e., $(X_{ik}, X_{jl}) \in \mathcal{C}$ defined in (12).

4 Numerical Experiments

We tested our algorithms for both the USAHCoP with distances from the AP¹ data set [10] and Turkish² highway data [15]. We tested the models with different threshold values of β . After solving a problem, the value of β is chosen for the next instance by multiplying β with 0.95 if the problem is feasible and by 1.25 otherwise. In this way, we were able to test the problem for different (loose/tight) threshold values. As an initial value of β , we used the average of the maximum distances of the nodes. If the threshold is too tight, the problem is infeasible and both approaches detected it quickly. Therefore, we did not include infeasible problem instances in the following tables. We used CPLEX 12.1 carried out on a Linux computer with four quad-core Intel Xeon processors running at 2.93 GHz and 64 GB of RAM.

First, we compared USAHCoP-r against SAQI-W2. Some preliminary analysis showed that CPLEX's cut generation at the root, while effective in raising the lower bound, generally made the overall solution times worse. Hence, we turned off all cut generation. To obtain root node values, we invoke CPLEX twice, first with branch and bound nodes limited to zero, then with a CPU time limit of 1800 s. Times reported below are for the total CPU time across all processors.

Numerical results are shown in Tables 1, 2, 3, 4, and 5. The labels of the columns are as follows: β = threshold value; p^* = optimal number of hubs; LB = the lower bound at the root node; t_{root} = time to solve the root node; t_{all} = total CPU time including model formulation (finding cliques); B&B = the number of nodes in the branch and bound tree; NZ = number of nonzero coefficients in this model. NZ appears to be better correlated with solve time than the number of rows or columns.

¹Available from the OR Library www.people.brunel.ac.uk/~mastjbb/jeb.

²Available at www.bilkent.edu.tr/~bkara/hubloc.htm (accessed Sep. 2016).

Table 1 AP data: 50 nodes, $\alpha = 0.75$. For USAHCoP-r, NZ = 17, 250

β	p*	USAHCoP-r					SAQI-W2					SAQI-Cliq				
		LB	B&B	t_{all}	t_{root}	LB	B&B	t_{all}	t_{root}	NZ	LB	B&B	t_{all}	t_{root}	NZ	
51174.7	5	5.0	0	0.09	0.06	5.0	0	0.1	0.08	11,994	5.0	0	0.46	0.17	30,210	
51308.8	5	5.0	0	0.09	0.06	5.0	0	0.12	0.1	14,431	5.0	0	0.88	0.53	38,324	
52102.6	5	5.0	0	0.09	0.06	5.0	0	0.13	0.11	18,404	5.0	0	2.21	1.66	50,545	
53047.4	4	4.0	0	0.12	0.07	4.0	0	0.19	0.17	21,751	4.0	0	2.7	2.08	63,707	
53868.1	4	4.0	0	0.1	0.07	4.0	0	0.32	0.3	28,131	4.0	0	3.41	2.6	82,562	
54009.3	4	4.0	0	0.19	0.09	4.0	0	0.36	0.33	28,866	4.0	0	4.1	3.28	85,306	
54844.9	4	4.0	0	0.18	0.08	4.0	0	0.61	0.52	35,624	4.0	0	12.14	11.03	10,8091	
55839.4	4	4.0	0	0.18	0.12	4.0	0	0.95	0.86	42,006	4.0	0	7.48	6.13	129,006	
56703.3	4	3.12	14	0.43	0.07	3.67	0	1.61	1.09	48,174	3.67	7	24.53	15.5	146,322	
56851.9	4	3.0	4	0.32	0.08	3.67	0	2.25	1.91	49,090	3.6	0	33.78	18.61	146,169	
57731.5	4	3.0	11	0.31	0.1	3.5	6	10.46	1.61	56,318	3.44	0	31.16	26.69	162,456	
58778.3	4	3.0	43	0.61	0.12	3.0	0	3.26	2.11	66,335	3.19	0	56.24	52.12	195,083	
59687.7	4	3.0	40	0.57	0.14	3.0	3	6.69	2.8	75,105	3.08	0	61.04	56.82	208,171	
59844.1	4	3.0	32	0.65	0.15	3.0	3	11.91	5.0	75,362	3.07	0	57.21	52.28	210,614	
60770.0	3	3.0	0	0.31	0.13	3.0	0	4.01	3.33	89,592	3.0	0	37.73	30.88	266,315	
61871.9	3	3.0	0	0.23	0.13	3.0	0	4.66	4.0	102,501	3.0	0	144.74	138.95	300,028	
62993.8	3	2.0	70	2.62	0.14	2.5	0	4.69	2.32	111,834	2.5	0	159.97	140.23	313,608	

Table 2 AP data: $\alpha = 0.75$. Comparisons of the SAQI-Min formulation for AP data sets with 50 and 100 nodes

n	SAQI-W2							SAQI-Min						
	β	p*	LB	B&B	t_{all}	t_{root}	NZ	p*	LB	B&B	t_{all}	t_{root}	NZ	
50	56703.3	4	3.67	0	1.55	1.09	48,174	4	3.67	0	3.71	1.59	32,073	
50	56851.9	4	3.67	0	2.21	1.91	49,090	4	3.67	0	1.99	1.67	32,784	
50	57731.5	4	3.5	6	10.4	1.61	56,318	4	3.33	0	2.81	2.2	36,989	
50	58778.3	4	3.0	0	3.19	2.11	66,335	4	3.11	0	2.36	1.88	42,916	
50	59687.7	4	3.0	3	6.61	2.8	75,105	4	3.0	0	4.57	2.74	48,635	
50	59844.1	4	3.0	3	11.83	5.0	75,362	4	3.0	0	10.53	2.7	48,861	
50	60770.0	3	3.0	0	3.93	3.33	89,592	3	3.0	0	4.51	3.88	56,938	
50	61871.9	3	3.0	0	4.57	4.0	102,501	3	3.0	0	22.57	5.62	64,164	
50	62993.8	3	2.5	0	4.59	2.32	111,834	3	2.5	0	9.96	5.63	70,015	
100	52376.0	7	7.0	0	4.72	4.51	158,901	7	7.0	0	4.84	4.65	102,934	
100	55132.6	5	4.43	5	1711.32	12.23	323,942	5	4.33	0	221.42	121.94	209,514	
100	58034.4	13 ^a	3.38	0	1800.62	120.78	581,868	4	3.5	0	672.35	421.54	363,459	
100	61088.8	4 ^a	3.0	0	1800.43	628.36	92,0721	11 ^a	3.0	0	1802.15	1047.7	572,353	

^aThe best heuristic value found in 1800 s

Table 3 AP data with 50 nodes $\alpha = 0.75$. Comparisons of all three SAQI variants using plain branch and bound (all preprocessing, cuts and heuristics turned off)

β	p*	SAQI-W2				SAQI-Cliq				SAQI-Min			
		LB	B&B	t_{all}	t_{root}	LB	B&B	t_{all}	t_{root}	LB	B&B	t_{all}	t_{root}
51174.7	5	5.0	2	1.88	0.12	5.0	0	0.68	0.36	5.0	0	0.3	0.1
51308.8	5	5.0	0	0.1	0.08	5.0	0	0.59	0.19	5.0	0	0.5	0.26
52102.6	5	5.0	0	0.25	0.22	5.0	0	0.75	0.2	5.0	0	0.61	0.32
53047.4	4	4.0	0	0.27	0.22	4.0	0	1.0	0.31	4.0	2	2.68	0.52
53868.1	4	4.0	0	0.27	0.24	4.0	0	1.46	0.56	4.0	0	0.96	0.42
54009.3	4	4.0	0	0.42	0.35	4.0	0	1.33	0.4	4.0	0	1.74	1.17
54844.9	4	4.0	0	0.56	0.48	4.0	1	3.46	1.5	4.0	0	0.89	0.21
55839.4	4	4.0	0	0.59	0.5	4.0	0	2.52	0.79	4.0	0	1.14	0.3
56703.3	4	3.5	2	14.27	0.61	3.67	4	30.82	1.61	3.67	3	5.32	0.37
56851.9	4	3.33	3	21.46	0.75	3.6	3	26.45	1.92	3.57	11	12.4	0.45
57731.5	4	3.12	10	24.28	1.0	3.44	4	50.97	2.59	3.25	7	10.18	0.53
58778.3	4	3.0	7	35.61	1.25	3.19	8	161.16	3.48	3.0	7	28.71	0.74
59687.7	4	3.0	104	756.79	1.04	3.08	7	226.02	5.5	3.0	15	63.2	0.78
59844.1	4	3.0	24	67.61	0.74	3.07	8	203.02	5.62	3.0	22	73.9	1.04
60770.0	3	3.0	11	29.41	1.16	3.0	0	9.31	5.71	3.0	2	13.71	0.8
61871.9	3	3.0	3	27.32	0.99	3.0	0	11.61	7.56	3.0	0	3.15	0.92
62993.8	3	2.12	4	48.69	2.03	2.5	3	253.75	8.51	2.5	5	22.82	2.23

Table 4 USAHCoP-r results for large AP data sets with 100 and 200 nodes, $\alpha = 0.75$

n	β	p^*	LB	B&B	t_{all}	t_{root}	NZ
100	52376.0	7	6.0	31	3.17	0.53	69,500
100	55132.6	5	4.0	36	4.73	0.7	69,500
100	58034.4	4	3.0	13	3.46	0.77	69,500
100	61088.8	3	3.0	78	23.19	1.2	69,500
200	57672.9	6	5.0	151	1167.1	8.08	279,000
200	60708.3	4	4.0	257	1189.37	12.84	279,000
200	63903.5	4	3.0	165	1871.56	11.01	279,000
200	64892.1	3	2.0	85	551.99	10.29	279,000
200	65062.2	3	2.0	183	1610.0	10.04	279,000
200	66068.8	3	2.0	78	536.8	14.82	279,000
200	67266.8	3	2.0	103	1483.32	18.41	279,000
200	68486.6	2	2.0	100	726.63	25.51	279,000
200	69546.1	2	2.0	4	69.75	30.37	279,000
200	70807.2	2	2.0	90	1195.72	26.49	279,000
200	73206.4	2	2.0	0	35.55	19.47	279,000
200	74533.9	2	2.0	51	350.14	42.52	279,000
200	77059.4	1	1.0	0	22.34	18.63	279,000

Comparison of SAQI formulation variants. The SAQI-W2 model has fewer variables than USAHCoP-r and in some cases, fewer nonzeros. Table 1 presents the results for AP instances with with 50 nodes. It shows that the solution time for the root node and hence overall solution times are competitive for SAQI-W2 when the number of nonzeros is less than for USAHCoP-r. However as NZ increases, the solution times slow down significantly. This is also true when going from SAQI-W2 to SAQI-Cliq which have identical number of constraints and variables but different number of coefficients due to the lifting in of additional variables into the clique constraints. Similar patterns were observed for 40-node data sets (not shown here).

In fact, the increase in computation costs is surprising. Comparing SAQI-W2 and SAQI-Cliq which have the same formulation except for the additional coefficients in the clique constraints, we see a threefold increase in the number of coefficients leading to an increase in the root node solve time by a factor of 10 or more.

There are also some peculiar instances in Table 1 such as for $\beta = 56851.9$ and $\beta = 57731.5$, where the lower bound at the root nodes is slightly larger for SAQI-W2 than for the tighter formulation SAQI-Cliq. While CPLEX has been prevented from adding cuts, it still carries out preprocessing. There are significant differences in how effectively the two formulations are preprocessed. For example, for $\beta = 57731.5$ the number of rows is reduced to 9,198 for SAQI-W2 but only to 16,517 for SAQI-Cliq even though both start off with 17,437 constraints initially. Interestingly CPLEX reports that after preprocessing, SAQI-W2's number of nonzero coefficients had increased by about 15% while for SAQI-Cliq it had reduced by about 17%. We

Table 5 USAHCoP-r results for the Turkish data with 81 cities. Columns SW and SM indicate the solution status for SAQI-W2 and SAQI-Min, respectively. *I* Infeasible; – Failed to complete even the root node; *R* Root node solved only; *H* Heuristic solution found; *O* Solved to optimality

β	$\alpha = 0.6$										$\alpha = 0.7$									
	p^*	LB	B&B	t_{all}	t_{root}	SW	SM	p^*	LB	B&B	t_{all}	t_{root}	SW	SM						
1518.4	4	2.0	1197	707.79	0.25	H	H	7	5.5	363	14.69	0.18	O	O						
1598.3	4	2.0	368	28.59	0.37	H	H	5	3.12	76	4.28	0.24	H	H						
1602.5	4	2.0	342	40.88	0.4	H	H	5	3.12	69	4.08	0.25	H	H						
1627.3	4	2.0	294	26.68	0.51	H	H	5	3.0	475	22.06	0.29	H	H						
1686.9	3	2.0	251	31.18	0.64	H	H	4	2.0	238	19.73	0.33	H	H						
1708.5	3	2.0	203	27.64	0.75	R	H	4	2.0	447	34.45	0.41	H	H						
1739.5	3	2.0	109	19.06	0.84	H	R	3	2.0	27	2.64	0.39	H	H						
1744.0	3	2.0	273	18.32	0.86	R	H	3	2.0	37	4.52	0.47	H	H						
1775.7	2	2.0	22	2.8	0.92	H	R	3	2.0	29	2.87	0.64	H	H						
1807.8	2	2.0	5	3.21	1.79	–	R	3	2.0	97	4.71	0.96	H	O						
1835.8	2	2.0	7	2.48	1.12	–	–	3	2.0	231	27.59	1.25	–	H						
1869.1	2	2.0	15	3.71	1.83	–	R	2	2.0	31	4.82	1.2	R	H						
1927.4	2	2.0	4	2.71	1.13	–	–	2	2.0	7	2.18	0.77	H	H						
1962.3	2	2.0	0	2.03	1.2	–	–	2	2.0	0	2.46	1.05	O	R						
1967.5	2	2.0	6	3.63	2.04	–	R	2	2.0	0	2.04	1.24	R	R						
2028.8	2	2.0	0	2.25	1.26	–	–	2	2.0	0	1.73	1.19	R	R						

(continued)

Table 5 (continued)

β	$\alpha = 0.6$										$\alpha = 0.7$											
	p^*	LB	B&B	t_{all}	t_{root}	SW	SM	p^*	LB	B&B	t_{all}	t_{root}	SW	SM	p^*	LB	B&B	t_{all}	t_{root}	SW	SM	
2071.0	2	2.0	11	4.14	2.12	-	-	2	2.0	0	1.95	1.32	-	R	2	2.0	0	1.95	1.32	-	R	
2180.0	1	1.0	0	1.39	0.96	-	O	1	1.0	0	1.32	0.9	-	-	1	1.0	0	1.32	0.9	-	-	
$\alpha = 0.8$																						
1686.9	6	5.09	0	0.46	0.22	O	O															
1708.5	6	4.0	46	1.44	0.22	O	O															
1739.5	6	4.0	568	33.34	0.26	O	O															
1744.0	5	4.0	256	6.39	0.23	H	H															
1775.7	4	3.0	222	13.42	0.35	O	O															
1807.8	4	2.0	99	2.85	0.28	H	O															
1835.8	3	2.0	38	2.83	0.45	H	O															
1869.1	3	2.0	83	13.88	0.67	H	H	4	4.0	0	0.45	0.25	O	O	4	4.0	0	0.45	0.25	O	O	O
1927.4	2	2.0	53	3.37	0.61	H	O	3	2.0	23	0.94	0.24	O	O	3	2.0	23	0.94	0.24	O	O	O
1962.3	2	2.0	11	1.91	0.92	H	H	3	2.0	25	1.36	0.37	O	O	3	2.0	25	1.36	0.37	O	O	O
1967.5	2	2.0	6	2.46	1.5	H	O	3	2.0	21	1.64	0.33	O	O	3	2.0	21	1.64	0.33	O	O	O
2028.8	2	2.0	47	2.95	0.87	O	H	2	2.0	15	2.11	0.75	O	O	2	2.0	15	2.11	0.75	O	O	O
2071.0	2	2.0	0	1.09	1.0	H	O	2	2.0	0	1.08	0.7	O	O	2	2.0	0	1.08	0.7	O	O	O
2180.0	1	1.0	0	1.16	0.77	O	O	1	1.0	0	0.92	0.6	O	O	1	1.0	0	0.92	0.6	O	O	O

conjecture that these differences in preprocessing are the causes for the exceptions in the lower bound and may partly be the reason why SAQI-Cliq performs so much worse than the original SAQI-W2.

The reduced SAQI Formulation. Empirical results suggest the possibility of improving the performance by taking the opposite approach. Carry out “inverse-lifting” to reduce the number of coefficients and minimize the size of the formulation at the expense of tightness. The formulation SAQI-Min uses constraints constructed as follows: (1) Generate constraints using Algorithm 2.1 as for SAQI-W2. (2) Extend these constraints into maximal cliques in a randomized way as for SAQI-Cliq but only add variables if they violate the threshold with at least one existing variable. (3) Go through all constraints in order of decreasing clique size and remove any variables that are not required for logical correctness. So, we remove a variable X_{ik} if for every other X_{jl} in the constraint the distance threshold (3) holds or the same pair X_{ik}, X_{jl} already appears in an earlier constraint.

Table 2 shows that while the reduced formulation size can have a positive effect on solution times, this is not always the case. There appears to be very little correlation between formulation size and the time taken to solve the root node. For example, the instance with $n = 50$, $\beta = 59844.1$ where the number of coefficients has been reduced by 35% and the root node run time nearly halved. On the other hand, $n = 50$, $\beta = 62993.8$ where the number of coefficients was reduced by a slightly larger percentage the root node solve time more than doubled. This is despite the fact that even after preprocessing, the SAQI-Min MILP was much smaller (12,482 rows, 1,834 columns, and 80,703 nonzeros) than the SAQI-W2 MILP (22,063 rows, 1,834 columns, and 127,210 nonzeros). Even where there are significant differences in the CPU times, these appear to be more due to “luck” in find a good heuristic solution with no obvious connection to properties of the two formulations.

Results for plain branch and bound. The curious anomalies mentioned above in the relationship between the types of constraints used, the root lower bound, and run time deserve further investigation. To eliminate the effects of some of the sophisticated preprocessing, cutting, and heuristic solution methods that are included in CPLEX, we decided to turn off all of these. In addition, we stopped CPLEX from choosing the root node solution algorithm automatically by fixing this to the primal simplex method.

The new results shown in Table 3 indicate that for this plain version of the MILP solver, the anomalies disappear. The strengthened constraints always produce a tighter lower bound. Interestingly, the reduced version in which coefficients were dropped from the maximum clique constraints still produce lower bounds that are at least as good and sometimes better than the original formulation. The run times for the root lower bound also agree more closely with the difference in the number of nonzero coefficients (note that the “NZ” columns have not been shown as they are identical to those in Tables 1 and 2). The overall run time is slightly less predictable since it partly depends on when the branch and bound finds the optimal solution. However, overall the SAQI-Min formulation with the reduced set of cuts appears to be the most effective.

Results for USAHCoP-r on large instances. Given the poor performance of the different SAQI variants, we only provide detailed results for large instances using the USAHCoP-r formulation. Indeed for 200-node AP data sets, none of the SAQI variants were able to solve any of the instances and in most cases failed to even solve the root node. Table 4 shows that the USAHCoP-r managed to solve all of these problems, though in the case of $n = 200$, $\beta = 63903.5$ CPLEX reported using slightly more CPU time than the time limit of 1800s given to it. As CPLEX was run with multiple threads, the elapsed (wall-clock) time is often significantly less than the CPU times. In fact, the only problem that required more than 500s of real time was $n = 200$, $\beta = 67266.8$ which took 707.55 s. The only 200-node instance for which SAQI-W2 solved the root node within the 1800s time limit was for $\beta = 57672.9$ where it obtained a lower bound of 5.67 in 1624.04 s.

The approaches have been tested on the Turkish data with β defined in the same way as for AP. For each β , we tried $\alpha = 0.6, 0.7, 0.8$, and 0.9 . For some combinations of α and β with no feasible solutions, the corresponding parts of the table are left blank. The results are in Table 5. For SAQI-W2 and SAQI-Min, we only show the solution status at the 1800s limit (i.e., whether CPLEX managed to solve the root node or to solve the instance to optimality). We indicate where we find at least a non-trivial heuristic solution. CPLEX starts with the trivial solution of making every node a hub and only after some time finds a better solution (with <10 hubs).

The results indicate that SAQI-Min tends to perform slightly better than SAQI-W2. However, the results are not consistent nor the differences very large. For example, for $\alpha = 0.7$, $\beta = 1962.3$, SAQI-W2 found the optimal solution but it took 1041.9s almost all of which were required to solve the root node requiring just 1s to find the optimal solution with a root node heuristic. On the other hand, SAQI-Min which had far fewer rows and nonzero coefficients took 1444.6s for the root node and found no heuristic solution in the remaining time. To get an indication of the difference in solution quality between the different formulations, we calculated the average number of hubs over all instances where both SAQI-W2 and SAQI-Min at least found a non-trivial heuristic solution. This gives 5.10 hubs for SAQI-W2 and 4.41 for SAQI-Min, though the optimal solutions found by USAHCoP-r require only 3.38 hubs on average for these instances.

It is clear that the USAHCoP-r formulation performed very well on a range of problems that could not be solved using SAQI-W2 and SAQI-Min. The only instance for which USAHCoP-r required more than 1 min of CPU time was with $\alpha = 0.6$ and $\beta = 1518.4$. Here, the lower bound was quite weak. However even though SAQI-W2 and SAQI-Min could both obtain a stronger lower bound (2.86 and 3.48, respectively), they each only found a heuristic solution with six hubs without being able to complete the branch and bound within the time limit.

5 Concluding Remarks

We have considered a previously published [16] formulation for the single allocation hub covering problem (USAHCoP) and shown that this could be tightened by lifting some of the constraints. We have also proven that the lifted constraints are facet-defining. However, in computational experiments, it is shown that this lifting of the constraints actually has a negative impact on the computational performance when solving the MILPs using a recent version of the CPLEX MILP solver. A better outcome can often be achieved by first lifting the constraints and then paring back the coefficients to get a minimal set of constraints. However in comparing different formulation variants empirically, the actual effectiveness of the formulation depends not only on their size and tightness but also on how it interacts with the CPLEX MILP algorithms including preprocessing, cutting, and heuristics.

A new formulation for USAHCoP has been proposed based on the radius concept. It uses auxiliary variables for the maximum distance between hubs and their nodes. This formulation, while slightly weaker than any of the others, is much more compact and was shown empirically to perform better, a similar conclusion found for other hub problems [9, 10]. Using the new formulation, instances with up to 200 nodes were solved that were previously out of reach for exact solution approaches.

Further work will be required to see whether the facet-defining inequalities for USAHCoP can be used to produce higher performing algorithms. For example, it may be possible to develop a branch and cut approach to exploit the stronger constraints without paying as larger a price for the exponential growth in the number of such constraints and nonzero coefficients.

References

1. Alumur, S.A., Kara, B.Y., Karasan, O.E.: The design of single allocation incomplete hub networks. *Transp Res Part B* **43**(10), 936–951 (2009)
2. Alumur, S.A., Kara, B.Y., Karasan, O.E.: Multimodal hub location and hub network design. *Omega* **40**(6), 927–939 (2012). Special Issue on Forecasting in Management Science
3. Atamturk, A., Nemhouser, G.L., Savelsbergh, M.: Conflict graphs in integer programming. *Eur. J. Oper. Res.* **121**, 40–55 (2000)
4. Calik, H.S., Alumur, A., Kara, B.Y., Karasan, O.E.: A tabu search based heuristic for hub covering problem over incomplete hub networks. *Comput. Oper. Res.* **36**(12), 3088–3096 (2009)
5. Campbell, J.F.: Integer programming formulations of discrete hub location problems. *Eur. J. Oper. Res.* **72**, 387–405 (1994)
6. Campbell, J.F., O’Kelly, M.E.: Twenty-five years of hub location research. *Transp. Sci.* **46**(2), 153–169 (2012)
7. Contreras, I.: Hub location problems. In: Laporte, G., Nickel, S., Gama, F.S.d. (eds.) *Location Science*, pp. 311–344. Springer International Publishing (2015). 00039
8. Ernst, A.T., Hamacher, H., Jiang, H., Krishnamoorthy, M., Woeginger, G.: Uncapacitated single and multiple allocation p -hub center problems. *Comput. Oper. Res.* **36**, 2230–2241 (2009)
9. Ernst, A.T., Krishnamoorthy, M.: Efficient algorithms for the uncapacitated single allocation p -hub median problem. *Locat. Sci.* **4**, 139–154 (1996)

10. Ernst, A.T., Krishnamoorthy, M.: Exact and heuristic algorithms for the uncapacitated multiple allocation p -hub median problem. *Eur. J. Oper. Res.* **104**(1), 100–112 (1998)
11. Kara, B.Y., Tansel, B.: On the single assignment p -hub center problem. *Eur. J. Oper. Res.* **125**(3), 648–655 (2000)
12. Kara, B.Y., Tansel, B.: The latest arrival hub location problem. *Manage. Sci.* **47**(10), 1408–1420 (2001)
13. Kara, B.Y., Tansel, B.: The single-assignment hub covering problem: models and linearizations. *J. Oper. Res. Soc.* **54**(1), 59–64 (2003)
14. Padberg, M.: On the facial structure of set packing polyhedra. *Math. Program.* **5**, 199–215 (1973)
15. Tan, P.Z., Kara, B.Y.: A hub covering model for cargo delivery systems. *Networks* **49**(1), 28–39 (2007)
16. Wagner, B.: Model formulations for hub covering problems. *J. Oper. Res. Soc.* **59**(7), 932–938 (2008)

Search Strategies for Problems with Detectable Boundaries and Restricted Level Sets

Hanyu Gu, Julia Memar and Yakov Zinder

Abstract The chapter is concerned with a class of discrete optimisation problems which includes a number of classical *NP*-hard scheduling problems. The considered solution method is an iterative procedure that at each iteration, it computes a lower bound on the optimal objective value and searches for a feasible solution attaining this bound. The chapter describes three search methods—descending search, ascending search, and their combination. These methods are illustrated by considering their implementations for the unit execution time unit communication delay maximum lateness problem with parallel identical machines. The resultant algorithms are compared by means of computational experiments.

Keywords Discrete optimization • Scheduling theory • Exact methods • Maximum lateness

1 Introduction

The class of discrete optimisation problems considered below has been originally introduced in [2]. This class includes a number of well-known *NP*-hard scheduling problems (see [2, 4]) and is defined by the following properties of the objective function and feasible region. The objective function $F(x_1, x_2, \dots, x_n)$ is a non-decreasing function defined on the n -dimensional hypercube of points with integer coordinates, satisfying the inequalities $0 \leq x_i \leq p(n)$, $1 \leq i \leq n$, where p is a polynomial. It is assumed that $p(n)$ is integer. The objective function F should be minimised on a subset X of the above hypercube, satisfying the condition stated below as

H. Gu · J. Memar (✉) · Y. Zinder
University of Technology, PO Box 123, Broadway, Sydney, NSW 2007, Australia
e-mail: julia.memar@uts.edu.au

H. Gu
e-mail: hanyu.gu@uts.edu.au

Y. Zinder
e-mail: yakov.zinder@uts.edu.au

Property 1. In addition, it is assumed that F has two properties, stated below as Properties 2 and 3.

Two of these three properties are based on the following notion of dominance. A point $a = (a_1, a_2, \dots, a_n)$ dominates point $b = (b_1, b_2, \dots, b_n)$ if $b_i \leq a_i$ for all $1 \leq i \leq n$ and at least one of these inequalities is strict. The property of the feasible region X is concerned with its boundary, where the boundary of X is the set of all points in X which do not dominate any other point in X .

Property 1 There is an algorithm which for any point in X in polynomial time determines whether or not this point is on the boundary of X .

The Property 2 uses the notions of a \bar{F} -dominant set and a level set. For any value \bar{F} of F , a set D in the domain of F is \bar{F} -dominant if $F(x_1, x_2, \dots, x_n) = \bar{F}$ for all $(x_1, x_2, \dots, x_n) \in D$, and if $F(y_1, y_2, \dots, y_n) = \bar{F}$ and $(y_1, y_2, \dots, y_n) \notin D$ imply that there exists a point in D which dominates (y_1, y_2, \dots, y_n) . For any value \bar{F} of F , a level set, denoted by $A(\bar{F}, F)$, is an \bar{F} -dominant set with the smallest cardinality among all \bar{F} -dominant sets. It can be shown (see [2, 4]) that for any value \bar{F} of F , the corresponding level set is unique.

Property 2 For any value \bar{F} of F , the corresponding level set can be found in polynomial time.

The third property, which specifies the considered class of discrete optimisation problems, is also related to F .

Property 3 For any value F' of F such that $F' < F(p(n), \dots, p(n))$, the smallest value of F , which is greater than F' , can be found in polynomial time.

The optimisation procedure, presented in [2, 4], is an iterative algorithm that at each iteration uses some lower bound on the optimal value of F . All lower bounds belong to the range of F . Of course, $F(0, \dots, 0)$ can be taken as an initial lower bound, but a tighter bound may improve the convergence. At each iteration with some lower bound \bar{F} , the optimisation procedure searches for a feasible point dominated by one of the elements constituting $A(\bar{F}, F)$. Property 2 guarantees that all elements of $A(\bar{F}, F)$ can be enumerated in polynomial time, and the optimisation procedure uses them in succession. If a feasible point, dominated by some element of $A(\bar{F}, F)$, has been found, the optimisation procedure terminates with this point as an optimal solution. Otherwise, using Property 3, the optimisation procedure finds a new lower bound and starts a new iteration.

Search for a feasible point, dominated by an element of $A(\bar{F}, F)$, can be conducted in several different ways. This gives rise to three different approaches—descending, ascending, and descending-ascending search methods. The approach, presented in [2, 4], will be referred to as descending. In all three approaches, each $(a_1, \dots, a_n) \in A(\bar{F}, F)$ initiates a search tree, where all nodes correspond to points in the domain of F . The difference between the descending, ascending, and descending-ascending approaches is in the method of constructing the search tree. These three methods are presented below.

2 Descending Method

According to the descending method, presented in [2, 4], the root of the search tree corresponds to $(a_1, \dots, a_n) \in A(\bar{F}, F)$. At each stage of construction of the search tree, the optimisation procedure chooses a node which does not have successors in the already constructed fragment of this tree and connects this node to one or several new nodes (branching). The new nodes correspond to points dominated by the point corresponding to the node at which branching occurs.

Let $d = (d_1, \dots, d_n) \notin X$ be a point which corresponds to a node without successors in the partially constructed search tree. Let

$$\rho(d_1, \dots, d_n) = \min_{(x_1, \dots, x_n) \in X} \max_{1 \leq j \leq n} [x_j - d_j].$$

Point d dominates at least one feasible point if and only if

$$\rho(d_1, \dots, d_n) \leq 0. \quad (1)$$

One of the problems that possesses Properties 1, 2, and 3 is the makespan minimisation problem with parallel identical machines, unit execution time (UET) tasks, and precedence constraints. Since this problem is NP-hard in the strong sense (see [1]), the question whether or not (1) holds is in general an NP-complete problem. Hence, instead of $\rho(d_1, \dots, d_n)$, one may attempt to calculate some $\underline{\rho}$ such that

$$\underline{\rho} \leq \rho(d_1, \dots, d_n). \quad (2)$$

The method of calculating $\underline{\rho}$ depends on F and X . Some examples can be found in [2, 4].

If $\underline{\rho} > 0$, then d is fathomed, i.e., no branching at d is required. If $\underline{\rho} \leq 0$ or $\underline{\rho}$ has not been calculated at all, then d can be projected onto X , where the projection of d onto X is a point with the smallest t among all points $(d_1 + t, \dots, d_n + t)$ satisfying $(d_1 + t, \dots, d_n + t) \in X$. Of course, the projection may not exist. It is easy to see, that if the projection $(d_1 + \tau, \dots, d_n + \tau)$ exists and $\tau \leq 0$, then d dominates this projection, and the optimisation procedure terminates because the projection is a feasible point.

If the projection $(d_1 + \tau, \dots, d_n + \tau)$ exists and $\tau > 0$, then this projection dominates d , and therefore, dominates any point dominated by d . Hence, if $(d_1 + \tau, \dots, d_n + \tau)$ belongs to the boundary of X , then d cannot dominate any feasible point and the corresponding node of the search tree should be fathomed. Furthermore, if the projection $(d_1 + \tau, \dots, d_n + \tau)$ belongs to the boundary of X and dominates a , then the same reasoning leads to the conclusion that the entire search tree should be fathomed, because a cannot dominate any feasible point.

The two remaining cases are when the projection $(d_1 + \tau, \dots, d_n + \tau)$ does not belong to the boundary of X and $\tau > 0$, and the case when the projection does not exist. In both cases (see for example [2]), there exists $(x_1, \dots, x_n) \in X$ and i such that

$$\max_{1 \leq j \leq n} [x_j - d_j] = \rho(d_1, \dots, d_n) \text{ and } x_i - d_i < \rho(d_1, \dots, d_n). \quad (3)$$

In general, neither index i nor $\rho(d_1, \dots, d_n) - [x_i - d_i]$ are known. The idea is to find a subset $B \subseteq \{1, \dots, n\}$ such that, for some $i \in B$, there exists $(x_1, \dots, x_n) \in X$, satisfying (3); to calculate a lower bound $0 < \delta \leq \rho(d_1, \dots, d_n) - [x_i - d_i]$; to introduce, for each $j \in B$, a new node corresponding to the point (d'_1, \dots, d'_n) , where

$$d'_e = \begin{cases} d_e - \delta & \text{if } e = j \\ d_e & \text{if } e \neq j \end{cases},$$

if (d'_1, \dots, d'_n) is in the domain of F , and to link each such new node with the node corresponding to d . Although $\{1, \dots, n\}$ is always a possible choice of B , smaller B may improve the convergence. It is easy to see that each (d'_1, \dots, d'_n) is dominated by d and therefore is dominated by the element of the level set corresponding to the root of the search tree. Furthermore, for at least one of these new points

$$\rho(d'_1, \dots, d'_n) = \rho(d_1, \dots, d_n).$$

Therefore, if there exist feasible points dominated by (d_1, \dots, d_n) , then at least one of them is dominated by one of the new points. Since $0 \leq a_e \leq p(n)$ for all $1 \leq e \leq n$, after a finite number of steps, the optimisation procedure either finds a feasible point dominated by the considered element of the level set and terminates with this feasible point as an optimal solution or establishes that the considered element of the level set does not dominate any feasible point.

In general, the methods of choosing B and calculating δ depend on F and X . Several examples can be found in [2–4].

3 Ascending Method

According to the ascending method, a search tree for each $a = (a_1, \dots, a_n) \in A(\bar{F}, F)$ emanates from the root corresponding to a point which is dominated by a and by all points in X . Although $(0, \dots, 0)$ is an obvious choice for the point associated with the root, a point with a larger value of the objective function may improve the convergence. As in descending method, all nodes in this search tree correspond to points in the domain of F and each of these points is dominated by a . In contrast to the descending method, each branching results in new nodes associated with points which dominate the point corresponding to the node at which branching occurred.

Let $b = (b_1, \dots, b_n) \notin X$ be a point associated with a node without successors in the partially constructed search tree, and let $(b_1 + \tau, \dots, b_n + \tau)$ be the projection of b onto X . Since a dominates b , if

$$\tau \leq \min_{1 \leq j \leq n} [a_j - b_j], \quad (4)$$

then a dominates $(b_1 + \tau, \dots, b_n + \tau)$ and the optimisation procedure terminates with the projection as an optimal solution.

Suppose that (4) does not hold and that the projection $(b_1 + \tau, \dots, b_n + \tau)$ belongs to the boundary of X . If $\tau \geq \max_{1 \leq j \leq n} [a_j - b_j]$, then the projection dominates a .

Taking into account that a is not a feasible point, this implies that a does not dominate any feasible point, because otherwise $(b_1 + \tau, \dots, b_n + \tau)$ will dominate this feasible point which contradicts the definition of the boundary. Hence, the entire search tree is fathomed. If the projection $(b_1 + \tau, \dots, b_n + \tau)$ belongs to the boundary of X and

$$\min_{1 \leq i \leq n} [a_i - b_i] < \tau < \max_{1 \leq i \leq n} [a_i - b_i],$$

then consider the set B of all indices i such that $b_i + \tau + 1 \leq a_i$. Since the projection $(b_1 + \tau, \dots, b_n + \tau)$ cannot dominate feasible points, for any feasible point (x_1, \dots, x_n) dominated by a (if such a point exists), there exists $i \in B$ satisfying the inequality $x_i \geq b_i + \tau + 1$. Hence, the node, associated with (b_1, \dots, b_n) , can be linked with $|B|$ new nodes (branching), one for every $i \in B$. Here, a new node corresponding to i is associated with (b'_1, \dots, b'_n) , where

$$b'_j = \begin{cases} b_j + \tau + 1 & \text{if } j = i, \\ b_j & \text{if } j \neq i. \end{cases}$$

The two remaining cases are when the projection $(b_1 + \tau, \dots, b_n + \tau)$ does not belong to the boundary of X and (4) does not hold and the case when the projection does not exist. Let $X(b, a)$ be the set of all feasible points that dominate b and are dominated by a . If $X(b, a) \neq \emptyset$, then in both mentioned above remaining cases, for any $(x_1, \dots, x_n) \in X(b, a)$, not all n differences $x_i - b_i$ are equal. Hence, there exists i such that,

$$x_i - b_i > \min_{1 \leq j \leq n} [x_j - b_j]. \tag{5}$$

In general, neither $(x_1, \dots, x_n) \in X(b, a)$ nor index i are known, and the idea is to find a subset $B \subseteq \{1, \dots, n\}$ such that if $X(b, a) \neq \emptyset$, then there exists $(x_1, \dots, x_n) \in X(b, a)$ and $i \in B$ such that (5) holds; to calculate a lower bound $1 \leq \delta \leq x_i - b_i - \min_{1 \leq j \leq n} [x_j - b_j]$; to introduce, for each $j \in B$, a new node corresponding to the point $b' = (b'_1, \dots, b'_n)$, where

$$b'_e = \begin{cases} b_e + \delta & \text{if } e = j \\ b_e & \text{if } e \neq j \end{cases},$$

if b' is dominated by a , and to link each such new node with the node corresponding to b . Similar to the descending method, although $\{1, \dots, n\}$ is an obvious choice for B , smaller B may improve the convergence.

It is easy to see that if $X(b, a) \neq \emptyset$, then for at least one $(x_1, \dots, x_n) \in X(b, a)$ there exists a new node and the associated point $b' = (b'_1, \dots, b'_n)$ such that

$$\min_{1 \leq j \leq n} [x_j - b'_j] = \min_{1 \leq j \leq n} [x_j - b_j] \geq 0.$$

Hence, if $X(b, a) \neq \emptyset$, then $X(b', a) \neq \emptyset$ for at least one new node. On the other hand, each (b'_1, \dots, b'_n) dominates b . Since all coordinates of all points are nonnegative integers bounded above by $p(n)$, after a finite number of steps, the optimisation procedure either finds a feasible point dominated by the considered element of the level set and terminates with this feasible point as an optimal solution or establishes that the considered element of the level set does not dominate any feasible point.

4 Descending-Ascending Method

As the name suggests, the descending-ascending method is a combination of the descending and ascending methods. Therefore, each node of the search tree for the currently considered $a = (a_1, \dots, a_n) \in A(\bar{F}, F)$ is associated with a pair of points. All these points are in the domain of F . The root of the search tree is associated with a pair where the first point in the pair is a point dominated by all points in X , i.e., by all feasible points, and by a , whereas the second point in the pair is a itself. For all other nodes of the search tree, the pair (b, d) of points, associated with a node, has the following property: $b \notin X$, $d \notin X$, d dominates b , and a dominates d .

Let b and d be a pair of points, associated with a node of the search tree that does not have successors in this tree. The search procedure attempts to find a feasible point that dominates b and is dominated by a or to determine that such feasible point does not exist, and hence, the node has to be fathomed, first by using the ascending method and ignoring d . If the ascending method cannot achieve this goal, the procedure ignores b and uses the descending method to find a feasible point dominated by d .

If both, ascending and descending, methods, using point b and point d , respectively, have failed to find a desired feasible point or to establish that such point does not exist, then branching occurs. Branching is generated either using the ascending method and the point b , or using the descending method and the point d , but not using both methods simultaneously. If the ascending method is selected for branching, this method is modified in order to satisfy the following condition: each resultant point b' should be dominated by d . If the descending method is selected for branching, this method is modified in order to satisfy the following condition: each resultant point d' should dominate b . The choice of what method among the two should be used for branching can be made in many different ways. For example, the selection criterion may be the cardinality of the sets B , used by the methods. Let $b = (b_1, \dots, b_n)$, $d = (d_1, \dots, d_n)$, $b' = (b'_1, \dots, b'_n)$, and $d' = (d'_1, \dots, d'_n)$, then another example is a selection criterion based on the comparison of $\max_{1 \leq i \leq n} (d_i - b'_i)$ and $\max_{1 \leq i \leq n} (d'_i - b_i)$.

5 Applications

As an illustration, consider the following scheduling problem

$$P|prec, c_{ij} = 1, p_i = 1|L_{max}, \tag{6}$$

where P indicates that a set of tasks $N = \{1, \dots, n\}$ is processed on parallel machines, $prec$ and $p_i = 1$ specify that tasks are subject to precedence constraints and that all processing times are one unit of time, and $c_{ij} = 1$ signify the unit communication delays. No preemptions are allowed; a feasible schedule σ is specified by tasks' completion times $C_i(\sigma)$, $1 \leq i \leq n$, which are assumed to be positive integers. Let m be the number of parallel machines. It is easy to see that even if the tasks are scheduled one at a time, $C_i(\sigma) \leq n$, $1 \leq i \leq n$. Thus, the feasible region X can be viewed as a set of points with integer coordinates $(C_1(\sigma), \dots, C_n(\sigma))$ satisfying:

- $1 \leq C_i(\sigma) \leq n$, $1 \leq i \leq n$;
- $|\{i : C_i(\sigma) = t\}| \leq m$ for all integer $1 \leq t \leq n$;
- $C_i(\sigma) \leq C_j(\sigma) - 1$ for all i and j such that $i \rightarrow j$;
- if $i \rightarrow j$ and $i \rightarrow g$, then $C_i(\sigma) \leq \max(C_j(\sigma), C_g(\sigma)) - 2$;
- if $i \rightarrow j$ and $h \rightarrow j$, then $C_j(\sigma) \geq \min(C_i(\sigma), C_h(\sigma)) + 2$.

The objective is to minimise maximum lateness

$$L_{max}(\sigma) = \max_{j \in N} (C_j(\sigma) - d_j), \tag{7}$$

where $C_j(\sigma)$ is the completion time of a task j in schedule σ and d_j is the task's due date, assumed to be integer. In what follows the time slot t is an interval $[t - 1, t]$. The time slot t is complete (in respect of the given priority μ_g) if there are m tasks j with priority $\mu_j \geq \mu_g$ and completion time $C_j(\sigma) = t$, otherwise the time slot is incomplete. Let $Q(i)$ be the set of predecessors of task i and $K(i)$ be the set of successors of the task i . Then, for each task $i \in N$ calculate the following:

- The lower bound for completion time c_i :

$$c_i = \begin{cases} 1, & \text{if } Q(i) = \emptyset \\ \max_{\underline{c} \leq c \leq \bar{c}} \left\{ c + \left\lceil \frac{|\{j : j \in Q(i) \text{ and } c_j \geq c\}| - 1}{m} \right\rceil + 1 \right\} & \text{otherwise,} \end{cases}$$

where \underline{c} and \bar{c} are the smallest and the largest c_j among $j \in Q(i)$.

- The priority μ_i :

$$\mu_i = \begin{cases} \max_{j \in N} d_j - d_i, & \text{if } K(i) = \emptyset \\ \max \left\{ \max_{j \in N} d_j - d_i, \max_{\underline{\mu} \leq \mu \leq \bar{\mu}} \left\{ \mu + \left\lceil \frac{|\{j : j \in K(i) \text{ and } \mu_j \geq \mu\}| - 1}{m} \right\rceil + 1 \right\} \right\} & \text{otherwise,} \end{cases}$$

where $\underline{\mu}$ and $\bar{\mu}$ are the smallest and the largest μ_j among $j \in K(i)$, and d_i is the task's due date.

It has been shown in [3], that for any schedule σ

$$L_{max}(\sigma) = \max_{i \in N} (C_i(\sigma) + \mu_i) - \max_{j \in N} d_j. \quad (8)$$

5.1 The Procedure

According to the optimisation procedure, described in Sect. 1, the first step is to calculate the initial lower bound \underline{L} . Taking into account (8), we have

$$\underline{L} = \underline{C} - \max_{q \in N} d_q, \quad (9)$$

where \underline{C} is the lower bound on $\max_{i \in N} (C_i(\sigma) + \mu_i)$. The next step of the procedure requires to determine the level set for the value of the objective function. It is easy to see that the level set consists of only one point (a_1, \dots, a_n) for any value \underline{L} of the maximum lateness function, where a_i , for $1 \leq i \leq n$, is defined as $a_i = \underline{L} + d_i$.

Thus, for the only point of the level set (a_1, \dots, a_n) , the procedure determines whether or not there exists a feasible point $(x_1, \dots, x_n) \in X$, which is dominated by (a_1, \dots, a_n) . In other words, is there a feasible schedule σ , such that

$$\max_{i \in N} (C_i(\sigma) - a_i) \leq 0 \quad (10)$$

Taking into account (8), (9) and the above definition of a_i ,

$$\begin{aligned} \max_{i \in N} (C_i(\sigma) - a_i) &= \max_{i \in N} (C_i(\sigma) - (\underline{L} + d_i)) = \\ &= \max_{i \in N} (C_i(\sigma) + \mu_i) - \max_{q \in N} d_q - (\underline{C} - \max_{q \in N} d_q) = \max_{i \in N} (C_i(\sigma) + \mu_i) - \underline{C}. \end{aligned}$$

Thus, the inequality (10) holds if and only if the following inequality holds:

$$\max_{i \in N} (C_i(\sigma) + \mu_i) \leq \underline{C}. \quad (11)$$

The lower bound \underline{C} is calculated as

$$\underline{C} = \max_{\underline{c} \leq c \leq \bar{c}} \left\{ \max_{\underline{\mu} \leq \mu \leq \bar{\mu}} \left\{ c - 1 + \left\lceil \frac{|\{j : c_j \geq c \text{ and } \mu_j \geq \mu\}|}{m} \right\rceil + \mu \right\} \right\}, \quad (12)$$

where \underline{c} and \bar{c} are the smallest and the largest c_i among $i \in N$ and $\underline{\mu}$ and $\bar{\mu}$ are the smallest and the largest μ_i among $i \in N$.

The procedure constructs a search tree in order to find a feasible schedule satisfying (11) for the current value of \underline{C} using descending, ascending, or descending-ascending methods. If the procedure determines that such a schedule does not exist,

it retains \tilde{C} , the next smallest value of $\max_{i \in N} (C_i(\sigma) + \mu_i)$ such that $\tilde{C} > \underline{C}$. The new iteration starts with the new lower bound $\tilde{C} > \underline{C}$. Once a schedule satisfying (11) for the value of \underline{C} is found, the optimal value L^* is calculated as $L^* = \underline{C} - \max_{q \in N} d_q$.

5.2 Descending Method

Consider the partially constructed search tree associated with the current lower bound \underline{C} . Each node of the search tree is associated with the set of priorities $\{\mu_1, \dots, \mu_n\}$ and the lower bound LB^μ calculated with the set of priorities according to (12). All current existing nodes are queued in the list in non-decreasing order of corresponding lower bounds. Let $C_{max}(\sigma) = \max_{i \in N} (C_i(\sigma) + \mu_i)$ and denote by \tilde{C} the smallest value of $C_{max}(\sigma)$ produced by the search tree so far and by $\tilde{\sigma}$ —the schedule such that $C_{max}(\tilde{\sigma}) = \tilde{C}$. Here are the steps of the descending method:

1. Select the node with the smallest lower bound LB^μ . If the list is empty and $\tilde{C} > \underline{C}$, the new iteration of the optimisation procedure starts for the new lower bound \tilde{C} .
2. Construct a schedule σ using List Algorithm and the list of tasks in non-increasing order of μ .
3. If $C_{max}(\sigma) \leq \underline{C}$, set $L^* = \underline{C} - \max_{q \in N} d_q$ and terminate the optimisation procedure.

Otherwise, go to the next step.

4. Select the task g with the smallest completion time $C_g(\sigma)$ among all tasks j such that $C_j(\sigma) + \mu_j = C_{max}(\sigma)$ and let τ be the first incomplete time slot (in respect of the priority μ_g) on the left of g in schedule σ . If $\tau \leq 1$, then σ is the optimal schedule for this set of priorities μ . If $C_{max}(\sigma) < \tilde{C}$, set $\tilde{C} = C_{max}(\sigma)$ and $\tilde{\sigma} = \sigma$. No further branching is required on the node, delete the node and go to the step 1. If $\tau > 1$ go to the next step.
5. Select set $U = \{u : \tau < C_u(\sigma) < C_g(\sigma) \text{ and } \mu_u \geq \mu_g\} \cup \{g\}$ and the sets:

$$T = \{b : K(b) \cap U \neq \emptyset \text{ and } C_b(\sigma) = \tau - 1\} \text{ and}$$

$$S = \{b : K(b) \cap U \neq \emptyset, Q(b) \cap T = \emptyset \text{ and } C_b(\sigma) = \tau\}.$$

Let the branching set $B = T \cup S$. It has been shown in [3] that there exist an optimal schedule σ^* and $j \in B$ such that $C_{max}(\sigma^*) > C_j(\sigma^*) + \mu_j$, and thus, the priority μ_j can be increased without changing the value of the criterion.

6. For each $i \in B$ calculate the new set of the priorities η as follows:

$$\eta_j = \begin{cases} \mu_j, & \text{if } j \neq i, \\ \eta_j = \mu_j + C_g(\sigma) + \mu_g - (C_j(\sigma) + \mu_j), & \text{if } j = i. \end{cases}$$

Calculate lower bound LB^η . If $LB^\eta \leq \underline{C}$, create a new node associated with the set of priorities η and the lower bound LB^η . Include the node in the list of nodes and re-arrange the list in non-decreasing order of nodes' lower bounds. If $\underline{C} < LB^\eta < \tilde{C}$, let $\tilde{C} = LB^\eta$. If all elements of the set B have been considered, delete the current node and go to step 1.

5.3 Ascending Method

The main difference in the ascending method from the descending method is that we will be increasing and branching on the sets of the lower bounds $\{c_1, \dots, c_n\}$ instead of increasing and branching on the sets of priorities $\{\mu_1, \dots, \mu_n\}$. In order to select the branching set, a schedule σ is constructed using “ascending” List Algorithm and the list of tasks in non-increasing order of c . The schedule is constructed from right to left starting from the time slot $t = n$, assigning the completion time to the first task i on the list such that $n - C_i(\sigma) \geq \mu_i$ and the completion times are assigned for all $j \in K(i)$ or $K(i) = \emptyset$. Thus, by construction

$$\max_{i \in N} (C_i(\sigma) + \mu_i) = n. \quad (13)$$

Let $\chi = \min_{j \in N} (C_j(\sigma) - c_j)$. Let σ' be a schedule derived from σ by shifting all completion times by χ to the left: $C_i(\sigma') = C_i(\sigma) - \chi, 1 \leq i \leq n$. Taking into account (13) and the definition of χ ,

$$\begin{aligned} \max_{i \in N} (C_i(\sigma') + \mu_i) \leq \underline{C} &\iff \max_{i \in N} (C_i(\sigma) + \mu_i - \chi) \leq \underline{C} \iff \\ n - \min_{j \in N} (C_j(\sigma) - c_j) \leq \underline{C} &\iff \min_{j \in N} (C_j(\sigma) - c_j) \geq n - \underline{C}. \end{aligned} \quad (14)$$

As shown above, if the schedule σ satisfies (14), then the corresponding σ' satisfies (11). Consider the partially constructed search tree associated with the current lower bound \underline{C} . Each node of the search tree is associated with the set of lower bounds on the tasks' completion times $\{c_1, \dots, c_n\}$ and the lower bound LB^c , where LB^c is calculated with the set of $\{c_1, \dots, c_n\}$ according to (12). All current existing nodes are queued in the list in non-decreasing order of corresponding lower bounds LB^c . Denote by $\chi(\sigma) = \min_{j \in N} (C_j(\sigma) - c_j)$. Let $\tilde{\chi}$ be the largest value of $\chi(\sigma)$ produced by the search tree so far and $\tilde{\sigma}$ be the schedule such that $\chi(\tilde{\sigma}) = \tilde{\chi}$. Here are the steps of the ascending method:

1. Select the node with the smallest lower bound LB^c . If the list is empty and $\tilde{\chi} < n - \underline{C}$, the new iteration of the optimisation procedure starts for the new lower bound $\tilde{C} = n - \tilde{\chi}$.
2. Construct a schedule σ using the “ascending” List Algorithm and the list of tasks in non-increasing order of cs .
3. If $\chi(\sigma) \geq n - \underline{C}$, set $L^* = \underline{C} - \max_{q \in N} d_q$ and terminate the optimisation procedure. Otherwise, go to the next step.
4. Select task g with the largest completion time $C_g(\sigma)$ among all tasks j such that $C_j(\sigma) - c_j = \chi(\sigma)$ and let τ be the first incomplete time slot (in respect of the priority c_g) on the right of g in schedule σ . If $\tau \geq n$, then σ is the optimal schedule for this set of $\{c_1, \dots, c_n\}$. If $\chi(\sigma) > \tilde{\chi}$, set $\tilde{\chi} = \chi(\sigma)$ and $\tilde{\sigma} = \sigma$. No further branching is required on the node, delete the node and go to the step 1. If $\tau < n$ go to the next step.

5. Select set $U = \{u : C_g(\sigma) < C_u(\sigma) < \tau \text{ and } c_u \geq c_g\} \cup \{g\}$ and the sets:

$$T = \{b : Q(b) \cap U \neq \emptyset \text{ and } C_b(\sigma) = \tau + 1\} \text{ and}$$

$$S = \{b : Q(b) \cap U \neq \emptyset, K(b) \cap T = \emptyset \text{ and } C_b(\sigma) = \tau\}.$$

Let the branching set $B = T \cup S$. Similar to the descending case, there exist an optimal schedule σ^* and $j \in B$ such that $\chi(\sigma^*) < C_j(\sigma^*) - c_j$, and thus, the c_j can be increased without changing the value of the criterion.

6. For each $i \in B$ calculate the new set of the priorities ζ as follows:

$$\zeta_j = \begin{cases} c_j, & \text{if } j \neq i, \\ \zeta_j = c_j + C_j(\sigma) - c_j - (C_g(\sigma) - c_g), & \text{if } j = i. \end{cases}$$

Calculate lower bound LB^ζ . If $LB^\zeta \leq \underline{C}$, create a new node associated with the set of priorities ζ and the lower bound LB^ζ . Include the node in the list of nodes and re-arrange the list in non-decreasing order of nodes' lower bounds. If $\underline{C} < LB^\zeta < n - \tilde{\chi}$, let $\tilde{\chi} = n - LB^\zeta$. If all elements of the set B have been considered, delete the current node and go to step 1.

5.4 Descending-Ascending Method

The descending-ascending method incorporates the elements of both descending and ascending methods. Consider the partially constructed search tree associated with the current lower bound \underline{C} . Each node of the search tree is associated with the sets $\{c_1, \dots, c_n\}$ and $\{\mu_1, \dots, \mu_n\}$, and the lower bound $LB^{(c, \mu)}$, where $LB^{(c, \mu)}$ is calculated according to (12). All current existing nodes are queued in the list in non-decreasing order of corresponding lower bounds $LB^{(c, \mu)}$. Denote by σ^d the schedule constructed by “descending” List Algorithm, and by σ^a —the schedule constructed by “ascending” List Algorithm. Denote by $\Delta^{(c, \mu)} = \min\{n - \chi(\sigma^a), C_{max}(\sigma^d)\}$. Let $\tilde{\Delta}$ be the smallest value of $\Delta^{(c, \mu)}$ produced by the search tree so far and $\tilde{\sigma}$ be the schedule that produced this value. Here are the steps of descending-ascending method:

1. Select the node with the smallest lower bound $LB^{(c, \mu)}$. If the list is empty and $\tilde{\Delta} > \underline{C}$, the new iteration starts for the new lower bound $\tilde{C} = \tilde{\Delta}$.
2. Construct a schedule σ^d with the “descending” List Algorithm and the list of tasks in non-increasing order of μ s and a schedule σ^a with the “ascending” List Algorithm and the list of tasks in non-increasing order of c s.
3. If $\chi(\sigma^a) \geq n - \underline{C}$ or $C_{max}(\sigma^d) \leq \underline{C}$, set $L^* = \underline{C} - \max_{q \in N} d_q$ and terminate the optimisation procedure. Otherwise, go to the next step.
4. Select task g^d and incomplete time slot τ^d for the σ^d similar to the step 4 of descending algorithm and select task g^a and incomplete time slot τ^a for the σ^a similar to the step 4 of ascending algorithm. If $\tau^a \geq n$ or $\tau^d \leq 1$, then either σ^a or σ^d is the optimal schedule for this set of $\{c_1, \dots, c_n\}$ and $\{\mu_1, \dots, \mu_n\}$. If $\Delta^{(c, \mu)} < \tilde{\Delta}$, set $\tilde{\Delta} = \Delta^{(c, \mu)}$. No further branching is required on the node, delete the node and go to the step 1. If $\tau^a < n$ and $\tau^d > 1$, go to the next step.

5. Select the “descending” and “ascending” branching sets B^d and B^a , repeating the steps 5 and 6 of the descending and ascending methods.
6. Choose the branching set B out of B^d and B^a according to some criterion. We implemented three criteria of selection of the set B :

Method da1: Choose the set of the smallest cardinality;

Method da2: For each element $h \in B^d$, calculate the new priorities $\{\mu_1^h, \dots, \mu_n^h\}$, and for each element $q \in B^a$, calculate the new set $\{c_1^q, \dots, c_n^q\}$ according to step 6 of the descending and ascending methods correspondingly. For each branching set, calculate the maximum “window”:

$$W(B) = \max_{j \in B} \{ \max_{i \in N} (\underline{C} - c_i^j - \mu_i^j) \}.$$

Choose the branching set with the smallest maximum window;

Method da3: Similar to the previous case, calculate the set of new priorities for B^d and B^a . Then, for each of the sets calculate the average “window”:

$$AV(B) = \frac{\sum_{j \in B} \sum_{i \in N} (\underline{C} - c_i^j - \mu_i^j)}{|B|}.$$

Choose the branching set with the smallest average window.

7. Calculate lower bound $LB^{(c,\mu)}$ for the new sets of cs and μs . If $LB^{(c,\mu)} \leq \underline{C}$, create a new node associated with the sets of priorities and the lower bound $LB^{(c,\mu)}$. Include the node in the list of nodes and re-arrange the list in non-decreasing order of nodes’ lower bounds. If $\underline{C} < LB^{(c,\mu)} < \tilde{\Delta}$, let $\tilde{\Delta} = LB^{(c,\mu)}$. If all elements of the set B be have been considered, delete the current node and go to step 1.

6 Computational Experiments

The computational experiments aimed to compare the descending, ascending, and descending-ascending algorithms. The computational experiments were conducted by the second author using Ubuntu 14.04 LTS, Intel Core @1.70 Ghz x 2. The partially ordered sets were obtained from <http://www.kasahara.cs.waseda.ac.jp/schedule/>, the Kasahara Laboratory website. It was assumed that all tasks have unit processing time, and there are unit communication delays. The three groups considered each consisted of 180 instances of 50, 100, or 300 tasks. For each group, the experiments were run for 3, 4, 5, and 6 parallel machines. The execution of each instance was terminated once the search went through 5000 nodes.

Table 1 represents the percentage of the instances solved to optimality. All algorithms solved 92–100% of the instances. At least one of the descending-ascending methods performed at the same level or better than descending and ascending algorithms. Table 2 compares descending and ascending methods. The number of

Table 1 Percentage of the instances solved to optimality

Machines	50 tasks				100 tasks				300 tasks			
	3	4	5	6	3	4	5	6	3	4	5	6
Descending	98.3	95.6	98.3	99.4	100	97.2	95.6	97.2	97.8	97.2	96.7	94.4
Ascending	97.2	94.4	95.6	97.8	100	96.7	96.1	96.7	98.3	97.2	95.0	92.2
da1	95.6	93.9	98.3	98.3	100	96.7	95.6	96.1	98.3	98.3	97.2	95.6
da2	98.3	95.6	98.3	99.4	100	97.2	95.6	97.2	97.8	97.2	97.2	95.0
da3	98.3	95.6	98.3	99.4	100	97.2	95.6	97.2	97.8	97.2	97.2	95.0

Table 2 Descending and ascending methods compared

Machines	50 tasks				100 tasks				300 tasks			
	3	4	5	6	3	4	5	6	3	4	5	6
Descending	12.2	8.9	10.6	7.2	3.3	10.0	6.1	10.0	1.1	1.7	4.4	7.8
Ascending	9.4	12.2	10.0	8.9	2.2	4.4	8.9	5.0	2.2	4.4	3.3	3.9

Table 3 Descending-ascending methods compared

Machines	50 tasks				100 tasks				300 tasks			
	3	4	5	6	3	4	5	6	3	4	5	6
da1	91.7	92.8	93.3	94.4	97.8	93.3	91.1	93.9	97.8	96.7	97.8	94.4
da2	92.2	90.0	93.3	93.3	97.8	96.1	92.2	95.6	98.9	96.7	97.8	97.2
da3	92.2	90.0	93.3	93.3	97.8	96.1	92.2	95.6	97.8	96.1	92.2	95.6

iterations required by each method to solve an instance to optimality was calculated. The Table 2 shows the percentage of instances where one method required less iterations than the other, indicating that the methods are sensitive to the structure of the tasks’ graphs and perform differently on the same instances. Table 3 compares the three descending-ascending methods. The number of nodes required by a method to solve an instance to optimality was calculated. The Table 3 shows the percentage of the instances where the number of iterations used by the considered descending-ascending method is not greater than that of descending or ascending method. Thus, in 92–98% of instances across all groups of instances and all tested number of machines, the descending-ascending methods perform at least as well as either descending or ascending methods.

7 Summary and the Further Research

In this chapter, we have shown that the optimisation procedure, presented in [2–4], can be viewed as a descending method and it can be complemented by ascending and descending-ascending methods. Application of all three methods to a schedul-

ing problem has been implemented. The computational experiments demonstrated that descending and ascending methods are solving similar number of instances; however, they perform differently on the same instances. We implemented three variations of the descending-ascending method which incorporates features of both descending and ascending methods. At least one of the descending-ascending methods performed at the same level or better than descending and ascending algorithms. The aim of the further research is to develop applications of the presented approach to new types of discrete optimisation problems. In particular, in addition to the problems considered in [2–4], this optimisation procedure is also applicable to scheduling problems with partially ordered UET tasks and embedded sets of dedicated machines. This class of scheduling problems includes job-shop and flowshop problems with unit execution time tasks.

References

1. Ullman, J.D.: NP-complete scheduling problems. *J. Comp. Syst. Sci.* **10**, 384–393 (1975)
2. Zinder, Y., Memar, J., Singh, G.: Discrete optimization with polynomially detectable boundaries and restricted level sets. In: Wu, W., Daescu, O. (eds.) *COCOA 2010. LNCS*, vol. 6508, pp. 142–156. Springer, Heidelberg (2010)
3. Zinder, Y., Su, B., Singh, G., Sorli, R.: Scheduling UET-UCT tasks: branch-and-bound search in priority space. *Optim. Eng.* **11**, 627–646 (2010)
4. Zinder, Y., Memar, J., Singh, G.: Discrete optimization with polynomially detectable boundaries and restricted level sets. *J. Comb. Optim.* **25**, 308–325 (2013)

Alternative Passenger Cars for the Australian Market: A Cost–Benefit Analysis

Jason Milowski, Kalyan Shankar Bhattacharjee,
Hemant Kumar Singh and Tapabrata Ray

Abstract Petrol or diesel powered cars (henceforth referred as conventional vehicles (CV)) have long been in existence, and currently, 75% of cars in Australia belong to this category. Hybrids (HEVs), i.e. a vehicle with an electric drive system and an internal combustion engine running on either petrol or diesel have gained significant market share in recent years. While hybrids are regularly presented as “greener alternatives”, their competitive edge is largely dependent on existing market conditions (gasoline prices, electricity prices, purchase price and maintenance costs) and the usage (commuting distances). A new breed of cars, i.e. fully electric vehicles (EVs), is becoming increasingly popular for city commuters and expected to feature prominently in “Smart Cities” of the future. This study aims to evaluate the performance of electric vehicles (EVs), hybrid electric vehicles (HEVs) and conventional vehicles (CVs) based on three major considerations: average gasoline consumption per day, average GHG emissions in kg-CO₂ equivalent (kg-CO₂-eq) per day and equivalent annualized cost (EAC), for a typical Australian scenario. Each of the three objectives are assessed across a range of gasoline prices, electricity tariffs and commuting distances. Four vehicles have been considered in this study (The models for analysis have been developed based on available open source data with simplifications and assumptions.): two EVs (Nissan LEAF and a BMW i3), one HEV (Toyota Prius) and one CV (Hyundai i30). For a typical city commute of 50 km/day, the average gasoline consumption varies between 0 to 2.30 litre per day, average GHG emission varies between 8.25 to 12.57 kg-CO₂ equivalent per day, and equivalent annualized cost (EAC) varies between 9.90 to 38.79 AUD per day. With such a variation, the choice of one vehicle over another is largely dependent on user preferences. The chapter also presents an approach to customize EVs i.e. effectively develop EV or HEVs to be attractive to a particular market segment.

Keywords Electric vehicle · Vehicle design · Greenhouse gas emissions · Optimization model

J. Milowski · K.S. Bhattacharjee (✉) · H.K. Singh · T. Ray
School of Engineering and Information Technology, University of New South Wales,
Canberra, ACT 2600, Australia
e-mail: k.bhattacharjee@student.adfa.edu.au

© Springer International Publishing AG 2018
R. Sarker et al. (eds.), *Data and Decision Sciences in Action*,
Lecture Notes in Management and Industrial Engineering,
DOI 10.1007/978-3-319-55914-8_12

1 Introduction

Emissions in the transport sector have grown by 50% over the last two decades and now account for 17.2% of Australia's total GHG emissions, totalling approximately 92.8 mega-tonnes of $CO_2(e)$ annually [1]. The Department of Environment's National Greenhouse Gas Inventory reports suggest that cars account for 48% of Australia's transport emissions [2]. A breakdown of Australia's Transport emissions is shown in Fig. 1. In order to reduce the overall emissions as well as our reliance on fossil fuels, there is an impetus towards development and adoption of cars that are more efficient and run on cleaner/renewable energy sources. However, for any consumer product, initial and maintenance costs are both important considerations that affect the product's viability in a competitive market. Recent advancements in lithium-ion batteries and charging technology have paved the way for electric vehicles (EVs) and hybrid electric vehicles (HEVs). EVs are similar to hybrid electric vehicles (HEVs) except that a EV has a larger lithium-ion battery pack with plug-in charging capability. While EVs are quite regularly used for city commutes (shorter distances with pre-charged batteries), HEVs offer the opportunity for an extended range of operation, for example a trip between two close cities. HEVs use electric power from the battery to power the vehicle at low speeds, whereas at higher speeds, it relies on a conventional engine combined with electricity from the battery to meet power demands [3]. Furthermore, if one opts for a HEV, she/he can avoid the daily (often twice daily) necessity of charging the batteries as required for EVs. This study aims to objectively evaluate the performance of EVs with other alternatives (HEVs and CVs) based on gasoline cost, GHG emission and equivalent annualized cost. Nissan LEAF and BMW i3 are the two representative EVs used in this study. Toyota Prius is selected as a representative model for HEV, and Hyundai i30 is used as the baseline CV model. Basic specifications of each vehicle are outlined in Table 1, followed by the details of the underlying model and assumptions.

Fig. 1 Australia's transport emissions

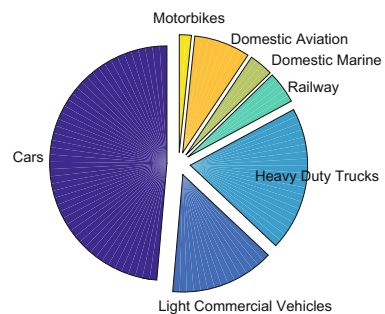


Table 1 Vehicle specifications

	Nissan LEAF	BMW i3	Toyota Prius	Hyundai i30
Type	5 door hatch	5 Door Hatch	5 door hatch	5 door hatch
Price (AUD)	39,990 AUD [4]	63,900 AUD [5]	26,133 AUD [6]	19,990 AUD [7]
Engine	80 kW electric motor [8]	125 kW electric motor [9]	1.8 L and 53 kW electric motor [10]	1.6 L [11]
Battery	24 kWh Li-ion [12]	22 kWh Li-ion [13]	1.3 kWh NiMH [10]	N/A
0–100 km/h (s)	8 [8]	7.2 [9]	10.9 [10]	11.1 [11]
Approx. Range (km)	130 [8]	190 [9]	1100 [10]	1000 [11]
Fuel tank capacity (l)	N/A	N/A	43 [10]	50 [11]
Gross weight (kg)	1900 [8]	1620 [9]	1775 [10]	1890 [11]
Battery charge time (h)	08:00 [8]	07:30 [9]	N/A	N/A

2 Model

The vehicle models used in this study have been derived from those reported in [14] (which used US data). The economic and usage parameters of the models have been updated based on Australian data. Furthermore, additional updates have been incorporated into battery-related data reflecting technological progress since the original study in 2010. We consider a typical mid-sized Australian city, Canberra, for this study. In order to study the objectives of interest (gasoline consumption, GHG emissions, annualized cost) over a variety of likely scenarios, the existing gasoline and electricity prices in Canberra are varied over a range of $\pm 20\%$ with daily distance of commute set as 25, 50, 75, 100 and 150 km. These values were chosen to represent typical distances travelled, the lower values representing a daily commute, and higher ones representing a trip to Goulburn.

The model of each vehicle is defined using four variables: the engine scaling factor (x_1), the motor scaling factor (x_2), the battery pack scaling factor (x_3) and battery energy swing (x_4). We have used the average values of the variables x_1 , x_2 , x_3 and x_4 for each vehicle type, since upper and lower bounds for each were reported in [14].

The decisions in this study are solely based on three objectives: average gasoline consumption per day, average GHG emissions in kg-CO₂ equivalent (kg-CO₂-eq) per day and equivalent annualized cost. Other aspects, such as aesthetics and popularity of a brand, are not considered in this study. For complete details of the models, interested readers are referred to [14]. The notations followed in this study are the same as those in [14] for easier interpretation and comparison. The parameters of the model that have been updated are listed below.

- κ is the battery energy capacity per battery cell. This parameter only affects the models of the EVs. For Nissan LEAF, battery energy capacity is 24 kWh [12] and the number of battery cells is 192 [12]. This leads to a κ value of 0.125 kWh/cell. Similarly, for BMW i3, the battery energy capacity is 22 kWh [13] and number of battery cells is 96 [13] which results in a κ value of 0.229 kWh/cell.
- η_B denotes the battery charging efficiency, a factor only affecting the EVs. In this study, η_B is taken as 90.5% [15] and 93.4% [16] for Nissan LEAF and BMW i3, respectively.
- v_E denotes the electricity emissions, which only applies for the EVs. The values for electricity emissions were taken from the U.S. Environmental Protection Agency report which states that Nissan LEAF produces an average of 194 g-CO₂/mile [17] and the BMW i3 produces an average of 175 g-CO₂/mile [17] from upstream electricity emissions.
The range, battery energy capacity and v_E values for Nissan LEAF are 134 km [18], 24 kWh [12] and 0.673 kg-CO₂/kWh. The corresponding values for BMW i3 are 160 km [19], 22 kWh [13] and 0.790 kg-CO₂/kWh.
- v_G denotes the gasoline life cycle emissions. Since EVs are fully electric, the values of v_G for Nissan LEAF and BMW i3 are considered as zero. For the HEV (Toyota Prius), v_G is 80 g-CO₂/km [10]. For the CV (Hyundai i30), v_G is 125 g-CO₂/km [11]. The fuel economy of Toyota Prius is 29.41 km/l [10] resulting in v_G of 2.352 kg-CO₂/l. Similarly, for Hyundai i30, the fuel economy is 21.7 km/l [11] which results in v_G of 2.717 kg-CO₂/l.
- v_{VEH} is defined in the model as life cycle GHG emissions associated with vehicle production. This parameter is kept same for all the vehicle types as 8500 kg-CO₂ [20].
- s_{LIFE} denotes the expected lifetime of the vehicle. We have used the period of warranty as the vehicle's life. For the Nissan LEAF [18], BMW i3 [19] and Toyota Prius [21], s_{LIFE} is considered as 100,000 km. For the Hyundai i30, s_{LIFE} is 160,000 km [22].
- D denotes the number of driving days per year. For all vehicles, this is assumed to be 300 days per year.
- c_{BASE} denotes the base cost of the vehicle. The price was taken as the drive away price from a dealer in Canberra in Australian Dollars (AUD). The c_{BASE} for the Nissan LEAF, BMW i3, Toyota Prius and Hyundai i30 are 39,990 AUD [4], 63,900 AUD [5], 26,133 AUD [6] and 19,990 AUD [7], respectively. c_{BAT} denotes the battery or the cost of replacement of a battery. This parameter is only relevant for the two EVs and the HEV. For the Nissan LEAF, BMW i3 and Toyota Prius, the values of c_B are 5,499 AUD [23], 13,725 AUD [24] and 2,400 AUD [25], respectively. Therefore, in our model, the base cost (c_{BASE}) has been modified for individual vehicles in such a way that the total vehicle related cost (c_{VEH}) for each individual vehicle is similar to the drive away price including the battery cost (c_{BAT}).
- r_N denotes the nominal discount rate, the value of which was taken directly from the Reserve Bank of Australia database. This value does not change between different vehicles. The value of r_N as of 26 March 2016 is 0.02 [26].

- r_I denotes the inflation rate. The value of r_I was taken directly from Reserve Bank of Australia database and does not change with the vehicle types. The value of r_I as of 26 March 2016 is 0.017 [27].
- c_E denotes the annual average residential electricity price. For the model discussed in this chapter, the current cost of electricity (c_E) was taken as 0.1727 AUD/kWh [28].
- c_G denotes the annual average gasoline price. The current cost of fuel is taken from ACT (Australian Capital Territory) Fuel Watch which was 1.02 AUD/l [29] on 27 March 2016.

3 Numerical Experiments

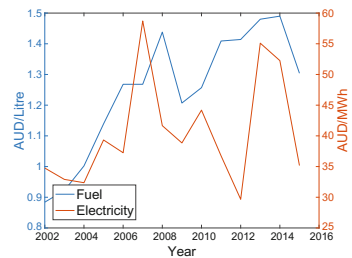
Having discussed the details of the vehicle models in the previous section, we present details of the analysis in this section. Specifically, we explore the performance of the vehicles under a range of different market scenarios, such as variations in gasoline and electricity, as well as for various commuting distances.

3.1 Experimental Set-Up

Figure 2 shows recent trends in fuel and electricity prices. Annual average data of fuel and electricity prices was taken from the Australian Institute of Petroleum [30] and the Australian Energy Market Operator [31], respectively.

The performance of the vehicles was assessed with the gasoline prices, and cost of electricity varying between $\pm 20\%$, i.e. values of c_E and c_G were varied between 0.13816/kWh to 0.20724/kWh and 0.816 AUD/l to 1.224 AUD/l, respectively, for each daily commuting distance of 25, 50, 75, 100 and 150 km.

Fig. 2 Australia’s recent trend in fuel and electricity prices



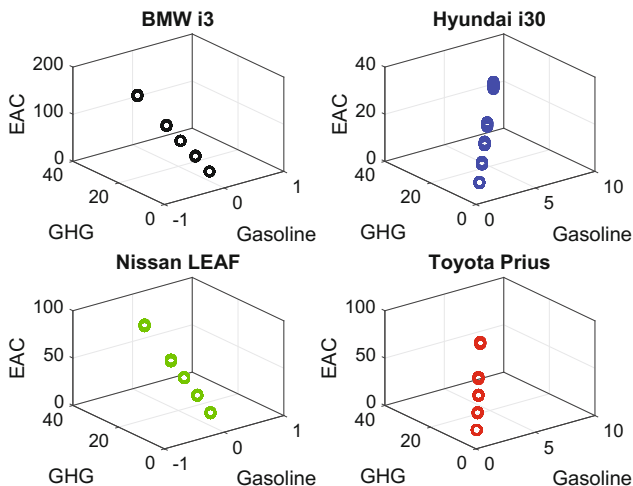


Fig. 3 Objective values for the four vehicles for various commute distances

3.2 Results and Discussion

The performance of the vehicles are presented in Fig. 3 for 605 instantiations i.e. 11 different values of c_E and c_G and 5 different values of commuting distances. One can clearly observe that BMW-i3 has significantly large value of EAC when compared with other alternatives. Not surprisingly, the gasoline consumption is zero for the EVs, followed by HEV and then the CV. It is interesting to take note that the GHG emissions are still quite high for EVs. While the manufactures state zero tailpipe emissions for vehicles running in EV mode, the upstream electricity emissions from each car are considered in this model and are found to be of noticeable value. One can also notice that BMW i3 has the highest GHG emission among all the types of vehicles considered by virtue of its larger battery pack.

Next, we present the spider plots for all distances in order to aid decision-making for a user among the four options, in Fig. 4.

For commuting distances up to 150 km/day, BMW-i3 is a “dominated” alternative, which essentially means that among the four alternatives, there is one alternative which is better in at least one and equal or better in all the other performance indicators. Thus, a choice except BMW i3, in such a situation, would need additional user preferences.

It is evident that the EAC is significantly higher for EVs. While advancement in battery technology is likely to bring this down over the years, such a large gap is likely to affect uptake of EVs in short term. It is also important to take note that gasoline prices do not affect EV’s commuting shorter distances, i.e. those that are within the battery range. A more detailed model of battery replacement would have provided better insights as the replacement cost is a part of what makes the life cycle

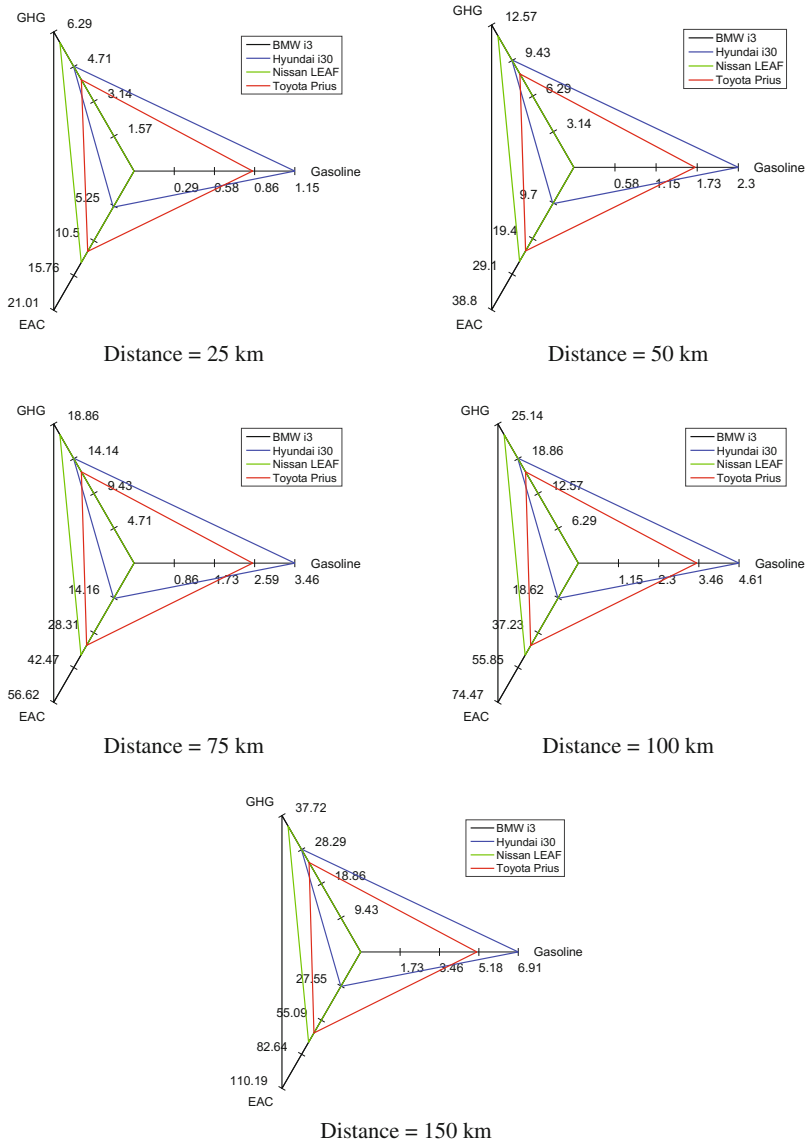


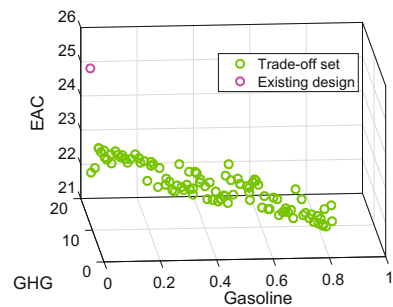
Fig. 4 Difference in objective values based on distances

cost of the two EVs so large. By not replacing these batteries periodically, but instead only when it is required, the life cycle cost of these vehicles could be brought down allowing them to compete with the other vehicles in the market.

4 Optimizing EVs for Different Market Segments

In the above analysis, the performance of each vehicle was analyzed across a range of operating conditions i.e. gasoline and electricity tariffs and driving distances. In this section, we illustrate the importance of modularity and opportunities for re-design to be attractive to a particular market segment. Once again we assume a simple scenario for illustration only, and the same principle can be used to re-design other EVs. Let us assume, one is interested to identify or offer alternative Nissan LEAF designs for individuals commuting an average daily distance of 50 km. Since this process considers a range of battery pack scaling factor, the cut-off distance will vary. Therefore, beyond the cut-off distance, the EVs have to consume gasoline. In this chapter, for this EV, the value of gasoline life cycle emission (v_G) beyond cut-off distance is considered to be the same as Toyota Prius i.e. the HEV. To achieve this, a population-based evolutionary optimization algorithm was run with a population size of 100 solutions evolving over 100 generations. The probability of crossover, probability of mutation, distribution index of crossover and mutation was set to 1, 0.1, 30 and 20, respectively, with the bounds of the variables x_1 , x_2 , x_3 and x_4 set as [0.5263, 1.0526], [0.9615, 2.1154], [0.2, 1] and [0, 0.8], respectively. The trade-off set of solutions are presented in Fig. 5, while the variation in optimal variable values (x_1 , x_2 , x_3 and x_4) are presented in Fig. 6. One can clearly observe that there is an opportunity to present an user with a design with an EAC of 21.51 AUD as opposed to the baseline EAC of 25.59 AUD for Nissan LEAF. While in this simple example, we have considered a fixed distance of commute of 50 km, one can use a probabilistic distribution that reflects the usage of the market segment. The design corresponding to EAC of 21.51 AUD is essentially a HEV design. Such an exercise also provides insights to upstream processes, i.e. effect of the variables on the performance indicators and their relationship.

Fig. 5 Trade-off set: Nissan



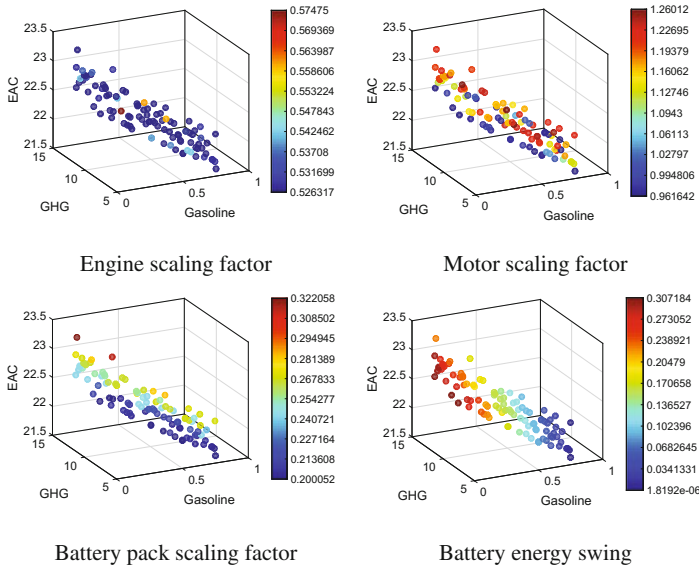


Fig. 6 Variation in optimal variable values

5 Summary and Future Work

Automobiles are one of the major contributors to greenhouse gas emissions. In order to reduce the detrimental effects on environment as well as reliance on fossil fuels for a sustainable future, greener alternatives such as EV and HEV are increasingly drawing attention. However, from a customers' point of view, other aspects such as initial and running/maintenance cost also play a major role in their choices. In this study, we evaluated the performance of EVs, HEVs and conventional vehicles (CVs) based on average gasoline consumption per day, average GHG emissions per day and equivalent annualized cost (EAC), in a typical Australian scenario. Towards this goal, we modified existing models based on US data reported earlier and incorporated updates based on battery technology developments since the original study. Using these models, we assessed the above three objectives for a range of variation in gasoline prices, electricity tariffs and driving distances for four representative cars: Nissan LEAF, BMW i3 (both EV), Toyota Prius (HEV) and Hyundai i30 (CV). It was observed that for distances up to 150 km, BMW i3 was dominated by one of the other alternatives. Interestingly, it was also observed that overall GHG emissions are still high for EVs due to upstream electricity emissions. At the same time, EAC is also high for EVs, implying that they are not currently attractive from a cost point of view, but have a possibility of being so with further advancement in technology or incentives. The second exercise illustrated the methodology to optimize any vehicle to make it more attractive for a market segment. A family of Nissan LEAF EV redesigns were generated that would be attractive for users commuting a daily dis-

tance of 50 kms. It is important to take note that some of the redesigned vehicles correspond to HEVs. It is clear that significant benefits can be offered through re-design and modularization which is expected to be a regular feature in next generation of vehicles. Apart from identifying alternative designs, the optimization exercise also offers interesting insights that can influence upstream processes.

Acknowledgements The third author would like to acknowledge the support from UNSW Early Career Research Grant.

References

1. Commonwealth of Australia: Australian national greenhouse accounts—quarterly update of Australia's national greenhouse gas inventory. https://www.environment.gov.au/system/files/resources/e18788bd-2a8a-49d1-b797-307a9763c93f/files/quarterly-update-september-2013_1.pdf (2014)
2. Australian government: national greenhouse gas inventory. <http://ageis.climatechange.gov.au/NGGL.aspx> (2014)
3. Mahapatra, S., Egel, T., Hassan, R., Shenoy, R., Carone, M.: Model-based design for hybrid electric vehicle systems. https://www.mathworks.com/tagteam/49376_2008-01-0085_Model_Based_Design_HEV_Final_1%2010%2008.pdf (2008)
4. Nissan: Nissan LEAF price and offers. <http://www.nissan.com.au/Offers/Offers> (2016)
5. BMW: BMW model compare price. <https://www.bmw.com.au/en/ssl/modelcompare.html> (2016)
6. Toyota: Toyota prius c. <http://www3.toyota.com.au/prius-c/prices> (2015)
7. Hyundai: Hyundai i30 price calculator. <http://www.hyundai.com.au/shop/calculator/quote?model=i30&variant=109&postcode=2612&pbuser=P&colour=Polar+White&options=> (2016)
8. Nissan: Nissan LEAF specifications. <http://www.nissanus.com/electric-cars/leaf/versions-specs/> (2016)
9. BMW: BMW i3 technical data. http://www.bmw.com/com/en/newvehicles/i/i3/2015/showroom/technical_data.html (2016)
10. Toyota: Toyota prius specifications. <http://www3.toyota.com.au/prius/specifications/prius-auto> (2016)
11. Hyundai: Hyundai i30 specifications. <http://www.hyundai.com.au/cars/small-cars/i30/specifications> (2016)
12. Cell, module, and pack for EV applications. http://www.eco-aesc-lb.com/en/product/liion_ev/ (2016)
13. Morris, C.: BMW i3. <https://chargedevs.com/newswire/bmw-demonstrates-stationary-storage-system-using-i3-battery/> (2013)
14. Shiau, C.N., Kaushal, N., Hendrickson, C.T., Peterson, S.B., Whitacre, J.F., Michalek, J.J.: Optimal plug-in hybrid electric vehicle design and allocation for minimum life cycle cost, petroleum consumption, and greenhouse gas emissions. *J. Mech. Des.* **132**(9), 091, 013–091, 013–11 (2010)
15. Laboratory, I.N.: Steady state vehicle charging fact sheet: 2015 Nissan LEAF. <https://avt.inl.gov/sites/default/files/pdf/fsev/SteadyStateLoadCharacterization2015Leaf.pdf> (2015)
16. Laboratory, I.N.: Steady state vehicle charging fact sheet: 2014 BMW i3 i3. https://avt.inl.gov/sites/default/files/pdf/fsev/SteadyStateLoadCharacterization2014BMW_i3.pdf (2014)
17. Agency, U.S.E.P.: Light-duty automotive technology, carbon dioxide emissions, and fuel economy trends: 1975 through 2014. <http://epa.gov/fueleconomy/fetrends/1975-2014/420r14023.pdf> (2014)

18. Nissan: 2015 Nissan LEAF owner's manual. <https://owners.nissanusa.com/content/techpub/ManualsAndGuides/LEAF/2015/2015-LEAF-owner-manual.pdf> (2015)
19. BMW: 2015 BMW i3 owner's manual. <https://carmanuals2.com/get/bmw-i3-2015-owner-s-manual-63429> (2015)
20. Samaras, C., Meisterling, K.: Life cycle assessment of greenhouse gas emissions from plug-in hybrid vehicles: implications for policy—supporting documentation. http://pubs.acs.org/doi/suppl/10.1021/es702178s/suppl_file/es702178s-file004.pdf (2008)
21. Toyota: Toyota prius brochure. <http://www3.toyota.com.au/prius-c/~media/toyota/vehicles/prius-c/files/prius-c-ebrochure.pdf> (2015)
22. Hyundai: Hyundai i30 warranty information. <http://www.hyundai.com.au/owning/icare/warranty> (2016)
23. Cole, J.: Nissan LEAF battery. <http://insideevs.com/breaking-nissan-prices-leaf-battery-replacement-5499-new-packs-heat-durable/> (2013)
24. Loveday, E.: BMW i3 battery. <http://insideevs.com/bmw-i3-battery-module-costs-1715-60-8-modules-per-car-total-cost-13725/> (2015)
25. Shop, T.H.: Toyota prius hybrid car battery prices & replacement costs. <http://www.thehybridshop.com/media/blogs/toyota-prius-hybrid-car-battery-prices-replacement-costs/> (2014)
26. Cash Rate. <http://www.rba.gov.au/statistics/cash-rate/> (2016)
27. Reserve bank of Australia. <http://www.rba.gov.au/> (2016)
28. ACTEWAGL: our act electricity prices 2015–2016. <http://www.actewagl.com.au/~media/ActewAGL/ActewAGL-Files/Products-and-services/Retail-prices/Electricity-retail-price> (2016)
29. ACT fuel watch. <http://actfuelwatch.com.au/> (2016)
30. Australian Institute of Petroleum: Pump prices retail. <http://www.aip.com.au/pricing/retail.htm> (2016)
31. Australian Energy Market Operator: Average electricity prices—historical. <http://www.aemo.com.au/Electricity/National-Electricity-Market-NEM/Data-dashboard#average-price-table> (2016)

A Quick Practical Guide to Polyhedral Analysis in Integer Programming

Vicky Mak-Hau

Abstract Polyhedral analysis is one of the most interesting elements of integer programming and has been often overlooked. It plays an important role in finding exact solutions to an integer program. In this paper, we will discuss what polyhedral analysis is, and how some constraints for an integer programming model are “ideal” in the sense that if the model contains all of these “ideal” constraints, then the integer optimal solution can be obtained by simply solving a linear programming relaxation of the integer program. This paper serves as a quick guide for young researchers and PhD students.

Keywords Polyhedral Analysis · Integer Programming · Combinatorial optimization

1 Introduction

Integer Programming (IP) has been widely used in real-life combinatorial optimization problems, such as routing, scheduling, rostering, and hub-locations. There are three major types of integer linear programs. Let c be a nonnegative vector in \mathbb{R}^n , g be a nonnegative vector in \mathbb{R}^p , A be a $m \times n$ matrix, D be a $m \times p$ matrix, and b a m -vector, with all elements in c , g , A , D , and b real numbers.

A *mixed integer linear programming problem* (MILP) is of the form:

$$\max\{cx + gy : Ax + Dy \leq b, x \in \mathbb{Z}_+^n, y \in \mathbb{R}_+^p\} \quad (1)$$

As with usual practice, we do not distinguish between row and column vectors in our notation. The focus of our paper will be on *pure integer linear programming problems* (ILPs):

V. Mak-Hau (✉)
School of Information Technology, Deakin University, Waurn Ponds,
Geelong, Australia
e-mail: vicky.mak@deakin.edu.au

$$\max\{cx : Ax \leq b, x \in \mathbb{Z}_+^n\}, \quad (2)$$

and in particular, *pure binary linear programming problems* (BIPs):

$$\max\{cx : Ax \leq b, x \in \{0, 1\}^n\}. \quad (3)$$

Of all aspects of an integer programming model, perhaps one is most interested in how well it performs in terms of finding the optimal solution(s). Without doubt, the solution methodology used (e.g., branch-and-bound, branch-and-cut, column generation etc.) plays a key role in the computational performance; however, the performance also largely depends on the strength of the constraints of the integer program.

Consider two pure general integer programs described below.

$$\text{IP1 : } \max\{cx + dy : 2x + 2y \leq 5, x, y \in \mathbb{Z}\} \quad (4)$$

$$\text{IP2 : } \max\{cx + dy : x + y \leq 2, x, y \in \mathbb{Z}\} \quad (5)$$

Both IP1 and IP2 contain the same set of feasible integer points:

$$X = \{(0, 0), (0, 1), (0, 2), (1, 0), (2, 0), (1, 1)\}.$$

But IP2 is better in the sense that by solving the LP relaxation of IP2, we get the integer solution for free and hence obtain the optimal solution to the integer program, whereas with IP1, depending on the values of c and d , we may get a fractional value when an LP relaxation is solved, in which case we obtain only an upper bound to the optimal value of the integer program. IP2 is, therefore, an *ideal formulation*. We now introduce the mathematical background, definitions, and notation.

Let $P = \{x \in \mathbb{R}_+^n : Ax \leq b\}$ be a polytope (a bounded polyhedron) containing the set of all integer solutions to the system of linear inequalities $Ax \leq b$. A point $x \in P$ is a convex combination of points in P if there exists x^i , for $i \in \{1, \dots, t\}$ such that $x = \sum_{i=1}^t \lambda_i x^i$, where $\sum_{i=1}^t \lambda_i = 1$ and $\lambda_i \geq 0$ for all $i = 1, \dots, t$. Let $X = \{x \in \mathbb{Z}_+^n : Ax \leq b\}$. In this case, P is the linear programming relaxation of X .

The *convex hull* of X denoted by $\text{conv}(X)$ contains all feasible convex combinations of the points in X . An integer programming model is *ideal* if $P = \text{conv}(X)$, in which case solving P will produce naturally integer solutions, hence the optimal solution for the integer program. In other words, there is no LP-IP (integrality) gap. There are very few classic combinatorial optimization problems that present no integrality gap, except for the ones for which the following property holds.

Proposition 1 ([1], Proposition 3.3) *A linear program $\max\{cx : Ax \leq b, x \in \mathbb{R}_+^n\}$ has an integral optimal solution and finite optimal objective value under the necessary and sufficient condition that A is totally unimodular, and that b is a vector of integers.*

One classic combinatorial optimization problem with such properties is the assignment problem.

We say that P is *full-dimensional* if $\dim(P) = n$, the number of decision variables, in which case, one can find $n + 1$ affinely independent points in P .

Consider again the system of linear inequalities $Ax \leq b$. Let $M^=$ be the index sets of equality constraints in $Ax \leq b$, we denote these constraints by $(A^=, b^=)$; and M^{\leq} be the index sets of inequalities of $Ax \leq b$, we denote these constraints by (A^{\leq}, b^{\leq}) . We assume that (A^{\leq}, b^{\leq}) cannot be written as a linear combination of $(A^=, b^=)$. We have that $M^= \cap M^{\leq} = \emptyset$ and that $M^= \cup M^{\leq} = M$, with M the index set of all constraints in $Ax \leq b$. Now, if P is not full-dimensional, then $\dim(P) = n - \text{rank}(A^=, b^=)$.

Let $X = \{x \in \mathbb{Z}_+^n : Ax \leq b\}$, if $\text{conv}(X)$ is full-dimensional, then there is a unique set of constraints that describes the $\text{conv}(X)$. If such a complete polyhedral description is found, then solving the linear programming relaxation will give us the optimal solution to the integer program for free.

In most real-life integer programming models, however, particularly the classic traveling salesman- and vehicle routing-family problems, as there are equality constraints (the degree constraints), the corresponding polytopes are not full-dimensional. In such cases, there are in fact infinitely many complete polyhedral descriptions. Take the following integer program as an example.

$$X = \{x_1, x_2 \in \mathbb{Z} \mid x_1 + x_2 = 6, 2 \leq x_1 \leq 5, 1 \leq x_2 \leq 4\}. \tag{6}$$

The only feasible points are: $X = \{(2, 4), (3, 3), (4, 2), (5, 1)\}$ and that $\text{conv}(X)$ is one-dimensional, with $(2, 4)$ and $(5, 1)$ the extreme points. Given these two extreme points given, one possible complete description of $\text{conv}(X)$ is:

$$X = \{x_1, x_2 \in \mathbb{R} \mid x_1 + x_2 = 6, x_1 \geq 2, x_1 \leq 5\}. \tag{7}$$

and another is:

$$X = \{x_1, x_2 \in \mathbb{R} \mid x_1 + x_2 = 6, x_2 \geq 1, x_2 \leq 4\}. \tag{8}$$

One can easily see that there are in fact infinitely many complete descriptions of $\text{conv}(X)$.

We now introduce a few terminologies regarding constraints of an integer program. Again, let $X = \{x \in \mathbb{Z}_+^n : Ax \leq b\}$. For simplicity, we will use (π, π_0) to represent a constraint defined by $\pi x \leq \pi_0$. We say that (π, π_0) is a *valid* constraint if $\pi x \leq \pi_0$ for all $x \in X$. We say that F defines a *face* of $\text{conv}(X)$ if $F = \{x \in X : \pi x = \pi_0\}$. A face is a *proper face* if $F \neq \emptyset$ and $F \neq \text{conv}(X)$.

A face is called a *facet* if $\dim(F) = \dim(\text{conv}(X)) - 1$. One way to show that (π, π_0) defines a facet is to use the following theorem.

Theorem 1.1 ([2], Theorem 3.6 in Sect. 1.4) *Let $P = \{x \in \mathbb{R}^n : Ax \leq b\}$, let $(A^=, b^=)$ be the equality set of $P \in \mathbb{R}^n$, and let $F = \{x \in P : \pi x = \pi_0\}$ be a proper face. We have that F is a facet of P , if and only if there exists $\alpha \in \mathbb{R}^1$ and $\mu \in \mathbb{R}^{|M^=|}$ such that $(\alpha\pi + \mu A^=)x = (\alpha\pi_0 + \mu b^=)$, for all $x \in F$.*

As an illustration, let:

$$X = \{x_1, x_2, x_3 \in \mathbb{Z}_+^3 : x_1 + x_2 \leq 6, x_1 \leq 5, x_2 \leq 4, x_3 = 3\}. \quad (9)$$

Suppose we want to show that $x_2 \leq 4$ is facet-defining for $\text{conv}(X)$. We have that $F = \{x \in X : x_2 = 4\}$, $(\alpha\pi + \mu A^\top) = (0, \alpha, \mu)$, with α, μ as unknowns, and for every $x \in F = \{(0, 4, 3), (1, 4, 3), (2, 4, 3)\}$, we have that $(0, \alpha, \mu)x = (\alpha\pi_0 + \mu b^\top) = (4\alpha + 3\mu)$. Hence $x_2 \leq 4$ is a facet for X .

The theorem is mathematically very elegant, however in practice, it is easier to just demonstrate that the dimension of F is one less than the dimension of $\text{conv}(X)$, by finding the rank of the matrix with each row representing a distinct $x \in F$.

A complete polyhedral description is made up of facets. However hard it may seem, the more facets we can find for an integer program, the more likely we will have a small integrality gap, and consequently the more likely the exact method based on the integer program will perform well.

2 The Double Description Methods and Open Source Tools

There are a few good open source software that can be utilized for polyhedral analysis. For polytopes that are full-dimensional, one can use, e.g., `cdd/cdd+` [3] and `PORTA` [4]. However, `PANDA` [5] can handle polytopes that are not full-dimensional. In any case, all software are based on the idea of double description of a polyhedron.

The double description method was first proposed in [6]. Essentially, the idea is that every polyhedron can be described in two equivalent ways: a complete polyhedral description $P = \{x \in \mathbb{R}^n : Ax \leq b\}$, or the set of all extreme points in P , and from one, we can deduce the other. The former is referred to as the H-representation and the latter, the V-representation.

To explain how `PANDA` works, consider the following example.

$$X = \{x, y \in \{0, 1\}^2 : 2x + 2y \leq 3\}. \quad (10)$$

We first enter the LP relaxation of (10) into `PANDA`, using the H-representation, as below.

```
Names:
x   y
Inequalities:
2x + 2y <= 3
x <= 1
y <= 1
x >= 0
y >= 0
```

We then run PANDA by entering the command `./panda Toy.in > Toy.ext`. In the output file `Toy.ext`, we have the V-representation of the extreme points of the LP relaxation of (10).

```
Vertices/Rays:
1  2  2
2  1  2
0  1  1
1  0  1
0  0  1
```

The points above are the extreme points $\{(\frac{1}{2}, 1), (1, \frac{1}{2}), (0, 1), (1, 0), (0, 0)\}$ for the LP relaxation of (10). For binary integer programs, to obtain the extreme points for $\text{conv}(X)$, one can simply remove the fractional extreme points.

To obtain the facets for $\text{conv}(X)$, one can enter the modified V-representation of the integer extreme points: $(0, 1)$, $(1, 0)$, and $(0, 0)$, as below:

```
Names:
x  y
Vertices:
0  1
1  0
0  0
```

with the command `./panda Toy1.ext > Toy1.in`. PANDA will then return the facets for $\text{conv}(X)$.

```
Inequalities:
-x <= 0
-y <= 0
x + y <= 1
```

Since $\text{conv}(X)$ is full-dimensional, the three constraints above define the complete description of the convex hull, and the description is unique.

In Fig. 1, we present an example of a basic formulation, in H-representation, of the Cardinality Constrained Multi-cycle Problem (CCMcP) [7] (see Model 4 therein), with only four vertices on the graph, and a cardinality restriction of three. (Readers are referred to the paper for the IP model, hence we do not repeat the description of CCMcP in this paper.)

When we execute PANDA, we obtain all the extreme points for the LP relaxation, including the fractional ones. After removing the fractional points, we obtain the set of extreme points in Fig. 2.

For pure binary integer programming problems, the extreme points of the convex hull are in fact the set of all feasible points. Let x_1^* and x_2^* be two distinct extreme points of a BIP; let $X = \{x \in \{0, 1\}^n : Ax \leq b\}$; and let $x = \alpha x_1^* + (1 - \alpha)x_2^*$, for $0 < \alpha < 1$, then $0 < x_j < 1$ for at least one $j \in \{1, \dots, n\}$, hence $x \notin X$. If we are able to systematically generate all the feasible points, then we have the set of all extreme points. (See, e.g., [8] for an example). When we do not know the set of all feasible integer points, we must carry out the steps described above. For most classic combinatorial optimization problems, however, in particular the TSP-family

Names:
x12 x13 x14 x21 x23 x24 x31 x32 x34 x41 x42 x43

Equations:
x14 +x24 +x34 -x41 -x42 -x43 = 0
x13 +x23 -x31 -x32 -x34 +x43 = 0
x12 -x21 -x23 -x24 +x32 +x42 = 0
-x12 -x13 -x14 +x21 +x31 +x41 = 0

Inequalities:
x12 +x13 +x14 <= 1
x21 +x23 +x24 <= 1
x31 +x32 +x34 <= 1
x41 +x42 +x43 <= 1

x21 +x31 +x41 <= 1
x12 +x32 +x42 <= 1
x13 +x23 +x43 <= 1
x14 +x24 +x34 <= 1

x12 +x23 +x34 <= 2
x23 +x34 +x41 <= 2
x12 +x34 +x41 <= 2
x12 +x23 +x41 <= 2

x12 +x24 +x43 <= 2
x24 +x31 +x43 <= 2
x12 +x31 +x43 <= 2
x12 +x24 +x31 <= 2

x13 +x24 +x32 <= 2
x24 +x32 +x41 <= 2
x13 +x24 +x41 <= 2
x13 +x32 +x41 <= 2

x13 +x34 +x42 <= 2
x21 +x34 +x42 <= 2
x13 +x21 +x42 <= 2
x13 +x21 +x34 <= 2

x14 +x23 +x42 <= 2
x23 +x31 +x42 <= 2
x14 +x23 +x31 <= 2
x14 +x31 +x42 <= 2

x14 +x32 +x43 <= 2
x21 +x32 +x43 <= 2
x14 +x21 +x32 <= 2
x14 +x21 +x43 <= 2

x12 >= 0
x13 >= 0
x14 >= 0
x21 >= 0
x23 >= 0
x24 >= 0
x31 >= 0
x32 >= 0
x34 >= 0
x41 >= 0
x42 >= 0
x43 >= 0

x12 <= 1
x13 <= 1
x14 <= 1
x21 <= 1
x23 <= 1
x24 <= 1
x31 <= 1
x32 <= 1
x34 <= 1
x41 <= 1
x42 <= 1
x43 <= 1

Fig. 1 H-representation of model 4 of CCMcP in [7], with 4 vertices on the graph, and a cardinality restriction of 3

Names:	x12	x13	x14	x21	x23	x24	x31	x32	x34	x41	x42	x43
Vertices:	0	0	0	0	0	1	0	1	0	0	0	1
	0	0	0	0	1	0	0	0	1	0	1	0
	0	0	1	0	0	0	1	0	0	0	0	1
	0	0	1	0	1	0	0	1	0	1	0	0
	0	1	0	0	0	0	0	0	1	1	0	0
	0	1	0	0	0	1	1	0	0	0	1	0
	1	0	0	0	0	1	0	0	0	1	0	0
	1	0	0	0	1	0	1	0	0	0	0	0
	1	0	0	1	0	0	0	0	1	0	0	1
	0	0	0	0	0	0	0	0	1	0	0	1
	0	0	0	0	0	0	0	0	0	0	0	0
	0	0	0	0	0	1	0	0	0	0	1	0
	0	0	0	0	1	0	0	1	0	0	0	0
	0	0	1	0	0	0	0	0	0	1	0	0
	0	0	1	1	0	0	0	0	0	0	0	1
	0	1	0	0	0	0	1	0	0	0	0	0
	0	1	0	1	0	0	0	1	0	0	0	0
	1	0	0	1	0	0	0	0	0	0	0	0

Fig. 2 Extreme points for the IP presented in Fig. 1

and VRP-family problems, as well as cycle and chain problems, we do know the set of all feasible integer solutions.

When we enter the V-representation of all the extreme points of a BIP, PANDA will return one complete description of the convex hull of the feasible integer points. Recall that if a polytope is full-dimensional, there is only one unique complete polyhedral description, otherwise, there are infinitely many. In Fig. 3, we have one of the complete polyhedral descriptions of the small CCMcP example returned by PANDA. So, even though we may have a class of constraints that we suspect is facet-defining, the fact that it does not appear in the output returned by the software does not mean that the constraint is definitely not facet-defining. The benefit of using a software for obtaining even one of the complete polyhedral description is that it can give us some constraints that we did not know are facet-defining, then we can proceed to establish the proofs.

Notice that the bound constraint $x \geq 0$ is often facet-defining, see, e.g., [9], these are considered trivial constraints. Notice also that sometimes a constraint is only facet-defining for small problems, so in the end we cannot prove that they are facet-defining for all problem sizes. A constraint can also be facet-defining for larger problems, not toy-sized ones, so they are not found by a software.

3 Proof Techniques

Direct proof For BIPs of small scale, when we have all the extreme points explicitly generated, to show that a constraint (π, π_0) is facet-defining, one needs to show that the set of extreme points (e.g., x^1, \dots, x^t , where each of x^j , for $j = 1, \dots, t$, is a n -dimensional vector) that satisfy $\pi x = \pi_0$ are of dimension $\dim(\text{conv}(X)) - 1$. This can be done by calculating the rank of $(x^1, -1), \dots, (x^t, -1)$. If the rank is exactly $\dim(\text{conv}(X))$, then there are $\dim(\text{conv}(X))$ affinely independent feasible solutions

Fig. 3 One complete polyhedral description of the convex hull of the small CCMcP example

```

Equations:
x14 +x24 +x34 -x41 -x42 -x43 = 0
x13 +x23 -x31 -x32 -x34 +x43 = 0
x12 -x21 -x23 -x24 +x32 +x42 = 0

Inequalities:
-x21 <= 0
x23 +x24 +x31 +x34 +x41 +x43 <= 2
-x32 <= 0
-x42 <= 0
x41 +x42 +x43 <= 1
-x21 -x23 -x24 +x32 +x42 <= 0
x31 +x32 +x34 <= 1
-x21 -x23 +x32 -x43 <= 0
x24 +x34 -x41 -x42 -x43 <= 0
-x21 -x24 -x34 +x42 <= 0
x24 +x31 +x34 -x42 <= 1
-x23 <= 0
x23 -x31 -x32 -x34 +x43 <= 0
-x23 +x31 +x32 +x41 <= 1
x23 -x32 +x41 +x43 <= 1
-x24 <= 0
-x23 -x24 +x31 +x32 +x34 +x42 <= 1
-x23 -x24 +x32 +x41 +x42 +x43 <= 1
x23 +x24 -x32 +x43 <= 1
-x24 +x31 +x41 +x42 <= 1
-x23 -x24 +x31 +2x32 +x34 +x41 +2x42 +x43 <= 2
x23 +x24 +x34 -x42 <= 1
-x31 <= 0
-x23 +x34 -x41 -x43 <= 0
x21 +x24 +2x31 +x32 +x34 +x41 -x42 <= 2
-x23 +x32 +x41 +x42 <= 1
x21 +x23 +x31 -x32 +2x41 +x42 +x43 <= 2
-x24 -x31 -x34 +x43 <= 0
-x34 <= 0
-x23 +x32 +x34 +x42 <= 1
x21 +x23 +2x24 +x31 +x32 +2x34 -x42 -x43 <= 2
-x41 <= 0
x21 +2x23 +x24 -x32 -x34 +x41 +x42 +2x43 <= 2
-x24 +x32 +x42 +x43 <= 1
-x43 <= 0
-x24 +x31 +x32 +x42 <= 1
x24 +x32 +x34 -x43 <= 1
x24 -x32 -x41 -x42 <= 0
x24 +x31 +x32 +x34 -x42 -x43 <= 1
x23 -x32 -x34 +x41 +x42 +x43 <= 1
x23 -x31 -x32 -x42 <= 0
x21 -x23 +x31 +x32 +2x41 +x42 +x43 <= 2
x23 -x34 +x42 +x43 <= 1
x21 +x24 +x32 +x34 +x41 +x42 <= 2
x21 -x24 +2x31 +x32 +x34 +x41 +x42 <= 2
x21 +x31 +x41 <= 1
x21 +x23 +x31 +x32 +x42 +x43 <= 2
x21 -x34 +x41 +x43 <= 1
x21 +x31 +x34 -x43 <= 1
x21 +x24 +x34 -x43 <= 1
x21 +x24 +x31 -x42 <= 1
x21 +x23 -x32 +x41 <= 1
x21 +x23 +x24 <= 1
x21 +x23 -x34 +x43 <= 1
x21 +x23 +x24 -x32 -x34 +x43 <= 1
x21 +x23 +x24 +x34 -x42 -x43 <= 1
2x21 +x23 +x24 +x31 +x34 +x41 -x43 <= 2
2x21 +x23 +x24 +x31 -x34 +x41 +x43 <= 2

```

that satisfy the constraint (π, π_0) at equality, that is, $\dim(F) = \dim(\text{conv}(X)) - 1$, and therefore (π, π_0) defines a facet.

For BIPs of large scale, we have to explicitly construct $\dim(\text{conv}(X))$ affinely independent feasible integer points that satisfy (π, π_0) at equality. One way is to make sure a new variable is used in each new solution. Examples of such direct proofs can be found in [10] for the ATSP and VRPs with time windows or precedence

constraints, and [11] for cardinality constrained quadratic knapsack problem and the quadratic selective TSP.

Mathematical induction A one-dimensional mathematical induction framework for the Asymmetric Travelling Salesman Problem was proposed in [12], and the concept is essentially to use vertex insertion and can be applied in many cycle-based combinatorial optimization problems. When there are side constraints, however, e.g., cycle-cardinality constraints, a two-dimensional mathematical induction is required, (see e.g., [13] in the context of the Asymmetric Travelling Salesman Problem with Replenishment Arcs (RATSP)).

Monotone polytope Let $P = \{x \in \mathbb{R}^n : Ax \leq b\}$ and lies in the positive orthant. The monotone polytope is defined by $\tilde{P} = \{\tilde{x} \in \mathbb{R}^n : 0 \leq \tilde{x} \leq x, \text{ for some } x \in P\}$. The monotone polytope is full-dimensional, hence easier to analyze, though one will still need the results for the original polytope that is not full-dimensional. Fortunately, the theoretical result presented in [14] enabled us to translate results from the monotone polytope to the original polytope of an integer program. See also [15] for background mathematics.

Definition 1 Let $\dim(\tilde{P}) = n$; N be the index set of variables, (π, π_0) be a valid inequality for \tilde{P} ; $N^0 = \{j \in N \mid \pi_j = 0\}$; A_0^- be the r by $|N^0|$ submatrix of A^- with only columns with indices in N^0 . The inequality (π, π_0) is said to be support reduced with respect to P if A_0^- has a full row rank. Further, w.l.o.g., let $N^r = \{j_1, \dots, j_r\}$ be the index set of the columns of a basis for A_0^- . If (π, π_0) satisfies the condition that for each $k \in N^0 \setminus N^r$, if $N^0 \setminus N^r \neq \emptyset$, there exists a pair $x^1, x^2 \in \{x \in P \mid \pi x = \pi_0\}$, such that

$$\{j_k\} \subseteq \{j \in N \mid x_j^1 \neq x_j^2\} \subseteq N^0 \setminus N^r$$

then (π, π_0) is strongly support reduced.

Consider again (9) and the inequality $x_2 \leq 4$. We have that $A^- = [0, 0, 1]$, $N^0 = \{1, 3\}$, and $A_0^- = [0, 1]$. As A_0^- has a full row rank, it is support reduced. The index set for its column basis is $N^r = \{3\}$. Now, let $F = \{x \in X \mid x_2 = 4\}$ (with X the feasible set for (9)). Consider $x^1, x^2 \in F$ with $x^1 = (0, 4, 3)$ and $x^2 = (1, 4, 3)$, we have that $\{j \in N \mid x_j^1 \neq x_j^2\} = \{1\}$, which is $\supseteq \{1\}$ and $\subseteq N^0 \setminus N^r = \{1\}$. Hence, $x_2 \leq 4$ is strongly support reduced.

Theorem 3.1 ([14]) *Let $\pi x \leq \pi_0$, where $\pi_0 \neq 0$, be facet-defining for the monotone polytope $\text{conv}(\tilde{X})$. If $\pi x \leq \pi_0$ is strongly support reduced with respect to $\text{conv}(X)$, then it is also facet-defining for $\text{conv}(X)$.*

Hence, $x_2 \leq 4$ is facet-defining for X in (9). An application of this theorem in the context of minimum-span graph labeling problem with integer distance constraints can be found in [16].

4 Literature and Research Directions

There are a number of rather good papers that one can consult before embarking on a polyhedral analysis project, e.g., [17] for the p -cycle polytope, [18] for the Cardinality Constrained Covering Traveling Salesman Problem, [19] on the cycle polytope of a directed graph and its relaxations, [20] on the k -cycle polytope, [21] on the circuit polytope, [22] on the Capacitated Vehicle Routing Problem, [12] on ATSP, and many more. One should also consult a few very good textbooks on polyhedral studies, e.g., [1, 2].

For polytopes that are not full-dimensional, to generate an alternative set of facets from the complete polyhedral description provided by a software may be a worthwhile exercise. Firstly, some constraints have better structures that make it possible to develop fast separation algorithms. Secondly, some constraints are simply easier to prove that they are facet-defining. Further, one should not give up so quickly and jump straight to (meta-) heuristics just because the full IP did not perform well on a commercial IP solver. One should always explore stronger constraints and experiment with different relaxations and decomposition methods, or even using these as part of a heuristic method.

References

1. Wolsey, L.A.: *Integer Program*. Wiley, New York (1998)
2. Nemhauser, G.L., Wolsey, L.A.: *Integer and Combinatorial Optimization*. Wiley, New York (1988)
3. cdd+ reference manual. <https://www.math.ucdavis.edu/~deloera/MISC/BIBLIOTECA/trunk/Fukuda/Fukuda1.pdf> (2010). Accessed 30 Sept 2010
4. Porta vers. 1.4.1. <http://www.iwr.uni-heidelberg.de/groups/comopt/software/PORTA/> (2010). Accessed 30 Sept 2010
5. Lrwald, S., Reinelt, G.: Panda: a software for polyhedral transformations. *EURO J. Comput. Optim.* **3**(4), 297–308 (2015)
6. Motzkin, T.S., Raiffa, H., Thompson, G.L., Thrall, R.M.: *The Double Description Method*. Princeton University Press, Princeton (1953)
7. Mak-Hau, V.: On the kidney exchange problem: cardinality constrained cycle and chain problems on directed graphs: a survey of integer programming approaches. *J. Comb. Optim.* 1–25 (2015)
8. Mak-Hau, V.: Polyhedral results for the cardinality constrained multi-cycle problem (CCMcP) and the cardinality constrained cycles and chains problem (CCCCP). In: *Proceedings of 21st International Congress on Modelling and Simulation (MODSIM, Nov 2015)* (2015)
9. Akartunali, K., Mak-Hau, V., Tran, T.: A unified mixed-integer programming model for simultaneous fluence weight and aperture optimization in vmat, tomotherapy, and cyberknife. *Comput. Oper. Res.* **56**, 134–150 (2015)
10. Mak, V., Ernst, A.T.: New cutting-planes for the time-and/or precedence-constrained ATSP and directed VRP. *Math. Methods Oper. Res.* **66**(1), 69–98 (2007)
11. Mak, V., Thomadsen, T.: Polyhedral combinatorics of the cardinality constrained quadratic knapsack problem and the quadratic selective travelling salesman problem. *J. Comb. Optim.* **11**(4), 421–434 (2006)

12. Balas, E.: The asymmetric assignment problem and some new facets of the traveling salesman polytope on a directed graph. *SIAM J. Discret. Math.* **2**(4), 425–451 (1989)
13. Mak, V., Boland, N.: Facets of the polytope of the asymmetric travelling salesman problem with replenishment arcs. *Discret. Optim.* **3**(1), 33–49 (2006). *The Traveling Salesman Problem*
14. Balas, E., Fischetti, M.: On the monotonicity of polyhedra. *Math. Program.* **78**(1), 59–84 (1996)
15. Pulleyblank, W.R., Grötschel, M.: Clique tree inequalities and the symmetric travelling salesman problem. *Math. Oper. Res.* **11**(4), 537–569 (1986)
16. Mak, V.: Polyhedral studies for minimum-span graph labelling with integer distance constraints. *Int. Trans. Oper. Res.* **14**(2), 105–121 (2007)
17. Hartmann, M., Özlük, Ö.: Facets of the p -cycle polytope. *Discret. Appl. Math.* **112**(13), 147–178 (2001). *Combinatorial Optimization Symposium, Selected Papers*
18. Patterson, R., Rolland, E.: The cardinality constrained covering traveling salesman problem. *Comput. Oper. Res.* **30**(1), 97–116 (2003)
19. Balas, E., Stephan, R.: On the cycle polytope of a directed graph and its relaxations. *Networks* **54**(1), 47–55 (2009)
20. Nguyen, V.H., Maurras, J.F.: On the linear description of the k -cycle polytope. *Int. Trans. Oper. Res.* **8**(6), 673–692 (2001)
21. Bauer, P.: The circuit polytope: facets. *Math. Oper. Res.* **22**(1), 110–145 (1997)
22. Cornuejols, G., Harche, F.: Polyhedral study of the capacitated vehicle routing problem. *Math. Program.* **60**(1), 21–52 (1993)

Towards a Feasible Design Space for Proximity Alerts Between Two Aircraft in the Conflict Plane

Mark Westcott, Neale Fulton and Warren F. Smith

Abstract In studying airspace it is necessary to have a model of how and when two aircraft come into proximity. There are two components: a kinematic description of the aircraft in flight, and a set of rules for deciding whether proximity has occurred. The focus in this paper is on the rules with the kinematics kept as simple as possible by utilizing the crossing track model. The aircraft are assumed to be flying straight-line paths at constant speed in a common plane towards a common waypoint A where the paths intersect. The kinematics is completely determined once the initial positions and the velocity vectors are known. A set of proximity rules are described which then permit partitioning of a constrained mathematical model for proximity. The partitioning is a function of parameter values derived from the proximity rules. It follows that the region where all constraints are satisfied defines a Feasible Design Space (FDS), and a different set of design variables is identified for describing the kinematics than is commonly used in current practice. The Compromise Decision Support methodology constructs permit the formalization of the analysis of how different designs for airspace management and communication might affect the occurrence of proximity between aircraft. The existence of proximity can be determined analytically once the kinematic variables are known. The use of the new FDS is applicable hierarchically from strategic planning through to real-time adaption required in actual in-flight operations. It is important as a visualization tool for simulation studies and decision support analyses.

Keywords Aircraft proximity • Feasible Design Space • Compromised Decision Support methodology

M. Westcott (✉) · N. Fulton
Data 61, CSIRO, Canberra, ACT, Australia
e-mail: mark.westcott@csiro.au

N. Fulton
e-mail: neale.fulton@csiro.au

W.F. Smith
School of Engineering and IT, UNSW, Canberra, ACT, Australia

1 Introduction

Conflict management (CM) is identified as one of the seven architectural pillars of the ICAO Global Air Traffic Management Operational Concept [1]. Conflict management is comprised of three functions: Proximity Specification, Conflict Detection and Conflict Resolution. In this paper, a Feasible Design Space (FDS) for proximity specification based on the Compromise Decision Support methodology [2, 3] is presented for use in the Conceptual Engineering specification process, detailed design and in operational management facilitation.

Netjasov [4] presents a set of risk assessment models for crossing tracks that identify a hierarchy of strategic, tactical and operational considerations. The model presented here is a more detailed and harmonized benchmark model for tactical [5], current day operational [6], in-flight planning and engineering design purposes. New activities in airspace such as the introduction of remotely piloted vehicles and the modernization of conflict management functions for existing conventionally piloted aircraft are placing demands for decision support models for engineering design and acceptance test that cover the total possible domains of operation.

However, historic development of crossing track models have only been partial and not achieved the degree of model integration and fidelity required for foreseeable operations. For example, ICAO [7] establishes a crossing (intersecting) track model for risk assessment purposes but this model and other published historic models are not complete in engineering epistemic terms for they lack definition of the total number of crossing kinematic modes that can exist. Nor have they adequately defined both spatial and temporal warnings. In this paper, the canonical parameters that govern proximate behaviour between aircraft pairs are identified in terms of both the kinematic modes of operation and the required spatial and temporal warnings. Further, the Feasible Design Space presented is based on a specific choice of canonical parameters that ensures smooth transitions of the loci of the operational point under dynamic changes in the kinematic variables.

Drawing from the discipline of optimal engineering design [2, 3], if a system can be modelled mathematically, the region where system constraints and bounds are satisfied defines the 'Feasible Design Space'. Using, in particular, the constructs of the Compromise Decision Support methodology if a FDS exists, it can be explored to find superior or so called satisficing designs, by mapping candidate solutions against specified system aspirations. For example, in the context of air traffic management, the design (or operational) feasibility might be defined by maintaining aircraft in adequately separated (non-proximate) relative positions. However, should aircraft move into more proximate relative positions the aspiration would be to find the most effective action to recover an adequately separated state.

The challenging aspect in any multi-objective design problem is the construction of a mathematical model with sufficient fidelity to provide useful results through model exploration processes, thus identifying the emergent system behaviours. Therefore, the focus of the research presented in this paper is on model construction. Given an engineering problem, what solution permits the identification of a

minimal canonical set of design variables, how are these variables bounded and how are they related to form constraints and objectives?

2 Definition of Proximity

The model of proximity has two components: a kinematic description of the aircraft in flight, and a set of rules for deciding whether proximity has occurred. Here, we focus on the rules while the kinematics is kept as simple as possible by use of the crossing track model [8–11]. This model assumes that there are two aircraft flying straight-line paths at constant speed in a common plane towards a common waypoint A . The paths intersect at A . The kinematics is completely known once the initial positions and the velocity vectors of the two aircraft are known.

Again, for simplicity, a Cartesian coordinate system is set in the plane with the origin at A and with one aircraft (Aircraft 1) travelling towards A along the positive x -axis. The other aircraft will be called Aircraft 2. The kinematics is then completely specified by five parameters:

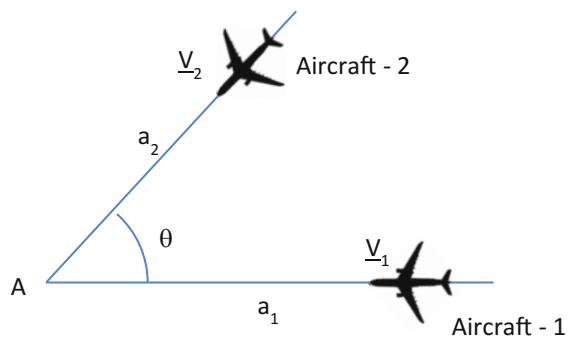
- The speeds of the two aircraft, v_1 and v_2 ;
- The initial distances from A , a_1 and a_2 ;
- The track intersection angle, θ , between the aircraft tracks.

Without loss of generality assume $\theta \in [0, \pi]$. Sometimes, it will be necessary to distinguish between the first quadrant $Q_1 (\theta \in [0, \frac{1}{2}\pi])$ and the second quadrant $Q_2 (\theta \in (\frac{1}{2}\pi, \pi])$. The kinematic model is shown in Fig. 1.

The basic idea is that unacceptable proximity occurs if either a time separation or a distance separation threshold is violated; that is, if the two aircraft ever get ‘too close’ in either space or time. We denote these thresholds by τ_{thresh} and d_{thresh} , respectively.

If unacceptable proximity occurs, it follows that some action must be taken to re-establish an acceptable level of proximity. The identification of feasible and possible alternative actions is more readily facilitated by the FDS approach.

Fig. 1 Kinematic model for flight towards a common waypoint



However, the focus of this paper is on describing the construction of the foundational model and constraints for a FDS approach.

The natural check for violation of the distance threshold is to identify the aircraft separation at the *Point of Closest Approach* (PCA). Our chosen check for time separation is the time between the aircraft arrivals at A , since at the moment of the first arrival one aircraft is directly in front of the other. If t_{Ai} ($i = 1, 2$) is the arrival time of Aircraft i at A , then clearly $t_{Ai} = a_i/v_i$. Formally, we now define:

$t_A = \min(t_{A1}, t_{A2})$ = 1st arrival time at A

$\tau_A = t_{A2} - t_{A1}$ = time between arrivals of Aircraft 1 and 2 at A

d_{PCA} = spatial separation at PCA

t_{PCA} = time when PCA occurs

Because τ_A is used extensively, hereafter we drop the subscript A . Note that τ is signed, since in general either aircraft could arrive first at A .

2.1 Proximity Check

The aircraft are in proximity if the disjunction of the conditions $|\tau| \leq \tau_{\text{thresh}}$ and $d_{PCA} \leq d_{\text{thresh}}$ holds true.

3 Alert Times Associated with a Proximity Event

If proximity is imminent, it is very desirable to give the aircraft sufficient warning of the occurrence so that the proximity can be managed safely. That is, the aircraft need a suitably long *alert time interval* before a proximity event. Then, using the definition of proximity, one end of the alert time interval is set as follows:

- For a time separation violation, the time alert interval precedes t_A .
- For a distance separation violation, the time alert interval precedes the time when the violation first occurs; that is, the time at which the aircraft separation first reaches the threshold value d_{thresh} .

We say that the other (earlier) end of the time alert interval defines the required *alert time* for the proximity event. To express these requirements mathematically, we need some more notation. Define:

τ_{alert} = length of alert time interval

t_{alert} = alert time

$t_{d\text{thresh}}$ = time at which separation first reaches d_{thresh}

If there is no distance separation violation, there is of course no $t_{d\text{thresh}}$. Then the alert requirements described above can be written as:

- For a time separation violation, $t_{\text{alert}} = t_A - \tau_{\text{alert}}$
- For a distance separation violation, $t_{\text{alert}} = t_{\text{dthresh}} - \tau_{\text{alert}}$

Note that if t_{dthresh} occurs, it always precedes t_{PCA} .

4 Partitions of the Feasible Design Space

Two different partitions of the FDS are presented: the first (Sect. 4.1 and Fig. 2) permits a closer semantic association with the operational scenario and the second (Sect. 4.2 and Fig. 3) permits a closer association with the continuity of the mathematics underpinning the alert requirements.

4.1 The Operational Partition

There are three times always associated with the engagement between the two aircraft: t_{A1} , t_{A2} and t_{PCA} . These lead to a natural logical partition (Sect. 4.2.2) of the possible engagements into four cases, defined by the relative magnitudes of t_A , $T_A \equiv t_A + |\tau|$ (the later arrival time at A) and t_{PCA} , and by which aircraft arrives first at A . We note that Haddad et al. [8] only suggested a subset of this formal definition:

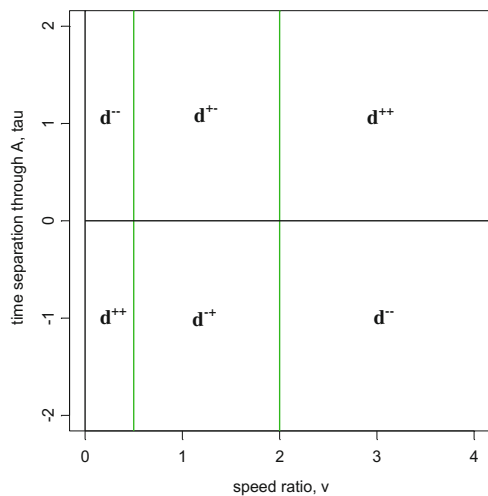
d^- is the case where $t_{\text{PCA}} < t_A$

d^{++} is the case where $t_{\text{PCA}} > T_A$

d^{+-} is the case where $t_A < t_{\text{PCA}} < T_A$ and Aircraft 1 reaches A first

d^{-+} is the case where $t_A < t_{\text{PCA}} < T_A$ and Aircraft 2 reaches A first

Fig. 2 Operational partition of the FDS, P, for $\theta \in Q1$. Here, $\theta = 60^\circ$. The vertical lines are at $v = \cos \theta$ and $v = \sec \theta$



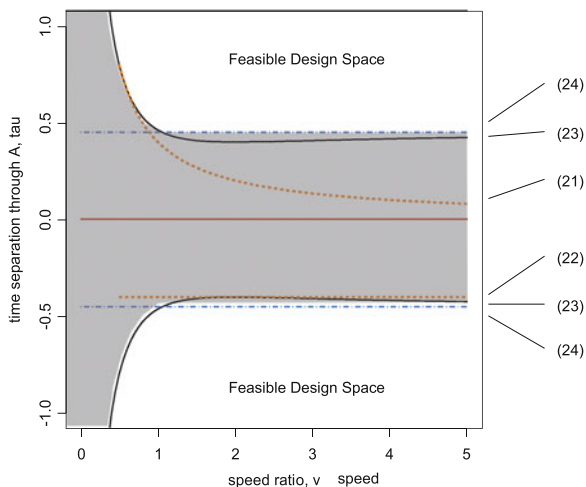


Fig. 3 Alert partition of the FDS, P , for $\theta \in Q1$. Equation numbers are shown on the *right*. Here, $\theta = 60^\circ$, $\phi_{\text{thresh}} = 0.4$, $\tau_{\text{thresh}} = 0.425$

So in d^- , PCA occurs before either aircraft reaches A ; in d^+ , PCA occurs after both aircraft have passed A ; in the other two regions, PCA occurs between arrivals at A , the distinction being which aircraft arrives at A first. While these four cases provide an important link to the spatial orientation of the aircraft with respect to the waypoint A for operational reasons, they are not natural boundaries for partitioning the FDS with respect to the alert boundaries: the functions delimiting alert transition are continuous across some of the operational boundaries.

4.2 The Alert Partition

From an alert perspective, the FDS partitions into two mutually exclusive regions: a normal (N) region of operation for which there are no alerts generated and a non-normal (not-N) region operation. The non-normal region also partitions. It is comprised of regions from the set of *Proximity Alert Regions* $\{T, D, TD, DT\}$. These are developed in Sect. 4.2. In terms of constructing the FDS, the mathematical task becomes:

1. Specify the FDS based on the kinematic parameters.
2. Find the Operational and the Alert partitions of the FDS.
3. Find the *Proximity Alert Regions* within the non-normal region. Not all kinds of *Proximity Alert Regions* may exist for a particular parameter set, so determine

the condition(s) on the parameters for the existence of each of the *Proximity Alert Regions*.

4. Identify the location of the operational point within the FDS with respect to the engagement cases, the Operational partition and, as required, the *Proximity Alert Regions*.

4.2.1 Choice of Parameters

The Operational partition (Sect. 4.1) is based on the relative magnitudes of the times t_{A1} , t_{A2} and t_{PCA} . The proximity alert regions in this section are based on the magnitudes of τ and d_{PCA} relative to their threshold values. The mathematical design question becomes:

Is it possible to find an economical set of parameters which can be used to describe all of these quantities?.

From the point of view of the display of results, two parameters would be ideal.

Remarkably, a reduction in the number is possible. To show this, we first need formulae for all of these quantities in terms of the basic kinematic parameters. Suppose we have two aircraft each travelling at constant velocity in a common (conflict) plane. Define the following symbols:

\mathbf{r}_i is the initial position vector of Aircraft i ($i = 1, 2$).

\mathbf{v}_i is the constant velocity vector of Aircraft i ($i = 1, 2$).

$\mathbf{r}_0 \equiv \mathbf{r}_2 - \mathbf{r}_1$ is the relative initial position vector of Aircraft 2.

$\mathbf{v}_R \equiv \mathbf{v}_2 - \mathbf{v}_1$ is the constant relative velocity vector of Aircraft 2.

The magnitude of a vector will be represented by the corresponding non-bold italic character; thus $v_R \equiv \|\mathbf{v}_R\|$. It is a standard result that t_{PCA} and d_{PCA} are calculated from:

$$t_{PCA} = -\frac{\mathbf{r}_0 \cdot \mathbf{v}_R}{\mathbf{v}_R \cdot \mathbf{v}_R} = -\frac{\mathbf{r}_0 \cdot \mathbf{v}_R}{v_R^2} \quad (1)$$

$$d_{PCA}^2 = \mathbf{r}_0 \cdot \mathbf{r}_0 - \frac{(\mathbf{r}_0 \cdot \mathbf{v}_R)^2}{\mathbf{v}_R \cdot \mathbf{v}_R} = r_0^2 - \frac{(\mathbf{r}_0 \cdot \mathbf{v}_R)^2}{v_R^2} \quad (2)$$

It is also easy to see that the separation between the aircraft decreases until PCA and then increases. For our parametric model and coordinate system, we have:

$$\mathbf{r}_1 = (a_1, 0), \quad \mathbf{r}_2 = (a_2 \cos \theta, a_2 \sin \theta), \quad \mathbf{v}_1 = (-v_1, 0), \quad \mathbf{v}_2 = (-v_2 \cos \theta, -v_2 \sin \theta)$$

It is routine to derive from (1) and (2) that:

$$t_{\text{PCA}} = \frac{a_1 v_1 + a_2 v_2 - (a_1 v_2 + a_2 v_1) \cos \theta}{v_1^2 + v_2^2 - 2v_1 v_2 \cos \theta} \quad (3)$$

$$d_{\text{PCA}} = \frac{|a_1 v_2 - a_2 v_1| \sin \theta}{\sqrt{v_1^2 + v_2^2 - 2v_1 v_2 \cos \theta}} \quad (4)$$

Recall that $\theta \in [0, \pi]$, so $\sin \theta \geq 0$. Also, note that, it is possible that t_{PCA} is negative when θ is in the first quadrant; this cannot happen for θ in the second quadrant, since then $\cos \theta \leq 0$ so the numerator in (3) must be positive (we assume about the signs of the a 's are positive). Now in (4), we have that

$$|a_1 v_2 - a_2 v_1| = v_1 v_2 |a_1/v_1 - a_2/v_2| = v_1 v_2 |t_{A1} - t_{A2}| = v_1 v_2 |\tau|,$$

so we can express d_{PCA} using only four parameters. This is not possible directly for t_{PCA} . However, a little algebra shows that, from (3),

$$t_{\text{PCA}} = t_{A1} + \frac{\tau v_2 (v_2 - v_1 \cos \theta)}{v_1^2 + v_2^2 - 2v_1 v_2 \cos \theta} = t_{A2} - \frac{\tau v_1 (v_1 - v_2 \cos \theta)}{v_1^2 + v_2^2 - 2v_1 v_2 \cos \theta} \quad (5)$$

So, the *difference* between t_{PCA} and t_{A1} or t_{A2} is a function of the same four parameters. And the differences are what are required for the mathematical description of the Operational partition. From (5), we see there is a further simplification possible, since the speeds v_1 and v_2 occur only as a ratio. So, if we define the *speed ratio* $v \equiv v_2/v_1$, we can write the difference between t_{PCA} and t_{A1} or t_{A2} as a function of just three parameters, τ , v and θ . So, we need just these three parameters to completely describe the Operational partition mathematically. Specifically,

$$t_{\text{PCA}} = t_{A1} + \frac{\tau v (v - \cos \theta)}{1 + v^2 - 2v \cos \theta} = t_{A2} - \frac{\tau (1 - v \cos \theta)}{1 + v^2 - 2v \cos \theta} \quad (6)$$

Note that v can take any positive value. To describe the proximity alert regions, we must study the inequalities associated with the proximity conditions. Time separation proximity is determined purely from the value of τ which is already a parameter. Distance separation is determined purely from the value of d_{PCA} . From (4), it is straightforward (see also [9–11]) to see that

$$d_{\text{PCA}} = v_1 \frac{|\tau| v \sin \theta}{\sqrt{1 + v^2 - 2v \cos \theta}} \quad (7)$$

The fact that d_{PCA} is proportional to $|\tau|$ might seem a fortuitous coincidence. It is actually very simply explained by a geometric argument in relative velocity space.

The special cases when $v = 1$ and/or $\theta = 0$, π are elementary and not further developed here.

From (7), we see that a fourth parameter is needed to describe d_{PCA} . This is obvious on dimensional grounds, since d_{PCA} has the dimension of length, which is not a dimension in any of the three earlier parameters. Then, to reduce the number of parameters required back to three, we convert the distance proximity check into a ‘time’ proximity check, by dividing through by v_1 . This turns the distances into the times it would take Aircraft 1 to travel those distances. These times are purely conceptual, except in a few special cases, but they are a convenient way, mathematically, to simplify the descriptions. The following notation is introduced:

$$\begin{aligned}\phi_{PCA} &\equiv d_{PCA}/v_1 \\ \phi_{\text{thresh}} &\equiv d_{\text{thresh}}/v_1\end{aligned}\quad (8)$$

Both ϕ_{PCA} and ϕ_{thresh} have the dimensions of time. The distance proximity check now becomes a ‘time’ check, namely $\phi_{PCA} \leq \phi_{\text{thresh}}$. To make the formulae explicit, from (7) we have

$$\phi_{PCA} = \frac{|\tau|v \sin \theta}{\sqrt{1 + v^2 - 2v \cos \theta}} \quad (9)$$

To display results graphically, we define the FDS as $P \equiv \{v \geq 1, \tau \in \mathbb{R}\}$ for any given value of θ . If we think of v as being plotted on the x-axis, this is the right half-plane in \mathbb{R}^2 .

4.2.2 Delineation of the Operational Regions

As noted earlier, the Operational partition (Sect. 4.1) is based on the relative magnitudes of the times t_{A1} , t_{A2} and t_{PCA} . These can easily be turned into a partition of P using (6). Then, because the denominator in (6) is positive except in the special case $v = 1$, $\theta = 0$, we can deduce that:

$$\begin{aligned}t_{PCA} \leq t_{A1} &\Leftrightarrow \tau(v - \cos \theta) \leq 0 \\ &\Leftrightarrow \tau \geq 0 \text{ and } v \leq \cos \theta \text{ or } \tau \leq 0 \text{ and } v \geq \cos \theta\end{aligned}\quad (10)$$

$$\begin{aligned}t_{PCA} \leq t_{A2} &\Leftrightarrow \tau(1 - v \cos \theta) \geq 0 \\ &\Leftrightarrow \tau \geq 0 \text{ and } v \cos \theta \leq 1 \text{ or } \tau \leq 0 \text{ and } v \cos \theta \geq 1\end{aligned}\quad (11)$$

The consequences of these formulas depend materially on whether θ is in the first or second quadrant. If $\theta \in Q2$ then $\cos \theta < 0$: the inequalities involving $\cos \theta$ in (10) and (11) are either trivially true (e.g. $v \geq \cos \theta$), or never true (e.g. $v \leq \cos \theta$). If $\theta \in Q1$, then all the inequalities in (10) and (11) are potentially active. This leads to the following characterization of the Operational partition.

Case 1. $\cos \theta \geq 0$ ($\theta \in Q1$)

$d^{- -}$. Here, $t_{PCA} < t_{A1}$ and t_{A2} , so:

$$d^{- -} \Leftrightarrow \tau > 0, v < \cos \theta \quad \text{or} \quad \tau < 0, v > \sec \theta \quad (12)$$

$d^{+ +}$. Here, $t_{PCA} > t_{A1}$ and t_{A2} . Reversing the inequality signs for τ in (10) and (11) gives:

$$d^{+ +} \Leftrightarrow \tau > 0, v > \sec \theta \quad \text{or} \quad \tau < 0, v < \cos \theta \quad (13)$$

$d^{+ -}$. Here, $t_{A1} < t_{PCA} < t_{A2}$. In this region, $\tau > 0$. From (10), reversing the inequality signs for τ , and (11):

$$d^{+ -} \Leftrightarrow \tau > 0, \cos \theta < v < \sec \theta \quad (14)$$

$d^{- +}$. Here, $t_{A2} < t_{PCA} < t_{A1}$. In this region, $\tau < 0$. From (11), reversing the inequality signs for τ , and (10):

$$d^{- +} \Leftrightarrow \tau < 0, \cos \theta < v < \sec \theta \quad (15)$$

Case 2. $\cos \theta < 0$ ($\theta \in Q2$)

The situation here is much more simple. As noted earlier, the $\cos \theta$ inequalities in (10) and (11) are either always true or never true. The ‘always true’ cases lead to:

$$t_{PCA} \leq t_{A1} \Leftrightarrow \tau \leq 0 \quad (16)$$

$$t_{PCA} \leq t_{A2} \Leftrightarrow \tau \geq 0 \quad (17)$$

So, we cannot have both inequalities on the left sides of (16) and (17) in the same direction, which means that the regions $d^{- -}$ and $d^{+ +}$ do not occur in this case. The only possibilities are:

$$d^{+ -} \Leftrightarrow \tau > 0 \quad (18)$$

$$d^{- +} \Leftrightarrow \tau < 0 \quad (19)$$

So, for each θ , the partition boundaries in the FDS (P) are always horizontal or vertical lines. For $\theta \in Q1$, they are shown in Fig. 2.

4.2.3 Delineation of the Proximity Alert Regions

The proximity alert regions are engagements where one or more of the proximity checks return a positive result; that is, one of the proximity check inequalities is

satisfied. This means that, at some point during the engagement, the two aircraft violate one or more of the separation standards. We now want to find where these regions are located in P.

A distance separation violation occurs when $d_{\text{PCA}} \leq d_{\text{thresh}}$. In Sect. 4.2.1, we noted that this can be redefined as a time inequality $\phi_{\text{PCA}} \leq \phi_{\text{thresh}}$, where ϕ_{PCA} is given by (9) and ϕ_{thresh} is a constant. This implies the following inequality between τ and v :

$$|\tau| \leq \phi_{\text{thresh}} \frac{\sqrt{1 + v^2 - 2v \cos \theta}}{v \sin \theta} \quad (20)$$

A time separation violation occurs when $|\tau| \leq \tau_{\text{thresh}}$. The boundaries of this region are horizontal lines in P. If a parameter point satisfies both these inequalities, then both types of separation violation occur and both types of alert are required. An important question then is which alert occurs first?

These distinctions show that there are five possible proximity alert regions in general.

- DT Both separation violations occur, distance alert occurs first.
- TD Both separation violations occur, time alert occurs first.
- D Only a distance separation violation occurs.
- T Only a time separation violation occurs.
- N No separation violation occurs.

By definition, the regions DT and TD must lie within both D and T. The distinction between DT and TD depends on the operational region within which the point lies. We examine each possibility in turn, *assuming that both separation violations occur*.

4.2.4 An Example of Alert Partitioning

An example of alert partitioning of the FDS is provided in Fig. 3.

d^- . Here, PCA is reached before either aircraft reaches A. So, t_{dthresh} always precedes t_A . Therefore, the distance alert will always be earlier; that is, there is no TD in this region.

d^+ . Here, PCA is reached after both aircraft have passed A. So, the question is whether t_{dthresh} precedes t_A . Suppose Aircraft 1 arrives first at A, so $t_A = t_{A1}$ and $\tau > 0$. At this time, the aircraft separation is $v_2\tau$. If this is less than d_{thresh} , then clearly $t_{\text{dthresh}} < t_A$, so the distance separation is violated earlier and the distance alert occurs earlier (DT); otherwise we are in TD. The boundary between them in P is

$$0 < \tau \leq \tau_{\text{thresh}}, \quad v\tau = \phi_{\text{thresh}} \quad (21)$$

If Aircraft 2 arrives first at A , $t_A = t_{A2}$, $\tau < 0$ and the separation at this moment is $v_1|\tau|$. As above, if this is less than d_{thresh} , then we are in DT; otherwise we are in TD. The boundary between them in P is

$$-\tau_{\text{thresh}} \leq \tau < 0, \quad |\tau| = \phi_{\text{thresh}} \quad (22)$$

\mathbf{d}^{+-} . Here, Aircraft 1 reaches A first, so $t_A = t_{A1}$, $\tau > 0$, and the separation is $v_2\tau$. Since PCA occurs before Aircraft 2's arrival, an identical argument to that in \mathbf{d}^{++} shows that the boundary in P between DT and TD is (21).

\mathbf{d}^{-+} . Here, Aircraft 2 reaches A first, so $t_A = t_{A2}$, $\tau < 0$, and the separation is $v_1|\tau|$. In the \mathbf{d}^{++} and \mathbf{d}^{+-} partitions, the arguments show that the boundary in P between DT and TD is (22).

Note the distinctions between the results in the four regions if both alerts might be required. In \mathbf{d}^{-} , the distance alert will always occur earlier; in the other regions, either alert could come first. The other distinction is the functional form of the boundary; when $\tau > 0$ it is a hyperbola (cf. (21)), when $\tau < 0$ it is a horizontal line (cf. (22)). This difference is due to our choice of the speed of Aircraft 1 as the scaling constant in (8).

In summary, then, there are three proximity alert region boundaries in P: between D and N; T and N; and TD and DT. These are defined by four equations. Two of these are (21) and (22), for the last boundary, depending on the sign of τ . For ease of reference, we write out the other two equations explicitly. Recall that $v > 0$ and $\theta \in [0, \pi]$.

$$\text{D and N boundary: } |\tau| = \phi_{\text{thresh}} \sqrt{1 + v^2 - 2v \cos \theta} / v \sin \theta \quad (23)$$

$$\text{T and N boundary: } |\tau| = \tau_{\text{thresh}} \quad (24)$$

The proximity alert regions are somewhat different for the two quadrants so they need to be treated as separate cases. For the description of these regions, we regard ϕ_{thresh} as fixed and consider what happens as τ_{thresh} increases.

5 Discussion: Operational Use of the Results

The partitioning of the FDS as shown in Fig. 3 has utility not only in decision support for strategic flight planning but also in real-time operational situations. From the latter point of view, for each proximity pair, it is possible to display P and the instantaneous operational point (ν, τ) in terms of the position of A and the values for v_i , a_i and θ . The adaption of the boundary curves, (21)–(24), as appropriate, can also be shown in real time. Given such a display, assuming constant velocity vectors, it would be very clear whether, at that moment, the current engagement had a risk of proximity violation for the predicted future progress of flight.

The engagement is, of course, dynamic; the aircraft positions are continually changing and the ground speeds associated with the tracks are also likely to change, for example, under wind shear. This phenomenon alone means that there is likely to be a reversal of which aircraft is the faster (has the higher ground speed) with a concomitant transition of (ν, τ) in the FDS. A second occasion when there will be a more abrupt change in the display is whether the arrival order at A of the two aircraft changes. In this case, τ will change sign, and the displayed DT/TD boundary curve will change its functional form from (21) to (22) or vice versa. In this case, however, the two aircraft will be transiting such that they are very close to a collision course with the concomitant distance separation standard being severely violated, signalling the essential attention needed to resolve the proximity situation. For many routine enroute situations, the display of FDS will, in fact, be essentially static, since none of τ , ν and θ will change significantly and the normalization by ν_1 in (8) will not change either. So, the instantaneous operational point and the boundaries of the engagement in P will slowly move on the display. Provided the rate of change of the display information is low, situational changes should be easily assimilated and interpreted by an operator, and the FDS will give useful information about a situation that is deteriorating from a proximity viewpoint.

A reason for the particular choice of independent variables for the construction of the FDS as presented in this paper was to ensure a smooth transition of (ν, τ) in these types of circumstances. The more conventional choice of parameters used to specify aircraft proximity in terms of distances and speed exhibits asymptotic behaviour and although the mathematics is correct the resultant behaviour means that the display of the operational point becomes erratic and therefore unusable in a human interface design. Similar difficulties would be encountered when interpreting decision support simulation results.

6 Conclusions

The aircraft crossing track problem has been a long-standing issue in airspace and air traffic management design. Although the problem has attracted research attention for over four decades, the collective published solutions have only been partial in a mathematical sense. Decision Support processes and Compromise Decision Support methodology, in particular, both require the ability to formulate solutions over the complete design domain through the construction of a Feasible Design Space (FDS). The FDS as presented in this paper has a canonical form, the attainment of which is required whether the complexity of future designs is to be contained and whether the value and insights associated with of decision support methodologies is to be enhanced for future operations.

The selection of the FDS design variables in canonical form is different from the conventional design variable selection used in air traffic management designs to date. Even when environmental changes such as wind shear and aircraft configuration changes (such as, flap settings and gear transitions) occur, the design variable

choice ensures that the instantaneous operating point transitions within the FDS in a smooth and stable manner thus broadening the potential use of the FDS to human-machine interface design. A further enhancement is that the FDS incorporates both spatial and temporal proximity alerts, a requirement in future designs. The FDS presented reduces epistemic errors associated with earlier modelling deficiencies and, thus, has the potential to improve risk assessments also used in the more strategic Decision Support modelling of the airways structures.

The principal contribution of this research, therefore, is to provide the mathematical form of the constraints governing aircraft proximity behaviour such that a FDS can be constructed. This leads to an opportunity to enhance the fidelity of decision-making in both strategic planning simulations and in the dynamic modelling of aircraft proximity in real-time operational situations.

References

1. ICAO Global Air Traffic Management Operational Concept (2005)
2. Mistree, F., Hughes, O., Bras, B.: The compromise decision support problem and the adaptive linear programming algorithm. In: Kamat, M.P., (ed.) *Structural Optimization: Status and Promise*, pp. 247–286. Washington, D.C., AIAA (1993)
3. Mistree, F., Smith, W.F., Bras, B.: A decision-based approach to concurrent design. In: Parsaei, H.R., Sullivan, W.G. (eds.) *Concurrent Engineering: Contemporary Issues and Modern Design Tools*. Chapman and Hall (1993)
4. Netjasov, F.: Conflict risk assessment model for airspace strategic planning. In: *Proceedings of 14th Air Transport Research Society Conference, Porto Portugal, 6–9 July 2010*
5. Netjasov, F.: Framework for airspace planning and design based on conflict risk assessment part 2: conflict risk assessment model for airspace tactical planning. *Trans. Res.-C* 24, pp. 213–226 (2012)
6. Netjasov, F., Babić, O.: Framework for airspace planning and design based on conflict risk assessment part 3: conflict risk assessment model for airspace operational and current day planning. *Trans. Res.-C* 32, pp. 31–47 (2013)
7. ICAO: Doc. 9689-AN/953. *Manual on Airspace Planning Methodology for the Determination of Separation Minima (First Edition, 1998), Amendment 1*, pp. 35I-35 N, (2002)
8. Haddad, R., Carlier, J., Moukrim, A.: A new combinatorial approach for coordinating aerial conflicts given uncertainties regarding aircraft speeds. *Int. J. Prod. Econ.* **112**, 226–235 (2008)
9. Dunlay, W.J.: Analytical models of perceived air traffic control conflicts. *Transp. Sci.* **9**, 149–164 (1975)
10. Schmidt, D.K.: On the conflict frequency at air route intersections. *Transp. Res.* **11**, 351–355 (1977)
11. Rome, H.J., Kalafus, R.: Impact of automatic dependent surveillance and navigation system accuracy on collision risk on intersecting tracks. In: *Proceedings of National Technical Meeting of The Institute of Navigation*, pp. 213–222 (1988)

Constructing a Feasible Design Space for Multiple Cluster Conflict and Taskload Assessment

Neale L. Fulton, Mark Westcott and Warren F. Smith

Abstract Appropriate management of proximity is required if aircraft are to be operated safely. Flight trajectories ranging from continental to very localized operations may become proximate causing multi-aircraft clusters to form within a flow. Clusters may emerge, dissipate in time, coalesce or be sustained (e.g. swarms). A collective characterization of multiple clusters within an air traffic flow, using a Number Theoretic approach, is presented in this paper. This complements earlier research that characterized the structure of individual clusters through Graph Theoretic techniques. A Feasible Design Space is constructed based on the number of aircraft generating the flow, the total number of clusters emergent in a flow, and the aggregated number of proximity-pairs across clusters. The system taskload demand is defined by the aggregated number of proximity-pairs. The engineering task of designing avionics, ergonomic interfaces, communication channels or ground-based facilities to manage proximity requires knowledge of the peak taskloads imposed on the various subsystems involved. Variation (inclusive of non-monotonic behaviour) in taskload during the growth and dissipation of the clusters is evident in the analysis presented. The mathematical basis underpinning the emergent proximity Feasible Design Space would enable these operational points to be identified a priori together with a suitable management strategy to avoid system saturation and to reduce the possibility of collision due to communication failure or task overload.

Keywords Aircraft • Conflict detection • Cluster • Proximity • Number partition • Taskload

N.L. Fulton (✉) · M. Westcott
CSIRO Honorary Fellow, Canberra, ACT, Australia
e-mail: neale.fulton@csiro.au

M. Westcott
e-mail: mark.westcott@csiro.au

N.L. Fulton · W.F. Smith
School of Engineering and IT, UNSW, Canberra, ACT, Australia

1 Introduction

Conflict Management is identified as one of the seven architectural pillars of the ICAO Global Air Traffic Management Operational Concept [1]. It is implemented through specified processes for Proximity Specification, Conflict Detection, and Conflict Resolution. The functional descriptions of each of these processes are integrally dependent on being able to identify and measure the real-time emergent proximity-pairs as aircraft trajectories come close to each other. Such assessment of proximity is a critical design issue whether discussing broad continental-scale flows or very local flow interactions such as near an airport or during a localized search and rescue mission.

The diversity of operations is evolving together with the diversity of communication modes available. This means that the aspects of airspace design underpinning Conflict Detection and Resolution (CD&R) must be supported by new mathematical approaches and by new engineering tools so that the planning, the scoping of design requirements, the design of heuristics for conflict management, and the monitoring of the real-time progression of an operation may all be approached in a systematic manner. Diversity of operation encompasses enroute continental traffic flows associated with air traffic control, through operations arising in uncontrolled regional airspace in remote parts of a continent, to swarming activity by micro-air vehicles (MAVs) associated with localized search and rescue operations. The number of MAVs participating in localized swarms is already circa 20–30 [2], as is the largest proximity cluster (cluster) reported in air transport operations in Europe only just over a decade ago [3]. Traffic flow behaviour in each of these contexts varies from persistent steady-state flows to flows exhibiting highly dynamic and sporadic behaviour.

Progressively, this diversity of flow is being modelled as a dynamic, complex networked system. Two networks are envisaged. The first is the network of aircraft using the airspace and its proximity relationships (or proximity-pairs). The second is the network of communication links established between the aircraft themselves or with ground-based service facilities. One objective of the authors is to establish certain canonical behaviours of the aircraft network and its proximity-pairs. This in turn provides a characterization of the demand (see Sect. 1.1, Taskload) placed on the second network by the first network. In particular, a Feasible Design Space modelling the demand on system components and human actors (aircraft crew, air traffic control personnel and other ground-based operators) is required.

Durand et al. [4] modelled single proximity clusters (a group of aircraft each of which contributes to at least one proximity relationship). The modelling requires the specification of the number of aircraft and the number of proximity-pairs within the cluster. A novel contribution of the authors is to extend the description of the individual cluster to that of a collection of clusters within a general flow through an appeal to Number Theory. Certain scale-invariant properties are revealed that characterize the bounds on the aggregate number of proximity-pairs generated during coalescence (or, merging, combination) and dissipation (or, split, dispersal)

of multiple clusters within the flow. The properties are defined through deterministic relationships extracted from otherwise sporadic behaviour associated with the evolving coalescence and dissipation of the multiple clusters.

1.1 Taskload

Taskload is measured as a system-level demand event that is derived directly from the generation of proximity-pair events that, in turn, are derived directly from the changing topologies of the clusters. In this research, the determination of taskload is extended beyond that associated with an individual cluster to that of an aggregated quantity over a number of clusters within a flow. The importance of this interpretation is that it can be used to set the performance bounds required to establish the design specification of a dependable communication system whose function is to reliably exchange information for multiple aircraft, thus ensuring that all airspace activity can be accomplished under the system design constraint of no collision.

In the context of imminent proximity, the integrity and continuity of information transfer between aircraft must be assured for the duration of the proximity-pair and for the time required for information exchange. This means that a design assessment of peak taskload (a scheduling concept) is required. Our use of the term *task* (hence *taskload*) is compatible with the definition of taskload in the iFly Project [5] and that in the NATO Guidelines on Human Engineering Testing and Evaluation [6]:

Workload can be defined as the portion of human resources an operator expends when performing a specified task.

The NATO guidelines distinguish between a *task*, considered here as an objective element of a physical process, and the associated transformation into *workload* as the measure of human endeavour (which itself will be dependent on a specific system design). The outcome then reflects the subjective cognitive ability of a pilot or controller in performing the assigned task. We note for clarity, and with respect to the context set by other research, that we only consider establishing system-level measures of taskload associated with conflict management and not with respect to other tasks such as coordination workload or those that pre-empt further monitoring [7].

We also note, as a caution, that *taskload* and *workload* are not yet used consistently in the broader airspace literature: they have been used synonymously with respect to either role captured in the NATO definition. Terms such as “subjective workload” [8] and “cognitive taskload” [9] have been used. Flener et al. [7] highlight the unfortunate implicit transposition of objective and subjective dimensionality through the measures captured in their survey: “workload measures” in various papers are expressed in terms of physical entities such as the “maximum number of aircraft in a sector”. It is clear that such definitions seek to coalesce a

complex concatenation of relational transformations without defining an objective foundation for modelling and interpretation and, in so doing, only confuse the matter further. Taskload as a physical event can be objectively determined, whereas workload remains a subjective relationship with respect to its canonical domain (viz. taskload). The measure of workload is a mathematical relation (vis à vis, a function) encompassing characteristics such as operator currency in performing the task, the level of developed competency, the influence of the working environment, operational priorities, etc.

2 Axiomatic Propositions for Cluster Management

Formally: *A proximity-pair relationship exists between two aircraft when physical separation criteria (either a spatial criterion or a temporal criterion or both) are infringed.*

The terms “conflict” and “proximity” are treated synonymously. Throughout the paper, proximity-pair (a binary relationship) is taken to be the elemental unit of taskload generation. If a proximity-pair exists, then a task must be allocated to manage that proximity. It is beyond the scope of the paper to address questions of communication efficiency: for example, “Can specific individual tasks be combined to improve overall system performance?”

2.1 Foundational Construct—The Feasible Design Space (FDS)

Given proximity-pairs occur, it follows that an effective design for managing the system with its emergent properties is required. Drawing from the field of optimal engineering design, feasible designs exist where there is a region (domain) within an n-dimensional design variable space where all the constraints including design variable bounds are satisfied. Two types of region are considered in practical approaches to systems engineering: regions(s) in which it is technologically feasible to provide services and to meet the system requirements (the so-called Feasible Design Space (FDS)), and regions(s) which are aspired to and where it is envisaged that future operations should be located. Preference for designs within the FDS is specified through the statement of goals or objectives. Collectively, the goals/objectives can be conceived to represent the aspiration for the design. Conceptually, the better designs are those that map closest to the aspiration space. Designers will consider trade-offs between possible satisfying design solutions while exploring the emergent properties of the system.

In terms of an aspiration space, it is not difficult in the context of the growth of MAV operations to foresee clusters of much greater complexity than have ever been experienced in the past with traditional uses of airspace.

2.2 Feasible Design Space (FDS)—The Assumptions

Twelve axiomatic propositions are put forward as definitions and assumptions in support of the construction of the FDS. Propositions P1–P6 describe the existing state of the art as published [3, 4]. Propositions P1–P6 are supported by Graph Theoretic approaches that have been used to analyse individual clusters with two or more aircraft.

- P1** A traffic flow is comprised of T flight paths.
- P2** In general, the traffic flow can be comprised of consistently repeated flight-path patterns, and simultaneously, of other flight-path patterns of a sporadic nature.
- P3** Proximity is a spatio-temporal relationship that may manifest between each pair of flight paths. A proximity-pair forms when two aircraft will be closer than prescribed minima in space or time or both.
- P4** An observational time interval is chosen such that aircraft pair can come into proximity at most once within the time interval.
- P5** Clusters within the flow emerge when a transitive closure [10] is applied to all the proximity-pair relationships.
- P6** A cluster is comprised of at least one proximity-pair.

The authors developed propositions P7–P12 to extend the existing theoretical model to include aggregate measures over multiple emergent clusters within a traffic flow

- P7** A unit cluster is defined as an aircraft not in a proximity relationship with another aircraft. (This new definition is required to permit an equivalence relationship between all aircraft within a flow and the parts in a partition under Number Theory).
- P8** For a unit cluster, the number of proximity-pairs is zero.
- P9** In the observational time interval, the traffic flow partitions into r clusters (including unit clusters).
- P10** P_A is the aggregate of all proximity-pairs over all clusters within the total flow.
- P11** The Feasible Design Space (FDS) is a Cartesian coordinate system with coordinates T, r and P_A .
- P12** Measures of Effectiveness (MoE) are, T, r, P_A , and the relative saturation of the total flow (the Graph Theoretic density), P_A/C_2^T .

We note, in the context of P12, and in general, a more preferred system state is gained by maximizing T and r (inclusive of unit clusters) and minimizing P_A and P_A/C_2^T .

3 Modelling Single and Multiple Clusters

3.1 Single Clusters

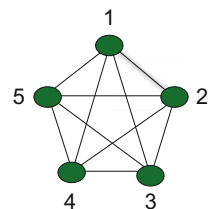
A cluster is most often modelled as a graph $G(V, E)$ with V nodes (aircraft in the cluster) and E edges (proximity-pairs). A cluster is a group of aircraft each with a proximity-pair relationship with at least one other aircraft in the group. A cluster graph shows all the aircraft that are related by a chain of one or more proximity-pairs.

The cluster relation between aircraft is reflexive and symmetric but not transitive [10 p. 547]. Formally, then, a cluster is an equivalence class whose elements are equivalent for the *pathwise transitive closing* of the proximity relationship between aircraft. For a given number of aircraft within a cluster, the number of proximity-pairs is not fixed because of the different patterns of interaction from which proximity can arise. However, the number of proximity-pairs does have a bounded range, the extremes of which are combinatorially complex (see Sect. 5).

Granger and Durand [3] characterized the complexity of historic traffic flow patterns by the sizes of the clusters that formed between aircraft in a given continental-scale flow. The emergence of clusters was reassessed every few minutes with the numbers and patterns of clusters recorded. The number of cluster topologies having the same cluster size (number of vertices, aircraft) was enumerated, and the number of different graphical sequences (degree sequences) possible for that size was identified.

A combinatorially saturated cluster graph for an arrangement of five aircraft is illustrated in Fig. 1. A practical limitation in this approach is that the cluster graph abstracts away the proximity zone information of where aircraft pairs might come into proximity and the degree of interaction at that location. A bipartite graph model for making this distinction explicit has been developed by the authors.

Fig. 1 A combinatorially saturated cluster graph for five aircraft



3.2 Multiple Clusters in a Flow

Typically, when historic data are analysed, the cluster is treated as a static instance with both V and E constant [3]. However, when swarms have been modelled [2, 11–13], the number of agents has been treated as constant, but the number of proximity-pairs has varied; that is, $E(t)$ varies with time.

In the present research, we consider clusters evolving with $V(t)$ and $E(t)$ both as functions of time. We also consider multiple clusters where each cluster will have its own individual graph. However, the properties of a multi-cluster echelon are better modelled based on the concept of the number partition from Number Theory. Number partitions identify the number of ways that a given integer number can be split into other lesser integer numbers (the parts). A correspondence between a part and a cluster (graph) size is made. However, to complete the correspondence, we define a unit cluster as being a single-node graph with no proximity relationship (the normative operational state). With this extension, we can completely and uniquely associate each of the parts in the number partition with the set of cluster graph sizes that has formed in the flow. Appropriate references within Number Theory are [14–18].

The problem formulation can then proceed by specifying each member of the set of aircraft as

$$\{A_i\}, |A| = T, 1 \leq i \leq T \quad (1)$$

with each aircraft having an associated flight path listed as a member of the total set of flight paths (typically a piecewise linear set)

$$\{l_1, \dots, l_i, \dots, l_T\}. \quad (2)$$

Any resultant proximity-pair between any two pairwise flight-path segments identifies an associated proximity zone, the total set of which is

$$\{P_1, \dots, P_m\}, 1 \leq m \leq C_2^T \quad (3)$$

Any one aircraft can potentially be in proximity with a number of other aircraft. Transitive closure of the proximity relationships (pairs) between aircraft gives rise to a set of r clusters

$$\pi = \{\lambda_1, \dots, \lambda_r\}, |\pi| = r, 1 \leq r \leq T \quad (4)$$

where π is the general partition set $\{\lambda_1, \lambda_2, \dots, \lambda_r\}$ of an integer T : λ_j the parts, and

$$\sum_{j=1}^r \lambda_j = T \quad (5)$$

The normative formulation of the situation is when $r = T$, $\lambda_j = 1 \forall j$ (i.e. no proximity-pairs). A non-unit cluster emerges when there is at least one $\lambda_j > 1$. For each λ_j , the j th cluster can be represented as a graph $G(V(j), E(j))$ where $V(j) \in \{A_i\}$ is the number of aircraft in the j th cluster and $E(j)$ is the edge set (proximity-pairs) associated with that cluster. The order of $G(V(j), E(j))$ is then

$$|V(j)| = \lambda_j \quad (6)$$

and the size

$$(\lambda_j - 1) \leq |E(j)| \leq C_2^{\lambda_j}. \quad (7)$$

In $G(V(j), E(j))$ the degree of the k th vertex, $deg(v_{j,k})$ is the measure of the number of proximity-pairs associated with that vertex (aircraft). The Degree Matrix, $D(\lambda_j)$, is a $\lambda_j \times \lambda_j$ matrix whose diagonal terms are the degree sequence of $G(V(j), E(j))$. The trace of $D(\lambda_j)$ is equal to $2|E(j)|$. The density of the graph, $\sigma(j)$, measures the relative completeness of the total possible number of edges in the graph:

$$\sigma(j) = |E(j)| / C_2^{\lambda_j} \quad (8)$$

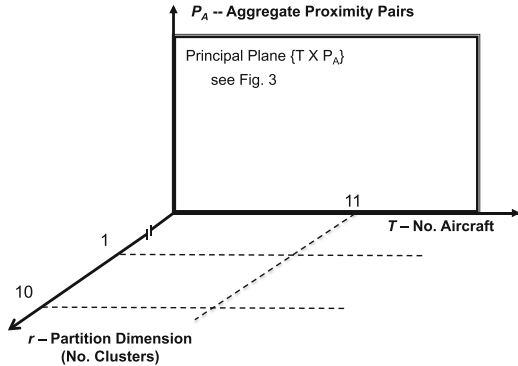
subject to Eq. (7). The total number of proximity-pairs emergent in the whole aircraft population across all r clusters is then equated to the fundamental measure of taskload:

$$\sum_{j=1}^r |E(j)| \equiv P_A(\pi) \equiv Taskload. \quad (9)$$

4 A Feasible Design Space (FDS) for Multiple Cluster Flows

The cluster relationships observed within a given time window arise from the total number of aircraft, T , the aggregate number of proximity-pairs, $P_A(\pi)$, across all clusters, and the number of clusters, r . The count $P_A(\pi)$ is then equated to the fundamental taskload and serves as a direct input (demand) to the communication scheduling requirements. The taskload temporal behaviour is characterized by time to point-of-closest-approach (PCA), transaction length, and the prioritization of transaction deadlines [19]. An adaption of the operational envelope capturing taskload information has been presented in [20]. Further discussion of pilot taskloads and communication link characteristics is provided in [19, 21]. A related study of the effect of geo-spatial communication structures on the processing of proximity warning is given in [22].

Fig. 2 Feasible Design Space (FDS) and Principal plane



A FDS is constructed to exhibit the aggregate number of proximity-pairs across all clusters, $P_A(\pi)$, and its relationship to the number of clusters r and to the number of aircraft, T (see Fig. 2). The FDS is a template so there is no measurement error considered in its construction or associated with any of the variables. We note for completeness that when actual measured data are plotted on the FDS template, appropriate error estimates must be considered.

Equations cast in the FDS are closed-form deterministic equations. The functions of interest are integer functions, but for ease of visual reference, some functions are plotted as the loci (or envelopes) of real functions. The FDS is then a three-dimensional space specified through the Cartesian product

$$FDS = \{T, r, P_A(\pi) \in R^+ : T \times r \times P_A(\pi)\} \tag{10}$$

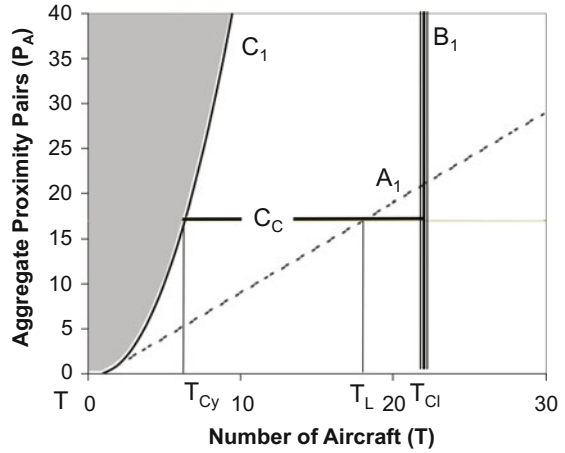
When the FDS is formulated for discrete integer functions, it is cast as a coincident three-dimensional space specified through the Cartesian product

$$FDS = \{T, r, P_A(\pi) \in N : T \times r \times P_A(\pi)\} \tag{11}$$

The visual presentation enabled by the FDS framework aids in the conceptualization of the fundamental properties exhibited by the aircraft interactions within a flow and also enables the behaviour of the bounds to be explored as the number of clusters, the cluster sizes, and the proximity-pair relationships vary. It provides a context for the measurement of the operational decision points. Operational and design questions such as the following can be explored:

1. In how many ways can the group of T aircraft be decomposed into subgroups (clusters) and how many subgroups of what sizes can be formed?
2. For given values of (T, r) , what is the range of the number of proximity-pairs, $P_A(\pi)$, that can be generated?
3. What is the maximum aggregate taskload, $P_A(\pi)$, that can be generated?
4. Is there sufficient communication channel capacity to service all the tasks?

Fig. 3 FDS Principal plane $\{T \times P_A\}$ template



4.1 The Principal Plane

The two-dimensional plane $\{T \times P_A(\pi)\}$ covering all possible operational (decision) points (OP) is called the Principal plane.

The plane $\{T, r, P_A(\pi) \in R^+ : T \times (r=0) \times P_A(\pi)\}$ does not have a physical meaning in the problem domain so we use this specific plane to locate the Principal plane $\{T, P_A(\pi) \in R^+ : T \times P_A(\pi)\}$. The Principal plane is illustrated in Fig. 3 in which the functions C_1 and A_1 derive from the plane $\{T, r, P_A(\pi) \in N : T \times (r=1) \times P_A(\pi)\}$, representing a single cluster.

In general, the number of aircraft operating in a given airspace, T , within a flow will partition into r clusters (Eq. 4) the sizes of which are written as a sequence, π , of positive integers, $(\lambda_1, \dots, \lambda_r)$, with the properties $\lambda_1 \geq \dots \geq \lambda_r$ and Eq. (5). The integers λ_j are the parts of a number partition. Then, r is the number of parts in the partition (the partition dimension).

The size of the j th part corresponds to the number of aircraft contributing to the j th cluster. Each individual cluster, $C_{c(j)}$, generates a number of proximity-pairs, $P(j)$, which when aggregated across all clusters yields $P_A(\pi)$. Aggregate data from each of the r cluster planes that contribute to $P_A(\pi)$ are then mapped onto the Principal plane. For notational simplicity, define $P_A \equiv P_A(\pi)$. In the following, both C_k^n and $C(n, k)$ are used as notation for the binomial coefficient.

C_1 is the binomial bound $C(T, 2)$; A_1 is the linear bound $(T - 1)$; and C_C is the communication channel capacity limit. The infeasible region is left of C_1 .

4.1.1 Constructing the FDS for Proximity-Pairs and Taskload

The aggregate number of proximity-pairs, P_A , that have formed from T aircraft in a specified time interval is governed by Eqs. (5) and (9). The analysis of various

relationships presented here arises from Number Theory as discussed in Eqs. (3)–(5). For a single cluster, T and λ can be used interchangeably.

4.1.2 The Constraint C_1

The upper (real) functional constraint is the binomial bound $C(T, 2)$.

$$C_1 = \{T \in R^+ : (T, T(T-1)/2)\} \tag{12}$$

It is the envelope of the maximum number of pairwise conflicts between T aircraft. This constraint is true in 3D space for an arrangement of flight paths represented by either infinite lines or line segments of finite length.

4.1.3 Defining the Aspiration Space, A_1

The aspiration locus is given by the (real) functional inequality

$$A_1 = \{T \in R^+ : (T, T(T-1))\} \tag{13}$$

It is the envelope of the maximal linear constraint. This is the bound for clusters to be represented as a tree structure in Graph Theoretic terms. An example is when $T-1$ aircraft are flying in parallel but the remaining aircraft crosses each of the $T-1$ flight paths. An aggregate of proximity-pairs $P_A = \sum_1^r |E(j)| < A_1$ may be feasible when each $\sigma(j) \ll 1$. Should the clusters coalesce, the range in the number of possible proximity-pairs for a single cluster, $T(=\lambda)$, is defined by the difference between the constraint C_1 and aspiration A_1 .

4.1.4 The Bound B_1

The bound B_1 , defined by the discrete set,

$$B_1 = \{(T_{Cl}, P_A) \in N^2 : T_{Cl} = \text{constant}\} \tag{14}$$

It is not a hard bound but is a reference value of T in a particular airspace that identifies the maximum cluster size observed or expected.

Example 1 The largest cluster reported in [3] was 21 aircraft. There were also over 200 clusters of 10 or more aircraft. Further, all of the possible 19 cluster configurations of 5 aircraft were recorded, showing the great variety of patterns possible. ■

Example 2 In a recent Australian Flight Safety magazine [23], a pilot on a short flight in Victoria from Geelong to Ballarat (~ 43 NM) experienced 11 other aircraft operating in the vicinity of Ballarat airport. The pilot decided to delay an approach to the airport to permit the congestion to clear. ■

4.1.5 The Bound C_C

The value of P_A for which a resource (e.g. a communication channel) will become saturated by taskload is given by the bound

$$C_C = \{C_C, k \in N: C_C = k = \text{constant}\} \quad (15)$$

Given this bound, the value of T that will saturate the resource capacity for combinatorially saturated and linearly saturated clusters, respectively, is defined by the functions:

$$T_{Cy} = \{T, k \in N: \text{int}[T(T-1)/2] = k, k = \text{constant}\} \quad (16)$$

$$T_L = \{T, k \in N: T = k + 1, k = \text{constant}\} \quad (17)$$

Example 3 The ICAO Manual on Required Communication Performance (RCP) [24] establishes the transaction time τ_{RCP} for various operational communication situations. As tabled, these times range from 10 to 400 s. In validating a transaction time, it is important to establish the constituent times that may include allowances for electromagnetic propagation, aircraft systems delays, and/or human response times as appropriate. This assessment will establish an RCP type with an associated τ_{RCP} . Many avionic and air traffic management systems are designed based on a specified update rate: a flight management system may have an update rate from 1 to 600 Hz dependent on aircraft type, and an air traffic management system may have update rates at sub-Hertz frequencies based on surveillance radar returns. Another consideration is the smallest period to be monitored such as in the Future Air Navigation System (FANS) project [25]. In this case, the observation interval was 6 min. When the system interval I_S is specified, then $C_C = I_S/\tau_{RCP}$ can be specified. ■

Example 4 Simple taskload situations have been managed in the past by “plain voice radio”, “see and avoid”, or a combination called “alerted see and avoid”. The transaction times for voice can be relatively long with an average of 40 s with range 7–70 s, so with only a few proximity-pairs the available channel capacity saturates. Data link can improve the situation dynamically as the end-to-end latency measured in the Smart Skies trial was of order 3 s [20]. ■

5 Canonical Properties of Cluster Aggregation and Disaggregation

The size of the airspace volume in which operations occur can vary quite substantially. Transcontinental operations may involve a sector hundreds of kilometres in lateral dimension, whereas a search and rescue operation may be very localized, a small valley, for example. The vertical extent can also vary from a few tens of metres to thousands of metres. Within this volume, aircraft may come into proximity. Aircraft can be grouped, or partitioned, into clusters, where each aircraft in a cluster is sufficiently proximate to others in the same cluster to be of potential operational concern. This physical grouping can be related to the Number Theory concept of an integer partition and the number of aircraft (size) within each cluster to the parts of the partition.

The properties of the number of subgroups or clusters that can form from T aircraft are equivalent to the properties of the partitions of T . The number of partitions can range from one, when each aircraft is in proximity with at least one other aircraft, to T , when no aircraft is in proximity with any other aircraft (all “clusters” are of size 1). Thus, we can show the rigorous extension of the cluster concept to capture behaviour at a sector level. Some results from partition theory are reviewed first.

5.1 Number Partitions, Clusters, and Proximity-Pairs

In the context of aircraft proximity, the partitions of T aircraft represent the possible sets of clusters that can occur with T aircraft.

The number, $P_A(\pi)$, is the number P_A now distinguished by reference to a specific partition, π , and is an MoE of operational behaviour, since it bounds the number of potential proximities that might need to be managed. It is not possible to say, a priori, whether any particular value of $P_A(\pi)$ or its extremes will be realized in practice, since the flight-path arrangements and a specific definition of the proximity relation have not been posed at the present level of abstraction. Nonetheless, general bounds on the extremes can be found.

5.2 Partitions of Dimension r

The functions C_2 , C_3 and C_4 are added to the Principal plane from the plane $\{T, r, P_A \in N: T \times (r=10) \times P_A\}$ in Fig. 4. The maximum values for $P_A(\pi)$ occurring in the plane $\{T, r, P_A \in N: (T=11) \times r \times P_A\}$ are shown in Fig. 5. A subset of the plane $\{T, r, P_A \in N: (T=11) \times r \times P_A\}$ is shown in Fig. 6.

Fig. 4 FDS Principal plane $\{T \times P_A\} : T < 30$, partition dimension, $r = 10$

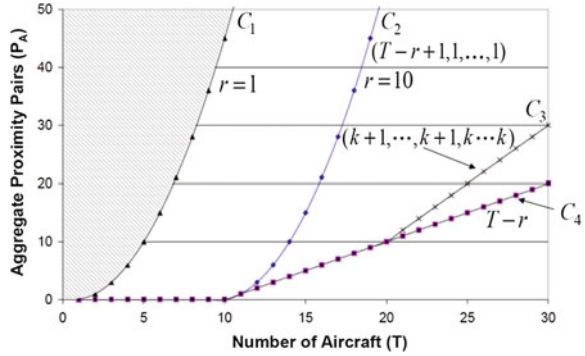
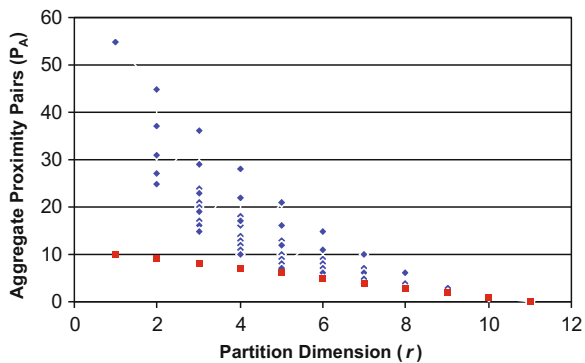


Fig. 5 FDS plane $\{(T = 11) \times r \times P_A\}$: Max. $P_A(\pi)$ for all partitions



Suppose there are r clusters of aircraft, so the partition of T has r terms. The bounds on the range of values for $P_A(\pi)$ can be found analytically. The lower bound is always $T - r$. The upper bound can itself assume a range of values. In essence, the more unequal the parts of the partition, the larger the value of the upper bound. Visualization of these characteristics can be assisted by the use of Fig. 4.

The constraint C_1 is defined by Eq. (12). Further constraints are specified as discrete sets but plotted as piecewise continuous functions for ease of visualization. The constraint

$$C_2 = \{(T, P_A) \in N^2 : P_A = C_2^{T-r+1}\} \tag{18}$$

shows the maximal $P_A(\pi)$ with $10 \leq T$ for a partition of dimension 10. The constraint

$$C_3 = \{(T, P_A) \in N^2 : P_A = 0 \text{ for } k=0, \\ \{P_A = \rho C_2^{k+1} + (r-\rho)C_2^k \text{ for } 1 \leq k\} \} \tag{19}$$

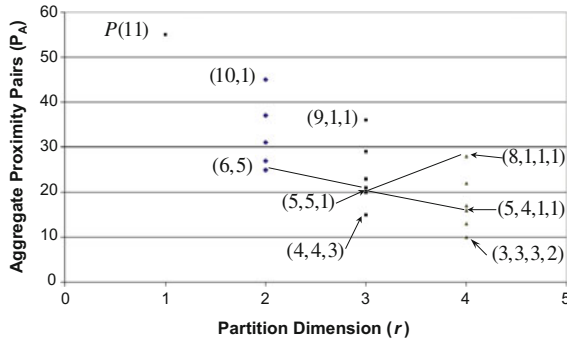


Fig. 6 Max. $P_A(\pi)$ for partition dimension (r) in the FDS plane $\{(T = 11) \times (r = 1(1) 4) \times P_A\}$

is the most uniform distribution of aircraft across r parts and represents the smallest $P_A(\pi)$ given that each part is combinatorially saturated. The constraint

$$C_4 = \{(T, P_A) \in N^2 : P_A = T - r\} \tag{20}$$

represents the minimum $P_A(\pi)$ for r clusters, where each cluster has the minimum number of proximities (the linear bound for $r = 1$ in Fig. 4). This is the situation where a cluster can be represented as a tree structure in Graph Theoretic terms. In Fig. 4:

C_1 —maximum bound $C(T, 2)$; C_2 —maximal P_A for r partitions; C_3 —most uniform distribution; C_4 —linear bound on P_A for r partitions.

Example 5 Aircraft are allocated time slots for operations during departure and arrivals at an airport. The number of available slots (r) is taken as 10 in Fig. 4. That is, the first 10 aircraft are each allocated a unique slot so proximity-pairs cannot build up. For these aircraft, the build-up of complexity is deferred until there are more than 10 aircraft. Beyond this, multiple aircraft would need to be allocated to the one slot (e.g. paired approach for a closely spaced runway system). In the above example for $T \geq 10$, the constraint C_2 shows the situation in which the extra aircraft are allocated to the same single slot, whereas C_3 shows the situation in which all slots are filled in the most uniform way. However, it can also be seen that if the slot system should fail, then the potential for conflict generation is significant as the system reverts from C_2 to C_1 in the worst case. ■

In the airspace context with multiple clusters, $P_A(\pi)$ is a measure of the aggregate complexity of the system. The more proximity-pairs there are, the more challenging is the problem of managing them all safely. Even for a fixed number of clusters, $P_A(\pi)$ can vary over a considerable range. This is evident in Fig. 5 where the horizontal axis is r , the dimension of the partition. For each r , minimum and maximum complexities for each of the $p(T, r)$ partitions of $T = 11$ are plotted. The ordering is from the smallest to largest values of the λ_j .

Complexity does not vary monotonically with cluster number r . It is clear from Fig. 5 that the ranges of the maxima for each r can overlap considerably. Note that proximity-pairs, for T aircraft distributed over r clusters, could have a dynamic range with a maximum complexity of $C(T-r+1, 2)$ while with $r-1$ clusters the complexity could be as low as $T-r+1$. Further, it is clear that the ranges of the maxima for each r can overlap considerably. This means that a partition of dimension r can have a considerably smaller complexity than one of dimension $r+1$. Splitting a cluster into new clusters of maximum complexity might actually lead to a considerable increase in proximity-pairs, hence taskload. This type of change would be indicated as an upward trajectory in Fig. 6.

Example 6 Consider the example where $T=11$. If $r=2$, there can be a partition with maximum complexity 25 (the partition (6, 5)), but for $r=3$, there can be a partition with complexity 36 (the partition (9, 1, 1)). Even for $r=4$, there can be a partition with complexity 28, namely (8, 1, 1, 1).

For design and operational management, it is important so as to be able to calculate the effect on $P_A(\pi)$ as π changes. This behaviour can be seen more explicitly in Fig. 6 which represents an expansion in detail of a line of constant T in the FDS. Every state of the system specified by $P_A(\pi)$ is shown. In this manner, transitions from one state to another become transparent, as do the consequences in change of taskload due to that transition. ■

Example 7 The point is illustrated by way of practical example. In Fig. 6, a subset of the partitions of $T=11$ is shown. In particular, two of the partitions illustrated are (5, 5, 1) and (5, 4, 1, 1) each of which contains at least one 5-cluster (of size five). Further, a 5-cluster of (5, 5, 1) being split into three is illustrated in Fig. 6, thus creating the partition (8, 1, 1, 1) of four clusters with a maximum $P_A(\pi) = 28$, whereas an alternative split results in a partition of (5, 4, 1, 1) also with four clusters but having a maximum $P_A(\pi)$ of only 16.

In summary, increasing r does not necessarily decrease $P_A(\pi)$, and conversely, decreasing r does not necessarily increase $P_A(\pi)$. This observation is critically important if the state (operating point) of the system is such that $P_A(\pi) \sim C_C$ in which case a change in partition and/or part size can change the operation with a potential of task saturation and the consequence of system failure with associated losses.

6 Discussion

The detailed study of cluster formation in European airspace by Granger and Durand [3] provides the total numbers of clusters of each size that form during a simulation of one day's traffic, but they do not say which clusters are present at any moment. Their research cannot be used directly to investigate multiple simultaneous clusters within a flow.

Characterization of the processes generating multiple clusters is required for taskload balancing and is a key engineering and operational issue. The FDS, as constructed [26], enables the analysis, modelling, and visualization of the bounds on the aggregate value of proximity-pairs, $P_A(\pi)$, for a general decomposition of the T aircraft into multiple clusters. A general conclusion is that $P_A(\pi)$ is largest when the cluster sizes are most unequal and smallest when the sizes are as close to equality as possible. The heuristic strategy of equalizing workload reported by Klein [27] and others is validated by the author's FDS analysis.

Taskload is shown not to behave monotonically with respect to either the number of clusters (r) or the size of the largest cluster (k). Taskload can therefore vary in non-intuitive ways. The range of values that the upper bound of $P_A(\pi)$ can take on, the non-monotonicity with respect to r and k and similar properties in other situations, show the potential danger of uninformed actions to reduce the taskload due to reorganization of aircraft both within a cluster and between different clusters. Neither increasing the number of clusters nor reducing the size of the largest cluster, both perhaps seemingly intuitively sensible, will always reduce the taskload. Great care in both design and operational decision-making is therefore required. The relationship between the objective measure of taskload and various subjective measures of workload remains an open research question.

First, in ongoing research, the behaviour of a partition with largest part, k , has also been investigated, but space does not permit an elaboration of this detail. However, as before, the maximum value occurs when the parts of the partition are as unequal as possible and the minimum occurs when they are as equal as possible. Second, proximity zones have been introduced to identify geographically where flight paths become physically proximate. A bipartite graph is used to provide a systematic way of accounting for the allocation of taskload demand. Finally, more detailed bounds associated with the scheduling of communication tasks are being developed. While the FDS facilitates a check of the first necessary condition that taskload must not exceed capacity, it does not directly address the important issue of task prioritization based on causality and physical feasibility considerations. The investigation of these three issues remains an open research endeavour.

7 Conclusions

The ability to accurately specify system-level taskload affects the assessment of the performance of pilots, air traffic controllers, and communication system link design. The introduction of the proposed FDS extends the abstraction of the single aircraft proximity cluster to include multiple clusters within a flow. The principal contribution of this research is to provide the mathematical form of the constraints governing the cluster behaviour. The number of clusters and the aggregation of proximity-pairs across all clusters are shown to be fundamental Measures of Effectiveness (MoE) that can then be used to specify and assess the taskload demand imposed on a Conflict Management system. The FDS thus provides the

foundation for the production of a dynamic model for real-time monitoring or for strategic assessment.

The FDS framework complements other approaches such as simulations and statistical methods for the fitting of historic data. As different heuristics are considered and data are obtained from actual operations, the loci of state behaviour associated with each heuristic can be plotted and evaluated. In this respect, the expression of nomic complexity has been refined through the analytic development of the intricacy of the laws governing the phenomenon of cluster interaction. As a visualization tool, the FDS enhances the ability to comprehend the combinatorial complexity and provides further comparative insight as to the MoE behaviour as traffic flows evolve.

References

1. ICAO.: Global Air Traffic Management Operational Concept. Doc 9854 AN/4854, 1st edn. International Civil Aviation Organization, Montreal, Canada (2005)
2. Leven, S., Zufferey, J.-C., Floreano, D.: Dealing with midair collisions in dense collective aerial systems. *J. Field Robot.* **28**, 405–423 (2011). doi:[10.1002/rob.20358](https://doi.org/10.1002/rob.20358)
3. Granger, G., Durand, N.: A traffic complexity approach through cluster analysis. Presented at 5th USA/Europe Air Traffic Management Research and Development Seminar, Paper 33. Budapest, Hungary, 23–27 June 2003
4. Durand, N., Bosc, J.-F., Alliot, J.-M.: Statistical Study of the French Airspace Congestion. Centre d'Etudes de la Navigation Aérienne, Ecole Nationale de l'Aviation Civile, Toulouse, France (1994)
5. Prandini, M., Piroddi, L., Puechmorel, S., Brazdilova, S.L.: iFly Deliverable D3.1, Complexity Metrics Applicable to Autonomous Aircraft, Safety, Complexity and Responsibility Based Design and Validation of Highly Automated Air Traffic Management. Project No. TREN/07/FP6AE/S07.71574/037180IFLY (2009)
6. NATO: NATO Guidelines on Human Engineering Testing and Evaluation. RTO-TR-021, AC/323(HFM-018)TP/19. Neuilly-sur-Seine, France (2001)
7. Flener, P., Pearson, J.: Automatic airspace sectorisation: a survey. arXiv preprint. [arXiv:1311.0653](https://arxiv.org/abs/1311.0653) (2013)
8. Manning, C., Fox, C., Pfeleiderer, E.: Relationships between measures of air traffic controller voice communications, taskload and traffic complexity. Presented at 5th USA/Europe Air Traffic Management Research and Development Seminar, Paper 93. Budapest, Hungary, 23–27 June 2003
9. Neerinx, M.: Cognitive task load analysis: allocating tasks and designing support. In: Hollnagel, E. (ed.) *Handbook of Cognitive Task Design*, pp. 283–305. CRC Press Inc, Boca Raton, Fla (2003)
10. Epp, S.S.: *Discrete Mathematics with Applications*, 2nd edn. Brooks/Cole Publishing Company, Pacific Grove, California (1995)
11. Torres, S.: Swarm theory applied to air traffic flow management. *Procedia Comp. Sci.* **12**, 463–470 (2012)
12. Martin, S., Girard, A.: Sufficient conditions for flocking via graph robustness analysis. In: *Proceedings of 49th IEEE Conference on Decision and Control*, pp. 6293–6298. Atlanta, Ga, 15–17 Dec 2010
13. Reynolds, C.W.: Flocks, herds, and schools: a distributed behavioural model. *ACM SIGGRAPH Comp. Graph.* **21**(4), 25–34 (1987)

14. Andrews, G.E.: *The Theory of Partitions*. Addison-Wesley, Reading, Mass (1976)
15. Andrews, G.E., Eriksson, K.: *Integer Partitions*. Cambridge University Press, Cambridge, UK (2004)
16. Abramowitz, M., Stegun, I.A.: *Handbook of Mathematical Functions*. 9th Printing National Bureau of Standards, Washington, D.C. (1970)
17. On-Line Encyclopedia of Integer Sequences. <http://oeis.org/Seis.html>, sequence A000041 (2010)
18. Weisstein, E.W.: *The CRC Concise Encyclopedia of Mathematics*. CRC Press Inc., Boca Raton, Fla (1999)
19. Fulton, N.L.: *Regional Airspace Design: A Structured Systems Engineering Approach*. Ph.D. Dissertation, University of New South Wales, Sydney, Australia (2002)
20. Fulton, N.L., Baumeister, R., Westcott, M., Estkowski, R.: An automated general aviation protection system for manned and unmanned aircraft. In: *Proceedings of 30th Digital Avionics Systems Conference*, pp. 5B2-1–5B2-16. Seattle, Washington, 16–20 Oct 2011. doi:[10.1109/DASC.2011.6096076](https://doi.org/10.1109/DASC.2011.6096076)
21. Fulton, N.L., Baird, J., Smith, W.: A compromise decision support problem approach to airspace design. Presented at 10th Australian International Aerospace Congress/14th National Space Engineering Symposium, AIAC2003-014. Brisbane, Australia, 29 July–1 August 2003
22. Fulton, N.L., Westcott, M., Emery, S.: Influences of communication structural complexity on operational safety in regional airspace design. *Saf. Sci.* **49**, 1099–1109 (2011)
23. CASA: Too many planes! Too many radio calls!. *Flight Safety Australia*, 80, 50–51 (2011)
24. ICAO Manual on Required Communication Performance (RCP). Doc 9869 AN/462, 1st edn., International Civil Aviation Organization, Montreal, Canada (2008)
25. ICAO: Special Committee on Future Air Navigation Systems, 3rd meeting. Doc. 9503, FANS/3, International Civil Aviation Organization, Montreal, Canada (1986)
26. Mistree, F., Smith, W.F., Bras, B.B., Allen, J.K., Muster, D. Decision-based design: a contemporary paradigm for ship design. In: *Proceedings of Annual Meeting of the Society of Naval Architects and Marine Engineers*, San Francisco, California, 31 October–3 November 1990
27. Klein, A.: An efficient method for airspace analysis and partitioning based on equalized traffic mass. Presented at 6th USA/Europe Air Traffic Management Research and Development Seminar, Paper 1, Baltimore, Md., 27–30 June 2005

Open-Pit Mine Production Planning and Scheduling: A Research Agenda

Mehran Samavati, Daryl L. Essam, Micah Nehring and Ruhul Sarker

Abstract Mining is a complex, expensive, yet lucrative business. Today's open-pit mines are huge projects in Australia. To keep the projects profitable, planners and schedulers are under constant pressure to make mine plans that are as accurate as possible and optimize production at all stages, from mine to market. In general, two different systems are available for extracting material in the mining industries: the traditional truck and shovel (T&S) and the modern in-pit crushing and conveying (IPCC) systems. While T&S has been extensively studied by operations research (OR) community, there are, however, almost no studies for optimizing the operations in IPCC systems. Despite great advantages of IPCC systems, mining companies are often reluctant to use it, due to the lack of an optimum strategic plan that makes it difficult, if not impossible, to estimate the costs of IPCC systems. In most cases, industry is still relying on the judgement or best estimate of experienced personnel in strategic decision making. This is without any guarantee of optimality and will be refined manually through multiple time-consuming iterations. This chapter introduces IPCC to the OR community and points out the need for OR research. Subsequently, we will develop a research agenda that provides an apt ground to study this system.

Keywords Open-pit mine · Production planning · Large-scale scheduling · In-pit crushing and conveying system

M. Samavati (✉) · D.L. Essam · R. Sarker
School of Engineering and Information Technology,
University of New South Wales, Canberra, Australia
e-mail: mehran.samavati@student.adfa.edu.au

M. Nehring
School of Mechanical and Mining Engineering,
University of Queensland, Brisbane, Australia

© Springer International Publishing AG 2018
R. Sarker et al. (eds.), *Data and Decision Sciences in Action*,
Lecture Notes in Management and Industrial Engineering,
DOI 10.1007/978-3-319-55914-8_16

1 Introduction

Mining is a significant primary industry and contributor to economy, particularly in Australia. The tight profit margins under which these mines operate and the nature of mineral markets require efficient ore removal schemes to ensure that the mine makes money.

In general, two different systems are available for extracting material in the mining industries: the traditional truck and shovel (T&S) and the modern in-pit crushing and conveying (IPCC) systems. While T&S has been extensively studied by operations research (OR) community, there are, however, almost no studies for optimizing the operations in IPCC systems. The only studies in this area are by Konak [2] and Rahmanour et al. [5]; these studies, however, are generally about allocating a location to the conveyors on which material is loaded to be carried out of the deposit (in IPCC systems), and do not take into consideration the scheduling aspects of material extraction.

The open-pit mine production scheduling problem (OPMPSP) in the traditional T&S system consists of scheduling the extraction of a mineral deposit that is broken into a number of smaller segments, or blocks, across a horizon of several periods in order to maximize the total discounted profit known as net present value (NPV) from the mining project subject to a variety of operational constraints. A similar optimization problem exists in the IPCC system. Even though the objective in both systems seeks to maximize NPV, introducing conveyors (in IPCC) into an open-pit operation introduces a number of additional sequencing and pit expansion constraints that are not required in traditional T&S systems. These constraints mainly relate to the geometric need for a fixed pit access location to accommodate the conveyor which thus restricts possible production sequencing in the deposit. This means that generating a schedule for extracting blocks is determined based on the location of conveyors, while finding the best location for conveyors is itself an optimization problem and can change the schedule. These additional constraints add further complexity to an already complex large-scale OPMPSP.

Many mining companies put in place a traditional operation, i.e., T&S, simply because they are looking for low risk and early payback on their investment. Mining specialists tend to believe that during the evaluation stage of a project, engineers should compare the costs and weigh up the benefits of an IPCC system to a traditional mining operation. However, lack of an optimum strategic plan makes it difficult, if not impossible, to estimate the costs of IPCC systems. In most cases, industry is still relying on the judgement or best estimate of experienced personnel in strategic decision making. This is without any guarantee of optimality and will be refined manually through multiple time-consuming iterations. Therefore, providing a strategic plan involving uncertainties and potential risks is something that mining companies require in order to approach the IPCC system more confidently. This

chapter discusses the benefits of IPCC system and points out the need for OR research. Subsequently, we will develop a research agenda for the OR community to study this system.

2 IPCC System

IPCC systems come from a few decades ago, first appearing in Germany in 1956. They were first applied to transport material out of a limestone quarry which was not possible by a truck and shovel operation due to the floor conditions [3]. In the current economic and political climate, high diesel prices, shortages of tyres for large off-highway trucks and labor, and high carbon emissions have reduced the attractiveness of a truck and shovel operation. While these factors are a limitation to the use of a truck and shovel system, they can also be seen as an opportunity to exploit an IPCC system for its reduced operating costs, severely reduced labor requirements, minimal reliance on large tyres for off-highway trucks, and decreased carbon emissions [4].

The benefits of an IPCC system revolve around operating expenses [1]. The costs for fuel, trucks, tires, labors, and carbon emissions can be significantly reduced if an IPCC system is installed.

In spite of these benefits, companies are still unwilling to use IPCC. One of the reasons is the fact that there are some factors that must be considered to justify the replacement of trucks with IPCC configuration. These factors, however, are totally related to the initial investment of the project, which cannot be precisely known without having an optimal strategic plan. For example, IPCC is capital intensive and requires a long-life operation in order to benefit from the reduced operating expenses. This means that a certain number of time periods (usually years) are required to payback the initial investment. However, lack of a precise estimation of the needed initial investment makes it difficult to estimate the number of these years. Investments in a mining project need to incorporate planning over several years. It must be known that, despite larger short-term capital expenses compared with T&S, the IPCC operation will return the investment quickly through lower operating costs.

Typically, IPCC operating costs are lower than normal truck and shovel operations; however, some factors such as fuel prices, size of the mine, materials mined, and the manpower required need to be analyzed and determined for the full life of the ore body to optimize the profit. Due to the lack of a methodology to obtain the best sequence of the extraction operations and an optimal schedule, these factors are analyzed based on strategic plan that only comes from the judgement of experienced personnel in strategic decision making.

In addition, the inherent risks of unforeseen factors affect the predictability of the operations. A well-developed strategic plan that takes into consideration the potential risk, when optimizing operations, can minimize potential uncertainties.

Therefore, one additional topic in mining optimization relates to developing a methodology to make a strategic plan for the use of IPCC. One possibility is to expand on the methods already developed for T&S by carrying out an initial investigation/development to add additional constraints that produce optimal pit limits when taking into consideration the use of IPCC systems. In the next section, we will introduce the potential research areas that relate to optimizing mine projects' operations with IPCC configuration.

3 Research Opportunities for the OR Community

As discussed above, certain factors, such as the estimation of the initial investment and the needed equipment, require a strategic production plan when using IPCC systems. In fact, there are a variety of aspects that must be optimized in order to develop such a plan. In this section, we introduce these aspects to OR community.

Despite identical objective in both systems, that is maximizing NPV, OPMPSP in the IPCC system differs from that of T&S due to the following reasons:

1. IPCC uses three different conveyors—main ‘trunk’ conveyor, transfer conveyor, and bench conveyor—instead of trucks to transfer material out of the pit. Finding the best location to accommodate these conveyors is of importance and must be considered alongside extraction scheduling.
2. There are new precedence relationships between the blocks, in addition to the traditional precedence relationship in T&S.
3. The new precedence relationships between blocks vary depending on the locations of conveyors that are a decision variable themselves.

Figure 1 shows the deepest level of a pit from a top view. Each square indicates a block, and the gray-shaded blocks represent those containing valuable material, known as ore blocks.

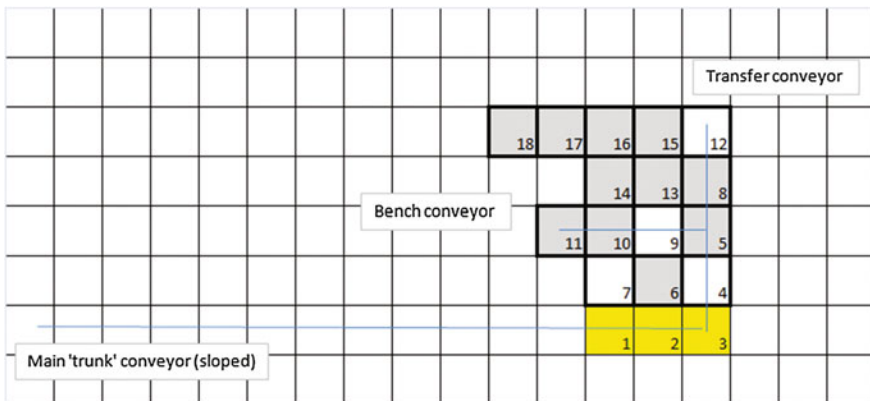


Fig. 1 A graphical view of the positions of conveyors in IPCC systems

In this figure, the transfer conveyor is placed in blocks 3, 4, 5, 8, and 12. All these blocks must be extracted to accommodate the transfer conveyor. Similarly, blocks 1, 2, and 3 (yellow-shaded blocks) must be removed to accommodate the flat section of the main 'trunk' conveyor. Note that the remaining section of this conveyor (i.e., the sloped section as can be seen in Fig. 1) goes into the upper level of the ore body, and no more blocks in this level need to be removed for this conveyor.

The best location for these conveyors is itself a decision variable and must be determined at the same time with scheduling the extraction. The third conveyor, bench conveyor, is mobile and can move to different rows.

Changing precedence relationship between blocks is another aspect that should be taken into consideration when performing the scheduling. To illustrate this, we give an example on Fig. 1. Assume that block 11 is selected to be extracted. After removing this block, the extracted material are poured in the bench conveyor and transferred through this conveyor to the transfer conveyor, and finally to the main conveyor. This means that blocks 10 and 9 must be extracted before block 11 to accommodate the bench conveyor. Thus, blocks 9 and 10 are the predecessors of block 11. However, this relationship may change by changing the location of either the transfer or main conveyor. For example, suppose that the best location for the transfer conveyor is selected to be the column starting with block 1, i.e., blocks 1, 7, 10, 14, and 16, in this case, there are no predecessors to block 11.

The preceding example describes one of the aspects in IPCC systems that should be optimized. There are, however, other aspects that can be considered in order to develop a strategic plan for the entire project.

- Integrating the metallurgical throughput/recovery relationship into the optimal pit limit and/or scheduling process
- Incorporating stockpiling into the pit limit and/or scheduling process (perhaps geological or market risk parameters)
- Incorporating uncertainty/risk aspects into the pit limit/scheduling process (perhaps geological or market risk parameters)
- Integrating waste dump scheduling (for encapsulating acid-bearing material) into the optimal pit limit/scheduling process

From a practical point of view, the first two aspects may be the most important ones to be considered. All these operational aspects also exist in the traditional T&S extraction system; from an OR point of view, integrating waste dump scheduling has been the most difficult aspect in the traditional system and, in fact, there are still no efficient algorithms to address this problem. The same may hold for the IPCC system, as incorporating waste dump requires considering the storing of extracted material alongside extraction scheduling.

4 Conclusion

In this chapter, we introduced a new optimization problem to the OR community. The traditional version of this problem is known as long-term open-pit mine production scheduling. This is a well-known optimization problem that has been considered by the OR community for a few decades. However, a new modern system, i.e., IPCC, is available for extracting material from mine ore bodies, and this gives rise to the need for OR specialist to modify the previous techniques applied to the traditional system so they can be applied to IPCC.

We introduced the new extracting system in such a way that is straightforward for OR community to understand and discussed the research areas coming from this system. Optimizing the operations of the modern extracting system can lead to a several thousand dollar increase in the profit of a company.

References

1. Foley, M.: In-pit crushing: wave of the future. *Aust. J. Min.* 46–53 (2012)
2. Konak, G., Onur, A.H., Karakus, D.: Selection of the optimum in-pit crusher location for an aggregate producer. *J. SAIMM* **107**, 161–166 (2007)
3. Koehler, F.: In-pit crushing system the future mining option. In: Twelfth International Symposium on Mine Planning and Equipment Selection, pp. 371–37. The Australian Institute of Mining and Metallurgy, Kalgoorlie (2003)
4. McCarthy, R.J.: In-pit crushing and conveying: fitting a square peg in a round open pit. In: Proceedings CIM Montreal 2011 Canadian Institute of Mining, Metallurgy and Petroleum Montreal (2011)
5. Rahmanpour, M., Osanloo, M., Adibee, N., AkbarpourShirazi, M.: An approach to locate an in pit crusher in open pit mines. *IJE Trans. C: Asp.* **27**(9), 1475–1484 (2014)

A Comparative Study of Different Integer Linear Programming Approaches for Resource-Constrained Project Scheduling Problems

Ripon K. Chakraborty, Ruhul Sarker and Daryl L. Essam

Abstract Over the last few decades, the resource-constrained project scheduling problem (RCPSP) has been considered a challenging research topic in operations research and computer science. In this paper, we have primarily proposed two different integer linear programming (ILP) models for RCPSPs. As the computational effort required for solving such models depends on the number of variables and constraints, our proposed mathematical models were carried out while attempting to reduce the required number of variables and constraints. For better demonstration, four other ILP models for RCPSPs were also considered so that they could be compared with our proposed models. That comparative study was conducted by solving standard benchmark instances while using a common objective function. The study provides interesting insights about the problem characteristics, model sizes, solution quality and computational efforts required for solving those ILP models.

Keywords Resource-constrained project scheduling problem • Mixed integer linear programming formulations • Mathematical formulations

1 Introduction

RCPSP has become an important problem for project scheduling over the last few decades [1]. The RCPSP assumes complete information of resource usage and activity duration, and determines a feasible baseline schedule which encompasses a list of activity starting times while minimizing the makespan [2]. Diversified applications of RCPSPs have stimulated many mathematical formulations from earlier researchers. From the last decades or so, CPM and PERT are the fundamental techniques to solve project scheduling problems. These two methodologies

R.K. Chakraborty (✉) · R. Sarker · D.L. Essam
School of Engineering and Information Technology, University of New South Wales,
Canberra 2600, Australia
e-mail: ripon.chakraborty@student.adfa.edu.au

study the temporal development of a project, while taking into account only precedence relationships among activities and considering that resources are unlimited. In RCPSP, it is assumed that resources are limited, which necessitate some of the other mathematical models. Again, for the conceptual validation of those models, there exist a large number of benchmark instances for RCPSP. In spite of there being criticism of those instances, popular instances are often taken from PSPLIB (project scheduling problem library). So, in this paper, we will consider instances with different numbers of activities, such as 30, 60, 90 and 120, to test our approaches.

To solve RCPSPs, integers linear programming (ILP)-based approaches are common in the literature. However, real-life projects with many activities are impossible to solve by using exact algorithms, as they involve a large number of variables and constraints. According to Herroelen and Leus [3] and Alcaraz et al. [4], many of the 60-activity and most of the 90- and 120-activity instances from PSPLIB are beyond the capability of exact methods. Koné et al. [5] have recently indicated that the MILP model can deal with up to 25–35 activities. For this reason, any mathematical model that can reduce the number of variables and constraints in representing RCPSP would be very useful in practice.

Due to the high degree of complexity of RCPSPs, numerous heuristic and meta-heuristic methods have also been proposed [6]. Although heuristics may produce good solutions within a reasonable computation time, they do not guarantee an optimal solution. Mathematical programming, especially MILP, because of its rigorousness, flexibility and extensive modelling capability, has become one of the most widely explored methods for solving scheduling problems [7]. However, considering the state of current computational capability, the conventional methods are incapable of solving MILP models with a large number of variables and constraints. In some models, the number of variables increases exponentially with the number of time periods, which encouraged us to develop alternative mathematical models which redefine variables to minimize the number of variables and constraints.

In this paper, we address a static RCPSP with the objective of minimizing makespan or project completion time. Two different mathematical formulations for RCPSPs are proposed that differ in how they handle time. One of them is discrete time-based (i.e. sequencing variable and flow-based formulation, SVFBB) and another one is continuous time-based (i.e. continuous time formulation allowing shifts, CTFAS). Four other state-of-the art mathematical models are also considered to be compared with our proposed models. For better analysis, each of those six formulations was solved using the same objective functions. Comprehensive analysis has also been carried out among those different approaches, particularly to see the relative efficiency of minimizing the number of variables to represent RCPSPs. Later on, the effectiveness of the mathematical approaches will be demonstrated with the results of extensive experimentation with different types of benchmark instances. In brief, this paper's key contribution over existing research on classical RCPSPs lies on the fact that it comes with two broad types of

mathematical formulations, namely, continuous and discrete time approaches that are shown to be competitive for different benchmark instances.

2 Problem Descriptions and Mathematical Models

The RCPSP under study is based on the following assumptions: (i) the activities composing a project have certain and known durations; (ii) all predecessors must be finished before an activity can start; (iii) resources are only renewable; (iv) activities are non-preemptive (i.e. cannot be interrupted when in progress); and (v) the main objective is to minimize project completion time. Let, I ($i = 0 \dots I + 1$) be the set of activities to be scheduled, R ($r = 1 \dots R$) be the number of available renewable resources. The activities constituting the project are represented by a set $\{0, \dots, I + 1\}$, where 0 and $I + 1$ are dummy nodes representing the start and end, respectively. The other important notations are depicted in the nomenclature. Each resource type has a certain capacity limit which should be utilized throughout a project's life without being exceeded. As in most project management studies, we also consider minimizing makespan as our sole objective. Throughout this section, we present several integer or mixed integer linear programming (MILP) models for RCPSPs, which we have solved with the branch and bound (B&B) method. In particular, Sects. 2.1 and 2.2 present existing discrete time formulations, while Sect. 2.3 is our novel discrete time formulation. Following them, Sect. 2.4 is our novel continuous time formulation, while Sects. 2.5 and 2.6 deal with existing techniques.

Nomenclature

Indices/Sets

- I set of activities, $i = 0 \dots I + 1$
 T set of time periods, $t = 0 \dots T$
 R set of renewable resources, $r = 1 \dots R$

Parameters:

- K_{rt} Capacity of resource r at time t
 U_{ir} Resource usage of activity i for resource r
 d_i Duration of activity i
 ES_i, LS_i Earliest & latest starting time, respectively, for activity i
 EF_i, LF_i Earliest & Latest Finish time, respectively, for activity i
 TSL_i Total Slack time of activity i
 T Total planning horizon/upper bound of project duration
 P_i Set of direct (and indirect) predecessors of activity i
 B_i Set of direct (and indirect) successors of activity i
 P_{prec} Represents the precedence set
 S_i Starting time continuous variable for activity i

f_{ijr}	<i>Quantity of resource r that is transferred from activity i (at the end of its processing) to activity j (at the start of its processing)</i>
$I + 1$	<i>Last job</i>
TI	<i>Transitive closure of pre-existing precedence relationship on activities</i>
U_{irt}	<i>Maximum availability of resource r for activity i at time t</i>
Y_k	<i>Capacity of resource K</i>

2.1 Discrete Time Formulation (DTF)

The fundamental mathematical concept of standard RCPSPs was first developed by Pritsker et al. [8] and Talbot [9]. Since this model is indexed by both activities and time, we will call it the basic discrete time formulation (DTF). The formulation is as follows:

Decision variables

$$x_{it} = \begin{cases} 1 & \text{if activity } i \text{ starts in period } t \\ 0 & \text{otherwise} \end{cases}$$

$$\text{Minimize } Z = \sum_{t=0}^T tx_{(I+1)t} \tag{1}$$

Constraints:

$$\sum_{t=0}^T x_{it} = 1 \quad \forall i \in I \tag{2}$$

$$\sum_{t=0}^T tx_{jt} \geq \sum_{t=0}^T (t + d_i)x_{it} \quad \forall (i, j) \in P_{prec} \tag{3}$$

$$\sum_{i=1}^I \sum_{q=t-d_i+1}^t U_{ir}x_{iq} \leq K_{rt} \quad \forall r \in R \text{ and } \forall t \in T \tag{4}$$

$$x_{it} \in \{0, 1\} \quad \forall i \in I, t = 1, \dots, T \tag{5}$$

Here, Eq. (1) represents the objective function of the project which is to minimize the makespan (i.e. minimize the starting time of the last dummy job). Constraint (2) represents that every job or activity must be handled exactly once. Constraint (3) ensures the precedence relationship among activities. Meanwhile, constraint set (4) represents the capacity constraints of the renewable resources.

2.2 Flow-Based Continuous Time Formulations (FCTF)

Incorporation of sequencing variables was the very first category of continuous time formulations. This flow-based continuous time formulation (FCTF) of Artigues et al. [10] involves three types of decision variables. Firstly, the starting time continuous variable, S_i and S_j , secondly, sequential binary variables, x_{ij} and finally, continuous flow variable f_{ijr} . This formulation can be written as follows:

$$x_{ij} = \begin{cases} 1, & \text{if activity } i \text{ is processed before activity } j \\ 0, & \text{otherwise} \end{cases}$$

$$\text{Min } S_{I+1} \quad (6)$$

Subject to

$$x_{ij} + x_{ji} \leq 1 \quad \forall (i, j) \in (I \cup \{0, n+1\})^2, i < j \quad (7)$$

$$x_{ik} \geq x_{ij} + x_{jk} - 1 \quad \forall (i, j, k) \in (I \cup \{0, n+1\})^3 \quad (8)$$

$$S_j - S_i \geq (d_i + M_{ij})x_{ij} - M_{ij} \quad \forall (i, j) \in (I \cup \{0, n+1\})^2 \quad (9)$$

$$f_{ijr} \leq \min(u_{ir}, u_{jr})x_{ij} \quad \forall (i, j) \in (I \cup \{0\}) \times I \cup \{n+1\}, \forall r \in R \quad (10)$$

$$\sum_{j \in I \cup \{0, n+1\}} f_{ijr} = u_{ir} \quad \forall i \in I \cup \{0, n+1\}, \forall r \in R \quad (11)$$

$$\sum_{i \in I \cup \{0, n+1\}} f_{ijr} = u_{jr} \quad \forall j \in I \cup \{0, n+1\}, \forall r \in R \quad (12)$$

$$f_{n+1,0,r} = U_r \quad \forall r \in R \quad (13)$$

$$x_{ij} = 1 \quad \forall (i, j) \in TI \quad (14)$$

$$x_{ji} = 0 \quad \forall (i, j) \notin TI \quad (15)$$

$$f_{ijr} \geq 0 \quad \forall (i, j) \in (I \cup \{0, n+1\})^2, \forall r \in R \quad (16)$$

$$S_o = 0 \quad (17)$$

$$ES_i \leq S_i \leq LS_i \quad \forall i \in I \cup \{n+1\} \quad (18)$$

$$x_{ij} \in \{0, 1\} \quad \forall (i, j) \in (I \cup \{0, n + 1^2\}) \tag{19}$$

Here, similar to previous approaches, the objective function (6) is to minimize the project makespan. Constraint set (7) states that for two distinct activities, either i precedes j or j precedes i, or i and j are processed in parallel. Constraint (8) expresses the transitivity of the precedence relations. Constraints (9) are so-called disjunctive constraints that link the start time of i and j with respect to variable x_{ij} . Constraint set (10) links the flow variables and the x_{ij} variables. If i precedes j, the maximum flow sent from i to j is set to $\min \{u_{ir}, u_{jr}\}$, while if i does not precede j, the flow must be zero. Constraints (11)–(13) are resource flow conservation constraints. Constraints (14) and (15) set the pre-existing precedence constraints. Constraints (18) restrict the start time of any activity $\forall i \in I \cup \{0, n + 01\}$ to lie between its earliest and its latest start time. Finally, constraints (16), (17) and (19) represent the basic definition of this FCTF model.

2.3 Sequencing Variable and Flow-Based Formulations (SVFBF)

Comparing with the conventional formulation, the research of Maravelias and Grossmann [11] is a crucial step forward which should be addressed first before moving to the proposed formulations. It uses a continuous representation of the time domain and allows the duration of each task to vary according to the number of resources allocated to it. Our proposed sequencing variable and flow-based discrete time formulations (SVFBF), which in addition to keeping track of the resources being used at each point in time, determine which activities take place in parallel. Meanwhile, it also calculates the total resource requirements of such activities and forces these requirements to be less than the available capacities. Here, the resources should be transferred on a flow basis and the variables are time dependent. The decision variables are as follows:

$$y_{it} = \begin{cases} 1 & \text{if activity } i \text{ starts in period } t \\ 0 & \text{otherwise} \end{cases}$$

$$x_{ij} = \begin{cases} 1 & \text{if activity } i \text{ is processed before activity } j \\ 0 & \text{otherwise} \end{cases}$$

Formulation:

$$\text{Min} = S_{T+1} \tag{20}$$

Subject to

$$\sum_{t=ES_i}^{LS_i} y_{it} = 1 \quad \forall i \in I \tag{21}$$

$$S_i = \sum_{t=ES_i}^{LS_i} t y_{it} \quad \forall i \in I \tag{22}$$

$$S_j - S_i \geq (d_i + M_{ij})x_{ij} - M_{ij} \quad \forall (i, j) \in (I \cup \{0, n + 1\})^2 \tag{23}$$

$$f_{ijr} \leq \min(u_{ir}, u_{jr})x_{ij} \quad \forall (i, j) \in (I \cup \{0\}) \times I \cup \{n + 1\}, \forall r \in R \tag{24}$$

$$\sum_{j \in I \cup \{0, n + 1\}} f_{ijr} = u_{ir} \quad \forall i \in I \cup \{0, n + 1\}, \forall r \in R \tag{25}$$

$$\sum_{i \in I \cup \{0, n + 1\}} f_{ijr} = u_{jr} \quad \forall i \in I \cup \{0, n + 1\}, \forall r \in R \tag{26}$$

$$f_{n+1,0,r} = U_r \quad \forall r \in R \tag{27}$$

$$x_{ij} = 1 \quad \forall (i, j) \in TI \tag{28}$$

$$x_{ji} = 0 \quad \forall (i, j) \notin TI \tag{29}$$

$$\sum_{i=1}^I \sum_{q=t-d_i+1}^t U_{ir} y_{iq} \leq K_{rt} \quad \forall r \in R \text{ and } \forall t \in T \tag{30}$$

$$f_{ijr} \geq 0 \quad \forall (i, j) \in (I \cup \{0, n + 1\})^2, \forall r \in R \tag{31}$$

$$S_o = 0 \tag{32}$$

$$ES_i \leq S_i \leq LS_i \quad \forall i \in I \cup \{n + 1\} \tag{33}$$

$$x_{ij} \in \{0, 1\} \quad \forall (i, j) \in (I \cup \{0, n + 1\})^2 \tag{34}$$

Here, like before, the objective function (20) is to minimize the project make-span. Constraint set (21) represents that each activity must start within its earliest and latest start times and start only once. Constraint set (22) defines the start time of each activity *i*. Meanwhile, the descriptions of constraint sets (23)–(29) and (31)–(34) are the same as for constraint sets (9)–(19), respectively, whereas constraint set (30) represents the capacity constraints of renewable resources.

2.4 Continuous Time Formulations Allowing Shifts (CTFAS)

In this section, we started by considering a basic formulation proposed by Pritsker et al. [8] employing binary variables x_{it} that allocate a feasible start time $t \in T$ to each activity $i \in I$. Furthermore, we extended the model proposed by Rieck et al. [12] to deal with general temporal constraints and renewable resources. Here, the total float, $TF_i = LS_i - ES_i$, is the maximum length of time, by which the start of activity i may be delayed beyond its earliest start time, without causing project completion to be delayed beyond the final deadline. Here, delaying activity start time is referred as shifting. Since this formulation considers the possibility of activity shifting under a continuous time frame, we name this formulation as continuous time formulations allowing shifts (CTFAS). Here, binary variable x_{iq} states the extent of shifting, $q \in \{1, \dots, TF_i\}$, of activity $i \in I$ beyond its ES_i . The decision variables are as follows:

$$x_{iq} = \begin{cases} 1 & \text{if activity } i \text{ is shifted } q \text{ time units after } ES_i \\ 0 & \text{otherwise} \end{cases}$$

$$s_{it} = \begin{cases} 1 & \text{if activity } i \text{ starts in period } t \\ 0 & \text{otherwise} \end{cases}$$

$$\text{Minimize } S_{T+1} \tag{35}$$

Subject to

$$\sum_{q=1}^{TF_i} x_{iq} \leq 1 \quad i \in I \tag{36}$$

$$\sum_{t=ES_i}^{LS_i} s_{it} = 1 \quad \forall i \in I \tag{37}$$

$$S_i = ES_i + \sum_{q=1}^{TF_i} qx_{iq} \tag{38}$$

$$ES_b - ES_i \geq \sum_{q=1}^{TF_i} qx_{iq} - \sum_{q=1}^{TF_b} qx_{bq} + d_i \quad \forall i \in I \cup \{0, n+1\}, b \in B_i \quad \text{or,}$$

$$\sum_{t=0}^T tx_{jt} \geq \sum_{t=0}^T (t + d_i)x_{it} \quad (i, j) \in P_{prec} \tag{39}$$

$$U_{irt} \geq \left(1 - \sum_{q=1}^{TF_i} x_{iq}\right) u_{ir} + \sum_{q=1}^{\min\{t-ES_i, TF_i\}} x_{iq} u_{ir} \quad \forall i \in I \cup \{0, n+1\}, r \in R, ES_i \leq t < EF_i \quad (40)$$

$$U_{irt} \geq \sum_{q=1+\min\{t-EF_i, TF_i\}}^{\max\{t-ES_i, TF_i\}} x_{iq} u_{ir} \quad \forall i \in I \cup \{0, n+1\}, r \in R, EF_i \leq t < EF_i + TF_i \quad (41)$$

$$U_{rt} \geq \sum_{i=1}^I U_{irt} - Y_k \quad r \in R, t \in T \quad (42)$$

$$x_{iq} \in \{0, 1\} \quad \forall i \in I \cup \{0, n+1\}, q \in \{1, \dots, TF_i\} \quad (43)$$

$$s_{iq} \in \{0, 1\} \quad \forall i \in I \cup \{0, n+1\} \quad (44)$$

Constraint (36) guarantees that the decision variables, x_{iq} , for an activity i will equal unity, at most, once (in the event that the activity is shifted, i.e. whenever $S_i > ES_i$). Constraint Eq. (37) represents that every job or activity must be handled exactly one time. Inequalities (38) and (39) ensure that the involved temporal or the precedence constraints will be satisfied. Constraint (40) ensures that the resource requirement will be met at every point in time $t \in \{ES_i, \dots, EC_i - 1\}$, where an activity i is not shifted beyond its earliest start time. Furthermore, if an activity i is shifted, inequalities (41) guarantee that the resource requirement will always be considered, while activity i is in progress at its temporarily shifted position. Finally constraints (42) and (43) ensure that the maximum allocation of resources is not exceeded.

2.5 Start/End Event-Based Continuous Time Formulations (SEECTF)

In the case of discrete time formulations, variables are indexed by time. In contrast to that formulation, two new event-based formulations were proposed by Koné et al. [5]: start/end-based and on/off-based. The start/end event-based continuous time formulation (SEECTF) considered only $(n + 1)$ activities as events. They used two types of binary variables, one for start event (x_{ie}) and the other one for its end (y_{ie}). A continuous variable t_e was also introduced to represent the date of event e , and a continuous variable r_{ek} was used for the quantity of resource k required immediately after event e ($e = 1 \dots \varepsilon$). Their formulation was as follows:

$$\text{Min } t_n \quad (45)$$

Subject to,

$$t_0 = 0 \quad (46)$$

$$t_f \geq t_e + p_i x_{ie} - p_i(1 - y_{if}) \quad \forall (e, f) \in \mathcal{E}^2, f > e, \forall i \in A \quad (47)$$

$$t_{e+1} \geq t_e \quad \forall e \in \mathcal{E}, e < n \quad (48)$$

$$\sum_{e \in \mathcal{E}} x_{ie} = 1 \quad \forall i \in A \quad (49)$$

$$\sum_{e \in \mathcal{E}} y_{ie} = 1 \quad \forall i \in A \quad (50)$$

$$\sum_{\tau=e}^n y_{i\tau} + \sum_{\tau=0}^{e-1} x_{j\tau} \leq 1 \quad \forall (i, j) \in E, \forall e \in \mathcal{E} \quad (51)$$

$$r_{ok} = \sum_{i \in A} b_{ik} x_{i0} \quad \forall k \in R \quad (52)$$

$$r_{ek} = r_{e-1,k} + \sum_{i \in A} b_{ik} x_{ie} - \sum_{i \in A} b_{ik} y_{ie} \quad \forall e \in \mathcal{E}, e \geq 1, k \in R \quad (53)$$

$$r_{ek} \leq B_k \quad \forall e \in \mathcal{E}, k \in R \quad (54)$$

$$ES_i x_{ie} \leq t_e \leq LS_i x_{ie} + LS_{n+1}(1 - x_{ie}) \quad \forall i \in A, \forall e \in \mathcal{E} \quad (55)$$

$$ES_{n+1} \leq t_n \leq LS_{n+1} \quad (56)$$

$$(ES_i + p_i) y_{ie} \leq t_e \leq (LS_i + p_i) y_{ie} + LS_{n+1}(1 - y_{ie}) \quad \forall i \in A, \forall e \in \mathcal{E} \quad (57)$$

$$t_e \geq 0 \quad \forall e \in \mathcal{E} \quad (58)$$

$$r_{ek} \geq 0 \quad \forall e \in \mathcal{E}, k \in R \quad (59)$$

$$x_{ie} \in \{0, 1\}, y_{ie} \in \{0, 1\} \quad \forall i \in A \cup \{0, n+1\}, \forall e \in \mathcal{E} \quad (60)$$

Constraint (46) stipulates that event 0 starts at time 0. Inequalities (47) ensure that activity i starts at event e and ends at event f . Any other combination of values for x_{ie} and y_{ie} yield either $t_f \geq t_e$ or $t_f \geq t_e - p_i$, which are redundant with constraint (48). Constraint (49) orders the events. Meanwhile, constraints (50) and (51) ensure that the start and end event must have a single occurrence, respectively. Constraint (51) describes the precedence relationship between activities. Constraint (52) gives for each resource, the total resource demand of the activities that start at event 0. Constraint (53) is a resource conservation constraint. Constraint (54) limits the demand of resources at each event to those that are available. Constraints (55)–(57) are valid inequalities based on activity time windows.

2.6 On/Off Event-Based Continuous Time Formulation (OOECTF)

In addition to the start/end event-based formulation, Koné et al. [5] also proposed another useful on/off event-based continuous time formulation (OOECTF). The earlier one needs more variables for representing events than the later one. Here, the number of events is exactly equal to the number of activities. The decision variable x_{ie} is set to 1 if activity i start at event e , or if it is still being processed immediately after event e . Another decision variable used here is a continuous one (t_e), which represents the date of event e . Their OOECTF was as follows:

$$\text{Min } C_{max} \quad (61)$$

Subject to,

$$\sum_{e \in \mathcal{E}} x_{ie} \geq 1 \quad \forall i \in A \quad (62)$$

$$C_{max} \geq t_e + (x_{ie} - x_{i,e-1})p_i \quad \forall e \in \mathcal{E}, \forall i \in A \quad (63)$$

$$t_0 = 0 \quad (64)$$

$$t_{e+1} \geq t_e \quad \forall e \neq n-1 \in \mathcal{E} \quad (65)$$

$$t_f \geq t_e + ((x_{ie} - x_{i,e-1}) - (x_{if} - x_{i,f-1}) - 1)p_i \quad \forall (e, f, i) \in \mathcal{E}^2 \times A, f > e \quad (66)$$

$$\sum_{e'=0}^{e-1} x_{ie'} \leq e(1 - (x_{ie} - x_{i,e-1})) \quad \forall e \in \mathcal{E} \setminus \{0\} \quad (67)$$

$$\sum_{e'=e}^{n-1} x_{ie'} \leq (n-e)(1 + (x_{ie} - x_{i,e-1})) \quad \forall e \in \mathcal{E} \setminus \{0\} \quad (68)$$

$$x_{ie} + \sum_{e'=0}^e x_{je'} \leq 1 + (1 - x_{ie})e \quad \forall e \in \mathcal{E}, \forall (i, j) \in E \quad (69)$$

$$\sum_{i=0}^{n-1} b_{ik}x_{ie} \leq B_k \quad \forall e \in \mathcal{E}, \forall k \in R \quad (70)$$

$$ES_i x_{ie} \leq t_e \leq LS_i(x_{ie} - x_{i,e-1}) + LS_n(1 - (x_{ie} - x_{i,e-1})) \quad \forall e \in \mathcal{E}, \forall i \in A \quad (71)$$

$$ES_{n+1} \leq C_{max} \leq LS_{n+1} \quad \forall e \in \mathcal{E}, \forall i \in A \quad (72)$$

$$t_e \geq 0 \quad \forall e \in \varepsilon \quad (73)$$

$$x_{ie} \in \{0, 1\} \quad \forall i \in A, \forall e \in \varepsilon \quad (74)$$

The objective function (61) is the minimization of makespan and is similar to others. Constraint set (62) ensures that each activity is processed at least once during a project. Constraint set (63) links the makespan to the event dates: $C_{max} \geq t_e + p_i$ if i is in process at event e but not at event $e-1$, i.e. if i starts at event e . Constraints (64) and (65) ensure event sequencing. Constraint set (66) links the binary optimization variable x_{ie} to the continuous variable t_e , and ensures that if activity i starts immediately after event e and ends at event f , then the date of event f is at least equal to the date of event e plus the processing time of activity i . Constraints (67) and (68) are called contiguity constraints which ensure non-pre-emption (i.e. the events after which a given activity is being processed are adjacent). Constraint set (69) maintains the precedence relationship. Constraint set (70) is the resource constraint that limits the total demand of activities in process at each event. Constraints (71) and (72) set the start time of any activity i to be between its earliest start time and its latest start time.

3 Solution Approach

Because of the rigorousness, flexibility and extensive modelling capability of MILP models, here in this paper, we have considered six different ILP/MILP models with some binary decision variables. For ILP/MILP, the B&B algorithm is so far the best for getting optimum results with less computational time [13]. Keeping this in mind, the above-mentioned mathematical formulations were coded in the LINDO optimization software (which uses B&B as a default solver) and were executed on an Intel Core i7 processor with 16.00 GB RAM and a 3.40 GHz CPU.

4 Experimental Results and Analysis

To compare our proposed two mathematical models with the others from Sect. 3, at first, a single-mode resource-constrained project is considered as an example. As evident from Fig. 1, the project network has nine activities with two dummy nodes (start and end nodes). The maximum allowable resource for the entire time duration is considered as 5 units. The proposed MILP formulations were implemented for the considered example and were solved by using the B&B algorithm with LINDO/LINGO optimization software. Since all formulations were solved by using an exact algorithm (i.e. B&B), they produced the same objective function value (i.e. makespan) equals to 7. Apart from SEECTF, the solving time for all of the other

Fig. 1 Project network

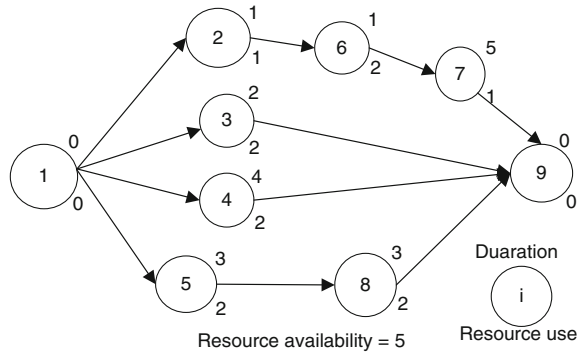


Table 1 Variable and constraint-based comparison among all mentioned approaches

Model name	Make span	N.V	N.C	CPU (s)
DTF	7	108	41	1
FCTF	7	215	938	1
SVFBB	7	135	54	1
CTFAS	7	179	189	1
SEECTF	7	212	955	15
OOECTF	7	190	972	1

mathematical formulations took approximately 1 s each. But, as shown in Table 1, for small project (here only for nine activities), DTF produces the least number of variables (N.V), while our proposed SVFBB and CTFAS are competitive to the others and placed second and third, respectively. Moreover, the number of constraints (N.C) for SVFBB and CTFAS was also significantly lower than the others, except for DTF. In summary, considering computing time, there is no significant difference among the different mathematical models for such a small number of activity project. Therefore, to develop better conclusions, we need to perform further demonstrations with different mixes of projects or benchmark instances.

Table 2 summarizes the comparative view of number of variables (N.V) and constraints (N.C) generated from the six considered mathematical models. Here, we employed four different benchmark sets. At first, we considered KSD instances for 30 activities taken from the PSPLIB website. These instances were first proposed and generated by Kolisch and Sprecher [14]. We also employed the KSD15_d and Pack_d instances proposed by Koné et al. [5]. Owing to the fact of having relatively short durations for most of the instances of KSD30, which could represent an advantage for MILP formulations indexed by time, Koné et al. [5] created two new types of instances (named Pack_d and KSD15_d). Furthermore, we also considered Patterson benchmark instances from the PSPLIB website. Details on these instances can be found from the work of Patterson [15]. To give a clear view, we considered 10 instances from each benchmark group, which were later solved with the B&B approach for our modified or proposed mathematical formulations. As mentioned

Table 2 Variable and constraint-based comparison among all mentioned approaches for different single-mode benchmark problems

Instance	Parameters	DTF	FCTF	SVFBB	CTFAS	SEECTF	OOECTF
KSD_30 (size: 30 activity)	N.V	1632	4571	1705	2032	2035	985
	N.C	313	38115	373	8530	19664	20723
	CPU (s)	1.00	3.00	1.37	1.85	2.50	2.25
KSD15_d (size: 15 activity)	N.V	8602	1430	1820	1527	588	270
	N.C	2083	6564	2113	5530	3426	2475
	CPU (s)	5.5	1.85	1.62	3.30	1.43	1.20
Pack_d (size: 22 activity)	N.V	14973	2091	7045	4862	1052	504
	N.C	2042	15732	2168	6042	7201	6804
	CPU (s)	5.80	3.52	4.93	4.53	2.50	2.00
Patterson (20 activity)	N.V	682	1669	787	822	962	460
	N.C	167	13306	287	2733	6772	6340
	CPU (s)	1.8	3.25	4.58	5.55	2.25	1.15

before, the KSD30 instances include 30 activities while for KSD15_d, Pack_d and Patterson instances, the numbers of activities on average are 15, 22 and 20, respectively. Expectedly, under each formulation, the solver produced the same average makespan with varied computational time (CPU in seconds). From Table 2, it is clear that the best MILP formulation, considering average number of variables for the KSD30 and Patterson 20 instances (which have low activity duration), is DTF. Whereas, our proposed SVFBB and CTFAS generated relatively fewer amounts of N.V compared to event-based and flow-based approaches. On the contrary, event-based models are better than the other models, for instances KSD15 and Pack_d (which have high activity duration time and are harder to solve). When the activity's durations are significantly higher (i.e. Pack_d instances), DTF produces substantial amounts of N.Vs which directly affects its computation time. In contrast with DTF, for these higher activity duration instances, our proposed formulations, SVFBB and CTFAS, only need small numbers of variables and can be solved with reasonable computational efforts. In a nutshell, the proposed mathematical models (i.e. SVFBB and CTFAS) are somewhat competitive to the others, even for both higher and lower project durations.

5 Conclusions

The objective of this research was to analyse and develop suitable mathematical models for single-mode RCPSPs. Two different ILP/MILP models were formulated that differ in their time dependency of decision variables (i.e. discrete and continuous). Those ILP/MILP models were then compared with some state-of-the-art mathematical models and were solved by implementing branch and bound

techniques in the LINDO platform. Different benchmark problems for different numbers of activities were considered for numerical experimentation. The experimental results show that for benchmark instances of smaller durations, discrete time-based approaches (i.e. DTF and SVFBB) are competitive to continuous time-based approaches considering both number of variables and computational times. However, for benchmark instances with higher activity durations, continuous time-based approaches (particularly event-based approaches and CTFAS) significantly outperformed the others. The suitability of this continuous time-based approach may be stronger if the number of activities for each instance is increased. From these results, practitioners have a summary of different alternative formulations with their strengths and weaknesses. These models can be easily implemented to solve a RCPSP on a real-time basis for small to big industrial sectors.

We assumed that the project activities are the same throughout the whole project life. But in reality, that may not always be true. To keep pace with ever changing trends, consideration of different uncertainties is a must. Therefore, proposing continuous time-based mathematical formulations that consider duration variability or resource breakdowns can be an important future research area.

References

1. Hartmann, S., Briskorn, D.: A survey of variants and extensions of the resource-constrained project scheduling problem. *Eur. J. Oper. Res.* **207**(1), 1–14 (2010)
2. Bruni, M.E., et al.: A heuristic approach for resource constrained project scheduling with uncertain activity durations. *Comput. Oper. Res.* **38**(9), 1305–1318 (2011)
3. Herroelen, W., Leus, R.: Project scheduling under uncertainty: survey and research potentials. *Eur. J. Oper. Res.* **165**(2), 289–306 (2005)
4. Alcaraz, J., Maroto, C., Ruiz, R.: Solving the multi-mode resource-constrained project scheduling problem with genetic algorithms. *J. Oper. Res. Soc.* **54**(6), 614–626 (2003)
5. Koné, O., et al.: Event-based MILP models for resource-constrained project scheduling problems. *Comput. Oper. Res.* **38**(1), 3–13 (2011)
6. Kyriakidis, T.S., Kopanos, G.M., Georgiadis, M.C.: MILP formulations for single- and multi-mode resource-constrained project scheduling problems. *Comput. Chem. Eng.* **36**, 369–385 (2012)
7. Koné, O., et al.: Comparison of mixed integer linear programming models for the resource-constrained project scheduling problem with consumption and production of resources. *Flex. Serv. Manuf. J.* **25**(1–2), 25–47 (2013)
8. Pritsker, A.A.B., Waiters, L.J., Wolfe, P.M.: Multiproject scheduling with limited resources: a zero-one programming approach. *Manage. Sci.* **16**(1), 93–108 (1969)
9. Talbot, F.B.: Resource-constrained project scheduling with time-resource tradeoffs: the nonpreemptive case. *Manage. Sci.* **28**(10), 1197–1210 (1982)
10. Artigues, C., Michelon, P., Reusser, S.: Insertion techniques for static and dynamic resource-constrained project scheduling. *Eur. J. Oper. Res.* **149**(2), 249–267 (2003)
11. Maravelias, C.T., Grossmann, I.E.: Optimal resource investment and scheduling of tests for new product development. *Comput. Chem. Eng.* **28**(6–7), 1021–1038 (2004)
12. Rieck, J., Zimmermann, J., Gather, T.: Mixed-integer linear programming for resource leveling problems. *Eur. J. Oper. Res.* **221**(1), 27–37 (2012)

13. Zhu, G., Bard, J.F., Yu, G.: A branch-and-cut procedure for the multimode resource-constrained project-scheduling problem. *INFORMS J. Comput.* **18**(3), 377–390 (2006)
14. Kolisch, R., Sprecher, A.: PSPLIB-a project scheduling problem library: OR software-ORSEP operations research software exchange program. *Eur. J. Oper. Res.* **96**(1), 205–216 (1997)
15. Patterson, J.H.: Alternate methods of project scheduling with limited resources. *Naval Res. Logist. Q.* **20**(4), 767–784 (1973)

A Recovery Model for Sudden Supply Delay with Demand Uncertainty and Safety Stock

Sanjoy Kumar Paul and Shams Rahman

Abstract In this paper, a recovery model is developed for managing sudden supply delays that affect retailers' Economic Order Quantity (EOQ) model. For this, a mathematical model is developed that considers *demand uncertainty* and *safety stock*, and generates a recovery plan for a finite future period immediately after a sudden supply delay. Solving recovery problems involve high commercial software costs, and their solutions are complex. Therefore, an efficient heuristic solution is developed that generates the recovery plan after a sudden supply delay. An experiment is conducted to test the proposed approach. To assess the quality and consistency of solutions, the performance of the proposed heuristic is compared with the performance of the Generalized Reduced Gradient (GRG) method, which is widely applied in constrained mathematical programming. Several numerical examples are presented and a sensitivity analysis is performed to demonstrate the effects of various parameters on the performance of the heuristic method. The results show that safety stock plays an important role in recovery from sudden supply delays, and there is a trade-off between backorder and lost sales costs in the recovery plan.

Keywords Demand uncertainty · Heuristic · Recovery plan · Safety stock

1 Introduction

In the competitive supply chain environment, sudden disruptions are one of the most common real-life problems [7]. In 2015, a survey conducted by the Business Continuity Institute [2] reported that seventy-four percent of the total 426 firms surveyed had experienced at least one disruption in their supply chain, with fifteen

S.K. Paul · S. Rahman
School of Business IT and Logistics, RMIT University, Melbourne, Australia

S.K. Paul (✉)
UTS Business School, University of Technology Sydney, Sydney, Australia
e-mail: sanjoy.paul@uts.edu.au

percent of those firms having 6–20 disruptions per year. The survey also revealed that the firms suffered financial losses of between fifty thousand to five hundred million Euros due to supply chain disruptions. Besides financial losses, supply chain disruptions also bring many other negative outcomes for organizations. For instance, according to the same report mentioned above, supply chain disruptions harmed the reputation of twenty-seven percent of companies, and reduced the projected revenue of thirty-eight percent of companies. From the above report, it is clear that supply chain disruptions can cause organizations to suffer enormous financial and reputational losses.

In real-life disruption cases, the most common consequence of a disruption is a supply delay to the customer. To overcome this consequence, some researchers developed recovery models that consider supply and delivery delays after disruption under a deterministic demand condition [7, 8, 27]. In reality however, the demand can be uncertain and most researchers have ignored this while developing their recovery models [21]. Moreover, most of the previous recovery models assumed no safety stock [21] in the ideal plan. Considering safety stock would be a more practical way to develop a recovery model for managing sudden supply delay. To fulfill this gap in the literature, in this paper, we develop a recovery plan for managing sudden supply delays in retailers' Economic Order Quantity (EOQ) model, considering demand uncertainty and safety stock in the ideal plan. Although, the proposed model can be solved by using existing commercial software, but generally it is quite expensive to use in practice [7]. In addition, computational solutions to large scale disruption problems can be very complex [21]. Therefore the problem becomes intractable, so we suggest a heuristic approach which can approximate recovery plan efficiently. To assess the performance and applicability of the proposed approach, we compare our heuristic solution with a standard search algorithm such as the Generalized Reduced Gradient (GRG) method [6].

2 Literature Review

Over the last two decades, one of the most important research areas in operations research and business management has been the modeling of supply chains. More specifically researchers have considered various supply chain issues such as coordination and integration [1, 10, 11, 28], uncertain demand [3, 13, 18], disruption risk [12, 23, 24, 26], and sudden disruption [9, 15, 16, 19, 22]. Recently, Snyder et al. [25], Paul et al. [21] and Fahimnia et al. [5] provided an extensive review of supply chain disruption models. We however, in this literature review we focus on the recent works of sudden disruption recovery models.

On the topic of supply chain disruption recovery planning, several studies were found in the literature. Most of these studies proposed recovery models by considering production, supply disruption and demand fluctuation. In production disruption recovery models, for example, Xia et al. [27] developed a general disruption

management approach for a two-stage production and inventory control system that incorporated a penalty cost for deviations of revised plans from original plans. To analyze disruption effects in detail, they divided the disruption interval into three parts: pre-disruption, in-disruption, and post-disruption. Later, the study was extended by Hishamuddin et al. [7] who developed a plan to recover from production disruption in a single-stage production-inventory system. It was further extended by developing real-time disruption recovery plans for both single and multiple production disruptions in a single-stage imperfect [14, 19], a two-stage imperfect [22] and a three-stage mixed [15] production-inventory systems. This was achieved by considering backorder, lost sales and/or outsourcing options, and by developing heuristics to solve their models.

Recently, Hishamuddin et al. [8] studied a supply disruption recovery model with backorder and lost-sales concepts for managing supply delays in a two-stage supply chains consisting of single supplier and retailer and a heuristic was developed to obtain the recovery plan. Subsequently, several studies extended this model to develop real-time recovery models for managing supply disruption in three-stage supply chains (with multiple suppliers and retailers) and also proposed some heuristics to solve their models [17]. Furthermore, the real-time recovery concept was also applied for managing sudden demand fluctuations in a supplier-retailer coordinated system [20]. This study considered both backorder and lost sales options to generate revised plans, within a finite future period, after a fluctuation occurs.

The earlier discussion demonstrates that most of the models considered production and supply disruptions. However, they have ignored the parameters of *uncertain demand* and *safety stock* [21]. In this study, we develop a model for recovery from a sudden supply delay in a retailers' EOQ model. We consider triangular fuzzy numbers for tackling uncertain demand, and we also consider safety stock in the ideal plan while developing the recovery plan. We develop a mathematical model and a new heuristic that generates the recovery plan, within the recovery window, after the occurrence of a sudden supply delay. The heuristic results are tested for quality and applicability on a number of random test problems generated using a uniform random distribution. To the best of our knowledge, this is the first model which develops a recovery model in a retailers' EOQ model that considers both uncertain demand and safety stock.

3 Problem Description

In this section, we describe the problem of sudden supply delay in a retailers' EOQ model. We use the following notations.

- Q Lot size in the ideal plan
- \tilde{D} Fuzzy demand
- D Total expected demand
- SS Safety stock

- H Holding cost (\$/unit/time)
- S Set-up cost (\$/set-up)
- B Per unit backorder cost (\$/unit/time)
- L Per unit lost sales cost (\$/unit)
- T_d Supply delay (time)
- N Maximum number of cycles in the recovery window
- B_q Backorder quantity
- L_q Lost sales quantity
- S_i Safety stock at the end of cycle i in the recovery window
- X_i Revised lot size of cycle i in the recovery window

In this study, we consider a retailers' EOQ model where demand is a fuzzy random variable and there is safety stock in the ideal plan. In Fig. 1, the solid line represents the ideal plan, where Q is the lot size. There is a safety stock (SS) in the ideal plan, which is a certain percent of the lot size, and which is decided by the management of the organization. In this ideal plan, we assume that there is no disturbance. This ideal system could face a sudden delay in the supply which could not be predicted. So, we develop a recovery plan for a finite future period (known as the *recovery window*), to minimize the impact of that sudden delay. After the occurrence of a sudden delay, the duration of which is known, T_d . The dashed line, shown in Fig. 1, presents the recovery plan after a sudden delay. We revise the plan within the recovery window so that the impact of the sudden delay can be minimized. We use both backorder and lost sales options to recover from a sudden delay, and optimize the recovery plan by minimizing total cost. The decision variables are: backorder quantity (B_q), lost sales quantity (L_q), revised lot size (X_i), and revised safety stock (S_i) within the recovery window.

The recovery plan incorporates both backorder and lost sales costs needed to recover from a sudden delay in supply. These two costs can be defined as follows.

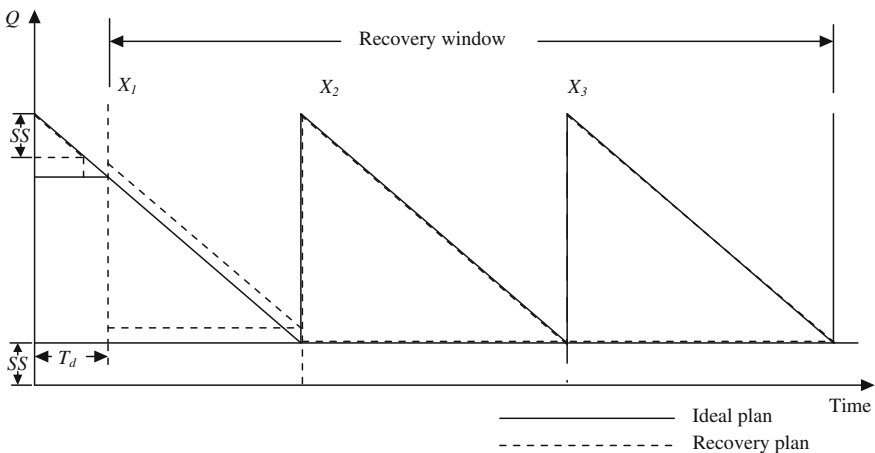


Fig. 1 A supply delay recovery plan within an EOQ model

- **Backorder quantity:** after the occurrence of a supply delay, the portion of demand that cannot be supplied on schedule but can be delivered at a later date when available [7, 15].
- **Lost sales:** the amount of sales lost when customers do not wait for stock to be replenished [7, 15].

In this study, we have made a number of assumptions, as follows.

- A single item is considered in EOQ model.
- Safety stock is assumed to be a percentage of lot size.
- Product demand is a triangular fuzzy number [3].
- The recovery plan starts immediately after a supply delay.
- The maximum number of cycles in the recovery plan is decided by the organization.

4 Model Formulation

In this section, we determine the equations for lot size and total expected demand considering fuzzy demand within the EOQ model. Then, we include safety stock in the final recovery model which generates the recovery plan after a sudden supply delay. The model is a constrained mathematical programming problem.

4.1 Considering Fuzzy Demand in EOQ Model

In this section, we determine the equations for lot size and total expected demand. These would be helpful to develop final recovery model. We know from the equation of total cost (TC) in the EOQ model, that:

$$TC = \frac{Q}{2}H + \frac{D}{Q}S \tag{1}$$

As demand is a fuzzy variable,

$$\widetilde{TC} = \frac{Q}{2}H + \frac{\widetilde{D}}{Q}S \tag{2}$$

In this paper, we consider demand data as triangular fuzzy numbers (TFN) [3]. Demand TFN and associated probabilities are taken as triplets $(\underline{d}_k, d_k, \overline{d}_k)$ and, $(\underline{p}_k, p_k, \overline{p}_k)$, respectively, where $k = 1, 2, 3, \dots, n$. We minimize the graded mean

integration value (GMIV) [4, 14] of total cost function and determine the optimal lot size and total expected demand (D) as presented in Eqs. (3) and (4) respectively.

$$\begin{aligned}
 Q^* = & \left[\frac{2}{H} \left\{ \sum_{k=1}^n \left[\frac{1}{2} d_k p_k + \frac{1}{3} d_k (p_k - p_k) + \frac{1}{3} p_k (d_k - d_k) \right. \right. \right. \\
 & \left. \left. \left. + \frac{1}{4} (d_k - d_k) (p_k - p_k) \right] \right\} \right. \\
 & \left. + \sum_{k=1}^n \left[\frac{1}{2} \bar{d}_k \bar{p}_k - \frac{1}{3} \bar{d}_k (\bar{p}_k - p_k) - \frac{1}{3} \bar{p}_k (\bar{d}_k - d_k) \right. \right. \\
 & \left. \left. \left. + \frac{1}{4} (\bar{d}_k - d_k) (\bar{p}_k - p_k) \right] \right\} S \right]^{\frac{1}{2}} \tag{3}
 \end{aligned}$$

$$\begin{aligned}
 D = & \sum_{k=1}^n \left[\frac{1}{2} d_k p_k + \frac{1}{3} d_k (p_k - p_k) + \frac{1}{3} p_k (d_k - d_k) \right. \\
 & \left. + \frac{1}{4} (d_k - d_k) (p_k - p_k) \right. \\
 & \left. + \sum_{k=1}^n \left[\frac{1}{2} \bar{d}_k \bar{p}_k - \frac{1}{3} \bar{d}_k (\bar{p}_k - p_k) - \frac{1}{3} \bar{p}_k (\bar{d}_k - d_k) \right. \right. \\
 & \left. \left. + \frac{1}{4} (\bar{d}_k - d_k) (\bar{p}_k - p_k) \right] \right] \tag{4}
 \end{aligned}$$

4.2 Objective Function and Constraints for Recovery Plans

In this section, we develop the mathematical model for generating recovery plans for sudden supply delays. To develop the model, we consider holding, set-up, lost sale and backorder costs during the recovery window. The final objective function is to minimize the total cost, subject to supply, demand, and quantity constraints. The holding cost (Eq. 4) is determined for both the revised lot and safety stock. The set-up cost (Eq. 5) is determined as cost per set-up multiplied by number of set-up. The lost sales cost (Eq. 6) is determined as unit lost sales cost multiplied by lost sales quantity [7]. The backorder cost (Eq. 7) is determined as unit backorder cost multiplied by backorder quantity and delay [7].

$$\text{Holding cost} = \frac{H}{2 \times D} \left[\sum_{i=1}^n X_i^2 \right] + \left(\frac{Q^*}{D} - T_d \right) S_1 H + \frac{H Q^*}{D} \sum_{i=2}^n S_i \tag{4}$$

$$\text{Set - up cost} = S \times N \tag{5}$$

$$\text{Lost sales cost} = L_q \times L \tag{6}$$

$$\text{Backorder cost} = \frac{B_q}{2} \times B \times \text{delay} \tag{7}$$

The objective function (Eq. 8), which is the total cost (TC), is determined by adding all the costs presented in Eqs. (4)–(7).

$$TC = \frac{H}{2 \times D} \left[\sum_{i=1}^n X_i^2 \right] + \left(\frac{Q^*}{D} - T_d \right) S_1 H + \frac{H Q^*}{D} \sum_{i=2}^n S_i + S \times N + L_q \times L + \frac{B_q}{2} \times B \times \text{delay} \tag{8}$$

It is subject to the following constraints, as presented in Eqs. (9)–(15).

$$X_i \leq Q^*; \forall i \tag{9}$$

$$S_i \leq SS + L_q; \forall i \tag{10}$$

$$B_q \leq \frac{L}{B} D \tag{11}$$

$$L_q \leq \left(T_d - \frac{SS}{D} - \frac{L}{B} \right) D \tag{12}$$

$$B_q + L_q = \left(T_d - \frac{SS}{D} \right) D; \text{ if } T_d > \frac{SS}{D} \tag{13}$$

$$B_q + L_q = 0; \text{ if } T_d < \frac{SS}{D} \tag{14}$$

$$X_i, S_i, B_q, \text{ and } L_q \geq 0 \forall i, \tag{15}$$

Equations (9) and (10) present the constraints for revised lot size and safety stock, respectively. Equations (11) and (12) are the constraints for backorder and lost sales quantities, respectively. The conditions of summation of backorder and lost sales quantities are presented in Eqs. (13) and (14). Finally, Eq. (15) presents the non-linearity condition of the decision variables.

5 Proposed Solution Heuristic

In this section, we develop a heuristic to solve the mathematical model presented in Sect. 4. The steps of the proposed solution heuristic are as follows.

- Step 1 Input parameters for ideal plan and fuzzy demand data.
- Step 2 Determine the plan for fuzzy demand using Eqs. (3) and (4).
- Step 3 Input supply delay (T_d) after its occurrence.
- Step 4 if $T_d \leq \frac{SS}{D}$
- $B_q = 0$
 - $L_q = 0$
 - $X_i = Q; \forall i$
 - $S_i = SS; \forall i$
 - Backorder cost = 0
 - Lost sales cost = 0
- Step 5 if $T_d > \frac{SS}{D}$
- Determine $y = T_d - \frac{SS}{D}$
 - Determine $x = \frac{L}{B}$
 - 5.1** if $x \geq y$
 - $B_q = y \times D$
 - $L_q = 0$
 - $X_i = Q; \forall i$
 - $S_i = SS; \forall i$
 - Backorder cost = $B_q \times B \times \frac{y}{2}$
 - Lost sales cost = 0
 - 5.2** if $x < y$
 - $B_q = x \times D$
 - $L_q = (y - x) \times D$
 - $X_i = Q; \forall i \neq 2$
 - $X_2 = Q - L_q$
 - $S_1 = SS + L_q$
 - $S_i = SS; \forall i \neq 1$
 - Backorder cost = $B_q \times B \times \frac{x}{2}$
 - Lost sales cost = $L_q \times L$
- Step 6 Determine different costs.
- Step 7 Record results.
- Step 8 Stop.

6 Results Analysis

In this section, we analyze the results of the recovery plan and run a comparison experiment to judge the quality of the heuristic solutions. We also perform a random experiment and a sensitivity analysis to reveal some important aspects of the model.

6.1 Recovery Plan

The recovery plan was generated by solving the mathematical model developed in Sect. 4. We have used the proposed heuristic, presented in Sect. 5, to solve the mathematical model. The fuzzy demand data for this analysis is presented in Table 1.

We used the following additional data for generating the recovery plan.
 $S = \$100$ per set-up, $H = \$0.8$ per unit per year, $B = \$0.6$ per unit per day,
 $L = \$12$ per unit, and $N = 3$.

The lot size (using Eq. 3) and safety stock in the ideal plan were determined as follows.

$Q^* = 2,563$ units, and $SS = 0.2 \times 2,563 = 513$ units.

Although we have experimented on many random test problems, for illustrative purposes we chose three sample instances by arbitrarily changing the supply delay data. The parameters are shown in Table 2.

The results for the three instances are presented in Table 3, which includes backorder and lost sales quantities, backorder and lost sales costs, and total cost. We observed that there was no backorder and lost sales costs in the recovery plan for instance number 1. This is because backorder and lost sales quantities were not incorporated in the recovery plan, and only safety stock was sufficient to generate the recovery plan from that delay. For instance number 2, we observed that only backorder cost was incorporated in the recovery plan. This is because the system was capable of recovering by using safety stock and incorporating only the backorder cost. For instance number 3, which have a longer supply delay, both backorder and lost sales were included in the recovery plan. This is because the system was not capable of recovering by using safety stock and only backorder. From Table 3, it can be seen that for the given data, the recovery plans use safety stock

Table 1 Fuzzy demand data

k	$\underline{d}_k, d_k, \overline{d}_k$	$\underline{p}_k, p_k, \overline{p}_k$ [3]
1	10000, 12000, 14000	0.045, 0.050, 0.055
2	15000, 17000, 19000	0.143, 0.150, 0.157
3	20000, 22000, 24000	0.292, 0.300, 0.308
4	25000, 27000, 29000	0.192, 0.200, 0.208
5	30000, 32000, 34000	0.092, 0.100, 0.108
6	35000, 37000, 39000	0.093, 0.100, 0.107
7	40000, 42000, 44000	0.094, 0.100, 0.106

Table 2 Three sample instances

Instance number	Supply delay (T_d)
1	0.01
2	0.05
3	0.08

Table 3 Recovery plan for three sample instances

Instance number	B_q (units)	L_q (units)	Backorder cost (\$)	Lost sales cost (\$)	Total cost (\$)
1	0	0	0	0	716.1
2	800	0	2670.1	0	3369.8
3	1439	149	8635.4	1788.6	11102.2

for smaller supply delays. With increasing supply delays, the recovery plans gradually incorporated backorder and lost sales costs alongside the use of safety stock. It was also observed that backorder were more attractive than lost sales for obtaining the optimal recovery plan.

6.2 Results Comparison

In order to evaluate the quality of the heuristic solutions, we compared them with those obtained by the GRG method, which is widely used to solve constrained mathematical programming problems [6], for 50 random test problems. To this end, we determined the results' average percentage of deviation using Eq. (16), which is commonly used in the literature [15, 17].

$$\text{Average percentage of deviation} = \frac{1}{M} \sum \left[\frac{|\text{Total cost from heuristic} - \text{Total cost from GRG}|}{\text{Total cost from GRG}} \times 100\% \right] \quad (16)$$

Here, M denotes the number of test problems.

The test problems were generated from a uniform random distribution by varying data in the following ranges.

$$B = [0.1, 0.8], \quad L = [5, 20], \quad SS = [100, 500], \quad \text{and} \quad T_d = [0.0001, 0.095].$$

The average percentage of deviation between the two approaches was only 0.00085%. This is negligible and may merely be because of rounding of the values of the decision variables.

6.3 Random Experimentation and Sensitivity Analysis

After evaluating the performance of the proposed solution heuristic, we performed a rigorous random experimentation and sensitivity analysis to better characterize the impacts of the important parameters on the final solutions. To this end,

we conducted random experimentation with a significant number of randomly generated problems. In this section we have analyzed the impacts of supply delay, backorder cost, lost sales cost, and safety stock on the recovery plan. This section presents a number of studies, in each of which only one variable is changed while the other parameters have the default values as presented in Sect. 6.1. For each study, 1,000 random test problems were generated by using a uniform random distribution. In what follows, we summarize the results obtained from the analysis.

Figure 2 presents the impact of supply delay on different costs. We observed that the total cost increases with supply delay, but the rate of increment is different. When supply delay is less than 0.0195, then total cost remains constant. This is because the system is capable of recovery by using only safety stock, so there is no backorder and lost sales costs when the supply delay is less than 0.0195. After that, the recovery plan incorporates only backorder cost until supply delay is 0.0743. In this range, the increment rate of total cost is higher because of incorporating backorder in the recovery plan. When supply delay is more than 0.0743, both backorder and lost sales are incorporated in the recovery plan and backorder costs become a constant amount. When incorporating both backorder and lost sales in the recovery plan, the total cost increases rapidly with increasing supply delay.

Figure 3 presents the impact of safety stock on different costs. We assume that the organization holds a maximum 20% of lot size as safety stock. We observed that the total cost decreases with increasing safety stock. This is because of the larger supply delay ($T_d = 0.08$) and the recovery plan that uses safety stock to determine its optimal plan. The backorder cost is constant but lost sales cost decreases with the

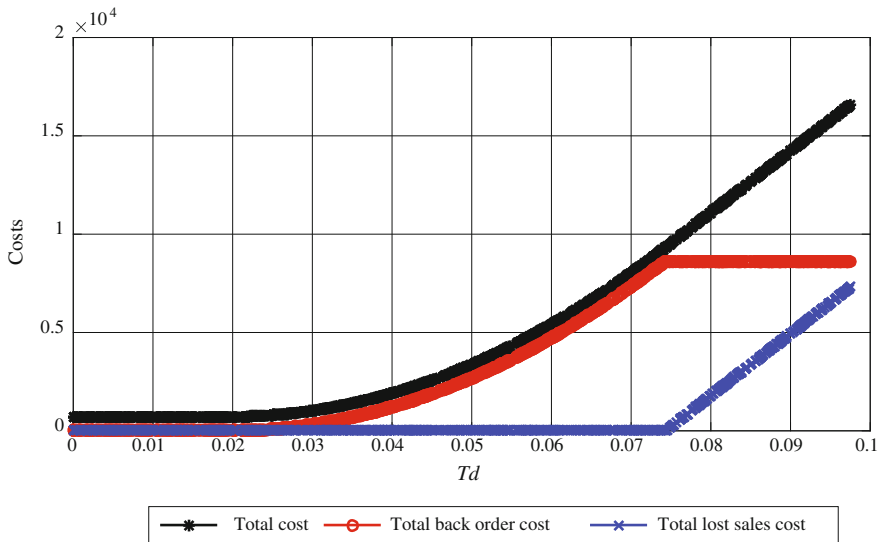


Fig. 2 Different costs versus T_d [$B=0.6, L=12, SS=513$]

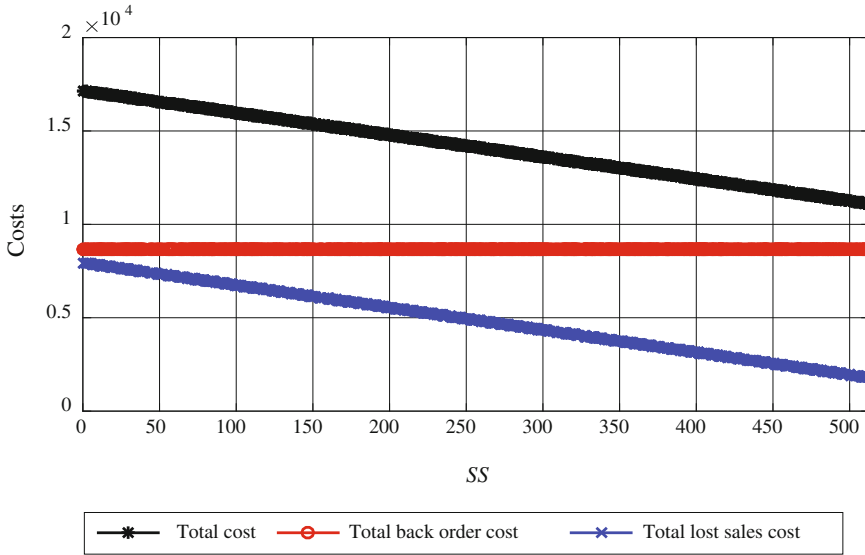


Fig. 3 Different cost versus SS [$B=0.6, L=12, T_d=0.08$]

amount of safety stock. This is because safety stock was used to decrease lost sales quantity, as lost sales were less attractive for generating this recovery plan.

The impact of backorder and lost sales costs on various costs are presented in Figs. 4 and 5, respectively. From Fig. 4, we observe that the total cost increases with per-unit backorder cost. When backorder cost is less than 0.543 per unit per day, then there is no lost sales cost in the recovery plan. This is because the system is capable of obtaining optimality by incorporating only backorder in its recovery plan. When backorder cost is more than 0.543 per unit per day, lost sales cost becomes included in the recovery plan and increases with increasing per-unit backorder cost. As lost sales costs increase when backorder costs are more than 0.543 per unit per day, backorder cost becomes less attractive in the recovery plan, hence it is decreasing.

The impact of per-unit lost sales cost on different costs is shown in Fig. 5. Total cost increases with per-unit lost sales cost when it is less than 13.38. After then it becomes a constant amount. When per-unit lost sales cost is less than 13.38, both backorder and lost sales are incorporated in the recovery plan. Total lost sales cost increases until per-unit lost sales cost is 6.73. After that, total lost sales cost decreases and backorder becomes attractive to obtain optimality in the recovery plan. When per-unit lost sales cost is more than 13.38, only backorder cost is incorporated in the recovery plan, as it becomes more attractive and also becomes a fixed amount. Then there is no lost sales cost in the recovery plan, as it becomes less attractive for generating recovery plan.

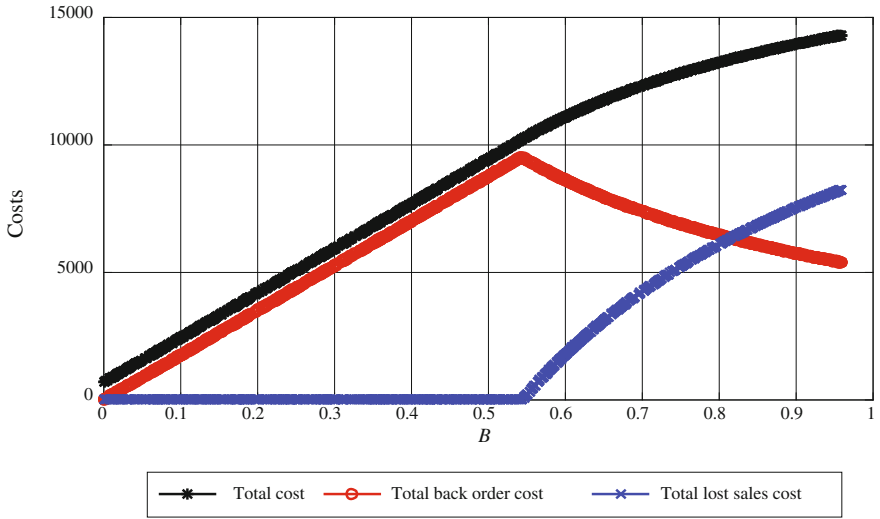


Fig. 4 Different costs versus B [$L = 12, SS = 513, T_d = 0.08$]

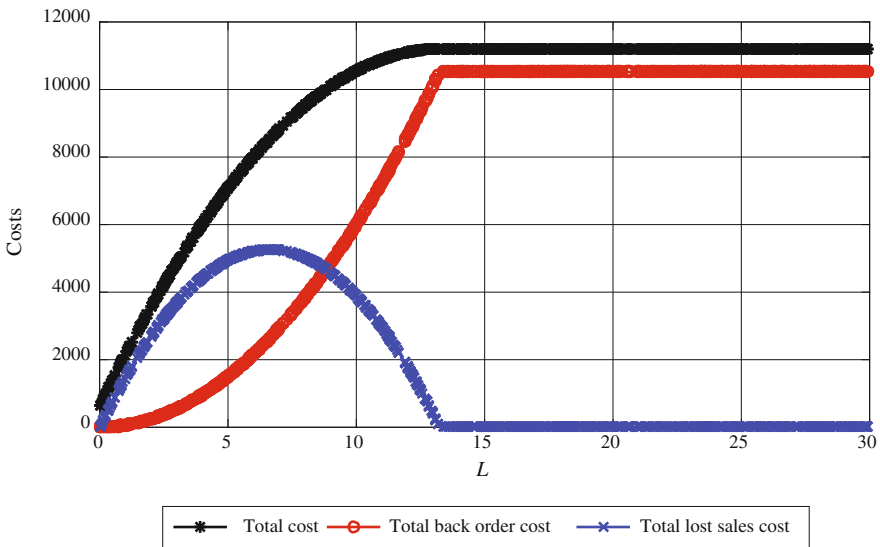


Fig. 5 Different costs versus L [$B = 0.6, SS = 513, T_d = 0.08$]

7 Conclusions

The main objective of this study was to develop a model (within a retailers' EOQ model) for recovery from a sudden supply delay that considers uncertain demand and safety stock. To fulfill this objective, firstly, we developed a constrained mathematical programming problem that considers fuzzy demand and safety stock. Considering the expensiveness of commercial software and computational complexity, we have proposed a solution heuristic to approximate the optimal recovery plan. To judge the quality of the heuristic, we compared the heuristic's solutions with another established solution technique—the Generalized Reduced Gradient (GRG) non-linear method. Comparisons were performed on 50 random test problems. The comparison experiment showed that the average percentage of deviation was only 0.00085%, which is insignificant deviation and may merely be because of rounding of the values of the decision variables. We also performed random experimentation to judge the capability of our proposed heuristic of solving all types of problems. Based on the experiments, it can be said that the proposed quantitative and heuristic approach offers a potentially very useful quantitative means of helping decision-makers arrive at prompt and accurate decisions regarding their recovery plan after a sudden supply delay.

There are several aspects that could be introduced to make the approach more comprehensive and practical. For example, investigating lead time factors and analyzing the effect of supply delays on lead times and recovery plans could be an interesting future research direction. Extending our approach to a multi-stage supply chain problem (with multiple suppliers, manufacturers, and retailers) would be a very interesting research direction. In addition, in the current study, we have modeled situations where only a single product is manufactured. Therefore, it would be worthwhile to investigate a more complex multi-tier supply chain system where multiple items are produced.

References

1. Agnetis, A., et al.: Set-up coordination between two stages of a supply. *Ann. Oper. Res.* **107**, 15–32 (2001)
2. Alcantara, P., Riglietti, G.: Supply chain resilience report, pp. 1–36. The Business Continuity Institute (2015)
3. Bag, S., et al.: A production inventory model with fuzzy random demand and with flexibility and reliability considerations. *Comput. Ind. Eng.* **56**(1), 411–416 (2009)
4. Chen, S.H., Hsieh, C.H.: Graded mean integration representation of generalized fuzzy number. *J. Chin. Fuzzy Syst.* **5**(2), 1–7 (1999)
5. Fahimnia, B., et al.: Quantitative models for managing supply chain risks: a review. *Eur. J. Oper. Res.* **247**(1), 1–15 (2015)
6. Gabriele, G.A., Ragsdell, K.M.: The generalized reduced gradient method: a reliable tool for optimal design. *J. Eng. Ind.* **99**(2), 394–400 (1977)

7. Hishamuddin, H., et al.: A disruption recovery model for a single stage production-inventory system. *Eur. J. Oper. Res.* **222**(3), 464–473 (2012)
8. Hishamuddin, H., et al.: A recovery mechanism for a two echelon supply chain system under supply disruption. *Econ. Model.* **38**, 555–563 (2014)
9. Hishamuddin, H., et al.: A recovery model for a two-echelon serial supply chain with consideration of transportation disruption. *Comput. Ind. Eng.* **64**(2), 552–561 (2013)
10. Kogan, K., Tapiero, C.S.: Coordination of co-investments in supply chain infrastructure. *J. Intell. Manuf.* **23**(6), 2471–2475 (2012)
11. Liao, C.J., et al.: An ant colony optimization algorithm for setup coordination in a two-stage production system. *Appl. Soft Comput.* **11**(8), 4521–4529 (2011)
12. Pal, B., et al.: A multi-echelon production–inventory system with supply disruption. *J. Manuf. Syst.* **33**(2), 262–276 (2014)
13. Panda, D., Maiti, M.: Multi-item inventory models with price dependent demand under flexibility and reliability consideration and imprecise space constraint: a geometric programming approach. *Math. Comput. Model.* **49**(9–10), 1733–1749 (2009)
14. Paul, S.K., et al.: A disruption recovery model in a production-inventory system with demand uncertainty and process reliability. *Lect. Notes Comput. Sci.* **8104**, 511–522 (2013)
15. Paul, S.K., et al.: A disruption recovery plan in a three-stage production-inventory system. *Comput. Oper. Res.* **57**, 60–72 (2015)
16. Paul, S.K., et al.: A quantitative model for disruption mitigation in a supply chain. *Eur. J. Oper. Res.* **257**, 881–895 (2017)
17. Paul, S.K., et al.: A reactive mitigation approach for managing supply disruption in a three-tier supply chain. *J. Intell. Manuf.* in press, 1–17 (2016)
18. Paul, S.K., et al.: Development of a production inventory model with uncertainty and reliability considerations. *Optim. Eng.* **15**(3), 697–720 (2014)
19. Paul, S.K., et al.: Managing disruption in an imperfect production-inventory system. *Comput. Ind. Eng.* **84**, 101–112 (2015)
20. Paul, S.K., et al.: Managing real-time demand fluctuation under a supplier-retailer coordinated system. *Int. J. Prod. Econ.* **158**, 231–243 (2014)
21. Paul, S.K., et al.: Managing risk and disruption in production-inventory and supply chain systems: a review. *J. Ind. Manag. Optim.* **12**(3), 1009–1029 (2016)
22. Paul, S.K., et al.: Real time disruption management for a two-stage batch production–inventory system with reliability considerations. *Eur. J. Oper. Res.* **237**(1), 113–128 (2014)
23. Qi, L.: A continuous-review inventory model with random disruptions at the primary supplier. *Eur. J. Oper. Res.* **225**(1), 59–74 (2013)
24. Salehi Sadghiani, N., et al.: Retail supply chain network design under operational and disruption risks. *Transp. Res. Part E Logist. Transp. Rev.* **75**, 95–114 (2015)
25. Snyder, L.V., et al.: OR/MS models for supply chain disruptions: a review. *IIE Trans.* **48**(2), 89–109 (2016)
26. Snyder, L.V.: A tight approximation for an EOQ model with supply disruptions. *Int. J. Prod. Econ.* **155**, 91–108 (2014)
27. Xia, Y., et al.: Real-time disruption management in a two-stage production and inventory system. *IIE Trans.* **36**(2), 111–125 (2004)
28. Xu, X., Meng, Z.: Coordination between a supplier and a retailer in terms of profit concession for a two-stage supply chain. *Int. J. Prod. Res.* **52**(7), 2122–2133 (2014)

Applying Action Research to Strategic Thinking Modelling

Leon Young

Abstract The versatility of the word strategy has created significant headaches for those looking to develop the area. The unfortunate position of the word strategy is that it has “acquired a universality which has robbed it of meaning”. Not only is strategy poorly understood and poorly used, but also the subservient capabilities that allow for the development of strategy, specifically strategic thinking, are equally mired in confusion and debate. Yet, despite this historical confusion, strategy and strategic thinking are often cited as the reason for organisational success or failure. Due to the inherent uncertainty within the subject, this paper seeks to use soft systems methodology to understand the problem. The problem of strategic thinking, specifically the development of a capability, is one of understanding rather than one of optimising. This chapter provides a broad review of a large research project on computational strategic thinking modelling. Importantly, we will examine the research methodology through the lenses of action research. We will outline the uncertain framework and summarise the finding that has notably increased our understanding of strategic thinking. This work confirms action research as a valid methodology for tackling uncertain situation and understanding what the problem is.

Keywords Strategic thinking • Soft systems methodology • Operations research

1 Introduction

How is it possible to solve a problem when the fundamental variables within the problem are not well understood? The field of strategy is diverse, and the use of the term is so varied as to be almost valueless. Notwithstanding this diffusion of the term, strategy still attracts significant attention both within business and government organisations. A simple online search revealed over 4.8 million articles

L. Young (✉)

Department of Defence, War Research Centre, Canberra, Australia
e-mail: L.Young@adfa.edu.au

containing the word strategy [1]. A total of 17,500 articles were created since 2015 with strategy in the title. Strategy is popular. But is it important? The Director of the Strategic Studies Institute, Douglas Lovelace, stated that “[no] subject is more essential in the preparation of national security professionals and military leaders than the teaching of strategy” [2]. While it is an understandable obsession within the security industry, Robynne Berg of Berg Consulting wrote that *strategy is fundamental to the success and sustainability of any organisation* [3]. The importance of strategy would be difficult to understate.

Equally, strategic thinking is often cited as being one of the most important abilities to foster within organisations. For instance, a recent report commissioned by the United Kingdom’s House of Commons into “Who does UK National Strategy?” stated that “*Strategic thinking is a valued skill in the Civil Service. It is one of the six core requirements in the Senior Civil Service competency framework*” [4]. This view is not new. Zabriskie and Huellmantel (1991) stated that “[s]trategic thinking is required to secure the long-term future of nations and organisations” [5]. However, despite the touted importance of both strategy and strategic thinking, the majority of CEOs cited the “*lack of strategic thinking as the main problem in their organisations*” [6]. This view has not changed since Zabriskie and Huellmantel’s study in the early 1990s. The UK Chief of Defence Staff, Sir Jock Stirrup, proclaimed that the UK had “*lost an institutionalised capacity for, and culture of, strategic thought*” [7].

Closer to home, several operational reports from the Middle Eastern campaigns demonstrated that the Australian Defence Force also lacked strategic thinking. For example:

- “...the Australian Defence Force (ADF) needs to identify and develop Commanders that think at the strategic (macro) level in order to design and implement effective campaign plans”, Operational report, 2012
- “...there is plenty of room to improve education of military planners and ... personnel to think in terms of effects”, Operational Report, 2011

It should be unsurprising then that there appears to be an inherent desire by organisations to foster strategic thinking. The broad intent of this research then was to investigate whether strategic thinking could be developed as a capability rather than an individual cognitive capability. In our case, we define capability as “the capacity to be or do or affect something” [8]. Thus, a strategic thinking capability is one where an organisation has the capacity to think strategically and develop appropriate strategies. Importantly, by developing strategic thinking as a capability, the organisation can remove the traditional dependence on specific individual strategic thinkers.

However, to develop strategic thinking as a capability, it would be useful if there was a common, foundational understanding of what strategy is, how strategic thinking is developed and how to quantify strategic thinking. Unfortunately, it became readily apparent that the field is mired in confusion and doubt. In fact, there appears to be widespread agreement that, due to its popularity, strategy has

“acquired a universality which has robbed it of meaning” [9]. Using the term strategy without contextualising, at least providing a definition, can then lead to confusion.

It should be no surprise then that strategic thinking is also poorly understood. According to Bonn (2001), there “*is no agreement in the literature on what strategic thinking is*” [10]. A decade later, Jelenc and Swiercz found that “*strategic thinking has turned into a synonym for almost all of the concepts with strategic as their first word*” [11]. It is these muddied waters that have created considerable debate and confusion in strategic thinking [12]. So we are now in a position where there is a recognised idea that is broadly considered to be extremely important yet there is no agreement on definition. While there are a small number of conceptual descriptions of strategic thinking, none actually measure strategic thinking using a quantitative metrics or cognitive logic [13]. Finally, a review conducted by the author in 2015 failed to reveal any literature on how to create strategic thinking as a capability.

While the initial motivation of this research was to investigate the optimal method for developing a strategic thinking capability, it became readily apparent that there existed too much confusion over terminology and methodology. Without a framework, this research would have been fruitless. Thus, it became apparent that this was a problem of understanding not one of optimising. This chapter demonstrates how a soft operational research methodology, specifically action research, can be successfully used to develop understanding of a problem.

2 Methodology

Peter Checkland once observed that studying purposeful human actions and interactions was not simply a matter of setting to work to discover “laws” governing the phenomena in question [14]. He went on to describe a rational thought process where theory led to practice and practice led to theory. However, Checkland proposed a modification to the natural science use of rational thought so as to incorporate the learning feedback loop common in most social research. This is illustrated in Fig. 1 [15].

You will note that this diagram contains three parts: the intellectual framework (F); the methodology (M) for using F; and the area of application (A). It is through the application of F, using M, onto A that we are able to learn about phenomena or problem of concern. In true “soft” tradition, we can regard the resultant system model as a model relevant for arguing *about* the world, not models *of* the world [16].

The rational thought model is actualised through a seven-step action research process [17]. These steps can be articulated as four broad questions that seek to address those ‘hostile’ questions commonly asked of action research.

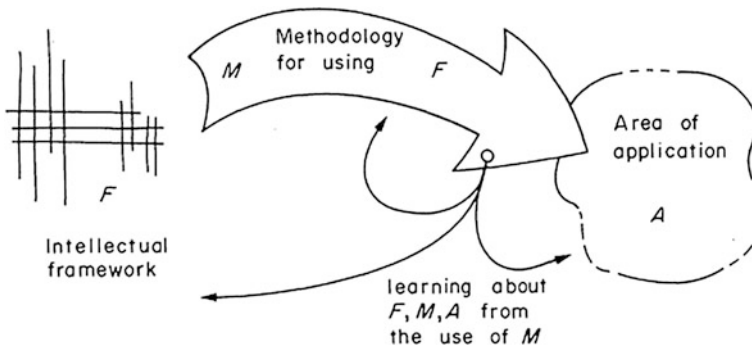


Fig. 1 Checkland's illustration of rational thought

- **What is being researched?** The broad theme being researched is the development of strategic thinking as a capability. This has required an examination of capability, strategy and strategic thinking.
- **Who is the researcher and who is the participant?** The explicit researcher is the author, however, we should recognise the potential melding of the researcher and the participant in the situation. In this case, it must be recognised that the researcher (the author) has been within the defence strategic environment for a number of years and could be considered a participant of the phenomenon being studied.
- **How do you know when to stop?** Action research deals with situations that may not be homogenous through time, and thus, it is difficult to know when to stop. As the nature of the research is modelling strategic thinking, the appropriate place to stop would be when we can explain the development of a strategic thinking capability through a model.
- **How can results be conveyed to others or transferred to other situations?** It is important to recognise that the research is often highly contextualised and may, or may not, be transferable to other situations. In this case, the research has concentrated on strategic thinking within the Australian Department of Defence. While it is hoped that the results are applicable across many organisations, the limitations, due to sample type, should be recognised from the outset.

This rational thought model is very useful in explaining this research as it allows the exploration and understanding of social problems. Strategic thinking is inherently a social problem as it involves humans and interactions between social groups. In our case, the framework is represented by the contemporary paradigms used for strategic thinking and capability development. These paradigms are elicited from a normal literature review. We then employ proven research methods (semi-structured interviews, surveys and experiment logic) as our methodology for interacting with the area of application. The area of application is broadly organisational strategic thinking capabilities; however, strategic thinkers are used as a proxy to limit the scope of this thesis.

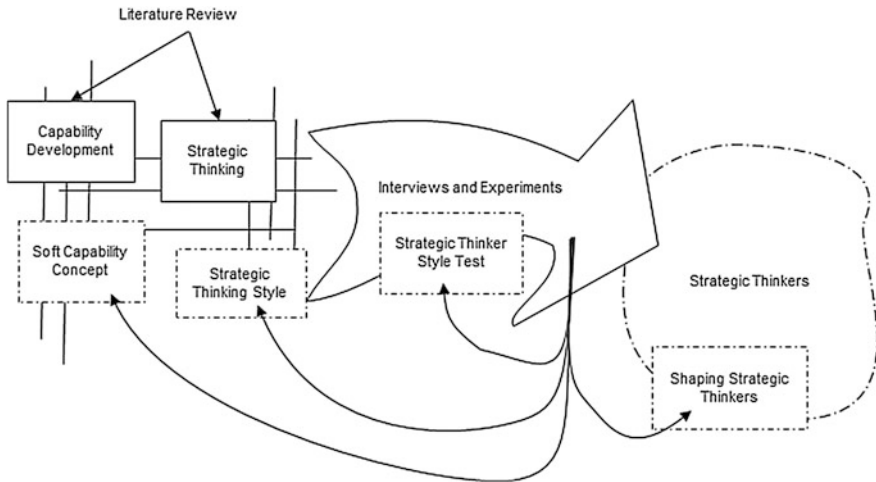


Fig. 2 Applying rational thought to strategic thinking modelling

The key advantage of using rational thought in action research is the recognition that intervention will create new knowledge or learning on F, M and A. Using this model, this research was able to build on the existing framework through the development of a soft capability concept and identification of strategic thinking styles. The methodology is built upon with the addition of an original strategic thinking style test. Finally, we explore a novel understanding of how a strategic thinking capability could be developed in the area of application (Fig. 2).

3 Research Results

As inferred earlier in this chapter, the existing theoretical framework was quite sparse. The traditional notions of capability and capability development did not appear to match or suit the development of strategic thinking. Similarly, the foundational concepts of strategic thinking were poorly understood and rarely agreed upon. Thus, the rational thought model is quite applicable in illustrating how our insights were gained. The following paragraph lists the understanding elicited to date through the research.

3.1 *Soft Capability Concept*

Due to the novelty of the subject and lack of published work, it was critical that the data were collected from individuals who could be considered subject matter

experts (SME) in the field of capability development and acquisition. The goal of the research then was to ensure that the data collected from the specialists within the field of capability and strategy were rich in detail. The methodology most suited for capturing data rich in detail was qualitative research, specifically through personal interviews. Personal interviews allowed a much greater depth of investigation (and thus quality of detail) compared with a survey or written correspondence. The style of interview combined aspects of a conceptual interview and discursive interviews [18]. In this style, the interviews are semi-structured and the interviewee is seen as a collaborative participant. Thus, the specific questions and examples discussed would vary between individuals as it is dependent upon the participant's experiences and knowledge. Common to all interviews were the set of guiding questions/themes that all conversations needed to cover.

The research uncovered a resident, intuitive understanding of soft capabilities with all of the SME [19]. Soft capability was, however, regarded by all participants as a true capability even though there are no published documents that specifically deal with the concept of soft capability. This understanding seemed to stem from people's exposure to other "soft-hard" dichotomies such as soft and hard power or soft and hard operations research. It became clear that humans are central to the concept of soft capability, and additionally, its intangibility was commented upon by almost all of the participants. Thus, we conclude with the understanding that while hard capability is characterised by major physical systems (such as plant equipment or vehicles), soft capability is characterised by the people.

3.2 Strategic Thinking Style Test

The first step in the action research framework is to understand the existing framework. As this is the foundation from which you can derive the methods and understanding of the area of application. Thus, while the term strategy was relatively simple to pin down and define, strategic thinking required a different approach due to the complete lack of consensus in the literature. In order to understand the epistemology of the term strategic thinking, a historical literature review was conducted. What was immediately clear is that the confusion over the meaning of strategy thinking has prevailed for decades. In all, 120 peer-reviewed articles and books were compiled and examined for definitions of strategic thinking. On completion of the table, the key concepts were then reviewed using a cluster analysis method. Essentially, all of the definitions were laid out and then grouped into like clusters. For example, there were a number of definitions that emphasised the importance of creating value for the organisation while other definitions emphasised that strategic thinking was a way of thinking about problems. Finally, the definitions were mapped across to a historical timeline along the previously identified domains. From this review, we could see that strategic thinking is a means-ends way of thinking that is future orientated and seeks to create value or an advantage for the system [20].

Once strategic thinking was defined, it became equally relevant to understand the characteristics of strategic thinkers. The importance is derived from an understanding that, as a soft capability, the strategic thinking capability was likely to reside in individual or collective cognitive characteristics. Due to the quantity and quality of literature regarding strategic thinkers, it was decided that the best way to understand what a strategic thinker is was through a comprehensive literature review. A total of 55 sources were found to provide detailed descriptions of the characteristics of a strategic thinker. These were reviewed and the characteristics mapped using a cluster analysis. What was revealed was that, despite different terms, there appears to be a broad consensus on four significant characteristics of a strategic thinker: visionary thinking, holistic intuition, creative thinking and systems thinking.

Fortunately, these four cognitive characteristics appeared to be measurable. This was an important step as a measurable capability is one that can purposively developed or improved. It became readily apparent that there has been little work in assigning metrics to strategic thinking abilities. While there were several relativistic models, these appeared to be quite subjective and context specific. Our model sorts to understand the generic measures of a strategic thinker in order to understand how they could be developed in the organisation.

Using the four cognitive characteristics (vision, intuition, creativity and systems thinking) as a guide, we looked to leverage and synthesis other cognitive trait specific assessments into a single assessment. Fortunately, several of the characteristics (creativity and intuition) are well studied with a range of applicable metrics that could be used. Visionary thinking, however, proved to be quite problematic as most tests were simple judgement-based binary assessments of a vision statement. This resulted in the development of an original assessment of visionary thinking based on the original literature review of visionary thinking as a strategic thinker characteristic. Similarly, the search for generic systems thinking assessment found little to go on. In the end, while a simple test was used, this area appears to be a significant gap in knowledge.

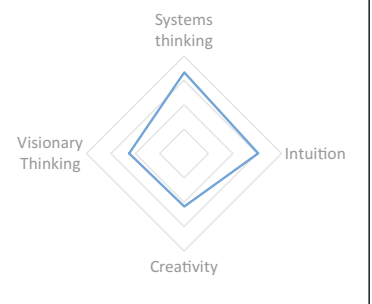
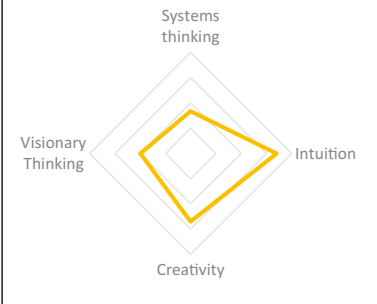
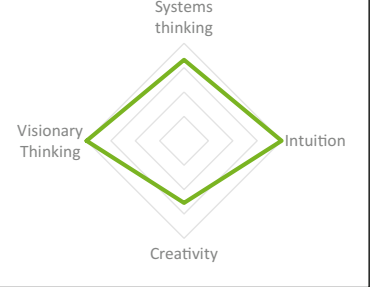
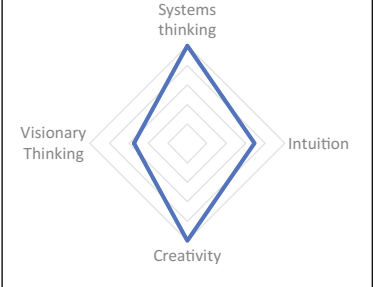
The test was designed to be given both online and in paper as this created flexibility. The online version was preferred due to ease of transcription. The test was piloted on about 15 military officers and non-military executives and took, on average, 26 min to complete. This included the range of discriminators designed to ascertain correlations in strategic thinking development (for instance, gender, age, experience and education). While the test utilised an original assessment for visionary thinking based on four attributes (articulated, plausible, desirable and actionable), the remainder of the test used existing assessments for:

- creativity (based on Shah et al. (2012) measuring fluency, flexibility, originality and quality) [21];
- intuition (TIntS by Pretz et al., 2014 measuring Inferential, Affective, Holistic Big-Picture and Holistic Abstract) [22]; and
- Systems thinking (simple assessment based on Cardenas et al. 2010) [23].

3.3 Strategic Thinking Style

The application of the strategic thinking style test in the pilot study found that there were at least four broad groups. Though noting the variables (four), one could theorise that there are up to 16 different combinations. Rather than classifying different styles as better strategic thinkers, though again, theoretically at least, this is possible, we felt it more appropriate to label the groups as styles. This recognises that most people could think strategically; however, some were more appropriate to certain situations. The visual advantage this test has is that the results can be

Table 1 Example of strategic thinking styles

<i>Type C</i>	<i>Type D</i>
	
<ul style="list-style-type: none"> ● Suited for: <ul style="list-style-type: none"> – Problem solving – Unusual problems ● Not suited for: <ul style="list-style-type: none"> – Absent of direction – Problem finding 	<ul style="list-style-type: none"> ● Suited for: <ul style="list-style-type: none"> – Problem finding – Normal problems ● Not suited for: <ul style="list-style-type: none"> – Abstract problems – Problem solving
<i>Type E</i>	<i>Type F</i>
	
<ul style="list-style-type: none"> ● Suited for: <ul style="list-style-type: none"> – Immediate operations – “strategic” problems ● Not suited for: <ul style="list-style-type: none"> – Abstract problems – Absent of direction 	<ul style="list-style-type: none"> ● Suited for: <ul style="list-style-type: none"> – Immediate operations – “tactical” problems ● Not suited for: <ul style="list-style-type: none"> – Absent of direction – High-level/strategic problems

mapped into a spider graph. This allows for an immediate recognition of the different style. Four examples are provided in Table 1. Interestingly, it also allows us to theorise the most appropriate work context for that individual—an application that could prove useful in the human resource and management sector. The table illustrates the thinking style, using a spider graph, and seeks to provide a context to the strategic thinking style evidenced by the test.

3.4 Shaping Strategic Thinkers

Through an understanding of soft capability and the inherent key characteristics of strategic thinking, we can hypothesise a developmental model for strategic thinking. In this case, we use the Thinking Capability Analysis Technique (TCAT) [24]. TCAT extends the Function Analysis System Technique (FAST) in System Engineering. FAST has demonstrated a great deal of success as a decision-aiding tool to map out functional interdependency for requirement engineering. T-CAT replaces the “how” question in FAST with “enablers”, it extends the notations to include “responsibility” or the “whom” question to simultaneously establish a line of accountability, and increases the flexibility of the representation to cover multiple scopes. While still in draft form, a proposed TCAT for strategic thinking capability is represented in Fig. 3.

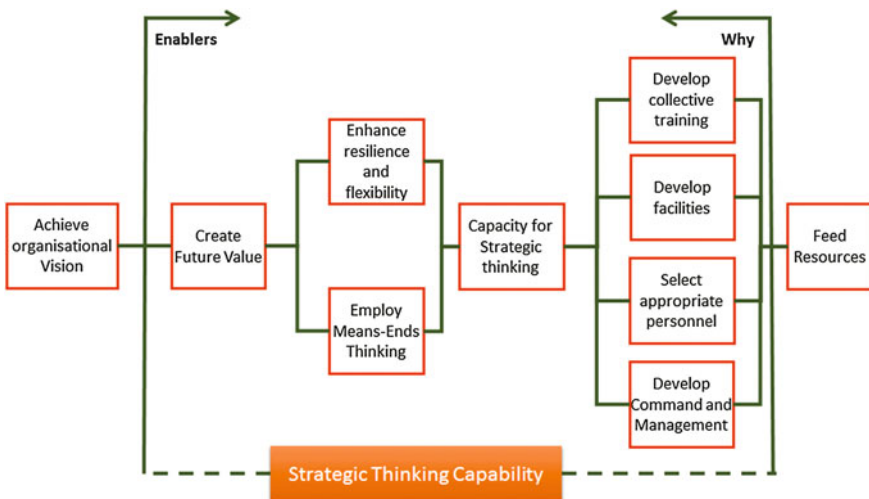


Fig. 3 TCAT for the development of a strategic thinking capability

4 Conclusion

The field of strategy is diverse, and the use of the term is so varied as to be almost valueless. Equally, strategic thinking is often cited as being one of the most important abilities to foster within organisations. Yet, despite this assumed importance, there is very little research on the quantitative development of strategic thinking as an organisational capability. Early in the research, it became apparent quantifying strategic thinking was impeded by not only a lack of common set of characteristics, but also because these cognitive characteristics were inherently difficult to measure. For example, the relativistic measures of visions were inappropriate for deliberate capability development.

It thus became apparent that there was little common agreement on foundational concepts. The biggest indicator was the diverse use of strategy and its subservient action, strategic thinking. Immediately it became important to utilise a methodology that was centred on problem understanding. Due to familiarity with operations research, the author explored a number of soft system methods before settling on action research as an appropriate methodology. On the whole, this has proven to be a good choice due to the inherent flexibility in the method. Importantly, the use of the rational thought logic has allowed a number of insights and key contributions to the fields of Systems Thinking, Management Science and Operations Research.

- **Systems Thinking.** This thesis contributes to the field of systems thinking through using social research methods to develop an original concept of capability. Capability is generally considered to be platform centric. This soft capability concept develops a framework for describing people-centric capability.
- **Management Science.** This thesis provides two key contributions in Management Science. The first is the identification of strategic thinking styles and the second is the development of a theoretical model of strategic thinking development as a capability within organisations.
- **Operations Research.** This research presents an original quantitative assessment for measuring strategic thinking styles.

This chapter sought to demonstrate a contemporary use of action research in the exploring an uncertain problem space. We have demonstrated that an action research methodology, specifically Checkland's flexible rational thought model, is extremely useful in developing key insights into clouded areas of interest where the phenomenon is dominated by human interaction.

References

1. Search conducted on 08 Jul 2016 using <https://scholar.google.com.au> with the search term "strategy"
2. Marcella, G.: *Teaching Strategy: Challenge and Response*, Strategic Studies Institute, U.S. War College, Carlisle, PA, page v (2010)
3. Berg, R.: 12 Sept 2011, Three Reasons Strategy is Important, Berg Consulting. http://bergconsulting.com.au/Berg_Consulting_Blog/three_reasons_why_strategy_is_important (2016). Accessed 8 Jul 2016
4. House of Commons, Who does UK National Strategy? The Stationary Office, London, p. 20 (2010). <http://www.parliament.uk/pasc>
5. Zabriskie, N.B., Huellmantel, A.B.: Developing strategic thinking in senior management. *Long Range Plan.* **24**(6) (1991)
6. Bonn, I.: Improving strategic thinking: a multilevel approach. *Leadersh. Organ. Dev. J.* **26**(5), 337 (2005). Emerald Group Publishing Limited
7. House of Commons, Who does UK National Strategy? The Stationary Office, London, p. 6 (2010). <http://www.parliament.uk/pasc>
8. Gaidow, S., Boey, S., Egudo, R.: A review of the capability options development and analysis system and the role of risk management. Technical report, DTIC Document (2006). <http://www.dtic.mil/cgi-bin/GetTRDoc?AD=ADA460076>
9. Strachan, H.: The lost meaning of strategy. *Survival.* **47**(3), 33–54 (2005)
10. Bonn, I.: Developing strategic thinking as a core competency. *Manag. Decis.* **39**(1), 63 (2001)
11. Jelenc, L., Swiercz, P.M.: Strategic thinking capability: conceptualization and measurement. In: The 56th Annual ICSB World Conference, Stockholm, Sweden, 15–18 June 2011. https://www.researchgate.net/profile/Lara_Jelenc/publication/265002736_Strategic_Thinking_Capability_Conceptualization_and_Measurement/links/544668ea0cf2f14fb80f38d8.pdf
12. Behm, A.: *Strategic Tides: Positioning Australia's Security Policy to 2050*. The Kokoda Foundation, Kokoda Paper No 6, p. iv (2007)
13. Dagher, M.M., Al Zaydie, K.I.H.: The measurement of strategic thinking type for top managers in Iraqi public organizations-cognitive approach. *Int. J. Commer. Manag.* **15**(1), 45 (2005)
14. Checkland, P.: From optimizing to learning: a development of systems thinking for the 1990s. *J. Oper. Res. Soc.* **757** (1985)
15. Checkland, P.: From optimizing to learning: a development of systems thinking for the 1990s. *J. Oper. Res. Soc.* **758** (1985)
16. Checkland, P.: From optimizing to learning: a development of systems thinking for the 1990s. *J. Oper. Res. Soc.* **765** (1985)
17. Checkland, P., Holwell, S.: Action research: its nature and validity. *Syst. Pract. Action Res.* **11**(1), 16 (1998)
18. Kvale, S., Brinkmann, S.: *Interviews: Learning the Craft of Qualitative Research Interviewing*. Sage (2009)
19. Young, L.D.: Defining and developing soft capabilities in defence. In: Weber, T., MCPhee, M.J., Anderssen, R.S. (eds.) *MODSIM2015, 21st International Congress on Modelling and Simulation*. Modelling and Simulation Society of Australia and New Zealand, Dec 2015, pp. 876–882 (2015). ISBN: 978-0-9872143-5-5. <http://www.mssanz.org.au/modsim2015/D3/young.pdf>
20. Young, L.D.: Towards a more comprehensive understanding of strategic thinking. *Aust. Def. Force J.* **199**, 55–64 (2016). ISSN 1320-2545. http://www.adfjournal.adc.edu.au/UserFiles/issues/199%202016%20Mar_Apr.pdf
21. Shah, J.J., Millsap, R.E., Woodward, J., Smith, S.M.: Applied tests of design skills-part 1: divergent thinking. *J. Mech. Des.* **134**(2), 1–10 (2012)

22. Pretz, J.E., Brookings, J.B., Carlson, L.A., Humbert, T.K., Roy, M., Jones, M., Memmert, D.: Development and validation of a new measure of intuition: the types of intuition scale. *J. Behav. Decis. Mak.* **27**(5), 454–467 (2014)
23. Cardenas, C., Sosa, R., Moysen, R., Martinez, V.: Sustaining sustainable design through systemic thinking. *Int. J. Eng. Educ.* **26**(2), p287 (2010)
24. Abbass, A.A., Young, L.D.: From systems thinking to capability thinking using the thinking capability analysis technique In: Weber, T., MCPhee, M.J. Anderssen, R.S. (eds.) MODSIM2015, 21st International Congress on Modelling and Simulation. Modelling and Simulation Society of Australia and New Zealand, Dec 2015, pp. 876–882 (2015). ISBN: 978-0-9872143-5-5. <http://www.mssanz.org.au/modsim2015/D3/abbass.pdf>

Regression Models for Project Expenditures

Terence Weir

Abstract This report discusses regression models to analyse planned and actual expenditure data from projects in an Australian Defence capital investment program. Variations in expenditure from that planned have the potential to create cash flow problems in Defence. Therefore, an understanding of the relationship between planned and actual expenditure will improve project planning and portfolio financial management. It is also useful to understand if families of projects behave differently to each other because differences may indicate varying management practices across project domains or differences in the nature of project families. The regression model accommodates project time and military domain effects, heteroscedasticity, repeated measures and nonlinear relations between planned and actual annual project expenditure. The nonlinear model is linearized into an additive lognormal model and fitted via a linear mixed models methodology that facilitates modelling the within project covariance structure. Generally, projects underspend against the plan early in their life and overspend in later years. For each year, there are significant differences in expenditure rates between domains, but the expenditure rate does not depend on planned expenditure. The model may be used by project and portfolio planners to test likely spending variations from plan and to then adjust expenditure plans accordingly; it, therefore, provides a tool to measure project and financial risk.

Keywords Mixed models • Longitudinal data • Project expenditures

T. Weir (✉)
Department of Defence, Defence Science and Technology Group,
Canberra Act, Australia
e-mail: terence.weir@dsto.defence.gov.au

1 Introduction

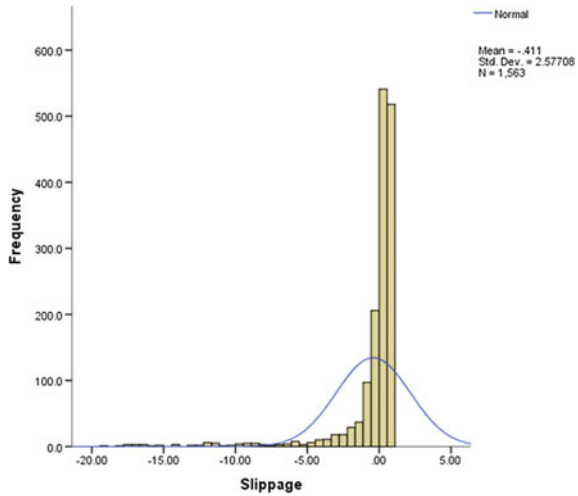
A significant proportion of Department of Defence (Defence) expenditure is for the approved major capital investment program (AMCIP). In most years, Defence budgets approximately \$4500 m for expenditure on major projects (Department of Defence [4]). Often project expenditure does not match its annual plan, resulting in expenditure variations. This can create cash flow problems for Defence (i.e. under- or overspending the allocated budget) and implies that resources are not being allocated efficiently and provides a source of frustration for Government. The reasons for the variations primarily stem from underestimation of both the scope and complexity of work in meeting the demands of the project schedule. Other factors may include reprogramming of a project due to external influences, such as changes to the Defence budget. Work not completed is generally postponed to later years but can then cause fluctuations in expenditure plans by Defence from year to year. Defence has typically tried to manage expenditure variations, in particular underspends, by planning for expenditure *slippage* using simple adjustments to expenditure plans; this is called a '*slippage model*'. Where applied, this treats projects similarly and does not reflect differences between project domains. Given that it plans for slippage, Defence has typically *overprogrammed* its capability acquisition plan to further mitigate the risk of underspending in a budget year (i.e. scheduling additional projects in case of slippage). Even so, Defence planners have expressed dissatisfaction that annual project expenditure differs from that planned and have undertaken a number of studies into expenditure slippage. This paper follows on from one of those studies by Weir and Malcolm [27].

Projects in the AMCIP are approved individually by the Australian Government. Each project approval also includes a proposed expenditure plan. Put simply these expenditure plans may be described as “year-wise expenditure spreads” for the (initially) assumed lifetime of the project. Following approval, the Defence Capability Acquisition and Sustainment Group (CASG)¹ manages the “actual expenditure” of the project as work is completed against planned budgets.

In every financial year, it is highly likely that several adjustments will be made to the (current) project expenditure plan. Therefore, the actual project expenditure pattern may be considerably different from the initial planned expenditure. Expenditure variations may be examined from a portfolio to individual project level, across various categorisations (such as project domain, project acquisition mode and project managing division), and against the initial plan or any subsequent plan. Because Defence manages a portfolio of projects, sometimes expenditure on some projects can be accelerated to make up for slippage in other projects. Nonetheless, it is Defence’s aim to minimize cash flow variations at the project and portfolio level, and subsequent under- or over- spending of the Defence budget in any year. Therefore, a better understanding of how actual variations in expenditure

¹Formerly Defence Materiel Organisation (DMO).

Fig. 1 Probability density of expenditure slippage (percentage change from baseline) rate observed in AMCIP expenditure data 1996/97-2012/13. Overlaid on this histogram is a Gaussian curve computed from the sample mean and sample variance



from plan occur would assist project planners and financial authorities in minimizing cash flow changes.

Defence has typically monitored expenditure against plan in the AMCIP using percentage change from baseline. Reporting a percentage change from baseline shows the results of a project’s expenditure behaviour in a form immediately accessible and comfortable for management. However, when compared to other statistical approaches, such as analysis of variance on the actual values, percentage change from baseline has the lowest statistical significance and is highly sensitive to changes in variance (see [25, 26]). Figure 1 demonstrates the non-normality in the distribution of slippage defined as percentage change from baseline observed in AMCIP data. Vickers suggests that analysis of variance is the most reliable approach to investigate the effects on costs, and it is this method that is employed later in this report. Lo et al. [16] demonstrate that more statistically robust but more complex techniques, as will be described in this paper, can be adequately represented in decision support tools for portfolio project management.

This paper models project expenditures for AMCIP projects in the period 1996/97 to 2012/13. Planned and actual expenditure in each AMCIP project in each year of its duration has been recorded by Defence for financial planning and reporting and provides the data set for analysis. The project financial data is accompanied by organizational data that identifies the domain of the investment, such as land, sea or air. Because variations from expenditure plans have the potential to create cash flow problems in Defence, developing a model that explains the relationship between planned and actual expenditure will improve project planning and portfolio financial management. The model may also provide better indicators to Defence of when a project needs management intervention to control expenditure variations from plan. From a Defence portfolio management

perspective, it is also desirable to understand if families of projects behave differently from each other because the differences may be due to varying management practices across project domains or to the nature of domains.

1.1 Data Form and Scope

The data set analysed here consists of 533 projects with 1404 matching observations of planned expenditure and actual expenditure. Expenditures have been adjusted for inflation, and project plans have been adjusted for scope changes that modified the original expenditure plan. Each project belongs to one of five domains—Air (AIR), Joint (JNT), Land (LND), Other (OTH) and Sea (SEA). Observations have been taken only from years one to 10 of a project’s duration.²

Our analysis can be considered as observational study of planned and actual expenditures by group with repeated measures. Scatter plots for planned versus actual expenditures shown in Fig. 2 exhibit considerable variability, but suggest an expected broad association between them. Most data exhibits slippage, but about one-third of the data is the case where actual expenditure is greater than that planned in a particular year. This is usually the result of work being brought forward from later years of a project’s plan. Examination of the data and known portfolio management practices show this can be in response to slippage in other projects.

2 An Overview of Previous Studies and Literature

Open Source Papers. Existing open source technical literature statistically examining project costs or expenditures is usually concerned with one of two domains of application: (1) large infrastructure projects (rail networks, etc.) and (2) large-scale building projects such as the construction of hotels or hospitals, etc. In contrast, very little open source literature exists on similar expenditure modelling or analysis for major Defence projects. Of these articles, very few discuss the issue of variations in planned and actual expenditures over the life of a project; none discuss in-year variations and their potential impact on cash flow.

In the articles by Love et al. [17–19], the approach of empirically fitting probability distributions to cost and schedule overrun data is explored. This approach has also been applied by Gill and de Visser [8] for temporal slippage in Defence projects.

²Some projects extend beyond 10 years in their execution, but the original plan is constrained to 10 years in AMCIP.

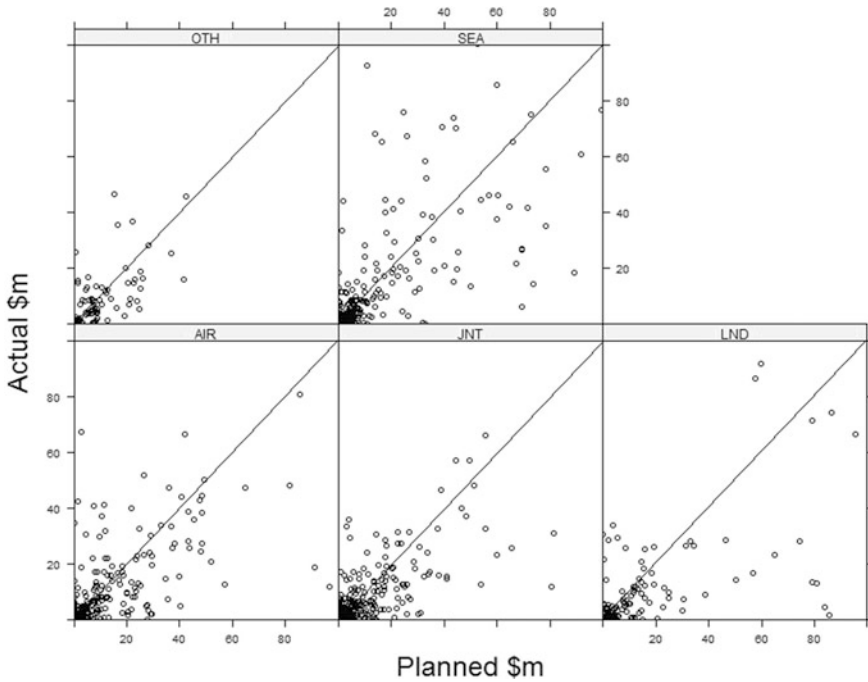


Fig. 2 Scatter plots for the planned versus actual project expenditures by domain. The line $y = x$ is shown

Anastasopoulos et al. [2] develop a model to compute the likelihood of project time-delay applied to highway construction projects. This model considers factors such as contract award price, planned project duration and project class or types.

Burgess et al. [3] develop a model for year on year cumulative expenditures of NASA projects by pooling expenditure data and fitting a Weibull distribution. The paper notes that there is an unanswered question as to “how strong is the correlation between cost and phasing” i.e. between actual in-year expenditure and planned expenditure.

Defence External Reports. Two external examinations of Defence project slippage have been conducted in recent years. The first examined expenditure variations defined as a difference between planned expenditure at the last budgeting adjustment in a given financial year (usually additional estimates), and the actual incurred expenditure for the corresponding year that cannot be explained by factors such as scope or price changes (this, therefore, includes expenditure slippage).

Here, the mechanics of the budget processes meant that the only time periods suitable to be considered in this analysis were the approximately six-month periods between planned spend and an actual spend. The report noted a lack a structure in the data relationships, suggesting that this precluded strong conclusive results. It found slippage is only weakly linked to type of project but its scale or volatility had

not changed over time. It highlighted that attempts to revise budgets in the budget cycle are not always successful, especially in the later parts of a project when a project will have considerable internal momentum.

A second consultant examined project slippage as a part of a wider review for Capability Development Group (CDG). Their approach was to examine cumulative spend spreads, comparing approved cumulative spread with actual cumulative expenditure. This approach may have an effect of smoothing slippage at each time interval, as deviations from planned spends may cancel out. It should be noted that this report only considered about 25% of AMCIP projects, which were generally of lower cost and shorter duration than typical AMCIP projects. The report found slippage is higher in the first half of a project's planned life.

Both consultants reported the determinism in Defence models of project expenditures is a weakness and suggests that it could be replaced by more statistical approaches that address differences in projects.

Defence Internal Reports. Weir and Malcolm [27] examined expenditure variations in the AMCIP from a number of perspectives.

An analysis of expenditure slippage at the aggregated project level (in terms of annual slippage rate (i.e. change from baseline)) shows there has been a consistent improvement in the reprogramming of AMCIP projects over the period that data is available, indicating that project expenditure performance has been strictly improving against the initial expenditure estimates. Variation in slippage appears to increase with duration of project, but the report found no statistical differences in the means of slippage across projects by year or by a measure of project complexity called ACAT Rating.³ Slippage is only weakly linked to project domain and acquisition mode. The data available for this study did not identify the exact underlying cause(s) of the slippage, only that it occurred in projects with certain characteristics.

Weir and Malcolm also developed a general linear model (GLM) (see e.g. [12]) of expenditures. This model assumed independence between and within project observations, which as we will see later in this report, is an unjustified simplification. Nonetheless, the model gives comparable results to those found here; actual expenditure is different across Year of Project with the same planned expenditure, and project domain is also a significant factor. Project acquisition mode was not found to be a significant factor.

By analysing project lifetimes using a proportional hazards model, Weir and Malcolm show all projects have an almost fixed propensity to slip in time and there is little difference between the behaviour of different projects.

In addition, some nonlinear parametric modelling and visualization of project spend spreads were developed by W.P. Malcolm and reported in Weir and Malcolm. This model could well be used to develop a metric on the collection of spend trajectories for a given project, that is, quantifying the difference between the planned spend trajectory and the actual spend trajectory.

³ACAT Rating data is very subjective and so has been ignored in this study.

The major recommendation of the report was for Defence to reduce its estimates of expenditure slippage when projects are presented for endorsement. Lo et al. [16] applied the modelling results of Weir and Malcolm in a program decision support and visualisation tool and favourably compared the GLM with a deterministic slippage model used in Defence. Peever et al. [20] recommended Defence cease expenditure slippage and overprogramming as management tools used on project and portfolio expenditure plans. History suggests this will require improved project planning to avoid expenditure variations. Modelling project expenditures could quantify the risk in project plans.

In summary, there has been little published work on the relationship between planned and actual expenditures over the life of a project; none discuss in-year variations and their impact on cash flows. As Burgess [3] has noted, research lacks an investigation into the relationship between planned and actual expenditure. Consultants have reported the determinism in Defence models of project expenditures is a weakness and suggests that it could be replaced by more statistical approaches that address differences in projects. The model developed in the next section addresses these issues.

3 Proposed Model of Project Expenditures

Scatter plots of log scale values at Fig. 3 show a more defined linear relationship between planned and actual expenditures. This suggests that a model involving logged data may be suitable for explaining the relationship.

With this in mind, Pretest/Posttest models (e.g. [1, 22, 23]) provide a template for modelling the expenditure data. The following characteristics are pertinent for the analysis of this type of problem.

- (1) Zero planned expenditure (x) implies a zero actual expenditure (y) (zero planned expenditure would only happen in the case of a project being extended and, therefore, would incur an actual expenditure without a planned expenditure; these cases are not considered here).
- (2) Planned and actual expenditures are nonnegative.
- (3) The data is possibly heteroscedastic.
- (4) The relation between planned and actual expenditure is possibly nonlinear.
- (5) The observations carried out on the same project are possibly correlated.

The model proposed is of the form:

$$y = \beta x^\gamma \varepsilon \tag{1}$$

where β is a coefficient of expenditure (and in our case will characterize a domain of projects), γ may be interpreted as a coefficient of uniformity of the expected expenditure and ε is a nonnegative random error.

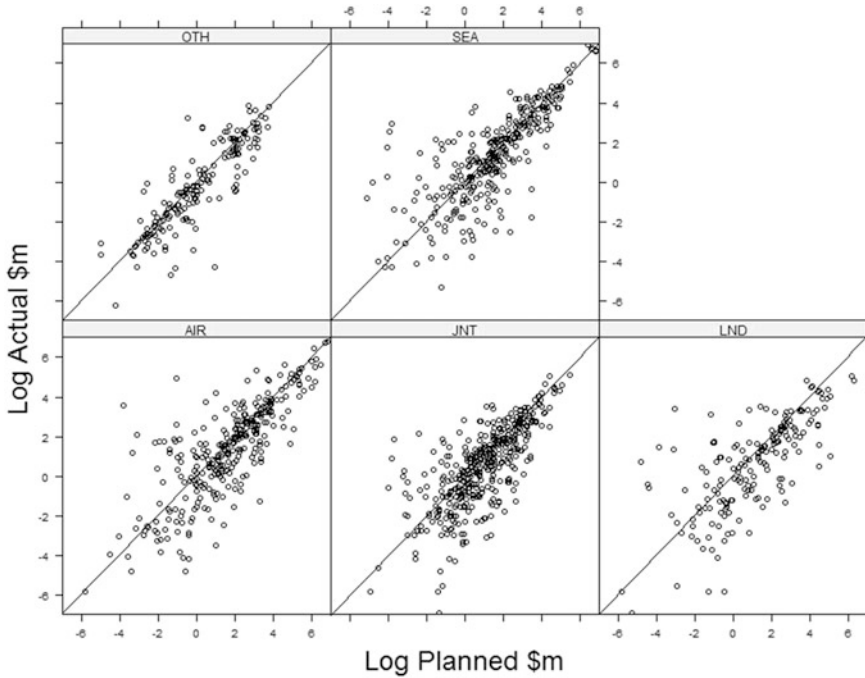


Fig. 3 Scatter plots for the log of planned versus log of actual project expenditures by domain. $\text{Log } y = \text{Log } x$ is shown

Under this model, $E(y)/x = \beta x^{\gamma - 1} E(\varepsilon)$ is the expected expenditure rate function (a measure of the actual expenditure per unit of planned expenditure). when $\gamma = 1$, the expected expenditure rate is consistent with planned expenditure; when $\gamma < 1$ ($\gamma > 1$), the expenditure rate is increasing (decreasing) with the planned expenditure; that is, the higher the planned expenditure, the higher (lower) is the actual expenditure. In addition, the expenditure efficiency of projects (i.e. how well a project meets its expenditure goals) is also proportional to β .

Note that, under this model, characteristics (1) and (2) are automatically satisfied. Furthermore, we have $\text{Var}(y) = (\beta x^{\gamma})^2 \text{Var}(\varepsilon)$, which allows for the possible heteroscedasticity mentioned in (3). If $\gamma \neq 1$, the nonlinear relation mentioned in (4) may also be accommodated. Finally, condition (5) can be addressed by imposing an adequate covariance structure on the errors ε .

The model at Eq. 1 may be fitted by linear mixed models (LMM). To do this, we transform (3.1) as

$$\log(y) = \log(\beta) + \gamma \log(x) + \log(\varepsilon) \tag{2}$$

Assuming that $\delta = \log(\varepsilon)$ follows a normal distribution with mean 0 and variance τ^2 is equivalent to assuming a lognormal distribution for ε . Using linear mixed

models for Eq. 2 leads to a lognormal linear mixed model (LNLMM) where $\log(y)$ is the response variable.

An inconvenience of the lognormal model is that the logarithmic transformation excludes zero values for x and/or y . The cases where x is zero can be disregarded, because it implies that a project has been extended. The cases where $x \neq 0$ and $y = 0$ are more problematic, because the elimination of such observations from the analysis will incur a loss of information. However, there is little option but to ignore these cases because they imply that either a project was deferred for a year or cancelled. In either case, management decisions, external to the project, were made; none of the cases imply that the planned actual expenditure is zero.

4 Linear Mixed Models

Mixed models differ from more familiar linear models (e.g. linear regression, ANOVA) through their ability to cope with correlated data and unequal variances. Mixed models are very useful to analyse data with a hierarchical structure, where measures from distinct units or subjects are independent and those from within subjects are correlated. Essentially, mixed models segment data into two parts: fixed effects and random effects. The expected values of the observations are described by the fixed effects, and the variance and covariances of the observations are described by the random effects. In particular, mixed models are appropriate to analyse repeated measures in longitudinal studies where each subject of the study is measured multiple times. In such studies, there are essentially two fixed effect factors, treatments and time. Random effects result from variation between subjects and from variation within subjects. Measures on the same subject at different times are almost always correlated, with measures taken close together in time being more highly correlated than measures taken far apart in time. Observations on different subjects are often assumed to be independent.

The objectives of repeated measures studies usually are to make inferences about the expected values of the observations; that is, about the means of the populations from which subjects are sampled.

This is done in terms of the treatment and time effects of the model. The classical linear mixed model considered by Laird and Ware [14] is expressed as

$$y_i = X_i\beta + Z_ib_i + e_i, i = 1, \dots, N \quad (3)$$

where y_i is the $(n_i \times 1)$ vector of responses for the i -th unit, X_i is the $(n_i \times p)$ fixed effects specification matrix, β is the corresponding $(p \times 1)$ vector of parameters, b_i is a $(q \times 1)$ vector of random effects with $E(b_i) = 0$ and $Var(b_i) = G$, Z_i is a $(n_i \times q)$ specification matrix for the random effects, and e_i is a $(n_i \times 1)$ vector of random errors independent of b_i , with $E(e_i) = 0$, $Var(e_i) = R_i$, where $G(q \times q)$ and

$R_i(n_i \times n_i)$ are symmetric positive definite matrices. The marginal expected response is $E(y_i) = X_i\beta$ and the conditional (on the individual effect b_i) expected response is $E(y_i) = X_i\beta + Z_i b_i$. The model [3] allows for correlation between the errors within subjects. According to Fitzmaurice et al. [6], the inclusion of random effects may account for heterogeneity of regression coefficients across sample units, possibly due to several unmeasured factors that affect the response variable.

It follows that (for details see e.g. Galecki and Burzykowski [7]) $\Sigma = \text{Var}(y_i) = Z_i G Z_i^T + R_i$, where the first and second summands correspond, respectively, to the inter- and intra-individual covariance structures. When $R_i = \sigma^2 I$, the model is termed a homoscedastic conditionally independent model, and correlation among observations on the same unit i arises from their sharing the unobservable (latent) variable b_i [5].

In the original formulation, Laird and Ware [14] assumed that b_i and e_i in Eq. 3 follow normal distributions. Unbiased and consistent estimators of the variance components may be obtained by maximizing the restricted likelihood function, and estimators of the fixed effects may be obtained via maximum likelihood (ML) Galecki and Burzykowski [7]. In practice, however, it is often not plausible to assume that the response is normally distributed. To bypass this problem, a possible strategy, as described in the previous section, is to consider a LNLMM, where the response is assumed to follow a multiplicative model with lognormal errors; the corresponding linearized model is additive and may be expressed as Eq. 3.

There are numerous references and guides on the application of linear mixed models. Surveys on linear and GLMM are presented in Jiang [13]. Longitudinal data analysis using mixed and marginal models is well described in Verbeke and Molenberghs [24]. ‘How to’ guide for mixed linear models using contemporary software include Galecki and Burzykowski [7], West et al. [28] and Heck et al. [11].

We fit LNLMMs to the AMCIP data. We show how some important characteristics of the data may be incorporated in the models, discuss the robustness of parameter estimators in the presence of outliers and comment on their computational implementation. In the next section, we conduct a preliminary exploratory analysis with the objective of identifying models for analysis. We then present the results of fitting the LNLMMs, detail their specification together with the estimation method and discuss diagnostic tools. Finally, we present some concluding remarks.

We note that there are other possible approaches to modelling the AMCIP data including panel data analysis (e.g. Wooldridge [29]) of the planned and actual expenditures over time and time series approaches such as regression analysis with lags. For a broader choice of response distributions rather than considering LNLMMs, models in which the parameters are estimated via generalized estimating equations (GEE) could be employed (see e.g. Liang and Zeger [15] and Rao et al. [21]). Another is to examine cumulative planned and actual expenditures as done by Burgess [3]. These approaches will be the subject of future work.

5 A Model for AMCIP Data

The model Eq. 1 may be extended to apply to the AMCIP data and can be specified by

$$y_{ijk} = \alpha_k \beta_j x_{ijk}^{\gamma_j} \varepsilon_{ijk} \quad (4)$$

where y_{ijk} is the actual expenditure for project i in domain j in year k and x_{ijk} is the corresponding planned expenditure $i = 1, \dots, 533, j = 1, \dots, 5, k = 1, \dots, 10$; α_k, β_j and γ_j are parameters to be estimated and ε_{ijk} are nonnegative random errors.

Model Eq. 4 may be linearized by taking logarithms,

$$\log(y_{ijk}) = \rho_k + \lambda_j + \gamma_j \omega_{ijk} + e_{ijk} \quad (5)$$

where $\rho_k = \log(\alpha_k), \lambda_j = \log(\beta_j), \omega_{ijk} = \log(x_{ijk})$ and $e_{ijk} = \log(\varepsilon_{ijk})$.

To identify whether random intercepts and/or slopes should be included, we started by fitting model Eq. 2 assuming uncorrelated errors, as described in Weir and Malcolm [27]. In Fig. 4a, we plot the residuals versus the rank of the mean residual (mean of the residuals for each project); some projects have all residuals larger than others, suggesting that there are subject-specific components affecting the response. This variability may be modelled by random intercepts. The variance function plot at Fig. 4b and individual profiles of $\log(y)$ versus $\log(x)$ plotted at Fig. 4c do not suggest that individual slopes are different so that random slopes are not required. Standardized residuals are plotted versus fitted values in Fig. 4d. Thirty-six outliers are observed (about 2.5% of all observations); these are distributed across 34 projects and occur in every Year of Project and in every project domain.

Evidence of reducing correlation for $\log(y)$ over time is displayed at the matrix plot of correlations at Fig. 5a where correlations between pairs of measurements decrease with the number of years between measurements. It can be observed that the measurements adjacent in time exhibit similar correlations. An examination of the residuals and their lagged values also shows a decreasing strength in linear relationship over time, suggesting that the residuals may exhibit a compound symmetry or autoregressive covariance structure.

The residuals at Fig. 5b do not exhibit significant differences in variance at each time point, so the residual covariance structure may be modelled accordingly by constant variance at each time point. This supports the assertion of a compound symmetry or autoregressive covariance structure but also suggests that an appropriate model may be one simply incorporating random intercepts and an independent error structure or even just an approach utilizing an independent error structure. Therefore, considerable experimentation is required to identify a suitable covariance structure.

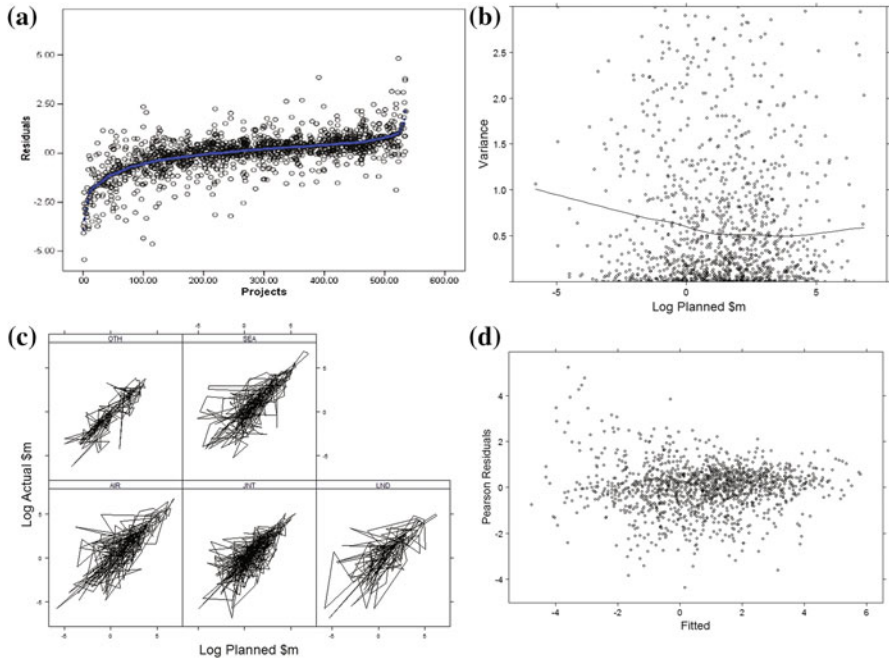


Fig. 4 **a** Residuals versus ranks of subject mean OLS residuals. **b** Variance function of OLS residuals. **c** Individual profiles of $\log(y)$ versus $\log(x)$. **d** OLS residuals versus fitted values

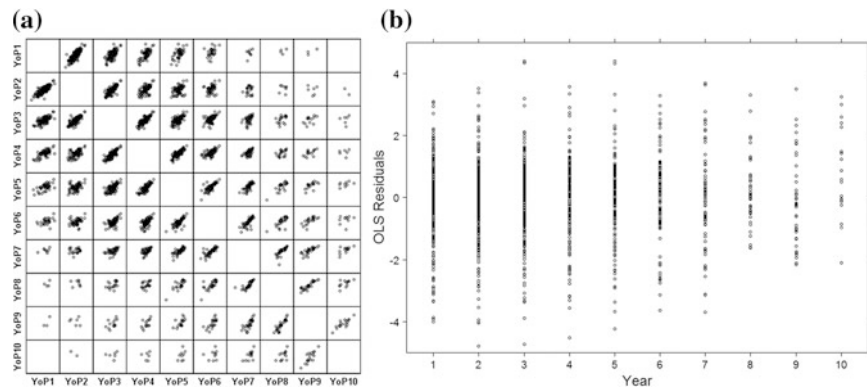


Fig. 5 **a** Correlations of $\log(y)$ across Year of Project (YoP). **b** OLS residuals over time (Year)

In order to find the most parsimonious model, we compare different models obtained by the following sequential attempts to simplify Eq. 4:

- (1) checking whether year effects α_k could be eliminated, that is, whether model Eq. 4 could be reduced to

$$y_{ijk} = \beta_j x_{ijk}^{\gamma_j} \varepsilon_{ijk} \quad (6)$$

- (2) testing whether there is a significant difference between domains, that is, whether model Eq. 4 could be reduced to

$$y_{ijk} = \alpha_k x_{ijk}^{\gamma_j} \varepsilon_{ijk} \quad (7)$$

- (3) checking whether a common growth coefficient of the expected costs ($\gamma_j = \gamma$) is acceptable; that is, whether model Eq. 4 could be reduced to

$$y_{ijk} = \alpha_k \beta_j x_{ijk}^{\gamma} \varepsilon_{ijk} \quad (8)$$

or

$$y_{ijk} = \alpha_k x_{ijk}^{\gamma} \varepsilon_{ijk} \quad (9)$$

5.1 Model Fitting

Here, we consider a LNLMM model of the form Eq. 5 that includes random effects to account for possible positive within-subjects correlations and also considers an error covariance matrix that incorporates the correlations observed in the previous section. Such models may be fitted via well-established linear mixed model methodology, where the location and the covariance structure may be modelled separately. The LNLMM, with random intercepts, may be expressed as

$$\log(y_{ijk}) = \rho_k + \lambda_j + \gamma_j \omega_{ijk} + u_i + e_{ijk} \quad (10)$$

where $u_i \sim N(0, \sigma_b^2)$ are independent random variables corresponding to the random effects of projects. The error vectors e_{ijk} are independent and follow $N(0, R_i)$ distributions, where, as suggested by the preliminary analysis, R_i has a first-order autoregressive structure AR (1) or heteroscedastic variance structure with variance r_k^2 .

The model was fitted via maximum likelihood (with restricted maximum likelihood for the within-subjects covariance parameters) using methods implemented in the *lme* function from the *nlme* library in *R*. Very similar results were derived in *SPSS*. Models incorporating both heteroscedasticity and autoregression failed to converge in *R*. So, as a first step in identifying an appropriate covariance structure, models separately incorporating autoregression or heteroscedasticity were examined. Plots of Pearson residuals from LNLMMs incorporating random intercepts and autoregression, heteroscedasticity, or independent errors are shown in Fig. 6,

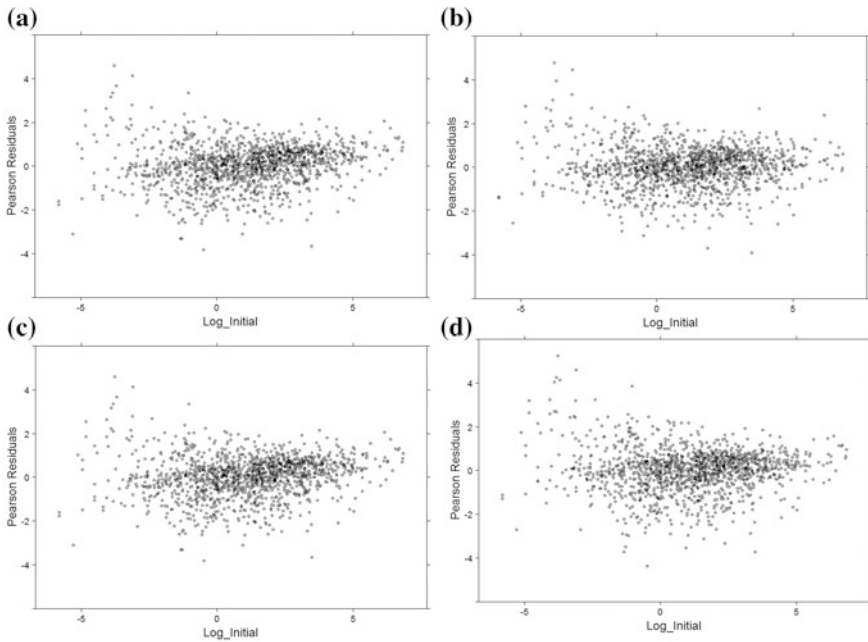


Fig. 6 Residual plots from LNLMM (model Eq. 4) with random intercepts **a** independent errors **b** heteroscedastic errors **c** AR1 errors **d** no random intercept, independent Errors

together with the residuals from the OLS model. The models were also assessed against the variance function⁴ $\nu_{ik} = \sigma_b^2 + r_k^2$.

Trials using likelihood ratio tests of different covariance structures incorporating independent errors, autoregression or heteroscedasticity in combination with residual diagnostics, showed that an autoregressive covariance structure provided a significantly better model fit in comparison with assuming independent errors (or compound symmetry) or heteroscedastic covariance structures and just as satisfactory residuals.

Key measures for each step of the modelling strategy under the LNLMM assuming random intercepts and an autoregressive error structure are summarized in Table 1, where each model was evaluated using maximum likelihood (ML) tests (for the fixed effects), restricted maximum likelihood (REML) (for the covariance structure), Akaike Information Criterion (AIC) and Bayesian Information Criterion (BIC) where appropriate.

Goodness of fit for different models, evaluated via the R^2 Marg summary measure from the marginal model, is provided for completeness. Guerin and Stroup [9] and Gurka [10] discuss ML, REML, AIC and BIC for model comparison.

⁴Random slopes were also considered for the LNLMM leading to a quadratic form for the variance function. This led to a poor fit to the observed variance from the OLS analysis.

Table 1 Estimates and standard errors (in brackets) for LNLMMs

Parameters	Model Eq. 4	Model Eq. 6	Model Eq. 7	Model Eq. 8	Model Eq. 9	Model Eq. 8 (Reduced data)
Σ_t	0.52 (0.19)	0.40 (0.34)	0.53 (0.17)	0.49 (0.21)	0.68 (0.11)	–
Σ	1.31 (0.06)	1.40 (0.06)	1.30 (0.05)	1.31 (0.06)	1.31 (0.05)	1.09 (0.56)
ρ	0.4304591	0.4932961	0.4200208	0.4307339	0.4184478	0.386
R^2 Marg	0.641	0.617	0.639	0.641	0.638	0.753
$-2\log\text{Lik}$	4729.548	4797.226	4735.442	4723.152	4728.264	3930.899
AIC	4771.548	4821.226	4769.442	4757.152	4754.265	
BIC	4881.465	4884.114	4858.472	4846.182	4822.384	

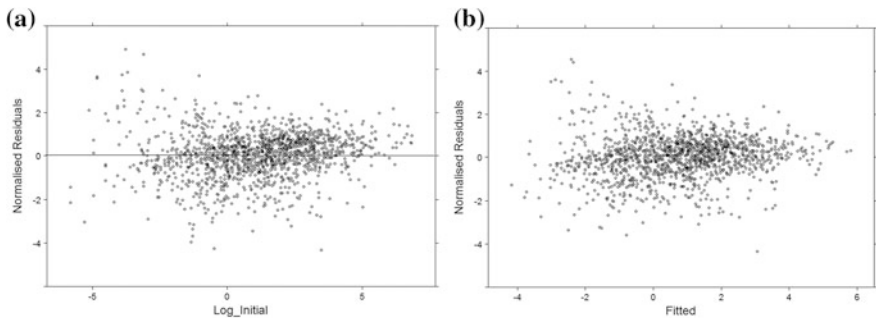


Fig. 7 Residual plots from final LNLMM with AR1 errors **a** Marginal residuals **b** Conditional residuals

Procedural examples for model selection may be found in West, Welch and Galecki [28] or Heck et al. [11] for example.

The preferred model is model Eq. 8. In particular, there is no evidence that any of the other models perform better, on examination of either likelihoods, AIC, BIC, R^2 Marg or residuals. Plots of residuals for model Eq. 8 are at Fig. 7. The plots show some tapering to the right, suggesting decreasing variability that may be a consequence of a slight overfitting by the lognormal model. Year of Project and project domain both affect the final cost for any given initial cost, and a constant power function relationship exists between planned and actual expenditure with the exponent less than unity. These results suggest that projects behave slightly differently across domains and departures from expenditure plans across projects are explained by domains (and not by planned expenditure). This is somewhat unexpected as common processes and management arrangements are in place for the management of AMCIP projects. On the other hand, differences in the effect of time on project expenditures are expected. In particular, the “pressure” on expenditure increases annually up to year eight and then declines in years nine and 10. This may reflect projects “ramping up” over time to a maximum effort and then slowly

subsiding. It certainly reflects the typical “S”-shaped curve for cumulative expenditure described in Weir and Malcolm [27]. The intra-class correlation coefficient is 70%; so over two-thirds of the observed variability comes from within projects, supporting the ramping up phenomenon, rather than between projects.

The model also suggests that projects underspend in the early years of their life; this reflects observed cash flow behaviour in Defence, as reported by Weir and Malcolm [27], reflecting over-optimistic project plans and constraints placed on projects by planned expenditure slippage and portfolio overprogramming.

Figure 8 presents strip plots of the residuals for each year and project domain; some slight variability in variance remains, especially for the later years (where there is less data) and in the Domain of “Other”.

The marginal residuals at Fig. 7a support the linear model but it and the conditional residuals at Fig. 7b suggest there are a number of outliers that warrant further attention. In order to evaluate the robustness of the estimators and the leverage of the outliers, the model was refitted to the reduced data obtained by omitting the outliers suggested in Fig. 8 (residuals larger, in absolute value, than the 97.5th percentile). Not much can be said about the outliers; they are unusual in the sense that they do not fit the model well, but, given the large amount of data, are expected. There is no apparent pattern to their nature. They are spread over both Years and project domains. A cursory review of the outliers suggests they reflect extreme departures in actual expenditure from planned expenditure. Some may result from accounting adjustments, but most are due to project and portfolio management interventions.

For the refitted model, an autoregressive error covariance structure was fitted to the data, but there was no need for a random intercept (i.e. the random intercept’s variance is zero). The results are presented in the final column of Table 1. As shown at Fig. 9 for the reduced data, the elimination of the outliers almost completely removes heteroscedasticity.

The major discrepancy between the remaining estimates for the complete and reduced data is a 20% difference in the estimate of the exponent γ (from 0.65 to 0.78 and so reflects that, without the outliers, expenditure better matches plan), but otherwise there is little difference. So, in summary, the outliers are influential with

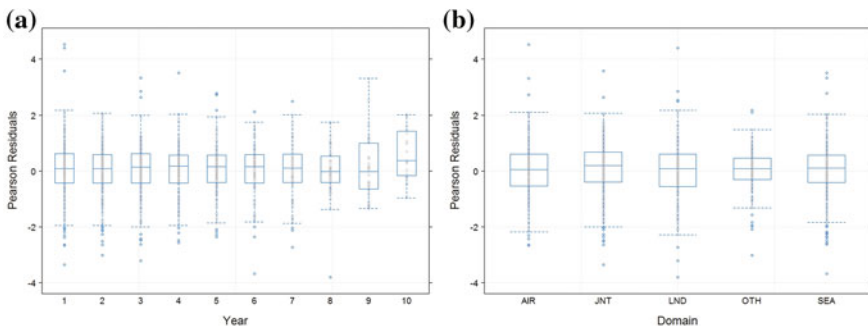


Fig. 8 Strip plots from final LNLMM with AR1 errors **a** Year **b** Domain

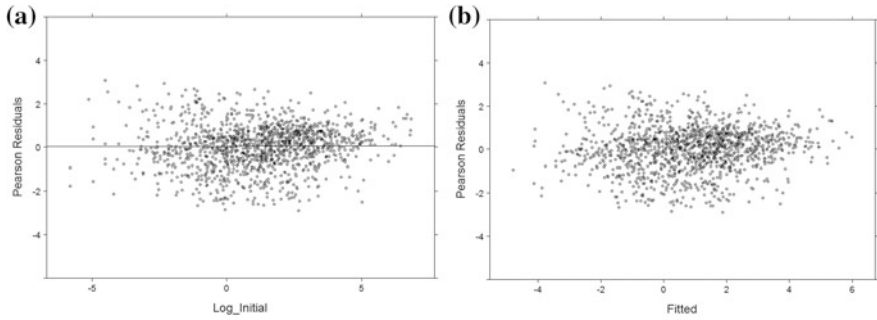


Fig. 9 Residuals for reduced data a Marginal b Conditional

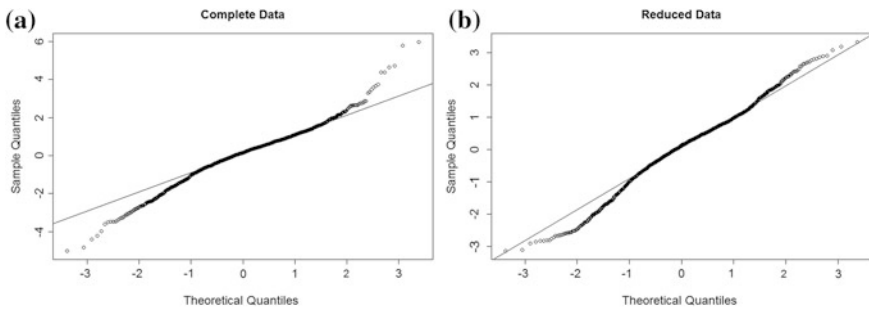


Fig. 10 Q-Q plots of conditional residuals for the preferred LNLMM. a Complete data. b Reduced data

respect to both the covariance parameters and the fixed part of the model. As expected, the estimated error variance (Σ^2) is smaller for the reduced data set. The Q-Q plots in Fig. 10a (complete data) and Fig. 10b (omitting outliers) suggest mild deviations from the normality assumption, especially for smaller residuals, but this is unlikely to jeopardize the results.

The estimated best linear unbiased predictors (EBLUPs) of the random effects of each project are plotted at Fig. 11a. There are apparently only a few projects with random effects that are smaller than the rest. The quantile plot at Fig. 11b suggests the random effects are approximately normally distributed. The plot identifies the small number of observations with the predicted random effects greater, in absolute value, than the 0.90 quantile of the standard normal distribution.

Plots of the (population) expected expenditure for the LNLMM models for planned expenditures between \$5 m and \$30 m are shown in Fig. 12.

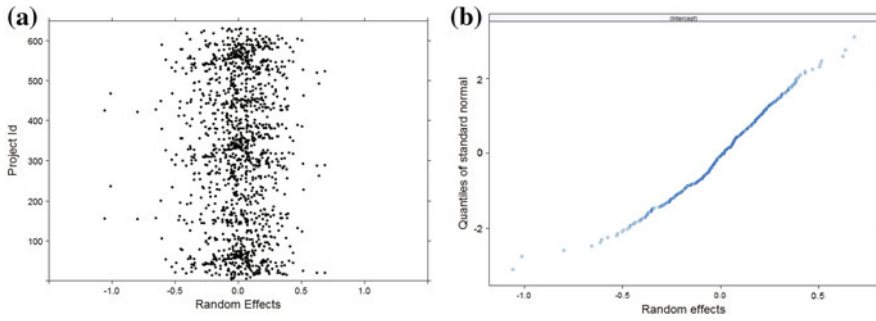


Fig. 11 **a** Dot plots of the predicted random effects (EBLUPs) for the projects. Complete data. **b** Normal Q-Q plots of the predicted random effects (EBLUPs) for the projects

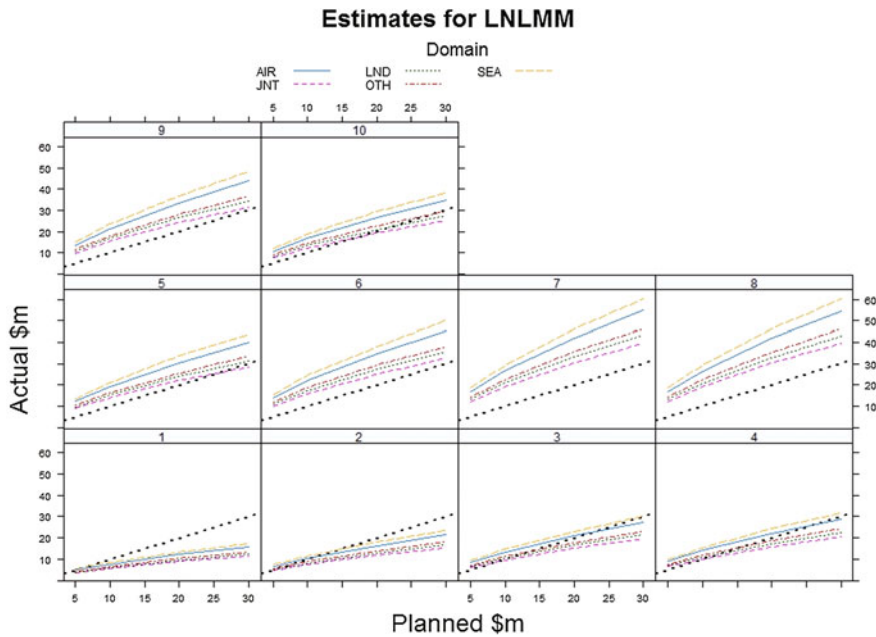


Fig. 12 Final model expected expenditure against planned expenditure by Year of Project for the preferred LNLMM. For this demonstration, annual planned expenditure is restricted to \$5–\$30 m. The bold dotted line is $y = x$ (i.e. where actual expenditure equals planned expenditure)

6 Conclusions

This report examined project expenditure for AMCIP projects in the period 1996/97 to 2012/13, based on the Government-approved expenditure plan. Actual expenditure was modelled as a multiplicative power function of planned expenditure using LNLMM. The LNLMM allows for a detailed modelling of the

within-subjects correlation structure and the prediction of individual random effects. The modelled within project correlation structure reflects the observed autocorrelation of within project expenditures. The random effects are at the project level and represented in the model as random intercepts. The modelling demonstrates that there are both Year of Project and project domain effects on planned expenditures and that the relationship between planned and actual expenditure is nonlinear, being exponential. The model has a constant negative coefficient of uniformity, so the expenditure rate for all projects is decreasing and departures from expenditure plans across projects are explained by project domains (and not by planned expenditure). This is surprising because of standardized project planning in Defence, but may reflect differences in management practices between project domains or some other factor in the nature of projects (which was not examined here). There are also significant differences in expenditure rates by Year of Project. As a general rule, projects underspend early in their lifetimes and overspend later, reflecting over-optimistic planning of projects and expenditure constraints. The data is consistent and infers that project spending is unlikely to go to plan. The impact of this may be mitigated by employment of models such as that developed here which can quantify expenditure variations from plan. Residual plots from the models show some tapering to the right, suggesting decreasing variability that may be a consequence of a slight overfitting of the models. Outliers exist in every Year of Project and project domain. The outliers influence both the fixed and random parts of the LNLMM, and their elimination removes most heteroscedasticity. The outliers may result from accounting adjustments but more likely project and portfolio management interventions. Further examination of these outliers, including a need to distinguish between project-internal factors and significant portfolio factors, is warranted in order to develop a stronger model. The model may be used by project and portfolio planners to test likely spending variations from plan and gives them the opportunity to adjust expenditure plans accordingly to reduce variations; hence, the model provides a measure of financial risk. Future work will consider panel data approaches to modelling the AMCIP data. Another approach is to examine cumulative planned and actual expenditures as done by Burgess [3].

Acknowledgements The author thanks C. Rowe, R. Willett, R. Kidson and two anonymous referees for their constructive comments in the preparation of this paper

References

1. Alencar, A.P., Singer, J.M., Rocha, F.M.M.: Competing regression models for longitudinal data. *Biom. J.* **54**, 214–229 (2012)
2. Anastasopoulos, P.C., Labi, S., Bhargava, A., Mannering, F.L.: Empirical assessment of the likelihood and duration of highway project time delays. *J. Const. Eng. Manage.* **138**(3), 390–398 (2011)
3. Burgess, E., Krause, C., Sterburzel, J., Elliott, D.: Phasing Estimation Relationships, NASA Cost Symposium. Pasadena, CA. http://www.nasa.gov/sites/default/files/files/08_PERFT_Cost_Symposium_Final_TAGGED.pdf (2013). Accessed 16 July 2016

4. Department of Defence: Defence Portfolio Budget Statements 2015–16, p 20. <http://www.defence.gov.au/budget/15-16/Pbs.asp> (2015). Accessed 16 July 2016
5. Diggle, P., Liang, K., Zeger, S.: *Analysis of Longitudinal Data*. Oxford University Press, Oxford (2002)
6. Fitzmaurice, G.M., Laird, N., Ware, J.: *Applied Longitudinal Analysis*. Wiley, New York (2004)
7. Gałecki, A., Burzykowski, T.: *Linear Mixed-Effects Models Using R: A Step-by-Step Approach*. Springer, NY (2013)
8. Gill, A., de Visser, G.: *Defence Project Schedule Slippage Modelling*, Defence Science and Technology Organisation DSTO TN1284 (2014)
9. Guerin, L., Stroup, W.W.: A simulation study to evaluate PROC MIXED analysis of repeated measures data. In: *Proceedings of the 12th Annual Conference on Applied Statistics in Agriculture*, pp. 170–203. Kansas State University, Manhattan (2000)
10. Gurka, M.J.: Selecting the best linear mixed model under REML. *Am. Stat.* **60**, 19–26 (2006)
11. Heck, R.H., Thomas, S.L., Tabata, L.N.: *Multilevel and Longitudinal Modeling with IBM SPSS*. Routledge, NY (2014)
12. Horton, R.L.: *The General Linear Model*. McGraw-Hill, Inc, New York (1978)
13. Jiang, J.: *Linear and Generalized Linear Mixed Models and Their Applications*. Springer, NY (2007)
14. Laird, N., Ware, J.: Random-effects models for longitudinal data. *Biometrics* **38**, 963–974 (1982)
15. Liang, K.Y., Zeger, S.L.: Longitudinal data analysis using generalized linear models. *Biometrika* **73**, 13–22 (1986)
16. Lo, E.H.S., Weir, T., Tay, N., Bulluss, G.J., Wang, Y.-J.: Improving project budgeting through slippage analysis in program viewer. In: *Proceedings of Systems Engineering Test Evaluation Conference*, Canberra, ACT, INCOSE (2015)
17. Love, P.E.D., Wang, X., Sing, C.P., Tiong, R.L.: Determining the probability of project cost overruns. *J. Constr. Eng. Manage.* **139**(3), 321–330 (2013)
18. Love, P.E.D., Sing, C.P., Wang, X., Edwards, D.J., Odeyinka, H.: Probability distribution fitting of schedule overruns. *J. Oper. Res. Soc.* **64**(8), 1231–1247 (2013)
19. Love, P.E.D., Sing, C.P., Wang, X., Irani, Z., Thwala, D.W.: Overruns in transportation infrastructure projects. *Struct. Infrastruct. Eng.* **10**(2), 141–159 (2014)
20. Peever, D., Hill, R., Leahy, P., McDowell, J., Tanner, L.: *Creating One Defence—The First Principles Review of Defence*, Department of Defence (2015)
21. Rao, C.R., Toutenburg, H., Shalabh, H.C.: *Linear Models and Generalizations*, 3rd edn. Springer, NY (2008)
22. Singer, J.M., Andrade, D.F.: Regression models for the analysis of pretest/posttest data. *Biometrics* **53**, 729–735 (1997)
23. Singer, J.M., Nobre, J.S., Sef, H.C.: Regression models for pretest/posttest data in blocks. *Stat. Model.* **4**, 324–338 (2004)
24. Verbeke, G., Molenberghs, G.: *Linear Mixed Models for Longitudinal Data*. Springer, NY (2000)
25. Vickers, A.J.: The use of percentage change from baseline as an outcome in a controlled trial is statistically inefficient: a simulation study. *BMC Med. Res. Methodol.* **1**(1), 6 (2001)
26. Vickers, A.J.: Parametric versus non-parametric statistics in the analysis of randomized trials with non-normally distributed data. *BMC Med. Res. Methodol.* **5**(1), 35 (2005)
27. Weir, T., Malcolm, W.P.: *A Statistical Analysis of Expenditure Slippage and Project Lifetimes in the Approved Major Capital Investment Program*, DSTO-CR-2013-2014 (2014)
28. West, B.T., Welch, K.B., Gałecki, A.T.: *Linear Mixed Models: A Practical Guide Using Statistical Software*, 2nd edn. Chapman and Hall/CRC (2015)
29. Wooldridge, J.M.: *Econometric Analysis of Cross Section and Panel Data*. MIT Press (2010)

SimR: Automating Combat Simulation Database Generation

Lance Holden, Richard M. Dexter and Denis R. Shine

Abstract Land simulation, experimentation and wargaming (LSEW) has long-used land combat simulation as a central tool to support its analysis of army modernisation studies. Combat simulations provide great utility through their ability to analyse the impact of equipment, structure and tactics within a force-on-force context. However, their extensive input data requirements create significant challenges in terms of data generation, verification and validation. Since 2012, LSEW has been developing the simulation repository (SimR), a database designed for the express purpose of managing and storing combat simulation input data. SimR was designed with a number of critical features in mind: a minimalist storage methodology, the concept of data provenance and the use of deterministic data generation algorithms to produce input data on demand. More recently, LSEW has introduced the feature of automated database generation. Focusing on the COMBATXXI [1] combat simulation as a target, SimR can now produce a working COMBATXXI land component performance database on demand with minimal human intervention. This is a significant advance over previous methods, which relied heavily on analysts to manually piece together databases from disparate sources, a time-consuming and error-prone approach. As a result, the latest COMBATXXI study uses a SimR-generated database.

Keywords Combat simulation · Validation and verification · Configuration management

L. Holden (✉) · R.M. Dexter · D.R. Shine

Land Simulation Experimentation and Wargaming, Land Capability Analysis,
Joint and Operations Analysis Division, DST Group, Edinburgh 5111, Australia
e-mail: lance.holden@dsto.defence.gov.au

R.M. Dexter
e-mail: richard.dexter@dsto.defence.gov.au

D.R. Shine
e-mail: denis.shine@dsto.defence.gov.au

1 Introduction

The generation, storage, verification and validation of combat simulation input data have been a long-standing challenge to LSEW. Combat simulations such as Close Action Environment (CAEn) [2] or COMBATXXI adjudicate aspects of combat using large lookup tables, where the probability of some kind of event (such as a hit, kill, or detection) need to be specified based on a number of circumstances (such as range, angle, elevation and time of day) [2]. These input parameters act as dimensions, creating a huge volume of data that needs to be specified.

Previous LSEW attempts to solve this problem have had mixed levels of success. In the early 2000s, the army experimental framework (AEF) database was built to centralise the input data for the CAEn, JANUS and CASTFOREM [3] combat simulations, but the implementation never made it out of the conceptual stage. At a similar time, the Foevvs tool was developed by LSEW as a means of generating vehicle vulnerability data; however, it was limited in its applicability in terms of modelling and output data generation.

2 Solution

The SimR solution is based on a number of design tenets which have helped drive its development path [4].

1. **Limited Scope.** SimR is intended only for the purpose of storing and generating data for combat simulations. It is not intended to store all information about military systems.
2. **Minimal Data Storage.** Minimise the data stored within SimR through making intelligent inferences or through storing base data and using algorithms to produce complex data on demand. This reduces the verification and validation burden.
3. **Traceability and Provenance.** SimR must keep a history of changes and allow the addition of metadata in order to improve data validity.
4. **Automation.** SimR must export a working combat simulation database with minimal human input, eliminating the error-prone process of building databases by hand.

This solution was heavily enabled by the development of a suite of data generation capabilities developed by LSEW which included direct and indirect fire vulnerability tools (Foevvs) and a sensor data generation tool based on NV-IPM, a popular sensor modelling tool. Tools such as these allow SimR to store entity-level data, with interaction data (such as probabilities of hit and kill between pairs of entities) to be generated on demand by trusted, deterministic software.

3 Implementation

This section describes how the current Simulation Repository implementation achieves the aim of the tenets described above.

3.1 Workspace

Central to the user experience with entering data is the concept of a workspace, which is a collection of entity definitions such as munitions, weapons, platforms or force allocations (Fig. 1). Each entity describes a particular component in a simulation, either physical, such as weapon, or conceptual, such as force allocation. SimR defines a fixed set of entities that the user can create and edit, and this set is closely tied to the needs of target simulations such as COMBATXXI. Depending on entity type, various fields are available, such as the calibre of a munition or speed of a vehicle. Not all fields require data during editing, but at export time missing data is identified by the selected exporter to ensure the usability of any generated simulation database. Many users may collaborate in the development of entities in a workspace. Entities can also be copied between workspaces. See the exporter section for more explanation.

Each workspace allows the simulation developers to explore different data values. They can explore concepts such as different armour configurations of vehicles or different armaments. Each change and the reasons for the change are isolated from other workspaces.

Fig. 1 Entities within a workspace

The screenshot shows a workspace interface with a filter bar at the top containing buttons for 'All (204)', 'A Vehicle (9)', 'Artillery (2)', 'B Vehicle (0)', 'Force Type (2)', 'Indirect Fire Weapon Mount (6)', 'Infantry (2)', 'Munition (63)', 'Posture Change Time Table (1)', and 'Self Propelle'. Below the filters is a table with three columns: Name, Category, and Creator. The table lists several entities, all created by 'Lance Holden'.

Name	Category	Creator
100mm_2A70_ATGM	Weapon	Lance Holden
100mm_2A70_CANNON	Weapon	Lance Holden
100mm_9M117M1_ATGM	Munition	Lance Holden
100mm_UOF17_HEFRAG	Munition	Lance Holden
105mm_PG29V_HEAT	Munition	Lance Holden
105mm_RPG29_ATRL	Weapon	Lance Holden
12.7mm_6P49_HMG	Weapon	Lance Holden
12.7mm_B32_API	Munition	Lance Holden

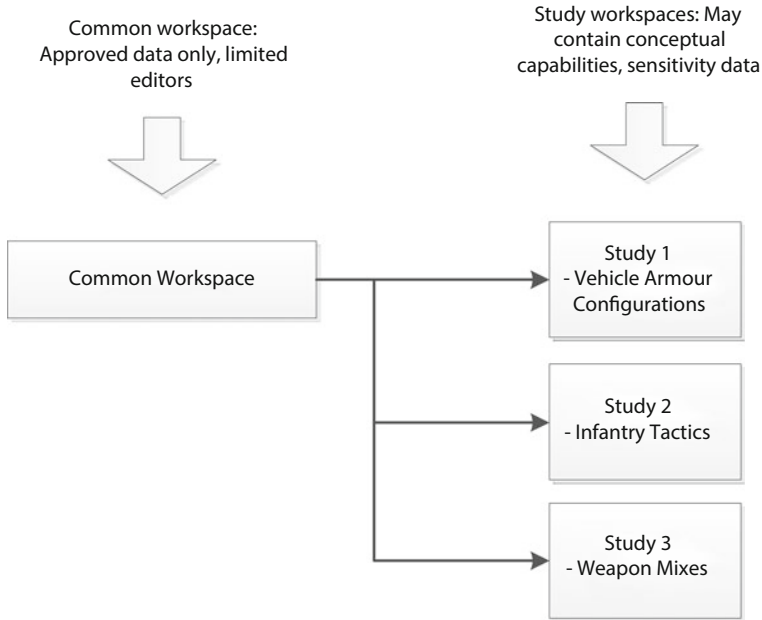


Fig. 2 Workspaces within SimR

A single well-defined workspace known as the Common Workspace acts as a repository of approved values. The Common Workspace stores “real” data, omitting entities that are developed for specific studies such as conceptual configurations that do not exist in reality. Edits to the Common Workspace are limited to a few users who have authorisation to make such changes, which are only made after an extensive review and justification of new values. Data from the Common Workspace can be imported directly into experiment workspaces to avoid the need to duplicate data entry and to inherit all of the data provenance and validation that has gone into maintaining the Common Workspace.

The workspaces are essential to the SimR solution for configuration management. They provide for the ability to explore different interactions and to provide the ability to review what and why data values were altered. Through a concept LSEW has termed views, all changes to workspaces are tracked to ensure traceability. They are also available for users at any time either by direct access to the contents or by viewing the workspace associated with any produced export. Figure 2 shows the concept of workspaces visually.

3.2 Entities

As described, an entity represents a collection of data to represent a physical item or conceptual structure. Some example entity types are explained below.

3.3 *Weapon Systems*

Several entity types are used to represent weapons. A munition type exists to record details of the munition being fired. The munition is independent of the weapon or delivery method at the time it is created; however, this information can be inferred from specifying the munition type (BALL, BOMB, ICM, etc.). Explosive or penetration data generation parameters are recorded on the munition.

The means of firing a munition are represented by weapon entities. A weapon identifies the type from a selection of options, for example RIFLE, MACHINE_GUN, CANNON and HOWITZER. It records details about the number of munitions that are activated on trigger pulls but not their performance.

Weapons and munitions are combined via the weapon mount entity type. This combination links a weapon entity with a mount point. A mount point is a description of how the weapon is held or stabilised when being fired, for example, a 7.62-mm PKT MMG can be mounted on both a BMP-3 BOW and COAX. Weapon mounts have two distinct types, direct fire weapons (where the ballistic projectile takes a straight flight to a visible target) or indirect fire weapons (where the round is launched in an arc against targets that may not be directly seen by the firer).

Weapon mounts contain all of the munitions that may be fired by the weapon type. Each of these associations contains extra Foevvs specific data that defines this pair working together. This can include muzzle velocity, ballistic coefficients and other performance data. More details on the use of this data can be found in: [5–7].

This weapon system structure was built because not all information exists at the munition level, as some performance aspects only become clear once combined with the weapon (i.e. in the case of muzzle velocity, which may change for the same munition depending on the weapon it is fired from), or the mount (different types of stabilisation produce different dispersions).

3.4 *Platforms*

Platforms in the system refer to entities that have a physical presence in the simulation and have behaviour associated with their use. One may assign types to an entity, which defines the type of data the entity requires. A single entity may have several types, such as self-propelled artillery which is both a vehicle and artillery type. Platforms contain a set of entity attributes that determine how it moves and what size it occupies. Shape files that described the entity as a 3D model are associated with platforms and used by the Foevvs routines when calculating system vulnerability.

Platforms attach weapons via weapon mount entities. Each weapon mount attachment contains extra information related to the pairing of these entities such as specifying how many rounds of the munitions used are ready and stowed. The weapon mounts on a platform also contain articulation and sensor information.

3.5 *Sensors*

Sensors are represented in SimR using basic characteristics such as magnification and field of view. On export, SimR calls NV-IPM [8], a sensor modelling tool developed by Night Vision and Electronic Sensors Directorate (NVESD) to generate the complex interaction data required for combat simulations.

3.6 *Provenance*

One of the key requirements for SimR is the ability to track why values are selected as much as what values are used. Each entity provides a set of fields that can record source material used to justify values. This can be stored as either hyperlinks to available resources or as embedded binary files. Combined with the change recording methods per view, SimR is able to query what changes were made and the justifications for them.

The design for SimR chose to use provenance per entity rather than per field. This was based on the fact that a single source of provenance may be attributable to several fields; therefore, the user imports the source data once and notes which fields it impacts upon. From an implementation view point, it also reduced the visual clutter on the data entry pages.

LSEW plans to improve the provenance concept in the future in two main ways. First, there is presently no system for allocating confidence levels in individual data sources. Once this is rectified, we will seek a way to aggregate individual confidence levels into a broader metric for the higher level entities.

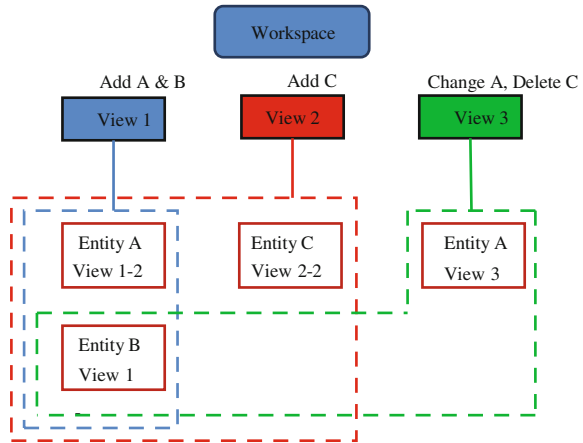
3.7 *Views*

Each workspace can contain any number of entities that can have any number of changes made to them. A key system requirement was to provide access to older states of data so that users can either reproduce data that has previously been generated or create a new export from the same historical data for a different simulation tool.

This is achieved in SimR through a concept called views. A view represents that state of a workspace at a given time. They are tracked by a version number starting at 1 and incrementing with each new view which is also tracked by a timestamp. Users can access old views by either the version number or entering a time. When a view has been created, the data in it can never be edited; any future changes create a new view.

The views concept has been heavily modelled on source code version control tools such as Apache Subversion (SVN) [9] but ignores the concept of branching

Fig. 3 Workspace to view to entity relationship



(being able to split into different workspaces data contents and merging the results afterwards). An ad hoc branch implementation is possible by creating a new workspace from the state of an existing workspace. Merging is not specifically implemented but entities can be copied between workspaces.

Each individual change to an entity will generate a new view of the entire workspace. When a new view is created, a message describing the reason for the change is recorded. The change messages are used to allow other users to understand why the change was made. The system can also highlight differences in values, so the user can track the changes to the workspace over time. Figure 3 shows a simple illustration of how views change as the workspace changes.

3.8 Data Alteration

Data alterations are passed through the workspace. The workspace knows how to create all the dependent data objects in the database. A view represents only a readable slice of the workspace at a time. All alteration requests must pass through the workspace.

When changes to one entity requires changes to another entity to keep consistent validity with the data representation, the user is able to preview the impact and accept them before the change is saved. An example occurs when altering the munitions on a weapon mount entity, any platform that uses the weapon mount needs to ensure its weapon mount munition is correct after the change. This ensures the data is always in a valid state for an export. Data may be altered so that is valid for the database but no longer valid of an exporter that was previously used. If attempting to export with the same settings, the exporter will generate a list of faults as part of the normal validation process.

3.9 Database Storage

The data structure of an entity is very different between data types. Additionally, the fields that define an entity type can change as the SimR system is further developed. Common approaches such as storing this data in a Structured Query Language (SQL) database would require modification to database table columns for every data change. This is a large undertaking, especially when a database has been in use for a significant amount of time and contains data that needs to be preserved. Additionally, the creation of a new entity type will require the creation of new database tables. Having entity data stored across multiple different tables makes it difficult to perform searches against common fields.

For this reason, SimR was instead built upon a NoSQL database. NoSQL databases provide a database that is document focused rather than the traditional table and row focus of SQL databases. This allows the data to be unstructured when saved and loaded and searched as a single item, which matched the data storage requirements for SimR. The MongoDB [10] database has been selected as preferred NoSQL implementation, due to the available supporting documentation, active development and integration with the Java language used by SimR.

MongoDB does not provide any support for transactions to protect the integrity of the data. The SimR system has developed a series of collections that allow for transactional processing to occur. The data is stored in three collections: workspace, entity and view. The workspace collection contains the document that describes the workspace and user permissions on it. The entity documents contain all of the details of an entity and the range of views they apply to. An entity document that refers to a specific version only occurs when that version is saved; the search functions ensure it is never examined before all the required data is saved to the database. A view document contains details of the change to the workspace. Each view document requires a unique and incrementing version number; the server provides this information in a safe manner, so one version number is never repeated. The order the view documents are saved does not matter.

Each complete version of an entity is saved. This increases the amount of storage space needed as entities change as complete versions are saved; however, this makes it easy to search through older views as the data is already complete in the database and does not need to be rebuilt from a change log.

4 Exporting to Target Simulations

Exporting is the process of taking a workspace view and generating data files that are compatible with a simulation tool. The exporting process takes the key data values that have been entered on entities and uses a set of deterministic algorithms to generate the remaining interaction data between entities (Fig. 4). The result of the export is stored on the SimR server for users to download.

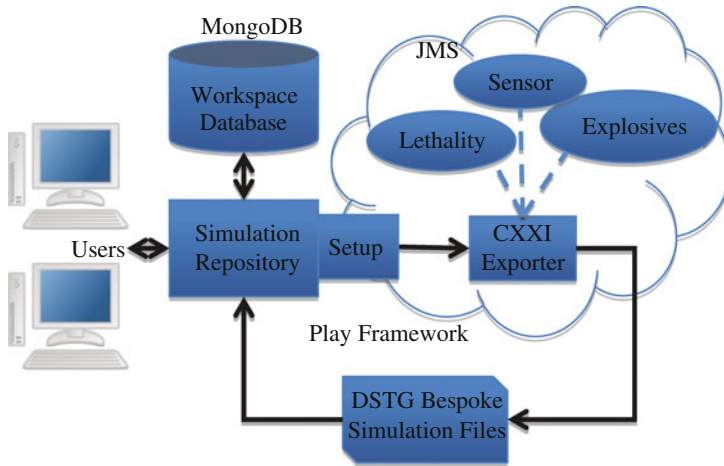


Fig. 4 Workflow from exporting a workspace to collecting simulation files

4.1 Set-up

Each export begins with a configuration step where the user sets the interactions to be generated. This allows the user to specify data that is not generic enough to belong in the workspace but is required for a simulation to function correctly. The most important component of set-up is the definition of valid weapon/target pairs, where one defines which pairings require some kind of lethality data to be generated as part of the export process. Export configurations can be copied from previous exports.

Each export configuration selects from the available exporters and a view from a workspace. This allows users to regenerate data. Exporters are also versioned, and old implementations remain available for selection. These two selection options give users the ability to generate data from the latest view with the latest exporter or to use different exporters or views, allowing the regeneration of data from previous studies or generating comparisons between data changes with different exporter versions for the same simulation tool.

4.2 Export

Exporters are implemented as separate processes from the SimR service. Each exporter responds to requests for work sent via messages from SimR. The export message contains the workspace view and all binary data associated with it. The exporters are implemented to break the task down into smaller components and to distribute these to the data generation processes. The results are gathered by the

exporter, formatted correctly for the target simulation and then transferred back to SimR as the final result. Exporters provide status updates as they are processing.

4.3 *Completeness Checking*

The first task of the exporter is to break the complete job into individual tasks. As each task is generated, the system checks the data to ensure it has the parameters needed. If there are any data errors detected, the export fails and the user is given a list of entities and fields that need to be corrected before the export can process.

Each exporter must provide this check at export time instead of during entity creation and editing. The entity data is a generic representation and may contain values that simulations do not need. Not having data is only an error at the time the exporter requires it.

This process removes a major source of error from database construction, reducing the number of errors that can be passed through to the simulation and reducing the time required for users to find the cause of data errors. It does not, however, check the data for correctness.

4.4 *Data Generation Services*

The interaction data required by the simulation is generated from the set of Foevvv services, an in-house lethality and vulnerability tool suite maintained by LSEW. Foevvv draws upon weapon and target data specified in SimR, generating interaction data such as probabilities of kill, formatted as specified by the exporter. Each of these services consumes significant computing resources (CPU and memory) which when run for multiple results at once exceed the capabilities of a single computer, requiring a distributed computing approach. More information on the lethality and vulnerability processes can be found in [5, 6].

The test environment is using a Blade server with Windows virtual machines executing the code that has been developed. The ActiveMQ [11] messaging service is used to communicate between the services, the exporter and SimR. Currently, services must be started manually and no load balancing is performed; future work planned with Deakin University will attempt to establish better methods for distributing both the work tasks and required software to any machine connecting to the processing network.

The COMBATXXI exporter breaks a job into tasks which are then processed in multiple threads. Each task is controlled by a software function that looks at the workspace and generates tasks that will generate simulation data. Some tasks may require new tasks to be created to generate their required input data, where possible generated data is shared with tasks that need the same data to prevent duplicate calculations occurring. Tasks that require generated input data wait until all the

generated data is available and then immediately process it to the required simulation format. This reduces the amount of memory needed by the computing process as the total data generation process can involve moving gigabytes of data between computers.

4.5 Generated Simulation Data

Once the data for each simulation is generated, it is stored in a zip file on the SimR server which is accessible to all users of the workspace. The design goal behind any exporter is to minimise further manipulation of the prepared data, so it can be used in the target simulation; ideally, exported data is “plug and play”.

Each export result contains a copy of the export request messages. This contains the workspace and view that was created and the export settings, giving the user enough information to regenerate the data on demand. It can also be stored for configuration management external to that provided by SimR.

5 Conclusion

Currently, SimR is able to produce the land component database tables required for the COMBATXXI simulation and some limited data for CAEn. The process of changing data takes only minutes for the operator, and the final database is automatically prepared without human error within hours. A process that could previously take weeks or months of data preparation is now reduced to approximately a day and will continue to improve as more verified entities are available in the Common Workspace and the exporter implementations have their execution speed improved.

The improved time to data generation combined with a greater ability to justify the input data increases the confidence and responsiveness of army modernisation activities supported by combat simulation, with the follow-on benefit of meeting the demanding timelines of decision-makers.

Future development for SimR will focus on completing the other domains of the COMBATXXI data that are currently not produced, reducing human configuration of distributed processing environment and exporting to multiple combat simulations.

SimR currently occupies a unique space in the world for management of simulation data. There are no known peers offering the same ability to allow easy configuration of simulation data and removing the burden of human error in data generation. Continued development of SimR will allow LSEW to be a world-leading example of data management for combat simulation tools.

References

1. COMBATXXI User's Guide: Crew and Mounted Expected Casualty Assessment Methodology (2015)
2. Shine, D.R., Dexter, R.M., Russack, S.J.: CAEn System Data User Guide v9.2. Defence Science and Technology Organisation DSTO-GD-0496 (2007)
3. Department of the Army: Combined Arms and Support Task Force Evaluation Model (CASTFOREM) Update: Executive Summary (2005)
4. Shine, D.R., et al.: A Methodology for the Generation, Storage, Verification and Validation of Performance Data for Modelling and Simulation. NATO MSG-111, Sydney (2013)
5. Mazonka, O., Shine, D.R.: Methods and Models in Preparing Weapon-Target Interaction Data for Combat Simulations. MODSIM 2013, Adelaide, South Australia (2013)
6. Mazonka, O., Shine, D.R.: Simple Physical Models in Support of Vulnerability and Lethality Data for Wargaming and Simulation Environments. SimTect 2012, Adelaide, South Australia (2012)
7. Roy, R.L., Cazzolato, F.: An Investigation of Hit Probability Calculations for JCATS. Centre for Operational Research and Analysis TM-2007-31 (2007)
8. NVESD.: Night Vision Integrated Performance Model (NV-IPM). http://www.cerdec.army.mil/inside_cerdec/nvesd/integrated_performance_model/ (2016). Accessed 25 July 2016
9. Apache Subversion: <https://subversion.apache.org/> (2016). Accessed 25 July 2016
10. MongoDB: <https://www.mongodb.com/> (2016). Accessed 25 July 2016
11. ActivMQ: <http://activemq.apache.org/> (2016). Accessed 25 July 2016

Battlespace Mobile/Ad Hoc Communication Networks: Performance, Vulnerability and Resilience

Vladimir Likic and Kamran Shafi

Abstract Dynamic self-forming/self-healing communication networks that exchange IP traffic are known as mobile ad hoc networks (MANET). The performance and vulnerabilities in such networks and their dependence on continuously changing network topologies under a range of conditions are not fully understood. In this work, we investigate the relationship between network topologies and performance of a 128-node packet-based network composed of four 32-node communities, by simulating packet exchange between network nodes. In the first approximation, the proposed model may represent a company of soldiers consisting of four platoons, where each soldier is equipped with MANET-participating radio. In this model, every network node is a source of network traffic, a potential destination for network packets, and also performs routing of network packets destined to other nodes. We used the Girvan-Newman benchmark to generate random networks with certain community structures. The interaction strength between the communities was expressed in terms of the relative number of network links. The average packet travel time was used as the proxy for network performance. To simulate a network attack, selected subsets of connections between nodes were disabled, and the performance of the network was observed. As expected, the simulations show that the average packet travel time between communities of users (i.e. between platoons) is more strongly affected by the degree of mixing compared to the average packet travel time within a community of users (i.e. within an individual platoon). While the conditions presented here simulate a relatively mild

V. Likic (✉)

Joint and Operations Analysis Division, Defence Science and Technology Group,
24 Scherger Drive, Canberra, ACT 2609, Australia
e-mail: vladimir.likic@dsto.defence.gov.au

K. Shafi

School of Engineering and Information Technology, University of New South Wales,
Canberra, Australia
e-mail: k.shafi@adfa.edu.au

K. Shafi

Australian Defence Force Academy, Campbell, ACT 2612, Australia

attack or interference, simulation results indicate significant effects on the average packet travel time between communities.

Keywords Mobile ad hoc networks (MANET) • Electronic warfare • Packet-based networks • Tactical communications • Network topologies • Network performance • Discrete event simulations • Computer simulations

1 Introduction

Future tactical communications must support highly mobile warfighters, potentially operating in remote areas that may or may not have a connection to a wider network backbone. Dynamic self-forming/self-healing communication networks that exchange IP traffic are known as mobile ad hoc networks (MANET). Each participating device in such networks is a host node that generates network traffic, potentially receives network traffic as a destination node, and acts as a router for traffic destined for other nodes. The last function increases network coverage and provides additional resilience [1]. Moreover, participating devices in MANET are frequently moving and the network is continuously self-configuring, implying that the network topology is changing frequently and unpredictably, as some links are lost and new links are established. We have yet to fully understand how the performance and vulnerabilities in such networks and how this may depend on the resulting network topologies under a range of conditions.

It is well understood that operating MANET is associated with significant security and performance challenges [2, 3]. Consequently, several researchers studied resilience in MANET [4, 5], while others have focused on proposing methods that improve resilience of such networks under specific operating scenarios [6]. Some authors investigated security issues in tactical MANET [7–9]. Our broader objective is to investigate the relationship between MANET network topologies and critical operational measures, such as performance and vulnerability. Specifically, we aim to understand the relationship between MANET topologies and:

- a. Performance, controlling events, and traffic anomalies; and
- b. Resilience and adaptability of such networks when under natural interference or deliberate attack.

We use computational models as experimentation tools for hypothesis testing, capturing the key parameters, and to enable the development of measures of robustness and threat/defence effectiveness under specific attack scenarios. In this paper, we summarise the first steps taken towards developing the computational framework suitable for addressing the above challenges and report on preliminary results that demonstrate the proposed approach.

In order to study the relationship between MANET topologies and network performance, several key problems need to be addressed. The first is concerned with the level of abstraction, a well-known problem in the domain of network simulations [10, 11], and computer simulations in general [12]. In the past, communication networks were studied at many different levels, from high level of granularity (where the realistic network protocols are modelled) to low level of granularity (where many realistic details are neglected to achieve required simulation scale or to fulfil some other specific purpose). For example, Balakrishnan et al. reported network simulations at a low level of granularity [13]. On the other hand, the simulations reported by Gadde and co-authors [11] as well as that of Nicol and Yan [14] used high level of abstraction. The work of Arrowsmith and co-authors is an example of network simulations conducted at an intermediate level of granularity [15, 16]. In these simulations, the full detail of the TCP was not modelled (e.g. the full TCP packet structure, TCP handshake and similar), while the exchange of network packets between nodes, basic routing protocols, the effect of transmit buffers and packet loss, and other properties of real packet exchange networks was simulated. For the purpose of this work, we have chosen an intermediate level of abstraction similar to the work of Arrowsmith and co-authors [15, 16]. This choice allowed us to consider different network topologies and analyse packet movement under different conditions, while allowing for each scenario to run multiple simulation repeats in order to collect appropriate statistics.

The second challenge addressed in this work is concerned with scenario generation. The optimal approach to this is highly dependent on the phenomenon of interest and objectives of the study [10]. Simulations of realistic network sizes require automated generation of complex network topologies, traffic patterns, and dynamic links, in this case consistent with the properties of MANET. In this work, we addressed this challenge by applying the graph theory and we exploited recent developments related to community structure in graphs [17, 18].

2 Method

The overall workflow. The proposed method consists of two main components: (1) a graph approach is adopted to generate MANET topologies; and (2) discrete event simulation method is applied to simulate network dynamics. The overall workflow used to construct network topology, prepare, run computer simulations, and analyse results is shown in Fig. 1.

Scenario. In a realistic military scenario, MANET would consist of hierarchical groups of users or communities. For example, an army company may consist of 3–6 platoons, each consisting of approximately 30 soldiers. In an actual deployment, the soldiers belonging to the same platoon may be located in close proximity, while different platoons may be more widely distributed geographically. As a result, soldiers belonging to the same platoon will be “networked” more tightly, with fewer links between the soldiers belonging to different platoons. We investigate this

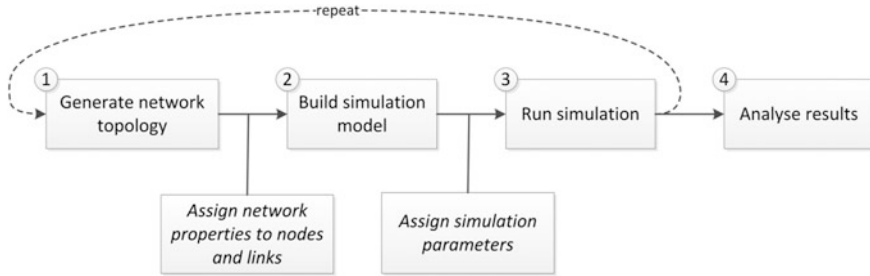


Fig. 1 Overall workflow used in this work. Simulation repeats were used to assess the stability of results, generated for different network topologies corresponding to the fixed network size and chosen community mixing. The steps were executed in the order as numbered, with steps 1–3 executed as a part of one simulation repeat

type of situation aiming to understand what might be the resulting network topologies, and how the network performance and resilience depend on the network topology. In the first approximation, we assume that each soldier carries a hand-held tactical radio device capable of sending/receiving packet-based messages and also participates in routing messages destined to other network nodes.

Preparation of network topologies. Network topologies were generated and handled as graphs. We chose to investigate the network of 128 nodes in total (corresponding to a company), consisting of four subnetworks of 32 nodes (each corresponding to a platoon). In order to model the links within platoons and between platoons, we exploit the theory of community structure in graphs [19]. A number of efficient algorithms for the detection of communities inherent in graphs were developed recently, and this in turn has led to the development of algorithms that can generate “benchmark” graphs for testing of community detection algorithms [17, 18, 20]. The algorithm proposed by Girvan and Newman [20] produces a graph consisting of 128 nodes, divided into four communities of 32 nodes each. Links between nodes are placed randomly, with certain probability that edge will belong to the same community, resulting in a graph with the expected degree of 16. We exploited this algorithm to generate random graphs with different degree of mixing between the communities. Two example networks consisting of four 32-node communities generated by the Girvan-Newman benchmark [20] are shown in Fig. 2; the mixing coefficients used for these graphs were 0.05 (plot (a)) and 0.20 (plot (b)).

We used the implementation of Girvan-Newman benchmark provided by Lancichinetti, Fortunato, and Radicchi (LFR) [17]. The LFR algorithm can generate a much wider range of benchmark graphs (not only Girvan-Newman type). It assumes power law distributions for both the degree and community size parameters and uses power law coefficients to control these parameters. The mixing coefficient is used to control the percentage of links shared between and within communities. The network is generated incrementally by adding nodes and links between them using the degree and community size coefficients. A rewiring step is

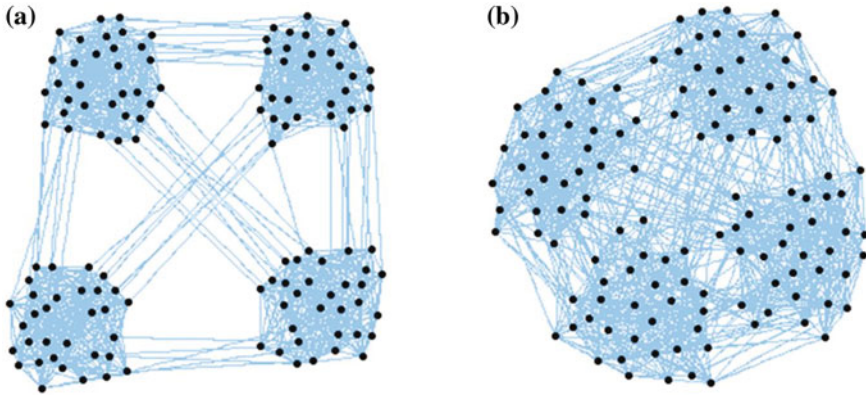


Fig. 2 Two 128-node networks composed of four 32-node communities generated by the Girvan-Newman benchmark [17, 20]. Plot (a) mixing coefficient between communities is 0.05; and plot (b) mixing coefficient between communities is 0.20

applied to balance the distribution of within and between community links based on the mixing coefficient.

For low mixing, the individual communities are nearly or completely isolated, with no communication between them. On the other hand, high mixing produces many links between different communities, and in this case it may not be possible to differentiate the individual communities visually (see Fig. 2). The mixing coefficient determines the fraction of total links between the communities. However, in both networks in Fig. 2, the total number of links is 1024, the average number of links per node is 16, and density is 0.13. The difference between the two networks is in the average path length, network diameter, and transitivity. For the network in Fig. 2, plot (a), the average path length is 2.47, diameter is 4, and transitivity is 0.41; for the network in Fig. 2, plot (b), the average path length is 2.14, diameter is 3, and transitivity is 0.24.

Simulation model. The network graph was turned into a simulation model by assigning network parameters to the nodes and links. The simulation model used in this work was inspired by the previously described model of packet-based network [15, 16]. The original model, Arrowsmith et al., is based on the following:

- I. The network consists of two types of nodes, *host nodes* and *router nodes*. Host nodes are sources and sinks of network traffic and also store and forward packets; router nodes only store/forward the packets;
- II. Host nodes create packets whose destination is another host node. Any host node creates its traffic independently of other host nodes;
- III. Each node maintains a queue of unlimited length where the packets are stored. Any packet generated by the host is placed at the end of the queue. The packet is discarded (packet sink) when it arrives at the destination; and

- IV. A node picks a packet from the head of its queue and forwards the packet to the next destination. The forwarding (and therefore the choice of the next-hop node) can be performed based on different algorithms.

The simulation model used in this work was broadly based on the above, with some significant differences. Firstly, only one type of node, tactical radio node, was implemented and was capable of both generating network traffic and routing network traffic. Since tactical radios are used for real-time communication, it was assumed that each radio would place the highest priority to locally generated network traffic, and any network packet generated by the node was placed at the front of the queue maintained by the node. Finally, in simulations described here, a discrete event network simulator was used in contrast to the original work [15, 16].

An internal structure of a single node used in the simulations is shown in Fig. 3, plot (a). A single node consists of a packet source, a forwarding queue, a packet forwarding module, and a packet sink. The incoming and outgoing connections are also highlighted. All packets generated by the packet source, as well as packets received from all incoming connections, are queued in the forwarding queue. Network packets generated internally by the node are placed at the front of the forwarding queue, to simulate the response to real-time communication traffic. The packet forwarding module processes packets from the forwarding queue based on the first-in-first-out (FIFO) regime. Packets destined for the current host are sent to the internal packet sink, while packets destined for other hosts are forwarded to the next-hop node based on the pre-calculated shortest path routing protocol. In Figure 3, plot (b) shows a simple network consisting of three nodes labelled “a”, “b”, and “c” organised in the linear arrangement a–b–c. The internal structure of the nodes is simplified. There are two node connections (a–b and b–c), each consisting of two directed communication links. For example, the connection b–c consists of directed connection links $b \rightarrow c$ and $c \rightarrow b$, shown in a dashed line.

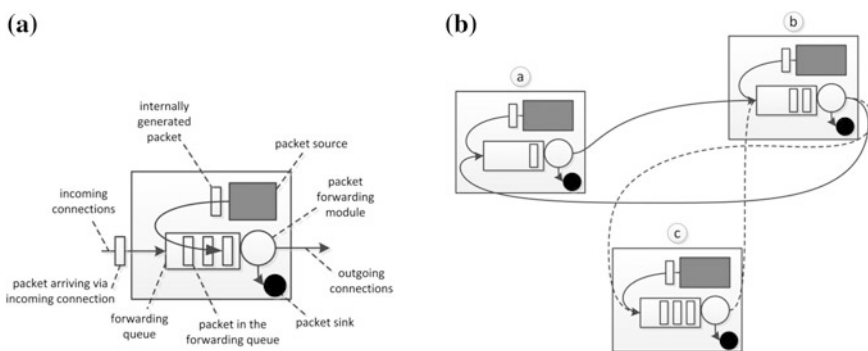


Fig. 3 Model of packet-based network implemented in this work is based on [15, 16] and references therein. Plot (a) shows the internal structure of a single network node; and plot (b) shows a simple network consisting of three nodes (labelled “a”, “b”, and “c”)

Simulation parameters. Each network node was assumed to generate network packets as simple Poisson process events with the average packet rate set to 19/time unit. Each node maintained a queue of packets, with a cut-off of 128. Any packet arriving, while the queue is full, is dropped. A packet forwarding process incurred a delay of 0.019, and each link incurred an additional transmission delay of 0.030 time units. Each individual simulation was run for 10 time units. For a given network (i.e. Girvan-Newman network with a specific mixing between communities), 16 simulation repeats were performed by generating a different network topology in each run while keeping the same mixing parameter. In the analysis phase, the averages and spreads for parameters of interest were estimated based on the 16 simulation repeats.

3 Results

In order to generate the network topology with a well-defined community structure, we used the Girvan-Newman benchmark [17, 20]. To simulate the effect of attack or interference, we disabled a fixed proportion of links, and investigated the effect on the average packet travel times, as the proxy parameter for network performance. For any given simulation, the average packet travel time was calculated over all network packets that arrived at the destination. For each mixing coefficient, 16 independent simulations were run, where each simulation was based on a different, randomly generated network. This provided the basis for the statistical analysis and served to smooth out any rare events, random network configurations, and randomness inherent in packet dynamics.

To generate the baseline, five batches of simulations were performed, for mixing coefficients $\mu = 0.05, 0.10, 0.15, 0.20,$ and 0.25 . The mixing coefficient determined the interaction strength between the four 32-node communities. For a given mixing coefficient, the simulation was repeated 16 times. For each simulation repeat, a different random network consisting of 128 nodes 1024 links was generated by the Girvan-Newman algorithm, keeping the mixing coefficient the same. The average packet travel time was defined as the time required for a packet to reach the destination node, regardless of the number of intermediate hops through routing nodes. The statistics were collected with network packets stratified into two categories: packet exchanged within a community (W-type packets) and packet exchanged between communities (B-type packets). For W-type packets, the destination node belonged to the same community as the packet generating node; for B-type packets the destination and source nodes belong to different communities.

In Figure 4, plot (a) shows the average packet travel time for W- and B-type packets for different mixing between the communities. For each mixing coefficient, the error bars were calculated from 16 independent simulations to average out the inherent uncertainty present due to random network topologies and random nature of packet generation and exchange. The average packet travel time is always greater

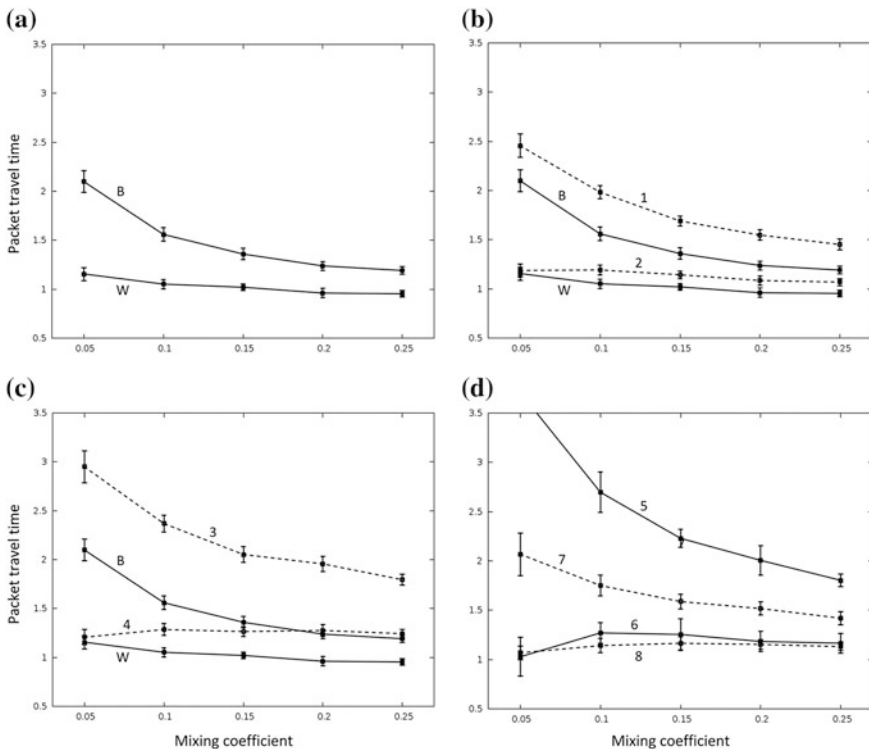


Fig. 4 Average packet travel time for different mixing coefficients. In each plot, the error bars shown were calculated as standard deviations across 16 independent simulation repeats. Plot (a) shows the average packet travel time for different mixing coefficients in the reference simulation (no link elimination); the plots for B-type and W-type packets are labelled. Plot (b): *dashed lines* show the average packet travel times for B-type (labelled 1) and W-type (labelled 2) packets where randomly chosen 15% of network links were disabled; the reference simulation plotted in *solid line*. Plot (c): *dashed lines* show the average packet travel times for B-type (labelled 3) and W-type (labelled 4) packets with 30% of network links disabled; the reference simulation plotted in *solid line*. In plot (d), 30% of network links were disabled, where all the disabled links belonged to the same community. The average packet travel times for B-type and W-type packets for the affected community are labelled 5 and 6, respectively; the average packet travel times for B-type and W-type packets averaged over the three unaffected communities are labelled 7 and 8, respectively

between communities than within communities, simply because each individual community is by definition more tightly “wired”. Over the examined range of mixing coefficient, the behaviour of B-type packets is distinctly non-linear. This would be expected as more links are created within each community at the expense of links between communities. Under the conditions examined, a distinctly non-linear behaviour for B-type packets was observed for $\mu < 0.15$.

Figure 4, plots (b) and (c) show the effect of disabling 15% and 30% of the network links, respectively, on the average packet travel time. The links to be

disabled were chosen randomly from the network, therefore affecting all four communities equally. Since this simply removes a fraction of paths that packets can travel from source to destination, it is expected that the net effect will be an increase of the average packet travel time. This is observed in Fig. 4, plots (b) and (c), which also shows that B-type packets are disproportionately affected. Therefore, under the conditions examined, an attack or interference with network links is expected to disproportionately affect the communications between different communities.

In Figure 4, plot (d) shows the effect of a directed attack affecting specifically one community. In this experiment, 30% of all network links were disabled but links were chosen in such a way that they involved only one community. The plots labelled 5 and 6 show the average packet travel time for the affected community (B-type and W-type packets, respectively), while plots 7 and 8 show the packet travel time averaged over the other three communities (B-type and W-type packets, respectively). The plots labelled 7 and 8 should be comparable to plots labelled 1 and 2. The plots labelled 5 and 6 suggest a severe network degradation compared to the reference experiment (plot (a)).

4 Discussion and Future Work

We investigate how the performance of a 128-node network, consisting of four 32-node communities of users, depends on the mixing strength (the number of links) between the communities. We used Girvan-Newman benchmark algorithm for community detection for generating network topologies to ensure the same network properties across different random network realisations regardless of the mixing coefficient between the communities. The resulting random networks each had 128 network nodes, 1024 links, and an average of 16 links per node. This is the key property that normalises all networks, allowing us to investigate the effect on the network when some links are disabled by network interference or attack.

In the first approximation, the proposed model represents a company of soldiers consisting of four platoons, where each soldier is equipped with MANET-participating radio and represents a network node. The defining characteristic of such a network is that each participating network node performs three different functions: generates network packets, receives network packets (as a destination node), and routes network packets destined for other nodes. In the simulation model, we have chosen an intermediate level of abstraction similar to that reported previously by Arrowsmith and co-authors [15, 16].

Two sets of experiments were carried out for each of the five different network topologies generated using Girvan-Newman graph generation algorithm [17, 20] with different mixing coefficients between communities. These correspond to running multiple simulations for each network topology with and without a simulated attack or interference. An attack was simulated by randomly disabling 15 and 30% of the links across the entire network and also from one of the network

communities. The average packet travel times were recorded within and between communities for each network topology in both scenarios, with and without interference.

The results suggest that:

- i. variation in mixing coefficient affects the average packet travel time both within and between communities, and more so for between communities;
- ii. the relationship between the two variables (mixing coefficient and average packet travel time) follows a non-linear trend, and this is especially pronounced for between communities traffic and $\mu < 0.15$;
- iii. the interference to the network structure by elimination of network links negatively affects network performance. For within community results, this effect seems to maintain a proportional relationship over the mixing parameter with the normal network performance; whereas for between community results, the effect shows a highly non-linear, asymptotic behaviour with decreasing mixing coefficient μ .

While the obtained results are quite intuitive, the variation in network performance even with a relatively simple set-up used in this study is remarkable and indicative of the importance of such a test bench to appropriately analyse the performance of tactical networks under a range of scenarios.

This work addressed the level of abstraction, the method for graph-based network generation, and translation to computer simulations, and demonstrates how the overall approach might be applied in the analysis of battlespace network performance under interference or attack scenarios. The simulation model presented here could be improved in several ways as follows:

- For traffic generation, we used simple Poisson process. More sophisticated traffic generators (e.g. long-range dependent) have been extensively investigated and shown to generate a more realistic traffic for TCP (transmission control protocol) networks [21].
- In the simulations presented here, network packets generated by the source node travel to the destination node and are potentially routed by the intermediate nodes. In real TCP/IP networks, TCP feedback is employed which significantly modifies the traffic patterns [22]. It has been shown that it is possible to simulate the essential characteristics of the TCP network in a simplified manner, thus still retaining a relatively high level of abstraction [15].

In summary, this work indicates the need to develop a high-fidelity simulation framework for benchmarking next-generation tactical battlefield network technologies, including MANET and those based on software-defined radio networks. This framework needs to integrate both predictive as well as prescriptive analytics to allow objectively measuring the vulnerability of next-generation network technologies under a variety of threat scenarios, as well as to provide recommendations for design improvements to address such threats. Additional graph generation methods need to be explored to better represent battlespace network configurations,

and new approaches may be required to define and simulate realistic threat scenarios.

Acknowledgements Authors are grateful to Richard Taylor, Yue Yi, and Richard Fleming for their comments on this work.

Approvals and Classification

This paper is APPROVED-FOR-PUBLIC-RELEASE.

References

1. O'Rourke, C., Johnson, S.B.: Mobile ad hoc networking revamps military communications. *COTS J.* **2011**, 34–42 (2011)
2. Wu, B., Chen, J., Wu, J., Cardei, M.: A survey of attacks and countermeasures in mobile ad hoc networks. In: *Wireless Network Security*, pp. 103–135. Springer (2007)
3. Conti, M., Giordano, S.: Mobile ad hoc networking: milestones, challenges, and new research directions. *Commun. Mag.* **52**(1), 85–96. IEEE (2014)
4. Zhang, D., Sterbenz, J.P.: Measuring the resilience of mobile ad hoc networks with human walk patterns. In: 2015 7th International Workshop on Reliable Networks Design and Modeling (RNDM), pp. 161–168. IEEE (2015)
5. Zhang, D., Cetinkaya, E.K., Sterbenz, J.P.: Robustness of mobile ad hoc networks under centrality-based attacks. In: 2013 5th International Congress on Ultra Modern Telecommunications and Control Systems and Workshops (ICUMT), pp. 229–235. IEEE (2013)
6. Voulgaris, S., Dobson, M., Van Steen, M.: Decentralized network-level synchronization in mobile ad hoc networks. *ACM Trans. Sens. Netw. (TOSN)* **12**(1), 5 (2016)
7. Holliday, P.: NOMAD a mobile ad hoc and disruption tolerant routing protocol for tactical military networks. In: 29th IEEE International Conference on Distributed Computing Systems Workshops, 2009 ICDCS Workshops' 09, pp. 488–492. IEEE (2009)
8. Ni, M., Zhang, L., Pan, J., Cai, L., Rutagemwa, H., Li, L., Wei, T.: Connectivity in mobile tactical networks. In: Global Communications Conference (GLOBECOM), 2014 IEEE 2014, pp. 4400–4405. IEEE (2014)
9. Perisa, D., Allwright, A., Pourbeik, P.: Structural dynamics of war game MANETs. In: 2007 ISIT'07 International Symposium on Communications and Information Technologies, pp. 830–835. IEEE (2007)
10. Breslau, L., Estrin, D., Fall, K., Floyd, S., Heidemann, J., Helmy, A., Huang, P., McCanne, S., Varadhan, K., Ya, X., et al.: Advances in network simulation. *Computer* **33**(5), 59–67 (2000)
11. Coarse-grained network simulation for wide-area distributed systems (2002)
12. Goldenfeld, N., Kadanoff, L.P.: Simple lessons from complexity, vol. 284 (1999)
13. Balakrishnan, H., Padmanabhan, V.N., Seshan, S., Katz, R.H.: A comparison of mechanisms for improving TCP performance over wireless links. *IEEE/ACM Trans. Netw.* **5**(6), 756–769 (1997)
14. Nicol, D.M., Guanhua, Y.: High-performance simulation of low-resolution network flows. *Simulation* **82**(1), 21–42 (2006)
15. Arrowsmith, D.K.A., Woolf, M.: Modelling of TCP packet traffic in a large interactive growth network. In: *Circuits and Systems, 2004 ISCAS '04 Proceedings of the 2004 International Symposium on Circuits and Systems*, 23–26 May 2004, vol. 475, pp. V-477–V-480 (2004)
16. Arrowsmith, D., Mondrag, R.J., Woolf, M.: Data traffic, topology and congestion. In: Kocarev, L., Vattay, G. (eds.) *Complex Dynamics in Communication Networks*, pp. 127–157. Springer, Berlin Heidelberg (2005)

17. Lancichinetti, A., Fortunato, S., Radicchi, F.: Benchmark graphs for testing community detection algorithms. *Phys. Rev. E* **78**(4) (2008)
18. Lancichinetti, A., Fortunato, S.: Community detection algorithms: a comparative analysis. *Phys. Rev. E* **80**(5), 056117 (2009)
19. Newman, M.E.J.: Modularity and community structure in networks. *Proc. Natl. Acad. Sci.* **103**(23), 8577–8582 (2006)
20. Girvan, M., Newman, M.E.J.: Community structure in social and biological networks. *Proc. Natl. Acad. Sci.* **99**(12), 7821–7826 (2002)
21. Rezaul, K.M., Grout, V.: An overview of long-range dependent network traffic engineering and analysis: characteristics, simulation, modelling and control. In: *Proceedings of the 2nd International Conference on Performance Evaluation Methodologies and Tools*. Nantes, France (2007)
22. Erramilli, A., Roughan, M., Veitch, D., Willinger, W.: Self-similar traffic and network dynamics. *Proc. IEEE*, 800–819 (2002)

Using Multi-agent Simulation to Assess the Future Sustainability of Capability

A. Gore and M. Harvey

Abstract The ability to make sound decisions in an area with many complex interactions, such as the sustainability of future capability, is limited by the tools available to emulate the system under study. Methods used to forecast maintenance capability and capacity to support future systems are typically static and deterministic in nature and hence cannot incorporate the true stochastic nature of maintenance events and the capability changes associated with the “growth” of personnel through their technical mastery journey. By comparison, discrete event simulations provide a dynamic platform within which we can emulate the randomness inherent in complex systems, and the extension to multi-agent simulations allows us to capture the effects of changes attributed to personnel. Using a simulation created to address the question of maintenance sustainability for future capability (Air Traffic Management System) for 44WG as a basis for analysis, this chapter compares the results of a discrete event simulation with no agent-based functionality against models containing successively greater multi-agent functionality. A consistent set of fictitious data was used in the analyses presented to run eight individual scenarios to allow fair comparison. From the analyses, we find the discrete event simulation provides overly optimistic results which would lead to understaffing of the maintenance team. In comparison, the multi-agent simulation results were closer to reality and therefore better suited to inform decision making.

Keywords Multi-agent modelling • Agent-based modelling • Discrete event modelling • Data-based decision making • Stochastic systems • Defence

A. Gore (✉)

Network Analytics, The University of Newcastle, Callaghan, Australia
e-mail: alan.gore@networkanalytics.com.au

M. Harvey

Network Analytics, Cardiff University, Cardiff, UK
e-mail: matt.harvey@networkanalytics.com.au

1 Introduction

Recently, Air Force has been undertaking Future Workforce Reviews and Operational Effectiveness Reviews to ensure they can efficiently and effectively support future capability. The latter of these reviews coincides with a transition to new Air Traffic Management equipment which required Logistics Engineering Leadership to reassess the technical workforce capability and capacity.

Historically, and from the Wing's perspective, technical workforce size requirements were determined using data from the flights on workload assessments. These have generally been based on the maintenance manager's determination which, in turn, is based on advice from their staff and a series of spreadsheets covering a multitude of flight resourcing and workload characteristics.

Reductions in staff numbers assist in minimising workforce costs in the short term but may impose significant capability risks in the longer term if internal maintenance capacity requirements cannot be met due to insufficient staff numbers or an inability to meet the required trade authorisation profile at each flight.

An accurate determination of maintenance capacity must incorporate factors from both the personnel side of the equation and the maintenance demands due to the equipment in place at each flight. Personnel factors include, but are not limited to, permanent air force (PAF) and civilian (APS) staffing levels, posting cycles, retention, training, leave and deployments, while the maintenance demand requires and understanding of each equipment item's preventative maintenance (PM) schedule and corrective maintenance (CM) profile.

While PM is scheduled and, therefore, remains relatively constant each year, temporal changes such as trade authorisation and rank progression, and interactions between each characteristic, coupled with the stochastic nature of CM place any true determination of workforce size well outside the realm of the largely static, isolated calculations found in spreadsheet-based solutions.

As in industry, the current trend towards a greater understanding of organisational design and its sensitivities to changes has led to more realistic modelling practices in alignment with the view that better information enables better decisions. The transition from discrete event to multi-agent modelling provides the ability to emulate evolving attributes of the agents (personnel) and the interaction of the agents with their environment (the system) and thereby incorporate the effects of these modifications.

A review of the literature focusing on the use of simulation to determine optimal workforce size reveals remarkably few publications, and no agent-based versions associated with the defence sector. Further, of those papers identified [1–5], only one [5] utilises multi-agent inclusions on discrete event models.

In accordance with latest practices, HQ44WG commissioned a multi-agent, discrete event simulation model to gain a comprehensive understanding of the long-term sustainability of flight maintenance teams and the sensitivity of system restoration times (SRTs), given a background PM load, overlaid with a random CM workload, and various workforce, progression and posting characteristics.

In this chapter, we use results from the discrete event simulation model, with and without various agent-based inclusions, to understand the implications on modelled workforce size and capability over time.

2 System Design

The objective of the simulation was to provide a tool to assess the forward capability of flights to meet maintenance SRTs and to better understand the effects on SRTs of changes in resource numbers, flight trade authorisation profiles and workload. In order to accommodate the objective, the model was initially conceptualised as being completely generalised. The ability to forecast for specific flights and create future scenarios was incorporated through input spreadsheets containing flight-related data and through “model user-interface” control selections.

The original data used for PM and CM tasking within the model were taken from the Networked Maintenance Activity Analysis and Reporting System (NET-MAARS) man-hours data report. This report contains a number of data fields from which we obtained the equipment item identifier, the number of personnel attending and the hours each resource allocated to travel, tool-time and administration on each maintenance task.

Unfortunately, unique equipment identifiers could only be recovered for just over half of the equipment items listed as scheduled events, and there was no clear distinction between those attending the task to undertake the work and those attending in a purely observational capacity. Differences in data input were also noted between flights, and clarification from key 44WG maintenance personnel was necessary to enable actual work requirements to be modelled with greater validity.

Flights were considered to have up to four key systems that could be included or excluded as required. These were radar, navigational aids, automation and communications. Input data allowed PM tasks to be assigned on an individual equipment item basis, but CM tasking could only be allocated at the system level, thus removing our ability to distinguish between complete and partial outages.

A series of workshops were held with key maintenance personnel to map the individual processes associated with PM, CM, the Technical Training Continuum and their interaction. PM tasking is undertaken daily in accordance with the complete PM schedule of tasks. CM is assigned and carried out at the earliest possible time following detection of the fault event. CM work is prioritised above PM, and should the resources with the appropriate trade authorisations required for a CM event be allocated to a PM event (with no other suitably qualified resources available), the requisite personnel will be released from their PM task to enable the higher priority CM to be undertaken. The abandoned PM task will remain on the task list be resumed by the next suitably qualified resource(s).

Trade authorisations are taken to be strictly hierarchical from tradesperson (TP), being the lowest level, through self-certifying tradesperson on PM (SCT-PM), self-certifying tradesperson on CM (SCT-CM), trade supervisor (TS) and finally

independent maintenance inspector (IMI). Note that the model was developed to better understand effects on SRTs and maintenance capability; consequently, the model was designed to reflect work effort only. That is, resources, and their individual trade authorisation levels, reflect an ability to conduct maintenance tasks with no authorisations carrying any level of supervisory requirement.

Note that the inclusion of resource posting imposes design decisions with regard to the authorisation level(s) of resources posting in. If the incoming resource assumes the authorisations of the outgoing resource, then the net change is zero and no impact occurs. If a specific resourcing profile is targeted for the flight, it imposes “necessary” authorisations on incoming personnel to ensure compliance with the final profile requirement; this was considered unrealistic due to the inability to satisfy all requirements for all flights. Hence, a less optimistic viewpoint was assumed in which all incoming resources carry no trade authorisations.

Allocation of resources to tasks is carried out so that task time is shared to the greatest extent possible within each trade authorisation level and with the lowest possible authorisation level assigned first. If no resource with the minimum authorisation is available to conduct the task, only then will the next highest authorisation level be requested. Hence, each trade authorisation level after SCT-CM is, in effect, a more senior SCT-CM technician.

In the typical discrete event model, resources with specific qualifications are added to the model as mentioned above, and these initial authorisations would remain unchanged throughout the duration of the simulation period. The addition of the multi-agent capability allows the resources to develop over time. Trade authorisation progression occurs on a duration in role basis for each of SCT-PM, SCT-CM, TS and IMI. However, the initial move TP to SCT-PM requires attendance at the associated system course(s) in addition to “on the job experience” implemented as one of either a specific duration in the role, a number of “buddy” event tasks or the duration of a specified number of “buddy” event hours.

Durations in any one trade authorisation (in any system) prior to trade progression are specified by the user but modified by the randomly assigned resource aptitude. The user specifies the percentage of resources with low, moderate and high aptitude and, once assigned, remains an attribute of the resource. In addition to affecting their speed of their trade progression, this attribute restricts low aptitude resources from attaining positions above SCT-CM.

A resource attending a maintenance task as a “buddy” is allocated to a task in addition to the minimum required authorised personnel to undertake the task. Buddy selection is system based with the total number of buddies allocated restricted to the user entered total number per task permitted. The selection of resources from the buddy list is randomised within systems, then amongst the candidates across systems prior to final selection. Buddy tasking was disabled across all model runs for this chapter to maintain the integrity of comparisons.

The rank profile of the team remains constant throughout the simulation period and, if agent-based inclusions are enabled, resources will be posted out upon completion of their user-specified, rank-based posting tenure. If the user enters nonzero values to indicate the percentage of posted positions to be filled from the

rank below, then resources are able to be promoted within the flight. Any positions unable to be filled via promotion are filled by posting in external resources. For the scenarios with posting enabled presented here, LAC, CPL and SGT have posting periods of 3 years while FSGT and WOFF are posted every 4 years.

All external resources posting in are given a TP authorisation in all systems and are randomly allocated one system as being “active”. This becomes the system in which they will commence their training. If cross-training is selected by the user, resources become available to commence training in other systems provided they reach the user-defined minimum authorisation level, and the system is identified as a “successor” system of any of the resource’s currently active systems. This functionality allows the user to utilise streaming of systems.

Daily maintenance activities are assumed to be conducted during any user-defined PM shift. However, for this chapter, we use a single PM shift per weekday only. CM is conducted at any time a notification of failure can be given. In general, this restricts CM to the technical operation and maintenance (TOM) console operator’s hours, which typically extend beyond the daily maintenance shift hours. If no TOM hours are specified, the notification period is restricted to the maintenance shift hours. Allocation of a TOM console operator requires a single resource (AC, LAC or CPL) for each shift. The ultimate effect is the removal of resources from the resource pool. Hence, the TOM is removed to ensure consistency of resourcing and results comparisons across models.

Annual leave is assumed to be evenly distributed amongst the resources and continuous for the user-specified number of days. Should the total duration of leave for the number of resources included exceed one year, resources’ leave will begin to overlap.

Despite the increase in modelling capability, we must be cognisant of the level of interaction between agents with other agents, with their environment, and changes within the agents themselves. Training of personnel increases their tasking capability in a stepwise fashion, but experience builds upon their capability nonlinearly. The former has been included in the models presented, the latter has not.

The model was validated using existing flight data and signed-off as accurately representing current performance indicators with respect to SRTs and the rotation and progression of personnel. The simulation model was developed and executed in the ExtendSim AT Suite program using, for this chapter, fictitious but realistic maintenance data with PM and CM profiles matching those of a selected flight.

In order to interrogate the action of agent-based effects such as posting, trade authorisation progression, training continuums, as is the intent of this chapter, a standard personnel profile of 8 members is introduced on each program execution. The initial trade authorisations, enabling of trade progression, posting and cross-training permissions are then altered as shown in Table 1 to create 8 individual scenarios. Scenarios 1 and 2 are discrete event only, while the remaining scenarios contain agent-based inclusions.

Establishing initial trade authorisation profiles to enable clear comparisons amongst the various scenarios requires some thought. Maintaining the respective maintenance team thresholds for each system with the inclusion of annual leave

Table 1 Scenario listing

Scenario	Initial resources		# Initial system authorisations	Trade progression	Posting	Cross-training (min auth)	# Cross-training systems
	SCT-PM	SCT-CM					
1	-	8	1	N	N	-	-
2	4	4	1	N	N	-	-
3	4	4	1	N	N	-	-
4	4	4	1	Y	Y	-	-
5	4	4	1	Y	Y	SCT-PM	2
6	4	4	1	Y	Y	SCT-PM @ 5 mths	4
7	4	4	1	Y	Y	SCT-CM @ 5 mths	4
8	4	4	1	Y	Y	SCT-CM @ 9 mths	4

imposes a minimum of 2 resources per system at SCT-CM level with fixed resources (as per scenario 1). However, the inclusion of agent interactions, which allows for development of resources, will not highlight significant differences in performance unless the ability to transition from non-functional to functional CM technician is introduced. Scenarios 1 and 2 reflect this with scenario 1 having $8 \times$ SCT-CM qualified resources (2 per system), while scenario 2 commences with $4 \times$ SCT-CM and $4 \times$ SCT-PM yet lacks trade progression. The remaining models (scenarios 3 through 8) include trade progression and commence with the same resourcing profile as scenario 2. Under these circumstances, the latter years of the 6-year simulation duration provide beneficial information for determining the long-term viability of the flight's maintenance capability.

Prior model execution reflected the real-world case of increased staff numbers reducing the time between task notifications to commencement while also reducing individual member's task utilisation (expressed as a percentage of each working day). Conversely, reducing personnel numbers results in extended times between notification and commencement and the consequent increase in daily utilisation.

Resourcing incorporates PAF only with the effects of APS inclusion replicated through the PAF resources with posting and other PAF-specific actions disabled.

3 Results

In order to compare the results of models across the various resourcing scenarios, we use the monthly tally of CM events completed within a set time from notification as the output measure. For the examples given below, a 4-h window is used. Clearly, a decrease in CM events completed within 4 h results in a commensurate increase in CM events completed in more than 4 h and, as CM takes precedence over PM, delays in CM completion times immediately impact PM commencement and completion times.

Scenario 1 reflects the standard discrete event model (no agent-based inclusions) which allows for CM and PM tasking and annual leave requirements and is used as the "base case" for comparison.

Scenario 1, with $8 \times$ SCT-CM qualified resources for the duration, performs exceptionally well throughout (see Fig. 1), while scenario 2, with $4 \times$ SCT-CM and $4 \times$ SCT-PM resources and no trade progression suffers with consistently lower performance over the time frame.

Scenario 2, while having a somewhat unrealistic personnel profile with no opportunity for posting or trade progression, highlights the impacts of these effects. The result of locking SCT-PM resources into that authorisation level is a drop in performance through an inability for both resources to undertake CM tasks, although the SCT-PM resources can assist on tasks if requested by the task resourcing requirement. Note also the annual drop in SRT as the SCT-CM authorised resource undertakes annual leave.

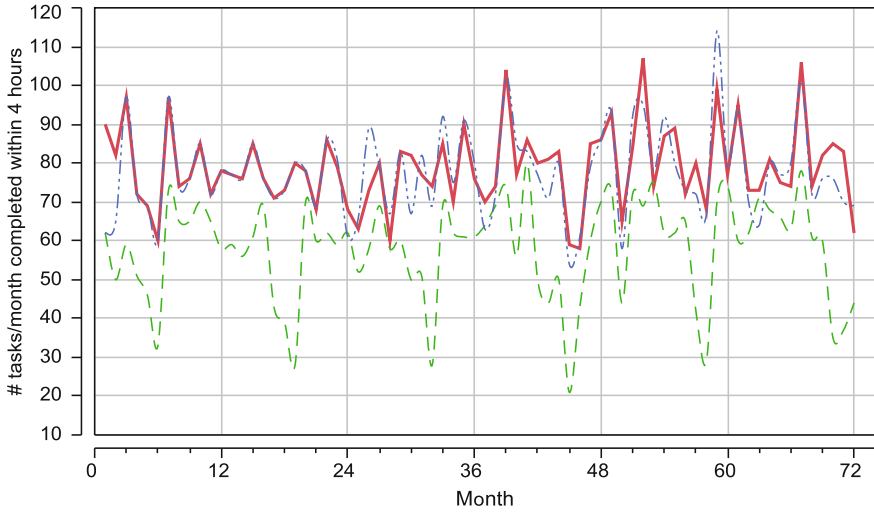


Fig. 1 Monthly task count of tasks completed within 4 h of notification. Scenario 1: solid line (red). Scenario 2: dashed line (green). Scenario 3: dash-dot-dot line (blue)

Scenario 3, using the same initial resource profile as scenario 2, performs almost identically to scenario 1 over the entire time frame despite some minor divergences.

The comparatively high performance of scenario 3 requires further explanation. The initial resourcing profile has $4 \times$ SCT-PM resources, two of which will almost immediately receive SCT-CM authorisations due to their earlier starting dates and immediate attendance on training programs. This additional capability in two of the systems provides sufficient capacity to maintain high-level coverage. After approximately 5 months, the duration at which SCT-PM authorised resources receive SCT-CM authorisations, the remaining two SCT-PM staff gain the higher-level qualification, but little improvement is possible on the already high-level coverage. As resources are not posted, the existing resources increase their authorisations above the SCT-CM level with no adverse effect on performance.

In Fig. 2, we compare the results of the discrete event model with $8 \times$ SCT-CM resources (scenario 1) against the $4 \times$ SCT-CM plus $4 \times$ SCT-PM models with trade progression and posting on a single system (scenario 4), and those with cross-training permitted following SCT-PM authorisation on two systems (scenario 5) and four systems (scenario 6).

Note the effect on performance of posting (scenarios 4 and 5) whereby the ability to maintain the 4-h restoration window decreases immediately after each 12 months of operation. Note also that the effect will be compounded by the availability of places on courses with only 2 places made available on each course. With an inability to meet the necessary training requirements, both the scenario 4 and 5 models (green and blue lines) suffer significantly after the 36-, 48- and 60-month postings indicating severe deficiencies in capability over those periods.

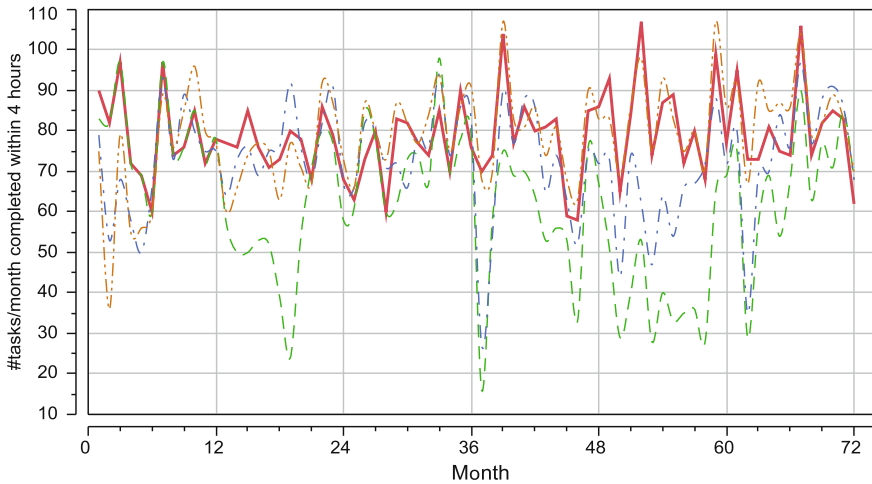


Fig. 2 Monthly task count of tasks completed within 4 h of notification. Scenario 1: solid line (*red*). Scenario 4: dashed line (*green*). Scenario 5: dash-dot line (*blue*). Scenario 6: dash-dot-dot line (*brown*)

The effects of cross-training are also apparent in the scenario 4 and 5 models as highlighted by the quicker recovery after the 48-month posting. In this instance, having some resources trained in an additional system reduces the depth of the dip in successful task count and provides a significant improvement for the remainder of that year.

Adding cross-training across all four systems (scenario 6) results in a system restoration profile largely matching, although in some areas improving on, that of scenario 1 and, consequently, scenario 3.

Modifying the requirement to permit the commencement of cross-training in other systems from SCT-PM to SCT-CM (see Fig. 3) under the currently accepted trade authorisation transition time has little impact on the overall capability when the required duration as SCT-PM is set to 5 months. The divergence after the 36-month posting will be due to insufficient SCT-CM numbers in any given system. This is likely the result of a, possibly unfortunate, combination of posting cycle changes, annual leave and training program attendance. The modelling process has no way of dealing with CM events that cannot be serviced and so they are tabled, awaiting completion when an authorised resource becomes available. The return to capability within the year indicates that a considered approach to resource planning would resolve such a situation in reality.

Extending the duration of authorisations from 5 to 9 months (scenarios 7 and 8), and moving the authorisation level at which cross-training in a new system can commence from SCT-PM to SCT-CM, gives greater opportunity for existing SCT-CM personnel be on leave while the lesser trade authorised personnel remain, incapable of being assigned to CM tasks. As a consequence, the CM task list quickly increases in length creating ever longer delays for task completion and

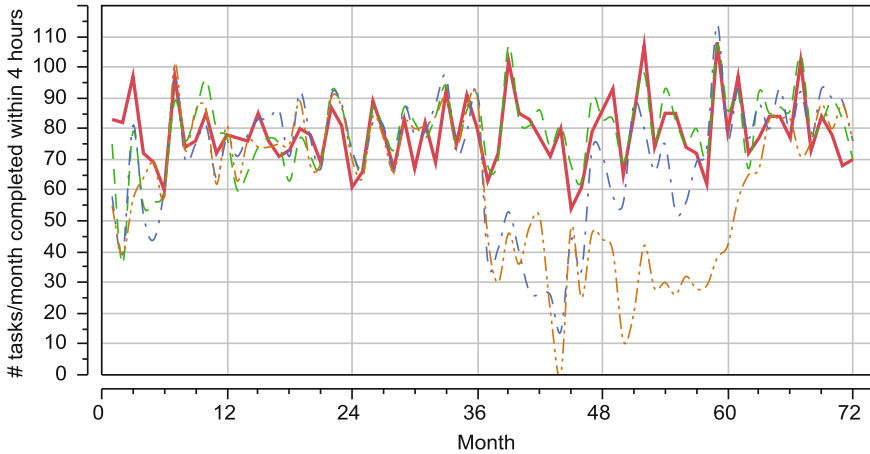


Fig. 3 Monthly task count of tasks completed within 4 h of notification. Scenario 3: solid line (*red*). Scenario 6: minimum SCT-PM at 5 months prior to cross-training with 4 systems enabled: dotted line (*green*). Scenario 7: minimum SCT-CM at 5 months prior to cross-training with 4 systems enabled: dash-dot line (*blue*). Scenario 8: minimum SCT-CM at 9 months prior to cross-training with 4 systems enabled: dash-dot-dot line (*brown*)

overall recovery to within acceptable restoration windows. In Fig. 3, this recovery occurs near month 60.

Scenario 1 has a static profile with two resources trained to SCT-CM level in each system making it approximately operationally equivalent to exclusively APS staff. As noted in other simulation runs (results not presented here), the addition of non-posting (APS) personnel adds significant stability to the workforce's capability to maintain its performance profile. The fact that the modelling above finds similar performance between scenarios 3 and 6 highlights the overly optimistic results provided by discrete event modelling when performance aspects are significantly altered by changes in agents yet agent-based functionality is not present in the model.

4 Conclusion

The results presented in this chapter emphasise the need to ensure that the type of modelling used and the level of detail incorporated are commensurate with critical factors directly associated with the outcome of interest, and those factors indirectly affecting the outcome of interest due to their effects on the overall operation. For example, with long-term sustainability of maintenance coverage as our outcome of interest, we must consider the number of personnel (for any given workload) as an example of a direct impact, while the changes in personnel through posting cycles, trade authorisation progression etc., have a significant impact through indirect means.

These findings show that discrete event modelling, in the absence of agent-based characteristics, provides an overly optimistic pattern of flight maintenance team performance. The initial team (scenario 1) equivalent to $8 \times$ APS resources at SCT-CM authorisation achieves approximately the same monthly rate of task completions as the team defined in scenario 6 which incorporates training throughout their posting tenure in up to the full complement of four systems, noting that the final authorisation state of each resource is dependent on their posting cycle, availability of training programs etc.

Changes in the authorisation level at which cross-training is permitted, e.g. changing from SCT-PM to SCT-CM in their current system prior to commencement of training in another system, carry a performance impact dependent on the time required to achieve the SCT-CM authorisation. At the current duration of approximately 5 months, little overall impact is noted.

Posting cycles impose a dramatic drop in overall performance capability, and while some resources posting in will carry trade authorisations, resources new to the Air Force are unlikely to carry any authorisations. In either case, the simulation identifies the extent of the impact and highlights the need for care when considering the overall trade authorisation profile due to posting cycle changes.

Further, the results shown above indicate that extended time in the role, such as through extended postings, and hence, the inclusion of long-term APS staff improves the overall stability of the workforce trade authorisations and the overall capability to achieve desired system restoration time frames.

This chapter has demonstrated that multi-agent modelling holds significant advantages over non-agent-based discrete event simulations for predicting workforce capability when the forecasting involves variability and interactions between agents and the system in which they operate. The greater the complexity, inherent variability and interaction within the system, the greater the benefit gained through the agent-based inclusions.

5 Study Limitations

The model design was deliberately narrow in its focus (44WG maintenance teams) to assist in the assessment of risk in relation to the maintenance teams' capacity and capability while transitioning to Air Traffic Management future equipment. It is acknowledged that the 44WG maintenance team is a sub-element of the wider Air Force maintenance capability, and therefore, changes within 44WG will have an impact on overall Air Force maintenance capability.

The following elements of the model would benefit from further development:

- A summative analysis for the ground technical workforce across Air Force to assess the impact of changes to the system on the wider organisation.
- Annual leave is currently algorithmic and therefore does not reflect the reality of leave being managed to minimise the impact on operations.

- Personnel posting into the simulation are assumed to be at the trade level of TP in one system only. Most maintenance personnel posted in, with the exception of those straight out of trade training, will arrive with some level of experience and/or authorisations.
- APS are treated in the same manner as PAF with regard to trade progression and cross-training. However, no ability for an APS member to leave the simulation is provided.

The ability to make better decisions, whether using a quantitative predictive model or a qualitative process, remains dependent on the quality of the available data. The use of better modelling methods promotes a greater acceptance of such models, and hence, an increased awareness of, and emphasis on, the type and quality of data to be collected.

References

1. Ntuen, C.A., Park, E.H.: Simulation of crew size requirement in a maintained reliability system. *Comput. Ind. Eng.* **37**, 219–222 (1999)
2. Robards, P.: Applying simulation to defence workforce modelling. In: Defence Human Sciences Symposium. <https://dhss.net.au/presentations/applying-simulation-defence-workforce-modelling-0> (2015). Accessed Sep 2016
3. Garza, R., Hill, R.R., Mattioda, D.D: Using simulation to analyze the maintenance architecture for a USAF weapon system. *Simulation* **89**, 294–305 (2013)
4. Oostrum, van J.M., et al.: *Int. Anesth. Res. Soc.* **107**, 1655–1662 (2008)
5. Feng, Y., Fan, W.: A hybrid simulation approach to dynamic multi-skilled workforce planning of production line. In: Tsinghua University Winter Simulation Conference (2014)

Application of Field Anomaly Relaxation to Battlefield Casualties and Treatment: A Formal Approach to Consolidating Large Morphological Spaces

Guy E. Gallasch, Jon Jordans and Ksenia Ivanova

Abstract Field anomaly relaxation (FAR) is a qualitative strategic planning technique useful for generating a range of alternative future scenarios in a complex, multi-dimensional problem space. It utilises the principles of general morphological analysis, in that a set of possible future scenarios are constructed by first defining the set of dimensions ('sectors') and their possible values ('factors'), then filtering out scenarios with combinations of parameters that are inconsistent with each other. This is an exercise that is inherently based on human judgement. As such, limitations on the dimensionality of the problem space being considered are generally required in order to keep the problem within the bounds of a human's cognitive processes. For example, the number of sectors and number of factors within each sector are generally restricted to no more than seven and five, respectively. Further, clustering of plausible scenarios that are 'similar' is generally performed to further reduce the resulting morphological space. This paper defines a mathematical framework for the computation of two heuristics, degree of overlap and degree of divergence, to assist humans in dealing with higher dimensionality, more complex problem spaces by helping to identify potential candidate sets of scenarios for clustering. We take a didactic approach to the concepts and mathematical formulation of these heuristics using a simple example, before briefly presenting the preliminary results of a case study on defining the scenario space for tactical battlefield casualty treatment. Ultimately, we wish to establish a comprehensive set of scenarios for high-level assessment of potential technologies for rendering enhanced battlefield casualty care and treatment.

Keywords Field anomaly relaxation • Morphological spaces • Battlefield casualty treatment

G.E. Gallasch (✉) · J. Jordans · K. Ivanova
Defence Science and Technology Group, Edinburgh, SA 5117, UK
e-mail: guy.gallasch@dsto.defence.gov.au

© Springer International Publishing AG 2018
R. Sarker et al. (eds.), *Data and Decision Sciences in Action*,
Lecture Notes in Management and Industrial Engineering,
DOI 10.1007/978-3-319-55914-8_24

327

1 Introduction

In the context of operations research, general morphological analysis (GMA) [1] refers to a systematic approach for multi-dimensional problem structuring [2]. The term ‘morphological space’ is used to describe a solution space: a set of all plausible configurations over the dimensions of the problem.

One widely known method for generating a morphological space is field anomaly relaxation (FAR) [3], a strategic planning technique that focuses on exploring alternative, comparably plausible future scenarios [4]. Although the terminology differs between GMA and FAR, both approaches comprise essentially the same key elements:

- Form an initial world view of the alternative future scenarios (in the case of FAR) that could unfold within the area of interest. Define the set of parameters (dimensions in GMA, sectors in FAR) that encompass the problem space. These are generally limited to seven plus or minus two, due to the limits of human working memory.
- Establish possible alternative values for the parameters (states or conditions in GMA, factors in FAR). The Cartesian product of parameters gives the set of all possible combinations of parameter values (configurations in GMA, whole field configurations or scenarios in FAR).
- Perform a cross-consistency assessment [2] to reduce the total set of possible configurations/scenarios by eliminating those that are not internally consistent (GMA) or manifestly inconsistent (FAR), i.e. those with parameter values that cannot coexist.

The result is a set of configurations/scenarios that are considered plausible. Cross-consistency assessment in FAR can be achieved by performing a pair-wise comparison of factors from different sectors. This step can substantially reduce the morphological space by filtering out anomalous scenarios. However, due to the combinatorial nature of these methods, this plausible set may still be substantial, so it is common for practitioners of FAR (e.g. [5, 6]) to perform an additional clustering of ‘similar’ scenarios to further reduce the dimensionality of the morphological space. Primarily, this is through aggregating ‘similar’ factors within a given sector. FAR then goes on to develop a so-called Faustian Tree that describes how the identified futures could evolve. We limit ourselves in this paper to the scenario generation steps.

While generation of the set of all possible scenarios is a well-known mathematical operation (Cartesian product of sectors), both assessing the consistency of fields on a pair-wise basis and subsequent clustering of similar scenarios remain largely based on human judgement. The latter can be problematic, particularly when the set of plausible scenarios remains large and does not easily fit within the limits of human cognition.

To address this limitation, we propose a mathematical framework and method for automating the assessment of ‘similarity’ of sets of scenarios. Our proposed

method does not automate the clustering process itself; rather, it provides the human with assistance in assessing similarity between sets of scenarios through two heuristics: degree of overlap and degree of divergence, between sets of scenarios. Ultimately, the human still makes the decision on which scenarios to cluster/aggregate. As alternatives, we briefly looked at related techniques for assessing ‘differences’ such as Hamming distance, run length encoding, Euclidean distances, and angles between higher dimensional vectors, but we felt that they were either not appropriate, overly complex, or not easily adapted to this specific problem.

Our interest in FAR stems from an interest in future technology solutions that can provide enhanced battlefield casualty treatment and desire a set of scenarios against which potential new technology solutions can be assessed. In this instance, the use of FAR is demonstrated through generation of possible future scenarios in which battlefield casualties may occur. We present some preliminary results of this FAR analysis towards the end of the paper.

2 Relaxation: An Introductory Example

2.1 Generating Plausible Scenarios

For illustrative purposes, suppose we are interested in constructing scenarios about future weather conditions. Based on our internal view of possible future contexts, one possible set of sectors and corresponding sets of factors are shown in Fig. 1a.

Formally, let:

- $S \in \mathbb{N}^+$ be the number of sectors,
- $Sectors = \{Sector_1, Sector_2, \dots, Sector_S\}$ be the set of sectors,
- $f_i \in \mathbb{N}^+$ be the number of factors in $Sector_i, f_i = |Sector_i|, i \in \{1, \dots, S\}$, and
- $Sector_i = \{factor_{i,1}, factor_{i,2}, \dots, factor_{i,f_i}\}$ is the set of factors comprising $Sector_i$,

Then:

- $Scenarios = Sector_1 \times Sector_2 \times \dots \times Sector_S$ is the set of all possible scenarios, and
- $\omega = (factor_{1,j_1}, factor_{2,j_2}, \dots, factor_{S,j_S}) \in Scenarios, j_i \in \{1, \dots, f_i\}$ is a single scenario from the set of possible scenarios.

In this example, $S = 3$ and the Cartesian product of the sectors gives a total of $f_1 * f_2 * f_3 = 4 * 4 * 3 = 48$ possible scenarios. It is usual when applying FAR to arrange sectors so that a memorable (and/or amusing) acronym can be created, and to refer to specific scenarios using a subscript notation applied to the acronym. For example, the acronym of sector names here is WRS, and the scenario comprising W2 (light breeze), R3 (shower) and S2 (partially cloudy) is identified by $W_2R_3S_2$.

(a)

Sectors:	(W)ind	(R)ain	(S)ky
Factors:	W1: still (no wind)	R1: no rain	S1: Clear (no clouds)
	W2: light breeze	R2: drizzle	S2: partially cloudy
	W3: strong breeze	R3: shower	S3: totally cloudy
	W4: gale	R4: heavy rain	

(b)

	W1	W2	W3	W4	R1	R2	R3	R4
R1	3	3	3	3				
R2	2	3	3	3				
R3	2	2	3	3				
R4	1	2	2	3				
S1	3	3	3	3	3	0	0	0
S2	3	3	3	3	2	2	2	2
S3	3	3	3	3	2	2	2	3

Fig. 1 Future weather: a Sector and factor definitions; and b pair-wise consistency ratings

Clearly, some of these are manifestly inconsistent, e.g. it is not reasonable to expect heavy rain when the sky is clear, while others are relatively independent, e.g. amount of cloud versus strength of wind. The pair-wise assessment of consistency of factors comprises 40 comparisons, shown in Fig. 1b using a matrix representation. Rather than a simple binary ‘consistent/inconsistent’ rating, it is common to extend the comparison of each pair of factors to a graduated rating. We have adopted a four-point scale: 0 (manifestly inconsistent), 1 (likely inconsistent), 2 (likely consistent), and 3 (manifestly consistent).

There are a number of ways this could be expressed formally. We choose a partial function representation. Let:

- *Ratings* = {0, 1, 2, 3} be a set of consistency ratings, corresponding to the ratings described above,
- *Factors* = $\bigcup_{i=1}^S Sector_i$ be the set of all factors, and
- *Score*: *Factors* × *Factors* → *Ratings* be a partial function that maps pairs of factors to a rating, such that
 - $\forall i_1, i_2 \in \{1, \dots, S\}, i_1 \neq i_2, \forall j_1 \in \{1, \dots, f_{i_1}\}, \forall j_2 \in \{1, \dots, f_{i_2}\}, Score(factor_{i_1, j_1}, factor_{i_2, j_2}) = rating \in Rating,$
 - $\forall i \in \{1, \dots, S\}, \forall j, k \in \{1, \dots, f_i\}, Score(factor_{i, j}, factor_{i, k})$ is undefined.

Then:

- $\omega = (factor_{1,j_1}, factor_{2,j_2}, \dots, factor_{S,j_S}) \in Scenarios$ is a plausible scenario if and only if $\forall i_1, i_2 \in \{1, \dots, S\}, i_1 \neq i_2, Score(factor_{i_1,j_{i_1}}, factor_{i_2,j_{i_2}}) > 0$, and
- $Scenarios_{plausible} \subseteq Scenarios$ is the set of plausible scenarios, such that $Scenarios_{plausible} = \{\omega | \omega \text{ is a plausible scenario}\}$.

For this example, there are three pair-wise comparisons required to assess each scenario: wind versus rain, wind versus sky and rain versus sky. A scenario is considered manifestly inconsistent if at least one pair of factors within the scenario is manifestly inconsistent. It turns out that there are 12 such scenarios, hence 12 of the 48 scenarios can be excluded from further consideration. An example is the scenario comprising $W_2R_3S_1$, where R3 (shower) versus S1 (no clouds) has been given a rating of 0 in Fig. 1b.

In addition to filtering out manifestly inconsistent scenarios, the four-point rating scale can be used to provide an indication (heuristic only, as it is based on qualitative assessment) of the overall internal consistency of each scenario, by taking the summation of the three pair-wise comparisons for each scenario.

Formally, let $InternalConsistencyScore: Scenarios \rightarrow \mathbb{N}$ be a function that computes the overall internal consistency score of a scenario, $\omega = (factor_{1,j_1}, factor_{2,j_2}, \dots, factor_{S,j_S}) \in Scenarios$, such that

$$InternalConsistencyScore(\omega) = \sum_{i_1=1}^{S-1} \sum_{i_2=i_1+1}^S Score(factor_{i_1,j_{i_1}}, factor_{i_2,j_{i_2}})$$

A histogram of overall consistency scores for plausible scenarios is given in Fig. 2a, with plausible scenarios shown in green and manifestly inconsistent scenarios shown in orange. The five most internally consistent scenarios (score of 9) comprise the four with no rain and clear skies, and the one with heavy rain, total

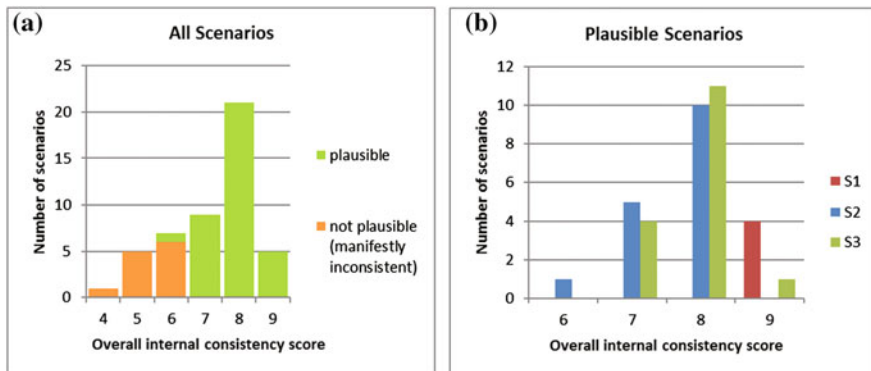


Fig. 2 Histograms of internal consistency scores: **a** plausible vs manifestly inconsistent scenarios, and **b** plausible scenarios broken down by sky sector factors

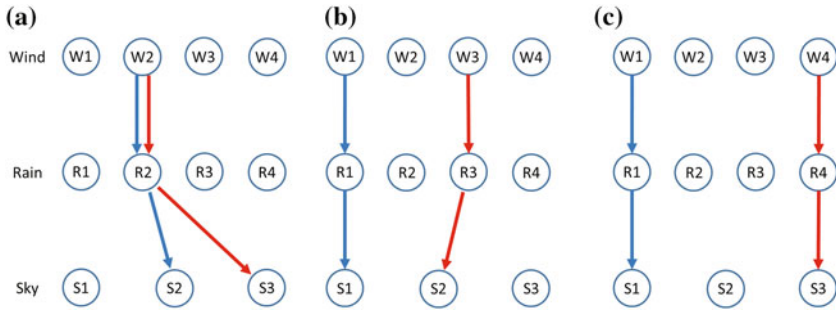


Fig. 3 Examples of scenarios that are **a** partially overlapping; and **b, c** non-overlapping

cloud cover and gale force winds. The least consistent scenario that is still plausible (score of 6) comprises heavy rain with only partial cloud cover and no wind. Intuitively, this makes sense, given our everyday observations of the weather (and hence our mental models of the weather) and how likely it is that particular factors from one sector will occur together with particular factors from other sectors.

Internal consistency, as the name suggests, is based on how likely individual pairs of factors will occur together, internally within a scenario. Despite this, it is tempting to equate the overall internal consistency heuristic with overall likelihood of occurrence. We advise caution in doing so. The scenario internal consistency (how well the factors within a scenario ‘fit together’) need not be directly related to the probability of occurrence of the scenario. For example, consider no rain with clear skies and a light breeze versus a bad storm with gale force winds, total cloud cover and heavy rain. Both are both equally internally consistent (score of 9), but in practice it may be that many more of the former are observed than the latter (One way around this is to consider marginal probabilities, as in [7, 8].).

2.2 Histograms as a Means of Exploring the Morphological Space

A method that we found useful for exploring the resulting set of plausible scenarios is the use of histograms. These provide some insight into the similarities and differences between sets of scenarios across the set of factors for a given sector, in terms of their overall consistency score. An example is given in Fig. 2b, in which histograms of the overall internal consistency scores are given across the three sky sector factors.

The differences between scenarios (in terms of internal consistency) across S1, S2 and S3 are evident in Fig. 2b. Scenarios containing S1 (clear skies) are in general more internally consistent than those containing S2 (partly cloudy) or S3 (complete cloud cover), and S2 scenarios tend to be less internally consistent than

S3 scenarios. Means and standard deviations can be calculated for the distributions of internal consistency scores, but there is a limit to the usefulness of this type of derived information: quantitative data derived from subjective assessments does not increase its objectiveness. It also says little about how similar the corresponding sets of scenarios are. A more insightful question may be to ask how similar/different the sets are, and hence how appropriate it would be to consider aggregating the corresponding factors, and hence clustering the scenarios. We present one possible way of answering this below.

3 Similarity Heuristics for Sets of Scenarios

We propose two heuristics for assessing the similarity of sets of scenarios. The first assesses the extent to which the two sets cover the same subsets of the morphological space. We call this heuristic the degree of overlap. The second is more subtle and assesses not just the extent to which scenarios in the two sets are different, but also how different. We call this the degree of divergence. We introduce and describe these two heuristics below.

3.1 *Similarity Heuristic 1: Degree of Overlap*

It is useful to think of the degree of overlap heuristic as ‘how much of the scenarios are the same between the two sets’.

3.1.1 Comparing Single Scenarios

Calculating the degree of overlap heuristic is relatively intuitive. To begin, let us consider two single scenarios, depicted diagrammatically in Fig. 3a: $W_2R_2S_2$ (blue) and $W_2R_2S_3$ (red). They differ only in the factor selected from the rain sector. Intuitively, as two of the three sectors overlap, we can say that these two scenarios have a degree of overlap of 0.667, or 66.7%.

Now, consider the two scenarios, $W_1R_1S_1$ (blue) and $W_3R_3S_2$ (red), depicted in Fig. 3b. These two scenarios do not overlap at any sector, hence we say that they have a degree of overlap of 0, or 0%. Further, consider the two scenarios in Fig. 3c. As in Fig. 3b, they also do not overlap on any sector, and hence have a degree of overlap of 0, but could be considered ‘more different’ than the two scenarios in Fig. 3b (We will come back to this notion of ‘how different’ when we describe the ‘degree of divergence’ heuristic.).

Formally, let:

- $FactorMatch: Factors \times Factors \rightarrow \{0, 1\}$ be a function that matches factors, such that $\forall factor_{i_1, j_1}, factor_{i_2, j_2} \in Factors,$

- $$FactorMatch(factor_{i_1, j_1}, factor_{i_2, j_2}) = \begin{cases} 1, & factor_{i_1, j_1} = factor_{i_2, j_2} \\ 0, & factor_{i_1, j_1} \neq factor_{i_2, j_2} \end{cases}$$

- $$s_1 = (factor_{1, j_1}, factor_{2, j_2}, \dots, factor_{s, j_s}) \in Scenarios,$$

and

- $$s_2 = (factor_{1, k_1}, factor_{2, k_2}, \dots, factor_{s, k_s}) \in Scenarios,$$

Then, $ScenarioOverlap: Scenarios \times Scenarios \rightarrow [0, 1]$ is a function that takes pairs of scenarios and returns the degree of overlap between those two scenarios, such that $\forall s_1, s_2 \in Scenarios,$

$$ScenarioOverlap(s_1, s_2) = \frac{\sum_{i=1}^S FactorMatch(factor_{i, j_i}, factor_{i, k_i})}{S}$$

Theoretically, a degree of overlap of 100% is possible only when comparing two identical scenarios, which is not a useful thing to do (Note that no two scenarios will ever be identical in the morphological space, as this is a mathematical property of the Cartesian product on sets).

3.1.2 Comparing Sets of Scenarios

When extending this concept to the degree of overlap between two sets of scenarios, we originally developed a sector-wise comparison of coverage of factors by the two sets. The number of factors in each sector that are members of at least one scenario in each set was calculated and normalised by the number of sectors. While simple, this is not particularly useful, as overlapping factor coverage in the two different sets may be by means of wildly differing scenarios. As an alternative, we propose a more straightforward, if more computationally expensive, extension of the single scenario comparison that works by computing the degree of overlap for each pair of scenarios across the two sets, and normalising the summation of all pair-wise comparisons by the number of pairs compared.

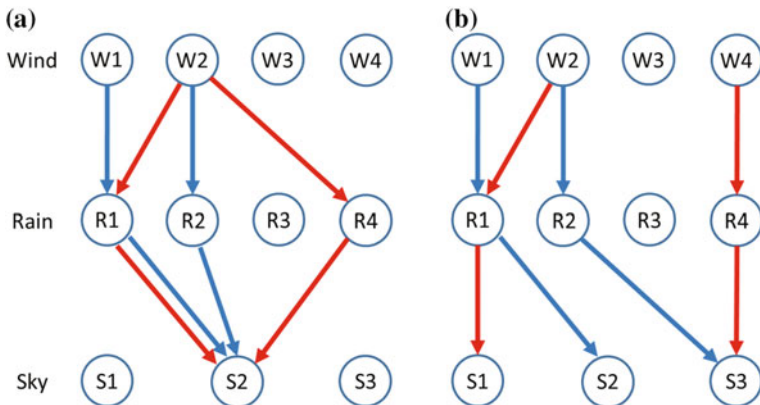


Fig. 4 Two examples of two sets of two scenarios (*blue* and *red*), with the same sector-wise degree of overlap but a different scenario-wise degree of overlap

To illustrate the difference between sector-wise comparison and scenario-wise comparison, consider the two examples of two sets of two scenarios given in Fig. 4, one set depicted in blue and the other in red. In both examples, the blue and red sets exhibit the same sector-wise degree of overlap (the two sets overlap by one factor only for each sector, giving $(\frac{1}{4} + \frac{1}{4} + \frac{1}{3})/3 = 0.278$) despite their visual appearance suggesting that the two sets in Fig. 4a overlap more than the corresponding two sets in Fig. 4b. Scenario-wise, there are four comparisons to be made: each of the blue scenarios against each of the red. This results in a scenario-wise degree of overlap of 0.583 for Fig. 4a, and 0.25 for Fig. 4b ($(\frac{2}{3} + \frac{1}{3} + \frac{2}{3} + \frac{2}{3})/4 = 0.583$ and $(\frac{1}{3} + \frac{0}{3} + \frac{1}{3} + \frac{1}{3})/4 = 0.25$, respectively).

Formally, let $S_1, S_2 \subset Scenarios$ be two non-empty sets of scenarios (i.e. $S_1, S_2 \neq \emptyset$, thus implying that $|Scenarios| > 0$). Then, *DegreeOfOverlap*: $2^{Scenarios} \times 2^{Scenarios} \rightarrow [0, 1]$ is a function that takes two sets of scenarios and returns the degree of overlap between those two sets of scenarios, such that $\forall S_1, S_2 \subset Scenarios$,

$$DegreeOfOverlap(S_1, S_2) = \frac{\sum_{s_1 \in S_1} \sum_{s_2 \in S_2} ScenarioOverlap(s_1, s_2)}{|S_1| * |S_2|}$$

As when comparing individual scenarios, it is only possible to obtain a degree of overlap of 100% when the two sets being compared are identical. While this is allowed, it is not useful to compare two identical sets, or even two sets that are not disjoint.

3.2 Similarity Heuristic 2: Degree of Divergence

The degree of overlap gives us a heuristic that tells us how much of two sets of scenarios are ‘the same’. We would also like to know not only that some proportion of the sets of scenarios overlap, but where they do not overlap, how ‘different’ they are (i.e. if they are different, then how different?). We call this the degree of divergence.

3.2.1 Comparing Single Scenarios

To do this, we can make some mild assumptions about the structure of factors within each sector. The first is that, generally, each sector comprises factors that cover a spectrum of possibilities, trending from ‘good’ through to ‘bad’ (or ‘bad’ to ‘good’, it does not matter which). All three sectors in our running example are such. The second is that there is a monotonic, equally spaced progression (based on whatever measure is appropriate) from one factor to the next within each sector, e.g. R1–R4 represents progressively heavier rain. Hence, if we consider a scale from 0 to 1 from one end of the spectrum (e.g. R1) to the other (e.g. R4), then we can say that the four rain factors divide the spectrum into three (equal) parts. The distance between factors then translates to a measure of difference between them.

With these mild assumptions in mind, let us return to Fig. 3. The two scenarios in Fig. 3a both contain W2, and so they differ by 0 for this sector. The rain sector also differs by 0 between the two scenarios. However, the sky sector differs by 0.5 (S2 vs. S3). Summing these together and normalising by the number of sectors give us an overall degree of divergence of $(\frac{0}{3} + \frac{0}{3} + \frac{1}{2})/3 = 0.167$. So we can say that these two scenarios have degree of overlap of 0.667, and a degree of divergence of 0.167. Alternatively, if the blue scenario contained S1 instead of S2, the degree of overlap would be the same (0.667), but the degree of divergence would increase from 0.167 to 0.333.

For Fig. 3b, c, the two scenarios both have the same degree of overlap (0) but degrees of divergence of $(\frac{2}{3} + \frac{2}{3} + \frac{2}{2})/3 = 0.778$ and $(\frac{3}{3} + \frac{3}{3} + \frac{2}{2})/3 = 1.0$, respectively, i.e. two scenarios in Fig. 3b are quite different, but the two in Fig. 3c are as different as it is possible to be.

Formally, $\forall i \in \{1, \dots, S\}, \forall j, k \in \{1, \dots, f_i\}$, let:

- The total order relation, \leq_{Sector_i} , be defined for each sector such that $factor_{i,j} \leq_{Sector_i} factor_{i,k}$ if and only if $j \leq k$
- *Difference: Factors* $\rightarrow [0, 1]$ be a function that maps from a factor to a value between 0 and 1 that indicates its position within the spectrum of its corresponding sector, such that $\forall factor_{i,j} \in Factors$,

$$\text{Difference}(\text{factor}_{i,j}) = \begin{cases} 1.0, & f_i = 1 \\ \frac{j-1}{f_i-1}, & f_i > 1 \end{cases}$$

Then, $\text{ScenarioDivergence}: \text{Scenarios} \times \text{Scenarios} \rightarrow [0, 1]$ is a function that takes pairs of scenarios and returns the degree of divergence between those two scenarios, such that $\forall s_1, s_2 \in \text{Scenarios}$,

$$\text{ScenarioDivergence}(s_1, s_2) = \frac{\sum_{i=1}^S |\text{Difference}(\text{factor}_{i,j_i}) - \text{Difference}(\text{factor}_{i,k_i})|}{S}$$

3.2.2 Comparing Sets of Scenarios

It is straightforward to extend the degree of divergence from single scenarios to sets of scenarios in the same way as the degree of overlap.

Formally, let $S_1, S_2 \subset \text{Scenarios}$ be two non-empty sets of scenarios as previously. Then, $\text{DegreeOfDivergence}: 2^{\text{Scenarios}} \times 2^{\text{Scenarios}} \rightarrow [0, 1]$ is a function that takes two sets of scenarios and returns the degree of divergence between those two sets of scenarios, such that $\forall S_1, S_2 \subset \text{Scenarios}$,

$$\text{DegreeOfOverlap}(S_1, S_2) = \frac{\sum_{s_1 \in S_1} \sum_{s_2 \in S_2} \text{ScenarioDivergence}(s_1, s_2)}{|S_1| * |S_2|}$$

To explain, lets return to Fig. 4a calculating the degree of divergence of each combination of blue and red scenarios and normalising against the number of comparisons give a degree of divergence of $((\frac{1}{3} + \frac{4}{3} + \frac{1}{3} + \frac{2}{3})/3)/4 = 0.222$ between the blue and red sets. Likewise, the degree of divergence for the sets in Fig. 4b is $((\frac{5}{6} + \frac{5}{2} + \frac{4}{3} + \frac{4}{3})/3)/4 = 0.5$. So, not only do the sets in Fig. 4b overlap less than those in Fig. 4a (0.25 vs. 0.583), they are also more divergent (0.5 vs. 0.222).

Two final notes. Firstly, each sector does not need to adhere to a scale from 0 and 1, and the progression from one factor to the next need not be linear (i.e. the factors need not be 'equally spaced' along that scale). A scale from 0 to 1 and a linear progression along this scale are by no means necessary and have been chosen only for the purposes of simplicity of explanation. In general, both can be arbitrarily chosen (presuming there is a good reason). Secondly, there may be occasions when a sector comprises categorical factors that cannot be easily compared in this way, e.g. {red, blue, yellow}. For such cases, we propose the sector be excluded from this analysis and defer to human judgement.

(a)

Sectors:	D: Access to medical support and patient information	R: Type of first responder	A: Complexity of access	S: Availability of supplies	T: Complexity of incident	I: Severity of injury	C: Combat conditions
	D1: Compromised access - 50+ minutes to next level of care, no access to medical voice or video support, no diagnostics or patient info	R1: Combatant responder	A1: Restricted - significant weather conditions, jungle, or heavy urban terrain, any integral evacuation options unavailable	S1: Basic field bandages and first aid kit	T1: High complexity - multiple casualties more than 5, or civilian and military, all ages including aged and children	I1: Priority 1 - life threatening	C1: Care Under Fire
	D2: Limited access - 10 - 50 mins to next level care, voice access to medical support, limited diagnostics - blood pressure and pulse	R2: Medic responder	A2: Moderately restricted - restricted access due to inclement weather, complex terrain, limited evacuation options integral to the unit and may be available	S2: Field medic supplies including limited clotting bandages, chest tubes and needles, pain medication	T2: Moderately high complexity - 2-4 casualties, or civilian and military	I2: Priority 2 - threat to limb	C2: Medium Level of Hostilities, no direct fire
Factors:	D3: High degree of access - in situ or within 5 mins to next level care, access to voice and video medical support, extensive diagnostics - ECG, blood pressure, laryngoscopy, ultrasound	R3: Medical Officer / Nursing Officer responder	A3: Easy - no weather impacts, clear terrain, evacuation options integral to the unit and available	S3: Field medic supplies plus extended medical supplies including blood (or blood agents), advanced drugs, oxygen, splints and spinal boards, defibrillator etc	T3: Medium complexity - 4 casualties, military only	I3: Priority 3 - minor casualty	C3: Permissive Environment
					T4: Low complexity - single casualty, military only		

Fig. 5 Preliminary results of FAR analysis for battlefield casualty occurrence

(b)

	D1	D2	D3	R1	R2	R3	A1	A2	A3	S1	S2	S3	T1	T2	T3	T4	I1	I2	I3
R1	3	1	0																
R2	2	2	2																
R3	0	2	3																
A1	3	1	0	3	1	0													
A2	1	3	1	3	3	0													
A3	0	1	3	2	2	2													
S1	3	1	0	3	1	0	3	3	2										
S2	2	3	2	0	3	1	2	3	3										
S3	0	1	3	0	1	3	0	1	3										
T1	3	3	3	2	3	3	2	2	3	3	3	3							
T2	3	3	3	2	3	3	2	2	3	3	3	3							
T3	3	3	3	3	3	2	3	3	3	3	2	2							
T4	3	3	3	3	3	1	3	3	3	3	2	1							
I1	3	3	3	3	2	1	3	3	3	3	2	1	3	3	3	3			
I2	3	3	3	3	2	1	3	3	3	3	2	1	3	3	3	3			
I3	3	3	3	3	2	1	3	3	3	3	2	1	3	3	3	3			
C1	3	2	1	3	2	3	3	2	1	3	3	0	3	3	3	3	3	3	3
C2	3	3	2	3	3	1	1	2	3	2	3	2	3	3	3	3	2	2	2
C3	1	2	3	3	2	2	0	2	3	1	2	3	3	3	3	3	0	0	0

(c)

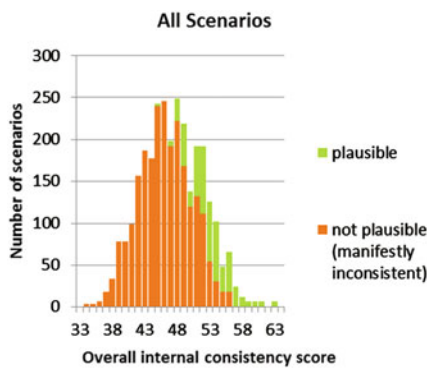


Fig. 5 (continued)

4 Application of FAR to Battlefield Casualty Occurrence

Figure 5 presents, in brief, our application of FAR to battlefield casualty occurrence, and some preliminary analysis on the resulting plausible scenarios. The sectors and factors, factor pair-wise comparison and histogram of scenario overall internal consistency scores (possible vs. plausible) are presented in Fig. 5a, b and c, respectively. In this example, our sectors produce the acronym DRASTIC.

A series of histograms broken down by factor (not shown here) suggests that ‘I: Severity of Injury’ has no impact on the overall internal consistency of a scenario, and ‘T: Complexity of incident’ has almost no impact. In hindsight, and with more practical experience, this can be inferred directly from the factor pair-wise comparisons in Fig. 5b. What is less obvious is that a permissive combat environment (C3) appears in no plausible scenarios whatsoever. Again, with hindsight and

experience, this is relatively obvious from the pair-wise comparisons, but is something that could easily be missed without appropriate computer tool support.

The next step is to test the efficacy of our degree of overlap and degree of divergence heuristics on this case study, to see if they accord with the above observations, and to see what additional insights can be gained in terms of the similarity and divergence of scenarios across factors.

Further, a detailed use case has been created corresponding roughly to the $D_1R_1A_1S_1T_3I_1C_2$ scenario (see [9] for details). The intent behind developing such use cases is to provide context to the selected automated and autonomous technologies and situate their use within army logistics. Use case development also helps to elicit issues for further examination. In this instance, a hypothetical capability able to project enhanced battlefield casualty treatment 'forward' into the battlespace is situated within this specific scenario.

Some issues that emerged from this use case include establishing the value proposition, asset availability and control, asset protection and security, noise and visual signature, and ability to function within a range of environments and weather conditions. It is also worth noting that many of these also hold true for the use of autonomy in other applications. Going forward, we wish to develop additional use cases that cover other, dissimilar, scenarios as a means of enhancing our understanding of the technology context and helping to elicit additional issues for further examination.

5 Discussion and Conclusions

Having established a mathematical formulation for our two heuristics allows them to be implemented in computer tools. One possible candidate is the Scenario Analysis Tool Suite [7, 8, 10], which provides additional methods for the treatment of sectors, factors and scenarios than those presented here. We believe our heuristics would be a nice complement to the factor compatibility-based clustering method, the probabilistic treatment given to scenarios (through the addition of marginal probabilities) and the integer linear programming methods for obtaining a balanced mix of scenarios in this tool.

As mentioned earlier, limits can be imposed on the dimensionality of the problem spaces that can be considered. The 'magic numbers' of seven sectors, and up to five factors per sector are often used. The suggestion is that these guidelines are primarily due to limits of human cognition. To a computer, however, thousands, and even millions, of scenarios are not necessarily problematic. This also exposes a limitation of FAR: scenarios that are less internally consistent have a higher tendency to be discarded. This has the potential to remove many of the less obvious/intuitive, and potentially more interesting scenarios from consideration, as the less obvious outliers tend to be those that correspond to black or grey swan events, with a higher disruptive potential than those more obvious ones down the 'middle of the road'.

Ultimately, we would like the results of the above FAR scenario generation process to feed directly into computer-based qualitative and quantitative models for assessing enhanced battlefield casualty treatment technology solution options, with sectors equating to model parameters, factors equating to parameter values and scenarios equating to instantiations of the model. As part of this future work, by avoiding the limitations of human working memory providing bottlenecks on the dimensionality or cardinality of the morphological space, we hope to avoid (or at least alleviate) elimination of less obvious but potentially more disruptive scenarios, and hence avoid one of the criticisms of the FAR method.

References

1. Zwicky, F.: *Discovery, Invention, Research—Through the Morphological Approach*. Toronto. The McMillan Company (1969)
2. Ritchey, T.: *General Morphological Analysis: A General Method For Non-quantified Modelling*. Swedish Morphological Society (2013)
3. Rhyne, R.: Technological Forecasting within alternative whole futures projections. *Technol. Forecast. Soc. Chang.* **6**, 133–162 (1974)
4. Rhyne, R.: Field anomaly relaxation: the arts of usage. *Futures* **27**(6), 657–674 (1995)
5. Stephens, A.K.W.: *Future urban states: a field anomaly relaxation study*. Technical Report, DSTO-TR-1910, Land Operations Division, Defence Science and Technology Organisation (2006)
6. Duczynski, G.A.: A practitioner's experience of using field anomaly relaxation (FAR) to craft futures. In: 18th International Conference of The System Dynamics Society, Bergen, Norway, 6–10 Aug 2000 (2000)
7. Nguyen, M.-T.: Strategic planning tool suite: an approach of combining scenario analysis methods. *ASOR Bull.* **27**(3), 2–11 (2008)
8. Nguyen, M.-T., Dunn, M.: Some methods for scenario analysis in defence strategic planning. Technical Report, DSTO-TR-2242, Joint Operations Division, Defence Science and Technology Organisation (2009)
9. Ivanova, K., Gallasch, G.E., Jordans, J.: Automated and autonomous systems for combat service support: scoping study and technology prioritisation. Technical Note, awaiting approval, Land Division, Defence Science and Technology Group (2016)
10. Dilek, C.: *The Scenario Analysis Tool Suite: A User's Guide*. General Document, DSTO-GD-0560, Joint Operations Division, Defence Science and Technology Organisation (2009)

Network Analysis of Decision Loops in Operational Command and Control Arrangements

Alexander Kalloniatis, Cayt Rowe, Phuong La, Andrew Holder, Jamahl Bennier and Brice Mitchell

Abstract In 2014, Commander Joint Task Force (JTF) 633 asked deployed operations analysts to examine information flow between deployed units of the Australian Defence Force (ADF) in the Middle East Region (MER) and to consider the contribution to decision-making of flows within and between the various deployed headquarters, Headquarters Joint Operations Command (HQJOC) and other strategic and coalition nodes. Data were collected across the theatre, using attributes such as frequency, means, network and type. Data were also collected on the *information function* of the interaction, which relates to the role of the communication within Boyd's Observe–Orient–Decide–Act (OODA) loop. Insights from these data were communicated to Commanders in theatre in late 2014 and early 2015. Further analysis used a representation of the C2 arrangements to generate a network diagram showing both information function and frequency. The network may now be visualised as a full socio-technical system, with nodes representing both organisational entities and information artefacts or systems, or as a

A. Kalloniatis (✉)

Behaviour & Control, Decision Sciences, Joint and Operations Analysis Division (JOAD),
Defence Science & Technology (DST) Group, Canberra, Australia
e-mail: alexander.kalloniatis@dsto.defence.gov.au

C. Rowe

Force Design, JOAD, DST Group, Canberra, Australia
e-mail: cayt.rowe@dsto.defence.gov.au

P. La · A. Holder

Behaviour & Control, Decision Sciences, JOAD, DST Group, Canberra, Australia
e-mail: phuong.la@dsto.defence.gov.au

A. Holder

e-mail: Andrew.holder@defence.gov.au

J. Bennier

Operations Support Centre, DST Group, Edinburgh, Australia
e-mail: jamahl.bennier@dsto.defence.gov.au

B. Mitchell

National Security & ISR Division, DST Group, Edinburgh, Australia
e-mail: brice.mitchell@dsto.defence.gov.au

© Springer International Publishing AG 2018

R. Sarker et al. (eds.), *Data and Decision Sciences in Action*,
Lecture Notes in Management and Industrial Engineering,
DOI 10.1007/978-3-319-55914-8_25

343

pure social network (human-to-human). This approach extends the Situation Awareness Weighted Network (SAWN) framework, creating an OODA Weighted Network model presented here as OODAWN. This paper will discuss the context for the work, the data collection techniques and the resulting network diagrams. We demonstrate the utility of the model by discussing insights regarding the C2 arrangements, both within theatre and from theatre back to Australia.

Keywords C2 • Information flow • Networks • OODA • Operations

1 Introduction

Command and control (C2) of a modern combined joint task force¹ is necessarily complex and continuously evolving. There will always be tension between the range of appropriate and important command chains, for example between national command and combined task force command, and also between joint functionality and specific environment management, such as air operations management. This is particularly pertinent for the Australian Defence Force (ADF) in the Middle East Region (MER), where there are a number of distinct operations relying on shared intelligence, logistics and other support elements and contributing to a range of combined task forces.

In late 2014, the Commander Joint Task Force (JTF) 633 asked deployed operations analysts for support in examining the C2 arrangements for ADF operations in the MER. This study set out to examine information exchange within and between the various deployed headquarters, Headquarters Joint Operations Command (HQJOC) and other strategic and coalition nodes. The study was undertaken soon after the commencement of Operation OKRA, which is Australia's contribution to the international effort to combat the Daesh (also known as ISIL) terrorist threat in Iraq and Syria [1]. The purpose of the work was to characterise the flow of information amongst ADF deployed units and back to Australian organisations and how this supported decision-making. An ability to describe the flow of information can provide insight into the effectiveness of organisational structures and help highlight opportunities to simplify the information flow.

The purpose of this paper is to document the scientific model and empirical method developed in the course of this study. To that end, we focus on how known properties of the C2 system may be detected in this network analysis in order to validate the model. First, we lay out the theoretical model and describe the data collection. We then present results as a set of network diagrams. We discuss the insights these offer into functioning of the C2 arrangements, particularly

¹Combined refers to a multiple nation force and Joint refers to force comprising multiple services such as the Army, Navy and Air Force.

highlighting how these compare with doctrinal or intended structures. The paper concludes with a picture of how this work may be folded into ongoing support to the ADF.

1.1 Theoretical Foundation

In this paper, we are concerned with quantifying the information flow through a system of individuals, units, staff and commanders in the administration and command of deployed forces, all of which may be seen as aspects of C2. Definitions of C2 are numerous and subtly varied, but ADF doctrine suffices: “C2 is the system empowering designated personnel to exercise lawful authority and direction over assigned forces for the accomplishment of missions and tasks” [2]. This draws attention not just to individuals, namely commanders, but to a *system*—pointing to a fundamentally distributed nature of C2. A scientific definition of C2 consolidates this: Pigeau and McCann separately define Command (creative exercise of will) and Control (structures and processes), then give C2 as “establishment of common intent to achieve coordinated action” [3, 4]. Implied here is that the intent should be common across all individuals, staff and commanders of the system and that the object of this is *action*. This final word links to the other popular military model for C2 that of John Boyd’s Observe–Orient–Decide–Act (OODA) loop. (Though originally promulgated by Boyd through the US DoD via briefing slides [5], the OODA model is now part of the academic literature, for example [6]. In recent years, the model has been extended from individuals to whole organisations [7].) Boyd’s C2 model compactly unites actions with the *cognitive* processes of the individual: *orientation and decision* are activities we readily associate with processes of individual human mind.

However, there is another approach which takes as unit of analysis distributed systems of staff and information displays. Hutchins’ Distributed Cognition holds that cognition is not purely “in the head” of an operator but manifested through a “computational ecology” of tools—such as for navigation, seen in the people and instruments of a ship’s Combat Information Centre (CIC) [8]. The ecological dimension of another common military term, *Situation Awareness (SA)*, has also been emphasised by Smith and Hancock [9]. Here, SA is “adaptive, externally directed consciousness” involving individual agents interacting with an environment, seeking knowledge about the environment and undertaking “directed action” within that environment. This approach invokes another type of “cognitive loop” to describe the dynamic between individual and environment, the Neisser’s Perception–Action Cycle [10], which enjoys strong support in the cognitive psychology literature. These ideas have been brought together by Stanton et al. [11] into a comprehensive empirical approach to *Distributed SA (DSA)* that provides the most direct antecedent to our approach in this paper. Again, the system is the unit of analysis here. SA is not resident in the head of an individual, rather emergent in interactions through the ecology of individuals and information objects and displays.

The empirical method associated with DSA involves data collection about three types of networks: the social network of communications between human individuals; the propositional network of relationships between information objects and functions; and finally the task network of activities that operators undertake within the system, be it a CIC, an air control centre or an energy control centre.

There is one more important model here that completes our survey of background theoretical constructs. The term Situation Awareness originates in the work of Endsley who was concerned with the challenges of fighter pilots in dealing with a rapidly changing environment and the multiple avionics displays in the cockpit of 1970s F-15s [12]. Her “three-level” model of SA has entered the lexicon of most military and civilian practitioners: SA is the “perception of environmental elements with respect to time or space, the comprehension of their meaning, and the projection of their status after some variable has changed”. Even though the Endsley model has been advanced to cover “team” and “shared” SA, it has been critiqued by proponents of DSA for its isolation of SA as being “in the head”. Though SA, particularly through the lens of Endsley’s model, is often associated with C2, the link is rarely explicitly stated. Endsley’s three levels sit within a larger model involving Decision, Action and other evaluation and control feedbacks. Each of Neisser’s, Boyd’s and Endsley’s models may be seen as equivalent with different levels of fidelity²: Boyd’s Observe and Orient equate to Endsley’s three levels Perception–Comprehension–Projection.

Previous work has unified the Endsley and Stanton models of SA into the Situation Awareness Weighted Network (SAWN) model [14, 15] and associated empirical method. As with DSA, SAWN collects and arranges data related to networks of interactions—though here social and information objects are combined into a single “socio-technical” network.

In this paper, we now expand SAWN to cover the entire OODA loop. To build a practical empirical approach, we simplify the SA scale to three levels and add two new levels to cover Decision and Action. In the following section, we describe a data collection instrument that collects network interactions—*who talks to whom*—but also assembles *how* (type of nature, type of information or social artefact), how often (frequency), and what we term the information *function*: Perception, Comprehension, Projection, Decision, and Action. This improved model has been termed the OODA Weighted Network or OODAWN model.

1.2 Data Collection

This study comprised two data collection activities: a preliminary survey followed by a more comprehensive survey across a broader set of respondents.

²Grant and Kooter [13] argue that “Orient” in Boyd’s OODA loop does not include Planning, whereas Endsley’s model does; we would argue that the Projection into future states is simply not as elaborated with Boyd’s level of fidelity.

The preliminary survey was a quick turnaround activity to support an immediate need of the Commander. The preliminary results indicated that a more systematic survey was warranted and it is this second data collection that is the subject of this paper.

The objective of this survey was to collect data from deployed ADF units and cells across the Middle East Region about who they communicate with, the form of the communication and the information function discussed above. The survey captured both information that was provided to another unit and information received from another unit. Respondents were requested to complete an Excel spreadsheet hosted on SharePoint.

Considerable effort was taken to construct a data collection spreadsheet that would enable consistent labelling of senders and recipients, as well as to minimise effort on part of the respondents. Senders and recipients were identified by a “Group”, “Unit” and “Position”. For example, “Group” could be “JTF633”, Unit might be “HQJTF633”, and Position might be “J1”. Thus, all inter-unit communication originating in the HQJTF633 J1 cell would then be captured against this sender. Condensing the full range of possible recipients into a three-level list was a non-trivial exercise and added considerable value to the quality of the data. The list of positions comprised the following: (i) relevant deployed individual positions or cells and (ii) other units and positions with which information flow was anticipated but were not part of the deployed ADF units of interest. Due to operational priorities, not all of the deployed units provided data for this survey. However, complete coverage of a core selection of units was achieved. The network of respondents can then be separated into the following:

- i. Core deployed units. Responses received from each relevant position (or cell) in these units so inferences can be drawn regarding any gaps in information flow within this core network.
- ii. Other deployed units. Some responses received from these units, but coverage is not complete. Inferences can be drawn regarding the nature of information flow, and care is required before assigning significance to any gaps.
- iii. Coalition units. Not surveyed. The data about information flow to and from these units have been provided by ADF deployed units.
- iv. Australian Strategic groups (these are groups and services in Australia, including HQJOC and units within the services). Not surveyed. The data about information flow to and from these units have been provided by ADF deployed units.

In addition to the three levels of identifiers (group, unit and position), respondents also selected a geographic location for each sender and recipient. This drop-down list was not context-dependent, so the location information provided a quality assurance check on the data.

Each information transmission was characterised (by the respondent) against five metrics: information function, information type, frequency, means and network, which are detailed in Tables 1 and 2. The data on means and network were used by the Theatre Information Manager to inform IT infrastructure planning.

Table 1 Characteristics of information exchange

Information type	This is the nature of the communication, including whether it is formal or informal
	Person to person (written incl email, letter, chat); meeting (incl VTC, telecon); SIGNAL, SITREP, incident report; standing instructions; minute; decision brief; noting brief; CONOPS; agenda, programme or schedule; RFI; RFI response; data or statistics; register; report; PowerPoint slides; form; contract or SOW; business case; other
Frequency	Hourly; daily; three times a week; twice weekly; weekly; fortnightly; monthly; quarterly; less than quarterly; other
Means	Email; SharePoint; network drives; in person; chat; video link; audio link; objective; other
Network	17 networks listed, covering different classifications and including coalition networks

Table 2 Information functions using the OODA Weighted Network Model

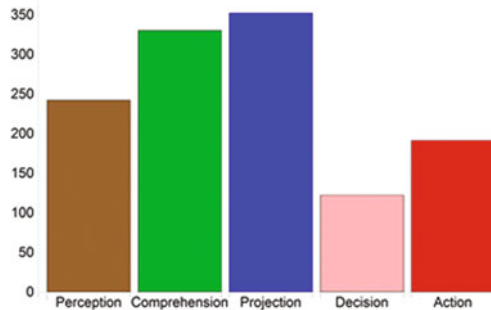
Information function	Description	Examples
Perception	Report of facts: What is there? When was it there? What is/was it doing?	Contact and detection reporting, log stats, personnel stats, incident reports
	Reporting of individuals, groups, platforms or environmental events of significance	
Comprehension	Provides analysis of detected individuals, groups, platform or environmental events, describing their current or recent activity	Providing analysis, e.g. Situation Report (SITREP)
	Comprehension is associated with understanding why these events and assets are where they are, and how they affect the surrounding region	
	Analysis of context, history of behaviours	
Projection	Analysis of activities of individuals, groups, platform or environmental events comparing their current or recent activity with a history or pattern in order to anticipate future developments or providing a schedule of future activities of Blue Force elements	Prediction, threat assessment, activity schedule, course of action analysis briefs, etc.
	This is the highest level of SA and draws together Perception and Comprehension, by making predictions on the future of the aforementioned events and assets	
	Deductions about future behaviours or statement of known future	

(continued)

Table 2 (continued)

Information function	Description	Examples
	activities based on a schedule or programme	
Decision	Brief providing recommended courses of action and/or seeking endorsement of an articulated decision from an approving authority, or issuing an endorsed decision	Decision briefs
Action	Orders requiring actions or tasks to be undertaken by assigned force elements	Task Orders (TASKORDs), Fragmentary Order (FRAGO)
	Drafting or issuing instructions to be undertaken by assigned units	

Fig. 1 Histogram of the number of links in the C2 network according to the information function; this representation also shows the colour allocations for the information function used in later network diagrams



1.3 Results and Discussion

These data were analysed within NetMiner as a network of positions, or nodes, and links, which are the instances of information flow identified by the respondents. Collected together the entire dataset represents a network of 351 nodes and 1237 links, which would generate an impenetrable diagram if shown as a whole. For this reason, we provide quite focused lenses on the network. Figure 1 shows the total number of links according to their information function. We see that the Endsley SA levels dominate, with Comprehension and Projection the most represented functions, the latter marginally higher.

By frequency, these break down into two primary groups: 323 occur daily or faster, and 586 occur within the weekly time frame (once, twice or three times per week) so that 70% of the data were in the weekly or faster frequency categories. This already paints a picture of what one may expect of C2 in the deployed context: fast time frames where information directly sensed from the environment plays a strong role and where decision-making needs to be a step ahead of the adversary so that anticipation is paramount, but also where the articulation of decisions as information artefacts is minimal.

With this in mind, we now zoom into the networks themselves. We give networks where nodes represent the transmitter (“from”) and recipient (“to”) of a communication, regardless of the method (document, face-to-face, email, chat). Links are coloured by information function according to the scheme used in Fig. 1 and have thickness according to the frequency, with thickest for the most frequent information exchanges.

We combine a set of networks in Fig. 2 where we have separated according to frequency: daily (or faster), weekly (or faster, but slower than daily), monthly (or faster, but slower than weekly) and slower than monthly. We observe in (a) that the fastest—daily—cycles are dominated by “Projection” and “Action” evident in the larger number of blue and red links in the first panel. Contrastingly, the weekly cycle in (b) is strongly dominated by Comprehension and Projection. We see moreover that in (a), Perception, though sub-leading, is more strongly linking between coalition and tactical units with brown links more visible in the lower left of centre parts of the diagram. Contrastingly, Comprehension strongly figures between the headquarters and Australian-based agencies seen in the number of links to the right of the diagrams for both the daily and weekly cycles. This pattern persists into the slower cycles (b)–(c), with Comprehension exclusively the domain of interchanges between the headquarters and domestic agencies but Projection across the entire space with coalition elements playing a significant role.

We now show in Fig. 3 a cut of the data only showing those nodes which directly provided data in the second collection—and therefore reflect fairly both

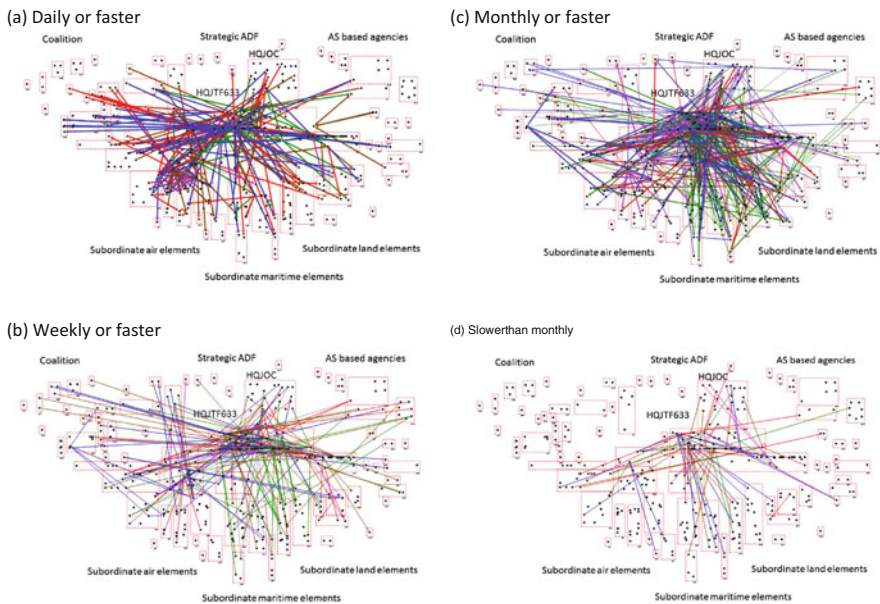
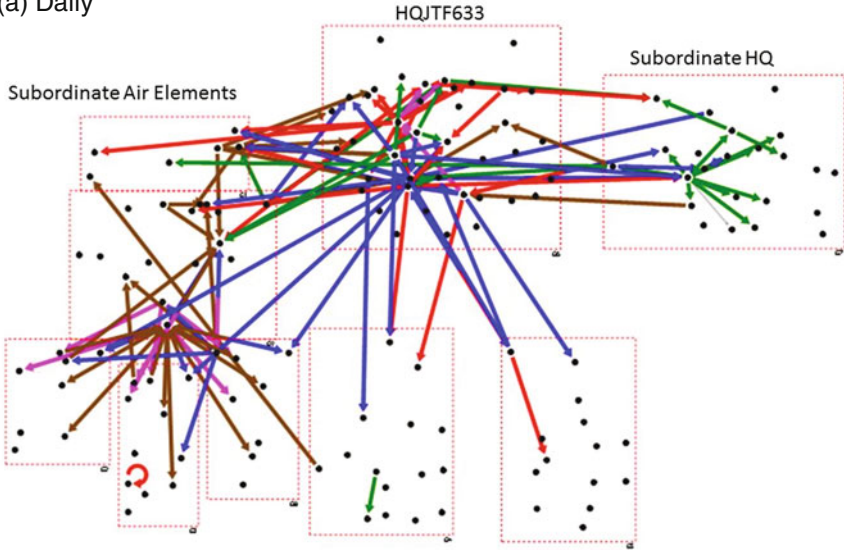


Fig. 2 Network diagrams for entire node set broken down according to frequency where link colour is according to the convention in Fig. 1

(a) Daily



(b) Weekly

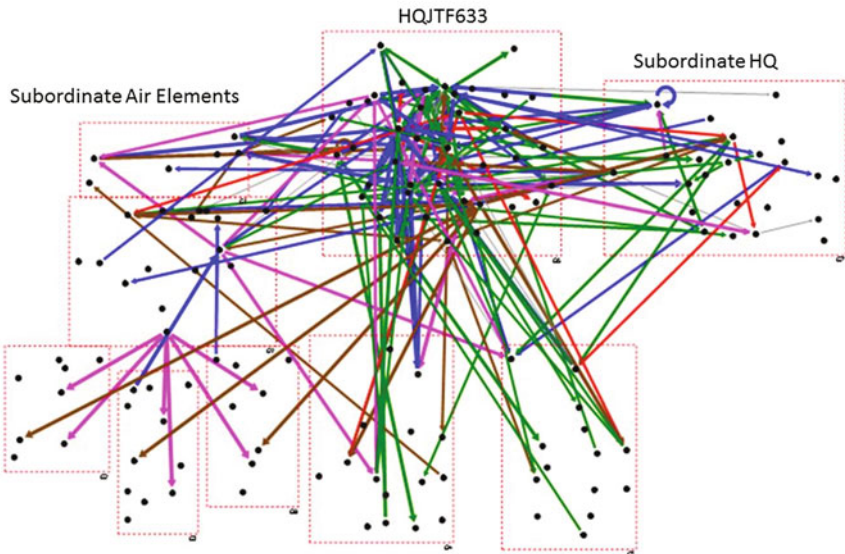


Fig. 3 Subset of nodes representing directly sampled individuals or units, separated into daily and weekly flows with colours again as in Fig. 1

inputs and outputs. Here, the large box in the top centre represents HQJTF633, with other HQs alongside and subordinate tactical elements below; of the latter, units overseeing various air platforms, to which we come later, are situated on the left-hand side. We only show the daily and weekly interactions in the two panels. Panel (a) shows a nearly clean separation of information functions: Perception in the air-based units, Projection linking HQJTF633 across all units, and Comprehension largely occurring between the headquarters. Panel (b) is quite different where now Decisions are propagating through the air units (as well as from HQJTF633 to immediate subordinate units) whilst Comprehension is occurring between HQJTF633 and its subordinate units. Projection, though less copious than Comprehension here, occurs largely at the HQJTF633 level. We therefore observe very different parts of the OODA cycle at different tempos and between different parts of the overall C2 system: air elements largely on a daily cycle focused around Perception and Decision; the rest of the system at the weekly tempo focused around Comprehension and Projection.

Focussing in on C2 for air operations in Fig. 4, see the above observations repeated: Perception largely confined to the lowest level subordinate air elements, Projection within HQJTF633 and across to its immediate subordinates,

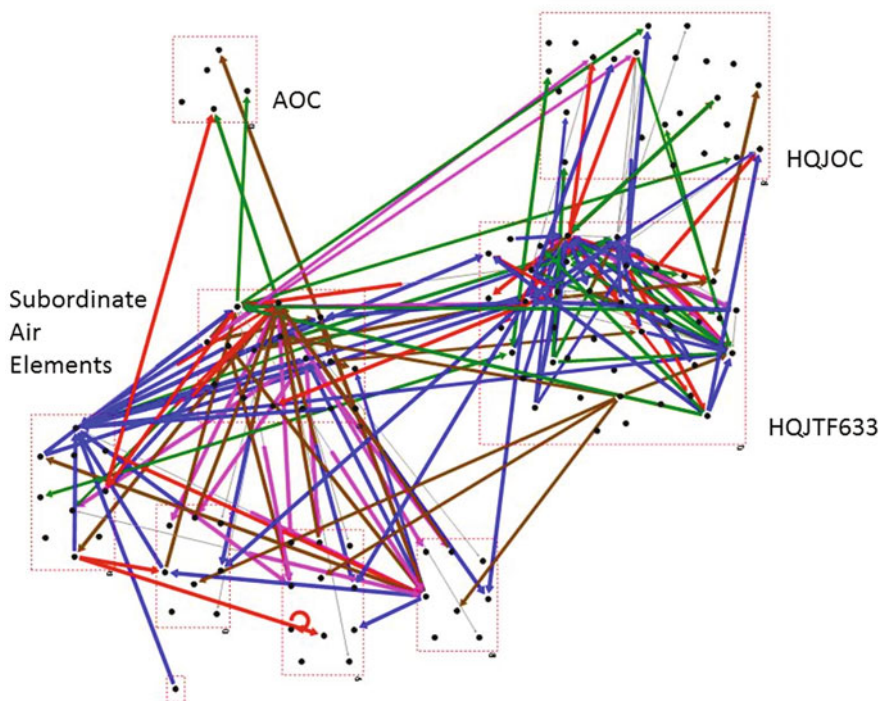


Fig. 4 Subset of nodes focused on command and subordinate air elements and the two main headquarters—only daily and weekly information exchanges are shown

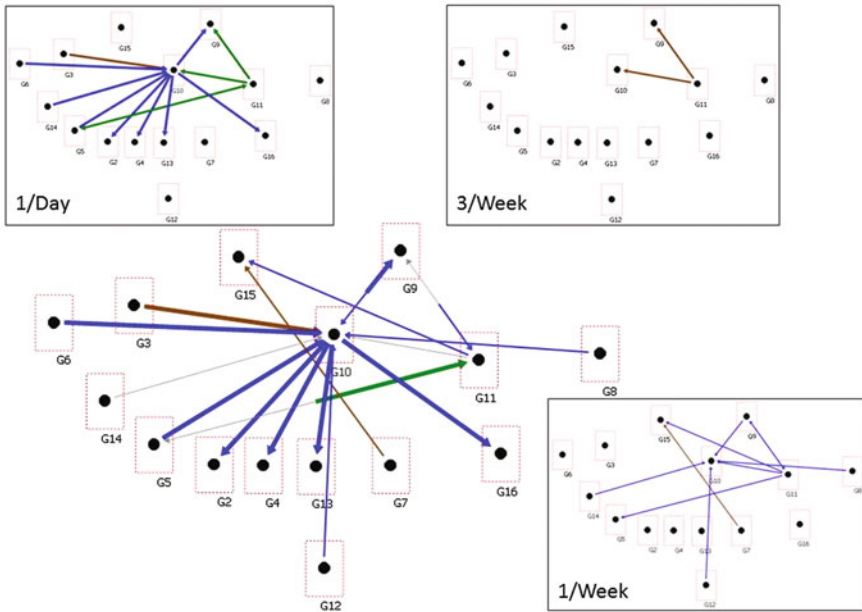


Fig. 5 Nodes representing intelligence officers across the entire network with the main diagram combining daily, 3 times per week and weekly and the individual sets inset

and Comprehension largely directed across the top and upwards. However, we additionally observe a Perception link on the daily tempo between a subordinate air element up to a node in the box placed in the top left part of the diagram. This box represents the Air Operations Centre (AOC)—physically located within HQJOC—but through which DGAIR in their operational role manage air operations on behalf of CJOPS [16]. The detection of this link is consistent with the RAAF doctrinal principle of “centralised control, decentralised execution”.

Finally, we focus in Fig. 5 on information flow between intelligence cells, as this key staff function is heavily reliant on timely and accurate exchange of information. The inset figures show the results across three time scales: daily, weekly and monthly. There is a clear dominance of Projection across these nodes, which is a key contributor to the exchange of Projection information in all the preceding diagrams. Of course, the intelligence function is the military discipline that is fundamental to a commander’s decision-making, providing the highest levels (in the generic sense) of situational awareness. The daily tempo indeed covers all three Endsley SA levels—with a tactical level intelligence officer providing raw Perception to the J2 of HQJTF633, Comprehension building through interactions with other nodes, and then Projection promulgated to subordinate units. We see then a succinct network representation of the deployed Intelligence Preparation of the Battlespace (IPB) process (see, e.g. Joint Publication 5-0 [17] (2011) and Field Manual 34-130 [18] for analogous US elaboration of these activities).

2 Conclusions

This study was a unique opportunity to collect rich data on the information flow in a complex military operational environment. The lexicon developed to describe information exchange in terms of the function, type, means and network provides an elegant breakdown of the key characteristics. This paper discusses inferences drawn regarding decision loops in command and control. However, these data have also been used for planning theatre information infrastructure and analysis of formal versus informal communications.

The Observe–Orient–Decide–Act Weighted Network (OODAWN) model was found to be extremely valuable for characterising the flow of information within deployed ADF units in the Middle East Region. The network representation was useful to illustrate known processes and also to identify situations where the information flow conflicted with the command and control arrangements. There is much more that can be extracted from the data, such as quantitative network metrics and the significance of informal communication. However, the sensitivity of these insights precludes their inclusion in this paper. For the first time, we have quantified the tempo and interactivity of deployed C2 networks that may be built on in future work. In particular, the method is now available for ongoing evaluation and analysis of ADF operations, offering commanders both a quick turnaround on the state of their current C2 structure and longitudinal data on its evolution.

Acknowledgements The authors would like to acknowledge the senior leadership of HQJTF633 from October 2014 to May 2015. This leadership team initiated the study and provided Command directives to facilitate data collection. Sincere thanks to the deployed ADF personnel who took time to provide quality and considered input to this study. The authors would also like to acknowledge the MER Theatre Information Manager for her input to the study design and data collection. Thanks also to Robert Graham, the other half of the deployed analyst team, for his excellent advice and general support with the data collection, and Mathew Zuparic for assistance with NetMiner in processing the preliminary dataset.

References

1. Department of Defence. Operation OKRA. <http://www.defence.gov.au/operations/okra/> (2016). Accessed 23 June 2016
2. Department of Defence (2009) Command and Control. ADDP 00.1, Australia
3. Pigeau, R., McCann, C.: Re-conceptualizing command and control. *Can. Mil. J.* **3**(1), 53–63 (2002)
4. Pigeau, R., McCann, C.: Redefining command and control. In: Pigeau, R., McCann, C. (eds.) *The Human in Command: Exploring the Modern Military Experience*, pp. 163–184. Kluwer Academic/Plenum, New York (2000)
5. Boyd, J. R. (1987) Organic design for command and control. (Unpublished briefing)
6. Osinga, F.: Getting a discourse on winning and losing: a primer on boyd's 'theory of intellectual evolution'. *Contemp. Secur. Policy* **34**(3), 603–624 (2013)
7. Dumbill, E.: *Planning for big data: a CIO's handbook to the changing data landscape*. O'Reilly Media, Sebastopol, California (2012)

8. Hutchins, E.: *Cognition in the Wild*. MIT Press, Cambridge MA (1995)
9. Smith, K., Hancock, P.A.: Situation awareness is adaptive, externally-directed consciousness. In: Gilson, R.D., Garland, D.J., Koonce, J.M. (eds.) *Situation Awareness in Complex Systems*, pp. 59–68. Embry-Riddle Aeronautical University Press, Daytona Beach, Florida (1994)
10. Neisser, U.: *Cognition and reality: principles and implications of cognitive psychology*. Freeman, San Francisco, CA (1976)
11. Stanton, N.A., Stewart, R., et al.: Distributed situation awareness in dynamic systems: theoretical development and application of an ergonomics methodology. *Ergonomics* **45**, 1288–1311 (2006)
12. Endsley, M.R.: Design and evaluation of situation awareness enhancement. In: *Proceedings of the Human Factors Society 32nd Annual Meeting*. Human Factors Society, Santa Monica, CA (1988)
13. Grant, T., Kooter, B., Comparing OODA and other models as operational view C2. In: *Proceedings of the 10th International Command and Control Research and Technology Symposium (ICCRTS)*, McLean, VA, 13–16 June (2005)
14. Ali, I., Kalloniatis, A., et al.: The situation awareness network (SAWN) model. In: *Proceedings of the 19th International Command and Control Research and Technology Symposium (ICCRTS)*, Alexandria, VA, 16–19 June (2014)
15. Kalloniatis, A., Ali, I., et al. The situation awareness weighted network (SAWN) model and method: theory and application. *Appl. Ergon* (2016)
16. Department of Defence: *Command and control in the Royal Australian air force*. AAP **1001**, 1 (2009)
17. USA Department of Defense: *Joint operation planning*. Joint Publication 5–0 (2011)
18. USA Department of the Army: *Intelligence preparation of the battlefield*. Field Man. 34–130, Washington DC (1994)

Impact of Initial Level and Growth Rate in Multiplicative HW Model on Bullwhip Effect in a Supply Chain

H.M. Emrul Kays, A.N.M. Karim, M. Hasan and R.A. Sarker

Abstract Bullwhip effect (BWE) in a supply chain, attributed as the amplification of variance of demand along its route of propagation, compels a manufacturer to bear additional costs in the form of non-optimal resource usage. An accurate forecasting approach for demand prediction can be instrumental in mitigating the BWE. Numerous researchers have attempted to assess the impact of several forecasting approaches such as Moving Average, Single, Double and Triple Exponential Smoothing models, ARIMA, AI-based methods on BWE. However, Multiplicative Holt-Winters approach in mitigating the BWE is not widely exploited particularly with respect to the influence of the initial values of the level and growth rate of this approach. Hence, in this research endeavour, an attempt is made to study the impact of these parameters of the Multiplicative Holt-Winters model on the bullwhip effect in a two-echelon supply chain. Accordingly a simulation is performed in MS Excel along with ANOVA to reveal the significance of the parametric values. The preliminary results demonstrate that the initial values of the level have a significant impact over the bullwhip effect whereas the initial values of the growth rate maintain a U-type relationship. Thus, a scope is revealed for further study to improve the widely adopted Multiplicative Holt-Winters forecasting approach for tackling the BWE through exploration of optimal conditions.

H.M. Emrul Kays (✉) · A.N.M. Karim (✉)

Faculty of Engineering, Department of Manufacturing and Materials Engineering,
IIUM, Gombak, Selangor, Malaysia
e-mail: h.m.emrul.kays@gmail.com

A.N.M. Karim

e-mail: mustafizul@iium.edu.my; anmkarim@gmail.com

M. Hasan (✉)

School of Mechanical and Manufacturing Engineering, UNSW, Sydney, Australia
e-mail: m.hasan@unsw.edu.au

R.A. Sarker (✉)

School of Engineering and Information Technology (SEIT), UNSW, Canberra, Australia
e-mail: r.sarker@adfa.edu.au

© Springer International Publishing AG 2018

R. Sarker et al. (eds.), *Data and Decision Sciences in Action*,

Lecture Notes in Management and Industrial Engineering,

DOI 10.1007/978-3-319-55914-8_26

Keywords Bullwhip effect • Forecasting • Multiplicative Holt-Winters model • Supply chain • ANOVA

1 Introduction

Due to the frequent technological advancements and operational changes as experienced nowadays, the competition, complexities and challenges have increased drastically [15]. At this time of globalization, easier international market access, prompt technological advancement and increased demand of higher quality product, have complicated the scenarios for the contemporary manufacturers. Hence, to contend in this fiercely competitive environment, the manufacturing companies have no choice other than gratifying their customers' needs on time as well as managing their demand and supply process properly. In this context, the urge for a more accurate and reliable forecasting approach, along with an effective management of the supply chain (SC) cannot be overlooked.

However, in managing the SC effectively, perhaps most of the manufacturers are likely to suffer due to the emergence of uncertainty in its demand and supply process [3]. Among which, the uncertainty associated with the supply process is to appear due to the variations in lead times, processing times, transportation times, production rates and employee performance, etc. Whereas, the inaccurate prediction of customer needs, caused by the ill forecasting practices, raises the uncertainty in demand. This inaccuracy in prediction, in turn, feeds into the shared information among the different echelons of a SC and adversely impacts its operational performance [3, 13]. Additionally, an inaccurate estimate amplifies the demand variations while propagating towards the upstream of SC as they are used to forecast the future events within different stages [9, 18]. In the literature, this phenomenon of demand amplification in supply chain is known as the bullwhip effect [14, 16, 5, 22].

The existence of bullwhip effect was first introduced by Forrester [10] as an irrational behaviour of SC. He also identified the lead time variations and the inaccurate forecasts as the main causes of bullwhip effect. Besides for the realistic comprehension of bullwhip effect, Sterman [19] proposed a 'beer distribution game' in the literature. In his research, it is reported that the poor understanding of industrial dynamics and the inappropriate decision-making amplifies the bullwhip effect further. Meanwhile, Lee et al. [14] also attempted to investigate the causes of bullwhip effect in an exemplary SC and observed the usages of inaccurate demand forecasts, the inappropriate order batching, the rapid price fluctuation and the shortage gaming as the most influential parameters. Apart from these endeavours, several other researchers such as Adenso-Díaz et al. [1], Metters [16], Geary et al. [11], Paik and Bagchi [17] have also attempted to realize the sources of bullwhip effect and found the inaccurate forecasts, lack of information sharing, longer production and information lead time, inappropriate anticipation of shortages, price variability and improper lot size as the significant causes.

Despite the recognition of all these sources, a number of researchers have emphasized on the demand forecasting as one of the most significant causes of bullwhip effect [12]. Therefore, it is not unexpected to find numerous research works proposing various forecasting models and methods to assess their impacts over the BWE. For instance, the impact of moving average forecasting method on the bullwhip effect was assessed by Chen et al. [6] in 2000. Whereas, on the same year, Chen et al. [7] also proposed another analytical method to evaluate the impact of simple and double-exponential smoothing techniques on the bullwhip effect. Since there was no realistic analytical solution, the researchers adopted the simulation technique for solving the model and observed a strong dependency among the bullwhip effect and the smoothing constants. They also observed that the more sophisticated forecasting approach could reduce the bullwhip effect significantly. Zhang [24] assessed the impact of moving average, simple exponential smoothing and minimum mean square error method on the bullwhip effect by using the analytical models. Meanwhile in 2005, the impact of moving average, simple exponential smoothing and minimum mean square error method on bullwhip effect were also assessed by Sun and Ren [20].

However, most of this class of proposed analytical impact assessment approaches are largely dependent on the smoothing constants, which limit their scope of assessing the impact of any improved exponential smoothing method on the bullwhip effect. Therefore, nowadays, a number of researchers are relying on the simulation techniques for assessing the impact of different parameters on the bullwhip effect. For instance, Wright and Yuan [23] used a simulation approach to evaluate the impact of Holt's method and Brown's double-exponential smoothing model on the bullwhip effect for a four-echelon supply chain. Barlas and Gunduz [2] adopted a system dynamics approach to assess the impact of simple exponential smoothing model on bullwhip effect by simulation. Even though the bullwhip effect cannot be eliminated entirely by using these sophisticated forecasting models, the researchers were able to mitigate the BWE significantly (approximately by 55%).

Apart from the single and double-exponential smoothing techniques, Bayraktar et al. [3] analysed the impact of additive Winters model on the bullwhip effect of a typical electronic supply chain by featuring the seasonal demand. In addition to the values of smoothing constants, the researchers also attempted to investigate the influences of seasonality and lead time over the bullwhip effect which demonstrated strong relationship. Whereas Chiang et al. [8] have assessed the impact of multiplicative Holt-Winters model on the bullwhip effect. Nevertheless, in both of the last two endeavours, even though the researchers investigated the impact of Holt-Winters model and some of their associated parameters on the bullwhip effect, the impact of the initial values of the level and trend, as evident from the literature, have not yet been investigated. Therefore, to fulfil this potential research gap, an attempt has made in this endeavour to comprehend the influence of smoothing constants, initial level and trend components of the Multiplicative Holt-Winters' model on the bullwhip effect. In this regard, a simulation is performed in MS Excel along with ANOVA analysis to reveal the significance of the parametric values. Subsequent sections of this paper are arranged as follows:

Sect. 2 presents the simulation model. Section 3 highlights the experimental design, while Sect. 4 summarizes the results and discussions. Finally, in Sect. 5, the relevant concluding remarks are made.

2 The Simulation Model

A typical two-echelon automotive supply chain having a single manufacturer and a single retailer is considered in this paper. At the starting of each time period- t , the manufacturer supplies the required goods to the retailer which was ordered L period (lead time = 1 week) ahead. In the meantime, the customers also place their demand which is satisfied by the retailer from on hand inventory. However, if the retailer's stock of an inventoried item is less than the customer demand, the additional amount to meet the shortage is backlogged. After fulfilling the customer demand D_t , the retailer checks the historical demands, forecasts the future requirements and places an order O_t for getting the new supply from the manufacturer. For this typical SC, let us also assume that the order-up-to inventory policy is followed by the retailer. Under which, the order-up-to point Y_t is computed by using Eq. (1).

$$Y_t = \widehat{D}_t^L + z\widehat{\sigma}_{et}^L \quad (1)$$

Here, \widehat{D}_t^L is the forecasted demand over L period, $\widehat{\sigma}_{et}^L$ is the estimated standard deviation of forecast error and the z is a constant relevant to intended service level. Usually, in the literature, the term z is defined as the safety factor. Interestingly, in this typical supply chain as the retailer use the Multiplicative Holt-Winters model to know the forecast- \widehat{D}_t^L , occurrence of variability in computing order-up-to point Y_t is inevitable. In the literature, this amplification in variance is defined as the bullwhip effect caused by forecasting. Nevertheless, in Eq. (1), the term $\widehat{\sigma}_{et}^L$ is the estimator of the standard deviation of forecast error σ_{et}^L , and it is calculated by using the simple exponential smoothing model. Whereas, the retailer's order to the customer O_t is computed by using Eq. (2)

$$O_t = Y_t - Y_{t-1} + D_{t-1} \quad (2)$$

2.1 Multiplicative Holt-Winters Model

The multiplicative Holt-Winters model for seasonal demand forecasting consists of an iterative process by incorporating the estimated level (L_T) defined as:

$$L_T = \alpha(d_T/SN_{T-l}) + (1 - \alpha) * (L_{T-1} + b_{T-1}) \tag{3}$$

Here, d_T is the actual demand for period T , SN_{T-l} represents the seasonal index for period $T - l$, where l denotes the seasonal length and b_T is the growth rate expressed as follows:

$$b_T = \beta(L_T - L_{T-1}) + (1 - \beta)b_{T-1} \tag{4}$$

In Holt-Winters method, the seasonal factors are updated at each iteration. Thus, the seasonal indices, SN_T and SN_{T-l} , respectively, for the periods T and $T - l$, are updated by using following equation:

$$SN_T = \gamma(d_T/L_T) + (1 - \gamma)SN_{T-l} \tag{5}$$

Parameters α , β and γ in Eqs. (3), (4) and (5) represent the smoothing constants. Starting from a certain period and available initial data, the Holt-Winters method is capable to forecast for the next one or more periods. Supposing that τ be the number of such periods and T be the initial period, the forecasted demand ($Y_{T+\tau}$) can be expressed as:

$$Y_{T+\tau} = (L_T + \tau * b_T)SN_{T+\tau-l} \tag{6}$$

The next period's demand (Y_{T+1}), corresponding to $\tau = 1$, by virtue of Eq. (6), could be expressed as:

$$Y_{T+1} = (L_T + b_T)SN_{T+1-l} \tag{7}$$

2.2 Customer Demand Generation

In this research, it is assumed that the customer demand (D_t) exhibits the changing mean, growth rate and multiplicative seasonal patterns. As proposed by Tratar [21] such a data set is generated by using Eq. (8).

$$D_t = base + slope \times t + season \times \sin\left(\left(\frac{2\pi}{season\ cycle}\right) \times t\right) \times t \tag{8}$$

$$+ noise \times snormal() \times t$$

In Eq. (8), $snormal()$ represents the normal random number generator, and the values of the demand parameters base, slope, season and noise are 1000, 100, 50 and 100, respectively.

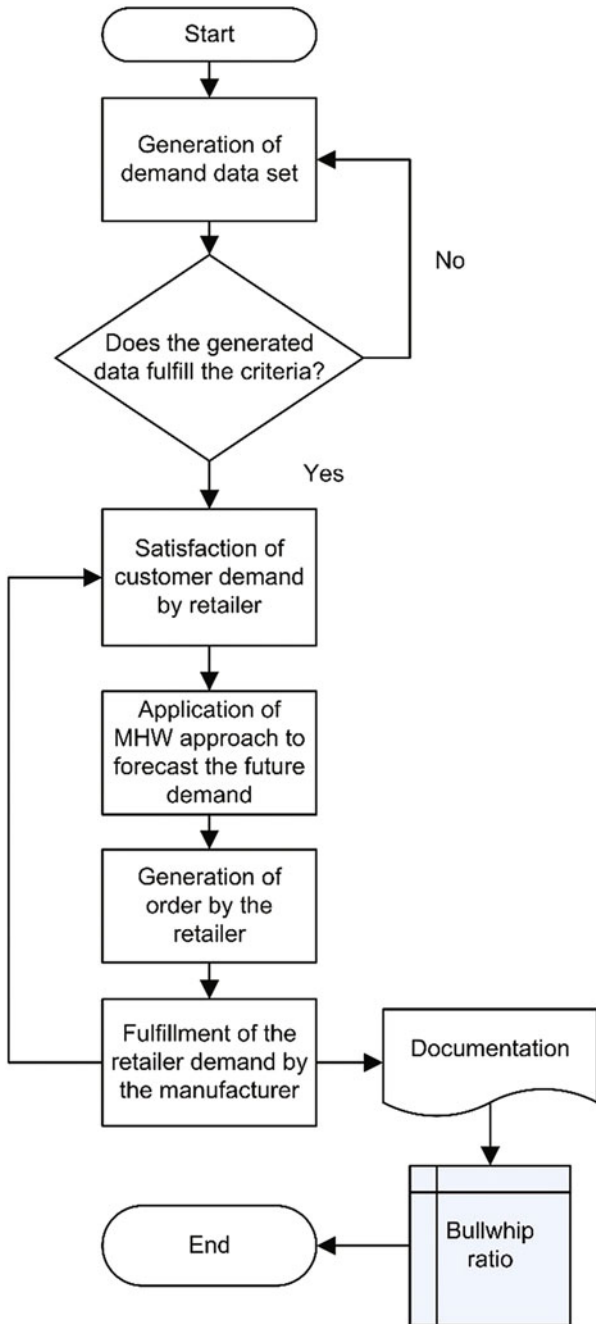


Fig. 1 Flow chart showing the key steps adopted for simulation

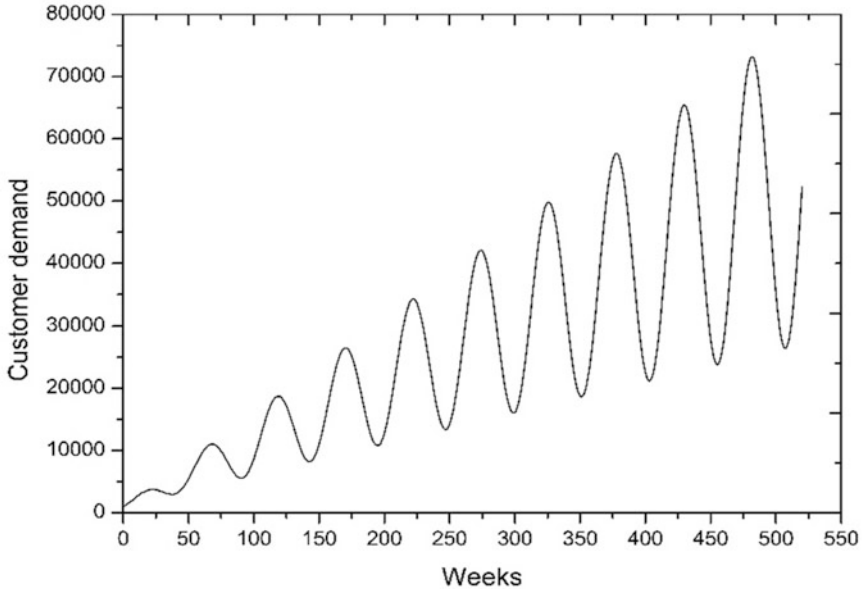


Fig. 2 Generated demand data having the base, slope, seasonality and noise

2.3 Initial Simulation

At this stage, the typical two-echelon supply chain is considered and simulated on MS Excel. The steps of the simulation are represented by the flowchart on Fig. 1.

To conduct the simulation, the demand data for 520 weeks are generated by using Eq. (8) and plotted in Fig. 2. From this data set, the first 156 weeks' data are used to estimate the initial parameters while the remaining 364 weeks' data are utilized to obtain the outputs.

3 Experimental Design

This research endeavour is intended to explore the impact of the parametric values of Multiplicative Holt-Winters model on the bullwhip effect. Hence, in experimental design, the smoothing constants, the initial values of the level and trend are considered as the independent factors. Among these, as adopted in the research work of [3], the values of three smoothing constants are also kept below 0.5. Meanwhile, for the initial level and growth rate, the ranges have been set by

Table 1 Values of independent factors used in the ANOVA test

Smoothing constants			Initial values of level	Initial values of growth rate
Alpha	Beta	Gamma		
0.10	0.10	0.20	1000	50
0.25	0.25	0.30	1500	200
0.50	0.50	0.40	2000	350

encompassing the intercept and slope of the initial data obtained by least squares method (Bowerman [4]). The Bullwhip ratio, which is computed by Eq. 9, has been taken as the dependent factor.

$$Bullwhip = \frac{Var(Order)}{Var(Demand)} \quad (9)$$

The independent variables and three levels of their values that have been used in experimentation are presented in Table 1. Thus, the whole experiment comprises of 243 parametric combinations.

4 Results and Discussion

To assess the autonomous and the combined impact of the smoothing constants, initial values of the level and trend on bullwhip effect, we conducted an ANOVA test. The results obtained by comparing the means through ANOVA analysis in SPSS are summarized in the following subsections.

4.1 Main Effects

The results obtained by ANOVA for bullwhip ratio are summarized in Table 2. It shows that four out of five independent variables considered (i.e. three smoothing constants and the initial value of the level) have significant impacts (since, $p < 0.05$) over the bullwhip effect whereas the impact of initial value of the growth rate is found to be 'not significant' (since, $p > 0.05$) at 95% C.I.

In order to analyse the obtained results, the multiple comparison tests were conducted using the Tukey's procedure. The results are summarized in the Table 3. The obtained results demonstrate that the bullwhip ratio is amplified with any increment of any of the considered independent factors, except for the initial values of the growth rate. However, the bullwhip effect converges to a lower value when the initial growth rate increases from 50 to 200. Interestingly, for any further increment in growth rate ranging from 200 to 350, bullwhip effect diverges towards a higher value. Based on experiments for the 243 parametric combinations,

Table 2 Selected output of ANOVA analysis

Source	Mean square	F	Sig.
Alpha	0.003	133.644	0.000
Beta	0.000	8.795	0.000
Gamma	0.001	24.238	0.000
IniLevel	0.000	17.248	0.000
IniGrowthrate	2.319E-005	1.022	0.362
Alpha * Beta	0.000	19.756	0.000
Alpha * Gamma	0.000	17.394	0.000
Alpha * IniLevel	0.000	10.510	0.000
Alpha * IniGrowthrate	2.355E-005	1.038	0.389
Beta * Gamma	0.000	15.055	0.000
Beta * IniLevel	5.997E-005	2.643	0.035
Beta * IniGrowthrate	0.000	6.232	0.000
Gamma * IniLevel	6.944E-005	3.060	0.018
Gamma * IniGrowthrate	2.757E-005	1.215	0.306
IniLevel * IniGrowthrate	3.734E-007	0.016	0.999
Alpha * Beta * Gamma	0.000	19.547	0.000

Table 3 Selected output of multiple comparison tests

Factors	Level	N	Subsets		
			1	2	3
Alpha	0.1	81	1.001211	1.012494	
	0.25	81	1.002751		
	0.5	81			
Beta	0.1	81	1.003744	1.005922	
	0.25	81		1.006790	
	0.5	81			
Gamma	0.2	81	1.002937	1.005374	1.008145
	0.3	81			
	0.4	81			
Initial value of level	1000	81	1.003464	1.005167	1.007825
	1500	81			
	2000	81			
Initial value of growth rate	50	81	1.005252	1.005107	1.006098
	200	81			
	350	81			

maximum deviation in the bullwhip ratio is found to be 6.54%. The optimal parametric values corresponding to the minimum bullwhip effect are determined as 1000 for initial level, 350 for initial growth rate, 0.1 for alpha, 0.1 for beta and 0.4 for gamma.

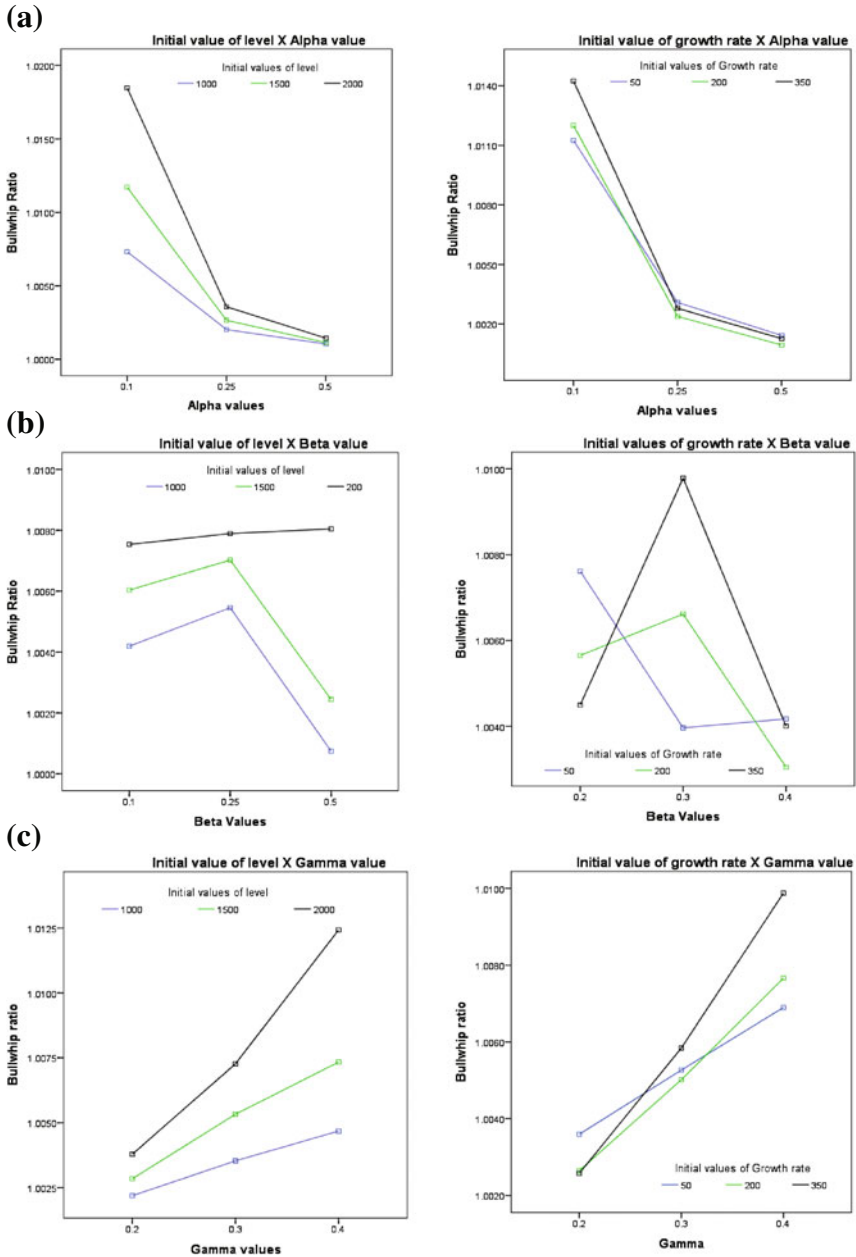


Fig. 3 Interrelation among the **a** alpha, **b** beta, **c** gamma, initial values and bullwhip effect

4.2 *Interactions Among the Smoothing Constants, Initial Values and the Bullwhip Effect*

The interrelation among the smoothing constants, the initial values of level and the initial values of the growth rate are shown in Fig. 3. From the Fig. 3a-c, it is evident that at any particular alpha, beta and gamma value, the bullwhip effect increases with the increment of initial values of level. Whereas, the initial values of the growth rate maintains a U-type relationship with the smoothing constants and the bullwhip ratio. However, this complex U-type interrelations emerged into the sight, perhaps due to the consideration of the ranges of smoothing constants and/or the assumption of the lead time as similar as the demand data updating periods.

5 **Concluding Remarks**

Due to the uncertainty in customer demand, the bullwhip effect is inevitable in supply chain. However, an appropriate forecasting approach is able to minimize the bullwhip effect and can thus play a vital role for the managers or decision makers in using more precisely predicted demand values. Since complete elimination of bullwhip effect from any SC is not possible, an endeavour should be always underway to propose or modify the conventional forecasting techniques for leaning the bullwhip effect. From this perspective, this research endeavour provides a clear insight about the impact of various parameters of Multiplicative Holt-Winters seasonal demand forecasting model on the bullwhip effect. For instance, the smoothing constants and the initial values of the level parameter of Multiplicative Holt-Winters model have a significant influence over the bullwhip effect whereas the influence of the initial values of the growth rate is found to be insignificant. But to secure a generalized stand, it will be interesting to assess our current findings for the various ranges of demand parameters (i.e. base, slope and noise) and the lead times. Despite the complex interaction among the smoothing constants, the initial values of the growth rate and the bullwhip effect, the present observation also invites for further investigation to frame the optimal scenarios. It is to be noted that realization of our research outcomes has also paved an opportunity for improving the widely adopted Multiplicative Holt-Winters approach by featuring the initial values of the level and the growth rate.

Acknowledgements This study was conducted under the FRGS project (FRGS14-102-0343) funded by Ministry of Higher Education (MOHE), Malaysia. The authors are grateful to MOHE and Research Management Centre (RMC), IIUM for their support.

References

1. Adenso-Díaz, B., Moreno, P., Gutiérrez, E., Lozano, S.: An analysis of the main factors affecting bullwhip in reverse supply chains. *Int. J. Prod. Econ.* **135**(2), 917–928 (2012)
2. Barlas, Y., Gunduz, B.: Demand forecasting and sharing strategies to reduce fluctuations and the bullwhip effect in supply chains. *J. Oper. Res. Soc.* **62**(3), 458–473 (2011)
3. Bayraktar, E., Koh, S.L., Gunasekaran, A., Sari, K., Tatoglu, E.: The role of forecasting on bullwhip effect for E-SCM applications. *Int. J. Prod. Econ.* **113**(1), 193–204 (2008)
4. Bowerman, B.L.B., O’Connell, A.B., Koehler, B.L.: *Forecasting, Time Series, and Regression*, 4th edn. Curt Hinrichis, USA (2005)
5. Chatfield, D.C.: Underestimating the bullwhip effect: a simulation study of the decomposability assumption. *Int. J. Prod. Res.* **51**(1), 230–244 (2013)
6. Chen, F., Drezner, Z., Ryan, J.K., Simchi-Levi, D.: Quantifying the bullwhip effect in a simple supply chain: The impact of forecasting, lead times, and information. *Manage. Sci.* **46**(3), 436–443 (2000)
7. Chen, F., Ryan, J.K., Simchi-Levi, D.: The impact of exponential smoothing forecasts on the bullwhip effect. *Nav. Res. Logist. (NRL)* **47**(4), 269–286 (2000)
8. Chiang, C.Y., Lin, W.T., Suresh, N.C.: An empirically-simulated investigation of the impact of demand forecasting on the bullwhip effect: Evidence from US auto industry. *Int. J. Prod. Econ.* **177**, 53–65 (2016)
9. Das, D., Dutta, P.: A system dynamics framework for integrated reverse supply chain with three way recovery and product exchange policy. *Comput. Ind. Eng.* **66**(4), 720–733 (2013)
10. Forrester, J.W.: Industrial dynamics—a major breakthrough for decision makers. *Harv. Bus Rev.* **36**(4), 37–66 (1958)
11. Geary, S., Disney, S.M., Towill, D.R.: On bullwhip in supply chains—historical review, present practice and expected future impact. *Int. J. Prod. Econ.* **101**(1), 2–18 (2006)
12. Jaipuria, S., Mahapatra, S.S.: An improved demand forecasting method to reduce bullwhip effect in supply chains. *Expert Syst. Appl.* **41**(5), 2395–2408 (2014)
13. Koh, S.L., Gunasekaran, A.: A knowledge management approach for managing uncertainty in manufacturing. *Ind. Manag. Data Syst* **106**(4), 439–459 (2006)
14. Lee, H.L., Padmanabhan, V., Whang, S.: The bullwhip effect in supply chains. *MIT Sloan Manag. Rev.* **38**(3), 93 (1997)
15. Mao, J.: Customer brand loyalty. *Int. J. Bus. Manag.* **5**(7), 213 (2010)
16. Metters, R.: Quantifying the bullwhip effect in supply chains. *J. Oper. Manag.* **15**(2), 89–100 (1997)
17. Paik, S.K., Bagchi, P.K.: Understanding the causes of the bullwhip effect in a supply chain. *Int. J. Retail Distrib. Manag.* **35**(4), 308–324 (2007)
18. Pati, R.K., Vrat, P., Kumar, P.: Quantifying bullwhip effect in a closed loop supply chain. *Opsearch* **47**(4), 231–253 (2010)
19. Sterman, J.D.: Modeling managerial behavior: Misperceptions of feedback in a dynamic decision making experiment. *Manage. Sci.* **35**(3), 321–339 (1989)
20. Sun, H.X., Ren, Y.T.: The impact of forecasting methods on bullwhip effect in supply chain management. In: *Proceedings of the 2005 Engineering Management Conference*, vol. 1, pp. 215–219 (2005)
21. Tratar, L.F.: Forecasting method for noisy demand. *Int. J. Prod. Econ.* **161**(1), 64–73 (2015)
22. Wang, X., Disney, S.M.: The bullwhip effect: Progress, trends and directions. *Eur. J. Oper. Res.* **250**(3), 691–701 (2016)
23. Wright, D., Yuan, X.: Mitigating the bullwhip effect by ordering policies and forecasting methods. *Int. J. Prod. Econ.* **113**(2), 587–597 (2008)
24. Zhang, X.: The impact of forecasting methods on the bullwhip effect. *Int. J. Prod. Econ.* **88**(1), 15–27 (2004)

The p -Median Problem and Health Facilities: Cost Saving and Improvement in Healthcare Delivery Through Facility Location

Michael Dzator and Janet Dzator

Abstract The importance of health to economic growth and development is an undisputed fact. Modern advancement in technology and healthcare has contributed to improved health and productivity, but there are many people who cannot access healthcare in a timely fashion. Factors affecting delays in accessing healthcare include inadequate supply, poor location, or lack of healthcare facilities all of which can be exacerbated by increasing healthcare costs and scarcity of resources. In this study, we develop a simple two-stage method based on the p -median problem to investigate the location and access to healthcare (emergency) facilities in urban areas. We compare the results of our new method with the results of similar existing methods using 26-node, 42-node, and 55-node data. We also show the efficiency of our method with exact methods using 150-node random data. Our method compares favorably with optimal and the existing methods.

Keywords Healthcare · Facility location · Costs · Emergency

1 Introduction

The location of facilities is crucial in healthcare delivery. For efficient and effective health care, facilities should be properly located. The implication of poor location of healthcare centers has a great cost in healthcare delivery. The utilization of health facilities is poor if they are not well located. This might lead to increase in morbidity and mortality. Therefore, the facility models have a greater importance in accessing critical dimensions such as distance and response time in healthcare

M. Dzator (✉) · J. Dzator
Central Queensland University, Rockhampton, QLD, Australia
e-mail: m.dzator@cqu.edu.au

J. Dzator
e-mail: Janet.Dzator@newcastle.edu.au

M. Dzator · J. Dzator
The University of Newcastle, Callaghan, NSW, Australia

facility usage. Moreover, efficient location of health facilities can reduce cost and improve utilization.

Healthcare services can be classified as essential or not essential. The distance to be covered by patients depends on whether the services are necessary or not. Patients will travel to any facility that provides essential services if that is the only facility in the area. However, patients will only use facilities of limited distance for nonessential services such as screening checks.

A critical factor for locating or operating emergency facilities is the response time to calls. Since the response time is dependent on the distance between the emergency facilities and the emergency sites, minimization of the average (total) distance separating users or nodes and facilities is paramount in locating emergency facilities [14].

Dzator and Dzator [14] argued that response time is one of the measures of effectiveness of emergency services and because the location of facilities affect response time, the utility derived from using emergency facilities is likely to increase as the distance between the facilities and users decrease. That is to say that facility effectiveness and efficiency decrease with increase travel distance or increase response time. We respect the fact that people will seek and use the closest facility when the need for emergency service arises regardless of distance or travel time. However, modernization and advanced technology have improved survival rates and reversal of incapacitation caused by catastrophic health events such as cardiovascular diseases if only patients could be reached or receive lifesaving interventions within a limited time of disease episode. Increased population, urban sprawl, and vehicular density are all modern realities that could increase travel or response time and diminish the effectiveness of emergency services offered by existing facilities. The p -median problem offers opportunity to review travel distance and/or response time and identify potential minimum response and travel time that could improve the effectiveness of service delivery.

The p -median problem is about locating p facilities, in this case emergency facilities, with the aim of minimizing the weighted distance between a user (demand point) and facility. Solving a p -median problem is time consuming, so it is said to be computationally difficult or “ NP -hard” on general networks [23]. The computational difficulty has been considered by many researchers leading to the increased use of heuristic approaches [11, 12, 37].

Other authors including Carson and Batta [3] in New York, McAleer and Naqvi [26] in Belfast, Serra and Marinov [37] in Barcelona, and Dzator and Dzator [14] in Perth have used the p -median model to locate or relocate emergency facilities. Recently, Dzator and Dzator [15] discuss the use of p -median problem in improving emergency facilities in developing countries.

In this study, we use the p -median problem to determine the effectiveness of emergency service for a given number of facilities. We measure the effectiveness by evaluating the average distance between the customers and facilities. The p -median approach is generally preferred in congested area such as urban areas because of our focus on minimizing the average distance and/or response time between potential users and the emergency facilities.

The rest of the paper is organized as follows. In Sect. 2, we present a brief overview of locating emergency facilities in the cities of the world over the past four decades. We discuss the p -median problem, the branch and bound method (BBM), and the vertex substitution solution method in Sect. 3. Section 4 follows with a discussion on the two-stage hybrid method as a tool for optimal location of additional healthcare facilities. The data, methods, and results are discussed in Sect. 5, and we conclude in Sect. 6.

2 Emergency Facility Location in Cities from 1969 to 2016

In the location of emergency facilities, one of the earliest applications of ambulance location was by Savas [34] in New York where emergency ambulance services have been provided since 1870. Savas [34] used a simulation model in solving the ambulance location problem and noted an improvement in the ambulance service by examining the number and location of ambulances. The simulation study showed that the combination of adding ambulances in a district and relocating ambulances closer to the demand point improved the level of service in terms of average response time.

In another early study on ambulance location, Fitzsimmons [17] and Swoveland et al. [38] used probabilistic models to study ambulance location in Los Angeles and Vancouver, respectively. The study in Los Angeles found the deployment of ambulances that minimizes the average response time. The ambulances were deployed such that no location in the area would be more than 2.5 miles from the ambulance station. This corresponds to a five-min average response time. In Vancouver, the study aimed at developing a methodology for locating ambulance depots. The methodology adopted was based on simulation. The study also aimed to find out whether relocating ambulances would improve the average response time. The simulation method that was used to locate ambulance stations performed well when compared to the existing locations.

The two studies also relate ambulance location to minimization of transportation cost. Fitzsimmons [17] said that the minimization of transportation cost is equivalent to the average response time of an ambulance system. In addition, Swoveland et al. [38] assume the ambulance location problem to be a p -median problem in which the closest ambulance is always available. They realized, however, that this is not necessarily so in practice.

Table 1 outlines the studies of location of emergency facilities from 1969 to 2016. The table discusses the location of emergency facilities in terms of the year of study, type of facility, and the problem considered. The type of model or method and major findings are also discussed. The studies in the table have located the emergency facilities to address mainly the problem of response time and coverage. Some of the studies that we have outlined have either reduced the response time of the emergency vehicle or increased the coverage. Furthermore, some of these studies were also conducted to assess the performance of the emergency system in a city.

Table 1 Summary of facility location problems—emergency facilities

City/study/model	Type of facility/problem considered	Findings/remarks
Santiago/Perez, Maldonado, and Ospina [28]/deterministic	Emergency—a fleet assignment model was used	Results show an increase in fleet use between 6 and 20%.
Vienna/Schmid [36]/deterministic and probabilistic	Emergency—approximate dynamic programming (ADP) was applied	The application of the model shows that by altering the dispatching rules of the emergency vehicles, the response time was reduced by 12.89%.
Adana/Coskun and Erol [7]/deterministic	Emergency—an optimization model was used	Optimal solution was obtained in 130 regions
Riyadh/Alsalloum and Rand [1] deterministic	Emergency—a bi-objective formulation of the covering problem was used to determine emergency centers	Optimal location of emergency centers was addressed
Montreal/Gendreau, Laporte and Semet [19]/Heuristic	Emergency—a heuristic method was used to solve an ambulance location problem	The method was very efficient in improving ambulance coverage in modern cities
Dubai/Badri, Mortagy, and Alsayed [2]/deterministic	Emergency—a multi-criteria model was used	The model seems to be an ideal technique that is applicable to the real-world fire station location problem
Bangkok/Fujiwara, Makjamroen, and Gupta [18] deterministic and simulation	Emergency—the ambulance deployment policies of Bangkok, Thailand, were examined in the study	The reduction of ambulances from 21 to 15 does not have any negative effect on the level of service provided
Victoria/Uyeno and Seeberg [40]/deterministic and simulation	Emergency—a p-median model and a simulation model were applied to ambulance location system in Victoria	The p-median model and simulation model showed reduction in average response time for paramedic, emergency, and regular ambulance transfers
Austin/Daskin and Stern [10]/deterministic	Emergency—a set covering problem was used	Efficiency was attained by the use of less vehicles as well maximum zone coverage
Baltimore/Schilling, Elzinga, Cohon, Church, and ReVelle [35] deterministic	Emergency—a modified covering models which took into account the distribution of specialized equipment or man power among location sites was used for the study of fire protection system	The city specified the construction of six new stations in its five-year capital improvement programs of 1976 and 1977
Denver Plane and Hendrick [29] Deterministic	Emergency—a deterministic model was used to find the location fire stations	The study resulted in the recommendation that may reduce annual cost by more than one million dollars

(continued)

Table 1 (continued)

City/study/model	Type of facility/problem considered	Findings/remarks
Detroit Hall [21] Probabilistic	Emergency—the allocation and distribution of ambulances are studied in the city of Detroit	The results were used in predicting the performance of both single function recovery systems and dual (police-ambulance) systems
New York Carter and Ignall [4] Simulation	Emergency—a simulation model was used	Additional units were allowed in peak demand hours
New York Savas [34] Simulation	Emergency—Improvement in ambulance service was considered by using a simulation model	The study concluded that low-cost improvements in ambulance could be achieved by redistributing ambulances

This assessment often leads to relocation (as seen from Table 1) of the emergency facilities. The relocation of the facilities often leads to a reduction of the response time and sometimes results in the reduction of the number of facilities without a reduction in the level of service as illustrated by Fujiwara et al. [18]. A study by Rajagoplan and Saydam [31] in Charlotte also focuses on the reduction of response time for which a deterministic model was applied to 200 emergency call data.

A number of authors included in the studies also addressed problem of accessibility and other important factors which are crucial to emergency service delivery. The other studies in the major cities include: Repede and Bernado [32], McAleer and Naqvi [26], Goldberg et al. [20], Liu and Lee [25], Eaton et al. [16] and Daskin [9].

These authors have not addressed the problem of locating additional emergency facilities due to population increase adequately. The focus of our paper is to examine the problem of locating additional facilities.

3 The p -Median Problem (Minimum Distance Problem)

Following the standard p -median problem, we specify our distance function as

$$\text{Min } \sum_{i=1}^m \sum_{j=1}^n a_i d_{ij} x_{ij}, \tag{3.1}$$

subject to

$$\sum_{j \in J} x_{ij} = 1, \forall i \in I \tag{3.2}$$

$$\sum_{j \in J} y_j = p \tag{3.3}$$

$$x_{ij} \leq y_j \forall i \in I, \forall j \in J \tag{3.4}$$

$$y_j \in \{0, 1\} x_{ij} \in \{0, 1\} \tag{3.5}$$

where

- $I = \{1, \dots, m\}$ is a set of demand or customer points
- $J = \{1, \dots, n\}$ are the potential facility sites
- $d_{ij} =$ the minimum distance that the patient is required to travel from point i (demand point) to a healthcare facility at point j
- $x_{ij} = 1$ if the patient at demand point i is assigned to a healthcare facility at node j , 0 otherwise
- $y_j = 1$ if a healthcare facility is located at point j , 0 otherwise
- $p =$ the required number of healthcare stations that will deliver efficiency or the targeted minimum response time/distance and
- $a_i =$ the total demand node i or the population in the service area

Equation (3.1) seeks to minimize the distance between patients and their closest healthcare facility subject to constraints 3.2–3.5 where constraint 3.3 specifies the required number of healthcare facilities, constraint 3.4 assigns patients according to located facilities, and constraint 3.5 defines the problem as a binary integer program.

There have been extensions of the p -median models in the extant literature with most seeking to improve the efficiency of the model. For example, Weaver and Church [41], Fitzsimmons [17], and Swoveland et al. [38] have extended the p -median problem to account for its stochastic nature.

Assuming there are n communities or suburbs, to locate p healthcare facilities, the total number of facilities of possible solutions is $C_p^n = \frac{n!}{p!(n-p)!}$. Mathematically, the search space explored in the minimization of distance problem using the p -median optimization model grows “factorially” as the number of facilities to locate and the communities to serve increase.

3.1 Branch and Bound Method (BBM)

Generally, combinatorial optimization problems can be stated more easily than solved. These problems form part of a large number of real-world planning problems, but they are not easy to solve. The method of branch and bound can be used effectively to solve computationally difficult problems. According to Dzator [13], a basic approach to solving a computationally difficult problem is to divide the solution set into smaller units and place bounds on the objective function of each subset. The bounds are then used to eliminate all solutions that are not feasible. The

branching process is carried out by selecting the branching variable. The branching process stops when we have a solution to the original problem which has an objective function value, in the case of minimization problem, less than or equal to all lower bounds of the generated subsets. Exact methods, such as branch and bound, usually give an optimal solution when applied to solve the facility location problem, but unfortunately a large amount of time is needed to solve large problems, and this is a limitation.

3.2 Vertex Substitution Method (VSM)

The vertex substitution method (VSM) is one of the early and simple heuristics used to solve the p -median problem. Teitz and Bart [39] developed the heuristic and applied it to select the initial set of p nodes for the p -median problem solution. The solution proceeds with the substitution of subsequent nodes that do not belong to original solution. Solutions or objective value resulting from each substitution is compared. The best result is obtained from the substitution that delivers the biggest decrease in the objective function [14].

The simplicity of the Teitz and Bart [39] heuristic makes it attractive for use in solving location problems. Firstly, it frequently converges to the optimum solution and it performs very well when compared with exact methods and other heuristics (see Rosing et al. [33]). Secondly, the problem size does not affect the accuracy of the solution obtained. Thirdly, the heuristic is able to solve other problem formulations apart from the p -median problem [22]. Fourthly, the heuristic is not tied to any particular data structure or implementation strategy. However, optimal results are not always guaranteed.

4 The Hybrid Method (HM) for Locating Additional Healthcare Facilities Optimally

In this section, we assume that healthcare facilities are already located and we need to expand the number of facilities due to population increase. The first part of the hybrid method involves the location of the existing facilities which is outlined below.

Step 1: Identify all the nodes (n) of the weighted distance matrix arranged in ascending order and note the number of distance nodes f_i for $1 \leq i \leq n$ for each column.

Step 2: Reduce the number of nodes for each column. The reduction variable ∂ is a function of n and p which is defined as: $\partial = F(n, p)$ such that $1 \leq \partial \leq \frac{np}{10}$.

Step 3: Choose the first p nodes after summing and arranging in ascending order.

Step 4: The cost corresponding to a patient at the selected nodes who uses a health facility at the selected nodes is set zero.

Step 5: Choose the minimum node after summation and arrangement in ascending order and swap with first p nodes initially chosen.

Step 6: Select the set with the lowest objective value and swap all the nodes which have not been used before. Keep the minimum set.

Step 7: Continue the process and use every node repeatedly till the objective value is stable.

As population increase and there is demand for more health care, there will be a need to locate additional facilities. We describe below the procedure for adding new facilities to the existing ones.

Step 8: We consider columns which correspond to the final solution set denoted as $\{1, 2, 3, \dots, p\}$ as the original facilities to serve the communities.

Step 9: Locate and add the facility with the largest drop in the total cost when patients are assigned to their closest facilities.

Step 10: We continue this process until the required number of additional facilities are obtained.

For example, if we have 10 existing facilities and we want to locate an additional facility, then we will locate a facility at a suburb for self-usage at that suburb that result in the largest reduction of total cost of using these facilities.

We propose this method because it is expensive to use exact method such as branch and bound (BB). The execution time for the BBM is far more compared to the hybrid heuristic procedure described above as the problem size increase (Our method needs further testing for future studies).

4.1 Data for Cities or Communities

The data used for the 55-node problem came from 55 communities in the Washington D.C (USA) area and is obtained from Colome et al. [6]. We calculated the distance matrix which was used in our heuristics.

The data used for 42-node problem came from 42 cities in the USA. The data was compiled by Dantzig et al. [8] and available in their paper. We assume uniform demand for all of these problems. Authors including Khumawala [24], Church and Meadow [5], Neebe [27], Rahman and Smith [30], and Dzator and Dzator [14] have also used this data.

The 26-node data set represent 26 communities from Perth, Western Australia. This data was also used by Dzator and Dzator [14] and Dzator and Dzator [15].

5 Computational Results and Discussions

We use the 2013 C++ program to determine the assumed existing facilities and the additional facilities. We used the Lagrangian relaxation method from the SITA-TION Location software [11] to determine the optimal solutions. We also obtained the values of the existing VSM from SITA-TION [11]. The 55-node data, the 42-node data, and the 26-node data described earlier were used for the computations. The computer used for the analyses had Intel[®] Core[™] i5-6500 CPU with 3.20 GHz and 7.86 GB of RAM. The percentage deviation value is obtained when we subtract the optimal value from the heuristic value all divided by the optimal value and multiplied 100.

Ten facilities are located at nodes 1, 2, 4, 8, 9, 13, 14, 17, 23, and 25 using 26-node problem. We assume that 10 healthcare facilities are already located at Armadale, Kelmscott, Belmont, Willetton, Canning Vale, Gosnells, Thornlie, Byford, Como, and East Victoria. To locate additional facilities one by one, we will locate the facilities such as adding a facility that will result in the greatest reduction of cost in accessing the facilities. A facility will be chosen from nodes 3, 5, 6, 7, 10, 11, 12, 15, 16, 18, 19, 20, 21, 22, 24, and 26. That is from the following suburbs namely Westfield, Rivervale, Cloverdale, Kewdale, Bentley, Cannington, Maddington, Serpentine, Oakford, Mundijong, Darling Down, South Perth, Kensington, Victoria Park, and Carlisle. The additional facility is located at node 15 (Serpentine) which results in the largest reduction of cost of accessibility if the eleven facilities are located. We continue to locate other additional facilities to give 12, 13, 14, and 15 facilities. Similarly, the 42-node data and the 55-node data were used for the computations and the results are shown in Table 2.

The results in Table 2 shows that the percentage deviation (cost) from the optimal in locating 11 to 15 facilities using the hybrid method is optimal, while the VSM ranges from 5.43 to 10.37% for 26-node problem. For 42-node problem, the VSM is optimal, while the HM ranges from 1.16 to 2.87%. The 55-node problem results in the optimal when the hybrid method is used, but the VSM gives results which range from 0.27 to 0.88%. The average percentage deviation from the optimal for the hybrid method is 0.76% and that of VSM is 2.15% as shown in Table 3.

Table 2 Results for three literature problems

Facilities	Deviations (%) from optimal for HM and VSM					
	HM	VSM	HM	VSM	HM	VSM
	26-node problem		42-node problem		55-node problem	
11	0	5.43	1.16	0	0	0.71
12	0	6.28	2.27	0	0	0.77
13	0	6.79	2.45	0	0	0.82
14	0	10.37	2.65	0	0	0.88
15	0	0	2.87	0	0	0.27

Table 3 Average deviations from the optimal

–	HM	VSM
Average Deviation	0.76	2.15

Table 4 Average deviation and CPU time for the 150-node problem

–	Objective value		CPU time (s)	
Facilities	HM	BB	HM	BB
3	0.33	0	3.14	417.78
10	1.28	0	143.29	26,620.18

To confirm the efficiency of our method, we compare our method with BBM using a problem size of 150 of 20 different weighted distance matrix problems generated randomly on [10, 100] to locate three and 10 facilities. The results are shown in Table 4 which shows that the HM is 0.33% within the BBM but is 0.08% of the BBM computational time for three facilities. For locating 10 facilities from nine existing facilities using the first stage of the hybrid method to locate existing facilities, the HM is 1.28% within the BBM but is 0.54% of the BBM computational time.

6 Conclusion

We have discussed the importance of healthcare centers and outline how to locate them optimally. We have presented the study of the location of emergency facilities in cities around the world from 1969 to 2016. A new hybrid method is developed and applied to three literature data. The results showed that our method performed better in two out of three literature problems. The average percentage deviations of our method from the optimal is 1.28% that of the existing method. We also confirmed the efficiency of our method by applying and comparing our results with those from the BBM. We observed a far less computational time for a 150-node problem using our method compared to the time it took BBM to run the same problem. The objective value of our method on average is within 1.5% of the optimal.

Our method has given encouraging results, but further tests with different problems and comparison with similar methods are needed to confirm the effectiveness of our method.

References

1. Alsalloum, O.I., Rand, G.K.: Extensions to emergency vehicle location models. *Comput. Oper. Res.* **33**, 2725–2743 (2006)
2. Badri, M.A., Mortagy, A.K., Alsayed, C.A.: A multi-objective model for locating fire stations. *Eur. J. Oper. Res.* **110**, 243–260 (1998)

3. Carson, Y. Batta R.: Locating an ambulance on Amherst campus of State university of New York at Buffalo. *Interfaces* **20**, 43–49 (1990)
4. Carter, G., Ignall E.: A simulation model of fire department operations. *IEEE Syst. Sci. Cybern.* **6**(4) (1970)
5. Church, R.L. Meadows M.E.: Location modeling utilizing maximum distance criteria. *Geogr. Anal.* **11**, 358–373 (1979)
6. Colome, R., Lourenco, H.R., Serra, D.: A new chance-constrained maximum capture location problem. *Ann. Oper. Res.* **122**, 121–139 (2003)
7. Coskun, N.: Erol and R.: An optimization model for locating and sizing emergency medical service stations. *J. Med. Syst.* **34**, 43–49 (2010)
8. Dantzig, G.B., Fulkerson D.R., Johnson S.M.: Solution of a large-scale traveling salesman problem. *Oper. Res.* **2**, 393–410 (1954)
9. Daskin, M.S.: Application of an expected covering location model to EMS design. *Decis. Sci.* **13**(3), 416–439 (1982)
10. Daskin, M.S., Stern E.H.: A hierarchical objective set covering model for emergency medical service vehicle deployment. *Transp. Sci.* **15**(2), 137–152 (1981)
11. Daskin, M.S. *Network and Discrete Location: Models, Algorithms and Applications*. Wiley, New York (1995)
12. Densham, P.J., Rushton, G.: A more efficient heuristic for solving large P-median problems. *Papers in Regional Science* **71**, 307–329 (1992)
13. Dzator, M.: *The Optimal Location of Emergency Units within Cities*, PhD Thesis, Curtin University of Technology (2007)
14. Dzator, M., Dzator, J.: An effective heuristic for the P-median problem with application to ambulance location. *Opsearch* **50**(1), 60–74 (2013)
15. Dzator, M. Dzator and J.: Health emergency facilities and development: Locating facilities to serve people and development better. *J. Dev. Areas* **50**, 131–142 (2016)
16. Eaton, D.J., Daskin, M.S., Simmons, D., Bulloch, B., Jansma, G.: Determining emergency medical service vehicle deployment in Austin, Texas. *Interfaces*, **15**, 96–108 (1985)
17. Fitzsimmons, J.A.: A Methodology for emergency ambulance deployment. *Manage. Sci.* **19**, 627–636 (1973)
18. Fujiwara, O., Makjamroen, T., Gupta, K.K.: Ambulance deployment analysis: a case study of Bangkok. *Eur. J. Oper. Res.* **31**, 9–18 (1987)
19. Gendreau, M., Laporte, G., Semet, F.: Solving an ambulance location model by Tabu search. *Locat. Sci.* **5**, 75–88 (1998)
20. Goldberg, J.R., Dietrich, R., Cheng, J.M., Mitwasi, M.G., Valenzuela, T., Criss, E.: Validating and applying a model for locating emergency medical vehicles in Tucson, AZ (case study). *Eur. J. Oper. Res.* **49**, 308–324 (1990)
21. Hall, W.K.: Management science approaches to the determination of urban ambulance requirements. *Socio-Econ. Plan. Sci.* **5**, 491–499 (1971)
22. Hillsman, E.L.: The P-median structure as a unified model for location-allocation analysis. *Enviro. and Plan. A.* **3**, 305–318 (1984)
23. Kariv, O., Hakimi, S.L.: An algorithmic approach to network location problems II: the P-medians. *SIAM J. Appl. Math.* **37**, 539–560 (1979)
24. Khumawala, B.M.: An efficient algorithm for the P-median problem with maximum distance constraints. *Geogr. Anal.* **5**, 309–321 (1973)
25. Liu, M., Lee, J.: A simulation of a hospital call system using SLAM II. *Simulation* 216–221 (1988)
26. McAleer, W.E., Naqvi, I.A.: The relocation of ambulance stations: a successful case study. *Eur. J. Oper. Res.* **75**, 582–588 (1994)
27. Neebe, A.W.: A procedure for locating emergency service facilities for all possible response distances. *J. Oper. Res. Soc.* **39**, 743–748 (1988)
28. Perez, J., Maldonado, S., Lopez-Ospina, H.: A fleet management model for the Santiago fire department. *Fire Saf. J.* **82**, 1–11 (2016)

29. Plane, D.R.: Hendrick, and T.E.: Mathematical programming and the location of fire companies for Denver fire department. *Oper. Res.* **25**, 563–578 (1977)
30. Rahman, S., Smith, D.K.: A comparison of two heuristic methods for the P-median problem with and without maximum distance constraints. *Int. J. Oper. Prod. Manag.* **11**, 76–84 (1991)
31. Rajagopalan, H.K., Saydam, C.: A minimum expected response model: Formulation, heuristic solution, and application. *Socio-Econ. Plan. Sci.* **43**, 253–262 (2009)
32. Repede, J.F. Bernando, J.J.: Developing and validating a decision support system for locating emergency medical vehicles in Louisville, Kentucky. *Eur. J. Oper. Res.* **75**, 567–581 (1994)
33. Rosing, K.E., Hillsman, E.L.: Rosing-Vogelaar, and H.: A note comparing optimal and heuristic solutions to the P-median problem. *Geogr. Anal.* **11**(1), 86–89 (1979)
34. Savas, E.: Simulation and cost-effectiveness analysis of New York's emergency ambulance service. *Manage. Sci.* **15**, 608–627 (1969)
35. Schilling, D., Elzinga, D.J., Cohon, J., Church, R. and C. ReVelle: The TEAM/FLEET for simultaneous facility and equipment siting. *Tranp. Sci.* **2**, 163–175 (1979)
36. Schmid, V.: Solving the dynamic ambulance relocation and dispatching problem using approximate dynamic programming. *Eur. J. Oper. Res.* **219**, 611–621 (2012)
37. Serra, D., Marianov, V.: The P-median problem in a changing network: the case of Barcelona. *Locat. Sci.* **6**, 383–394 (1998)
38. Swoveland, C., Uyeno, D., Vertinsky, I., Vickson, R.: Ambulance location: a probabilistic enumeration approach. *Manage. Sci.* **20**, 687–697 (1973)
39. Teitz, M.B., Bart, P.: Heuristic methods for estimating generalized vertex median of a weighted graph. *Oper. Res.* **16**, 955–961 (1968)
40. Uyeno, D.H., Seeberg, C.: A practical methodology for ambulance location. *Simulation* 79–87 (1984)
41. Weaver, J.R., Church, R.L.: A median location model with nonclosest facility service. *Transp. Sci.* **19**, 58–74 (1985)

A Bi-level Mixed Integer Programming Model to Solve the Multi-Servicing Facility Location Problem, Minimising Negative Impacts Due to an Existing Semi-Obnoxious Facility

Ahmed W.A. Hammad, David Rey and Ali Akbarnezhad

Abstract We propose a bi-level multi-objective model to solve the multi-facility location problem with traffic equilibrium constraints. The main facility location problem within our proposed model consists of locating a set of buildings with varying sensitivity thresholds due to the negative impacts propagating from an existing semi-obnoxious facility. The traffic routing problem is modelled as a user equilibrium which is embedded using its Karush-Kuhn-Tucker optimality conditions. We use the convex scalarisation approach to deal with multiple objectives. Two solution methods are then contrasted: in the first method we solve our linearised model using an off-the shelf Mixed Integer Programming solver. In the second solution approach we use Benders Decomposition algorithm to improve computational tractability. Numerical results highlight the superiority of the decomposition approach when solving a realistic-sized instance.

Keywords Facility Location Problem · Aircraft · Conflict detection · Cluster, proximity · Number partition · Taskload

1 Introduction

The problem of locating a set of semi-obnoxious facilities in a region has been well studied in the literature, particularly during the last decade. Studies reviewed tend to locate the semi-obnoxious facilities under the assumption that other sensitive servicing facilities (i.e. ones providing a service to customers) already occupy fixed

A.W.A. Hammad (✉) · D. Rey · A. Akbarnezhad
School of Civil and Environmental Engineering,
The University of New South Wales, Sydney, Australia
e-mail: a.hammad@unsw.edu.au

© Springer International Publishing AG 2018
R. Sarker et al. (eds.), *Data and Decision Sciences in Action*,
Lecture Notes in Management and Industrial Engineering,
DOI 10.1007/978-3-319-55914-8_28

381

positions within the region [18]. The literature is abundant with studies that address the problem from a discrete modelling point of view [3, 5, 23] and from a continuous setting [17, 18]. In this paper we adopt discrete modelling, though we take a different avenue where we assume that the location of the semi-obnoxious facility is already known and fixed, while a set of facilities sensitive to the negative impacts resulting from the semi-obnoxious facility are to be located within its vicinity. Examples of such problems are highly relevant particularly in the field of urban design, where a situation arises that requires the siting of facilities around existing semi-desirable facilities including hospitals, airports and wireless stations. We therefore believe that tackling the problem of facility location around semi-obnoxious facilities is integral for urban design, given challenges that cities face nowadays in coping with the increased mandate of ensuring the sustainable development of their underlying structure.

Existing models of semi-obnoxious facility location problems are generally formulated as a single or as bi-objective models [13, 15, 16]. It is commonly the case that the mini-max model is deployed for obnoxious facilities whereas the max-min model is used when a facility is considered to be desirable [7, 20]. Our model is different to what is present in the current literature due to two main reasons: firstly, the sensitive facilities are assumed to be traffic demand inducing, hence imposing a change to the traffic assignment of the underlying road network. In this work we therefore focus on both the induced traffic assignment changes that are associated with the location decision of the sensitive facilities along with the requirements of ensuring adequate serviceability of the underlying network, through reducing the traffic congestion. In this paper, the traffic assignment problem is modelled as a User Equilibrium (UE). Consequentially, this requires us to model our problem as a bi-level model, where the upper level represents the planner's decision, while the lower level models users' route choice. This class of multi-level optimisation problems can be represented as a Leader-Follower or Stackelberg game, where an optimisation problem is embedded within another one [4]. Solving such types of problems is challenging due to the difficulty in appropriately capturing the reaction function linking the upper and lower level decision variables. As such, bi-level problems are NP-hard even for the linear cases [1]. Current literature where the facility location problem is considered in conjunction with the traffic assignment one is limited to studies on disaster management where distribution centres are desired to be located [9, 21]. Such studies do not account for the traffic that is induced to the network and the focus is mostly on the congestion created at the located distribution facilities.

Secondly, the sensitive facilities which we desire to locate are assumed to be servicing facilities, which need to satisfy demand of existing population centres in the regions. As a result, we are also interested in maximising the coverage of the located facilities to the demand points that require to be serviced. To do so we implement the concept of facility coverage [6, 12, 14] which depends on the Euclidean distance between the servicing facilities and the service-demanding regions [13].

The main contributions of this paper can be summarised as follows:

- We propose a novel bi-level model for locating multiple facilities around an existing semi-obnoxious facility, where facilities are assumed to be traffic demand inducing.
- We account for the bi-level nature of the problem by representing the traffic equilibrium model using its Karush-Kuhn-Tucker (KKT) optimality conditions. The multi-objective nature of our model is addressed by adopting a scalarisation approach.
- We contrast two solution methods; namely a Mixed Integer Program (MIP) model approach and a Benders Decomposition (BD) approach for solving the multi-facility location problem around a semi-obnoxious facility.

The organisation of this paper is as follows. In the next section we outline our proposed bi-level multi-facility location model in the presence of an existing semi-obnoxious facility. In order to handle the bi-level nature of the model, we adopt the KKT equivalent conditions to convert it to a single level model. We then outline the solution approach which we adopt, which includes the linearisation of bi-linear terms in the model and the use of a decomposition approach. Comparison of the decomposed and MIP models then ensues, through applications of the developed methods to a case example. We conclude the paper with our main findings and future work endeavours.

2 Model

In this section we define the basic elements of our network representation and we present our multi-objective bi-level model. The network representation is shown in Fig. 1. First we define the notation adopted in the model. We let N denote the set of

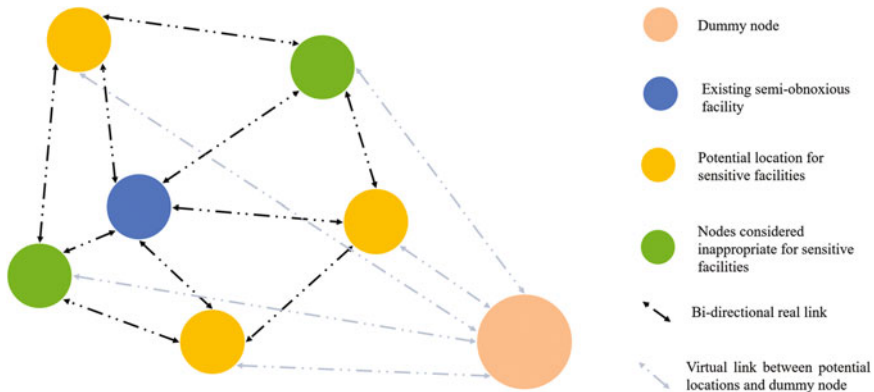


Fig. 1 Network representation after incorporation of dummy node

all nodes within the region under consideration, exemplifying population node districts and potential locations for positioning the facilities. Let the set $P \subseteq N$ be the set of all potential sensitive facility locations. We also define the population centroids that are to be visited as $D \subseteq N$. We denote the set of facilities as F and the set of all origin-destination (OD) pairs as W . We introduce a dummy node into our network, labelled E , to link all flows associated with the sensitive facilities to be positioned and the population nodes. The set L_{real} represents the set of all “real” links and is defined as follows:

$$L_{real} \subseteq N \times N$$

the set $L_{virtual}$ denotes the set of all “virtual” links, defined as:

$$L_{virtual}: = \{(r, s): r, s \in P \cup \{E\}, r = E \text{ or } s = E, r \neq s\}$$

Using this formulation, locating a sensitive facility is equivalent to connecting the selected population node to host the sensitive facility with the dummy node E . We define the set of links as $L = L_{real} \cup L_{virtual}$. We adopt the travel time function provided by the Bureau of Public Roads [19] to model the impact of traffic volume on link travel times. The BPR function is convex yet non-linear, and it is given as:

$$t_{ij}(x_{ij}) = T_{ij}^0 \left(1 + \eta_{ij} \left(\frac{x_{ij}}{c_{ij}} \right)^\phi \right) \quad \forall (i, j) \in L_{real} \tag{1}$$

where $t_{ij}(x_{ij})$ denotes the travel time function which depends on the flow on link $(i, j) \in L_{real}$, T_{ij}^0 is the free flow travel time, c_{ij} is the capacity of the link and η_{ij} and ϕ are BPR model parameters.

Let the parameters AN_r , τ_f , POP_r and q_{ir} denote the average level of obnoxiousness emitted from the semi-obnoxious facility as measured at node $r \in N$, the threshold of the sensitive facility $f \in F$, the population at node r and the total demand between origin $i \in N$ and destination $r \in D$, respectively. We also define the binary matrix δ_{rs} to equal 1 if the distance between nodes r and s is less than a coverage threshold distance defined, and zero otherwise. As variables of the model we define x_{ij}^r and z_j^s to denote the flow on link $(i, j) \in L$ for each destination $r \in D$ and a binary variable which equals one if a sensitive facility is placed at location $s \in P$, respectively. To measure whether a node is covered or not we define the binary variable γ_{rs} to equal one if node r is covered by node s , and zero otherwise. Our model is then represented through Eqs. (2)–(19).

$$\min_{\mathbf{z}} \quad g_1 = \sum_{(i,j) \in L_{real}} x_{ij} t_{ij}(x_{ij}) \tag{2}$$

$$\min_{\mathbf{z}} \quad g_2 = \sum_{f \in F} \sum_{r \in N} z_r^f (AN_r - \tau_f) \tag{3}$$

$$\max_{\mathbf{z}} \quad g_3 = \sum_{r \in N} \sum_{s \in D} POP_r \gamma_{rs} \quad (4)$$

subject to

$$\sum_{s \in P} z_s^f = 1 \quad \forall f \in F \quad (5)$$

$$\sum_{f \in F} z_s^f \leq 1 \quad \forall s \in P \quad (6)$$

$$\gamma_{rs} = \delta_{rs} \sum_{f \in F} z_s^f \quad \forall r \in N, s \in P \quad (7)$$

$$\sum_{s \in P} \gamma_{rs} \leq 1 \quad \forall r \in N \quad (8)$$

$$\gamma_{rs} \in \{0, 1\} \quad \forall r, s \in P \quad (9)$$

$$z_f^s \in \{0, 1\} \quad \forall f \in F, \forall s \in P \quad (10)$$

$$\min_{\mathbf{x}} \quad \sum_{(i,j) \in L_{real}} \int_0^{x_{ij}} t_{ij}(\omega) d\omega \quad (11)$$

subject to

$$\sum_{\substack{j \in N: \\ (i,j) \in L}} x_{ij}^r - \sum_{\substack{j \in N: \\ (j,i) \in L}} x_{ji}^r = q_{ir} \quad \forall i \in N, \forall r \in D, i \neq r \quad (12)$$

$$\sum_{\substack{s \in N: \\ (s,E) \in L_{virtual}}} x_{sE}^E = \sum_{\substack{r \in N: \\ (r,E) \in W}} q_{rE} \quad (13)$$

$$\sum_{\substack{s \in N: \\ (E,s) \in L_{virtual}}} \sum_{r \in D} x_{Es}^r = \sum_{\substack{k \in N: \\ (E,k) \in W}} q_{Ek} \quad (14)$$

$$x_{sE}^E \leq \sum_{f \in F} z_s^f \sum_{\substack{r \in N: \\ (r,E) \in W}} q_{rE} \quad \forall s \in P: (s,E) \in L_{virtual} \quad (15)$$

$$x_{Es}^r \leq q_{Er} \sum_{f \in F} z_s^f \quad \forall s \in P, \forall r \in D: (E,s) \in L_{virtual} \& (E,r) \in W \quad (16)$$

$$x_{sE}^r = 0 \quad \forall s \in N, \forall r \in D \setminus \{E\}: (s,E) \in L_{virtual} \quad (17)$$

$$x_{ij} = \sum_{r \in N} x_{ij}^r \quad \forall (i,j) \in L \quad (18)$$

$$x_{ij}^r \geq 0 \quad \forall (i,j) \in L, \forall r \in D \quad (19)$$

The upper level, defined by Eqs. (2)–(10), is described first. Equation (2) minimises the total system travel cost of the road network considered. Equation (3) minimises the total penalty due to sensitive facility threshold exceedance, resulting from the location of the facility close to the negative impacts propagating from the existing semi-obnoxious facility. Equation (4) maximises the coverage of all population nodes in the network. Equation (5) ensures that each sensitive facility is located and Eq. (6) requires that each node only accommodates a maximum of one facility. Equation (7) states that the coverage variable can only equal one if a facility is positioned within a specified distance threshold, while Eq. (8) requires coverage to be only counted once for any node r . The domain of the variables of the upper level are defined through Eqs. (9) and (10).

Our lower level UE model is defined by Eqs. (11)–(19). The objective function of the lower level is given by Eq. (11), which minimises the individual travel times on the links of the network. Flow conservation on all links is ensured through Eq. (12). Equations (13)–(17) target the flow conservation on the virtual links, while Eq. (18) is a definitional constraint which gives the sum of flow on each link of the network. Finally, the domain of the lower level variable is defined by Eq. (19). We note that the representation of the UE traffic assignment problem corresponds to a multi-commodity flow formulation [9].

3 Solution Approach

In this section, we present the proposed solution approach to solve our urban facility location problem. Since our problem is bi-level in nature, and given that bi-level problems are NP-hard and difficult to solve [8], we adopt a solution methodology whereby we convert the bi-level formulation into a single level one. In Sect. 3.1 we outline how this is achieved, i.e. replacing the lower level model with its KKT conditions. In Sect. 3.2 we present the piece-wise linearisation of the convex BPR function. Our model is then converted from a Mixed Integer Non-Linear Program (MINLP) to a MIP. In Sect. 3.3 we linearise the quadratic terms in the objective functions of the upper level model, while in Sect. 3.4 we describe how we deal with the multi-objective nature of the model through the adoption of a scalarisation technique. Finally, in Sect. 3.5 we describe how we apply a Benders Decomposition approach.

3.1 Traffic Equilibrium as KKT Conditions

We replace the lower level problem in our original BLP model with its KKT conditions. This is plausible due to the convexity of our lower level model, where equivalent equilibrium requirements can be stated through first order conditions. The KKT conditions replacing the lower level UE model, Eqs (11), (12) and (19), are defined in Eqs. (20)–(27). We note that the complementarity constraints, integral to the KKT conditions below, have been linearised.

$$\sum_{\substack{j \in N: \\ (i,j) \in L}} x_{ij}^r - \sum_{\substack{j \in N: \\ (j,i) \in L}} x_{ji}^r = q_{ir} \quad \forall i \in N, \forall r \in D, i \neq r \tag{20}$$

$$\sigma_{ij}^r = t_{ij}(x_{ij}) - v_i^r + v_j^r \quad \forall (i,j) \in L_{real}, \forall r \in D \tag{21}$$

$$x_{ij}^r \leq \omega_{ij}^r \bar{X} \quad \forall (i,j) \in L_{real}, \forall r \in D \tag{22}$$

$$\sigma_{ij}^r \leq (1 - \omega_{ij}^r) \bar{T} \quad \forall (i,j) \in L_{real}, \forall r \in D \tag{23}$$

$$\sigma_{ij}^r \geq 0 \quad \forall (i,j) \in L_{real}, \forall r \in D \tag{24}$$

$$\omega_{ij}^r \in \{0, 1\} \quad \forall (i,j) \in L_{real}, \forall r \in D \tag{25}$$

$$x_{ij}^r \geq 0 \quad \forall (i,j) \in L, \forall r \in D \tag{26}$$

$$v_i^r \in \mathbb{R} \quad \forall i \in N, \forall r \in D \tag{27}$$

Equations (20) and (26) are the same as Eqs. (12) and (19) in the lower level model, respectively. The dual variables, represented by v_i^r , refer to the Lagrangian multipliers of Eq. (12). Equations (21)–(25) linearise the complementarity constraints of the KKT conditions. The multipliers' signs are unrestricted, as indicated by Eq. (27).

3.2 Linearising the Link Cost Function

The BPR function is non-linear with respect to the flow variable x_{ij} only; it is a convex function [19]. We approximate the BPR function, Eq. (1), using piece-wise linearisation. We partition the range of each flow variable, set by the limiting bounds, into s segments, with corresponding a priori points within the range of the flow variable from ξ_{ij}^1 to ξ_{ij}^{s+1} . We introduce the continuous variables $\lambda_{ij}^1, \dots, \lambda_{ij}^{s+1}$, as Special Ordered Sets of Type 2 (SOS2), to act as disaggregate convex combination weights.

We let \tilde{t}_{ij} be a variable that approximates the time function. We let H be the set of elements from 1 to $s + 1$, while another set containing one less element, namely \hat{H} , is defined as:

$\hat{H} = \{\alpha \in H: \text{ord}(\alpha) < |H|\}$. We introduce the binary variables ζ_{ij}^α to mimic SOS2 variable behaviour. To implement the piece-wise linearisation, we define the following set of equations:

$$x_{ij} = \sum_{\alpha \in H} \lambda_{ij}^\alpha \zeta_{ij}^\alpha \quad \forall (i, j) \in L \quad (28)$$

$$\tilde{t}_{ij} = \sum_{\alpha \in H} \lambda_{ij}^\alpha T_{ij}^0 \left(1 + \eta_{ij} \left(\frac{\zeta_{ij}^\alpha}{c_{ij}} \right)^\beta \right) \quad \forall (i, j) \in L \quad (29)$$

$$\sum_{\alpha \in H} \lambda_{ij}^\alpha = 1 \quad \forall (i, j) \in L \quad (30)$$

$$\lambda_{ij}^\alpha \leq \zeta_{(ij)\alpha-1} + \zeta_{(ij)\alpha: \alpha \in \hat{H}} \quad \forall \alpha \in H, (i, j) \in L \quad (31)$$

$$\sum_{\alpha \in \hat{H}} \zeta_{(i,j), \alpha} = 1 \quad \forall (i, j) \in L \quad (32)$$

$$\tilde{t}_{ij} \geq 0 \quad \forall (i, j) \in L \quad (33)$$

$$\lambda_{ij}^\alpha \geq 0 \quad \forall (i, j) \in L, \forall \alpha \in H \quad (34)$$

$$\zeta_{(i,j), \alpha} \in \{0, 1\} \quad \forall (i, j) \in L, \forall \alpha \in H \quad (35)$$

Equations (28) and (29) define the approximation of the flow variable and the approximated time function, respectively. Equations (30)–(32) imitate the SOS2 variable behaviour, while Eqs. (33)–(35) define the domains of the variables.

3.3 Linearisation of the Total System Travel Cost

The nonlinearity in Eq. (2) can be dealt with by replacing Eq. (2) with a linearised objective function that models the same concept of the system travel time. Given that the dual prices, v_i^r , represent the shortest travel time from origin i to destination r , and since we already have the demand values q_{ir} defined, an equivalent linear version of Eq. (2) can thus be defined as:

$$\min g_1' = \sum_{r \in C} \sum_{i \in D} v_i^r q_{ir} \quad (36)$$

3.4 *Scalarisation Technique*

In order to deal with the multi-objective (MO) nature of our model, we combine the three objectives into a single function. To do so we firstly define a scaling factor for each objective function based on its individual optimal solution. The multi-objective optimisation then takes place in a non-dimensional unit-less space. We aim to derive a sample of the overall solutions on the Pareto front; hence we do not focus heavily on methods for choosing appropriate weight vectors to establish a correspondence between the weights and the solutions. We do note that in the MO scalarisation method, the choice of a weight combination for the three objectives does not necessarily correspond to the level of importance of either objective relative to the decision maker. The choice that we make for the weight vector is solely based on incrementing the weights from a small value to a large one to allow us to capture as much of the solutions on the Pareto front. Our feasible solution space, which is a representation of the set of values of the objective functions we are interested in optimising, is non-convex, and this is due to the integrality conditions enforced in our model. Non-convex parts of the Pareto front will not be covered due to the convex nature of the scalarisation approach.

We let g_w^* denote the optimal value of each single objective function u , and we let $\psi_u \geq 0$ denote the weight assigned for each objective function, such that $\sum_u \psi_u = 1$. Our overall optimisation model can then be presented as:

$$\min_{z,x} \psi_1 \frac{g_1'}{g_1^*} + \psi_2 \frac{g_2}{g_2^*} + \psi_3 \frac{-g_3}{g_3^*} \tag{37}$$

subject to

Equations (5)–(10), (20)–(35)

$$\sigma_{ij}^r = \tilde{t}_{ij} - v_i^r + v_j^r \quad \forall (i,j) \in L, \forall r \in D \tag{38}$$

3.5 *Benders Decomposition*

After linearising our original problem, we get a single level MIP model, which we can solve using BD algorithm [2]. BD often relies on formulating a master problem, containing complicating integer variables, while a set of sub-problems, containing continuous variables, are solved. We fix the values of the integer variables and we solve the sub-problem to generate a set of either feasibility or optimality cuts, passed on to the master problem. The solution of the sub-problem gives the upper bound value (for a minimisation problem). The master problem is then solved and its solution is compared to the lower bound. This process of iterating between the

master problem and the sub-problem continues until convergence between the upper bound and the master problem optimal value is achieved.

To describe the concept involved behind the BD algorithm which we apply, we present the following mathematical example, adopting the notation set of [11]

Assume that our model can be simplified into the following MIP representation:

$$\begin{aligned} \min_{x,y} \quad & c^T x + f^T y \\ Ax + By \geq & b \\ y \in & Y \\ x \geq & 0 \end{aligned} \tag{MIP - 1}$$

where c^T, f^T, A, B, b are all parameters.

If the integer variable is attached to a fixed configuration, the problem that we will be interested in solving is:

$$\begin{aligned} \min_x \quad & c^T x \\ Ax \geq & b - B\bar{y} \\ x \geq & 0 \end{aligned} \tag{P - SP}$$

This represents our primal sub-problem (P-SP). For each constraint defined in the primal model, we can obtain its dual price, as an extreme point, if the primal problem is feasible, or through an extreme ray, if the sub-problem is infeasible. These prices then allow us to define our Master problem (MP) as follows:

$$\begin{aligned} \min_y \quad & l \\ l \geq & f^T y + (b - By)^T \bar{u}_{extreme} \\ (b - By)^T & \bar{u}_{ray} \leq 0 \\ y \in & \{0, 1\} \\ l \geq & 0 \end{aligned} \tag{MP}$$

where l is a continuous variable defined in the master problem and which is the only term in the objective function of the master problem that is optimised (minimised if the original problem is a minimisation problem).

We can now present the BD algorithm which we adopted, Algorithm 1. As the first step in the algorithm, we fix the integer variables in the sub-problem to a feasible solution. We initialise the upper bound and lower bounds. We then solve the sub-problem. If the sub-problem is found to be infeasible then we add the feasibility cuts to the master problem. Else the sub-problem is optimally solved, the upper bound is updated, and in the case that the algorithm has not converged yet,

we add an optimality cut to the master problem. The master problem is solved and the lower bound is updated to check the convergence condition.

```

Initialise  $y := 1, LB := -\infty, UB := \infty$ 
while  $UB - LB > 0.0001$ 
  solve sub-problem
  if sub-problem unbounded then
    add feasibility cut to Master problem
  else
    add optimality cut to Master problem
     $UB := \min\{UB, f^T y + C^T x\}$ 
  solve Master problem
   $LB := z$ 
    
```

Algorithm 1. Benders Decomposition

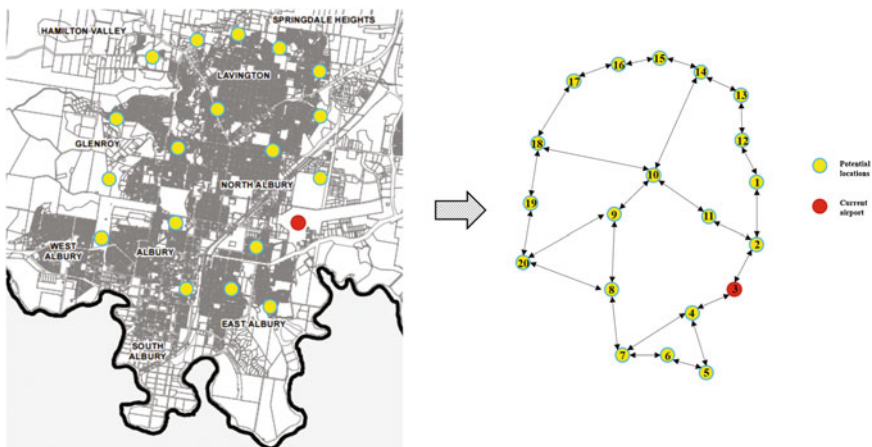


Fig. 2 Simplified network, Albury

4 Numerical Example

We test our proposed model and solution methodologies on a hypothetical scenario involving the siting of several sensitive facilities in the city of Albury, Australia, where the aircraft noise impacts due to Albury Airport, considered as the existing semi-obnoxious facility, are accounted for. The region under study is shown in Fig. 2, along with a simplified road network of Albury which we consider. We make the following assumptions: (1) all nodes in the network are potential suitable locations that need to be assessed; all these nodes represent population nodes too;

Table 1 Facility properties

Facility	Threshold noise limit τ (dB(A))
F1	40
F2	42
F3	60
F4	52
F5	51
F6	45
F7	55
F8	70

Table 2 Link properties

Tail node	Head node	T_{ij}^0	c_{ij}	Tail node	Head node	T_{ij}^0	c_{ij}
1	2	4	470	11	10	5	625
2	1	4	470	10	14	8	1800
2	3	2	370	14	10	8	1800
3	2	2	370	10	18	7	1460
3	4	3	410	18	10	7	1460
4	3	3	410	11	2	3	700
4	5	5	490	2	11	3	700
5	4	5	490	1	12	4	650
4	7	6	640	12	1	4	650
7	4	6	640	12	13	3	550
5	6	3	350	13	12	3	550
6	5	3	350	13	14	3	600
6	7	3	380	14	13	3	600
7	6	3	380	14	15	2	600
7	8	5	710	15	14	2	600
8	7	5	710	15	16	2	610
8	9	7	1100	16	15	2	610
9	8	7	1100	16	17	3	770
8	20	6	1050	17	16	3	770
20	8	6	1050	17	18	5	1200
9	10	4	670	18	17	5	1200
10	9	4	670	18	19	4	1300
9	20	7	770	19	18	4	1300
20	9	7	770	19	20	4	1200
10	11	5	625	20	19	4	1200

(2) the facilities to be located are sensitive to noise, and these all provide the same service to people. Table 1 gives the noise thresholds of each facility to be located, where dB(A) are A-weighted decibels, defining the units of measurement of noise.

(3) Noise levels resulting from the operation of Albury Airport are obtained after assessing the Australian Noise Exposure Forecast chart associated with Albury Airport, obtained from Air-services (“WebTrak|Airservices,” [22] and deriving the maximum noise levels resulting due to aircraft flyovers at each node. (4) The capacities and free flow travel times for the underlying network, shown in Table 2, have been determined through extrapolations, relying on the inferred road classes within Albury. Table 3 gives the locations, the noise assessment and the population at each node of the network.

A total of 8 noise sensitive facilities are to be sited across the city of Albury. The size of the network is composed of 21 nodes and 76 links (of which 38 are virtual links). In total there exists 30,474,662,40 solutions, thus highlighting the highly combinatorial nature of the urban location problem we are solving.

The MIP model along with the BD algorithm were implemented in AMPL and were solved on an Intel core i7 CPU, 4 GB RAM. The calculations were performed for two values of segments s introduced in Sect. 3.2, namely 3 and 6. Computational results are shown in Table 4, where we contrast the performance of BD with a pure

Table 3 Node properties

Node	Max noise due to airport (dB(A))	Population	Coordinates	Node	Max noise due to airport (dB(A))	Population	Coordinates
1	71	7000	(16,10)	11	71	7000	(14,7)
2	83	9000	(17,7)	12	72	7000	(15,12)
3	–	3000	(15,5)	13	59	5000	(15,16)
4	81	8000	(13,4)	14	40	4000	(13,18)
5	69	7000	(14,1)	15	42	5000	(9,19)
6	69	7000	(13,3)	16	43	4000	(4,18)
7	71	8000	(6,2)	17	45	4000	(3,17)
8	68	7000	(5,5)	18	47	5000	(2,12)
9	55	5000	(4,7)	19	51	5000	(15,7)
10	62	6000	(4,10)	20	45	5000	(1,6)

Table 4 Computational results

	Weight assignment	MIP		BD	
		Time (s)	Objectives (g_1, g_2, g_3)	Time (s)	Objectives (g_1, g_2, g_3)
$s = 3$	1	223	(81000,85,7843)	41	(81000,85,7843)
	2	213	(92000,81,8813)	37	(92000,81,8813)
	3	214	(93000,75,7921)	32	(93000,75,7921)
$s = 6$	1	–	(83200,63,11233)	342	(94200,75,7921)
	2	–	(86400,65,10653)	324	(95000,75,7921)
	3	–	(64300,75,12433)	298	(95300,75,7921)

MIP approach applied on the single level formulations. We limit the run times to 1000 s and the optimality gap was set at 0.1%. CPLEX was deployed to solve the linear Program and MIP in both models. Samples of the Pareto points on the front are obtained by altering the weighting given to each objective function in Eq (37), and this is shown in Table 4, through various weight configurations. The 1st set of weights is (0.4, 0.5, 0.1); 2nd set is (0.1, 0.2, 0.7); and the 3rd set is (0.5, 0.3, 0.2). These have been chosen arbitrarily for the purpose of demonstrating the ability of our approach to yield different solutions on the Pareto front. The computation time of BD for the case where $s = 3$ was comparatively lower than the time taken to solve the pure MIP. The advantage of applying BD can particularly be noticed for the case where $s = 6$, as the instances are always solved when BD is deployed. The pure MIP fails to achieve a result within the time limit specified for instances where $s = 6$. We observed that most of the time spent in BD algorithm was on solving the primal sub-problem. From the results of Table 4 we can also deduce that the time taken by MIP and BD depends on the segment value adopted; the greater the segments the higher the computation effort required. Solutions obtained correspond to non-dominated points where a trade-off between maximising facility coverage, minimising noise impacts and minimising total system travel time exists.

5 Conclusion

In this paper, we proposed a bi-level multi-objective model for the multi-facility location problem in the presence of a semi-obnoxious facility, where the facilities to be located are assumed to be demand inducing. As a result, we included the impacts of introducing the facilities on the underlying traffic network. The bi-level model is converted into a single level one by replacing its lower level UE convex program with associated KKT conditions. We then implemented a BD algorithm to solve the NP hard model for a realistic instance. BD proved to be more effective than simply adopting a pure MIP approach.

Several limitations exist in our study including: (1) the large time taken to solve the sub-problem of BD; (2) demand is assumed fixed rather than elastic. Future research avenues could comprise the development of faster decomposition approaches to the multi-facility urban design problem in the presence of semi-obnoxious facility, and the use of elastic demand to model the impact of the introduced facilities.

References

1. Bard, J.F.: Practical Bilevel Optimization: Algorithms and Applications. Springer Science & Business Media (2013)
2. Benders, J.F.: Partitioning procedures for solving mixed-variables programming problems. *Numer. Math.* **4**, 238–252 (1962). doi: [10.1007/BF01386316](https://doi.org/10.1007/BF01386316)

3. Berman, O., Wang, Q.: Locating semi-obnoxious facilities with expropriation: minisum criterion. *J. Oper. Res. Soc.* **58**, 378–390 (2007)
4. Bracken, J., McGill, J.T.: Mathematical programs with optimization problems in the constraints. *Oper. Res.* **21**, 37–44 (1973). doi:[10.1287/opre.21.1.37](https://doi.org/10.1287/opre.21.1.37)
5. Carrizosa, E., Conde, E.: A fractional model for locating semi-desirable facilities on networks. *Eur. J. Oper. Res.* **136**, 67–80 (2002). doi:[10.1016/S0377-2217\(01\)00030-3](https://doi.org/10.1016/S0377-2217(01)00030-3)
6. Church, R., Velle, C.R.: The maximal covering location problem. *Pap. Reg. Sci.* **32**, 101–118 (1974). doi:[10.1111/j.1435-5597.1974.tb00902.x](https://doi.org/10.1111/j.1435-5597.1974.tb00902.x)
7. Contreras, I., Fernández, E., Reinelt, G.: Minimizing the maximum travel time in a combined model of facility location and network design. *Omega, Spec. Issue Forecast. Manag. Sci.* **40**, 847–860 (2012). doi:[10.1016/j.omega.2012.01.006](https://doi.org/10.1016/j.omega.2012.01.006)
8. Dempe, S.: *Foundations of Bilevel Programming*. Springer Science & Business Media (2002)
10. Even, S., Itai, A., Shamir, A.: On the complexity of time table and multi-commodity flow problems. In: Presented at the 16th Annual Symposium on Foundations of Computer Science, 1975, pp. 184–193 (1975). doi: [10.1109/SFCS.1975.21](https://doi.org/10.1109/SFCS.1975.21)
11. Gutjahr, W.J., Dzubur, N.: Bi-objective bilevel optimization of distribution center locations considering user equilibria. *Trans. Res. Part E Logist. Trans. Rev.* **85**, 1–22 (2016). doi:[10.1016/j.tre.2015.11.001](https://doi.org/10.1016/j.tre.2015.11.001)
9. Kalvelagen, E.: *Two Stage Stochastic Linear Programming with GAMS*. Amsterdam Optimization Modeling Group LLC, Washington DC (2003)
12. Matisziw, T.C., Murray, A.T.: Siting a facility in continuous space to maximize coverage of a region. *Socioecon. Plan. Sci. The contributions of Charles S. Reville* **43**, 131–139 (2009). doi:[10.1016/j.seps.2008.02.009](https://doi.org/10.1016/j.seps.2008.02.009)
13. Melachrinoudis, E., Xanthopoulos, Z.: Semi-obnoxious single facility location in Euclidean space. *Comput. Oper. Res.* **30**, 2191–2209 (2003). doi:[10.1016/S0305-0548\(02\)00140-5](https://doi.org/10.1016/S0305-0548(02)00140-5)
14. Murawski, L., Church, R.L.: Improving accessibility to rural health services: The maximal covering network improvement problem. *Socioecon. Plann. Sci. The contributions of Charles S. Reville* **43**, 102–110 (2009). doi:[10.1016/j.seps.2008.02.012](https://doi.org/10.1016/j.seps.2008.02.012)
15. Ohsawa, Y.: Bicriteria Euclidean location associated with maximin and minimax criteria. *Nav. Res. Logist.* **47**, 581–592 (2000). doi:[10.1002/1520-6750\(200010\)47:7<581:AID-NAV3>3.0.CO;2-R](https://doi.org/10.1002/1520-6750(200010)47:7<581:AID-NAV3>3.0.CO;2-R)
16. Ohsawa, Y., Plastria, F., Tamura, K.: Euclidean push–pull partial covering problems. *Comput. Oper. Res. Part Special Issue: Recent Algorithmic Advances for Arc Routing Problems* **33**, 3566–3582 (2006). doi:[10.1016/j.cor.2005.03.034](https://doi.org/10.1016/j.cor.2005.03.034)
17. Ohsawa, Y., Tamura, K.: Efficient location for a semi-obnoxious facility. *Ann. Oper. Res.* **123**, 173–188 (2003). doi:[10.1023/A:1026127430341](https://doi.org/10.1023/A:1026127430341)
18. Plastria, F., Gordillo, J., Carrizosa, E.: Locating a semi-obnoxious covering facility with repelling polygonal regions. *Discret. Appl. Math.* **161**, 2604–2623 (2013). doi:[10.1016/j.dam.2013.05.010](https://doi.org/10.1016/j.dam.2013.05.010)
19. Sheffi, Y.: *Urban Transportation Networks: Equilibrium Analysis With Mathematical Programming Methods*. Prentice-Hall (1984)
20. Skriver, A.J.V., Andersen, K.A.: The bicriterion semi-obnoxious location (BSL) problem solved by an ϵ -approximation. *Eur. J. Oper. Res.* **146**, 517–528 (2003). doi:[10.1016/S0377-2217\(02\)00271-0](https://doi.org/10.1016/S0377-2217(02)00271-0)
21. Sun, H., Gao, Z., Wu, J.: A bi-level programming model and solution algorithm for the location of logistics distribution centers. *Appl. Math. Model.* **32**, 610–616 (2008). doi:[10.1016/j.apm.2007.02.007](https://doi.org/10.1016/j.apm.2007.02.007)
22. WebTrak!Airservices [WWW Document]. <http://www.airservicesaustralia.com/aircraftnoise/webtrak/> (2016). Accessed 5 June 16
23. Yapicioglu, H., Smith, A.E., Dozier, G.: Solving the semi-desirable facility location problem using bi-objective particle swarm. *Eur. J. Oper. Res.* **177**, 733–749 (2007). doi:[10.1016/j.ejor.2005.11.020](https://doi.org/10.1016/j.ejor.2005.11.020)

Can Three Pronouns Discriminate Identity in Writing?

David Kernot

Abstract In a study of three female and two male contemporary authors, five thousand words from each was obtained by accessing 30 freely available news articles, Web articles, personal blog posts, book extracts, and oration transcripts on the Internet. The data was anonymised to remove identity. All 25,000 words were aggregated across the 30 articles by word frequency and 29 personal pronouns extracted and normalised by sample size. Using logistic regression, each sample was tested to determine if it were possible to identify the author's gender using a subset of personal pronouns. The study found that it is possible to identify gender with 90% accuracy using the three pronouns 'my', 'her', and 'its. The technique was tested against six independent samples with 84% accuracy and could support the identification of adversaries on the Internet or in a theatre of war.

Keywords DOMEX • Identity • Authorship analysis • Pronouns • Logistic regression

1 Introduction

The anonymity of the Internet makes it an attractive platform for those wishing to conduct various crimes, including terrorism, where perpetrators mask their true name, age, and gender [1]. Outside of the Internet, document and media exploitation (DOMEX) supports a wide range of intelligence activities, provides critical intelligence unavailable through any discipline, and at its heart aims to exploit an adversaries' documents and other media [2]. Being able to attribute the authorship of a document or media record to an individual, such as an insurgent or a bomb maker can be just as important as the content [3–6].

D. Kernot (✉)

Joint and Operations Analysis Division, Defence Science Technology Group,
Edinburgh, Australia
e-mail: david.kernot@dsto.defence.gov.au

Here, we provide some background into authorship analysis and focus on gender. Authorship analysis examines the characteristics of a document and stems from stylometry, which is the statistical analysis of writing styles [7]. Groc [8] suggests that ‘authorship analysis’ can capture the writing styles of anonymous senders. Three subcategories exist within the general stylometry domain, and they are each used to identify different elements of an author or their writing style. Today, stylometry is used in similarity detection (to detect plagiarism), in authorship identification (to find anonymous authors), and authorship characterisation (for criminal investigations within the forensic linguistic domain) [7, 9–13].

The selection of the descriptors that characterise both text and the author is critical within stylometry and best described as ‘author’s invariant’, a text property that is similar across all texts an author creates but is different for each author. Establishing these properties is difficult [14], and the techniques are still being optimised [15, 16]. Current studies suggest that the area of debate around a writer’s invariant is in determining which text properties should be used. Word lengths, average word or sentence length, frequency of nouns, or verb or adjective use, the richness of vocabulary, specific usage, or frequency of function words, have been considered [17]. The word types that appear as a writer’s invariant words can be divided into function words and content words. Here, we focus on function words.

Function words are pronouns, conjunctions, prepositions, auxiliary verbs, and some adverbs. Function words have little lexical (or carry ambiguous) meaning and signal the structural relationships words have with each another, but their value is that they carry the mood and attitude of the writer [18]. Function words within texts can determine authorship identification, and there are not many of them in the English language that may help authorship identification [19, 20]. Analysis of the use of function words shows promise because they are used unconsciously by authors [16]. Fewer than 400 English speaking words are function words, less than 0.04%, and account for more than half of the words used in daily speech [21–24].

There are also sex differences in the use of virtually all function words, which includes pronouns [23]. People have a sense of personal uniqueness, and the expression of that sense appears in their use of pronouns, to the point the pronouns have attributes of the person writing [25]. Children’s conversational styles differ as they begin to socialise [26]. While girls develop an interest in conjunctions, boys tend to prefer nouns; when they grow up, women are more likely to use the first person singular pronouns, such as, ‘I’, ‘you’, and ‘she’, while men tend not to [26, 27]. Men use more common and proper nouns, such as ‘he’, ‘him’, ‘his’, and ‘himself’ [28]. Articles and prepositions are used significantly more by male bloggers, while personal pronouns, conjunctions, and auxiliary verbs are used significantly more by female bloggers [11, 29]. These points highlight the way people use pronouns and are a reflection of our speech and early socialisation, and this difference can indicate gender.

Overall, pronoun use is used more by females than males in both fiction and non-fiction, and while there are exceptions, this is true using 29 gender-specific first person, second person, and third person pronouns in both fiction and non-fiction samples [11]. Prediction of author gender from function word studies gave

accuracies of between 79.3 and 80.5%, and the results are consistent with classification studies on author gender in other types of texts [28–31].

A Naïve-Bayes classifier written with the assistance of the Natural Language Processing Toolkit (NLTK) subsequently trained provided 69% accuracy at predicting gender [32]. This does not achieve the same accuracy as the Argamon et al. study of author gender of formal texts (80%) [28]. Herring and Paolillo [33] achieved a higher accuracy of 95%, but they used blog authors, and their study used the Gender Genie website which is a derivation of the original Argomon et al. [28] machine learning algorithm. Another more recent study by Kagstrom et al. [34] suggested they also achieved 95% on blogs using a Naïve-Bayes classifier also, but after testing, Lai [32] believes their algorithm made mistakes on texts about programming by female authors and classified it as 65% effective. The multinomial Naïve-Bayes is a probabilistic learning method, popular for text classification, as is the multivariate Bernoulli model. Both attempt to classify text and are more complex due to their training requirements and in defining document representation [35].

In these more recent studies, it is important to note that they were used on blogs and that nobody achieved results higher than the way Argamon et al. [28] classified texts, but we believe that a subset of the significant data [28] can classify both formal texts and blogs better than 80%.

While it is possible to determine subtle differences between people by studying similarity of word patterns, semantic choices, word distribution and frequency of word choice [36], rely on basic statistical correlations, word counts, collocated word groups, or keyword density [37–40], we focus on gender. Gender identity masking is made easier because there are differences between a person’s biological sex and their socially constructed gender, not all women’s gender-related language is feminine, nor are all men’s masculine [1]. While little work has been done in gender identification from text since 2002 [1], our study [4] builds on Argamon et al.’s [28] analysis of 25 million words in 604 documents across the British National Corpus and suggests that the problem of identity masking is a wider DOMEX problem that extends outside of the Internet.

2 Methodology

Beginning with a hypothesis that ‘gender-based words in a given text can be used to discriminate between different authors’, we see if we can identify a writer’s gender from their use of personal pronouns using logistic regression analysis.

2.1 Preprocessing

We follow Argamon et al. [28] and limit each author’s work to six articles, but rather than use of fiction and non-fiction (natural science, applied science, social

science, world affairs, commerce, arts, belief/thought, and leisure), we sourced a range of freely available news reports, Web articles, personal blog posts, book extracts, and an oration transcript, for a sample size of 30 written samples from five contemporary Australian author's writing (three females and two males). While there are differing views held about the adequacy of a sample size of 30, we draw on the results of Argamon et al.'s [28] significant results using a sample of 640 articles. Linacre [41] suggests that it is feasible to develop a well-designed pilot study to a confidence value of 95% with a minimum sample size range between 16 and 36 (poor to best targeting), and a sample of 30 is the size for most purposes.

All identifying features were removed from the articles, including stop words (punctuation and numbers), so that each author contributed exactly 5,000 words across their six article contribution (article size: min 480, max 1289, average 834 words). A consolidated list of all unique words was created from the 25,000-word corpus, and each of the 30 articles was reduced to a word frequency list. Each list was given a unique identifier (1–30), author's gender (M or F), and each author's work identified as A–E only. Each of the 30 articles was normalised (all word frequency count lists were divided by the sample (article) size so that all 30 samples carried the same weight, and the values were divided by ten so that the range fell between 0 and 1). The sample was then randomly reordered to mask identity further. We reduce our word sample to 1,981 words using the gold standard for gender in use since 2003 (the 29 personal pronouns identified in the Argamon et al. [28] study that contributes to gender in Table 1).

2.2 *Article Selection Criteria*

To ensure the results were not skewed from their onset, a mix of both male- and female-authored articles was collected such that two of the authors are male and two female. The decision to choose an additional female author was driven by the ease of finding a third female author with a wide mix of article types, and hence adds more sample variety. For this study, each author contributes 5,000 words to the sample, even if that means cutting articles short. Each author contributes six articles of varying size that, where possible, includes at least one: book or extract, blog post, and newspaper article. These were chosen to obtain possible variations in writing styles.

The authors of articles selected were residents of Australia. However, ethnicity was not considered in determining authorship, because it would reduce the impartiality of the test. Personal data about each author (identified by a unique number only) is limited to gender. The only criterion was that the texts had to be written in English. Each author's contribution is divided into six random contemporary written texts extracted from the Internet. Criteria used in selection was as follows: The sources of written text are from a range of assorted contemporary literature, such as newspaper articles, magazine articles, books, and website sources; Proquest ANZ Newsstand is a major source of material; In selecting articles

Table 1 English language pronouns by assumed gender

Pronouns	Tag	Female $\mu \pm \text{stderr}$	Male $\mu \pm \text{stderr}$	t-test	Female median	Male median
he	M	271 ± 9.3	305 ± 11	$p < 0.05$	276	305
her	F	53.8 ± 5.1	18.5 ± 3.5	$p < 0.0001$	29.8	5.60
hers	F	53.8 ± 5.1	18.5 ± 3.5	$p < 0.0001$	29.8	5.60
herself	F	53.8 ± 5.1	18.5 ± 3.5	$p < 0.0001$	29.8	5.60
him	M	271 ± 9.3	305 ± 11	$p < 0.05$	276	305
himself	M	271 ± 9.3	305 ± 11	$p < 0.05$	276	305
his	M	271 ± 9.3	305 ± 11	$p < 0.05$	276	305
I	F	149 ± 14	86 ± 8	$p < 0.0002$	66.7	50.2
it	F	89.1 ± 2.8	86.7 ± 2.4	n/s	85.3	82.9
its	M	15.3 ± 0.93	19.0 ± 0.79	$p < 0.005$	12.2	19.0
me	F	149 ± 14	86 ± 8	$p < 0.0002$	66.7	50.2
mine	F	149 ± 14	86 ± 8	$p < 0.0002$	66.7	50.2
my	F	149 ± 14	86 ± 8	$p < 0.0002$	66.7	50.2
myself	F	149 ± 14	86 ± 8	$p < 0.0002$	66.7	50.2
our	F	149 ± 14	86 ± 8	$p < 0.0002$	66.7	50.2
ours	F	149 ± 14	86 ± 8	$p < 0.0002$	66.7	50.2
ourselves	F	149 ± 14	86 ± 8	$p < 0.0002$	66.7	50.2
she	F	53.8 ± 5.1	18.5 ± 3.5	$p < 0.0001$	29.8	5.60
their	F	97.8 ± 4.6	81.8 ± 2.7	$p < 0.005$	83.9	78.8
theirs	F	97.8 ± 4.6	81.8 ± 2.7	$p < 0.005$	83.9	78.8
them	F	97.8 ± 4.6	81.8 ± 2.7	$p < 0.005$	83.9	78.8
themselves	F	97.8 ± 4.6	81.8 ± 2.7	$p < 0.005$	83.9	78.8
they	F	97.8 ± 4.6	81.8 ± 2.7	$p < 0.005$	83.9	78.8
us	F	149 ± 14	86 ± 8	$p < 0.0002$	66.7	50.2
we	F	149 ± 14	86 ± 8	$p < 0.0002$	66.7	50.2
you	F	63.9 ± 8.0	30.0 ± 5.2	$p < 0.0005$	16.7	3.9
your	F	63.9 ± 8.0	30.0 ± 5.2	$p < 0.0005$	16.7	3.9
yours	F	63.9 ± 8.0	30.0 ± 5.2	$p < 0.0005$	16.7	3.9
yourself	F	63.9 ± 8.0	30.0 ± 5.2	$p < 0.0005$	16.7	3.9

determine which authors had a published book, and then newspaper articles; Popular authors are chosen with a focus on articles that are only written by that person; Articles written in the first person, where possible, although this was not always the case; 5000 words per author are randomly collated; The articles cover a broad range of subject matter; Where articles are longer the sample starts from the beginning of each article until all the words for that author total 5000, averaging about 800 words per article.

2.3 Stemming

Porter's popular stemming algorithm was initially considered [35] as was the Lancaster stemming algorithm [42] and then discarded. According to Hooper and Paice [42], *stemming* attempts to reduce a word to its *stem* or root form. This reduces dictionary size and can speed up processing time. Stemming can reduce the size of the reference library and subsequently the size of the bag of words, but with such a small sample size, this was not considered important. Stemming can also introduce and contribute to errors into the sample, due to over or under stemming [43, 44], it can also group words that do not have the same flavour [35]. These disadvantages would make a larger impact on such a small sample size, and therefore a larger, un-stemmed, but more accurate sample was preferred, but in this case, the personal pronouns 'hers', 'ours', 'theirs', and 'yours' were stemmed by the removal of the 's'.

2.4 Logistic Regression Testing

Logistic regression is determined to be the most appropriate statistical test, given the small sample size, and it allows prediction of a categorical dependent variable by two predictor or independent variables [45], such as gender. The form of the logistic regression equation or function is as follows:

Equation 1 Logistic Regression Equation

$$\text{logit}(p) = a + b_1X_1 + b_2X_2 + b_3X_3 + \dots + b_iX_i \quad (1)$$

where:

- (*p*) the probability that a case is a particular category,
- a* the constant of the equation, and
- b* the coefficient of the predictor variables.

The data is tested using R, a free software environment for statistical computing and graphics package. The method of testing the data was with the lrm—logistic regression models.

3 Gender Testing

From the 29 personal pronouns (minus the four stemmed words) identified in the Argamon et al. [28] study (see Table 1), a 25×30 matrix of personal pronouns was fed into the lrm package within R to conduct logistic regression analysis and determine if the gender is identifiable.

The 25 personal pronouns correctly match 11 of the author's gender, for an accuracy of 36%. The least statistically significant words are iteratively removed and logistic regression conducted each time to achieve a maximum of 28 correctly

identified articles by gender (93%) from five words (“my/her/its/themselves/them”). Several further tests are conducted with removal of statistically significant words.

The least significant word ‘its’ is removed and the test is run again resulting in 26 successful gender identifications from the list of 30 (87%) highlighting a smaller score. With ‘her’ removed (i.e. only ‘my’ remaining), results are 13 out of 30 (43%) correctly identified articles by gender. The decrease in scoring indicated that ‘its’ and ‘her’ should be returned to the successful word pool.

The next most significant word ‘themselves’ is included with ‘my/her/its’ and tested with 28 instances (93%) where the gender is successfully identified. The next most significant word ‘them’ is added to ‘my/her/its/themselves’ and tested with 28 instances (93%) of successful gender identification. These two cases (“my/her/its/themselves”, and ‘my/her/its/themselves/them’) have identical scores, and the two documents unable to be successfully matched are the same. For both cases of ‘my/her/its/themselves/them’, the estimate of probability was further away from the real gender results than without ‘them’, and it was therefore discarded. ‘Themselves’ was also discarded by its *p*-value being greater than 0.05 at the expense of one extra gender match.

Subsequent testing using the three most statistically significantly words (‘my’, ‘her’, and ‘its’) showed improvements, correctly identifying 27 of the 30 articles by gender (90%). A summary of the results is provided in the following two tables. In Table 2, the significant aspects of this analysis are shown from a pronoun match and accuracy perspective. In Table 3, the logistic regression formula values are provided, along with the *p*-values for the three most significant words. The coefficient value is the coefficient of the predictor variable, also known as the beta value, and the intercept is the intercept constant. The results of all of the testing are summarised in Appendix A (see Table 5), and the results from them are grouped in order of author for the pronouns ‘my’, ‘her’, ‘its’ (see Table 4).

In Tables 4 and 5, gender is the actual gender of the author. BLR is the binary logistic regression score, and if the score is equal to or greater than 0.5, the author gender is assumed to be male (M). CLASS refers to the classification M or F based

Table 2 Listing of gender-based pronoun matching accuracy

Pronouns	Matches	Accuracy
All 25 words	11	36.6
My/her	26	86.6
My/her/its	27	90.0
My/her/its/themselves	28	93.3
My/her/its/themselves/them	28	93.3

Table 3 Logistic regression values

Pronoun	Coefficient	<i>p</i> -value
My	-451.86	0.0000161
Her	322.47	0.01
Its	129.83	0.03
Intercept	-0.93	
P	0.0000158	

Table 4 Gender results by author

my/her/its						
Author	Gender	BLR	CLASS	MATCH	Article size	Article type
1	F	0	F	True	770	News
1	F	0	F	True	800	Blog
1	F	0	F	True	753	Blog
1	F	0	F	True	931	News
1	F	0	F	True	746	News
1	F	0	F	True	1000	Book extract
2	F	0.4818	F	True	968	Web
2	F	0.2831	F	True	711	Blog
2	F	0	F	True	1017	News
2	F	0	F	True	610	Book extract
2	F	0.6668	M	False	911	Web
2	F	0.1533	F	True	783	Web
3	F	0	F	True	799	News
3	F	0	F	True	909	News
3	F	0.0727	F	True	867	News
3	F	0.1427	F	True	1182	Book extract
3	F	0	F	True	480	Blog
3	F	0	F	True	763	Blog
4	M	0.9102	M	True	1096	Book extract
4	M	0.9962	M	True	1029	News
4	M	0.9999	M	True	938	Essay extract
4	M	0.6668	M	True	596	News extract
4	M	1	M	True	774	News
4	M	0.9983	M	True	567	Web extract
5	M	0.1989	F	False	1289	Book extract
5	M	0.957	M	True	588	News
5	M	0.4762	F	False	830	Web extract
5	M	0.9962	M	True	668	News
5	M	1	M	True	1124	Web extract
5	M	1	M	True	501	News

on the BLR. MATCH refers to the claim that CLASS and gender equate. If the results of BLR and CLASS are incorrect, the column is highlighted in red as FALSE. The results show that Author 1 was correctly matched as female for 100% of the time, Author 2 female for 83.4% of the time, Author 3 female for 100% of the time, Author 4 was identified as male for 100%, and Author 5 was correctly matched as male for 67% of the time.

4 Discussion

The results of this experiment indicate that there is a strong correlation for determining gender if the following words, ‘my’, ‘her’, ‘its’, ‘them’, and ‘themselves’ are used. The results also indicate that a higher relative use of the word ‘my’ meant it was more likely to be a female author. A higher relative use of the words ‘her’ and ‘its’ meant the author was more likely to be male. Of the five most significant words that accounted for 93% accuracy (see Table 2), ‘themselves’ and ‘them’ have *p*-values > 0.05, and for this reason are discarded. While this lowered the overall accuracy, it did so with a more statistically robust model.

Using the logistic regression equation in Eq. 1 Logistic Regression Equation and the resultant data in Table 3 (where the coefficient value is the coefficient of the predictor variable, also known as the beta value, and the intercept is the intercept constant), we can create a gender equation to identify the gender of an author from word samples between 480 and 1289 words using the pronouns ‘my’, ‘her’, and ‘its’. By normalising the data (dividing each pronoun count by the document size divided by 10), the normalised pronoun can identify gender as follows:

Equation 2 Gender Formula

$$(p) = \frac{\exp(-0.93 - (451.86 * \text{My}') + (322.47 * \text{Her}') + (129.83 * \text{Its}'))}{1 + \exp(-0.93 - (451.86 * \text{My}') + (322.47 * \text{Her}') + (129.83 * \text{Its}'))} \quad (2)$$

where: male gender (*p*) ≥ 0.5 and female gender (*p*) < 0.5

We test the gender equation on the original data and find that it replicates the logistic regression results (Table 5) and categorises the articles as male and female the same way, but there is some minor variation in the logistic regression values. We conduct sensitivity testing on the algorithm by changing the normalisation variable (normally set to 10, but tested at 0, 100, and 1000). Instead of dividing the article size by ten so that the article sizes now range between 48 and 129, we use the original article sizes (480–1289 words) and find that the mismatched genders assignments increase from three to eight. We then divide the article size by 100 and

find one of the articles for the male author (see Table 5 ID 11) incorrectly assigned as female becomes a male article (was 0.46 becomes 0.99), and one of the articles allocated to a female author (ID 4) correctly assigned as female becomes a male article (was 0.44 becomes 0.99). However, we still correctly match 27 of the 30 articles, even though more of our logistic regression scores are now 1 (there were two articles with a score of one, but now there are ten) and 0 (there were no articles but now there are four). When we divide the article size by 1000, the results are the same as using a value of 100; however, we find that our logistic regression scores change again, and there are even more polarised with more scores 1 or higher (there are now 13 with some being classed as undefined) and 0 (now 12). We select new independent data, four different works of a female author, and one single work from another male and female author for a sample size of six (range 450–750 words, average size of 637 words) and apply our gender algorithm to it. We find that it correctly matches five of the six articles (84% accuracy).

5 Conclusion

In this study, we have tested thirty articles written by five different authors to see if they can be identified through gender. We find that authors differ in their use of gender-based words, and it is possible to use logistic regression analysis to determine an author's gender from their use of the pronouns 'my', 'her', and 'its' with an accuracy of 90%. Further, independent testing showed it is possible to differentiate the signature of an author based on the logistic regression scores to an accuracy of 84%. More importantly, while the use of the male and female categories provides a simple categorisation of a person, we believe the gender-related identity score can better identify key individuals from insurgent and other networks through DOMEX, and critical intelligence can be obtained using the logistic regression value because of the fidelity of the scores. We further suggest that using a normalisation value against the document size of either ten or one hundred would achieve satisfactory results for the gender component of gender identity.

Acknowledgements This work formed part of a Master of Philosophy thesis through the University of New South Wales [4] and acknowledges the support of two former supervisors, Robert Stocker and Edward Lewis. We thank Andrew Gill for his help with the logistic regression programming within the R environment. This research is supported by the Defence Science Technology Group.

Table 5 Logistic regression testing results

ID	Gender	All 25 pronouns		Match	my/her/its			my/her			my/her/its/themselves		
		BLR	CLASS		BLR	CLASS	MATCH	BLR	CLASS	MATCH	BLR	CLASS	MATCH
1	F	0.9999	M	False	0	F	True	0	F	True	0	F	True
2	M	0	F	False	0.1989	F	False	0.2634	F	False	0.6843	M	True
3	F	0	F	True	0	F	True	0	F	True	0	F	True
4	F	0.0001	F	True	0.4818	F	True	0.1883	F	True	0.2428	F	True
5	F	1	M	False	0.2831	F	True	0.7555	M	False	0.1667	F	True
6	M	0	F	False	0.9102	M	True	0.7555	M	True	1	M	True
7	F	0.9999	M	False	0	F	True	0	F	True	0	F	True
8	M	0	F	False	0.957	M	True	0.9436	M	True	0.9482	M	True
9	F	0	F	True	0	F	True	0	F	True	0	F	True
10	F	0.9998	M	False	0.0727	F	True	0.5567	M	False	0.023	F	True
11	M	1	M	True	0.4762	F	False	0.5324	M	True	0.1548	F	False
12	M	0	F	False	0.9962	M	True	0.7555	M	True	0.996	M	True
13	F	1	M	False	0	F	True	0	F	True	0	F	True
14	M	0.9999	M	True	0.9999	M	True	0.7555	M	True	0.9999	M	True
15	M	0	F	False	0.9962	M	True	0.7555	M	True	0.996	M	True
16	F	0	F	True	0	F	True	0	F	True	0	F	True
17	F	1	M	False	0	F	True	0	F	True	0	F	True
18	M	0.0001	F	False	0.6668	M	True	0.7555	M	True	0.9964	M	True
19	F	0.0001	F	True	0	F	True	0	F	True	0	F	True
20	F	1	M	False	0.1427	F	True	0.106	F	True	0.2006	F	True
21	M	0.0001	F	False	1	M	True	1	M	True	1	M	True
22	F	0.0002	F	True	0	F	True	0	F	True	0	F	True
23	F	0	F	True	0.6668	M	False	0.7555	M	False	0.5422	M	False

(continued)

Table 5 (continued)

ID	Gender	All 25 pronouns		Match	my/her/its			my/her			my/her/its/themselves		
		BLR	CLASS		BLR	CLASS	MATCH	BLR	CLASS	MATCH	BLR	CLASS	MATCH
24	F	0.9999	M	False	0	F	True	0.0004	F	True	0	F	True
25	M	0.0003	F	False	1	M	True	0.9891	M	True	1	M	True
26	F	0	F	True	0	F	True	0	F	True	0	F	True
27	F	1	M	False	0	F	True	0	F	True	0	F	True
28	M	0.0001	F	False	0.9983	M	True	0.9436	M	True	0.9984	M	True
29	F	0.9997	M	False	0.1533	F	True	0.1883	F	True	0.0507	F	True
30	M	1	M	True	1	M	True	0.9996	M	True	1	M	True

References

1. Cheng, N., Chandramouli, R., Subbalakshmi, K.P.: Author gender identification from text. *Digit. Invest.* **8**(1), 78–88 (2011)
2. Cox, C.J.M.: DOMEX: the birth of a new intelligence. *Mil. Intell.* **22**
3. Garfinkel, S.L.: Document and media exploitation. *Queue* **5**(7), 22–30 (2007)
4. Kernot, D.: The identification of authors using cross-document co-referencing. http://www.unsworks.unsw.edu.au/primo_library/libweb/action/dlDisplay.do?vid=UNSWORKS&docId=unsworks_12072 (2013)
5. Kernot, D., Ward, K., Gill, A.: Novel Quantitative Methods for Analysing Questionnaire Data from Afghanistan: Application to the Cultural Compatibility Study. Defence Science Technology Organisation (DSTO), Commonwealth of Australia (2013)
6. Megill, T.A.: Terrain and intelligence collection. Army Command and General Staff Coll Fort Leavenworth KS School Of Advanced Military Studies (1996)
7. Zheng, R., Li, J., Chen, H., Huang, Z.: A framework for authorship identification of online messages: writing-style features and classification techniques. *J. Am. Soc. Inform. Sci. Technol.* **57**(3), 378–393 (2006)
8. Groc, I.: The online hunt for terrorists. PCMag.com. <http://www.pcmag.com/article2/0,2817,2270962,00.asp> (2012). Accessed 9 July 2012
9. Hayes, J.H., Offutt, J.: Recognizing authors: an examination of the consistent programmer hypothesis. *Softw. Test. Verif. Reliab.* **20**(4), 329–356 (2009)
10. Argamon, S., Sarie, M., Stein, S.S.: Style mining of electronic messages for multiple authorship discrimination: first results. In: Proceedings of the 9th ACM SIGKDD Conference on Knowledge Discovery and Data Mining, pp. 475–480. ACM Press (2003)
11. Koppel, M., Argamon, S., Shimoni, A.R.: Automatically categorizing written texts by author gender. *Lit. Linguist. Comput.* **17**(4), 401–412 (2002)
12. Sreeraj, M., Idicula, S.M.: A survey on writer identification schemes. *Int. J. Comput. Appl.* **26**(2), 23–33 (2011)
13. Stanczyk, U., Cyran, K.A.: Can punctuation marks be used as writer invariants? Rough set-based approach to authorship attribution. In: 2nd European Computing Conference (ECC'08), Malta, Sept 2008, pp. 11–13 (2008)
14. Stanczyk, U., Cyran, K.A.: Machine learning approach to authorship attribution of literary texts. *Int. J. Appl. Math. Inform.* **1**(4), 151–158 (2007)
15. Abbasi, A., Chen, H.: Writeprints: a stylometric approach to identity-level identification and similarity detection in cyberspace. *ACM Trans. Inf. Syst.* **26**(2), Article 7, 29 pp. (2008)
16. Chakraborty, T.: Authorship identification in Bengali literature: a comparative analysis. In: Proceedings of COLING 2012: Demonstration Papers, Dec 2012, pp. 41–50 (2012)
17. Nosary, A., Heutte, L., Paquet, T., Lecourtier, Y.: A Step Towards the Use of Writer's Properties for Text Recognition. Laboratoire Perception, Systèmes, Information (PSI), Université de Rouen (2006)
18. Klammer, T.P., Schulz, M.R., Volpe, A.D.: Analyzing English Grammar, 6th edn. Longman (2009)
19. Khmelev, D.V.: Disputed authorship resolution through using relative empirical entropy for markov chains of letters in human language text. *J. Quant. Linguist.* **7**(3), 201–207 (2000)
20. Khmelev, D., Tweedie, F.: Using Markov chains for identification of writers. *Lit. Linguist. Comput.* **16**(4), 299–307 (2001)
21. Allport, G.W.: Pattern and growth in personality. Holt, Rinehart and Winston, New York (1961). Chung, C., Pennebaker, J.: The psychological functions of function words. In: Fiedler, K. (ed.). *Social Communication*, pp. 343–359. Psychology Press, New York (2007)

22. Baayen, R.H., Piepenbrock, R., Bulickers, L.: The CELEX lexical database [CD ROM]. Linguistic Data Consortium, University of Pennsylvania, Philadelphia (1995). Chung, C., Pennebaker, J.: The psychological functions of function words. In: Fiedler, K. (ed.) *Social Communication*, pp. 343–359. Psychology Press, New York (2007)
23. Chung, C., Pennebaker, J.: The psychological functions of function words. In: Fiedler, K. (ed.) *Social Communication*, pp. 343–359. Psychology Press, New York (2007)
24. Rochon, E., Saffran, E.M., Berndt, R.S., Schwartz, M.F.: Quantitative analysis of aphasic sentence production: further development and new data. *Brain Lang* **72**, 193–218 (2000). Chung, C., Pennebaker, J.: The psychological functions of function words. In: Fiedler, K. (ed.) *Social Communication*, pp. 343–359. Psychology Press, New York (2007)
25. Harré, R.: The rediscovery of the human mind: the discursive approach. *Asian J. Soc. Psychol.* **2**(1), 43–62 (1999)
26. McGrath, C.: Sexed texts. *The New York Times*, 10 Aug 2003. <http://www.nytimes.com/2003/08/10/magazine/10WWLN.html> (2003). Accessed 5 Aug 2011
27. Newman, M.L., Pennebaker, J.W., Berry, D.S., Richards, J.M.: Lying words: predicting deception from linguistic style. *Pers. Soc. Psychol. Bull.* **29**, 665–675 (2003). Chung, C., Pennebaker, J.: The psychological functions of function words. In: Fiedler, K. (ed.) *Social Communication*, pp. 343–359. Psychology Press, New York (2007)
28. Argamon, S., Koppel, M., Fine, J., Shimoni, A.R.: Gender, genre, and writing style in formal written texts. *Text* **23**(58) (2003)
29. Argamon, S., Koppel, M., Pennebaker, J.W., Schler, J.: Mining the blogosphere: age, gender and the varieties of self-expression. *First Monday* **12**(9). http://firstmonday.org/issues/issue12_9/argamon/index.html (2007)
30. De Vel, O., Anderson, A., Corney, M., Mohay, G.: Mining e-mail content for author identification forensics. *ACM Sigmod Rec.* **30**(4), 55–64 (2001)
31. Hota, S., Argamon, S., Koppel, M., Zigdon, I.: Performing gender: automatic stylistic analysis of Shakespeare’s characters. In: *Proceedings of Digital Humanities, July 2006* (2006)
32. Lai, C.-Y.: Author gender analysis. Final project: from I 256 Applied Natural Language Processing, University of California, Berkeley, California, fall 2009. Accessed 11 Nov 2013. http://courses.ischool.berkeley.edu/i256/f09/Final%20Projects%20write-ups/LaiChaoyue_project_final.pdf (2009)
33. Herring, S.C., Paolillo, J.C.: Gender and genre variation in weblogs. *J. Sociolinguist.* **10**(4), 439–459 (2006)
34. Kågström, J., Kågström, E., Karlsson, R.: Classify Gender Analyzer_v5. http://www.uclassify.com/browse/uClassify/GenderAnalyzer_v5 (2009)
35. Manning, C.D., Raghaven, P., Schütze, H.: *An Introduction to Information Retrieval*. Cambridge University Press, Cambridge (2009)
36. Rosenstein, M., Foltz, P. W., DeLisi, L. E., & Elvevåg, B.: Language as a biomarker in those at high-risk for psychosis. *Schizophrenia Res.* (2015)
37. Lamb, A., Paul, M.J., Dredze, M.: (2013). Separating fact from fear: tracking flu infections on twitter. In: *HLT-NAACL*, pp. 789–795
38. Leech, N.L., Onwuegbuzie, A.J.: An array of qualitative data analysis tools: a call for data analysis triangulation. *School Psychol. Q.* **22**(4), 557 (2007)
39. Matsuo, Y., Ishizuka, M.: Keyword extraction from a single document using word co-occurrence statistical information. *Int. J. Artif. Intell. Tools* **13**(01), 157–169 (2004)
40. Stamatatos, E.: A survey of modern authorship attribution methods. *J. Am. Soc. Inform. Sci. Technol.* **60**(3), 538–556 (2009)
41. Linacre, J.M.: Understanding Rasch measurement: optimizing rating scale category effectiveness. *J. Appl. Meas.* **3**(1), 85–106 (2002)
42. Hooper, R., Paice, C.: The Lancaster Stemming Algorithm. Lancaster University Summer 2005. <http://www.comp.lancs.ac.uk/computing/research/stemming/general/> (2005). Accessed 19 Nov 2013

43. Paice, C.D.: An evaluation method for stemming algorithms. In: Croft, W.B., van Rijsbergen, C.J. (eds.) Proceedings of the 17th ACM SIGIR Conference held at Dublin, 3–6 July 1994, pp. 42–50 (1994)
44. Paice, C.D.: A method for the evaluation of stemming algorithms based on error counting. *J. Am. Soc. Inf. Sci.* **47**(8), 632–649 (1996)
45. Brace, N., Kemp, R., Snelgar, R.: *SPSS for Psychologists (Versions 12 and 13)*, 3rd edn. Lawrence Erlbaum Associates, Mahwah, New Jersey & London (2006)

Author Index

A

Akbarnezhad, Ali, 381
Aleti, Aldeida, 91
Aracena, Claudio, 27

B

Baatar, Davaatseren, 133
Banerjee, Soumya, 27
Bennier, Jamahl, 343
Bhattacharjee, Kalyan Shankar, 163
Borhan, Nazanin, 27

C

Chakraborty, Ripon K., 227
Chircop, Paul A., 117

D

Davey, Nicholas, 71
Dexter, Richard M., 103, 291
Dunstall, Simon, 71
Dzator, Janet, 369
Dzator, Michael, 369

E

Emrul Kays, H.M., 357
Ernst, Andreas T., 43, 133
Essam, Daryl L., 221, 227
Evertsz, Rick, 13

F

Fulton, Neale L., 187, 201

G

Gallasch, Guy E., 327
García-Flores, Rodolfo, 27
Gore, A., 315
Grossmann, Georg, 103
Gu, Hanyu, 81, 149

H

Halgamuge, Saman, 71
Hammad, Ahmed W.A., 381
Harvey, M., 315
Hasan, M., 357
Holden, Lance, 291
Holder, Andrew, 343

I

Ivanova, Ksenia, 327

J

Jiang, Houyuan, 133
Jordans, Jon, 327

K

Kalloniatis, Alexander, 343
Karim, A.N.M., 357
Kernot, David, 397
Konstantinou, Charalambos, 1
Krishanmoorthy, Mohan, 43, 133

L

La, Phuong, 343
Likic, Vladimir, 303
Ly, Thanh, 13

M

Mak-Hau, Vicky, 91, 175
Mathews, George, 27
Mayer, Wolfgang, 103
Mazonka, Oleg, 1
Memar, Julia, 149
Milowski, Jason, 163
Mitchell, Bruce, 343
Moser, I., 91

N

Nehring, Micah, [221](#)
Niraj Ramesh, D., [43](#)

O

Owen, Kerryn R., [103](#)

P

Paul, Sanjoy Kumar, [243](#)

R

Rahman, Shams, [243](#)
Ray, Tapabrata, [163](#)
Rey, David, [381](#)
Rowe, Cayt, [343](#)

S

Samavati, Mehran, [221](#)
Sarker, Ruhul, [221](#), [227](#), [357](#)
Selway, Matt, [103](#)
Shafi, Kamran, [303](#)
Shine, Denis R., [291](#)

Singh, Hemant Kumar, [163](#)
Smith, Warren F., [187](#), [201](#)
Stumptner, Markus, [103](#)

T

Thangarajah, John, [13](#)
Thorne, Brian, [27](#)
Tyshetskiy, Yuriy, [27](#)

V

Vacher, Blandine, [27](#)

W

Weir, Terence, [271](#)
Westcott, Mark, [187](#), [201](#)

Y

Young, Leon, [259](#)

Z

Zinder, Yakov, [149](#)